

# SOLAR POTENTIAL IN EARLY NEIGHBORHOOD DESIGN A Decision-Support Workflow Based on Predictive Models

THÈSE N° 7058 (2016)

PRÉSENTÉE LE 24 AOÛT 2016

À LA FACULTÉ DE L'ENVIRONNEMENT NATUREL, ARCHITECTURAL ET CONSTRUIT  
LABORATOIRE INTERDISCIPLINAIRE DE PERFORMANCE INTÉGRÉE AU PROJET  
PROGRAMME DOCTORAL EN GÉNIE CIVIL ET ENVIRONNEMENT

ÉCOLE POLYTECHNIQUE FÉDÉRALE DE LAUSANNE

POUR L'OBTENTION DU GRADE DE DOCTEUR ÈS SCIENCES

PAR

Émilie NAULT

acceptée sur proposition du jury:

Prof. M. Bierlaire, président du jury  
Prof. M. Andersen, Prof. E. Rey, directeurs de thèse  
Prof. R. Compagnon, rapporteur  
Prof. K. Steemers, rapporteur  
Prof. B. Cache, rapporteur



ÉCOLE POLYTECHNIQUE  
FÉDÉRALE DE LAUSANNE

Suisse  
2016



# Acknowledgements

I am truly grateful to the many people who contributed to the realization of this research project. I would like to thank in particular:

Prof. Marilyne Andersen for giving me the opportunity to conduct this work within LIPID, for her trust and support, and for her astute guidance from which I greatly learned and benefited.

Prof. Emmanuel Rey, for co-supervising this work and for giving me the chance to participate in the Green Density and Urban Recovery albums, experiences which were very fruitful to my research.

The jury members, Prof. Koen Steemers, Prof. Raphaël Compagnon and Prof. Bernard Cache, for accepting to take on the role of examiner and for reading and commenting on this manuscript with great care and attention. Prof. Michel Bierlaire for kindly accepting to fulfill the role of president of the jury.

The École polytechnique fédérale de Lausanne (EPFL) for the financial support and work environment. The EuroTech Universities Alliance and the SECURE (Synergistic Energy and Comfort through Urban Resource Effectiveness) project funded by the CCEM (Competence Center Energy and Mobility) for the financial support and our colleagues at the ETH and Empa (Zurich) for the fruitful meetings and exchanges.

Task leaders in the International Energy Agency (IEA) Task 51 - Solar Energy in Urban Planning - for giving me the opportunity to participate in this project, and all participants for their advice.

Igor Andersen and Camille Leviel at Urbaplan for their collaboration, interest and very relevant contributions to the project.

Peter Moonen for his trust and collaboration.

Mélanie Huck for her dedication and essential contribution that made it possible to conduct workshops with practitioners, who I also thank for their feedback, which was very beneficial to the completion of this work.

Friends and colleagues who offered of their time to review parts of this thesis and help with some graphics: Martine Laprise, Giuseppe Peronato, Carlos Becker, Sergi Aguacil,

## Acknowledgements

---

Maria Amundadottir, Judith Drouilles, Miguel Bermudez and Minu Agarwal.

Everyone at LIPID and LAST: my fellow colleagues, our senior researchers and our in-house IT expert for their support and helpful advice throughout the project, and our administrative assistants Joëlle Eaves and Martine Tiercy for their precious help. Each one contributed to creating a friendly and stimulating work atmosphere.

Many others have played a role in making this PhD experience so enriching, as it encompasses all spheres of life and extends beyond the campus. I thank each and every one of them - musicians, mountaineers and skiers, board gamers, cat-sitters...I hope you can all recognize yourself.

Finally, my warmest thanks to my inspirational and ever supporting and loving family.

*Lausanne, 30 June 2016*

E. N.

# Abstract

In light of the acknowledged need for a transition toward sustainable cities, neighborhoods and buildings, urban planners, architects and engineers have to comply with evermore demanding energy regulations. These decision-makers must be supported early-on in their process by adequate methods and tools. Indeed, early-design decisions, which concern parameters linked to the building form and urban layout, strongly dictate the solar exposure levels of buildings, in turn influencing their energy need (e.g. for heating and cooling) and production potential (e.g. through on-site active solar systems). Despite the spread of existing digitalized performance assessment methods, limitations remain, withholding their integration into the early design process. These considerations lay down the context within which this doctoral research was carried out.

The main objective of this thesis is the development of a performance-based workflow to support decision-making in early-design neighborhood projects. The performance is here defined through three criteria: (i) the daylight potential, quantified by the spatial daylight autonomy achieved on the ground-floor level (likely to represent a conservative value), (ii) the passive solar potential, quantified by the annual energy need for space heating and cooling (given certain assumptions e.g. on the insulation level), and (iii) the active solar potential, quantified by the annual thermal and photovoltaic energy production on site.

The research process consisted of two main phases. First, the development of a performance assessment engine allowing real-time evaluation of an ensemble of buildings. Second, the integration of this method into a decision-support workflow, taking the form of a digital prototype that was tested among practitioners. The work particularly focused on the Swiss context in terms of design practices and climate, although its extension to other locations is considered straightforward.

For the first phase, a metamodeling approach was adopted to circumvent the limitations associated to simulations involving solving physics-based equations. Mathematical functions were obtained to predict the daylight and energy performance of a neighborhood, from a series of geometry- and irradiation-based parameters, easily computable at the early-design phase. To derive these functions (or metamodels), a neighborhood modeling and simulation procedure was executed to acquire a dataset of reference cases, from which the metamodels were trained and tested. The resulting multiple-linear regression functions, combined to an algorithm for quantifying the active solar potential from the irradiation levels, formed our performance assessment engine. This core and novel part of the research also brought forward some knowledge on precautions to take when using certain performance indicators

## Abstract

---

or analyzing and interpreting simulation data.

To assess its usability and relevance, the workflow was implemented as a prototype, supported by existing 3D modeling and scripting tools. Inspired by the emerging performance-driven and non-linear design paradigms, a multi-variant approach was adopted for this implementation; from the space of possible designs defined by a small set of user-inputs, a series of neighborhood variants are generated through a random sampling algorithm. Results of their evaluation by the core engine are displayed to allow a comparative assessment of the variants in terms of their morphology and solar potential. Having been tested among practitioners during workshops, the prototype appears promising for providing design decision-support. Direct feedback gathered from participants support the relevance of the approach and reveals multiple avenues for further improvement. Results collected during the workshops also allowed probing the validity boundaries of the metamodels, by applying them on the professionals' designs and comparing the predictions to the simulation outputs, taken as reference. The prediction accuracy achieved attests the potential of the approach as an alternative to more complex methods, less adequate for exploring early-phase design alternatives.

Key words: early-phase neighborhood design, passive and active solar potential, design decision-support, predictive mathematical model, multi-criteria performance assessment, parametric modeling, energy and daylight simulation

## Résumé

De par la nécessité d'une transition vers la durabilité des villes, quartiers et bâtiments, les urbanistes, architectes et ingénieurs font face à des normes énergétiques de plus en plus exigeantes. Ces décideurs doivent être supportés tôt dans leur processus par outils adéquats. En effet, les décisions prises en phase initiale de conception, qui concernent des paramètres liés à la forme et disposition des bâtiments, affectent fortement l'exposition solaire des bâtiments, qui à son tour influence leur demande et potentiel de production énergétique. Malgré un développement accru d'outils informatisés, des limitations demeurent particulièrement au niveau de leur intégration au sein du processus de design. Ces considérations définissent le contexte à l'intérieur duquel cette recherche doctorale a été développée.

L'objectif principal de cette thèse est le développement d'une méthode d'aide à la décision en phase initiale de conception de projets de quartiers axée sur la performance. Cette performance est ici définie selon trois critères : (i) le potentiel en éclairage naturel, quantifié par l'autonomie au niveau du rez-de-chaussée (correspondant à une estimation prudente), (ii) le potentiel solaire passif, lié à la demande en chauffage et refroidissement des espaces (selon certaines hypothèses e.g. sur l'isolation thermique), et (iii) le potentiel solaire actif, quantifié par la production in-situ d'énergie thermique et photovoltaïque.

La recherche s'est réalisée en deux principales phases. Un système d'évaluation en temps réel de la performance d'un ensemble de bâtiments a d'abord été développé, suivi de sa mise en oeuvre sous forme de prototype informatisé d'aide à la décision, qui a été testé par des praticiens. Le travail s'est focalisé sur le contexte Suisse en terme de pratiques de design et du climat. L'extension à d'autres contextes est toutefois directement envisageable.

Dans la première phase, une approche basée sur la métamodélisation a été adoptée afin d'éviter les limitations associées aux simulations impliquant la résolution d'équations physiques. Des fonctions mathématiques ont été obtenues pour prédire la performance énergétique et en éclairage naturel d'un quartier à partir d'une série de paramètres liés à la géométrie et au niveau d'exposition solaire des bâtiments. Ces fonctions (ou métamodèles) ont été dérivées depuis une base de données de référence, acquise suivant une procédure de modélisation et simulation. Les fonctions de régression linéaire multiples ainsi obtenues ont été complétées par un algorithme pour quantifier le potentiel solaire actif. Cette partie centrale et novatrice de la recherche a également fourni de l'information sur les précautions à prendre lors de l'utilisation de certains indicateurs de performance ou de l'analyse et l'interprétation de données de simulation.

Pour évaluer son utilisabilité et pertinence, ce moteur d'évaluation a été intégrée dans une

## Résumé

---

méthode d'aide à la décision. Inspiré par la vision émergente du processus non-linéaire guidé par la performance, une approche multi-variante a été adoptée pour la mise en oeuvre ; à partir de l'espace de solutions possibles définie par quelques données en entrée de l'utilisateur, une série de variantes de quartiers sont générées aléatoirement. Les résultats de leur évaluation par le moteur permettent une comparaison des variantes au niveau de leur morphologie et potentiel solaire. Les tests menés par des praticiens lors de workshops ont révélé le potentiel et la pertinence du prototype comme outil d'aide à la décision. Les données recueillies ont permis d'identifier de multiples pistes d'améliorations futures et de sonder les limites de validité des métamodèles en les appliquant sur les designs des professionnels. Le niveau atteint de précision des prédictions approuve le potentiel de l'approche comme alternative aux méthodes plus complexes, moins adaptées à l'exploration d'alternatives de design initial.

Mots clefs : phase initiale de conception de quartiers, potentiel solaire passif et actif, aide à la décision et au design, modèle mathématique prédictif, évaluation multicritères de la performance, modélisation paramétrique, simulation énergétique et d'éclairage naturel



# Contents

|  |            |
|--|------------|
| <b>Acknowledgements</b>  | <b>i</b>   |
| <b>Abstract (English/Français)</b>   | <b>iii</b> |
| <b>List of figures</b>   | <b>xi</b>  |
| <b>List of tables</b>  | <b>xxi</b> |
| <b>1 Introduction</b>  | <b>1</b>   |
| 1.1 Energy and the built environment . . . . .                                     | 1          |
| 1.2 Urban planning and design process . . . . .                                    | 4          |
| 1.3 Motivation and targeted gap . . . . .  | 9          |
| 1.4 Thesis structure and research approach . . . . .                               | 10         |
| <b>2 State-of-the-art in decision-support methods applied to design</b>            | <b>13</b>  |
| 2.1 Overview and current use in practice . . . . .                                 | 13         |
| 2.2 Assessment methods . . . . .   | 21         |
| 2.2.1 Planning instruments for solar access in urban settings . . . . .            | 21         |
| 2.2.2 Morphological parameters as performance indicators . . . . .                 | 24         |
| 2.2.3 Physics-based simulation . . . . .   | 28         |
| 2.3 Analysis support . . . . .   | 36         |
| 2.3.1 Generative design . . . . .  | 36         |
| 2.3.2 Sensitivity analysis . . . . .   | 38         |
| 2.3.3 Design optimization frameworks . . . . .                                     | 39         |
| 2.3.4 Guidance through expert systems . . . . .                                    | 42         |
| 2.4 Synthesis - The need for a new approach . . . . .                              | 44         |
| <b>3 Validity assessment of existing metrics through neighborhood case studies</b> | <b>49</b>  |
| 3.1 Experimental method . . . . .  | 49         |
| 3.1.1 Selected metrics . . . . .   | 49         |
| 3.1.2 Case studies . . . . .   | 51         |
| 3.1.3 Modeling . . . . .   | 56         |
| 3.1.4 Simulation . . . . .   | 60         |
| 3.2 Results . . . . .  | 69         |
| 3.2.1 Geometry-based versus reference metrics . . . . .                            | 69         |
| 3.2.2 Irradiation-based versus reference metrics . . . . .                         | 77         |

## Contents

---

|          |  |            |
|----------|--|------------|
| 3.2.3    | Correlation between geometry- and irradiation-based metrics and relative influence . . . . . | 83         |
| 3.2.4    | Conflicting performance criteria . . . . .   | 84         |
| 3.3      | Discussion and limitations . . . . .   | 86         |
| 3.4      | Towards a novel performance assessment method . . . . .                                      | 87         |
| <b>4</b> | <b>Metamodel development</b>   | <b>89</b>  |
| 4.1      | Theoretical framework and overview of approach . . . . .                                     | 89         |
| 4.2      | Data collection . . . . .  | 92         |
| 4.2.1    | Base case neighborhood designs . . . . .   | 96         |
| 4.2.2    | Parametric modeling of design variants . . . . .   | 97         |
| 4.2.3    | Computation of predictors (inputs) . . . . .   | 106        |
| 4.2.4    | Simulation of responses (outputs) . . . . .  | 108        |
| 4.3      | Selection of metamodel form . . . . .  | 111        |
| 4.4      | Data analysis . . . . .  | 112        |
| 4.4.1    | Distributions . . . . .  | 112        |
| 4.4.2    | Correlations . . . . .   | 116        |
| 4.5      | Metamodel training and testing . . . . .   | 122        |
| 4.5.1    | Overview of fitting procedure . . . . .  | 122        |
| 4.5.2    | Particularities of deterministic simulations and consequences on meta-modeling . . . . .     | 122        |
| 4.5.3    | Model selection and inputs reduction - Stepwise linear regression . . . . .                  | 123        |
| 4.5.4    | Fitting the predictive functions - Ridge regression . . . . .                                | 130        |
| 4.5.5    | Interpretation . . . . .   | 136        |
| 4.5.6    | Additional metamodel version . . . . .   | 140        |
| 4.5.7    | Further investigation . . . . .  | 141        |
| 4.6      | Complementary algorithm: active solar criterion . . . . .                                    | 145        |
| 4.7      | Summary - Achievements, limitations and future work . . . . .                                | 145        |
| 4.7.1    | Reduction of computational cost . . . . .  | 146        |
| 4.7.2    | Solution space sampling . . . . .  | 146        |
| 4.7.3    | Effect of simulation settings . . . . .  | 147        |
| 4.7.4    | Error sources . . . . .  | 148        |
| <b>5</b> | <b>Application to the design process</b>   | <b>149</b> |
| 5.1      | Implementation as a design decision-support workflow . . . . .                               | 149        |
| 5.1.1    | Related work and objectives . . . . .  | 149        |
| 5.1.2    | Implementation process and structure of workflow . . . . .                                   | 150        |
| 5.1.3    | Example application . . . . .  | 159        |
| 5.2      | Preparation of workshops with practitioners . . . . .  | 160        |
| 5.2.1    | Objectives and phases . . . . .  | 160        |
| 5.2.2    | Questionnaires . . . . .   | 162        |
| 5.2.3    | Design task . . . . .  | 163        |

|                              |   |            |
|------------------------------|---|------------|
| <b>6</b>                     | <b>Appraisal of developed prototype</b>                                     | <b>169</b> |
| 6.1                          | Workshop outcome . . . . .  | 169        |
| 6.1.1                        | Initial questionnaire . . . . .   | 169        |
| 6.1.2                        | Performance of variants . . . . .   | 170        |
| 6.1.3                        | Ranking success rate . . . . .  | 175        |
| 6.1.4                        | Final questionnaire . . . . .   | 178        |
| 6.1.5                        | Synthesis - Potential of the prototype as design decision-support . . . . . | 182        |
| 6.2                          | Testing the metamodels' performance and boundaries . . . . .                | 185        |
| 6.2.1                        | Computation of inputs and reference outputs for the test set . . . . .      | 185        |
| 6.2.2                        | Assessment of prediction accuracy . . . . .                                 | 187        |
| 6.2.3                        | Synthesis - Generalization potential of metamodels . . . . .                | 188        |
| <b>7</b>                     | <b>Discussion</b>   | <b>191</b> |
| 7.1                          | Prediction error and fitting technique . . . . .                            | 191        |
| 7.2                          | Sensitivity to simulation settings . . . . .                                | 193        |
| 7.3                          | Averaging effect and extension to existing context . . . . .                | 198        |
| 7.4                          | Refining the dataset . . . . .  | 198        |
| 7.5                          | Increase in design flexibility . . . . .                                    | 199        |
| 7.6                          | Enhanced guidance and informative features of workflow . . . . .            | 199        |
| 7.7                          | Revised workshop plan . . . . .   | 201        |
| <b>8</b>                     | <b>Conclusion</b>   | <b>203</b> |
| 8.1                          | Main outcomes and achievements . . . . .                                    | 203        |
| 8.2                          | Application potential . . . . .   | 205        |
| 8.3                          | Outlook . . . . .   | 206        |
| <b>Appendix A Metamodels</b> |   | <b>209</b> |
| A.1                          | Data analysis - Distributions and correlations . . . . .                    | 209        |
| A.2                          | Stepwise selection . . . . .  | 212        |
| A.3                          | Interpretation - Main effects . . . . .                                     | 217        |
| <b>Appendix B Prototype</b>  |   | <b>219</b> |
| B.1                          | Implementation . . . . .  | 219        |
| B.2                          | Static demo of prototype . . . . .  | 222        |
| <b>Appendix C Workshop</b>   |   | <b>227</b> |
| C.1                          | Questionnaires . . . . .  | 227        |
| C.2                          | Slides . . . . .  | 233        |
| C.3                          | Supporting material . . . . .   | 239        |
| C.4                          | Results per participant . . . . .   | 243        |
| <b>Acronyms</b>              |   | <b>261</b> |
| <b>Bibliography</b>          |   | <b>280</b> |
| <b>Curriculum Vitae</b>      |   | <b>281</b> |



# List of Figures

|     |  |    |
|-----|--|----|
| 1.1 | Sector-specific CO <sub>2</sub> emissions in Switzerland in 2010 and projected for 2020 and 2050 according to the Energy Strategy 2050 scenario based on a new energy policy (data from OFEN and DETEC [2013]). . . . .  | 3  |
| 1.2 | Comparison of continuous power (primary energy) per person in the world, with respect to the 2000 Watts Society objective for 2100 (data from SuisseEnergie [2016]). . . . .   | 3  |
| 1.3 | Distribution of final energy consumption per sector (a) in the European Union in 2013 (data from European Commission [2015]) and (b) in Switzerland in 2014 (data from OFEN [2014]). . . . .   | 3  |
| 1.4 | The land planning procedure - Example for the Canton of Vaud, Switzerland <sup>1</sup> . SAT: <i>Service de l'aménagement du territoire</i> (planning service), CE: <i>Conseil d'état</i> (state council), TA: <i>Tribunal administratif</i> (administrative court). . . . .   | 5  |
| 1.5 | Urban project for the district of Les Plaines du Loup: (a) example timeline (non-exhaustive) [Ville de Lausanne, 2013] and (b) master plan of the Plan Directeur Localisé (PDL) <sup>2</sup> . . . . .   | 6  |
| 1.6 | There is a large freedom in early-design decisions, which hold the most effective energy savings potential. Building performance simulation (BPS) typically occurs at the advanced design stage (adapted from E Source [2006]; Hensen and Lamberts [2011]; McLean et al. [2013]). . . . .  | 8  |
| 1.7 | Distribution of primary energy consumption per sector in the United States in 2010 (data from U.S. Department of Energy [2011]). Residential and non-residential (e.g. commercial, service) buildings consume about 40% of the world's energy, the main end-uses being space and water heating, space cooling, and lighting. . . . . | 8  |
| 1.8 | Flowchart representation of the research approach with reference to the thesis structure and including the main components in the design decision-support workflow. . . . .  | 11 |
| 2.1 | Results from a survey among Flemish architects, reflecting their selection to different multiple choice questions [Verdonck et al., 2011; Weytjens and Verbeek, 2010]. . . . .   | 16 |
| 2.2 | Results from an online survey among building professionals across 14 countries [Kanters et al., 2014a]. . . . .  | 18 |

## List of Figures

---

|      |  |    |
|------|--|----|
| 2.3  | The ‘future’ design environment as seen by Milne [1991], composed of four components. . . . .  | 19 |
| 2.4  | Synthetic overview of main design decision-support (DDS) methods and tools typically used from urban planning to architectural design for various purposes. This matrix was developed by intersecting and merging elements found in the reviewed literature. . . . .   | 20 |
| 2.5  | Solar Envelope [Knowles, 2003] example for a parcel located in a built context, ensuring solar access to surrounding buildings between 11am and 1pm throughout the year at a latitude of 46°N. Image generated using the Solar Envelope (SE) component of DIVA-for-Grasshopper [Jakubiec and Reinhart, 2011]. . . . .  | 22 |
| 2.6  | The (a) passive zone concept, applied in the (b) Lighting and Thermal (LT) method, both proposed by Baker and Steemers [2000]. . . . .   | 26 |
| 2.7  | Results from a study investigating the impact of urban typology on energy and daylight performance and the correlation between (a) density, energy use (light gray line) and compactness (dark gray line), and (b) density, daylight autonomy (dark gray line) and solar gain (light gray line). Figures reprinted from Sattrup and Strømman-Andersen [2013], used with the permission of Peter Sattrup and Locke Science Publishing Company, Inc. . . . . | 27 |
| 2.8  | Different versions of the rule-of-thumb for predicting the daylit area from the window height. Image adapted from Reinhart [2005]. . . . .   | 27 |
| 2.9  | Example products based on the SOLARCHVISION method [Samimi and Nasrollahi, 2014] post-processed from Environment Canada’s long-term climate data at Montreal station (reprinted with the kind permission of Mojtaba Samimi). . . . .   | 31 |
| 2.10 | Visualization methods developed by Leidi and Schlüter [2013]. Red represents higher values; [0y] refers to the actual situation (a future case is also shown in the paper from which these graphs were directly taken [Leidi and Schlüter, 2013]). . . . .   | 31 |
| 2.11 | Interface of various existing urban-scale tools. . . . .   | 34 |
| 2.12 | Urban morphology (left) and its corresponding notional grid (right), which is evaluated in the UEIB method of Rodríguez-Álvarez [2016]. Images reprinted with the permission of Elsevier. . . . .  | 35 |
| 2.13 | Constraints decision plot from which solutions achieving the required daylight performance and density level can be identified. Source of image: Peronato [2014]. . . . .  | 37 |
| 2.14 | Pareto front of the solution space in a multi-criteria optimization problem where two functions are to be minimized. . . . .   | 39 |
| 2.15 | Solutions proposed by Bruno et al. [2011]’s workflow, corresponding to four different optimization functions. Image reprinted with the kind permission of Michele Bruno. . . . .   | 40 |
| 2.16 | Typical expert system structure. The shell of the system (within the dashed border) represents the generic, non-domain specific components. Image adapted from Luger [2005] with modifications. . . . .  | 42 |

|      |  |    |
|------|--|----|
| 2.17 | Commonly used metrics (center) typically used as quantifiers for various performance criteria (bottom) along the design process (top), and evaluated through different methods and tools (left). The schema loosely summarizes the detailed review of section 2.2. The numbered metrics are further investigated in chapter 3.   | 44 |
| 2.18 | Main steps and tasks (a) in a traditional, linear design assessment process versus (b) an alternative, generation-based approach. . . . .  | 47 |
| 3.1  | Schematic master plan of the six urban visions (delimited by a green border), and the existing built context (outside of the delimitation) in the <b>BE</b> case study. The sample surrounded by a dashed red line represents the simulated portion of each design. The shade of gray of the unbuilt buildings gives an indication of their height: darker = higher. Location: Waldstadt district, Bern, Switzerland. Images adapted from Rey [2013], in which the designs are referred to by their name here displayed. . . . . | 53 |
| 3.2  | Schematic master plan of the eight urban visions (black) and the existing immediate (gray) and surrounding (light gray) built context in the <b>YLB</b> study. Location: Gare-Lac sector, Yverdon-les-Bains, Switzerland. Images adapted from Rey [2015], in which the designs are referred to by their name here displayed. . . . .   | 53 |
| 3.3  | Left: Schematic shadow plan of the <b>YLB-PDL</b> base case. Due to practical considerations, only buildings G, H and I were simulated (red), taking into account their surroundings. Right: Annual irradiation map of two example variants. Source of images: Peronato [2014]. . . . .  | 54 |
| 3.4  | Illustrative master plan of the <b>LN-PDL</b> study, with example plots (framed in red) on which the design variants created from M1 and M2 or the specific designs of M3 (top) could be located. Plan adapted from Urbaplan [2015]. . . . .   | 54 |
| 3.5  | Experimental approach and tools used for acquiring the data necessary to compare the selected metrics. Results obtained for the simpler metrics of categories (i) and (ii) are compared with the full climate- and geometry-based metrics (iii) taken as reference values. The level of complexity and of detail of the obtained output increases along with the computational cost from top to bottom. . . . .  | 55 |
| 3.6  | Example models used for the thermal and daylight simulation using different tools. . . . .   | 57 |
| 3.7  | Rhino and Grasshopper (partial) set-up for the parametric modeling of variants and computation and simulation of metrics. Example for the M2A case in the LN-PDL study. . . . .  | 57 |
| 3.8  | Illustration of design variations in the YLB-PDL study. Source of image: Peronato [2014]. . . . .  | 58 |
| 3.9  | Grid for simulating the irradiation and resulting map using DIVA [Jakubiec and Reinhart, 2011]. . . . .  | 62 |
| 3.10 | False-color map of the (a) heating need (average per zone) and (b) Daylight Autonomy (DA) for design 1-LYN in the YLB study. . . . .   | 66 |

## List of Figures

---

|   |    |
|---|----|
| 3.11 Map of the DA results produced by Urban Daylight [Dogan et al., 2012] for all designs in the BE study. . . . .   | 69 |
| 3.12 Energy production by (a) photovoltaic (PV) and (b) solar thermal (ST) systems on facades and roofs against each geometry-based metric for BE. . . . .  | 70 |
| 3.13 Energy production against each geometry-based metric for YLB. . . . .  | 70 |
| 3.14 Energy production by (a) PV and (b) ST systems on facades (F, top) and roofs (R, bottom) against each geometry-based metric for the YLB-PDL designs. . . . .   | 71 |
| 3.15 Heating (top) and energy (including heating and cooling; bottom) need against each geometry-based metric for both the BE and YLB studies. . . . .  | 73 |
| 3.16 Heating (top) and cooling (bottom) need against each geometry-based metric for the YLB-PDL designs. . . . .  | 73 |
| 3.17 Correlation matrix and Pearson coefficient between each pair of geometry-based metrics for the LN-PDL designs. PR: plot ratio, SV: surface-to-volume, WF: window-to-floor. . . . .   | 74 |
| 3.18 Heating need against geometry-based metrics (except passive zone) for the LN-PDL designs. . . . .  | 75 |
| 3.19 spatial Daylight Autonomy (sDA) against each geometry-based metric for both the BE and YLB studies. . . . .  | 76 |
| 3.20 sDA against each geometry-based metric for the YLB-PDL designs. . . . .  | 76 |
| 3.21 sDA against geometry-based metrics for the LN-PDL designs. . . . .   | 76 |
| 3.22 Energy production by (a) PV and (b) ST systems on facades and roofs against each irradiation-based metric for BE. . . . .  | 78 |
| 3.23 Energy production against the average roof irradiation metrics for YLB. . . . .  | 78 |
| 3.24 Energy production by (a) PV and (b) ST systems on facades and roofs against each irradiation-based metric for the YLB-PDL designs. . . . .   | 79 |
| 3.25 Heating (top) and energy (bottom) need against each irradiation-based metric for both the BE and YLB studies. . . . .  | 80 |
| 3.26 Heating (top) and cooling (bottom) need against irradiation-based metrics for the YLB-PDL designs. . . . .   | 80 |
| 3.27 Heating need against irradiation-based metrics for the LN-PDL designs. . . . .   | 81 |
| 3.28 sDA against each irradiation-based metric for both the BE and YLB designs. . . . .   | 82 |
| 3.29 sDA against irradiation-based metrics for the YLB-PDL designs. . . . .   | 82 |
| 3.30 sDA against irradiation-based metrics for the LN-PDL designs. . . . .  | 82 |
| 3.31 Correlation matrix and Pearson coefficient between each pair of geometry- and irradiation-based metrics evaluated over the YLB-PDL designs. PR: plot ratio, SV: surface-to-volume, PZ: passive zone, WF: window-to-floor, MeanIrrad: mean envelope irradiation, IrradPerFA: envelope irradiation per floor area. . . . . | 83 |
| 3.32 Relative influence of geometry-based metrics over heating need and sDA for YLB-PDL and LN-PDL. Constant: intercept term in a linear regression (mean output when all parameters are 0). PR: plot ratio, SV: surface-to-volume, PZ: passive zone, WF: window-to-floor. . . . .  | 85 |



|  |     |
|--|-----|
| 3.33 sDA versus heating need for the YLB-PDL and LN-PDL designs, highlighting the conflicting nature of these two criteria. Pareto solutions are identified in red. . . . .  | 85  |
| 3.34 Proposed ‘hybrid’ approach situated mid-way between simple rule-of-thumb like and simulation-based methods. . . . .   | 88  |
| 4.1 Machine learning at the intersection of multiple domains. Figure adapted from Hall et al. [2014]. . . . .  | 91  |
| 4.2 Metamodeling concept: a metamodel is trained from a dataset of simulated cases (upper line), and applied to a new (unseen) case to obtain a predicted output*, without simulation (lower line). Figure adapted from Couckuyt and Dhaene [2016]; The MathWorks [2014]. . . . .  | 91  |
| 4.3 Overview of metamodeling procedure including data collection and analysis, model selection and training and testing. The main tools used at each phase are annotated: ML: Matlab, Rhino, GH: Grasshopper, DIVA, Archsim. For a description of each program, we refer the reader to chapter 3. References are provided in the text. . . . . | 96  |
| 4.4 Hypothetical designs proposed in the PDL for an area of Lausanne (Vernand) with a mixed program, highlighting the envisioned variations of building typology and layout for this mixed-used district. Source of images: Urbaplan [2015]. . . . .   | 98  |
| 4.5 Six example plans submitted to an urban design competition for an area of Lausanne (Malley) with a mixed program. Designs vary in terms of replicated versus mixed building typology (e.g. L-shape, cubic shape) and layout (e.g. different alignments, distances). Source of images: SDOL and Gauthier [2012]. . . . .                    | 98  |
| 4.6 Digital elevation models (DEMs) of the generic urban forms studied by Ratti et al. [2003] based on Martin and March [1972]. The shade of gray is indicative of the height (darker=higher). Top left to bottom right: pavilions, slabs, terraces, terrace-courts, pavilion-courts and courts. Source of image: Ratti et al. [2003]. . . . . | 99  |
| 4.7 Four typical building block designs identified and assessed by Kanters and Wall [2014]. Adapted from the original image found in the aforementioned source, licensed under CC BY 3.0. . . . .  | 99  |
| 4.8 Examples of models evaluated in Cheng et al. [2006] (source of the image). . . . .   | 99  |
| 4.9 Top view of base case Rhino design (left) from which variants are generated (examples on the right) for each case $M_i$ . . . . .  | 103 |
| 4.9 (Continued) Top view of base case Rhino design (left) from which variants are generated (examples on the right) for each case $M_i$ . . . . .  | 104 |
| 4.10 Sampling technique for M3-M5: 3-level Box-Behnken Design of Experiment, visually directly translatable to our x, y, z design variables (Table 4.4). . . . .   | 105 |
| 4.11 Parameters distribution for each case series ( $M_i$ ) for the <b>energy</b> [ $\text{kWh}/\text{m}_{\text{FA}}^2$ ] dataset. . . . .   | 113 |
| 4.12 Parameters distribution for each case series ( $M_i$ ) for the <b>daylight</b> [%] dataset. . . . .   | 114 |

## List of Figures

---

|      |   |     |
|------|---|-----|
| 4.13 | Histograms of the simulated energy need distribution for each case series and over all variants together (bottom right graph). The number in the top right corner represents the amount of data points in the respective histogram. Comparative ranges - existing office buildings [SIA, 2015] (hatch) and Société Suisse des ingénieurs et architectes (SIA) limits [SIA, 2009b] (light-gray histogram) - are shown in the background of the bottom right overall graph. . . . . | 117 |
| 4.14 | Histograms of the simulated spatial daylight autonomy distribution for each case series and over all variants together (bottom right graph). The number in the top right corner represents the amount of data points in the respective histogram. The nominally accepted 55% and preferred 75% thresholds defined by the IESNA [2012] are shown on the bottom right overall graph. . . . .  | 117 |
| 4.15 | Matrix of pairwise linear correlation coefficient between each combination of input parameters in the two datasets. From black (-1) to gray (0) to white (+1): negative to none to positive correlation. . . . .  | 119 |
| 4.16 | Relationship between the energy need output and each input in the energy dataset, with distinction between the different cases. . . . .   | 120 |
| 4.17 | Relationship between the sDA output and each input in the daylight dataset, with distinction between the different cases. . . . .   | 121 |
| 4.18 | Flowchart of the procedure for defining the predictors to use in the final predictive model fitting. Each block (top to bottom) is respectively detailed in sections 4.5.3 and 4.5.4. . . . .   | 122 |
| 4.19 | Flowchart of the procedure for selected the model form using the Matlab <i>stepwiselm</i> function with different settings. 'Fit stats' corresponds to the metrics described in Table 4.10. . . . .   | 124 |
| 4.20 | Results from the stepwise selection for each type of model for the energy (left) and daylight (right) metric. C: constant, L: linear, I: interactions, Q: quadratic. . . . .  | 126 |
| 4.21 | Flowchart of the iterative process for identifying influential inputs using <i>stepwiselm</i> on different training data subsets. . . . .   | 127 |
| 4.22 | Occurrence and coefficient value for each input over 50 iterations of the <b>energy</b> model. . . . .  | 128 |
| 4.23 | Occurrence and coefficient value for each input over 50 iterations of the <b>daylight</b> model. . . . .  | 129 |
| 4.24 | Flowchart of the iterative process for testing different input combinations using the Matlab <i>ridge</i> function and leading to the final predictors' selection. . . . .  | 131 |
| 4.25 | Predicted versus simulated energy need values (left) with associated residuals histogram (right) over all 25 iterations for each $\alpha$ (different subset of inputs included in each model), when training-testing using (a) the entire and (b) half of the dataset. The constant (intercept) is not counted in the displayed number of terms. Predicted, simulated and residual values are expressed in kWh/m <sub>FA</sub> <sup>2</sup> . . . . .                             | 133 |

4.26 Predicted versus simulated spatial daylight autonomy values (left) with associated residuals histogram (right) over all 25 iterations for each  $\alpha$  (different subset of inputs included in each model), when training-testing using (a) the entire and (b) half of the dataset. The constant (intercept) is not counted in the displayed number of terms. Predicted, simulated and residual values are expressed in %. 134

4.27 Flowchart of the final metamodel fitting procedure using ridge regression. . . . 135

4.28 Relative importance and effect of each input according to the **energy**  $f(x)$  metamodel structure. . . . . 138

4.29 Relative importance and effect of each input according to the **daylight**  $f(x)$  metamodel structure. . . . . 139

4.30 Fit and error metrics for each combination of data subsets, where a model trained on case  $M_i$  (x-axis) is tested on case  $M_j$  (color-coded bar). . . . . 142

4.31 Performance of the metamodels obtained by Gaussian Processes (GP) regression. For each metric: predicted versus simulated values (left) and residuals histogram (right). Each model contains the five input terms listed in Table 4.15. . . . . 144

4.32 Comparison of simulated floor-area-normalized heating need [ $\text{kWh}/\text{m}_{\text{FA}}^2$ ] between the current dataset and the LN-PDL results presented in chapter 3 for the adjacent M0 design series, in both orientations. . . . . 147

5.1 Implementation flowchart. The developed performance assessment engine (dashed boxes), detailed in chapter 4, is integrated with additional components to complete the workflow. Tools used, indicated by their logo, are presented in Fig. 5.2. . . . . 152

5.2 Tools used in the development of the prototype to produce the workflow of Fig. 5.1. UrbanSOLve consists in a Grasshopper plug-in (.gha file) that holds three components presented in Fig. 5.3. . . . . 152

5.3 Three custom Grasshopper components of the prototype (coded in C# by Mélanie Huck). These can be found in Grasshopper’s Component Tab ‘Extra’. Once selected, they must be placed in the current Grasshopper document and linked to/complemented by additional elements as explained in section 5.2.3 and Fig. 5.12. . . . . 152

5.4 Custom interface of the prototype (coded by Mélanie Huck), opened by double-clicking on the Parameters’ component (see Fig. 5.3). Boxes that are grayed-out correspond to variables that are currently fixed. . . . . 153

5.5 User-inputs are acquired through the custom interface (left) and the Rhino window (right, example user-defined configuration). . . . . 155

5.6 Irradiation map (left) and solution’s information (right) for two example design variants generated and evaluated by the prototype. . . . . 157

5.7 3D performance graph seen in 2D via three Rhino viewports. x-axis: active solar potential; y-axis: passive solar potential; z-axis: daylight potential. The 20 generated solutions are represented by numbered points (0-19). . . . . 158

## List of Figures

---

|      |  |     |
|------|--|-----|
| 5.8  | Results from the two example runs of the prototype with a different starting base case (see Table 5.1). Top: performance of each variant generated in the first (left) and second (right) run. Bottom: irradiation map of example variants generated in each run, with distinct performance outputs. . . . . | 158 |
| 5.9  | Workshop phases and tasks. . . . .   | 161 |
| 5.10 | Images of the design task: the ‘empty’ plot, selected from the hypothetical plan for an area of Vernand part of the Lausanne-Vernand - Romanel-sur-Lausanne PDLi ( <i>Plan Directeur Localisé intercommunal</i> ) [Urbaplan, 2015], and its modified context. . . . .  | 161 |
| 5.11 | Workshop physical set-up: four work stations (computers) with installed software, scale model of the context (prepared prior to event) and material for making a scale model of the design. . . . .  | 163 |
| 5.12 | Grasshopper script prepared for the workshops. The interface for gathering the user-inputs (see Fig. 5.4) is opened by double-clicking the circled (Parameters) component. The rest of the script is automated and does not require user intervention. . . . .   | 165 |
| 5.13 | Initial ranking sheet. . . . .   | 166 |
| 5.14 | Intermediate ranking sheet. . . . .  | 167 |
| 5.15 | Final ranking sheet. . . . .   | 168 |
| 6.1  | Participation in neighborhood-scale projects. PDL: (localized) master plan ( <i>Plan Directeur Localisé</i> ), PQ: district plan ( <i>Plan de quartier</i> ). . . . .  | 170 |
| 6.2  | Participants’ experience with tools. . . . .   | 171 |
| 6.3  | Participants’ experience with assessing different performance aspects. . . . .   | 171 |
| 6.4  | Drawings and calculations from one participant, from (a) Variant A to (b) Variant B. . . . .   | 172 |
| 6.5  | 3D models of some of the participants’ variant. . . . .  | 172 |
| 6.6  | Performance of each participant’s VA and VB with respect to each criteria, evaluated through simulation (left) and the predictive functions implemented in the prototype (right). . . . .  | 173 |
| 6.7  | Simulated values for the sDA versus energy need with the energy production coded in shades of gray, for all variants A and B created by the participants. . . . .  | 173 |
| 6.8  | Sign function where positive, null and negative values (x-axis) are respectively transformed to +1, 0 and -1 (y-axis). . . . .   | 176 |
| 6.9  | Ranking success rate computed through the (a) Kendall rank and (b) distance method, over all participants for each criterion and phase. . . . .  | 179 |
| 6.10 | Ranking success rate displayed as the color-coded (a) Kendall coefficient and (b) level of closeness, computed for each participant, criterion and phase. White squares correspond to no data. . . . .   | 179 |

|  |     |
|--|-----|
| 6.11 Distribution of answers to the final questionnaire, in terms of agreement level on a 5-point Likert scale with specific statements. A strong level of agreement is observed for most statements, while the disagreement instances are likely mainly caused by technical limitations of the tested prototype. . . . .  | 180 |
| 6.12 Hypothetical design to attempt to reproduce in the prototype. The three buildings must be inputted by selecting the same ‘simple volume’. The minimum intervals of dimensions to input to ensure covering the ranges found in the design are listed in the top right corner table. . . . .  | 183 |
| 6.13 Pre-workshop variants added to the participants’ designs to form the test set. .  | 184 |
| 6.14 Parallel coordinates plot showing the standardized value of the inputs and outputs corresponding to each test variants. Inputs in bold and starred are respectively the ones included in the full and reduced final versions of the metamodels.   | 186 |
| 6.15 Prediction accuracy of each energy (left) and daylight (right) metamodel version. For each figure: predicted against simulated performance values (left) and residuals (right) across the test variants. . . . .  | 189 |
| 6.16 Prediction accuracy of the (a) energy and (b) daylight GP metamodels. For each figure; predicted against simulated performance values (left) and residuals (right) across the test variants. . . . .  | 190 |
| 7.1 Simulated against predicted energy need [ $\text{kWh}/\text{m}_{\text{FA}}^2$ ] with 95% confidence intervals for predicted values, for one example iteration in the training-testing procedure (see Fig. 4.24), when fitting using the entire dataset (d=100%) and (a) 19 inputs, (b) 10 inputs, and (c) 3 inputs (see also section 4.5 and Fig. 4.25). These graphs were produced using the <i>predict</i> and <i>fitlm</i> functions in Matlab. . | 192 |
| 7.2 Schematic representation of the prediction uncertainty obtained with GP regression. From (a) to (b): when new reference points are added for a given x value, the prediction uncertainty decreases in the region around that value. . . . .  | 192 |
| 7.3 Heating, cooling, and total energy need in the medium (top) and low (bottom) U-value datasets (see Table 7.1), with distinction between the different M-cases. The difference between the maximum and minimum value is displayed ( $\Delta_{\text{max}}$ ).  | 195 |
| 7.4 Difference in the energy need between the medium and low U-value datasets (see Table 7.1), for each variant of each case series. The mean percentage difference, computed with respect to the medium U-value dataset, is displayed ( $\mu$ , see equation 7.1). . . . .  | 196 |
| 7.5 Relationship between the energy need output and each input in the (a) medium and (b) low U-value energy datasets (see Table 7.1), with distinction between the different M-cases. . . . .  | 197 |
| 7.6 Variation in the annual heating energy demand (normalized per floor area) obtained when increasing the window-to-wall ratio, for different glazing U-values, in the case of detached housing and compact urban block in Paris. Graphs made using data from [LSE Cities and EIFER, 2014]. . . . .   | 198 |

## List of Figures

---

|      |  |     |
|------|--|-----|
| 7.7  | New version of the custom interface for user-inputs (for comparison, see previous version in Fig. 5.4). . . . .  | 200 |
| 7.8  | Example graph for the new version of the performance visualization, with fixed axes allowing clearer comparison between the design variants from one run of the workflow, as well as between iterations starting with distinct initial user-inputs (for comparison, see previous version in Fig. 5.7). . . . .   | 200 |
| 8.1  | Vision for future development avenues. . . . .   | 207 |
| A.1  | Distribution of each input. Reference to these graphs is made in section 4.4.1. . . . .  | 210 |
| A.2  | Relationship between the output and each input. Reference to these graphs is made in section 4.4.2. . . . .  | 211 |
| A.3  | Main effects plot showing the estimated effect, on the energy metric, of each input, obtained when fitting using the entire dataset (d=100%) and (a) 19 inputs, (b) 10 inputs, and (c) 3 inputs (see also section 4.5 and Fig. 4.25). All values appearing on the graphs correspond to standardized data (inputs and output). The horizontal lines represent confidence intervals of 95% for these predictions, which are obtained by averaging over one input while changing the others. We observe that the effect of a given input changes from (a) to (c), e.g. the plot ratio whose effect goes from negative to positive. As mentioned in section 4.5.5, the influence of each input is dependent on the presence/absence of the others and as such, this data cannot be used e.g. as design guidelines. These graphs were produced using the <i>plotEffects</i> and <i>fitlm</i> functions in Matlab. . . . . | 217 |
| B.1  | Implementation diagram showing the chronological communication between the different parts composing the prototype (diagram by Mélanie Huck). . . . .  | 219 |
| B.2  | Alignment and rotation settings: explanation of effect on each building typology.  | 220 |
| B.3  | Irradiation cluster in Grasshopper, holding 20 instances of the DIVA irradiation simulation component. . . . .   | 221 |
| C.1  | Drawing base provided to participants in Phase A. . . . .  | 239 |
| C.2  | Rhino 3D model of the design task prepared for the workshops. Participants worked on the central empty parcel. . . . .   | 239 |
| C.3  | Variant submitted by participant 1. . . . .  | 244 |
| C.4  | Example variants produced by the prototype, showing the building dimensions issue (screenshots of recorded session). . . . .   | 244 |
| C.5  | Variants submitted by participant 2. . . . .   | 246 |
| C.6  | Variants submitted by participant 3. . . . .   | 248 |
| C.7  | Variants submitted by participant 4. . . . .   | 250 |
| C.8  | Variant submitted by participant 5. . . . .  | 252 |
| C.9  | Variant submitted by participant 6. . . . .  | 254 |
| C.10 | Variants submitted by participant 7. . . . .   | 256 |
| C.11 | Variants submitted by participant 8. . . . .   | 258 |

# List of Tables

|     |   |    |
|-----|---|----|
| 3.1 | Selected metrics to be compared for each performance criterion. Sources are listed in the text. PV: photovoltaic; ST: solar thermal; F: facades; R: roofs. . . . .  | 51 |
| 3.2 | Tools used in the modeling process in each project. Sources are mentioned in the text. . . . .  | 56 |
| 3.3 | Design variables and constants for generating variants in the YLB-PDL study, based on the PDL [Bauart Architectes et Urbanistes SA et al., 2010]. *Window-to-wall ratio was dictated by the window modeling done using constant intervals (e.g. between window bottom and floor). . . . .   | 58 |
| 3.4 | Design variables and constraints for generating variants in the LN-PDL study. *Window-to-wall ratio was dictated by the window modeling done using constant intervals (e.g. between window bottom and floor). bldg(s): building(s); cst: constant; var: variable. See Fig. 3.4 for a visual description of x, y, z and d. . . . .   | 59 |
| 3.5 | Overview of simulation tools and settings for each study for the <b>irradiation simulations</b> . References for tools: DIVA-for-Rhino/Grasshopper [Jakubiec and Reinhart, 2011], plug-in based on the simulation engines Radiance [Larson and Shakespeare, 1998] and Daysim <a href="http://daysim.ning.com/">http://daysim.ning.com/</a> ; GenCumulativeSky (algorithm) [Robinson and Stone, 2004]. . . . . | 62 |
| 3.6 | Overview of simulation tools and settings for each study for the <b>energy (thermal) simulations</b> . References for tools: UMI [Reinhart et al., 2013], Archsim <a href="http://archsim.com/">http://archsim.com/</a> , DIVA-for-Grasshopper [Jakubiec and Reinhart, 2011], plug-ins based on the simulation engine EnergyPlus [Crawley et al., 2000]. *Sources for settings: SIA [1999, 2009b] . . . . .   | 67 |
| 3.7 | Overview of simulation tools and settings for each study for the <b>daylight simulations</b> . References for tools: DIVA-for-Grasshopper [Jakubiec and Reinhart, 2011], Urban Daylight [Dogan et al., 2012], plug-ins based on the simulation engines Radiance [Larson and Shakespeare, 1998] and Daysim <a href="http://daysim.ning.com/">http://daysim.ning.com/</a> . . . . .                             | 67 |
| 4.1 | Comparative analysis of methods used for predicting building energy consumption, according to/adapted from Foucquier et al. [2013]; Zhao and Magoulès [2012]. Physical methods (above dashed line) are more common than machine learning techniques (below dashed line). . . . .  | 93 |

## List of Tables

---

|      |  |     |
|------|--|-----|
| 4.2  | Non-exhaustive overview of studies using machine learning techniques in the field of building performance prediction and sensitivity analyzes. *Sample size of complete dataset including training and testing subsets. (?): not clearly stated; bldg.: building; FAST: Fourier Amplitude Sensitivity Test; LHS: Latin Hypercube Sampling; NYC: New York City. . . . .   | 94  |
| 4.2  | (Continued) Non-exhaustive overview of studies using machine learning techniques in the field of building performance for prediction and sensitivity analyzes. *Sample size of complete datasets including training and testing subsets. (?): not clearly stated; bldg.: building; incl.: including; ANFIS: Adaptive Neuro-Fuzzy Inference System; SVR: Support Vector Regression; PMV: Predicted Mean Vote; GSA: Global Sensitivity Analysis. . . . . | 95  |
| 4.3  | Examples of relevant sources regarding studies on the impact of geometrical parameters at the urban scale on various performance metrics. . . . .  | 101 |
| 4.4  | Variables range (in initial grid orientation coded as 0°), constraints when present and constant parameters. bldg(s): building(s), fp: building footprint. See Fig. 4.9 for definition of x, y, z, a. . . . .  | 102 |
| 4.5  | Comparison values for office building dimensions from Deru et al. [2011]; SIA [2015]. . . . .  | 102 |
| 4.6  | List of geometry- and irradiation-based parameters representing potential performance predictors (inputs to the metamodels). Envelope includes all exposed facades and roof. TFA: total floor area; TEEA: total exposed envelope area . . .  | 107 |
| 4.7  | Settings for the energy need simulations with reference values for comparison. *[SIA, 2015], **[SIA, 2009b], ***[Deru et al., 2011]. . . . .   | 110 |
| 4.8  | Settings for the daylight simulation. . . . .  | 110 |
| 4.9  | Comparison values for some geometry-based parameters. Sources: (1) [LSE Cities and EIFER, 2014], (2) [Zhang et al., 2012a], (3) [Knowles, 2003], (4) [SIA, 2015], (5) [Steeners, 2003], (6) [Laëtitia et al., 2011]. . . . .   | 115 |
| 4.10 | Goodness-of-fit and error statistics used to compare and analyze results across the different fitting phases of Fig. 4.18. <i>N</i> : number of data points; <i>P</i> : number of input terms; <i>y</i> : simulated (reference) value; $\hat{y}$ : predicted (fitted) value; $\mu$ : mean. . . . .   | 124 |
| 4.11 | Model forms tested using the <i>stepwiselm</i> function with different settings. <i>y</i> : simulated (reference) value; $\beta_0$ : constant term (bias, intercept); $\beta_i$ : coefficient of input $x_i$ ; $\varepsilon$ : error term. . . . .   | 125 |
| 4.12 | Correlation level between the output metric and each input selected for fitting the corresponding full and reduced (bold) final predictive models. . . . .   | 135 |
| 4.13 | Full and reduced final fitted equations to be used for predicting the performance of new designs. . . . .  | 136 |
| 4.14 | Preliminary version of the predictive functions. . . . .   | 140 |
| 4.15 | Predictors found in the GP models along with their correlation level to the output metric. Bold terms denote predictors also contained in the final metamodels presented in section 4.5.4 (Table 4.13). . . . .  | 144 |



|   |     |
|---|-----|
| 4.16 Comparison of computational cost of evaluating the performance through a simulation versus the metamodel. These times were recorded for simulations run on an Intel i7-4820K (4 cores) 3.70GHz computer with 16 GB of RAM. Ranges correspond to the min-max value measured across the seven M cases that were simulated to generate the dataset. Daylight simulation on ground floor level only. | 146 |
| 5.1 User-inputs for the first and second example runs. . . . .  | 159 |
| 6.1 Terms that appeared in the justifications provided by participants when ranking the variants in the initial phase. . . . .  | 178 |
| 6.2 Summary of feedback gathered through the open-ended questions in the final questionnaire, re-structured according to positive and negative aspects along with suggestions regarding different features of the prototype. . . . .  | 181 |
| 7.1 U-values used in the energy need simulation for the medium and low U-value energy datasets. The medium setting corresponds to the dataset used to develop the metamodels in chapter 4. . . . .  | 195 |
| 7.2 Envisioned balance to compute an aggregated performance metric. . . . .   | 201 |
| C.1 Participant 1’s (a) answers to the initial questionnaire and (b) results in the ranking phases according to the simulated performance of each variant. . . . .  | 244 |
| C.2 Participant 1’s answers to the final questionnaire. . . . .   | 245 |
| C.3 Participant 2’s (a) answers to the initial questionnaire and (b) results in the ranking phases according to the simulated performance of each variant. . . . .  | 246 |
| C.4 Participant 2’s answers to the final questionnaire. . . . .   | 247 |
| C.5 Participant 3’s (a) answers to the initial questionnaire and (b) results in the ranking phases according to the simulated performance of each variant. . . . .  | 248 |
| C.6 Participant 3’s answers to the final questionnaire. . . . .   | 249 |
| C.7 Participant 4’s (a) answers to the initial questionnaire and (b) results in the ranking phases according to the simulated performance of each variant. . . . .  | 250 |
| C.8 Participant 4’s answers to the final questionnaire. . . . .   | 251 |
| C.9 Participant 5’s (a) answers to the initial questionnaire and (b) results in the ranking phases according to the simulated performance of each variant. . . . .  | 252 |
| C.10 Participant 5’s answers to the final questionnaire. . . . .  | 253 |
| C.11 Participant 6’s (a) answers to the initial questionnaire and (b) results in the ranking phases according to the simulated performance of each variant. . . . .   | 254 |
| C.12 Participant 6’s answers to the final questionnaire. . . . .  | 255 |
| C.13 Participant 7’s (a) answers to the initial questionnaire and (b) results in the ranking phases according to the simulated performance of each variant. . . . .   | 256 |
| C.14 Participant 7’s answers to the final questionnaire. . . . .  | 257 |
| C.15 Participant 8’s (a) answers to the initial questionnaire and (b) results in the ranking phases according to the simulated performance of each variant. . . . .   | 258 |
| C.16 Participant 8’s answers to the final questionnaire. . . . .  | 259 |



# 1 Introduction

*“Nous menons une guerre contre la nature. Si nous la gagnons, nous sommes perdus.”*

Hubert Reeves  
(astrophysicist, popularizer of  
science and environmentalist)

## 1.1 Energy and the built environment

In light of the current and critical issues related to climate change, resource scarcity, and energy efficiency, multiple initiatives and regulations have been launched by various governmental bodies across the world. At the European Union (EU) level, targets have been fixed for 2020, 2030 and 2050; the *2020 Energy Strategy* aims at 20% reduction in greenhouse gases (GHG), 20% energy efficiency improvement, and a share of renewable energy meeting at least 20% of the consumption, while the 2050 strategy aims at achieving a reduction of 80-95% in GHG (with respect to 1990)<sup>1</sup>.

Following the Fukushima nuclear disaster of 2011, Switzerland has developed its own *Energy Strategy 2050* to plan the required restructuring of its energy system, which will include decommissioning the existing five nuclear power plants as well as increasing the share of renewables and promoting energy efficiency<sup>2</sup>. Assuming the adoption of a new energy policy, the confederation has defined similar targets as the EU, with the goal of reaching GHG reductions ranging between 60-80% depending on the sector (see Fig. 1.1) [OFEN and DETEC, 2013]. These targets are reflected in the modified version of the Swiss Energy Law (*Loi sur l'énergie*, 2014), which includes reduction objectives in terms of average annual energy and electricity consumption per person [Confédération Suisse, 1998].

On the same grounds, non-legislative initiatives are also being launched. As an attempt to promote sustainability in a broader sense with a worldwide vision, the 2000 Watts Society concept was developed in Switzerland based on the idea that each human being 'has the right'

<sup>1</sup><https://ec.europa.eu/energy/en/topics/energy-strategy> (last accessed on January 25, 2016)

<sup>2</sup><http://www.bfe.admin.ch/themen/00526/00527/index.html?lang=en#> (last accessed on January 25, 2016)

## Chapter 1. Introduction

---

to 2000 watts in terms of primary energy and 1 ton/year of CO<sub>2</sub> emissions [SuisseEnergie, 2014]. To achieve these goals, a decrease of over 50% with respect to 2013 will be required in Switzerland, and a much larger drop in other developed countries, as shown in Fig. 1.2.

Due to the importance of buildings in the composition of the global energy consumption and GHG emissions (Fig. 1.3), the above-mentioned regulations, laws and initiatives also target specifically the built environment sector. For example, the 2000 Watts Society fixes target values in terms of primary energy consumption for new and renovated buildings. These values, along with a method to verify code-compliance, are contained in the SIA<sup>3</sup> norm 2040 [SIA, 2011].

In term of legal prescriptions, the general objectives laid out at the Swiss federal level are given a more tangible form through the cantonal and municipal regulations. For instance, the Energy Law has led to the energy regulations model (*Modèle de prescriptions énergétiques des cantons - MoPEC*), to be implemented in the cantons' legislations by 2018 [EnDK and EnFK, 2014]. This model contains prescriptive objectives, defined with reference to various SIA norms which set limit and target values, for example regarding building insulation requirements and energy consumption for heating and electricity.

Along with energy consumption reduction objectives, an increase in the share of renewable energy is also sought by various Swiss directives. These include cantonal-level laws such as, in the Canton of Vaud, the Law on Energy (LVLEne, [Canton de Vaud, 2014]), the Cantonal Master Plan (PDCn, [Canton de Vaud, 2015]) and the Regulations of the Planning and Construction Law (RLATC, [Conseil d'Etat du Canton de Vaud, 2014]). The objectives are to cover respectively 30%, 20% and 30% of the domestic hot water, electricity and final consumption of all new buildings with renewable energy sources by 2050. Financial incentives are also provided and an eased implementation process for small solar installations is granted.

This non-exhaustive overview illustrates the increasing spread and level of energy standards and regulations in the built environment. To achieve these European objectives and their national and local equivalents across western countries, a transition towards sustainable cities, neighborhoods and buildings is essential. In this sense, decision-makers, including policy-makers, urban planners, designers, architects, and engineers, have a key role to play, from the early stages of the strategic urban planning to the detailed building design level.

To better understand how they can fulfill this influential role, we must examine the process from the macro scale of urban planning to the architectural design level.

---

<sup>3</sup>The Société Suisse des ingénieurs et architectes (SIA) is a professional association for construction, technology and environmental specialists, which aims at promoting sustainable and high-quality design in the built environment in Switzerland (<http://www.sia.ch/en/the-sia/the-sia/>, last accessed on February 24, 2016).

## 1.1. Energy and the built environment

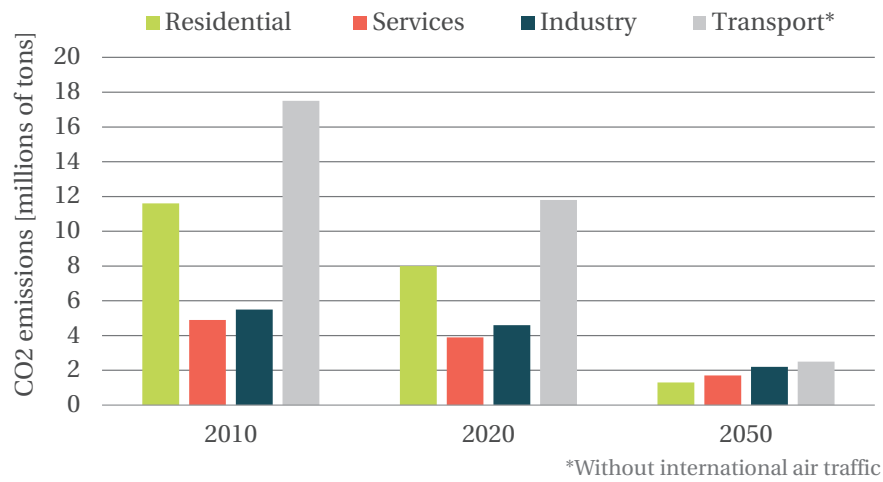


Figure 1.1 – Sector-specific CO<sub>2</sub> emissions in Switzerland in 2010 and projected for 2020 and 2050 according to the Energy Strategy 2050 scenario based on a new energy policy (data from OFEN and DETEC [2013]).

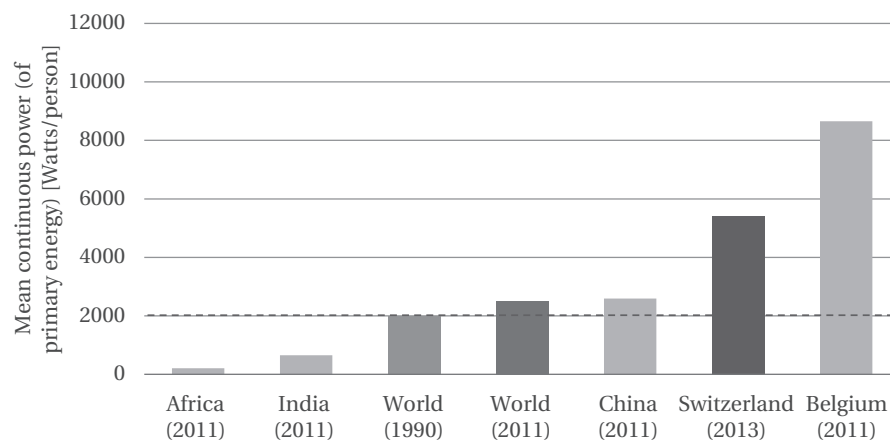


Figure 1.2 – Comparison of continuous power (primary energy) per person in the world, with respect to the 2000 Watts Society objective for 2100 (data from SuisseEnergie [2016]).

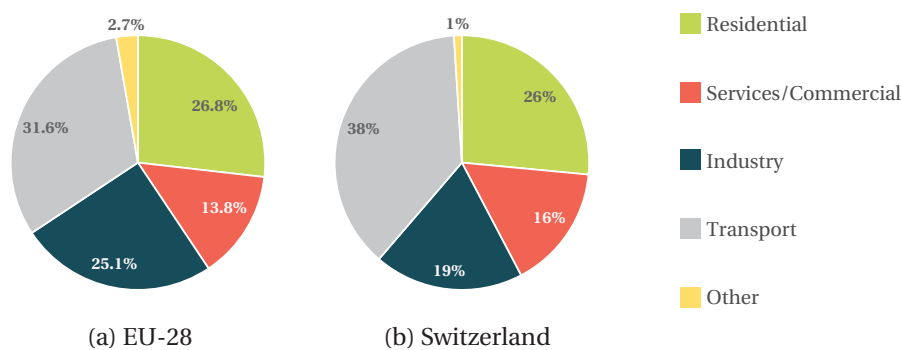


Figure 1.3 – Distribution of final energy consumption per sector (a) in the European Union in 2013 (data from European Commission [2015]) and (b) in Switzerland in 2014 (data from OFEN [2014]).

### 1.2 Urban planning and design process

Urban planning can be defined as “a dynamic profession that works to improve the welfare of people and their communities by creating more convenient, equitable, healthful, efficient, and attractive places for present and future generations”<sup>4</sup>. Other definitions mention the terms “a technical and political process”, “design of the urban environment”, “scientific, aesthetic, and orderly disposition of land, resources, facilities and services”<sup>5</sup>.

These definitions highlight the complexity and multidisciplinary nature of urban planning, which leads to the need for supporting and guiding instruments. In Switzerland, cantons and communities have the task to implement and further define their planning instruments, based on the general guidelines established by the confederation<sup>6</sup>. In the Canton of Vaud, two main types of planning documents exist, with their respective subjacent variants based on the targeted political level and spatial scale: master plans (*Plans directeurs*) and land use plans (*Plans d’affectation*). Documents of the former type allow political authorities to coordinate among each other, with no link to the landowners. They contain the main objectives and priorities. Based on these guidelines, the second type of documents, land use plans, are produced. These represent legally binding documents which define for a given territory the land use conditions (e.g. development purpose and size). For both types, the general procedure involves various actors and steps, as illustrated in Fig. 1.4.

At some point in the evolution of a project, a transition from planning to design will occur. Although the distinction between urban planning and urban design is not always clear, an attempt at distinguishing them was made by Reid Ewing, professor at the University of Utah:

*“Urban design differs from planning in scale, orientation, and treatment of space. Its scale is primarily that of the street, park, or transit stop, as opposed to the larger region, community, or activity center, which are foremost in planning. [...] The treatment of space in urban design is three-dimensional, with vertical elements as important as horizontal ones. Urban planning, on the other hand, is customarily a two-dimensional activity, with most plans visually represented in plan view, not model, section, or elevation.”* [Ewing, 2011, p.43]

In the case of the Canton of Vaud, the transition begins to occur through some of the above-mentioned planning instruments, such as the localized master plan (*Plan Directeur Localisé (PDL)*) or the district land use plan (*Plan de Quartier (PQ)*). These documents, drafted by the assigned agent, often an urban planning or design firm, contain objectives in terms of built and human density, program, energy efficiency and production goals, as well as morphological guidelines to a varying level of detail (e.g. from maximum allowed height only to building typology and layout). They set up the basis framework to be respected in

---

<sup>4</sup><https://www.planning.org/aboutplanning/whatisplanning.htm> (last accessed on January 26, 2016)

<sup>5</sup><https://www.mcgill.ca/urbanplanning/planning>, <http://www.cip-icu.ca/Becoming-a-Planner> (last accessed on January 26, 2016)

<sup>6</sup><http://www.vd.ch/themes/territoire/amenagement/guides-et-manuels/> (last accessed on January 27, 2016)

## 1.2. Urban planning and design process

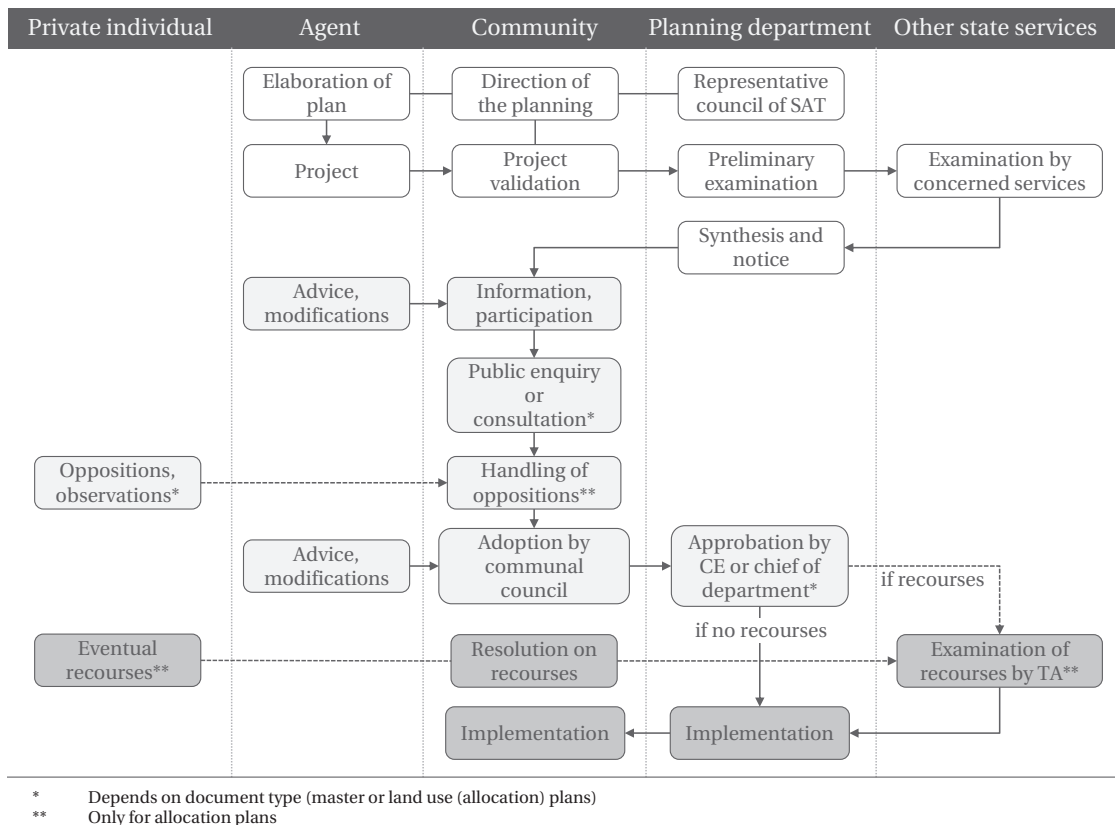


Figure 1.4 – The land planning procedure - Example for the Canton of Vaud, Switzerland<sup>7</sup>. SAT: *Service de l'aménagement du territoire* (planning service), CE: *Conseil d'état* (state council), TA: *Tribunal administratif* (administrative court).

subsequent, more detailed plans. They usually contain objectives based on norms, standards and/or labels, such as the SIA norms and Minergie label<sup>8</sup>. For example, the basic Minergie standard, linked to the SIA 380/1:2009 norm, requires a final energy consumption for space and water heating, electrical ventilation and air conditioning lower than 38 kWh/m<sup>2</sup>year for new collective housing and 40 kWh/m<sup>2</sup>year for new administrative buildings [Kesser, 2012]. For the latter, a reduction in the annual artificial lighting demand from the actual 19 kWh/m<sup>2</sup>year to a target value of 5 kWh/m<sup>2</sup>year is required by the SIA 2024:2015 norm [SIA, 2015].

Similar certification schemes such as DGNB in Germany [German Sustainable Building Council, 2013], BREEAM [BRE, 2013] in the United Kingdom (UK) and LEED [Welch et al., 2011] in the United States (US) are now extending to the urban level. Initially conceived for individual buildings, a neighborhood-scale version of the latter was launched in 2010 called LEED for

<sup>7</sup>Adapted from the "Schéma simplifié d'une procédure d'aménagement du territoire", accessible at <http://www.vd.ch/themes/territoire/amenagement/guides-et-manuels/> (last accessed on January 27, 2016).

<sup>8</sup>Minergie is a label for (new and existing) sustainable buildings which aims at ensuring occupant comfort with minimum energy consumption (<http://www.minergie.ch/basics.html>, (last accessed on January 25, 2016)). The label has grown in popularity in recent years and has evolved to include a set of labels with increasing requirements: Minergie, Minergie-P, Minergie-A, Minergie P-Eco and Minergie A-Eco.

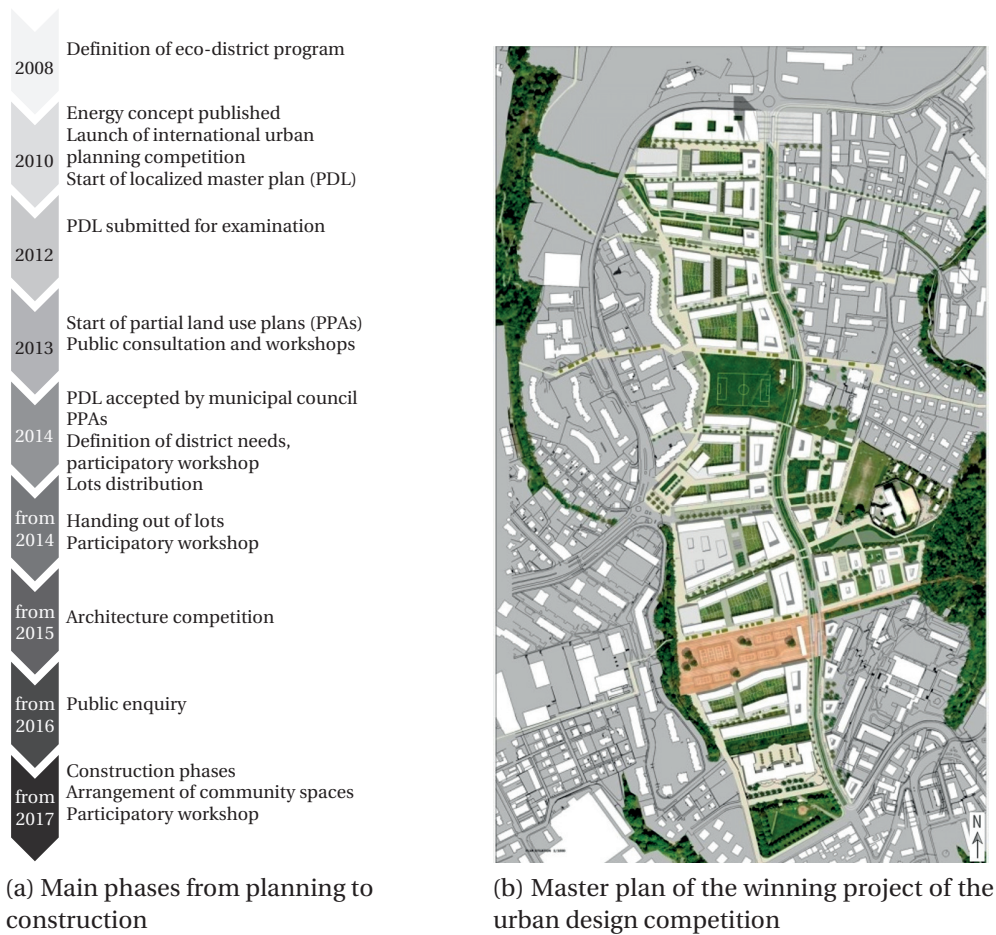


Figure 1.5 – Urban project for the district of Les Plaines du Loup: (a) example timeline (non-exhaustive) [Ville de Lausanne, 2013] and (b) master plan of the PDL<sup>9</sup>.

Neighborhood Development. Yet, it does not address the impact of urban and building morphology on energy performance [Eicker et al., 2015] and assigns a generally low weight to such considerations. Labels in themselves are still limited in terms of support brought to planners, decision-makers and designers.

To illustrate how an urban-scale project unfolds itself with reference to the above mentioned planning instruments, the timeline of an example project is shown in Fig. 1.5a. The master plan of this district-scale project for the city-owned area of Les Plaines du Loup in Lausanne, depicted in Fig. 1.5b, was introduced along with multiple guidelines and objectives in the PDL initiated in 2010 [Ville de Lausanne, 2013]. The plan proposes a dominant courtyard-based urban design, with a maximum height of six levels (with some exceptions). It aims at reducing the heating need to a minimum to reach the energy class A as defined in the SIA 2031 technical document [SIA, 2009a]. To do so, it recommends limiting the form factor to allow an optimal usage of solar gains.

<sup>9</sup>Adapted from <http://www.lausanne.ch/lausanne-en-bref/lausanne-demain/projet-metamorphose/sites/les-plaines-du-loup.html>, (last accessed on January 26, 2016).



These planning instruments thus define not only the general sustainability objectives (e.g. social mix, energy consumption), but also some early-design information (e.g. building shape) that can have a significant impact on the energy performance of the project. As illustrated in Fig. 1.6, early decisions, made particularly on building form, can lead to energy savings reaching up to 80% [Lechner, 2009]. Not only should the building form be determined based on performance considerations, but so should the urban form, which can be defined at different resolution levels (building/lot, street/block, city and region) [LSE Cities and EIFER, 2014; Moudon, 1997]. This change of scale is essential to take into account buildings interdependencies, which can have impacts as important as individual buildings on energy performance [Rickaby, 1987]. Decisions made on building and urban form strongly dictate the thermal exchanges of buildings with the environment and their level of solar exposure, which in turn influence the heating, cooling, and lighting required to ensure a thermally and visually comfortable environment for the occupants. These needs are major contributors in the energy consumption within residential and non-residential buildings, as shown in Fig. 1.7.

The early design stage is also the moment in the process when designers possess the greatest decisional freedom [Zeiler et al., 2007]. Decisions are made at each level, successively more detailed and specific than the previous, as we go from the early to the advanced design stages. Design problems are often characterized as ill-defined rather than well-defined [Andersen et al., 2008; Siret, 1997; Yezioro, 2009]. The problem statement and its solution evolve jointly throughout the process, during which alternative solutions are sought and weighted [Kalay, 1985; Marin et al., 2008]. This often translates into a cyclical ‘generate and test’ procedure, where form is given priority over performance [Oxman, 2009]. Despite the importance of early decisions and energy objectives contained in plans as stated above, it is at the later design stages, and thus detailed building-level, that performance assessment is typically conducted [Hensen and Lamberts, 2011]. After reviewing the design process through various case studies, Weytjens and Verbeeck [2009] noted that “*energy related issues are often more seen as ‘add-on’ components, which can be fixed in a later stage of the design*”. This is also highlighted by Kiel Moe, architect:

*“During this period [second half of the twentieth century], buildings became hermetically sealed, relied upon an increasingly layered approach to construction, and used increasing amounts of energy to serve their occupants. This approach was once understandable given its, now-distant, context of seemingly endless and relatively cheap energy sources. However, this is not a viable strategy for architecture in our current professional, economical, social, and ecological context.”* [Moe, 2008, p.7]

Recognizing this situation, the research and design community have come up with several design concepts, often sharing the same ideas and goals, sometimes differing by subtleties, and given different names such as ‘sustainable design/architecture’, ‘integrated design’, and ‘environmental design’. In addition to this surge in energy-conscious design, the important technological advances have led to the development and adoption of a large number of digital design-support tools in the past recent years, causing a shift from traditional to computer-

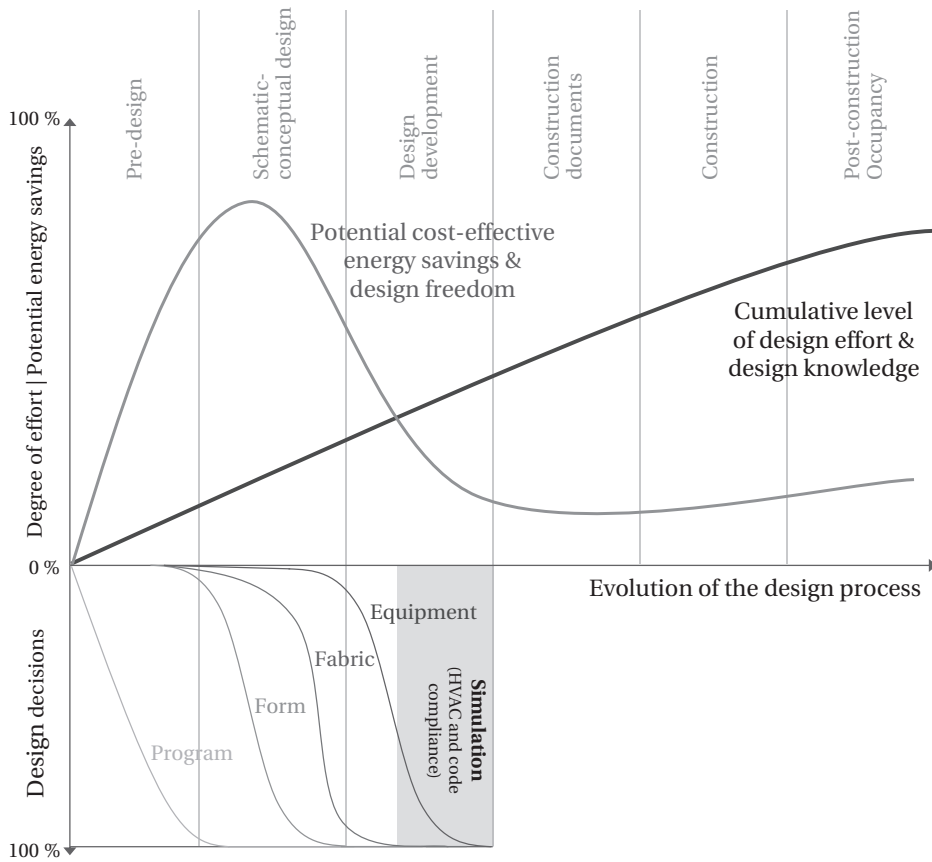


Figure 1.6 – There is a large freedom in early-design decisions, which hold the most effective energy savings potential. BPS typically occurs at the advanced design stage (adapted from E Source [2006]; Hensen and Lamberts [2011]; McLean et al. [2013]).

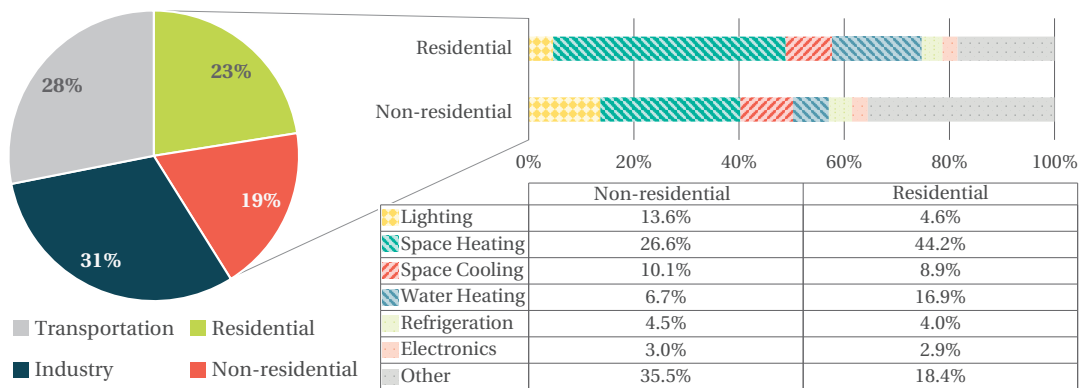


Figure 1.7 – Distribution of primary energy consumption per sector in the United States in 2010 (data from U.S. Department of Energy [2011]). Residential and non-residential (e.g. commercial, service) buildings consume about 40% of the world's energy, the main end-uses being space and water heating, space cooling, and lighting.

oriented architecture [Boeykens and Neuckermans, 2003]. This phenomenon allowed the accelerated examination of designs, facilitating and increasing the ability for drafting, modeling and elaborating forms, and providing means to rapidly generate and evaluate design alternatives [Grobman et al., 2010]. It also became possible to probe the macro scale, an area in perpetual evolution.

### 1.3 Motivation and targeted gap

Despite this increasingly favorable context, we are witnessing a low level of uptake of digital tools, particularly in the crucial early design phases of meso-scale projects.

*“The attention of research into energy-related aspects of the built environment has hitherto been focused at the scale of the individual building, or of the city as a whole.”* [Rickaby, 1987, p.43]

This remains a reality in the current context which is characterized, on one side, by extensively available detailed energy performance tools for assessing individual buildings, and on the other side, by models and methods for representing and analyzing the building stock at the macro level [Reinhart and Cerezo Davila, 2016]. There continues to be a need for additional developments addressed at the meso scale of the neighborhood, which is considered as particularly relevant and interesting nowadays regarding policies, scope and impact of design decisions, flexibility in the design, and the increasing number of urban renewal projects [Hachem et al., 2013; Peronato, 2014; Riera Pérez, 2016].

Moreover, the evaluation and comparison of design alternatives is still typically done in a manual and linear way [Grobman et al., 2010] and at the advanced building design stages as mentioned earlier [Hensen and Lamberts, 2011], with most existing tools conceived for analysis rather than design. Consequently, emerging design paradigms have been proposed, such as the ‘performance-based’ [Kalay, 1999], ‘performative’ [Oxman, 2009], and ‘non-linear’ [Grobman et al., 2010] design, respectively advancing multi-disciplinary and multi-criteria performance evaluation, intending to reverse the traditional design order by using performance goals as the form generation mechanism, and promoting simultaneous generation and evaluation of multiple design alternatives.

The emanating requirements are therefore shifting, not only temporally and spatially with respect to the design process, but also in terms of the priorities and fundamental approach to the design task. What appears to be lacking is a method that can provide performance feedback to practitioners in a non-disruptive yet novel way during the exploratory process of defining the buildings’ form and layout. This research seeks to address this gap, by providing the means for simultaneously evaluating multiple performance aspects of a whole neighborhood project, taking into consideration the impact of individual building-level design variables. The research focus is placed on the solar performance, defined in terms of the passive (heating, overheating mitigation, and daylight) and active (energy production) potential of new neighborhood developments in the Swiss context. However, the application and relevance of this work to

other cases, e.g. renewal and densification projects, and to other performance aspects, e.g. CO<sub>2</sub> emissions, is not excluded and is further discussed in the thesis.

### 1.4 Thesis structure and research approach

The research approach consists in a gradual investigatory and development process, culminating in a proposed decision-support workflow to provide guidance in early neighborhood design, with a focus on solar energy utilization. We are specifically concerned with the following questions:

1. How should we define the (energy/solar) performance of a (virtual) neighborhood and what metrics should be used to quantify each performance aspect, in a way that captures the interdependencies between buildings?
2. How can we efficiently evaluate these metrics considering the available (low) amount of early-design information, in the context of a real-time interactive computer-based workflow?
3. What are the essential features of a design decision-support system, built around the performance assessment engine (defined through the previous questions), that will make it in line with the ill-defined nature of the design process?

The workflow adopted to answer these questions is illustrated in the flowchart of Fig. 1.8, with reference to each chapter of the thesis, where the related main scientific challenges are identified.

We begin in **chapter 2** by exploring existing DDS methods and tools, revealing that novel approaches are needed in the development of digital tools to provoke a temporal spread of their use to the earlier design phases. The review underlines a gap to fill to provide adequate support to practitioners and push the shift towards performance-based design.

**Chapter 3** investigates the research literature to look at how the performance of a design is assessed. A selection of methods are tested by applying them to case studies. This preliminary study serves to define the performance criteria and associated *metrics (performance outputs)* of interest in this thesis. Limitations in current evaluation methods, linked e.g. to the lack of integration into the design process and high computational cost, lead us towards our proposed *performance assessment method*, based on *predictive models*<sup>10</sup>.

Developed in **chapter 4**, this core part of the thesis includes defining the set of *inputs* to the predictive model, consisting of parameters capturing design features that have an impact on the performance outputs. This link is exploited to develop multiple linear regression functions allowing a time-efficient estimation of the solar potential.

---

<sup>10</sup>The term predictive model refers to an equation-based model used to predict (or estimate) a certain value from a set of input parameters through the use of mathematical methods (<http://www.mathworks.com/discovery/predictive-modeling.html>, last accessed on April 18, 2016).

## 1.4. Thesis structure and research approach

In **chapter 5**, these pieces are assembled and complemented by additional components to create a workflow that is implemented as a computer-based tool and tested among practitioners through workshops. Influenced by the emerging paradigms mentioned earlier, the workflow follows a non-linear, performance-based design approach by generating and evaluating multiple design variants.

**Chapter 6** presents the results from the workshops and the appraisal (i) of the prototype in terms of its potential as a DDS tool and (ii) of the underlying performance assessment engine in terms of its predictive accuracy.

**Chapter 7** provides a discussion on limitations and foreseen improvements.

We conclude the thesis in **chapter 8** by highlighting the outcomes of the research along with their application potential and by providing an outlook.

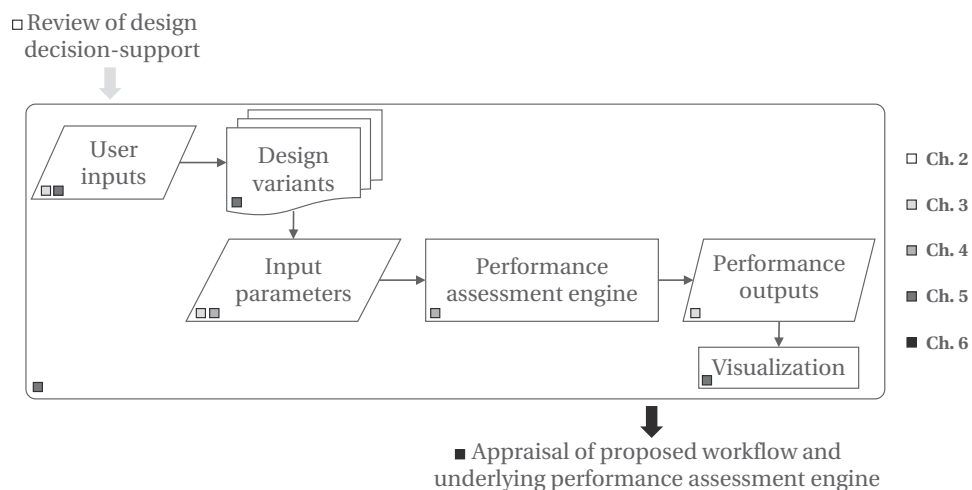


Figure 1.8 – Flowchart representation of the research approach with reference to the thesis structure and including the main components in the design decision-support workflow.



## 2 State-of-the-art in decision-support methods applied to design

*“At the scale of modern urban life, the ultimate constraints upon the system lie in nature.”*

Ralph L. Knowles  
(Professor of Architecture)

In this chapter, we look at the literature that has aimed at getting a better understanding of the interplay between urban to building morphology, climatic context and various performance aspects, with the objective of informing decision-makers by providing them with tools, in the form of simple guidelines and rules-of-thumb as well as more advanced computer-based programs.

We begin in section 2.1 with a general overview of design decision-support (DDS) methods and tools and how/when they are used along the design process. Studies including surveys and interviews among practitioners are summarized, bringing to light current barriers as well as requirements for overcoming them.

In the following sections, the key elements that compose DDS methods and tools and reflect the current research and development status are introduced. In section 2.2, detailed examples of *performance assessment* methods are presented according to the scale at which they are typically employed, from urban planning to building design. In section 2.3, we go over what we have termed *analysis support* concepts that can further guide decision-making.

We conclude by highlighting the most relevant elements, to our research context, from the literature review and on which we will build in the subsequent chapters.

### 2.1 Overview and current use in practice

The general domain of DDS methods and tools in the field of urban planning, urban design, and architectural design is practically unbounded and in continuous development. In the literature, reviews have been conducted to identify and sometimes categorize them, as well as highlight the barriers to their use in practice, through surveys among practitioners. Since the

## Chapter 2. State-of-the-art in decision-support methods applied to design

---

uptake of methods and tools is strongly linked to the design phases [Goodman-Deane et al., 2010], studies typically include this connection to the temporal evolution of the process (see Fig. 1.6).

Through a triangulated approach involving a literature review, case studies, interviews with experts, and surveys, Goodman-Deane et al. [2010] came up with a list of *commonly used design methods* in a general sense (i.e. with no reference to a specific design field), with an approximate indication of when they are used along the design process. Among others, methods based on observation, information search, and brainstorming were identified as often used at the early phase, while modeling, getting feedback from others, and testing occurred later. Visualization and sketching were noted as used throughout the design process. Time and cost were identified as two constraints significantly impacting design practice.

Similarly, but with a focus on architectural design, Verdonck et al. [2011] conducted a thorough review of a wide range of *design support tools* including various types of documentation - technical, standards, checklists, books - and methods for drawing - sketches, 2D-3D computer-aided (architectural) design/drafting (CA(A)D) software - simulation, evaluation, and analysis, as well as recourse to specialists. They defined the following roles of design support tools: evaluation/analysis, communication, knowledge-based, presentation, and modeling. Through a survey conducted among Flemish architects, they found that design decisions were mostly made based on practitioners' experience, clients' demands, and regulations, with design support tools used by only 22% of respondents, as shown in Fig. 2.1a. With respect to the design phases, they identified for which role additional support was requested in design support tools (Fig. 2.1b); at the early design phases, the need for better evaluation and analysis was predominant. When asked the reasons for not using *energy evaluation tools*, a majority of respondents answered that this was out of their competence domain and too time-consuming (Fig. 2.1c). Based on these observations, the authors defined an extensive list of requirements for "architect-friendly" building performance simulation (BPS) tools (here adapted from [Weytjens and Verbeeck, 2010]):

Usability in the design process: minimally interrupt the design process with in tune data-input; simplicity; minimal time required to operate the tool; adapted for use in early design; quickly obtain solutions and easily create, test and compare alternatives; real-time feedback on design decisions and changes; provide guidelines

Interface: visual communication of graphical user interface (GUI); clear, intuitive, and flexible navigation; clearly structured with a restrained set of functions (simplicity)

Data-input: limited; quick to provide (time to create model < 1h); input in the language of the architect; use of defaults to limit and facilitate data-entry; simple and intuitive input process; easy data review/change and creation of alternative designs/options; extensive library/database of building components; inputs consistent with early design phase (basic information); from general to detailed; graphical representation of building geometry; 3D modeler in simulation tool; possibility to import 3D CA(A)D files; input via drawing software (e.g. SketchUp)



## 2.1. Overview and current use in practice

---

Output: easy interpretation (language of architects); graphical representation of output; conformance with building codes and regulations; impact of decisions/parameters (uncertainty/sensitivity); simple but supportive information for design decisions; convincing output to communicate with clients; clearly indicate problem area(s); benchmarking; output displayed in 3D building model; generate reports for alternative designs/options; reliability of the output; adapted for different design phases

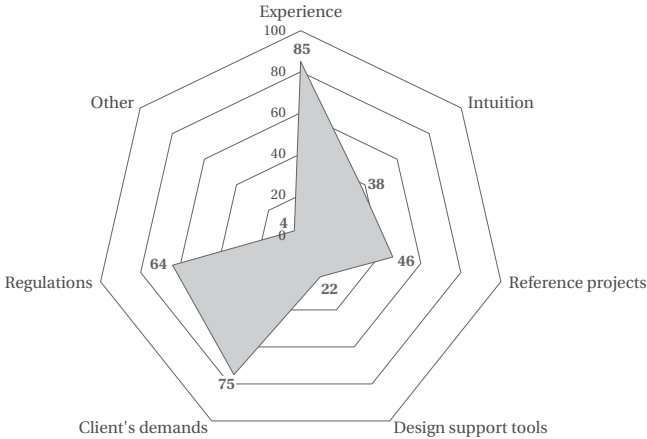
General: adaptable default values; highly visual; transparency of the tool; easy and intuitive to learn and use; short calculation time; adequate for local usage (units/materials/...); easy to use after long time of non-use

As will be seen in section 2.4 and ensuing chapters, we aim to comply with a large majority of these necessities through our proposed approach. Many of them are recurrently highlighted in other reviews and studies, as shown below.

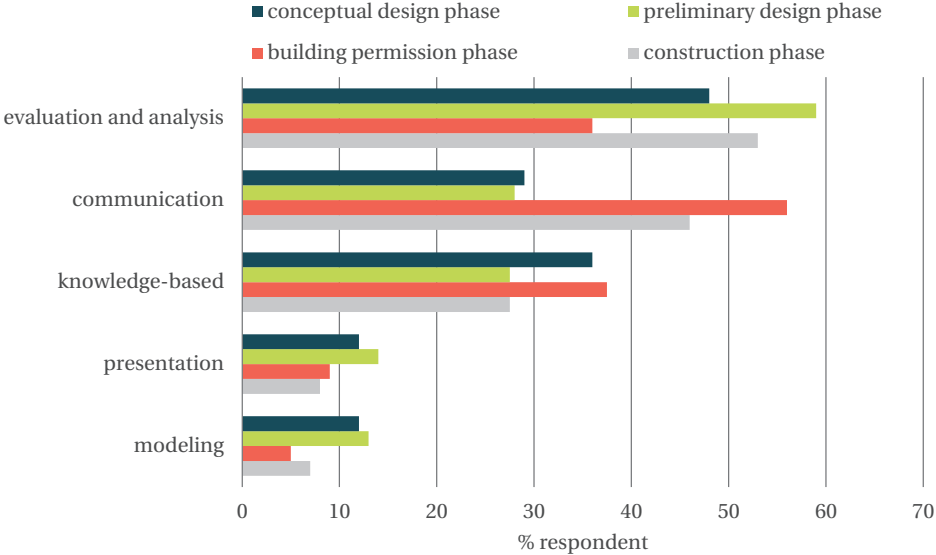
In the context of the International Energy Agency (IEA) Annex 31 [IEA, 2004], the following classification of *environmental tools* was proposed: (i) interactive software including life cycle analysis (LCA) tools and energy and ventilation modeling software, and (ii) passive tools including guidelines, checklists, case-studies, labels, regulations and more. Within another IEA project of the Solar Heating & Cooling programme (SHC), Task 41 “Solar Energy and Architecture”, 56 *computer-based tools* were reviewed from the perspective of their potential to support solar-oriented architecture from the early design phase. The software were classified as either (i) CA(A)D, e.g. ArchiCAD, Revit, Allplan, AutoCAD, SketchUp, Rhinoceros (ii) visualization, e.g. Flamingo, LuxRender, RenderWorks or (iii) simulation tools, e.g. DesignBuilder, Ecotect, Radiance, Daysim, PVSyst [Horvat and Dubois, 2012; IEA SHC Task 41, 2010]. It was observed that most CA(A)D tools allow photovoltaic (PV) and/or solar thermal (ST) system sizing, provide passive solar assessment - often through an integrated engine or plug-in conducting whole building energy simulation - and (day)lighting assessment, through visualization and (physically accurate) light rendering. The visualization tools were found to offer advanced (day)light simulation for high quality, post-design renderings. Software falling in the third category, simulation tools, were shown to provide passive solar gains and daylight availability estimation, as well as PV and ST sizing features.

What came out of the review is that most tools, regardless of the above classification, are more suited for the detailed rather than early design phase. Moreover, many are specialized in one of the performance criteria, for instance PV sizing only, as opposed to offering a more comprehensive assessment allowing to find balance between passive and active solar measures. Limitations in the outputs were also noted; most tools offer visualization of sunlight, shadow or incident irradiation on buildings, but lack in terms of numerical and informative feedback.

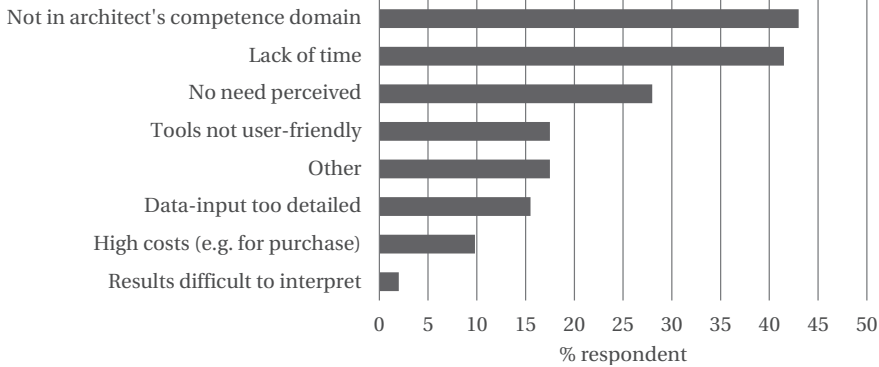
**Chapter 2. State-of-the-art in decision-support methods applied to design**



(a) Factors influencing design decisions (% respondent).



(b) Roles of tools for which more support (development) is required with respect to each design phase.



(c) Reasons for not using energy evaluation tools.

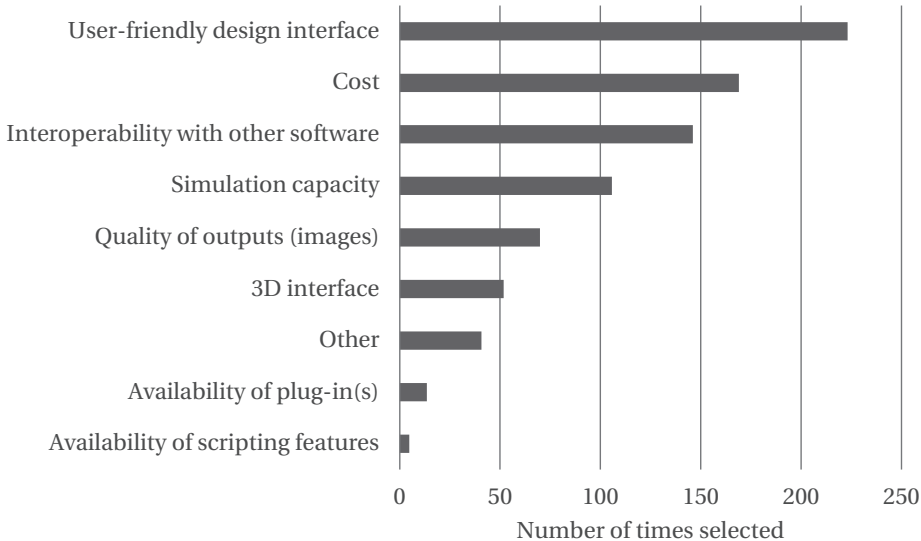
Figure 2.1 – Results from a survey among Flemish architects, reflecting their selection to different multiple choice questions [Verdonck et al., 2011; Weytjens and Verbeeck, 2010].

The work conducted within this IEA Task 41 also included a survey and interviews with practitioners [Horvat and Dubois, 2012; Kanters et al., 2014a]. Results allowed identifying factors that influence the choice of software: user-friendliness of the interface, cost and interoperability with other software were the most selected (see Fig. 2.2a). Concurring results were obtained regarding the main barriers to the use of existing tool, where complexity and cost prevailed, followed by time-consumption and lack of integration both into CA(A)D software and within the design workflow (Fig. 2.2b). These findings led the researchers to identify requirements for future BPS tools. The implementation of these tools into CA(A)D software is promoted as a way to make them function as *design tools* that could support comparisons between alternatives with respect to the energy need and production, in a way that can help architects. They state that appropriate early design phase (solar) tools should embrace the intuitive and iterative features intrinsic to this stage in the process, by allowing variations in building geometry and providing explicit feedback on solar-related performance aspects. The importance of communication-supporting features is also highlighted, e.g. to show to the client the consequences of design decisions on the building's energy performance.

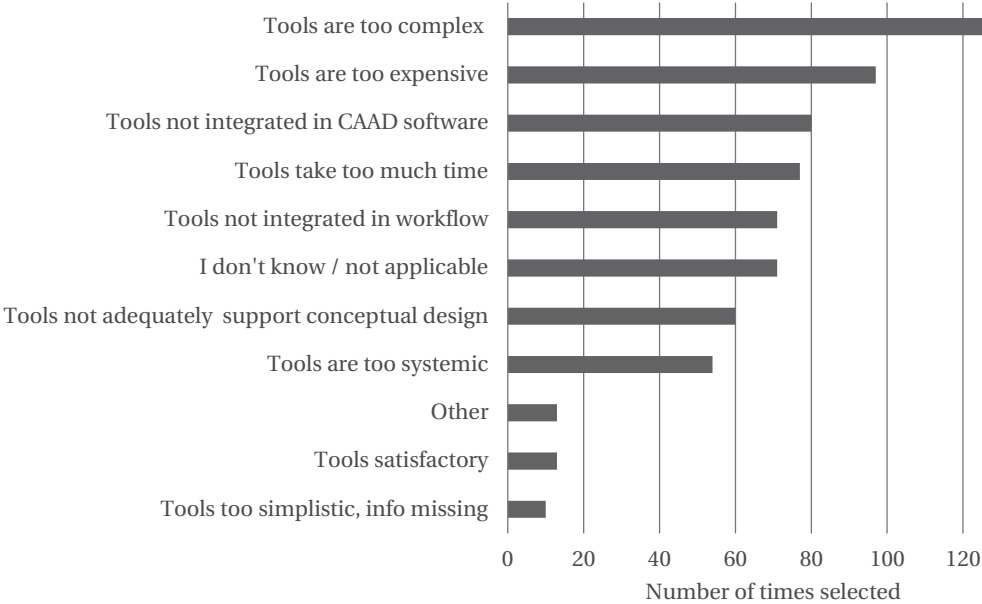
This lack of design-oriented tools was also brought up by Attia et al. [2012] who found that out of the 392 BPS tools listed as of 2011 on the US Department of Energy (DOE) website, less than 40 were targeting the early architectural design phases. The others were mainly identified as post-design and engineer-oriented evaluation tools. In that same study, barriers to the integration of BPS tools in the context of decision-making at the early design phases of Net Zero-Energy Building (NZEB) were identified: geometry representation, filling the inputs, providing informative support for decision-making, results interpretation, evaluative performance comparisons, and informed iteration.

The limited use of BPS tools as a general design decision-support is in fact recurrently highlighted in the literature [Alsaadani and De Souza, 2012; Hensen and Lamberts, 2011]. Based on research involving visits to architecture and engineering offices, Smith et al. [2011] affirm that *whole building energy analysis tools* are too complex and time-consuming to be used at the early design phase. These restrictions, combined with model exportation problems and detailed data requirements, discourage architects to use such tools who instead prefer hiring an expert, at a higher cost, to perform the energy analysis. Architects want tools better suited to their modeling applications that can quickly generate energy models while allowing comparison of various design alternatives. As such, relative values (between options) are considered more important than accurate figures. The missing tool is seen as complementary to the engineering consultant, providing energy-related knowledge to the architect who can then better communicate with the expert, which is likely to appear later in the process [Smith et al., 2011].

**Chapter 2. State-of-the-art in decision-support methods applied to design**



(a) Factors identified as the ones most influencing the choice of software to use, according to answers (3 selected factors max per respondent) by 826 respondents.



(b) Barriers to the use of available tools related to architectural integration of solar design, according to answers (multiple selections possible) by 685 respondents.

Figure 2.2 – Results from an online survey among building professionals across 14 countries [Kanters et al., 2014a].

The possibility of comparing design alternatives is a need further emphasized by Branko [2003] who defines an “*active design space exploration*”, where a defined building typology would be “*subjected to dynamic, metamorphic transformation*”, stemming from an optimizer. He also mentions that intuitive ‘low-resolution’ BPS tools are necessary for a more effective use in the conceptual design phase.

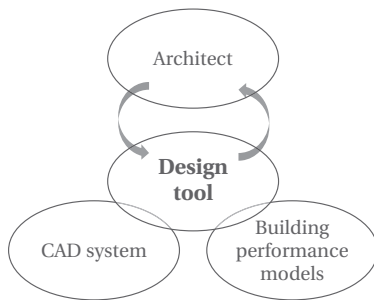


Figure 2.3 – The ‘future’ design environment as seen by Milne [1991], composed of four components.

The studies cited above seem to all eventually converge to computer-based software designed for evaluating the performance of buildings. The use of this subset of DDS tools is not spread among practitioners despite its great potential, already envisioned by Milne [1991] in the early 90’s when he stated that the (desired) *design tool* should be “*a piece of software that is easy and natural for architects to use, that easily accommodates 3D representations of the building, and that predicts something useful about building’s performance.*”[p.485]. He defined the following five categories of requirements for ‘future design environment’ consisting of the four

components shown in Fig. 2.3: (i) establishment of initial design conditions, (ii) simplified 3D data input, (iii) building performance prediction models, (iv) techniques for communicating complex data, and (v) automatic data conversion routines.

Despite the evolution of the field since then, the above review demonstrates that emphasis has remained on analytical and engineering tools as opposed to methods supporting design. There is thus still a need for improvement, particularly in the early phases when practitioners wish to explore the design solution space. As Beckers and Rodriguez [2009] put it:

*“[...] most programs are oriented to analysis and not to design. Thus, they are mainly used at the final step of the project, when the principal ideas are already defined, and all their possibilities are not apprehended.”* [p.475]

Clearly there is a general consensus on what are, on one side, the issues of existing DDS tools and on the other side, the requirements or features these should have. To summarize, the **main shortcomings** recurrently pointed out among existing tools regarding their use at the early design stage are [Branko, 2003; Horvat and Dubois, 2012; IEA SHC Task 41, 2010; Smith et al., 2011; Zhao and Magoulès, 2012]:

- too complex; out of competence domain; conceived for expert-users
- requiring detailed/high-resolution inputs
- time-consuming to learn and use
- specialized, which prevents a holistic performance assessment and creates the need for tool-specific model (remodeling for each evaluation done in a different environment)
- lacking in user and decision-making guidance

## Chapter 2. State-of-the-art in decision-support methods applied to design

These challenges contribute to the motivation behind this thesis, as further detailed later on, and are the mirror of many of the requirements highlighted earlier.

Figure 2.4 provides an overview in terms of the main DDS methods and tools encountered in this section. Their approximate position along the process from urban planning to architectural design intrinsically reflect the barriers unveiled; only a few, e.g. CA(A)D and guidelines, are used throughout, while simulation-based methods are commonly reserved for building-scale assessment at the detailed phase. Moreover, we observe that an ensemble of methods is usually required to fulfill all roles.

This section has inquired into the practitioners' stance in regard to the available supporting instruments. In the next section, we present a deeper investigation of methods and tools, providing concrete examples for each category found in Fig. 2.4.

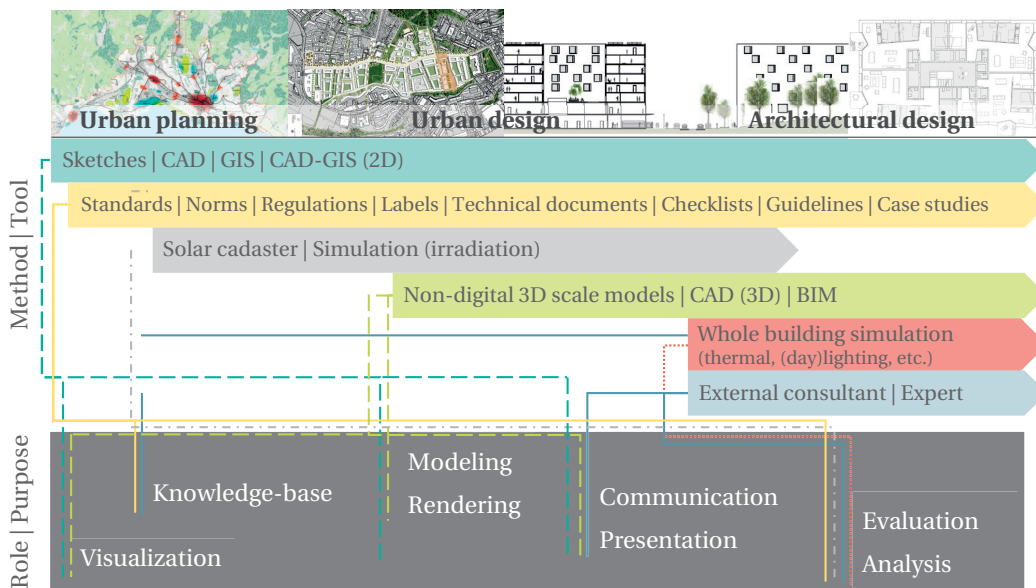


Figure 2.4 – Synthetic overview of main DDS methods and tools typically used from urban planning to architectural design for various purposes. This matrix was developed by intersecting and merging elements found in the reviewed literature.

## 2.2 Assessment methods

As highlighted in chapter 1, the design process is increasingly embracing the concept of *performance*, which has become a guiding design principle with the uptake of digital decision-support tools and emergence of sustainability objectives [Branko, 2003; Kalay, 1999; Oxman, 2009]. In the following, we loosely delimit the space of DDS methods and tools to examine more closely the computer-based and solar and energy performance assessment subset. Zooming in on the above-mentioned categories, we gradually unveil instances for each type of approach. Following the temporal and spatial timeline illustrated, we start from urban planning instruments to finish with building-scale tools.

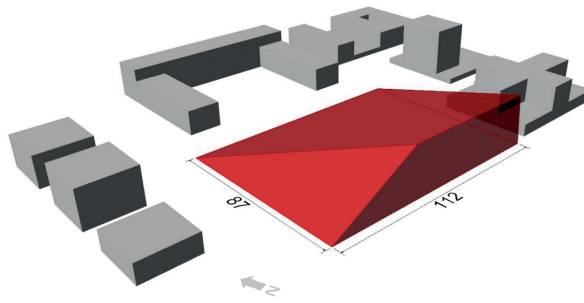
### 2.2.1 Planning instruments for solar access in urban settings

While a historical account on the evolution of theories related to the perception of the sun with respect to urban planning, design and architecture is out of the scope of this thesis, it is worth mentioning a few key elements of the past, before fast-forwarding to more recent developments. Thoughts on natural light in relation with urban form emerged in the 19th century, when light from the sky was perceived as a purifying fluid, stemming particularly from the hygienist movement (Siret [2013] and Harzallah [2007] as cited in Montavon [2010]). Divergent theories on facade exposure, orientation and building height were eventually proposed, motivated by different reasons linked for instance to health, psychological, cultural, social and thermal considerations [Montavon, 2010]. This diversity of motives has persisted, despite an increasing emphasis placed on solar exposure for daylight and thermal heat gains and avoidance, affecting comfort and health.

#### Solar envelopes and associated concepts

Geometrical methods were historically and are still employed to look at solar access and daylight availability in urban environment, often with density considerations. Focusing on the right of individual buildings to solar exposure, the Solar Envelope (SE) concept, first developed in the late 1970's [Knowles, 1999, 2003], consists in defining some geographical boundaries (around a hypothetical building) to ensure urban solar access to the space of interest and its surroundings. This concept was adapted by (and inspired) many to contribute to the development of zoning and planning regulations. Raboudi and Saci [2013] introduced the Solar Bounding Box, a spatially delimiting volume that respects urban rules (e.g. set backs, alignment, distance between buildings) and includes the SE. Pereira et al. [2001] applied the SE to ensure desirable insolation (in terms of thermal comfort) and skylight availability in Brazil. Obstruction angles for the city of Florianopolis were found based on the satisfaction of at least two out of three criteria based on the exclusion/acceptance of undesirable/desirable radiation (e.g. 1.5-2 hrs of insolation during winter). A stereographic obstruction mask and pondered radiation method were used to obtain the criteria-related values. A computer code called MascaraW was developed for visualization. SEs were derived from the obstruction angles and showed the potential use of this concept as a regulation and guideline-generating tool.

Figure 2.5 – Solar Envelope [Knowles, 2003] example for a parcel located in a built context, ensuring solar access to surrounding buildings between 11am and 1pm throughout the year at a latitude of 46°N. Image generated using the SE component of DIVA-for-Grasshopper [Jakubiec and Reinhart, 2011].



The SE concept has been implemented also in CityZoom, an urban planning decision support tool combining computer-aided (architectural) design/drafting (CA(A)D) with geographic information system (GIS), which generates buildings based on inputted master plan parameters (e.g. building height) and allows environmental assessments using SEs [Grazziotin et al., 2004; Turkienicz et al., 2008]. The DIVA-for-Grasshopper plug-in also allows generating and visualizing SEs (see Fig. 2.5) [Jakubiec and Reinhart, 2011].

Similarly, Faucher and Nivet [2000] proposed incorporating in a CA(A)D tool urban regulations and the design intents of the user, linked to sunlight and visibility, both considered as constraints on 3D volumes. This approach, termed ‘declarative modeling’, was also adopted by Gallas et al. [2011 a,b], where users must declare their intentions in terms of the desired daylighting atmosphere.

Based on the SE, Capeluto and Shaviv [2001] introduced new envelopes: the solar rights and collection envelopes which respectively represent the maximum building heights that can be achieved without violating solar rights and the lowest point where window/solar collectors are not shaded by the surroundings. From those envelopes, a Solar Volume (SV) is defined, containing the building heights allowing solar access to all nearby buildings. All of those parameters are determined for a given period of time. Using the SV to ensure maximum solar insolation, an investigation was done to determine the urban fabric (street orientation, distance between buildings) that allowed the densest urban setting, for the city of Tel Aviv (Israel) [Capeluto and Shaviv, 1999]. The simplified section lines, which define the SE respecting the required exposition hours in each direction, are also presented as an easier tool to be used by planning authorities, although more geometrically limiting [Capeluto et al., 2005, 2006].

The Solar Envelope and Solar Volume approaches allow freedom in building design and flexibility in criteria selection. Although they address the urban scale, Littlefair [1998] stated they may be too strict for dense urban areas and that their use requires the collaboration between urban designers and experts. The value of the SE concept has also recently been questioned through a study based on typical buildings in the US and focused on energy use and plot density [Niemasz et al., 2011]. The results suggest that direct solar exposure may affect energy performance in a significantly different way according to the climate and construction. The SE concept as a zoning tool had some negative impact on both energy use and achievable density for the building type considered in the study. The authors argue that “*there is obviously*



*a need for more climate-specific guidelines and standards that holistically integrate the concerns of solar access and developable density” [Niemasz et al., 2011].*

Addressing the need for a year-round approach focusing both on winter and summer seasons, Okeil [2010] proposed a specific residential urban shape, the Residential Solar Block, maximizing (respectively minimizing) solar energy on facades (resp. roofs and ground). In response to the SE’s lack of energy considerations, Morello and Ratti [2009] introduced iso-solar surfaces, 3D envelopes receiving equal amounts of solar energy. Similar to the envelopes introduced earlier, iso-solar rights and collection surfaces were defined, respectively representing the maximum height for buildable volumes preserving a certain amount of irradiation on surrounding sites, and the lowest possible surface for collecting a given amount of solar radiation. The same authors also addressed the computational limitations of applying the SE on extensive and irregular areas by proposing an approach using digital elevation models (DEMs) and image processing techniques.

### **Sky opening factors**

The abstract nature of early urban designs, proper to their ill-defined problem solving characteristic introduced in chapter 1.2, fosters the use of simple assessment methods. In addition to the volume-based approaches listed above, metrics are also derived from geometrical analyzes to quantify solar availability. As an indicator of urban daylight potential and radiation exchanges, the sky view factor (SVF) is often used, either defined as the proportion of visible sky from a point to the overall sky dome (geometrical definition) or the ratio between the radiation received by a planar surface and by the entire hemisphere (cosine-weighted definition, associated to the urban heat island (UHI) effect) [Zhang et al., 2012a]. Ratti et al. [2003] computed average SVFs at different facade heights, taking these values as a measure of the daylight condition inside buildings. Looking at different urban squares of London using DEMs, Chatzipoulka et al. [2015] found a negative correlation between density and mean facades SVF. Zhang et al. [2012a] adapted the SVF by computing the facade area falling within a SVF range and normalizing it by the floor area, using this metric as an environmental performance indicator. Compagnon [2004] presented a visualization technique displaying the facade area per orientation weighted by its corresponding SVF, forming an orientation rose useful as a planning tool allowing to compare various hypothetical urban forms. Robinson [2006] tested the validity of the SVF as well as two other related urban geometrical parameters: street canyon height-to-width ratio and urban horizon angle (mean elevation of the skyline from a facade). He found that the validity of such indicators is actually limited and that raw irradiation data are preferred.

Another daylight availability indicator is the Preferable Sky Window, representing the sky zone with the greatest daylight potential with respect to a horizontal indoor plane [Pereira et al., 2009]. Through a case study in Brazil, Pereira et al. [2009] applied this metric to establish guidelines (e.g. in terms of building height and spacing) ensuring urban daylight access on the winter solstice. A correlation was found with the illuminance values in a room model simulated

## **Chapter 2. State-of-the-art in decision-support methods applied to design**

---

with the Apolux software [Claro et al., 2005]. Seong et al. [2006] addressed the question of solar rights standardization in the Korean context with the development of a tool (HELIOS), based on the WALDRAM diagram method that calculates the sunshine duration in each housing unit of a building then declared satisfactory or not. Yezioro et al. [2006] proposed a methodology for deriving design recommendations and guidelines allowing proper insolation of urban squares (courtyards), based on the ratio between the exposed and total surface area, termed the Geometrical Insolated Coefficient.

### **Appraisal**

The above-mentioned concepts have been used in case-studies to demonstrate their relevance for urban planning as they allow defining - SE and derivatives - and assessing - indicators such as the SVF - the urban fabric with regards to 'proper' (varying definition) solar exposition. The case-specific nature of many of those methods, with assumptions and criteria to be pre-defined according to the objectives, make them challenging to implement and use by decision-makers. While they remain early-phase friendly due to the low level of detail of the required design information, for the same reason they offer little assurance as to global energy outcome, with the focus placed mainly on insolation duration and sky view. Many are by default spatially and temporally static; their evaluation is done for a specific moment and land parcel/point. Moreover, it is difficult to find any validation studies correlating the outcome of these methods to actual energy consumption or interior daylight levels, restraining our conviction about their value in the context of this thesis' objectives.

In the following section, we pursue our review with studies that have taken a closer look at urban form, captured through different parameters that have been linked to performance criteria.

### **2.2.2 Morphological parameters as performance indicators**

Due to the time and knowledge required to evaluate performance through modeling and simulation, as well as the need to make educated guesses regarding unknown design information at the early phase (factors which are amplified with the size of the project), multiple investigations have attempted to link morphological parameters, e.g. density and shape, to various performance aspects in order to identify potential indicators of the latter, more easily computable.

#### **Density and compactness**

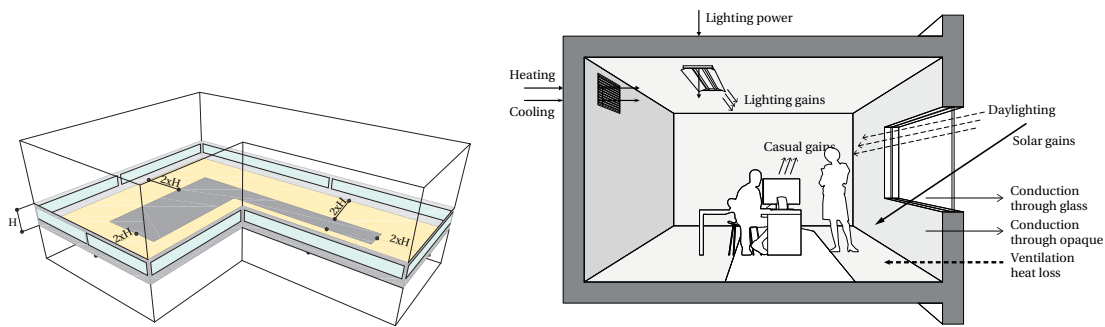
A prevailing parameter is the urban density, defined in terms built volumes (e.g. Floor Area Ratio (FAR): total floor area over site area) [Cheng, 2010]. Studies conducted have however come to divergent conclusions [LSE Cities and EIFER, 2014], challenging the often accepted notion that increasing density leads to energy efficiency [Laëtitia et al., 2011; Rodríguez-

Álvarez, 2016]. Careful case-specific analyzes are instead advocated [Mindali et al., 2004], adopting a more holistic point of view to include for instance daylight and transport-related energy consumption [Stemers, 2003]. Similar debates have been on-going regarding the compactness of cities - as an inverse of the urban sprawl - in relation with their sustainability [Burton et al., 2003].

A stronger consensus has been reached on the compactness parameter measured at the building scale, the rule-of-thumb being its maximization for increasing the thermal performance in winter. Compactness is quantified by slightly different metrics such as the surface-to-volume ratio [Knowles, 1974], also known as the shape parameter (exposed envelope surface / enclosed volume), and the relative compactness ( $6 \cdot \text{volume}^{2/3} / \text{exposed envelope area}$ ) introduced by Mahdavi and Gurtekin [2002]. Assuming a fixed volume, the most compact shape is the one with the least exposed surface area. Knowles [1974] demonstrated the correlation between the surface-to-volume ratio, which was referred to in that early study as the coefficient of susceptibility of a built arrangement, and the stress expressed as a function of variation of the environmental forces acting on this built domain. Based on certain assumptions related e.g. to thermal transmittance of facades, Martin and March [1972] concluded that the shape minimizing heat losses was that of a half cube [Ratti et al., 2005]. The value of the shape factor has been questioned in various studies where its correlation to energy consumption was shown to vary significantly for different climates and design features (e.g. glazing ratio) [Danielski, 2011; Depecker et al., 2001; Laëtita et al., 2011; Pessenlehner and Mahdavi, 2003]. Referring to the relative compactness as a potential indicator of overheating, Pessenlehner and Mahdavi [2003] concluded that it does *“not appear to capture the geometry of a building to the extent necessary for the predictive assessment of the overheating risk”*.

Although computed at the building level, compactness metrics are also applied in macro-scale studies [Taleghani et al., 2013]. Questioning the value of compactness as an indicator of the global energy performance (as opposed to the heating energy only), Ratti et al. [2005] conducted a study comparing the surface-to-volume ratio to the energy consumption for heating, cooling, ventilation and lighting, computed using the same default assumptions (including same London climate) for areas in London, Berlin and Toulouse. They tested another metric, derived from the passive zone concept initially proposed by Baker and Stemers [2000]: the passive to non-passive zone ratio, where a passive zone is defined as the area within twice the floor to ceiling distance (approximately 5.5-6 m) from an exposed facade. Illustrated in Fig. 2.6a, this concept is based on the fact that spaces closer to a facade can better benefit from daylight, natural ventilation and solar gains. The proportion of passive zones is thus considered an energy performance indicator. The outcome of Ratti et al. [2005]’s study showed that the ratio of passive to non-passive zones is a better indicator of urban energy consumption than the surface-to-volume ratio. The LT method was employed to predict the annual energy use for heating, cooling, lighting and ventilation. Originally developed by Baker and Stemers [2000], the aim of this method is to offer a simplified approach to energy performance assessment. It is based on a mathematical model - the LT model - derived from simulations over a room module, taking into consideration the energy flows illustrated in Fig. 2.6b. It consists in curves

## Chapter 2. State-of-the-art in decision-support methods applied to design



(a) The passive zone concept where the yellow area is considered passive and the dark gray core zone non-passive.  $H$  = height of one story. (b) Energy flows considered in the LT model. Image adapted from Baker and Steemers [2000].

Figure 2.6 – The (a) passive zone concept, applied in the (b) LT method, both proposed by Baker and Steemers [2000].

displaying the monthly net heating and cooling load for different glazing ratios. Multiple assumptions are made for deriving these curves by fixing default values to the LT model (e.g. insulation, lighting). Its application in practice consists in (i) identifying the passive and non-passive zones in a building, (ii) extracting the annual primary energy consumptions (heating, cooling and lighting) per floor area from the LT curves for the relevant glazing ratio, (iii) applying the correction factor for shading, and (iv) multiplying the resulting energy values by the corresponding building zones (passive/non-passive). Many LT models exist for various climates and building types: 1.2 for office buildings in Europe [Baker, 1992], 3.0 for southern Europe [Baker and Steemers, 1996] and the urban version [Ratti et al., 2000]. The latter couples the LT method with DEMs, used to extract the required information (e.g. urban horizon angle). However, the effect of the built context on the solar exposure (i.e. shading effect) is not taken into account through this method.

In a study exploring the link between various high-density urban forms and their level of solar radiation in the context of Singapore, Leung and Steemers [2009] put in question common conceptions and concluded that *“the application of broad-brush design concepts do not always guarantee real effect. Simplified computer-aided design methods that provide real-time feedbacks on solar irradiance on building facades are therefore desirable for the conceptual design stage”* [p.438].

The use of heuristics also becomes problematic when conflicting criteria are considered. In an investigation of the impact of block typologies of varying density on their solar gain, energy and daylight performance, Sattrup and Strømman-Andersen [2013] identified an optimal region of density demonstrating the need for a trade-off between the performance criteria. Their results, illustrated in Fig. 2.7, show the conflict between energy and daylight. They moreover found differences of 16% and 48% in terms of total energy use and daylight autonomy respectively between the designs, emphasizing the importance of incorporating such considerations into the decision-making process early-on.

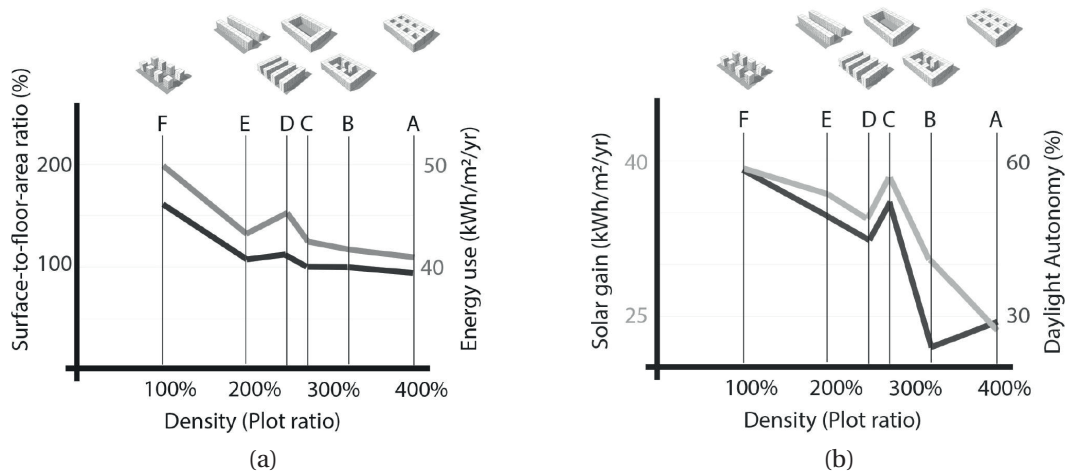


Figure 2.7 – Results from a study investigating the impact of urban typology on energy and daylight performance and the correlation between (a) density, energy use (light gray line) and compactness (dark gray line), and (b) density, daylight autonomy (dark gray line) and solar gain (light gray line). Figures reprinted from Sattrup and Strømmand-Andersen [2013], used with the permission of Peter Sattrup and Locke Science Publishing Company, Inc.

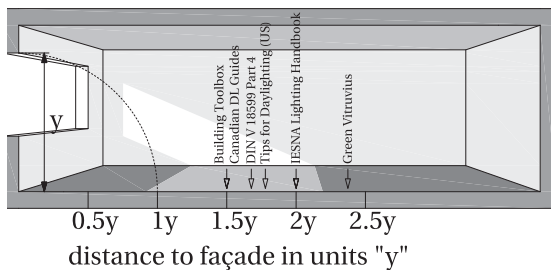


Figure 2.8 – Different versions of the rule-of-thumb for predicting the daylit area from the window height. Image adapted from Reinhart [2005].

### Additional geometry-based heuristics

At the building or room level, simple geometrical rules-of-thumb are applied with the aim of ensuring proper daylight levels. Despite a lack of standardized and validated rules [Galasiu and Reinhart, 2008; Reinhart and LoVerso, 2010], a commonly used example is based on the height of the window top and the room depth [Reinhart, 2005]. The daylit area is estimated as extending from the window facade to a certain factor of the window height, as illustrated in Fig. 2.8. Following a simulation-based experiment, Reinhart [2005] asserted the validity of such heuristics, however stating that daylight simulations should be conducted in specific cases such as for taking into account the potential obstructing impact of the surrounding context. Focusing on diffuse daylight, Reinhart and LoVerso [2010] proposed a rule-of-thumb design workflow for deriving the window-to-wall ratio and room dimensions from a defined performance target expressed in terms of the Daylight Factor (DF). The DF is a static metric defined as the ratio between the internal illuminance measure at a point inside a building and the external horizontal illuminance obtained assuming an overcast sky (Moon and Spencer [1942] as cited in Reinhart et al. [2006]). The simple workflow bypasses the need for calculating the DF.

## Chapter 2. State-of-the-art in decision-support methods applied to design

---

Simple geometry-based guidelines are also used to assess the energy production potential, notably the optimal tilt and the orientation of surfaces on which active solar systems are to be installed. This allows bypassing the need for full radiation simulations. However, multiple values can be found in the literature, e.g. setting the tilt equal to or 10 degrees below the latitude [Cronemberger et al., 2012]. In a study conducted over 78 cities in Brazil, Cronemberger et al. [2012] have shown that these various recommendations are not valid for such low latitudes, highlighting the need for climate-based indicators.

### Appraisal

From this review arises the need for methods finely balanced between case-specificity and generalizability. While many studies target the same fundamental question of finding the optimal building or urban form, slight differences in the objective function(s) they are aiming at maximizing/minimizing and the context they are looking at (e.g. climate, building function) lead to divergent results. This situation casts doubt on the applicability of simple geometrical parameters as proxies of performance metrics. In line with this concern, more comprehensive methods have been developed exploiting computational tools, in some cases resulting in indicators similar to the geometry-based ones, but derived from simulation outputs such as irradiation levels.

### 2.2.3 Physics-based simulation

#### Solar exposure

The technological advances brought about new possibilities for approaching performance evaluation through visualization techniques and simulation of incident solar radiation. A large majority of the methods involving simulation of solar exposure rely on the extensively validated and highly trusted Radiance engine, an open-source ray tracing<sup>1</sup> software used for lighting analysis and visualization [Larson and Shakespeare, 1998]. While a detailed software review is not the focus of this chapter, this particular program is worth mentioning since it is used in many of the studies and applications listed below.

Various CA(A)D tools are nowadays used for modeling, visualization and renderings (e.g. AutoCAD<sup>2</sup>, SketchUp<sup>3</sup>, Rhinoceros<sup>4</sup>). Many directly integrate or are linked to, e.g. via plug-ins, performance assessment engines, for which examples are given further. More recently, geographic information systems (GISs) are being used to visualize the solar exposure levels of building roofs, in the form of solar maps or cadasters [Kanters et al., 2014c]. These allow

---

<sup>1</sup>Radiance's lighting simulation engine employs a hybrid approach consisting in a Monte Carlo and deterministic ray tracing, starting from a measurement point from which light rays are traced backwards to the sources (<http://radsite.lbl.gov/radiance/framew.html>, last accessed on April 18, 2016).

<sup>2</sup><http://www.autodesk.com/products/autocad/overview> (last accessed on March 9, 2016)

<sup>3</sup><http://www.sketchup.com/> (last accessed on March 20, 2016)

<sup>4</sup><https://www.rhino3d.com/> (last accessed on March 20, 2016)

obtaining an estimate of the solar potential for ST and PV systems. Such maps are continuously being developed for specific regions, such as the city of Cambridge in the US<sup>5</sup> and some zones of Switzerland<sup>6</sup>.

As seen earlier with geometry-based parameters, illuminance- or irradiation-based metrics are also used as performance indicators. Irradiation thresholds are often applied to quantify the active solar potential. These diverge between countries and sources, often influenced by financial parameters. For example, Cronemberger et al. [2012] found that the ratio of available to maximum irradiation considered as acceptable - for an optimally inclined and oriented surface - ranges from 55% to 80%.

Compagnon [2004] defined irradiation- and illuminance-based thresholds to assess the performance in a more holistic way. A value was defined for the passive thermal, daylight and active (PV and ST) potential, and the exposed surface areas with a level exceeding the respective threshold was identified. This method was adopted in other studies [Cheng et al., 2006; Montavon et al., 2004b] including Swiss [Robinson et al., 2005] and European [Compagnon, 2000] projects.

As an indicator of the daylight conditions inside a building, the vertical Daylight Factor (DF) is used, measured on external facades and equivalent to the typical DF measured inside a building (introduced earlier). When computed for dense urban arrays of 25 buildings varying in terms of height, Ng [2005] concluded that larger building height differences could increase the vertical DF. The same author proposed a simplified method to evaluate the vertical DF, exploiting its correlation with the Unobstructed Vision Area, a geometrical parameter easier to compute [Ng and Cheng, 2004]. Requirements in terms of building height were defined. This method is used by the Government of Hong Kong for regulatory control of daylight performance. Concerned with linking external daylight levels with the interior building spaces, Zhang et al. [2012b] proposed a facade vertical DF per unit floor area, measuring the average amount of daylight on the facade that could affect the usable floor space.

In addition to indicators, some methods also produce specific types of images. The irradiation mapping for complex urban environment (ICUE) developed by Mardaljevic and Rylatt [2003] produces maps of annual/monthly sun and sky irradiation incident on building facades, taking into account shading and reflection by/between buildings. The creation of the 3D irradiation images, done in Radiance, is however very time-consuming.

Developed and exposed through case studies in [Samimi and Nasrollahi, 2014], SOLARCHVISION is an analysis tool aiming at helping planners integrate climatic and solar considerations in their decision-making process. Focusing on both active and passive solar strategies, it allows visualizing sun path diagrams of different metrics such as the 'degree of need to shade/shine', computed from the difference between the hourly outdoor temperature and a fixed indoor comfort temperature, and the 'positive/negative effects of the sun', depending on the amount

---

<sup>5</sup><http://www.mapdwell.com/en/cambridge> (last accessed on March 30, 2016)

<sup>6</sup><http://www.bfe-gis.admin.ch/sonnendach/?lang=fr> (last accessed on March 30, 2016)

## Chapter 2. State-of-the-art in decision-support methods applied to design

---

of solar radiation and the need to shade/shine degree. An example of each image for the climate of Montreal and an indoor temperature of 18°C are illustrated in Fig. 2.9.

Compagnon et al. [2015] developed a climate- and site-specific tool for guiding designers and policy makers, aiming to ensure sufficient day/sunlight access to both open spaces and buildings. The tool produces two types of stereographic images, starting from a simple 3D model (master planning type) and using Radiance: a multishading mask indicating the percentage unobstructed area toward each direction of the sky vault, and an effective envelope area picture displaying the total projected envelope area seen from the sky vault [Compagnon et al., 2015]. A series of daylight and sunlight availability indicators for open spaces and buildings' envelope can then be computed from these images: sky view factor (SVF), partial sunlight exposure, mean irradiation and others.

Similarly, various types of images (e.g. stereographic, isochronal) along with solar access metrics (e.g. solar flux, sky opening) are produced by many urban-adapted software including TownScope [Teller and Azar, 2001], Heliodon [Beckers and Rodriguez, 2009], SOLENE [Miguet, 2007] and Apolux (building-scale) [Claro et al., 2005] which have their own background sky modeling algorithm often based on the radiosity<sup>7</sup> method.

Leidi and Schlüter [2013] developed new analytical and visualization methods for urban conceptual design. The Volumetric Insolation and Visibility Analysis (VIA and VVA) methodologies were proposed and combined with computational fluid dynamics (CFD) to offer various representations over an unoccupied volume located in an urban environment, as shown in Fig. 2.10 (upper row). Additional constraints can be applied on the volume such as setbacks and occupation targets, as seen in the second row of Fig. 2.10.

Until now, we have seen methods that produce images and evaluate geometry-, irradiation- and illuminance-based indicators while remaining at the exterior surfaces of buildings. In the following, we go over approaches and tools that require more detailed building models to assess the performance from within. With this shift we see that indicators used to substitute established performance metrics are abandoned, as the goal of the following methods is to directly evaluate these more accurate metrics.

### Building behavior

In this section we will see that while an extensive amount of building-scale tools have been developed, many of them represent front-ends to a much smaller set of performance assessment engines. Some of these main underlying programs are Radiance (previously introduced) and Daysim<sup>8</sup>, a Radiance-based program, for annual irradiation and illuminance simulation, and EnergyPlus [Crawley et al., 2000] and DOE-2 [Birdsall et al., 1990] for dynamic thermal

---

<sup>7</sup>Radiosity-based algorithms involve subdividing surfaces in a scene into patches for which radiosity values are computed iteratively until sufficient illumination is obtained within the scene [Müller et al., 1995].

<sup>8</sup><http://daysim.ning.com/> (last accessed on March 20, 2016)



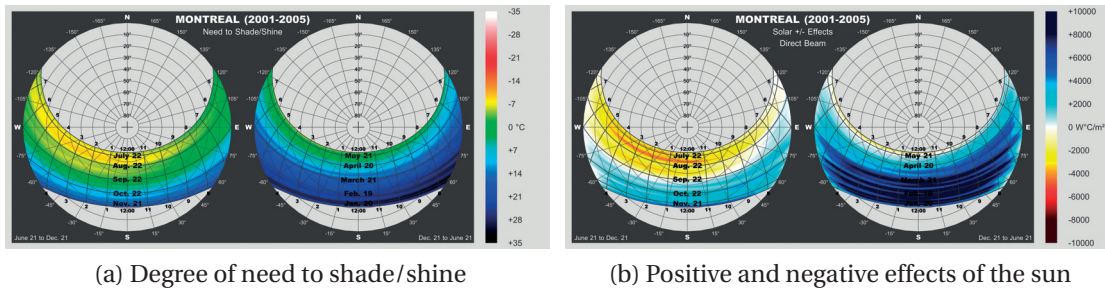


Figure 2.9 – Example products based on the SOLARCHVISION method [Samimi and Nasrollahi, 2014] post-processed from Environment Canada’s long-term climate data at Montreal station (reprinted with the kind permission of Mojtaba Samimi).

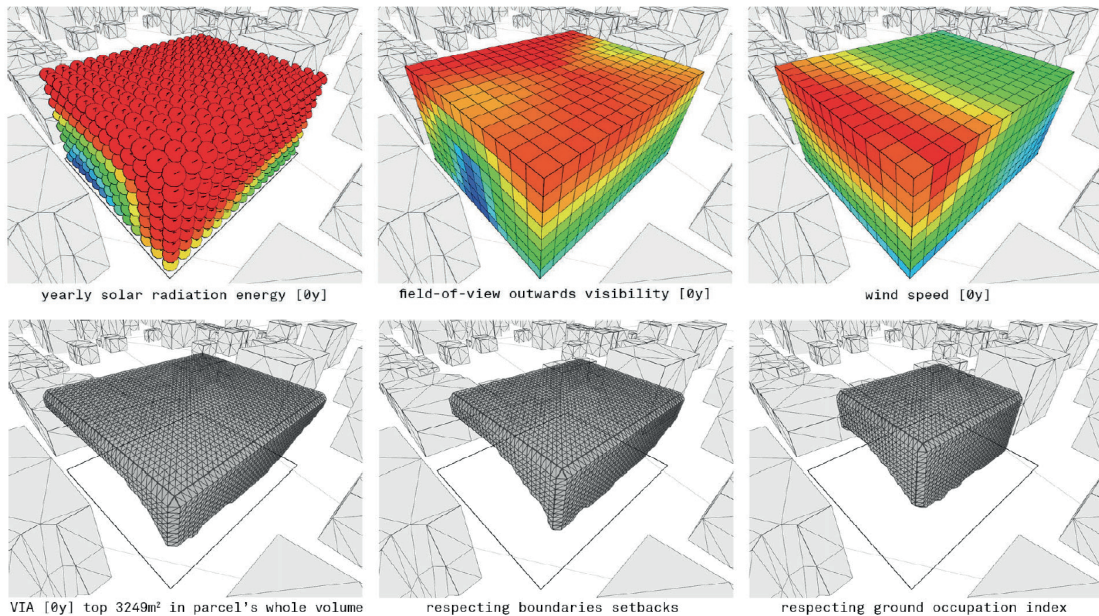


Figure 2.10 – Visualization methods developed by Leidi and Schlüter [2013]. Red represents higher values; [0y] refers to the actual situation (a future case is also shown in the paper from which these graphs were directly taken [Leidi and Schlüter, 2013]).

simulations. The goal of the front-end software are to embed these engines into a more user-friendly format complemented with a 3D modeler/visualizer, an interface for user-inputs and outputs, etc. The 3D modeler is either based on CA(A)D or building information modeling (BIM), fundamentally different in their approach. The former concept represents a digital version of the traditional pencil-sketched drawing, while the latter, more recent, consists in a parametric model embedding the physical and logical characteristics of the building elements [Graphisoft, 2016]. However, according to Hermund [2009], the use of BIM prompts a linear workflow that restricts the typical creative iterations of architects, and it currently concerns more the construction than architecture domain. Many programs are plug-ins for existing CA(A)D/BIM software such as Rhino and SketchUp, or they extend the modeling capacities of

## Chapter 2. State-of-the-art in decision-support methods applied to design

---

an integrated CA(A)D/BIM tool to incorporate a performance assessment engine. Instead of attempting to review individual existing tools, which is out of the scope of this thesis, we here identify features and general approaches of interest.

Since the 3D model and building information required are different between a daylighting and a thermal simulation, these two performance aspects are sometimes separated. Daylight metrics such as illuminance levels, the Daylight Factor (DF) and the climate-based DA are calculated inside a room or building by many tools such as Apolux [Claro et al., 2005], Daylight 1-2-3 [Reinhart et al., 2007], Daylighting Dashboard [Reinhart and Wienold, 2011] and DIVA-for-Rhino [Jakubiec and Reinhart, 2011]. The latter, a plug-in for the 3D modeler Rhino, continues to be developed and is increasingly used particularly in education and research [Elghazi et al., 2014; Sherif et al., 2013]. In addition to its daylighting and glare assessment features, based on Radiance and Daysim, it also allows a thermal simulation using EnergyPlus, but with an adapted building model slightly different than the daylighting model<sup>9</sup>. The DIVA package also includes a plug-in for Grasshopper<sup>10</sup>, a Rhino-based graphical algorithm editor. The latest version of DIVA (4.0) contains a multi-zone energy simulation component for Grasshopper called Archsim<sup>11</sup>, based on EnergyPlus, which combines seamlessly with the daylighting assessment model requirements.

Multiple other plug-ins exist for both Rhino and Grasshopper, documented on the Food4Rhino webpage<sup>12</sup>. Examples for Grasshopper are Mr. Comfy, allowing visualization of thermal/daylight simulation results (provided by an EnergyPlus-/Daysim-based program) [Doelling, 2014] and Ladybug+Honeybee for weather data analysis and simulation based on EnergyPlus, Radiance, Daysim and OpenStudio [Roudsari et al., 2013].

Other comprehensive stand-alone, plug-in or web-based tools allow evaluating both daylighting and thermal performance metrics, varying from simple to more complex in term of interface and assessment engine, e.g. Ecotect<sup>13</sup> [Roberts and Marsh, 2001]; Sefaira<sup>14</sup>, a plug-in for Revit and SketchUp based on EnergyPlus, Radiance and Daysim; DIAL+ [Paule et al., 2011] for lighting, natural ventilation and cooling, based on Radiance and the ISO 13791 dynamic thermal calculation; OpenStudio<sup>15</sup>, a plug-in for SketchUp, and DesignBuilder<sup>16</sup>, both based on EnergyPlus and Radiance.

---

<sup>9</sup>In DIVA-2.0: <http://diva4rhino.com/user-guide/simulation-types/thermal-analysis> (last accessed on March 11, 2016)

<sup>10</sup><http://www.grasshopper3d.com/> (last accessed on March 20, 2016)

<sup>11</sup><http://archsim.com/> (last accessed on March 20, 2016)

<sup>12</sup><http://www.food4rhino.com/> (last accessed on March 3, 2016)

<sup>13</sup>Although no longer available, some of Ecotect's features will be integrated into Revit products (<http://usa.autodesk.com/ecotect-analysis/>, last accessed on March 18, 2016).

<sup>14</sup><http://sefaira.com/> (last accessed on February 29, 2016)

<sup>15</sup><https://www.openstudio.net/> (last accessed on February 29, 2016)

<sup>16</sup><http://www.designbuilder.co.uk/> (last accessed on February 29, 2016)

A drastically small yet increasing amount of more comprehensive tools are conceived for meso- to macro-scale assessment. Notable examples are introduced below and illustrated in Fig. 2.11.

The master-planning analytical tool CityCAD<sup>17</sup> allows visualizing a sketched or imported city model along with extracted and computed values from user-inputs such as electricity and land and water use indicators (see Fig. 2.11a).

The urban modeling interface (UMI, Fig. 2.11b) is a Rhino plug-in conceived for neighborhood to city level assessment of energy use (embodied and operational) through EnergyPlus, walkability and daylight potential through Daysim [Reinhart et al., 2013]. Its main advantages lie in the simple workflow, user-friendly interface and semi-automated modeling features (e.g. windows automatically modeled from a given window-to-wall ratio). An effort was also made to accelerate the simulation time, by implementing simplified methods. For instance the daylight evaluation is done through the Urban Daylight program, which simulates hourly solar radiation levels on all facades via Daysim, that get converted into interior illuminance distributions with a generalized impulse response [Dogan et al., 2012].

The ArchiWIZARD<sup>18</sup> software offers a thermal, solar and lighting (based on ray-tracing) evaluation of an imported 3D (CA(A)D or BIM) model, with comparison to the French RT 2012 (thermal regulations). Results can be viewed in many tabular and graphical forms, such as the example illustrated in Fig. 2.11c.

CitySim (Fig. 2.11d), successor of SUNtool [Robinson et al., 2007], simulates urban energy flows with four core models: thermal, radiation, behavioral and plant/equipment [Robinson et al., 2009]. It was employed in the context of an energy concept for a master plan [Ville de Lausanne, 2010], but has however mainly remained in research until now [Thomas et al., 2014; Vermeulen et al., 2013].

As seen in section 2.1, the uptake of such tools is hampered notably by a lack of user-friendliness and guidance and a level of complexity judged too high. Some features attempted to mitigate one or many of these shortcomings are highlighted in the following.

To facilitate the simulation procedure, some tools such as the MIT Design Advisor [Urban and Glicksman, 2006] have implemented an editable database of default values that is used to reduce the amount of inputs demanded to the user. An important feature of those tools is that they offer a gradual exposure to details and can therefore be used at various stages throughout the design process. To support interpretation of results, code-compliance checks are offered by some tools, typically created for a specific climatic and political context, e.g. Lesosai<sup>19</sup> for Europe/Switzerland (EN ISO 13790 and SIA 380/1 norms as well as different labels) and ArchiWIZARD for France (RT 2012 regulation).

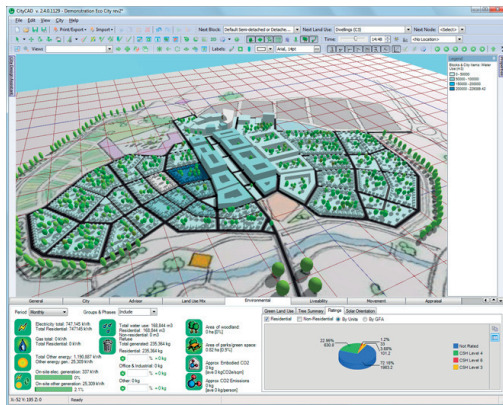
---

<sup>17</sup><https://www.holisticcity.co.uk/index.php/citycad> (last accessed on February 26, 2016)

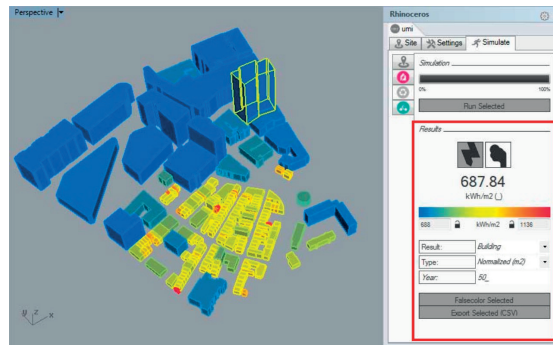
<sup>18</sup><http://www.graitec.com/fr/archiwizard.asp> (last accessed on March 20, 2016)

<sup>19</sup><http://www.lesosai.com/en/> (last accessed on March 20, 2016)

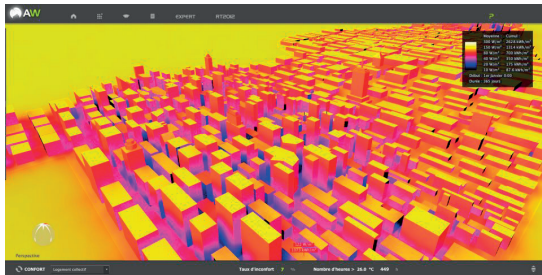
## Chapter 2. State-of-the-art in decision-support methods applied to design



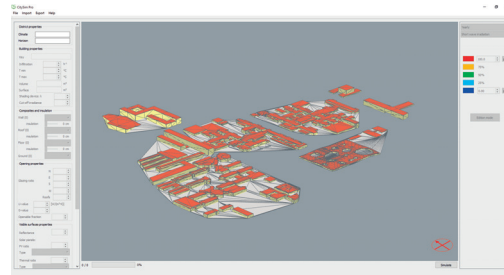
(a) CityCAD: urban design software tool for conceptual 3D master-planning. Source of image: <https://www.holisticcity.co.uk/index.php/citycad> (last accessed on February 26, 2016).



(b) Umi [Reinhart et al., 2013]: Rhino-based design environment for modeling the environmental performance of neighborhoods and cities. Source of image: <http://urbanmodellinginterface.ning.com/> (last accessed on April 14, 2016).



(c) ArchiWIZARD: 3D thermal simulation software. Source of image: <http://www.graitec.com/fr/archiwizard.asp> (last accessed on April 11, 2016).



(d) CitySim [Robinson et al., 2009]: simulation and optimization of energy fluxes of urban districts. Source of image: <http://www.kaemco.ch/download.php> (last accessed on April 14, 2016).

Figure 2.11 – Interface of various existing urban-scale tools.

Other features of interest are linked to support in the 3D model generation and interpretation. Developed by a team at Autodesk, Revit's Conceptual Energy Analysis tool automatically generates an energy model from the massing model of the architect, while also ensuring that both are in sync if modifications are made by the user to the massing model [Smith et al., 2011]. Automatic zoning, glazing and shading as well as surface determination are done based on assumptions, editable default values, metrics and mapping logic. For example, the window-to-wall percentage metric is used as a control method, with defaults for the target percentage. This allows the definition of all surfaces, thermal zones and shading objects. Conceptual constructions characteristics are then assigned as well as 'intelligent' defaults for occupancy and internal gains based on documents and studies from the American Society of Heating, Refrigerating and Air-Conditioning Engineers (ASHRAE) and codes for California. Comparison between alternatives can also be done. While the energy model is automatically generated, it remains the task of the user to manually modify the massing to create a design variant to be compared.

Similarly, focusing on facilitating the modeling particularly for urban-scale assessment, Dogan et al. [2015] developed Autozoner, an algorithm that automates the separation of buildings into thermal zones in preparation for an energy simulation [Dogan et al., 2015].

A large majority of the simulation tools introduced in this chapter are based on physical methods that solve equations describing the behavior of buildings or radiation from the sky. This makes them intrinsically accurate to some degree depending on the complexity of the engine and information provided and taken into account. In our context of interest of early neighborhood design, information is scarce and simulation is computationally expensive.

Attempting to address these issues, Rodríguez-Álvarez [2016] recently proposed the Urban Energy Index for Buildings (UEIB), a thermal and lighting model for facilitating energy considerations at the planning stage. Existing in both a spreadsheet and GIS-integrated format, the method incorporates a procedure for simplifying an urban morphology to a notional grid of repeated buildings as illustrated in Fig. 2.12. The heating, cooling and lighting loads are estimated through a simplified method, based on default values that can be edited by the user (e.g. materials' characteristics). Similar to the notional grid concept is the parametric street network generation and block subdivision method by Schneider et al. [2011], which is built from existing and custom-developed Grasshopper components. CitySim's thermal model, analogous to an electrical circuit, is another example of an alternative representation of buildings and of their behavior for reducing simulation time [Robinson et al., 2009].

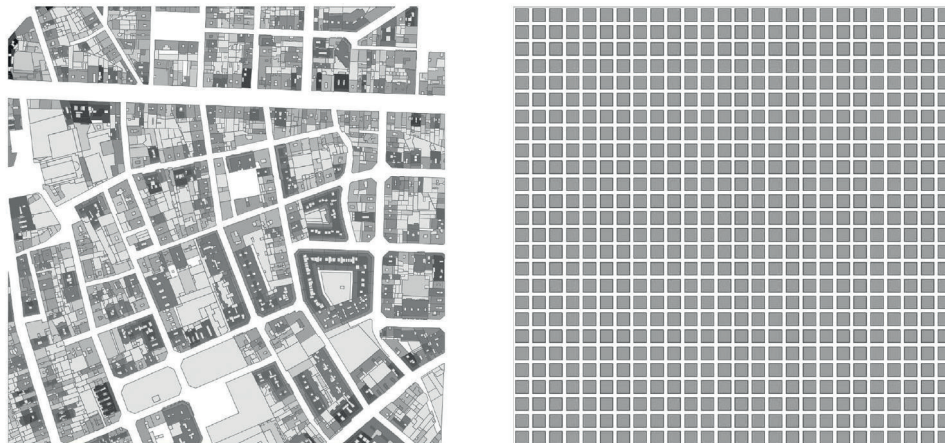


Figure 2.12 – Urban morphology (left) and its corresponding notional grid (right), which is evaluated in the UEIB method of Rodríguez-Álvarez [2016]. Images reprinted with the permission of Elsevier.

An alternative path to physics-based methods is to resort to techniques coming from the fields of computer science, artificial intelligence and statistics. The LT method introduced earlier was developed using such techniques, resulting in a mathematical model used to cheaply predict, from simple inputs, the energy performance. Multiple other examples can be found, mainly focused on the building scale [Ekici and Aksoy, 2009; Foucquier et al., 2013; Tsanas and Xifara, 2012]. As will be seen in chapters 3 and 4, this topic will become central to this thesis and will be further discussed in chapter 4 along with more examples found in the literature.

### Appraisal

Most simulation-based tools are often referred to in the literature as ‘generate-and-test’ or ‘trial-and-error’ and often criticized for being poorly integrated into the design process [Oxman, 2009; Petersen and Svendsen, 2010]. Despite the variety of graphical outputs offered by most tools, additional guidance is required for interpreting the results. As Prazeres and Clarke [2003] state: “*Copious amounts of data are generated by contemporary building simulation programs and the translation of these data to information that may be acted upon is problematic.*” These issues can be mitigated by allowing comparing design alternatives (e.g. SOLENE [Miguet, 2007], MIT Design Advisor [Urban and Glicksman, 2006], Building Design Advisor [Papamichael et al., 1997], Home Energy Efficient Design (HEED) [Milne et al., 2001]) or conducting sensitivity analyzes (e.g. iDbuild [Petersen and Svendsen, 2010]), therefore reducing the need for repeated manual evaluation while increasing the knowledge gained by users.

Such approaches bring us toward emerging design paradigms that promote a restructuring of the traditional linear process. As introduced in chapter 1, adopting a ‘non-linear’ flow involving the simultaneous generation and multi-criteria evaluation of multiple design alternatives can provide more guidance to the user [Grobman et al., 2010]. Example approaches that follow this notion are presented in the next section.

## 2.3 Analysis support

As seen in the above review, what we have termed assessment methods are at the core of any performance-based DDS. They vary in complexity and in the characteristics of the framework within which they must be embedded to be used by practitioners. In this section, we take a closer look at different or additional features these frameworks can have to further support users in making informed decisions. We use the term analysis support to convey this extra step toward producing and facilitating the interpretation of results from pure evaluation tools.

### 2.3.1 Generative design

Grobman et al. [2008] proposed a non-linear, performance-based tool, Generative Performance Oriented Design (GenPOD), allowing to generate and evaluate multiple design alternatives. Based on a morphing algorithm, building forms are generated to populate a design solution space, based on different performance aspects (e.g. sun shading/exposure, visibility).

Similarly, Mahdavi and Gurtekin [2002] observed that BPS tools, despite being able to provide significant amounts of data, do not effectively support the exploration of this data, or the navigation into the ‘design-performance space’. To address this shortcoming, they proposed a workflow involving the generation of alternatives through parametric variations of variables from an initial design, conducting a performance simulation on these design variants to be represented as a performance space landscape that can be interactively explored to identify the preferred alternatives.

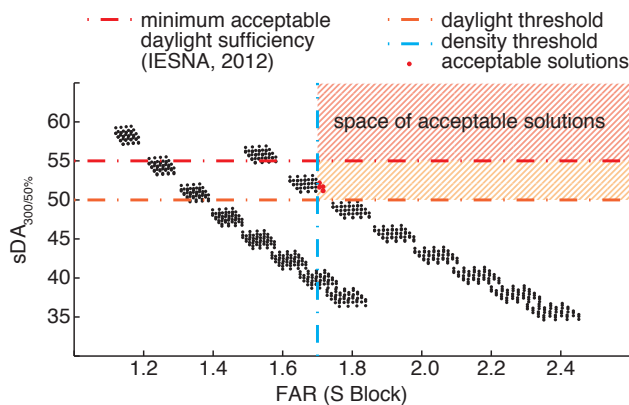


Figure 2.13 – Constraints decision plot from which solutions achieving the required daylight performance and density level can be identified. Source of image: Peronato [2014].

Lagios et al. [2010] developed an Animated Building Performance Simulation (ABPS) design workflow combining Rhino, Grasshopper and Radiance/Daysim. Allowing the evaluation of various performance indicators including solar radiation maps and daylight metrics, two simulation approaches are offered: the single versus multiple variant analysis. In the latter, design variables such as window size can be varied automatically using Grasshopper's parametric modeling features and slider component allowing to iteratively go through a range of numerical values. An animation is then generated by compiling the result images captured for each design variant.

Along the same line and also based on parametric modeling using Rhino, Grasshopper and simulation plug-ins, Peronato et al. [2015] developed a design-based method for assessing and visualizing various building performance criteria at the neighborhood scale. In this approach, elaborated in the context of a master's thesis conducted in part at LIPID [Peronato, 2014], parameters such as building set-back and height are varied one at a time, generating a series of design alternatives that are evaluated. Results are displayed through various graphs and images allowing to visualize the effect of specific parameters on a given performance output (e.g. energy need and active solar suitability of building surfaces). Optimal solutions can be identified by plotting the values associated to two criteria in addition to specific constraints, as illustrated in Fig. 2.13.

Populating this type of graph can be done through a formal mathematical method, optimization, used to identify highly performing design alternatives. Before addressing this field, we introduce a technique that is often adopted to identify the most influential parameters prior to or in combination with developing a parametric or optimization framework.

### 2.3.2 Sensitivity analysis

Considering a set of input parameters whose exact value is uncertain, sensitivity analysis can serve to identify which of these inputs most determine the uncertainty in a given output [Saltelli et al., 2004].

Martins et al. [2014] investigated the impact of varying urban and building parameters, e.g. the height, glazing U-value and plot ratio, on the irradiation and illuminance levels on the envelope. They then used the results to define the constants (less significant factors, e.g. U-value and glazing ratio) and variables (highly significant, e.g. albedo and aspect ratio) for an urban design optimization problem. Other studies, mainly at the building scale, have adopted a similar approach, often in combination with regression techniques [Capozzoli et al., 2009; Eisenhower et al., 2012; Hygh et al., 2012], or for investigating the sensitivity of a building to different climates based on its properties e.g. U-value and thermal mass [Rastogi, 2016].

Kavgic et al. [2013] identified the following four most influential factors out of 14 on the space heating energy consumption of a dwelling: mean indoor temperature, efficiency of heating system, external air temperature, and window U-value. They concluded that *“if there is a large error/uncertainty associated with these parameters, it is very likely that model predictions will be inaccurate”*. They however also stated that knowing the exact value for those inputs was still insufficient for obtaining accurate results, since the sensitivity analysis showed differences in the relative influence of parameters based on the examined building’s form and construction year.

Results that can be retrieved from a sensitivity analysis are dependent upon the context under study (e.g. climate, scale), the defined range for each variable, as well as the number and type of performance output(s) considered. This limits any generalization of the outcomes and highlights the need for robust methods that can be applied to different cases rather than specific studies.



### 2.3.3 Design optimization frameworks

Where other methods leave the search for the most satisfying solution and at least part of the interpretation of the results in the hands of the user, optimization explicitly directs the latter toward optimal conditions [Papalambros and Wilde, 2000]. To optimize a design means to find the settings, e.g. in terms of design parameters, that lead to minimizing or maximizing a certain criterion. For instance, in the simple case where one would like to maximize the daylight surface inside a room (objective function), the optimal solution would consist in the values of the design variables (e.g. whatever can be modified such as room and/or window dimensions) leading to the highest achievable daylight area.

Formally, the optimization of a design consists in defining a vector from the design variables:  $\mathbf{x} = (x_1, x_2, \dots, x_n)$  and the objective as a function of these variables:  $f(\mathbf{x})$ , with some potential constraints being described by functional relations such as  $h(\mathbf{x}) = 0$  [Papalambros and Wilde, 2000]. Multi-criteria or multi-objective optimization is when more than one objective function is defined or when constraints are present in addition to the objective(s) function(s). In such cases, a Pareto set of solutions can be obtained, consisting of Pareto optimal solutions in the form of  $\mathbf{x}$  vectors. This concept is illustrated in Fig. 2.14 for a minimization problem with two objective functions. A point  $A$  is considered a Pareto optimum if and only if there is no other point that equals or minimizes all functions ( $F_i(A) \leq F_i \forall i$ ) and  $A$  minimizes at least one function ( $F_i(A) < F_i$ ) [Papalambros and Wilde, 2000]. All points beyond the Pareto front are dominated by the Pareto set [Forrester et al., 2008].

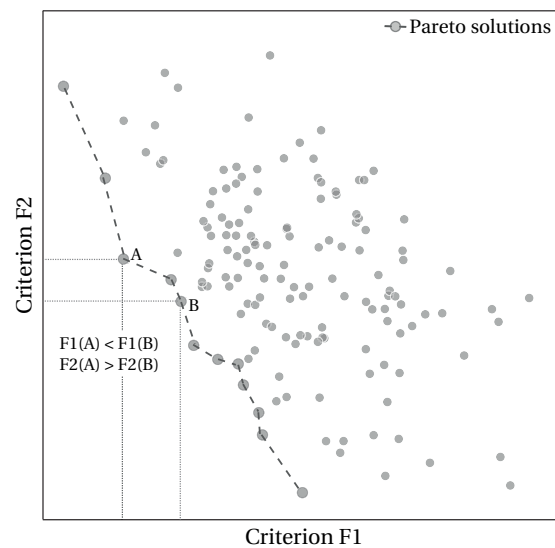


Figure 2.14 – Pareto front of the solution space in a multi-criteria optimization problem where two functions are to be minimized.

While optimization-based approaches are commonly criticized for their ‘black-box’ nature and low user-interaction [Gagne, 2011], exploiting the Pareto solutions can mitigate these issues by providing multiple design alternatives to the user as opposed to a unique optimal solution. The latter case is likely to be not well embraced by practitioners.

Optimization algorithms broadly fall into two categories: local optimizers (or hill-climbers) and global searches [Forrester et al., 2008]. Methods in the former group include gradient-based optimizers and direct search methods. In the second group we find for instance genetic algorithms (GA) and simulated annealing. While a detailed explanation of optimization methods is out of the scope of this review, it is worth mentioning that in the field of sustainable

## Chapter 2. State-of-the-art in decision-support methods applied to design

building design, genetic algorithms (GA) and direct search methods are the most common [Evins, 2013]. While optimization, in particular multi-objective optimization, is increasingly applied in this field, it is still mostly found in research, academia and engineering practices [Attia et al., 2013b; Evins, 2013]. We here give some examples focused on supporting performative design.

Oliveira Panão et al. [2008] employed a powerful optimization technique, GA, to search for the building shapes maximizing (respectively minimizing) the absorptance in winter (resp. summer), a parameter influenced by the solar irradiation on facades. In a case-study limited to a uniform urban layout - i.e. all buildings and street of same dimensions - optimal urban forms, as defined by the fitness function, for a specific latitude were identified. Similarly, Martins et al. [2014] applied multi-objective optimization to minimize (resp. maximizing) irradiation on facades (resp. roofs), with constraints linked to density and facade illuminance levels.

Bruno et al. [2011] combined the program Catia, used for parametric modeling, with Mode Frontier, an evolutionary computational software, to conceive a workflow for urban district optimization. A Multi-Objective Genetic Algorithm (MOGA-II) scheduler designed for rapid Pareto convergence is used to optimize different functions based on building program, location and density. Abstract cylindrical building shapes are modeled. Example solutions found for individual objective functions in a case study in Masdar are presented in figure 2.15.

Similarly, Mashood et al. [2007]'s GALOP system combines a knowledge base (concept introduced in the next section) with a GA optimization method, to be applied at the building layout planning stage. Focusing on three objectives - maximizing rental area, maximizing circulation grade and minimizing heat gain - and incorporating constraints both from the user and the knowledge base, the system searches the solution space for Pareto optimal configurations (e.g. orientation, shape), which are presented to the user. A decision-maker module also aids the designer in selecting a final design, by considering a priori knowledge and user preferences.

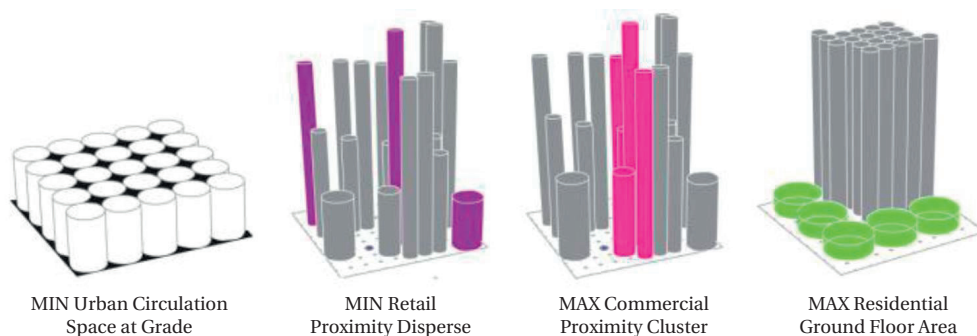


Figure 2.15 – Solutions proposed by Bruno et al. [2011]'s workflow, corresponding to four different optimization functions. Image reprinted with the kind permission of Michele Bruno.

Caldas [2006] developed an Evolutionary-based Generative Design System (GENE-ARCH), combining a GA with the DOE2.1E engine to optimize buildings thermal and lighting performance. Various case-studies have been published [Caldas, 2008; Caldas and Norford, 2002], including one conducted at the urban scale incorporating a shape grammar of the patio house typology in Marrakech [Caldas, 2011]. In this study, the methodology is applied with the goal of varying dimensional parameters, while respecting the typology of the patio houses, in order to minimize the energy consumption. Highly influencing geometrical factors on the energy consumption are also identified. The authors argue that through its goal-oriented generative design approach involving constraints and rules, the generation of non-intuitive optimal solutions can contribute to the user's creativity.

Marin et al. [2008] proposed an evolutionary design tool that evaluates the solar passive quality of evolving shapes through the Unified Day Degree method. Taking into account the subjective preferences of the designer, its aim is to explore the solution space of shapes for optimality regarding heating needs in winter.

Another optimization framework was recently proposed by Zemella et al. [2011]: the Evolutionary Neural Networks Design (ENN-Design) applied to building facades. Two approaches are presented: a single-objective optimization for minimizing the CO<sub>2</sub> emissions and a multi-objective optimization for minimizing both cooling and lighting energy consumptions. In the latter, a Pareto front illustrating the trade-off curve between both objectives is derived. Assumptions are made for the internal environment (temperature, gains, etc.) and facade thermal transmittances, while the glazing ratio, and window and solar protection type are taken as variables.

An example software, previously introduced, that integrates an optimizer is CitySim [Robinson et al., 2009], which relies on a hybrid evolutionary algorithm (CMA-ES/HDE) [Kämpf and Robinson, 2009, 2010]. Another software is GenOpt [Wetter, 2001], which includes a library of optimization algorithms that it links to various simulation software (e.g. EnergyPlus, DOE-2) to determine the parameter settings leading to the minimization of a thermal energy objective function. New input parameters are iteratively defined and sent to the program until the function's minimum has been found. Similarly, Opt-E Plus, developed at the National Renewable Energy Laboratory (NREL) as an in-house tool, uses multivariate and multi-objective optimization to identify the Pareto front related to total cost and energy savings (objective functions) using EnergyPlus [Long et al., 2010].

The main limitations of such optimization tools are their computational cost and detailed information required, as a large amount of design configurations must be fully simulated in often many runs to achieve convergence. However, the multi-objective approach is promising due to the possibility of generating a Pareto front from which multiple design options can be presented to the user, making it better suited and thus more seamlessly integrated into the design process.

Most optimization-based methods are somewhat disconnected from the field in which they

are applied and can sometimes act as a black-box with limited explanation brought to - and involvement of - the user [Gagne, 2011]. A more transparent approach for supporting the decision-making process consists in embedding expert knowledge into the performance assessment framework.

### 2.3.4 Guidance through expert systems

A typical expert system is structured as illustrated in Fig. 2.16. At its core is a knowledge-based problem solver containing general and case-specific knowledge about the domain of interest [Luger, 2005]. It can for instance be rule-based in the form of if...then... rules. This knowledge is applied to solve problems through the inference engine and information about the reasoning of the system is provided to the user by the explanation subsystem.

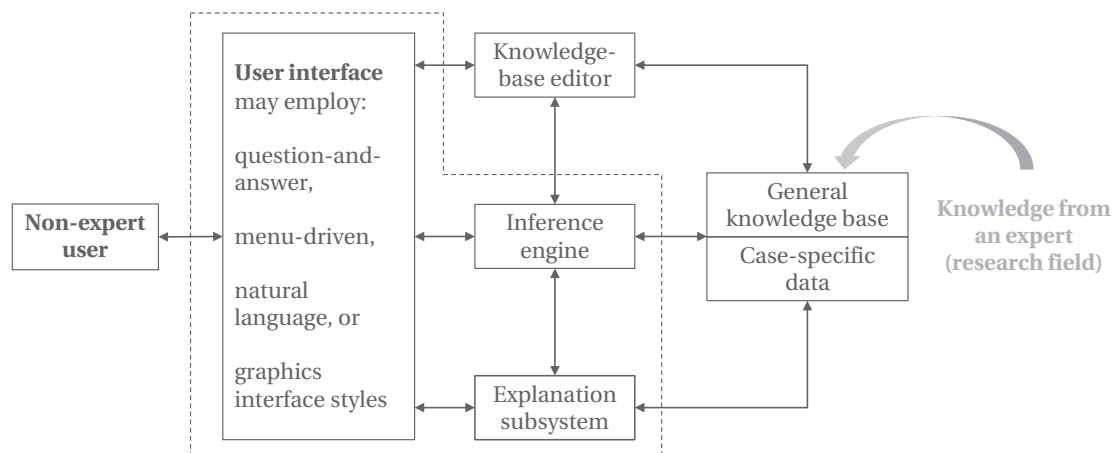


Figure 2.16 – Typical expert system structure. The shell of the system (within the dashed border) represents the generic, non-domain specific components. Image adapted from Luger [2005] with modifications.

A distinction must be made between databases of system-related data and the knowledge base containing the problem solving information. Knowledge is defined as “facts, information, and skills acquired by a person through experience or education; the theoretical or practical understanding of a subject” while data are “facts and statistics collected together for reference or analysis”<sup>20</sup>. For instance, material properties found in a software database does not represent a knowledge base in the sense of an expert system, which could contain rules such as *if* room overheating *and* material thickness is over code-compliance *then* decrease material thickness still respecting code-compliance.

Integrating an expert system allows generating and proposing advices to the user for improving their design, as done for instance in DIAL+ (based on a fuzzy-logic rule-based inference engine) [De Groot et al., 2003] and Lightsolve [Gagne, 2011]. More examples can be found in research, many of which were developed for Israel.

<sup>20</sup>Definitions taken from the Apple Mac OS New Oxford American Dictionary.

Shaviv et al. [1996] proposed combining a knowledge base and procedural simulation to be used with any CA(A)D tool and containing an energy (thermal performance) and a shading module. The knowledge base contains heuristic rules that were defined through case studies in Israel related to the design of passive solar buildings. An early example of a building design knowledge-based system, BEADS, was proposed by Fazio et al. [1989]. From the user inputs (location, building/wall/roof types, fenestration area and wall/roof thicknesses), feasible alternatives are proposed, respecting the performance requirements contained in a knowledge base, related to thickness, R-value, condensation and energy consumption, which also contains building code constraints. An additional database of material properties is implemented and design alternatives are produced and checked against the constraints. In this program, the knowledge is implemented in the form of schema rather than rules, containing attributes and values for the specification of performance characteristics.

Kalay also contributed to the development of rule-based expert systems early on for application to performance-based building-scale design [Kalay, 1985, 1998, 1999, 2001]. Yezioro [2009] developed a two-fold approach for passive solar architecture called PASYS. The first part addresses the pre-conceptual stage to help users determine the best combination of climatic design strategies. The resulting scenario is used as an input to the second (conceptual) stage during which the passive systems are selected and sized using a knowledge base.

NewFacades offers alternative design parameters (e.g. U-value, shading controls) following the input of a simple building description in the form of design intentions rather than a 3D model [Ochoa and Capeluto, 2009]. Explanations regarding the selection of the alternatives can be viewed. The program integrates the EnergyPlus engine for which a library of default values for component characteristics is used. The user is gradually exposed to details of the design and can eventually edit those values. The expert rule-based system is built from Israel's prescriptive directive, therefore ensuring the code-compliance of the designs.

The use of expert systems at the building, room or facade level appears promising, as proven by the above examples. However, envisioning their application at larger scales is not straightforward. Indeed, expert systems are for a reason typically used in specialized domains with clear solutions [Luger, 2005]. The fact that they are manually encoded requires an extensive amount of work and knowledge, in turn linked to a large quantity of data. For instance, coming back to our room optimization example (section 2.3.3), it is conceivable that a rule-based expert system be developed to guide the search for the optimal design with rules such as *if* daylit area is below target *and* window area is below max allowed *then* increase window area by x%. Acquiring the data to code such a knowledge base seems feasible. However, if we extend the room to a neighborhood, the jump in scale is matched with a surge in complexity.

## 2.4 Synthesis - The need for a new approach

In this chapter we have reviewed how the performance of a design is defined and evaluated, and how this information can be conveyed to and used by decision-makers. We have looked at the research and development side as well as the practitioners' perspective.

In Fig. 2.17, we have attempted to summarize how building performance is typically measured along the design process, according to our review. We here define **performance metrics** as quantitative measures of one or more **performance criteria** that are obtained using specific **evaluation methods**. For instance, wind flow is a quantity computed through CFD simulation and typically used to measure outdoor and internal thermal comfort and air quality.

This synthetic view allows us to better see which metric is mostly used at the early urban design phase: geometrical parameters and rules-of-thumb, Solar Envelopes (SEs) and similar concepts based on angles and volumes, and to a certain extent (but mostly in research) wind analysis, irradiation levels and derived metrics. There does not appear to be any established metric or set of metrics used to assess a specific performance criterion. At the detailed building

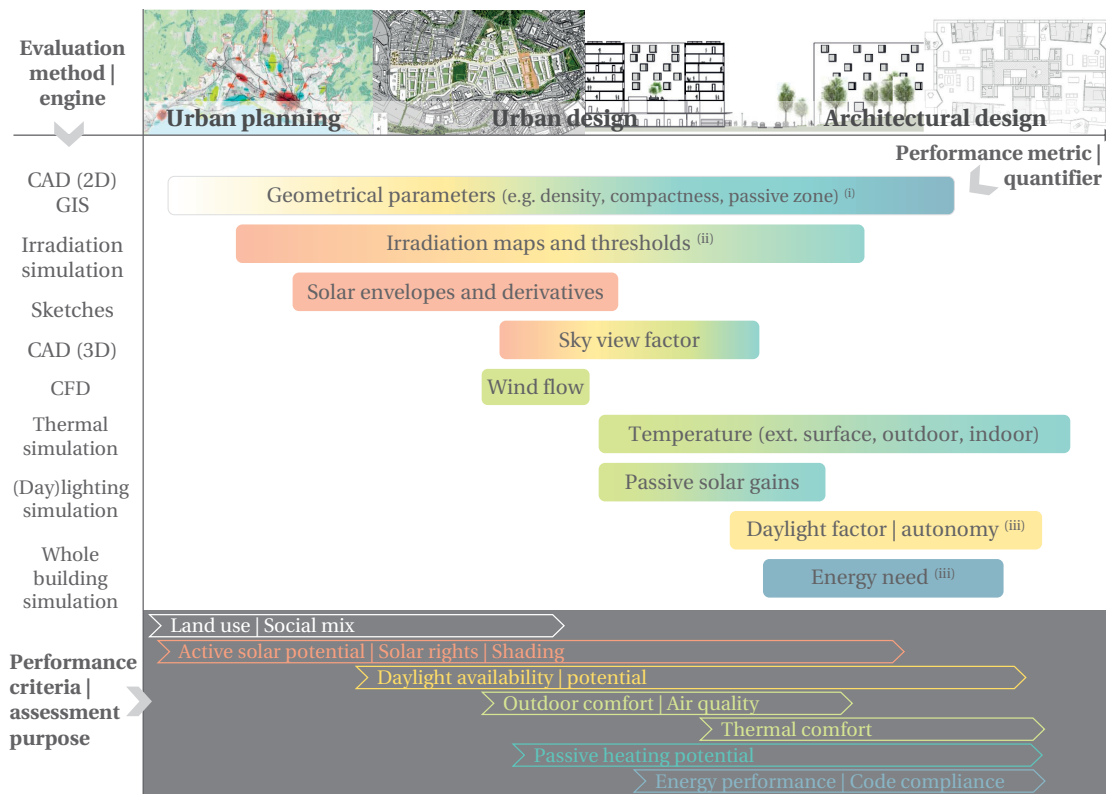


Figure 2.17 – Commonly used metrics (center) typically used as quantifiers for various performance criteria (bottom) along the design process (top), and evaluated through different methods and tools (left). The schema loosely summarizes the detailed review of section 2.2. The numbered metrics are further investigated in chapter 3.

scale, more complex methods associated to more accurate quantities are employed. However, their application in early urban design is not straightforward: the information required and computational complexity engendered make them inadequate, leading to the shortcomings highlighted in section 2.1.

What is not apparent in the schema of Fig. 2.17, although highlighted previously, is the often partial view of building performance. That is, multiple studies as well as developed methods and tools focus or allow evaluating only one criterion at a time, preventing a holistic view of the performance. This is however important, especially since optimizing for one criterion - e.g. heating need - may be detrimental to another valuable aspect - e.g. daylight.

*“[...] two conflicting exigencies for energy conservation appear: reducing the building envelope, which is beneficial to heat losses, and increasing it, which is favorable to the availability of daylight and natural ventilation. Which of the two phenomena prevails in the global budget of buildings? The above question is not likely to have an absolute answer.” [Ratti et al., 2005, p.768]*

This issue naturally leads to adopting a multi-objective, climate-based approach. Looking at only one performance criterion may be valid when assessing an existing environment, e.g. when a city wants to identify surfaces appropriate for installing solar systems. However, when dealing with the design of new buildings, which is the focus of this thesis, we argue that a more comprehensive view is of order, since passive measures are exploitable; the morphology and layout of buildings are yet to be defined and can lead to significant differences in terms of energy and daylight performance, as previously highlighted in studies such as the one presented in Fig. 2.7. This comprehensive view also means considering the interdependencies between buildings, a need also highlighted by Ratti et al. [2005]:

*“[...] they [current energy models and techniques] tend to consider buildings as self-defined entities, neglecting the importance of phenomena that occur at the urban scale. In particular, the effect of urban geometry on energy consumption still remains understudied and controversial. [...] Even software developed to simulate energy consumption at the city scale tend to neglect the effects of urban geometry.” [p.762]*

This situation is likely caused in part by the complexity induced by incorporating considerations extending beyond a building. Yet, the effect of urban morphology, and its consequences on solar exposure levels, on various performance criteria has been acknowledged, as brought out in section 2.2.

The question now is: can we address this issue by coming up with a performance assessment method satisfying the needs for its integration into a DDS workflow, addressing the challenges exposed in section 2.1? To answer this question, we begin in the next chapter with a test on a selected set of methods, by applying them on neighborhood case studies. The idea behind this first step is to deepen our understanding of the implications associated with evaluating a neighborhood design, while simultaneously probing the validity of existing performance

## Chapter 2. State-of-the-art in decision-support methods applied to design

---

metrics chosen from the literature. These fall into the categories that have been numbered in Fig. 2.17 and range from parameters computed on a simple geometrical model, often used as rules-of-thumb (e.g. compactness), to values obtained by simulating a more detailed building geometry (e.g. energy need). In line with the goal of having a more comprehensive solar/energy-performance assessment, we will focus on criteria related to both the passive and active solar potential of a neighborhood design.

This preliminary study, described in chapter 3, will guide us toward developing our performance assessment method, a process which is described in chapter 4. As foresight, our proposed workflow employs a technique at which we have glimpsed in this chapter: mathematical modeling, which allows predicting the performance without the need for a full thermal or daylight simulation.

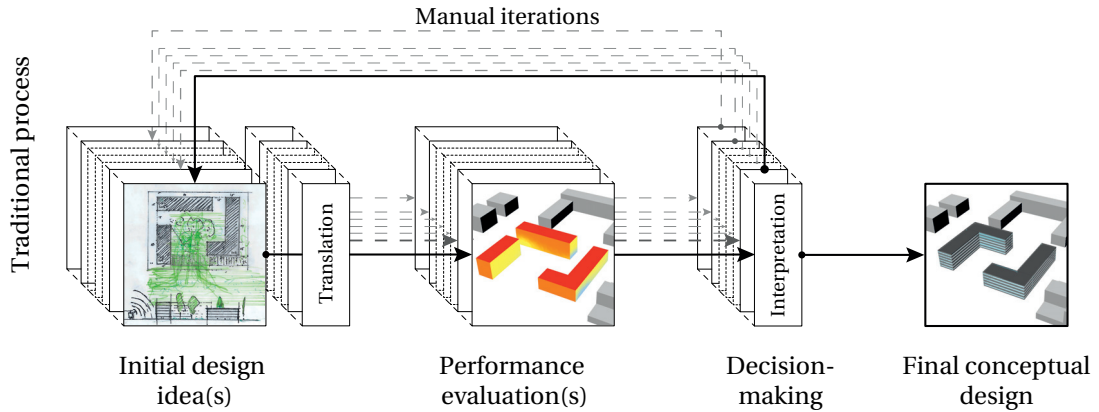
Forming the core contribution of this research, this method will then have to be integrated into a framework allowing it to be tested by practitioners. This transformation into a DDS prototype occurs in chapter 5, where we continue to build upon findings from this review.

As previously emphasized, we observe that a large majority of the tools publicly available induce a generate-and-test process, leaving the interpretation of results to the user. This linear process, depicted in Fig. 2.18a, also involves the translation of the initial design idea into a format that can be evaluated, e.g. by one or more specific performance assessment tools. This task can represent an important barrier from the practitioner's side. So does the need for manual repetitions when a comparative exploration of design alternatives is sought.

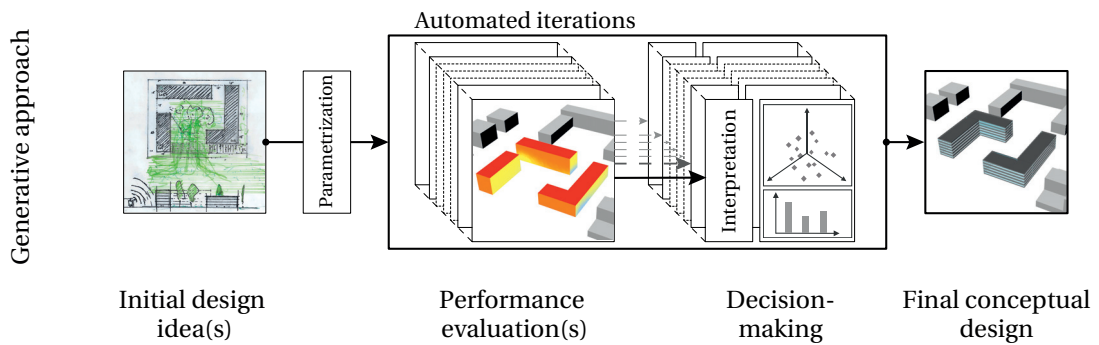
Addressing some of these issues are features offering more guidance to users as exposed in section 2.3, for instance by providing means to compare alternative designs or optimize specific parameters. The alternative assessment process induced by such features is illustrated in Fig. 2.18b. In this workflow, the initial design idea is expanded to a realm of possible solutions, by parameterizing design variables that practitioners typically wish to explore at a given moment in the design process, and that are likely to influence performance. User-defined ranges and objectives can then be used by an automated system to sample the solution space, generating and evaluating design variants in a way that supports decision-making.

In this research, we adopt this generative performance-driven approach when developing our DDS workflow, supported by existing tools, with the aim of fulfilling the requirements for a seamless integration into the early-design of neighborhood projects. Further motivated and detailed in chapter 5, the application potential of our approach is explored in chapter 6.





(a) Linear ‘generate-and-test’ workflow induced by many of the existing performance assessment methods and tools. The initial design idea must be translated into a model understood by the evaluation engine, after which an interpretation of the result must be made by the practitioner. This process is often manually repeated for evaluating different performance aspects (possibly using different tools), to enable comparing design variations, and until a satisfying solution is found.



(b) Non-linear ‘generative’ workflow. The translation of the initial design is replaced by a parametrization, where design variables and their corresponding range are defined by the user to depict a solution space from which an automated procedure samples to generate design variants. Once evaluated, interpretation of the results is supported by a (multi-criteria) performance-based representation of the solution space and/or suggestions on modifications with information on the effect of specific changes.

Figure 2.18 – Main steps and tasks (a) in a traditional, linear design assessment process versus (b) an alternative, generation-based approach.



# 3 Validity assessment of existing metrics through neighborhood case studies

Following the review of chapter 2, we here investigate if we can build on existing approaches to develop a performance assessment method addressing the challenges unveiled in section 2.1. Through case studies, a test is conducted on a selected set of existing methods. This preliminary investigation serves to define the performance criteria and associated metrics of interest in this thesis<sup>1</sup>. The outcomes lead us toward our proposed performance assessment method, based on predictive models.

## 3.1 Experimental method

### 3.1.1 Selected metrics

The selected metrics, abstractly introduced in section 2.4, are explicitly listed in Table 3.1 and further detailed in the following sections. They fall into the following categories:

- (i) **Geometry-based:** metrics computed from the morphology of the buildings, based uniquely on the 3D model. These are simple and early-design phase friendly, requiring a low level of modeling detail. They include the glazing ratio [Danielski, 2011; Pessenlehner and Mahdavi, 2003], the passive zone [Ratti et al., 2005], the plot ratio (a measure of density also known as Floor Area Ratio (FAR)) [Martins et al., 2014] and the compactness measure [Martins et al., 2014; Miguët and Groleau, 2007; Pessenlehner and Mahdavi, 2003; Ratti et al., 2003].
- (ii) **External solar- and geometry-based:** metrics computed from the level of solar exposure of external surfaces expressed in terms of irradiation (kWh/m<sup>2</sup>) or illuminance (lux), thus taking into account the interaction of buildings and their geometry. These require an irradiation simulation on a simple model and are commonly used [Otis, 2012; van Esch et al., 2012], sometimes including threshold values, identified by an ‘I’ in Table 3.1 [Cheng et al., 2006; Compagnon, 2000, 2004; Kanters et al., 2014b; Martins et al., 2014]. From now on, we adopt the abridged name of **irradiation-based metrics** to refer to this category.

---

<sup>1</sup>A large portion of this chapter has been summarized in Nault et al. [2015b, 2013].

### **Chapter 3. Validity assessment of existing metrics through neighborhood case studies**

---

**(iii) Full climate- and geometry-based:** metrics which are obtained through a more complex and computationally expensive yet conventional simulation, accounting for the climate and geometry in more detail (e.g. thermal zoning). These are established metrics such as the simulated energy need, and are here taken as the reference (ground truth).

The goal of this preliminary experiment is to investigate the validity of the early-phase-friendly metrics in categories (i) and (ii) as performance indicators of neighborhood designs. To infer their validity as ‘true’ indicators, we make the assumption that the full climate- and geometry-based metrics (category (iii)) are to be considered as the reference values. For conciseness, we refer to this set as the **reference metrics**.

Thus, results obtained by applying metrics from the first two categories should reflect the results obtained for the reference metrics. These were selected so as to cover the following performance criteria:

**Passive solar potential:** related to the passive performance of buildings, i.e. the potential to benefit from passive solar heating and from natural daylight while mitigating the risk of overheating.

**Active solar potential:** expressing the potential energy production by active solar systems (PV and ST).

The chosen reference metrics are, in the case of the passive criteria, more accurate, conventional and well-acknowledged performance indicators obtained through either daylight or thermal simulations. The dynamic climate-based sDA metric is used for quantifying the daylight potential [IESNA, 2012], while the space heating and cooling needs are obtained as a measure of the passive thermal potential. As seen in chapter 1, such metrics are the target of many regulations and labels due to the major share of the need for heating, cooling and artificial lighting in both non-residential (administrative, commercial, etc.) and residential buildings. Although an air conditioning system for cooling is not always present, the then hypothetical need for cooling still reflects the distance to a comfortable temperature range. For the active solar criterion, additional calculations from the irradiation data (cat. (ii)) provide an estimated energy production by active solar systems. All metrics are described in detail in sections 3.1.3 and 3.1.4.

While the sDA and energy need are not adequate metrics for early-design phase assessments due to the factors introduced earlier (e.g. computational cost, required information not yet known), they are valuable for proving or disproving the validity of alternative metrics, which are simpler and easier to calculate. This approach is based on the thinking that if we are to trust any one metric as being a performance indicator, it should effectively ‘indicate’ following the same trend as (i.e. go hand in hand with) the performance itself, which is quantified here by more transparent metrics closely tied to the physical thermal and radiation processes. These metrics are evaluated for a series of neighborhood designs presented in the next section.

Table 3.1 – Selected metrics to be compared for each performance criterion. Sources are listed in the text. PV: photovoltaic; ST: solar thermal; F: facades; R: roofs.

| Performance criteria |                       | (i) Geometry-based metrics | (ii) External solar- and geometry-based metrics          |  | (iii) Full climate- and geometry-based metrics  |
|----------------------|-----------------------|----------------------------|--|--|---|
| Passive solar        | Solar heat gains      | Density                    | Envelope area with irradi. > $I_{\text{heat gains}}$ (%) | Annual irradiation per envelope or floor area ( $\text{kWh/m}^2_{\text{FA}}$ ) | Annual heating need per floor area ( $\text{kWh/m}^2_{\text{FA}}$ )                     |
|                      | Overheating avoidance |                            | Envelope area with irradi. < $I_{\text{heat avoid}}$ (%) |  | Annual cooling need per floor area ( $\text{kWh/m}^2_{\text{FA}}$ )                     |
|                      | Daylight              |                            | Facade area with illumin. > $I_{\text{daylight}}$ (%)    |  | Spatial daylight autonomy (%)   |
| Active solar         | PV-F                  | Compactness                | Facade area with irradi. > $I_{\text{PV-F}}$ (%)         | Annual roof/facade irradiation per floor area ( $\text{kWh/m}^2_{\text{FA}}$ ) | Annual energy production on roof/facade per floor area ( $\text{kWh/m}^2_{\text{FA}}$ ) |
|                      | ST-F                  |                            | Facade area with irradi. > $I_{\text{ST-F}}$ (%)         |  |   |
|                      | PV-R                  | Passive zone               | Roof area with irradi. > $I_{\text{PV-R}}$ (%)           |  |   |
|                      | ST-R                  |                            | Roof area with irradi. > $I_{\text{ST-R}}$ (%)           |  |   |
|                      |                       | Glazing ratio              |  |  |   |

### 3.1.2 Case studies

The research presented in this chapter originated from different analyzes conducted in the context of four projects. The work done for these projects provided us with an opportunity to further exploit the data, by looking at it from another angle for the purpose of the current study. A series of 3D models used as case studies were the outcomes of each project:

- EPFL studios<sup>2</sup>, 2010-2012: bachelor-level architecture studios and summer workshops that resulted in six student visions that were analyzed and presented in the Green Density album [Andersen and Nault, 2013; Rey, 2013]. The schematic master plans of the projects, elaborated for the Waldstadt district in the city of Bern, Switzerland, are shown in Fig. 3.1. We will refer to this study by the acronym **BE** which stands for its location.
- EPFL studios<sup>3</sup>, 2012-2014: similarly, eight student designs developed in the same studio, but for the Gare-Lac area of Yverdon-les-Bains (Switzerland), were analyzed in the context of the Urban Recovery album [Nault et al., 2015a; Rey, 2015]. Their master plan is illustrated in Fig. 3.2. This study will be referred to by the acronym **YLB**.
- Master thesis [Peronato, 2014], 2013-2014: during a joint master's thesis between EPFL and IUAV conducted by Giuseppe Peronato whom we co-supervised in our laboratory (LIPID), multiple design variants were generated based on the master plan of the Gare-Lac sector in Yverdon-les-Bains [Bauart Architectes et Urbanistes SA et al., 2010]. Figure

<sup>2</sup>DENSE AGAIN (Yearbook 2010-2011) and URBAN MIX (Yearbook 2011-2012). Du projet urbain au détail constructif. Studio of Prof. Emmanuel Rey (EPFL, LAST).

<sup>3</sup>URBAN LAKESIDE (Yearbook 2012-2013) and URBAN REGENERATION (Yearbook 2013-2014). Du projet urbain au détail constructif. Studio of Prof. Emmanuel Rey (EPFL, LAST).

### Chapter 3. Validity assessment of existing metrics through neighborhood case studies

---

3.3 shows a schematic shadow plan of the master plan (base case design) along with two example variants (irradiation maps) [Peronato, 2014]. The acronym **YLB-PDL**<sup>4</sup>, standing for the location and master plan type (*Plan Directeur Localisé (PDL)*) will serve to distinguish this study from the previous one conducted on the same area.

- Comparative study, 2014: through collaboration with a Swiss urban design firm<sup>5</sup>, a study was conducted to compare design variants during the elaboration of a master plan document (*Plan Directeur Localisé Intercommunal* [Urbaplan, 2015]) for an area in the north of Lausanne (Switzerland), illustrated in Fig. 3.4 along with the base case designs (M1, M2) from which the variants were generated. Six specific designs (M3 A-F) provided by the firm were also analyzed. We assign to this project the acronym **LN-PDL** standing for its general location (Lausanne-Nord) and master plan context.

For all cases, the experimental approach for obtaining the data that allow us to compare the selected metrics is illustrated in Fig. 3.5 and further detailed in the following sections. The first step is to model the geometry at a Level of Detail (LoD)<sup>6</sup> 1 to extract the geometry-based metrics. The Level of Detail (LoD) 1 model corresponds to buildings modeled as blocks with a flat roof. An irradiation simulation, executed on the same model, allows us to compute the second category of metrics. The reference metrics are obtained either through further processing of results from the second phase (active solar) or full simulations on slightly more detailed models that include thermal zones and windows.

Most of the outputs associated with each phase of this workflow were obtained in the course of the four individual projects. In some cases, further work was done to complete the data for the purposes of the current analysis. We here make use of this data by looking at the correlation degree between specific pairs of metrics. Different tools (or versions of) were used between studies, as well as distinct modeling and simulation assumptions or settings. This is due to the fact that the four projects occurred consecutively and in distinct contexts. These discrepancies are not considered an issue here, as the intention of this chapter is not to compare absolute results between the studies, but rather investigate the outcome of applying the selected set of metrics to different neighborhood designs. The diversity of cases and simulation assumptions can rather be seen as an advantage. In the first two studies, BE and YLB, we have a small number of designs, quite different in terms of building typology and layout. The third study, YLB-PDL, includes a much larger number of designs created from small variations applied to a base case. LN-PDL is an in-between case, containing both multiple variants generated by applying moderate variations to two base case designs (M1 and M2), as well as six specific and distinct designs (M3 A-F).

---

<sup>4</sup>To avoid any confusion, it should be noted that this study has been presented in a previous publication using the acronym YLB [Nault et al., 2015b], here assigned instead to the Urban Recovery project.

<sup>5</sup>Urbaplan: <http://www.urbaplan.ch/> (last accessed on March 20, 2016)

<sup>6</sup>The Level of Detail (LoD) is a concept defined by the City Geography Markup Language (CityGML) to classify building models on a scale from 0 to 4 [Kolbe et al., 2005].

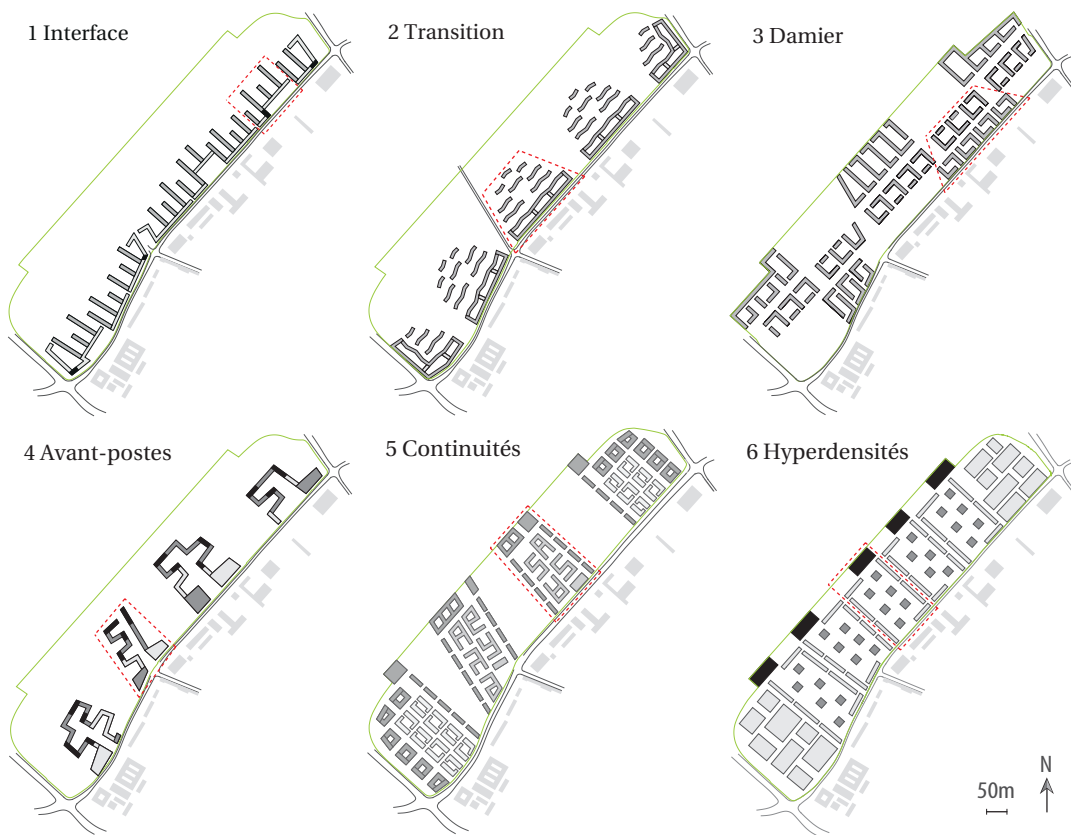


Figure 3.1 – Schematic master plan of the six urban visions (delimited by a green border), and the existing built context (outside of the delimitation) in the **BE** case study. The sample surrounded by a dashed red line represents the simulated portion of each design. The shade of gray of the unbuilt buildings gives an indication of their height: darker = higher. Location: Waldstadt district, Bern, Switzerland. Images adapted from Rey [2013], in which the designs are referred to by their name here displayed.

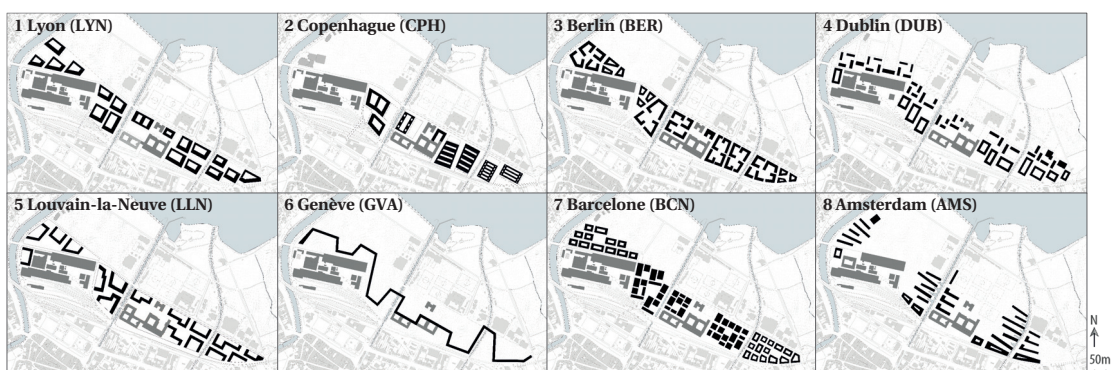


Figure 3.2 – Schematic master plan of the eight urban visions (black) and the existing immediate (gray) and surrounding (light gray) built context in the **YLB** study. Location: Gare-Lac sector, Yverdon-les-Bains, Switzerland. Images adapted from Rey [2015], in which the designs are referred to by their name here displayed.

Chapter 3. Validity assessment of existing metrics through neighborhood case studies

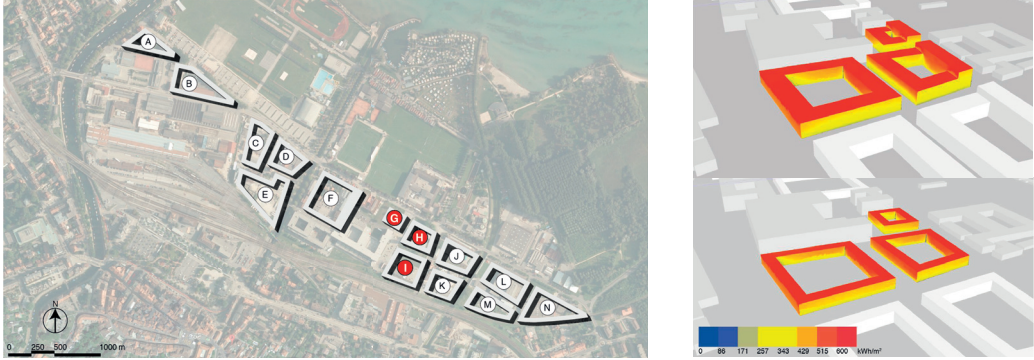


Figure 3.3 – Left: Schematic shadow plan of the YLB-PDL base case. Due to practical considerations, only buildings G, H and I were simulated (red), taking into account their surroundings. Right: Annual irradiation map of two example variants. Source of images: Peronato [2014].



Figure 3.4 – Illustrative master plan of the LN-PDL study, with example plots (framed in red) on which the design variants created from M1 and M2 or the specific designs of M3 (top) could be located. Plan adapted from Urbaplan [2015].



### 3.1. Experimental method

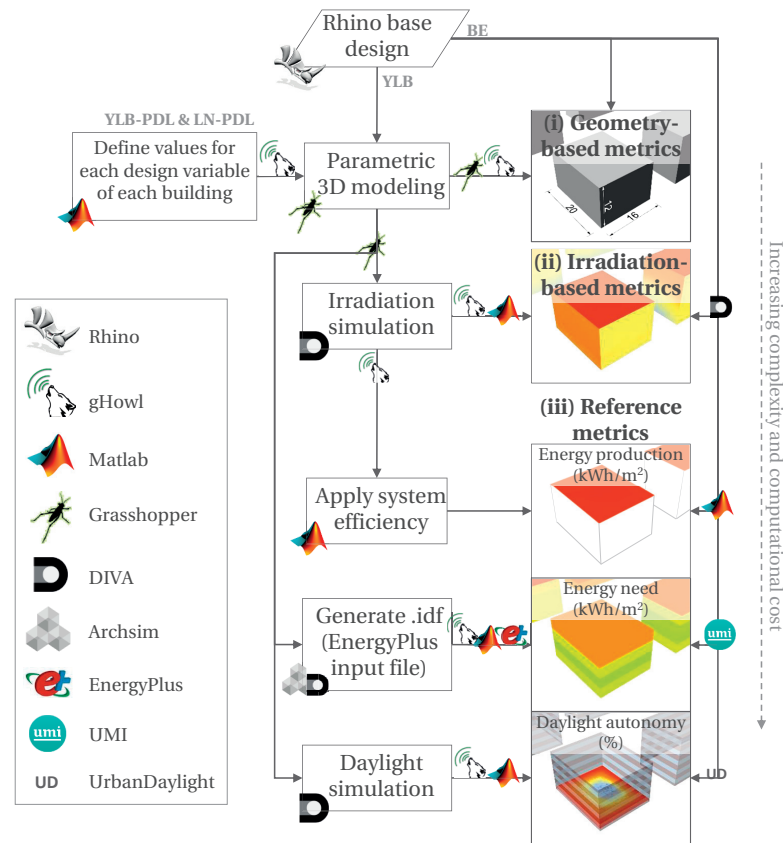


Figure 3.5 – Experimental approach and tools used for acquiring the data necessary to compare the selected metrics. Results obtained for the simpler metrics of categories (i) and (ii) are compared with the full climate- and geometry-based metrics (iii) taken as reference values. The level of complexity and of detail of the obtained output increases along with the computational cost from top to bottom.

The interest of having this diversity of cases lies in the fact that these represent various situations that could be found in practice. For instance, the student visions of BE and YLB could emanate from a design exploration phase or from an urban design competition, while the extensive series of variants in the YLB-PDL study would come up at a subsequent phase, after fixing the building typology. The fourth project occurred (in reality) in the context of a master plan elaboration. All of these situations moreover correspond to the applications and audience at which our proposed DDS workflow, developed in the next chapters, is addressed.

**3.1.3 Modeling**

**Tools and LoDs**

Table 3.2 summarizes the tools used in the 3D modeling of the designs for each study. Rhino<sup>7</sup> was used as the base 3D modeler and for visualization. The first version of UMI [Reinhart et al., 2013], a plug-in for Rhino, was used to facilitate the translation of the BE designs into thermal models. The window-to-wall ratio was fixed to 0.5 and 0.45 for BE and YLB respectively, with values falling within that range for the other two studies. Each story was defined as a thermal zone, except for YLB-PDL, where each bar (or block) composing the courtyards was modeled as a thermal zone without internal floors, due to limitations of Viper, the DIVA-for-Grasshopper component allowing an EnergyPlus simulation (described later).

As mentioned earlier, the modeling was done at different Level of Details (LoDs); buildings were first modeled as simple boxes for extracting all geometry-based metrics (except the window-to-floor ratio) and running the irradiation simulation. An example can be seen in Fig. 3.7. For computing the window-to-floor ratio and executing the thermal and daylight simulations, thermal zones were defined and windows were added, in a different layout according to the tool used, as illustrated in Fig. 3.6 and detailed further on.

Table 3.2 – Tools used in the modeling process in each project. Sources are mentioned in the text.

| <b>Tool</b>                     | <b>Role</b>   | <b>BE</b> | <b>YLB</b> | <b>YLB-PDL</b> | <b>LN-PDL</b> |
|---------------------------------|---|-----------|------------|----------------|---------------|
| Rhino                           | 3D modeler  | x         | x          | x              | x             |
| UMI                             | Thermal modeling support                                    | x         |            |                |               |
| Grasshopper                     | Parametric modeling   |           | x          | x              | x             |
| Matlab                          | Script for defining design variable values                  |           |            |                | x             |
| gHowl                           | Import/export of data between Excel, Grasshopper and Matlab |           |            | x              | x             |
| <b>Total number of variants</b> |   | <b>6</b>  | <b>8</b>   | <b>768</b>     | <b>1008</b>   |

**Parametric modeling**

For YLB-PDL and LN-PDL, a parametric modeling approach was adopted. Parametric modeling means generating a series of design variants that are linked through one or more mathematical relationship(s), forming a space that contains multiple related yet distinct shapes [Lagios et al., 2010]. The parametric modeling was done using Grasshopper<sup>8</sup>, a graphical scripting program for Rhino that allows automating, in an iterative sequence, the application of changes to a design. A screenshot is shown in Fig. 3.7. The added-value of this program also lies in the multitude of plug-ins continuously developed for it. One of them is gHowl<sup>9</sup>, used

<sup>7</sup><https://www.rhino3d.com/> (last accessed on March 20, 2016)

<sup>8</sup><http://www.grasshopper3d.com/> (last accessed on March 20, 2016)

<sup>9</sup><http://www.grasshopper3d.com/group/gHowl> (last accessed on March 20, 2016)

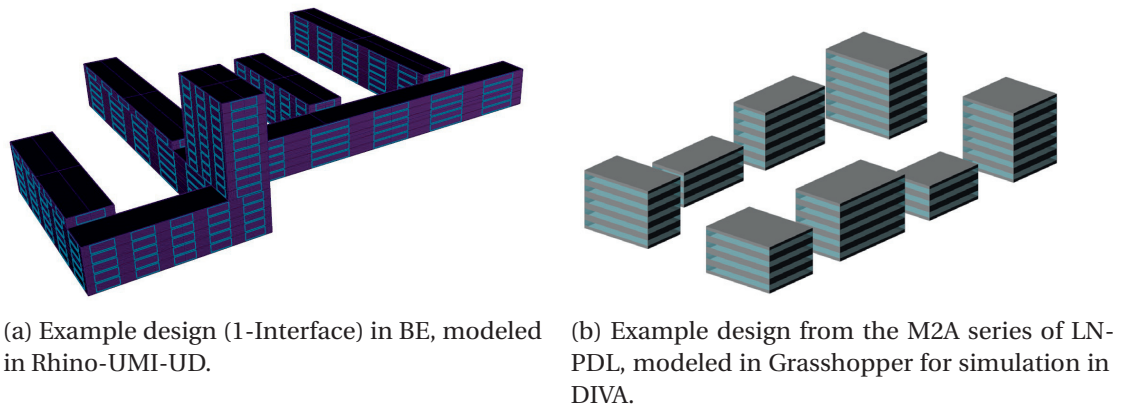


Figure 3.6 – Example models used for the thermal and daylight simulation using different tools.

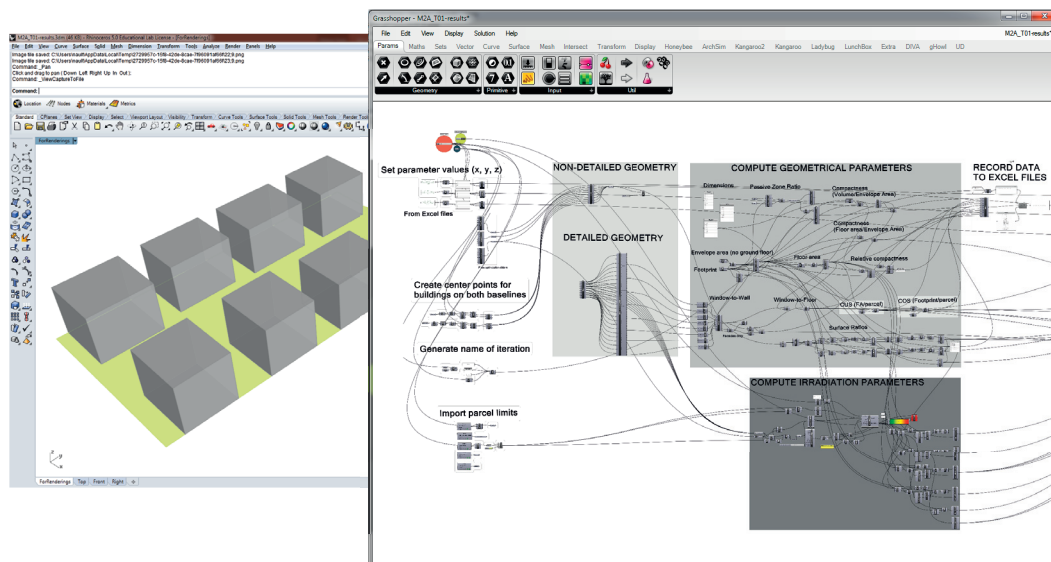


Figure 3.7 – Rhino and Grasshopper (partial) set-up for the parametric modeling of variants and computation and simulation of metrics. Example for the M2A case in the LN-PDL study.

here to exchange data between the software in the form of Excel files. Finally, Matlab<sup>10</sup> was used in the LN-PDL study, for which a script was developed to randomly assign values to each design variable and building for the series of M1 and M2 variants. Validity checks were also performed to ensure that models were realistic (e.g. no overlapping buildings) and respected the constraints (e.g. minimum density).

Parameters that were varied, kept constant or taken as constraints for YLB-PDL and LN-PDL are listed in Tables 3.3 and 3.4 respectively. In the former, geometrical modifications were done by varying the height of buildings within the range of values prescribed by the master plan [Bauart Architectes et Urbanistes SA et al., 2010], and by setting their depth and setback

<sup>10</sup><http://www.mathworks.com/products/matlab/> (last accessed on March 20, 2016)

### Chapter 3. Validity assessment of existing metrics through neighborhood case studies

to values expected to be representative of possible design choices. These variations, illustrated in Fig. 3.8 were simultaneously and iteratively applied on each courtyard block, leading to 768 design variants covering all possible combinations of parameter settings. To reduce simulation time, only buildings G, H and I in Fig. 3.3 were simulated, taking into account their surrounding context (terrain and buildings' reflectance/shading effect). The variations were applied equally on all three buildings, i.e. within each variant all buildings have the same depth, setback, and height value, with the exception of additional stories located on the northern facade of buildings G and H. Despite these uniform parameter values, we obtain three distinct building sizes due to the initial outer perimeter being different for each block. This can be better understood by looking at the annual irradiation map of the two example variants in Fig. 3.3.

In LN-PDL, the design variables and their range were specified by the urban design firm who provided the base case models. As mentioned, a random sampling algorithm was used to select building dimensions from the ranges. M2 was eventually split into M2A and M2B, to explore two different spans of (partially overlapping) building heights, the other settings being equal. A total of 144 (M1), 190 (M2A) and 164 (M2B) variants were generated and simulated for two orientations (N-S and E-W alignments), resulting in 1008 variants altogether, including M3.

In both projects, the window modeling was based on fixed values, e.g. the distance between the window base and the floor and the window height. This generated similar window-to-wall ratios among design variants, specified in Tables 3.3 and 3.4 in the constants' section.

Table 3.3 – Design variables and constants for generating variants in the YLB-PDL study, based on the PDL [Bauart Architectes et Urbanistes SA et al., 2010]. \*Window-to-wall ratio was dictated by the window modeling done using constant intervals (e.g. between window bottom and floor).

| Variable                     | Min:Step:Max |
|------------------------------|--------------|
| Setbacks (N-S/E-W)           | 0:1:3 m      |
| Block width                  | 10:1:17 m    |
| Number of stories            | 2:1:3        |
| Additional stories on N side | 0:1:2        |
| Constant                     | Value        |
| Window-to-wall ratio*        | ~0.48        |
| Story height ground floor    | 3.95 m       |
| Story height other floors    | 2.95 m       |

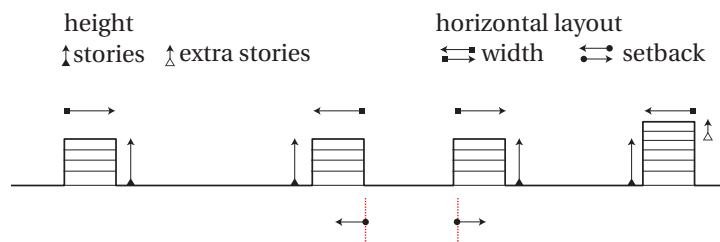


Figure 3.8 – Illustration of design variations in the YLB-PDL study. Source of image: Peronato [2014].

### 3.1. Experimental method

Table 3.4 – Design variables and constraints for generating variants in the LN-PDL study. \*Window-to-wall ratio was dictated by the window modeling done using constant intervals (e.g. between window bottom and floor). bldg(s): building(s); cst: constant; var: variable. See Fig. 3.4 for a visual description of x, y, z and d.

|                                 | <b>M1</b>                                  | <b>M2A</b>           | <b>M2B</b>           |
|---------------------------------|--|----------------------|----------------------|
| Variable                        | Min:Step:Max                               | Min:Step:Max         | Min:Step:Max         |
| x                               | 8:1:15 m                                   | 10:2:20 m            | 10:2:20 m            |
| y                               | 6:1:24 m                                   | 12:2:24 m            | 12:2:24 m            |
| z                               | 6:3:12 m                                   | 9:3:18 m             | 12:3:24 m            |
| d                               | (cst)                                      | 6:1:20 m             | 6:1:20 m             |
| Number of bldgs per side        | 8:1:14                                     | (cst)                | (cst)                |
| Orientation                     | 0° (N-S alignment) and 90° (E-W alignment) |                      |                      |
| Constant/Constraint             | Condition/Value                            | Condition/Value      | Condition/Value      |
| d                               | 0 m  | (var)                | (var)                |
| Number of bldgs per side        | (var)                                      | 4                    | 4                    |
| Window-to-wall ratio*           | 0.44-0.46                                  | ~0.46                | ~0.46                |
| Plot ratio                      | > 0.9                                      | > 0.9                | > 0.9                |
| Total floor area per bldg       | > 50 m <sup>2</sup>                        | > 200 m <sup>2</sup> | > 200 m <sup>2</sup> |
| Distance between neighbor bldgs | (0 m by default)                           | 6 m < dist < 20 m    | 6 m < dist < 20 m    |

#### Computation of (i) geometry-based metrics

Once we have achieved a simple LoD 1 modeling of the designs, the geometry-based metrics are computed, either manually via Rhino and Excel (for BE) or via automated operations directly scripted in Grasshopper (all other studies), as noticeable in Fig. 3.7. The exact definition of each metric is as follows:

**Plot ratio:** Density measure also known as the FAR and computed as the ratio between the total floor area and the plot area (constructible parcel of land). Common urban morphological parameter [Martins et al., 2014], linked to energy consumption and production [Steemers, 2003].

**Surface-to-volume:** Compactness measure computed as the ratio between the total exposed envelope area and the total enclosed volume. Indicative of heat losses; the smaller the surface-to-volume, the more compact the building, and the lower the heat losses due to a smaller exposed surface area [Ratti et al., 2003]. In northern climates, this ratio should generally be minimized to avoid heat losses which dominate over heat gains in winter, and to limit heat gains by having a smaller collecting surface in summer [Miguet and Groleau, 2007].

**Passive zone:** Ratio between the total area of passive zones (within 6 m of an exposed facade) and the total floor area [Steemers, 2003]. Quantifies the potential of a space to use daylight, sunlight and natural ventilation, and was found to be a better indicator than the surface-to-volume ratio for total energy consumption (heating, cooling, ventilation and lighting) [Ratti et al., 2005].

## Chapter 3. Validity assessment of existing metrics through neighborhood case studies

---

**Window-to-floor:** Measure of the glazing ratio, computed as the total window area divided by the total floor area. Used instead of the more common window-to-wall ratio which was kept approximately constant in the case studies. Glazing proportion characterizes heat gains and losses, natural ventilation, daylight, as well as other aspects not treated in this study such as glare [Ochoa et al., 2012].

These values are computed over the whole neighborhood, i.e. for an ensemble of buildings, leading to one value per design variant.

### 3.1.4 Simulation

Due to practical reasons linked to modeling and simulation time and resources, in the BE study only a sample of each design judged representative of the whole was simulated. These samples are highlighted in Fig. 3.1. Similarly for YLB-PDL, where the analysis was limited to the three courtyard buildings identified in Fig. 3.3. In all cases, the surrounding context is taken into account in the simulations, in terms of shading and reflectance of both existing and designed buildings.

All simulations are climate-based, that is, they all make use of the provided weather file from which some data (e.g. dry-bulb temperature) is extracted and used in the simulation. The weather files are the one for Bern for the BE study [Meteotest, 2012], Yverdon-les-Bains for both YLB and YLB-PDL [Meteotest, 2012] and Geneva for the nearby LN-PDL project [EnergyPlus, 2014].

### Computation of (ii) external solar- and geometry-based metrics

Running an irradiation simulation on the same LoD 1 models as in the previous step allows us to compute the second category of metrics (see also Table 3.1):

**Annual average irradiation:** Total annual irradiation received on a certain exposed surfaced divided by the area of that surface. Direct measure of solar availability.

**Floor-area-normalized annual irradiation:** Total annual irradiation received on a certain exposed surface divided by the total floor area. Direct measure of solar availability.

**Threshold-based daylight/passive/active solar potential:** Percentage envelope or facade area receiving an irradiation or illuminance level above (or below for heat avoidance criterion) the corresponding threshold, as listed in Table 3.5. Adapted from a method developed by [Compagnon, 2000].

The tools used, displayed in Fig. 3.5, as well as the settings applied when conducting the irradiation simulation are listed in Table 3.5. The values of the irradiation and illuminance thresholds for the calculation of the threshold-based metrics are also included the table.

In the four studies, the irradiation simulation is done via the DIVA plug-in for both Rhino and Grasshopper [Jakubiec and Reinhart, 2011], which relies on the Radiance [Larson and

Shakespeare, 1998] and Daysim<sup>11</sup> simulation engines. DIVA uses in particular a cumulative sky method based on the GenCumulativeSky Radiance module [Robinson and Stone, 2004] to obtain annual direct and diffuse irradiation levels on a grid of nodes (or sensor points) located on the exposed building envelope areas and oriented outwards with respect to the enclosed volume. An example grid is shown in Fig. 3.9a, for a 1 m resolution (distance between points). Results can be visualized through a false-color irradiation map, as shown in Fig. 3.9b.

The node-specific values are exploited in the calculation of the threshold-based metrics, which come from a method developed by Raphaël Compagnon in the context of a European project called PRECis [Compagnon, 2000] and further applied in subsequent studies [Compagnon, 2004; Montavon et al., 2004a]. Distinct threshold values are defined for assessing the passive heating, daylight and active solar potential. We have added to this list the heat avoidance threshold, for assessing the risk of overheating. These metrics have been computed in the BE and YLB-PDL studies only, the latter not including the added heat avoidance threshold. The origin of the threshold values, listed in Table 3.5, is explained below.

The **passive heating threshold** represents the amount of solar energy (kWh/m<sup>2</sup>) collected over the heating period - defined as September 15 to May 14 for the Swiss climatic context<sup>12</sup> - required to compensate the heat losses through glazing [Compagnon, 2000]:

$$I_{\text{heat gains}} = \frac{24 \cdot DD \cdot U}{1000 \cdot g \cdot \eta} \quad (3.1)$$

where

DD: heating degree days for Bern and Yverdon-les-Bains ( $DD_{BE} = 2906\text{K}\cdot\text{day}$  [Meteotest, 2012],  $DD_{YLB} = 2874\text{K}\cdot\text{day}$  [MétéoSuisse 2000-2013 average])

$U$ : thermal transmission coefficient for a typical double glazing (1.3 W/m<sup>2</sup>K)

$g$ : solar energy transmission coefficient for a typical double glazing (0.75)

$\eta$ : utilization factor taking into account occupants and building's dynamic behavior (0.7)

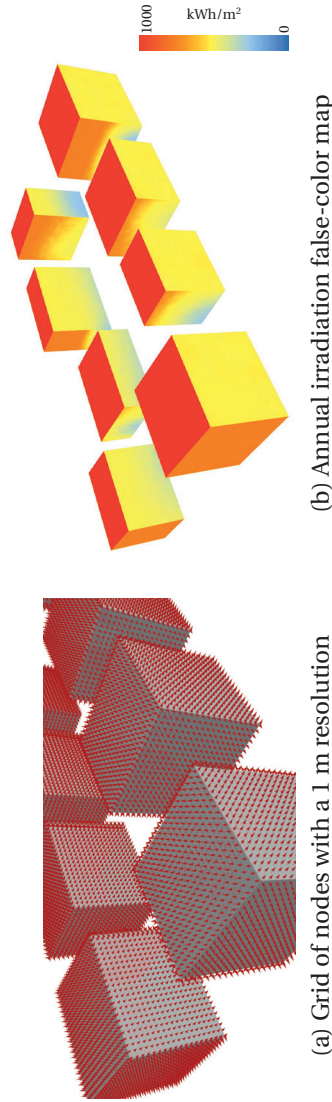
The **heat avoidance threshold** is defined in a simpler manner based on the fact that to mitigate the risk of overheating, the solar exposure in summer should be minimized. To allow a comparison among the BE designs to which this metric is applied, an upper limit has been set based on the energy received on average on all surfaces of all designs over the non-heating period (May 16 to September 14). This value does not represent the amount of energy that will lead to an overheating of the buildings, which would have required many assumptions and full energy analyzes to be determined. However, it still represents a case-specific approach worth investigating.

<sup>11</sup><http://daysim.ning.com/> (last accessed on March 20, 2016)

<sup>12</sup><http://www.hausinfo.ch/home/fr/droit/droit-bail/utilisation/chauffage.html> (last accessed on March 11, 2016)

Table 3.5 – Overview of simulation tools and settings for each study for the **irradiation simulations**. References for tools: DIVA-for-Rhino/Grasshopper [Jakubiec and Reinhart, 2011], plug-in based on the simulation engines Radiance [Larson and Shakespear, 1998] and Daysim <http://daysim.ning.com/>; GenCumulativeSky (algorithm) [Robinson and Stone, 2004].

|   | <b>BE</b>   | <b>YLB</b>           | <b>YLB-PDL</b>  | <b>LN-PDL</b>        |
|---|---|----------------------|---|----------------------|
| Tool  | DIVA-for-Rhino  | DIVA-for-Grasshopper | DIVA-for-Grasshopper  | DIVA-for-Grasshopper |
| Algorithm   | Daysim hourly   | GenCumulativeSky     | GenCumulativeSky  | GenCumulativeSky     |
| Grid resolution   | 3 m   | 2 m                  | 1 m   | 1 m                  |
| $I_{\text{heat gains: passive heating (lower) threshold}}$  | 172.7 kWh/m <sup>2</sup> over heating period                | -                    | 140 kWh/m <sup>2</sup> over heating period                  | -                    |
| $I_{\text{heat avoid: overheating risk (upper) threshold}}$ | 46.8 kWh/m <sup>2</sup> over non-heating period             | -                    | -   | -                    |
| $I_{\text{daylight: daylight (lower) threshold}}$           | 10 klux over yearly occupied hrs                            | -                    | 10 klux over yearly occupied hrs                            | -                    |
| $I_{\text{PV-R/F: PV (lower) thresholds}}$                  | 1000 (R: roof) and 800 (F: facade) kWh/m <sup>2</sup> -year | -                    | 1000 (R: roof) and 800 (F: facade) kWh/m <sup>2</sup> -year | -                    |
| $I_{\text{ST-R/F: ST (lower) thresholds}}$                  | 600 (R: roof) and 400 (F: facade) kWh/m <sup>2</sup> -year  | -                    | 600 (R: roof) and 400 (F: facade) kWh/m <sup>2</sup> -year  | -                    |



(a) Grid of nodes with a 1 m resolution (b) Annual irradiation false-color map

Figure 3.9 – Grid for simulating the irradiation and resulting map using DIVA [Jakubiec and Reinhart, 2011].



The **active solar system thresholds** are split per surface orientation - roofs versus facades - and technology - photovoltaic (PV) panels and solar thermal (ST) collectors. They represent the amount of energy collected throughout the year, considered as 'reasonable' levels, based on economic and technical factors for existing systems and the Swiss climatic context [Compagnon, 2004].

The **daylight threshold** is computed from the following equation [Compagnon, 2000]:

$$I_{\text{daylight}} = \frac{E_i}{\text{CU}} \quad (3.2)$$

where

$E_i$ : mean indoor illuminance on workplace, typically fixed at 500 lux for the working hours (8am-6pm)

CU: coefficient of utilization taking into account construction details (e.g. glazing ratio), typically of about 0.05 for vertical openings

For each threshold, a performance metric is computed, expressed as the percentage of exposed surface respecting the criteria-specific threshold condition:

$$\text{Potential}_{\text{crit}} = 100 \times \left( \frac{\sum_{i=1}^n \alpha_i}{n} \right) [\%] \quad \text{with} \quad \alpha_i = \begin{cases} 1 & \text{if } (I_i - I_{\text{crit}}) > 0 \quad (< 0 \text{ for heat avoidance}) \\ 0 & \text{otherwise} \quad (1 \text{ for heat avoidance}) \end{cases} \quad (3.3)$$

where  $I_i$  is the annual irradiation (or illuminance) value at node  $i \in [1, n]$  and  $I_{\text{crit}}$  is the criterion-specific threshold as defined above.

#### Computation of (iii) full climate- and geometry-based metrics

Through additional mathematical operations and simulations on a more detailed model, the final category of metrics, our reference values, are obtained:

**Energy production:** Estimate of the energy produced by facade- and roof-mounted PV panels and ST collectors, computed by further processing the irradiation data previously acquired.

**Energy need:** Annual heating and cooling need of the entire neighborhood, normalized by its total floor area, representative of the energy required to maintain comfort.

**Spatial daylight autonomy:** Measure of the interior space that receives a specified amount of daylight over a given period of time over the year.

Each metric is further detailed below.

#### Energy production

For BE and YLB-PDL, the energy production is computed by differentiating between each system and surface. A value is obtained for PV and ST on roofs and on facades. This metric builds upon the results from the irradiation-threshold metrics by making use of the surfaces (nodes) identified as adequate for each system, based on the same threshold value given in Table 3.5. As such, this metric does not require any additional simulation. However, we consider that it provides more trustworthy or realistic results, as the efficiency of each system is considered as well as the actual amount of irradiation of each node which exceeds the relevant threshold. It is computed through the following equation:

$$E_{\text{sys}} = \frac{\sum_{i=1}^{m_{\text{sys}}} I_i \times A_n \times \eta_{\text{sys}}}{\text{FA}} \quad [\text{kWh}/\text{m}_{\text{FA}}^2] \quad (3.4)$$

where

sys: combination of active system and installation surface (PV-F, PV-R, ST-F, ST-R)

$m_{\text{sys}}$ : nodes for which the irradiation threshold is achieved for surface and system sys

$I_i$ : annual irradiation of node  $i \in [1, m_{\text{sys}}]$  [kWh]

$A_n$ : average node area [ $\text{m}^2$ ]

$\eta_{\text{sys}}$ : efficiency of system (0.15 for PV-F/R, 0.70 for ST-F/R)<sup>13</sup>

FA: total floor area [ $\text{m}^2$ ]

In the YLB study, a different method is used to compute the energy production, developed by Giuseppe Peronato, PhD student at LIPID. The production metric corresponds to the electricity generated by PV panels installed on available roof surfaces, where areas reserved to ST collectors have been discarded. The algorithm is as follows.

First, the energy required to cover 50% of the annual Domestic Hot Water (DHW) needs, brought back to a period of 8 months corresponding to the heating season (September 15 to May 14), is computed:

$$\text{DHW} = 0.5 \times \text{FA} \times (\text{rres} \times \text{Qhw1} + (1 - \text{rres}) \times \text{Qhw5}) \times \frac{8}{12} \quad (3.5)$$

where

FA: the total floor area [ $\text{m}^2$ ]

Qhw1 and Qhw5: annual energy need per floor area for DHW for multi-family housing (75 MJ/ $\text{m}^2$ ) and commercial buildings (25 MJ/ $\text{m}^2$ ) respectively [SIA, 2009b], converted to kWh/ $\text{m}^2$

rres: ratio of residential surface, ranging between 0.5 and 0.9 among the YLB projects, with the remaining areas assigned to a commercial usage.

<sup>13</sup>These values respectively correspond to standard polycrystalline-based panels and flat-plate collectors (<http://www.swissolar.ch/fr/lenergie-solaire/photovoltaique/technologie/>, [http://www.minergie.ch/tl\\_files/download\\_fr/ad\\_cs.pdf](http://www.minergie.ch/tl_files/download_fr/ad_cs.pdf), last accessed on April 18, 2016).

The energy production from each node is computed for both ST and PV systems:

$$E_{ST,i} = I_{w,i} \times A_n \times \eta_{ST} \quad E_{PV,i} = I_{y,i} \times A_n \times \eta_{PV} \quad (3.6)$$

where

$I_{w,i}$ : total irradiation over winter season for node  $i$

$I_{y,i}$ : total irradiation over year for node  $i$

$A_n$ : average node area [ $\text{m}^2$ ]

$\eta_{\text{sys}}$ : efficiency of system (0.15 for PV, 0.70 for ST)

The production by PV is then sorted from highest to lowest, and the same order is applied to the series of ST production values. The latter are summed until the DHW need is achieved. The nodes thus ‘used’ for covering the DHW are removed from the PV series. Among the remaining nodes, the production is computed as:

$$E = \frac{\sum_{i=1}^m E_{PV,i}}{\text{FA}} \quad [\text{kWh}/\text{m}_{\text{FA}}^2] \quad (3.7)$$

where  $m$  nodes achieve the irradiation threshold for PV systems (set to  $1000 \text{ kWh}/\text{m}^2$  in this thesis as in [Compagnon, 2004]), excluding the ones reserved for covering the estimated DHW demand.

#### Energy need

The tools and settings used in the thermal simulation to obtain the heating and cooling needs are listed in Table 3.6. In all studies, a front-end for the EnergyPlus engine [Crawley et al., 2000] is used, where an ideal loads air system is assumed. This *ZoneHVAC:IdealLoadsAirSystem* object is modeled as an ideal Heating, Ventilation and Air Conditioning (HVAC) system that supplies conditioned air to the defined zone to meet all requirements (e.g. setpoint temperature) while consuming no energy in itself<sup>14</sup>. That is, no additional energy is required to meet the demand, as the ideal HVAC has an efficiency of 100%.

The outputs recorded, the total (sensible and latent) heating and cooling energy added to each zone, are summed over all zones and buildings within a design and divided by the total floor area. Figure 3.10a illustrates, for an example design of the YLB study, the annual heating need per floor area on average in each story, considered a thermal zone. Simulated via Archsim/EnergyPlus, the total needs per zone are summed over the whole design and divided by its total floor area. The same is done for cooling (when recorded). We refer to this metric as the *energy, heating or cooling need*, which is here equivalent to the *consumption* or the *Energy Use Intensity* (EUI), which is the total energy consumed by one (or a group of) building(s) in one year divided by the total gross floor area.

The main differences in the settings between the studies are found in the building function (or

<sup>14</sup><http://nrel.github.io/EnergyPlus/InputOutputReference/02-HVACTemplates/> (last accessed on March 11, 2016)

### Chapter 3. Validity assessment of existing metrics through neighborhood case studies

program), either defined as office or residential, the infiltration rate and loads, as well as the materials heat transfer coefficient. Sources consulted are noted in the table for the relevant studies. In some cases, default values provided by the tool were used, despite their inadequacy for the study's climate and context. For instance, the Archsim plug-in, then still in its early development status, was used for the first time in the LN-PDL study. A residential function was assigned, with a very high occupancy ratio, internal loads and U-values. This combination of parameters, obtained by overlooking default values in the plug-in, does not represent a realistic situation. In that same study, the *Zone Ideal Loads Zone Total Heating Energy* output, extracted from the .csv file generated by EnergyPlus, was the one used to compute the heating need metric. However it was later found that this value does not include the energy required to warm up the outdoor (fresh) air (*Zone Ideal Loads Outdoor Air Total Heating Energy*)<sup>15</sup>.

Learning from this early experiment, more realistic settings were used in the thermal simulation for other studies in which Archsim was employed, by processing the .idf it generated in Matlab to adjust settings before running the simulation in EnergyPlus. The total amount of heating including the proportion required for the outdoor air was used for computing the energy need, by extracting the *District Heating* output provided in EnergyPlus' Table file. As we will see in the next section, the mixed settings in LN-PDL and the exclusion of the outdoor air energy, which is conditioned by the function, occupancy and internal loads, somehow compensate each other to a certain degree, e.g. through the combined and opposite effect of high internal loads and low insulation.

Although some values are outside their typical range or do not represent best practice construction materials, the comparative nature of the study attenuates the importance of the settings accuracy, as we do not aim at obtaining accurate absolute energy need values. As mentioned earlier, it is rather interesting to investigate the effect on the results of these discrepancies in the settings among studies.

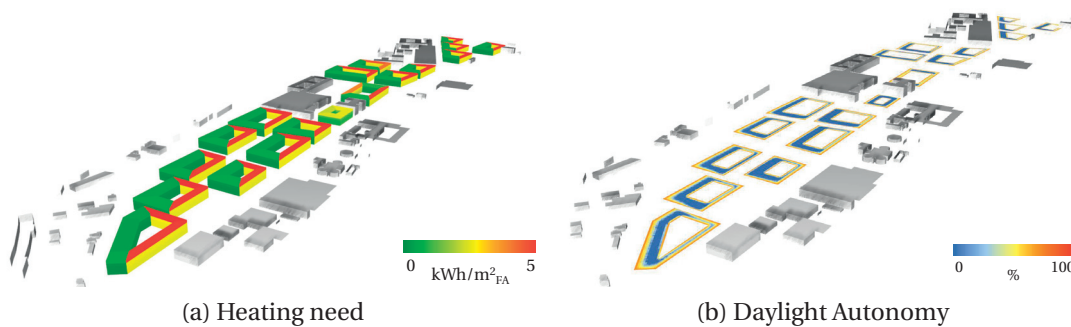


Figure 3.10 – False-color map of the (a) heating need (average per zone) and (b) DA for design 1-LYN in the YLB study.

<sup>15</sup>More information on the definitions of all output values can be found at <http://bigladdersoftware.com/epx/docs/8-0/input-output-reference/page-032.html> (last accessed on March 17, 2016).

Table 3.6 – Overview of simulation tools and settings for each study for the **energy (thermal) simulations**. References for tools: UMI [Reinhart et al., 2013], Archsim <http://archsim.com/>, DIVA-for-Grasshopper [Jakubiec and Reinhart, 2011], plug-ins based on the simulation engine EnergyPlus [Crawley et al., 2000]. \*Sources for settings: SIA [1999, 2009b]

|                          | <b>BE</b>  | <b>YLB</b>  | <b>YLB-PDL*</b>   | <b>LN-PDL</b>                                     |
|--------------------------|--|---|---|---|
| Tool                     | UMI  | Archsim   | Viper component of DIVA   | Archsim   |
| Included                 | Heating and cooling (ideal loads)                | Heating and cooling (ideal loads)                 | Heating and cooling (ideal loads)                               | Heating (ideal loads)                             |
| Occupancy                | Office, 0.045 people/m <sup>2</sup>              | Residential, 0.03 people/m <sup>2</sup>           | Mixed (80% residential, 20% office), 0.03 people/m <sup>2</sup> | Residential, 0.2 people/m <sup>2</sup>            |
| Heating setpoint         | 20°  | 20°   | 20°   | 20°   |
| Cooling setpoint         | 26°  | 26°   | 26°   | -   |
| Ventilation              | 0.0003 m <sup>3</sup> /sm <sup>2</sup>           | 0.00011 m <sup>3</sup> /sm <sup>2</sup>           | 0.0002 m <sup>3</sup> /sm <sup>2</sup>                          | 0.0002 m <sup>3</sup> /sm <sup>2</sup>            |
| Infiltration             | 0.5 ach  | 0.1 ach   | 0.0002 m <sup>3</sup> /s  | 0.1 ach   |
| Blinds                   | Activated when irradiation > 75 W/m <sup>2</sup> | Activated when irradiation > 180 W/m <sup>2</sup> | -   | Activated when irradiation > 180 W/m <sup>2</sup> |
| Equipment loads          | 8 W/m <sup>2</sup>                               | 7 W/m <sup>2</sup>                                | 6.6 W/m <sup>2</sup>  | 12 W/m <sup>2</sup>                               |
| Lighting loads           | 11 W/m <sup>2</sup>                              | 3 W/m <sup>2</sup>                                | 0 W/m <sup>2</sup>  | 12 W/m <sup>2</sup>                               |
| U <sub>ground/roof</sub> | 0.39 W/m <sup>2</sup> K                          | 0.24 W/m <sup>2</sup> K                           | 0.17 W/m <sup>2</sup> K   | 2.9 W/m <sup>2</sup> K                            |
| U <sub>wall</sub>        | 0.39 W/m <sup>2</sup> K                          | 0.19 W/m <sup>2</sup> K                           | 0.17 W/m <sup>2</sup> K   | 3.64 W/m <sup>2</sup> K                           |
| U <sub>window</sub>      | 1 W/m <sup>2</sup> K                             | 1 W/m <sup>2</sup> K                              | 1 W/m <sup>2</sup> K  | 2.7 W/m <sup>2</sup> K                            |

Table 3.7 – Overview of simulation tools and settings for each study for the **daylight simulations**. References for tools: DIVA-for-Grasshopper [Jakubiec and Reinhart, 2011], Urban Daylight [Dogan et al., 2012], plug-ins based on the simulation engines Radiance [Larson and Shakespeare, 1998] and Daysim <http://daysim.ning.com/>.

|                      | <b>BE</b>  | <b>YLB</b>              | <b>YLB-PDL</b>  | <b>LN-PDL</b>           |
|----------------------|--|-------------------------|---|-------------------------|
| Tool                 | Urban Daylight                                   | DIVA-for-Grasshopper    | DIVA-for-Grasshopper                                    | DIVA-for-Grasshopper    |
| Blinds               | Activated when irradiation > 75 W/m <sup>2</sup> | -                       | Activated when direct sunlight on more than 2% of nodes | -                       |
| Window transmittance | 65%  | 65%                     | 78%   | 65%                     |
| Grid resolution      | 2 m  | 2 m                     | 2 m   | 2 m                     |
| Occupancy            | 8am - 10pm                                       | 8am - 10pm              | 8am - 6pm   | 8am - 10pm              |
| Grid plane height    | 0.8 m from each floor                            | 0.8 m from ground floor | 0.8 m from ground floor                                 | 0.8 m from ground floor |
| Illuminance goal     | 300 lx   | 300 lx                  | 300 lx  | 300 lx                  |

### Spatial daylight autonomy

The sDA, detailed in [IESNA, 2012], is a climate-based metric that describes the annual sufficiency of daylight levels inside a building. It is quantified by the percentage of an interior horizontal area that meets a minimum illuminance target  $t$  over a certain fraction  $x$  of the occupied hours of the year. The sDA is thus a spatially ‘condensed’ version of the temporal Daylight Autonomy (DA) metric. The recommended parameter values are  $t = 300$  lux and  $x = 50\%$ , denoted by  $sDA_{300/50\%}$  [IESNA, 2012]. The analysis grid is set at 30” (76.2 cm) above the floor with a resolution of 24” (61 cm between nodes), the period from 8am - 6pm, with blinds operated hourly to block direct sunlight according to a procedure described in the aforementioned reference. While these are the official settings for measuring the sDA, we partly deviate from them in the four studies, in particular regarding the blinds modeling for which we met technical limitations linked to the tools used.

In all studies, the analysis grid is placed at 0.8 m above the floor, with a node resolution of 2 m. This distance, larger than the specified 61 cm, is to reduce computational time, significant at the scale of our studies (~hours for multiple buildings). The occupancy hours are extended to 8am - 10pm in three of the studies, to cover a larger range of possible daylight hours while detaching ourselves from a fixed building function. As mentioned for the energy simulation, these settings do not prevent us from comparing designs within a same study.

The tools and full list of settings for the daylight simulation are given in Table 3.7. The background engines common to all tools are Radiance and Daysim. Results for the BE study were obtained directly from Urban Daylight<sup>16</sup>, which produced the binary DA maps shown in Fig. 3.11 and provided the overall sDA through its interface. The maps display the daylit (white) versus non-daylit (black) areas, where daylit is defined as zones achieving a  $DA_{300/50\%}$ , i.e. with an illuminance level above the 300 lux threshold over 50% of the occupied hours. Only in this study was the sDA computed on all floors. For reasons linked to computational time, in the other three projects only the ground floor was considered, as a worst-case situation (most potentially shaded out of all floors).

The format of the simulation outputs is different for the other studies for which Grasshopper was used as an intermediary, to facilitate the modeling, between Rhino and the simulation plug-ins. Figure 3.10b shows the raw results obtained via DIVA-for-Grasshopper, plotted as a false-color DA map, for an example design of YLB. The sDA is computed by processing this data in Matlab to obtain the percentage space achieving a  $DA_{300/50\%}$ . The same procedure was followed for the parametric studies. In YLB-PDL, only 32 variants out of the 768 were simulated, due to the high computational cost of the daylight simulation.

---

<sup>16</sup>Urban Daylight converts hourly solar radiation levels on all facades simulated via Daysim into interior illuminance distributions through a generalized impulse response [Dogan et al., 2012].

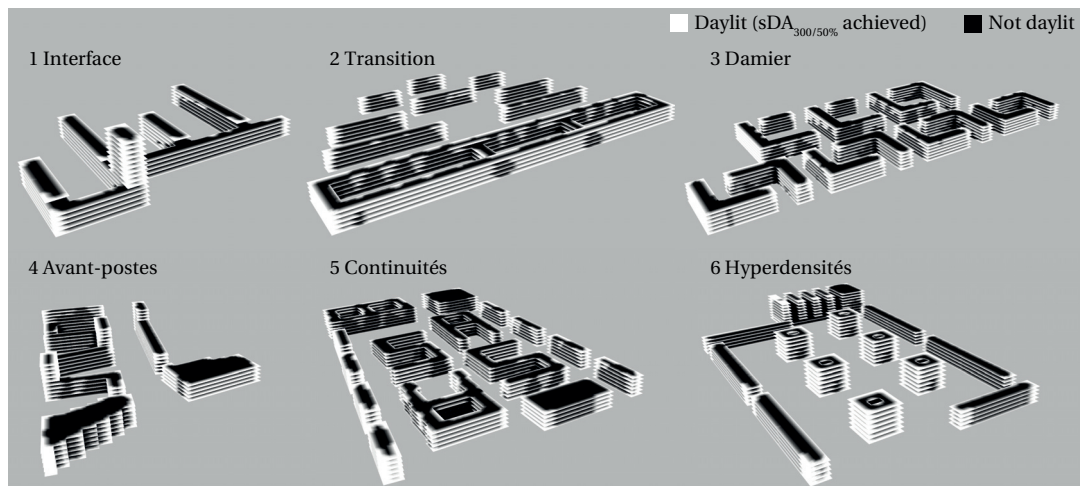


Figure 3.11 – Map of the DA results produced by Urban Daylight [Dogan et al., 2012] for all designs in the BE study.

## 3.2 Results

We here present the results through scatter plots showing the computed reference values (y-axis) against, on the x-axis, each (i) geometry-based metric in section 3.2.1 and (ii) external solar- and geometry- (or irradiation-) based metric in section 3.2.2. In each section, a subdivision is made to look at the three performance criteria: energy production, energy need and spatial daylight autonomy. Results for the first two smaller sized studies, BE and YLB, are often merged and presented together in the graphs, followed by YLB-PDL and LN-PDL. This sequence is repeated for each pair of metrics compared, with studies excluded in parts where no results were measured, e.g. LN-PDL for the energy production, not computed in that project. As motivated earlier, we want to investigate whether metrics (i) and (ii) are correlated to the reference values (iii), in order to judge of the ability of the former to establish a ranking among design alternatives with respect to a specific performance criterion.

The relationship between each pair of metrics is quantified by the linear coefficient of determination ( $R^2$ ), displayed only in graphs where it was found to be higher than 0.70. In the results for YLB-PDL, we have identified an example cluster through colored points, matching across all graphs for this study. Each cluster consists of variants with identical block depth, i.e. equivalent surface-to-volume and passive zone ratio, but distinct setbacks, window-to-floor and plot ratio. This allows visualizing where the same data points fall in the different graphs and will be used throughout this section to facilitate highlighting certain behaviors.

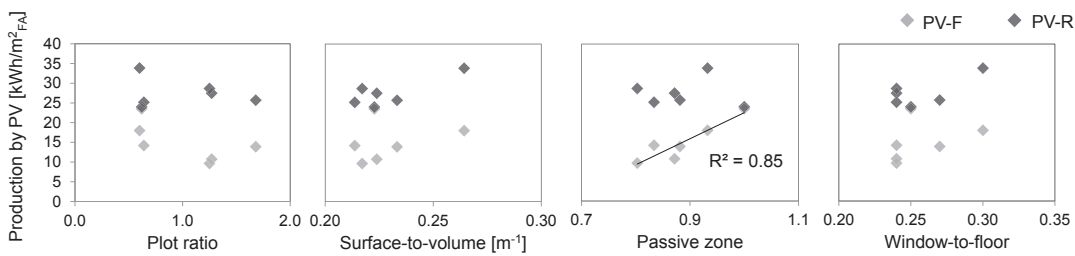
### 3.2.1 Geometry-based versus reference metrics

#### Energy production

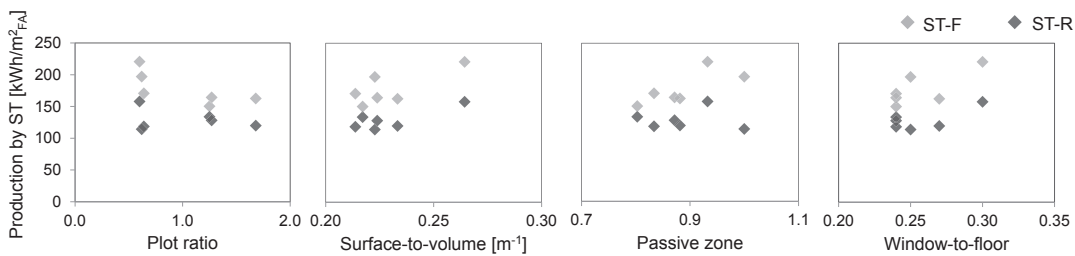
Figures 3.12, 3.13 and 3.14 present the comparison between the energy production (reference metric) and the geometry-based metrics respectively for the BE, YLB and YLB-PDL studies.

### Chapter 3. Validity assessment of existing metrics through neighborhood case studies

The abstract trends decipherable in the graphs of BE and YLB are more clearly seen for the much larger dataset of YLB-PDL (Fig. 3.14), showing patterns particularly for facade-mounted systems (PV-F and ST-F). In those cases, a linear relationship is found across all metrics, strongest for the window-to-floor ratio. This is explained by the fact that larger ratios mean more facade (i.e. collecting) surfaces for a certain enclosed floor area, the latter being the same normalization basis as the energy production value ( $\text{kWh}/\text{m}_{\text{FA}}^2$ ). For systems on roofs (PV-R, ST-R), we observe a spread with higher values associated to designs with 2-story buildings. The irradiation on roofs is likely to be very similar between designs with 2- and 3-story buildings, as this change affects all buildings so there is no increased shading. Thus, the floor area normalized irradiation level is higher for lower buildings, due to their smaller total floor area.



(a) Photovoltaic (PV) on facades (F) and roofs (R)



(b) Solar thermal (ST) on facades (F) and roofs (R)

Figure 3.12 – Energy production by (a) PV and (b) ST systems on facades and roofs against each geometry-based metric for BE.

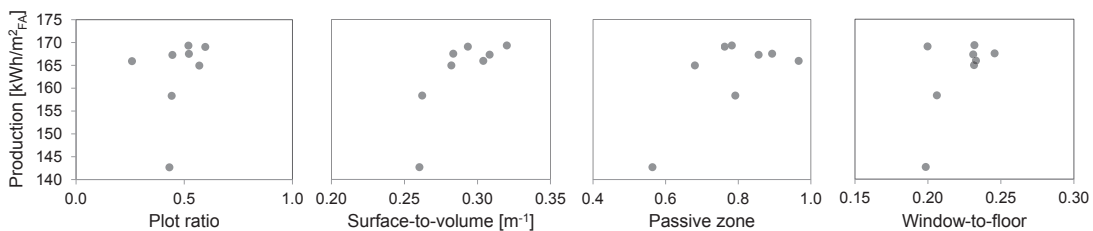


Figure 3.13 – Energy production against each geometry-based metric for YLB.



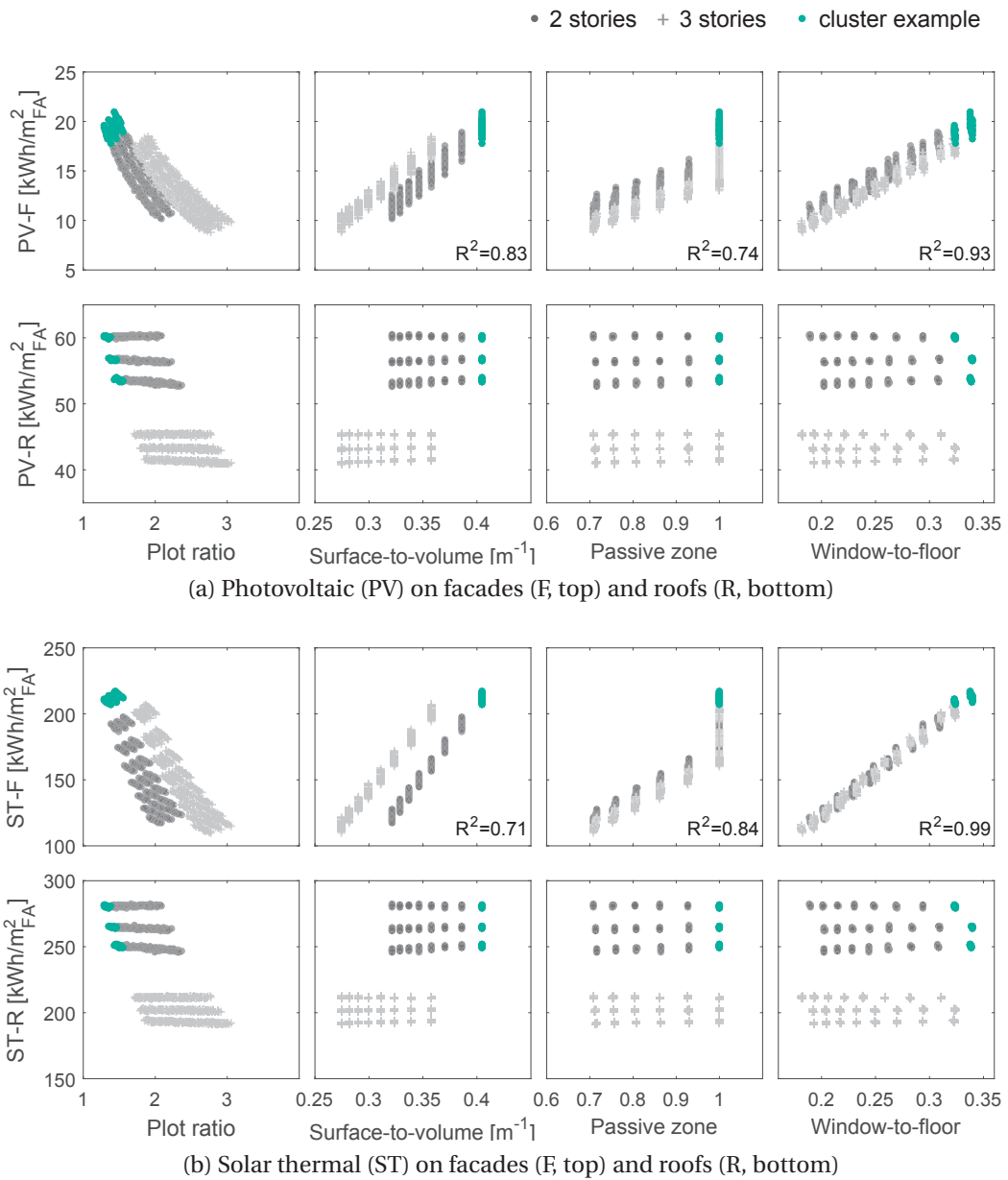


Figure 3.14 – Energy production by (a) PV and (b) ST systems on facades (F, top) and roofs (R, bottom) against each geometry-based metric for the YLB-PDL designs.

### Energy need

Figure 3.15 shows the heating need (top) and the energy need (including heating and cooling; bottom) against each of the four geometry-based metrics, for studies BE and YLB. Results for the cooling need are not separately shown as they were found to be very small for the BE case and displaying no trend for both BE and YLB. While the heating need is about twice as high for BE than YLB mainly due to the simulation settings, e.g. differences in infiltration rate and U-values, the total energy values are similar due to the cooling need contributions. Yet,

### Chapter 3. Validity assessment of existing metrics through neighborhood case studies

---

only BE displays high correlations for the surface-to-volume and window-to-floor ratios. The positive direction of the correlations are to be expected for this heating-dominated climate, with higher heat losses associated to both a larger window-to-floor ratio and a lower level of compactness (higher surface-to-volume). We speculate that the lack of trends for the YLB dataset may be caused by the combined effect of low U-values and the diversity of building orientations - and in some cases typologies - in the designs. In this study, a higher number of buildings spread over a larger surface area was included in the simulation (see Fig. 3.2) compared to the other studies. This may have led to an averaging effect limiting the differences in energy need and simultaneously fading out the influence of geometry-based metrics.

The same comparison is shown in Fig. 3.16 for the heating (top) and cooling (bottom) need of YLB-PDL. Designs with 2 versus 3 stories are separated particularly in the plot ratio and surface-to-volume graphs. For a same surface-to-volume ratio, 2-story designs perform better than the ones with 3 stories. Strong patterns are found across all geometry-based metrics for this larger dataset, with an  $R^2$  consistently above 0.70 except for the cooling versus plot ratio. These correlations are likely due to the way variants were generated through the parametric modeling, causing a dependency between the four geometry-based metrics. For example, when increasing the building depth design variable, all metrics are affected: the surface-to-volume, passive zone and window-to-floor augment while the plot ratio diminishes. Figure 3.17a shows an analysis of these four metrics through a correlation matrix, including the histogram of each parameter, displaying the Pearson correlation coefficient<sup>17</sup> between each pair. The correlation is strongest between the plot ratio (PR) and surface-to-volume (SV). The consequence of this interdependency is that if any one of the geometry-based metrics correlates with the heating need (positively or negatively), as expectedly occurs for the surface-to-volume ratio for instance, all other metrics will correlate as well. This observation puts us on guard regarding 'indirect' correlations, which are difficult to detect. Caution must also be used when drawing conclusions on the cause of the observed trend, as in the famous saying *correlation does not imply causation*.

The slope of each relationship indicates whether the metric should be minimized or maximized to achieve a better performance. The same directionality between heating and cooling means that both outputs can be minimized through the same geometrical features out of the ones considered. The positive slope for the passive zone is contradictory to the concept being it, where non-passive zones should theoretically potentially consume more than passive ones.

Indeed, in our case, variants with values of 1, for which 100% of the space is passive, show the highest heating and cooling need. However, it must be noted that total energy consumption for heating, cooling, ventilation and lighting is used in the passive zone concept [Ratti et al., 2005; Steemers, 2003]. Include these contributions and converting to primary energy values would allow a better comparison with the sources cited above.

---

<sup>17</sup><http://www.mathworks.com/help/matlab/ref/corrcoef.html> (last accessed on March 20, 2016)

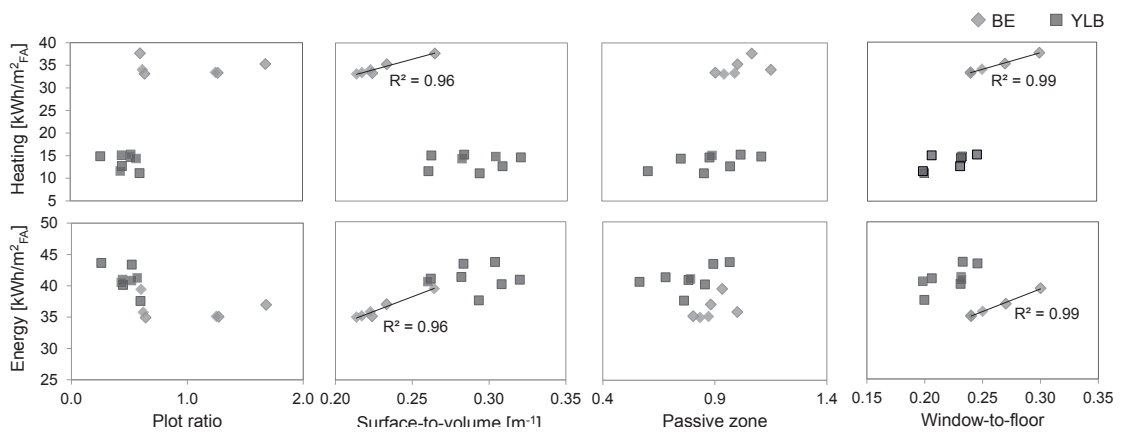


Figure 3.15 – Heating (top) and energy (including heating and cooling; bottom) need against each geometry-based metric for both the BE and YLB studies.

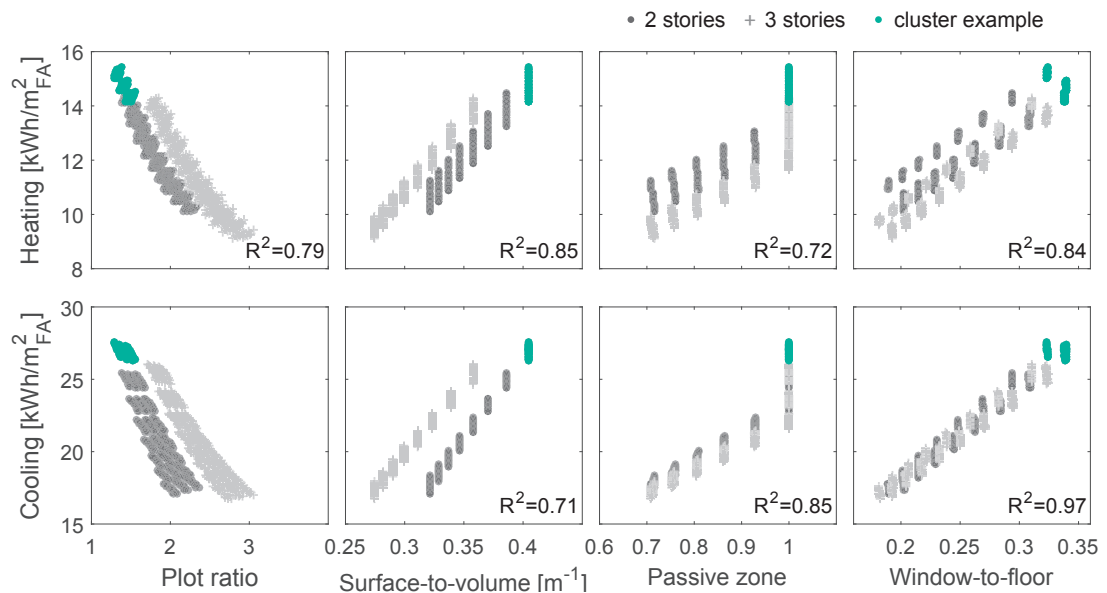


Figure 3.16 – Heating (top) and cooling (bottom) need against each geometry-based metric for the YLB-PDL designs.

When looking beyond the overall pattern of each graph, we observe that clusters are showing different or no trends, e.g. the group of colored dots. The overall positive correlation with the window-to-floor ratio is not observed within this group; the highest heating need is associated with a window-to-floor ratio of about 0.32, which is not the maximum value for this parameter. At constant surface-to-volume, the influencing factor appears to be the higher heat gains provided by larger glazed area, as opposed to the general trend in the window-to-floor ratio graph. Any one parameter is not sufficient to clearly rank the design alternatives, as we still observe clusters of points with identical values but different heating and cooling needs. This observation highlights the importance of considering multiple parameters in parallel.

### Chapter 3. Validity assessment of existing metrics through neighborhood case studies

Results obtained in the LN-PDL study for the heating need versus the geometry-based metrics (except the passive zone which was not computed) are shown in Fig. 3.18. Separations between the design series are observed, with  $0^\circ$  and  $90^\circ$  cases closely located. M1 designs present higher heating needs while M2A and M2B partly overlap. The overall trends are similar to the ones observed for YLB-PDL, particularly for the plot ratio and surface-to-volume. As for YLB-PDL, these two metrics are here also correlated, as shown in the correlation matrix of Fig. 3.17b where a Pearson coefficient of -0.92 is obtained.

Despite the differences in the simulation settings between YLB-PDL and LN-PDL as explained earlier (see also Table 3.6), it is interesting to compare these two studies. The heating need values are generally higher for LN-PDL, although these include only a part of the full amount of energy required, which is the value used in YLB-PDL, as explained in section 3.1.4. However, the cumulative effect of the LN-PDL settings - higher U-value, presence of blinds, etc. compared to the YLB-PDL settings - make the heating needs higher for this study. The LN-PDL values also span a wider range, from approximately 15 to over  $55 \text{ kWh/m}_{\text{FA}}^2$ , likely due to the larger diversity in the designs in terms of building typology and layout, but also dimension variations in the parametric modeling set-up. Yet, the ranges spanned by the geometry-based metrics - x-axes - in both studies are very similar. One hypothesis for explaining the larger differences seen in LN-PDL, as well as the weaker trend with the window-to-floor, is that by excluding the energy needed for providing and heating up the outdoor fresh air, the effect of morphological parameters on the heating need may be enhanced. What would be interesting to investigate is if the relative positioning or ranking of the design alternatives is changed when different simulation settings are used and the full energy need is taken as the reference metric. This is a question to which we will come back in the next chapter (section 4.7.3).

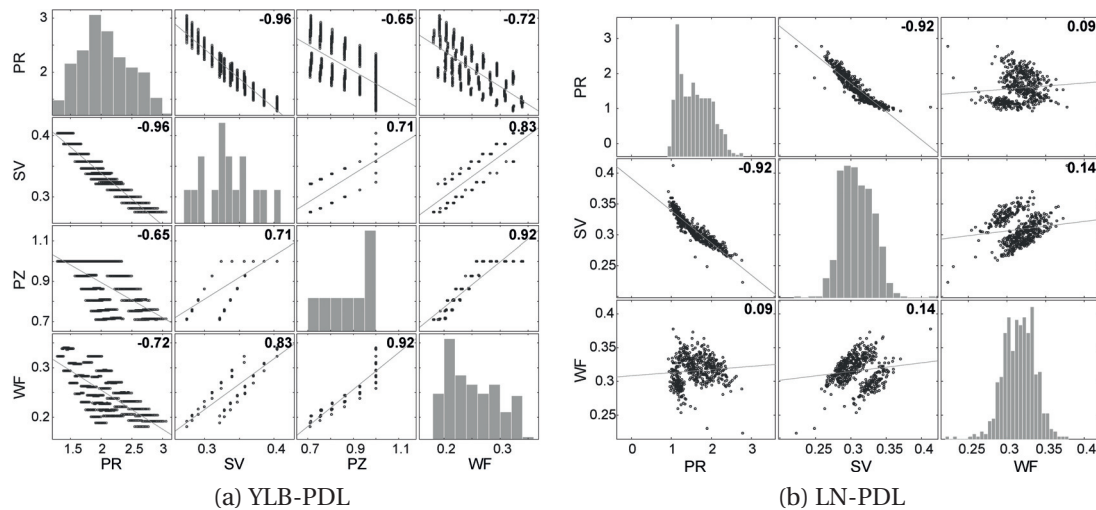


Figure 3.17 – Correlation matrix and Pearson coefficient between each pair of geometry-based metrics for the LN-PDL designs. PR: plot ratio, SV: surface-to-volume, WF: window-to-floor.

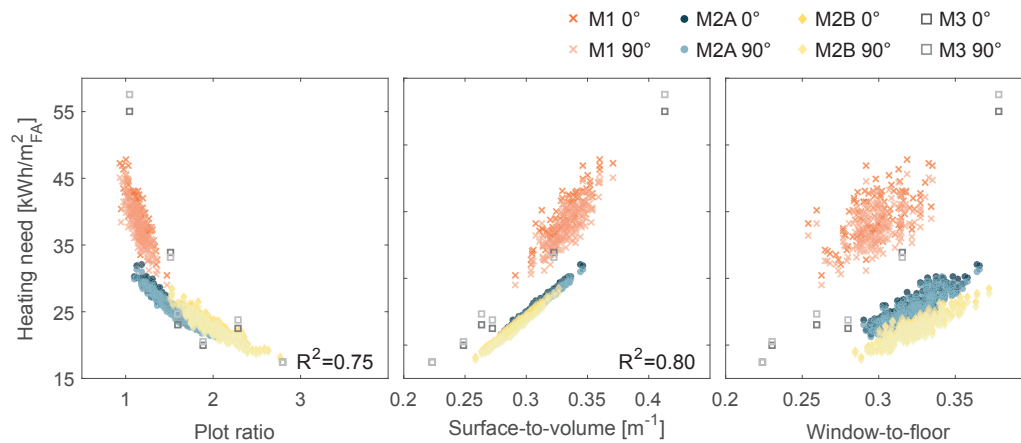


Figure 3.18 – Heating need against geometry-based metrics (except passive zone) for the LN-PDL designs.

### Spatial daylight autonomy

Trends are also observed between the sDA and the geometry-based metrics for some datasets. Figure 3.19 presents the graphs for the BE and YLB studies, the former showing a linear correlation for the surface-to-volume and window-to-floor metrics.

Results for YLB-PDL, shown in Fig. 3.20, also display such positive trends, despite the disparity in the data caused by reducing the simulated designs to 32 variants. As mentioned earlier, the sDA was obtained only for a sample of the 768 variants due to the computational cost of daylight simulations. This sample was chosen so as to capture extremes in terms of design variables, reflected in the results with the gap between high and low sDA values. The passive zone and window-to-floor show the highest positive correlation levels.

The same general effects are found for the larger dataset of LN-PDL, shown in Fig. 3.21. Designs that are denser, less compact, with larger window-to-floor ratios are linked to higher sDA values. However, the strength of the overall relationship between each pair is weaker as in no case have we reached an  $R^2$  of 0.70. When looking at individual design series, we do however obtain high correlation coefficients: 0.75-0.72 (M3 0°-90°) for the plot ratio, from 0.72 (M3 90°) to 0.86 (M2B) for the surface-to-volume and from 0.75 (M3 90°) to 0.90 (M2A-B) for the window-to-floor.

While results show patterns similar to the energy need, the actual indicative trend should be interpreted inversely: higher sDA values are indicative of a better performance (not accounting for possible glare issues), as opposed to the energy need which is to be minimized. This means that the passive zone here presents an overall behavior in accordance with its definition. Designs for which buildings are fully passive (value of 1) present a higher output. This result is in line with the various rules-of-thumb defining the ratio between window-head-height and daylit zone depth. The general statement behind such rules is that “*the depth of the daylit area usually lies between 1 and 2 times the size of the window-head-height*” [Reinhart, 2005]. Where

### Chapter 3. Validity assessment of existing metrics through neighborhood case studies

this rule becomes weaker is when the inter-building shading effect is noticeable. In the case of YLB-PDL, this does not seem to be the case, since height variations are small and applied to all three assessed buildings and thus the shading is relatively constant between design variants (if present at all). However, the shading may explain the weaker relationship with the passive zone observed for BE and YLB, considering the diversity in these designs (see Fig. 3.1 and 3.2).

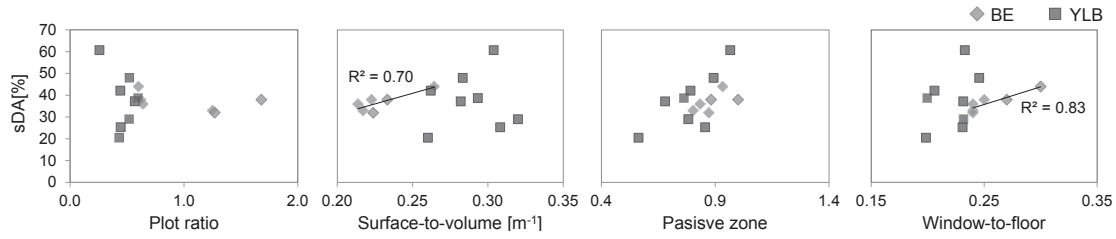


Figure 3.19 – sDA against each geometry-based metric for both the BE and YLB studies.

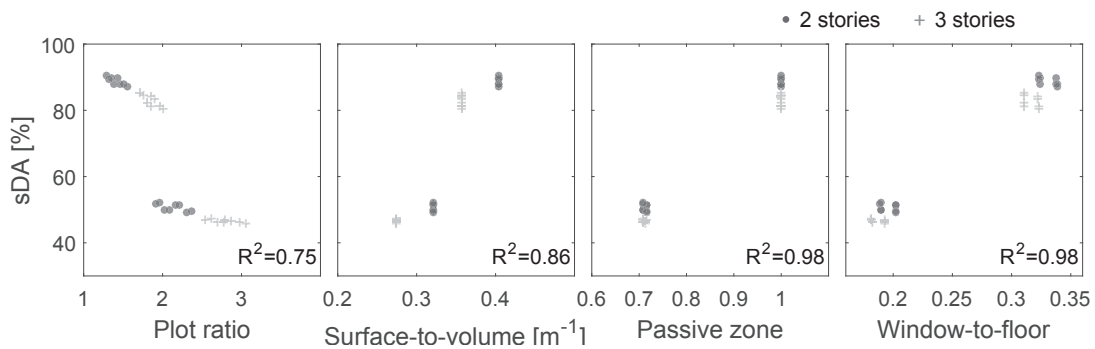


Figure 3.20 – sDA against each geometry-based metric for the YLB-PDL designs.

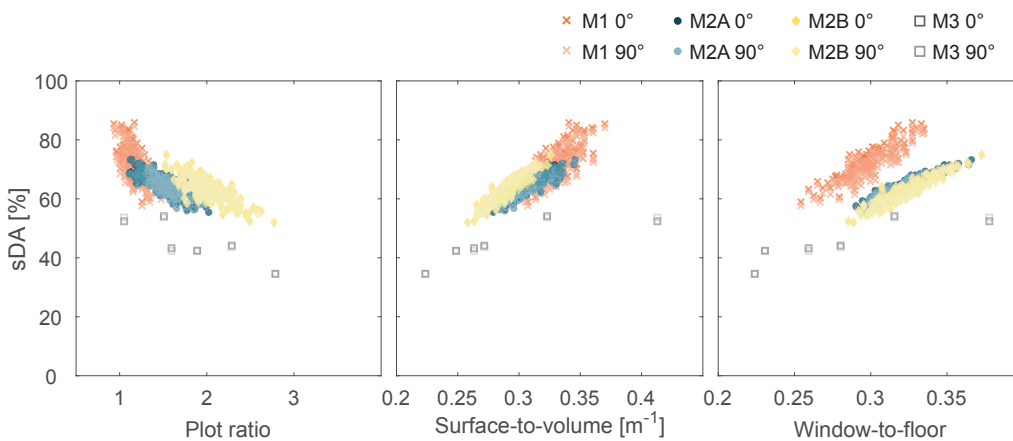


Figure 3.21 – sDA against geometry-based metrics for the LN-PDL designs.

### 3.2.2 Irradiation-based versus reference metrics

We now look at the correlation results for the second category of metrics, compared to the same reference values.

#### Energy production

Figures 3.22, 3.23 and 3.24 show, for BE, YLB and YLB-PDL respectively, the energy production against the threshold-based irradiation metric (left) and the annual irradiation averaged over the collecting surface (middle) and total floor area (right). As explained in section 3.1.4, a different threshold is applied for each system and surface, denoted as PV-F/R and ST-F/R where F stands for facade and R for roof. The same notation is used for the average irradiation metrics, which are computed for the corresponding surface (F/R) as opposed to the overall envelope. For YLB, only the average irradiation metrics are shown, computed over the roof to account only for the surfaces that contribute to the production (see eq. 3.7). Despite the discontinuous spread of data, a correlation is found for the mean roof irradiation.

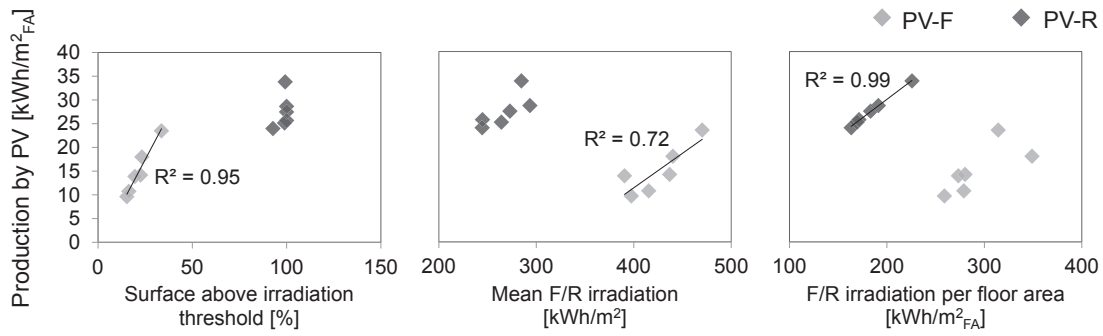
For BE and YLB-PDL, the annual irradiation per floor area is the best indicator with  $R^2$  values close to 1 for both systems installed on the roof. This is not surprising considering the calculation of the energy production (see eq. 3.4). The only difference between the compared metrics in the right-most graph is a multiplication factor (efficiency of system) and the exclusion of eventual shaded roof areas (nodes not achieving threshold). The floor area irradiation metric also shows the best correlation for facade-mounted systems except in the case of PV for BE, where we observe a higher correlation for the surface percentage and annual irradiation per envelope area.

#### Energy need

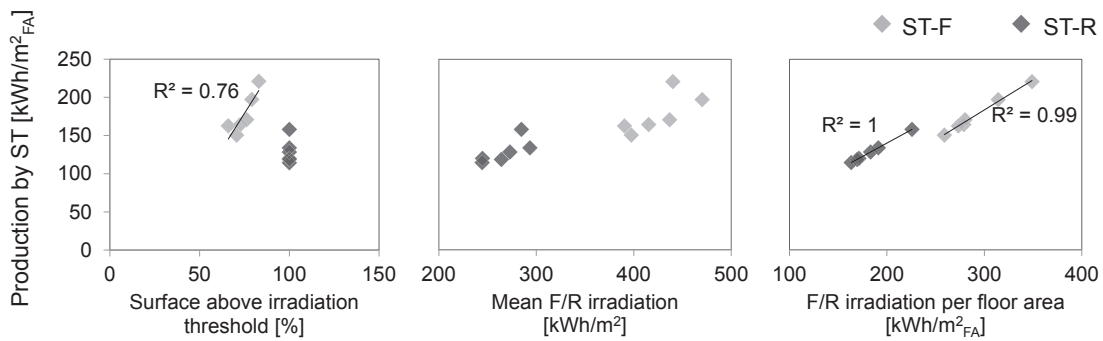
The threshold-based metric does not show a clear pattern with respect to the heating need, as seen in the left graph of Fig. 3.25 and 3.26 for the BE and YLB-PDL datasets respectively. In fact, the overall trend for YLB-PDL is opposite to what it ought to be considering that a higher surface percentage (x-axis) should correspond to a better performance, but is instead associated here with a higher heating need (lower performance). However, the trend within variants of equal surface-to-volume ratio illustrates the ‘correct’ correlation, highlighting the adequacy and validity of the metric for evaluating existing built environments, where the building shape cannot be changed, rather than for comparing hypothetical designs where more freedom exists.

In Fig. 3.26, the overall relationships between heating and cooling are the same for both averaged irradiation metrics. For instance, larger floor-area-normalized irradiation values are associated to both higher heating and cooling needs. If this metric was to be used to select a design, one would normally aim at maximizing its value, assuming it would decrease the heating need. In the current context, that would lead to the opposite.

**Chapter 3. Validity assessment of existing metrics through neighborhood case studies**



(a) Photovoltaic (PV) on facades (F) and roofs (R)



(b) Solar thermal (ST) on facades (F) and roofs (R)

Figure 3.22 – Energy production by (a) PV and (b) ST systems on facades and roofs against each irradiation-based metric for BE.

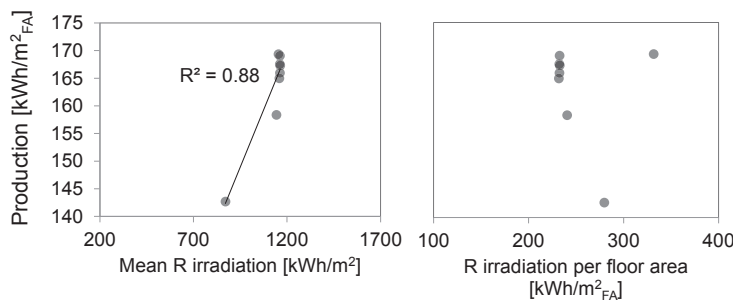
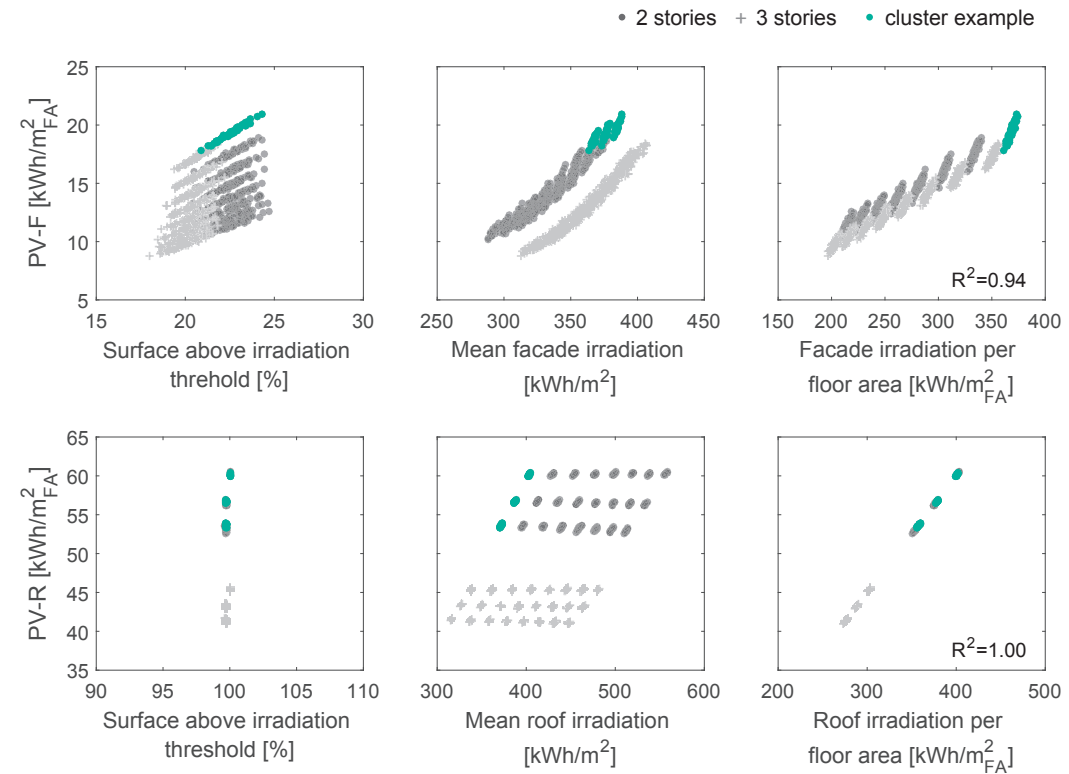
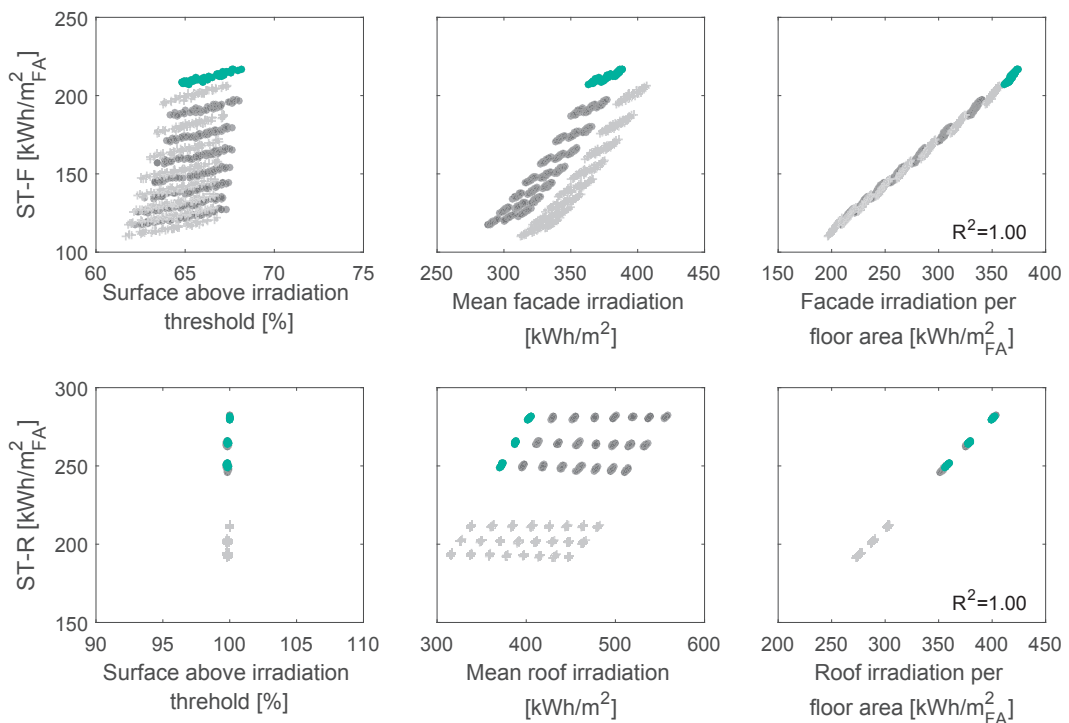


Figure 3.23 – Energy production against the average roof irradiation metrics for YLB.





(a) Photovoltaic (PV) on facades (F, top) and roofs (R, bottom)



(b) Solar thermal (ST) on facades (F, top) and roofs (R, bottom)

Figure 3.24 – Energy production by (a) PV and (b) ST systems on facades and roofs against each irradiation-based metric for the YLB-PDL designs.

### Chapter 3. Validity assessment of existing metrics through neighborhood case studies

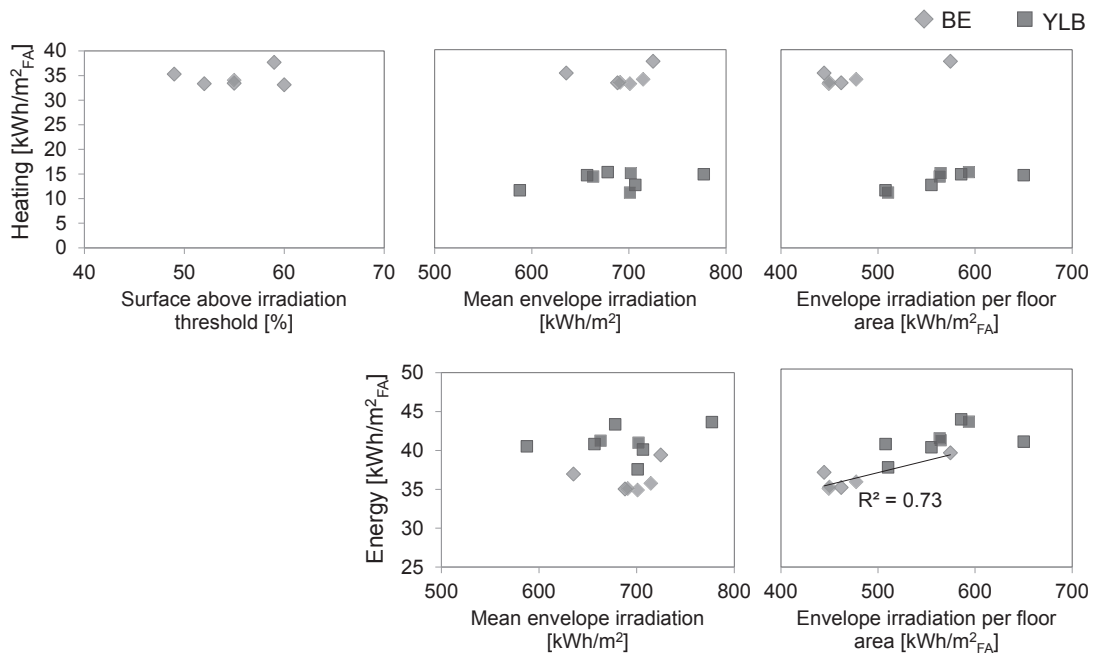


Figure 3.25 – Heating (top) and energy (bottom) need against each irradiation-based metric for both the BE and YLB studies.

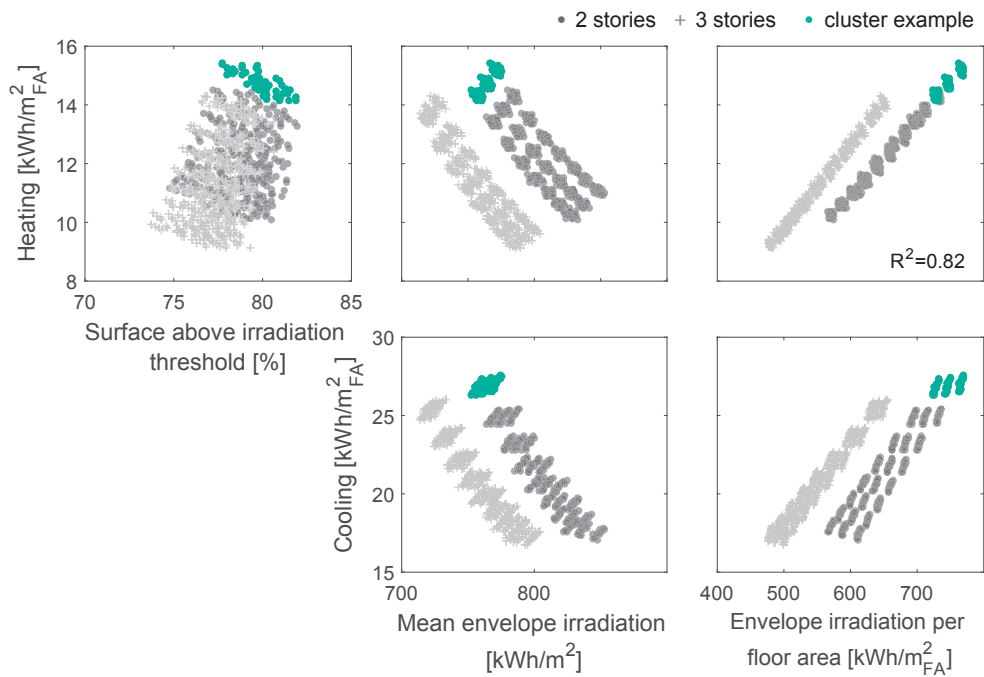


Figure 3.26 – Heating (top) and cooling (bottom) need against irradiation-based metrics for the YLB-PDL designs.

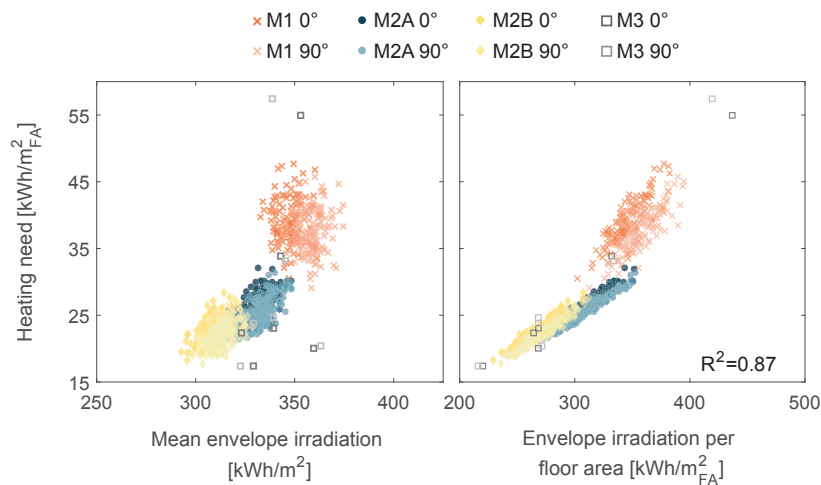


Figure 3.27 – Heating need against irradiation-based metrics for the LN-PDL designs.

Stronger correlations are found for the average irradiation metrics, particularly for the floor area normalized irradiation in the YLB-PDL study ( $R^2 = 0.82$ ), and similarly for LN-PDL (Fig. 3.27,  $R^2 = 0.87$ ). The mean envelope irradiation graph for YLB-PDL shows a double behavior with respect to the heating need: a negative versus positive trend for the overall versus clustered data. More irradiation per envelope area leads to a lower heating need as one would expect, except at constant surface-to-volume ratio, where lower exposure levels are preferred, likely due to the effect of the window-to-floor ratio as seen previously. For LN-PDL, a general positive curvature is observed for that metric, with clouds of points for each design series with a slight shift between  $0^\circ$  and  $90^\circ$  cases. This shift is more important for M1 and M3, less symmetrical than the M2 series.

The right-most graph for YLB-PDL shows more consistency, with the heating need increasing with the annual irradiation per floor area within and across clusters. However, this trend is opposite what one would expect, as observed for the BE case study as well. This can be explained by the fact that more irradiation per floor area means more exposed surface area and less compact buildings: heat losses dominate over solar gains for this climate.

### Spatial daylight autonomy

Results are less clear for the sDA; Fig. 3.28 to 3.30 show dispersed data points, the latter hinting at a positive relationship between the output and the facade irradiation per floor area, stronger for the M2 design series of LN-PDL. The orientation difference is more noticeable than in previous graphs, particularly for M1 and M3 due to their asymmetric layout.

**Chapter 3. Validity assessment of existing metrics through neighborhood case studies**

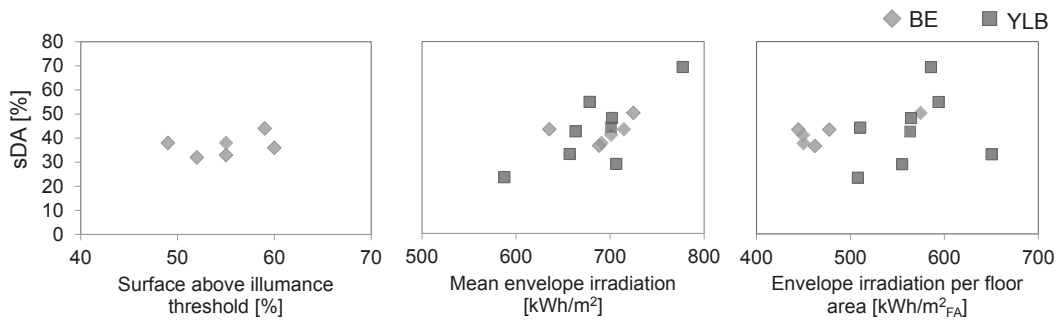


Figure 3.28 – sDA against each irradiation-based metric for both the BE and YLB designs.

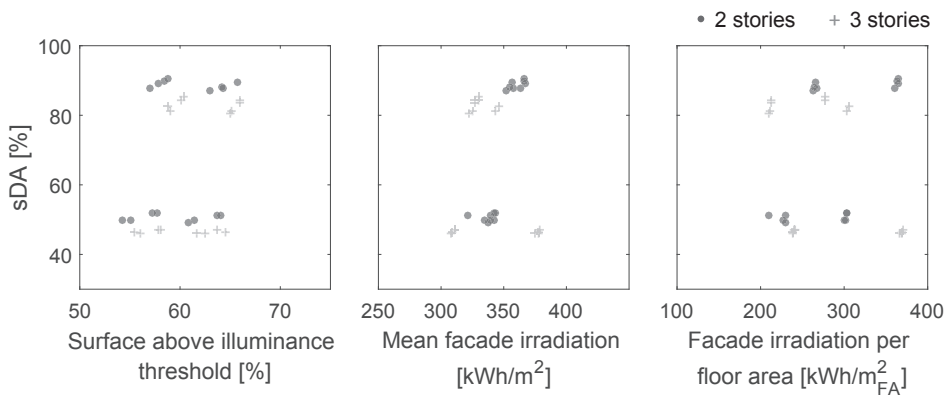


Figure 3.29 – sDA against irradiation-based metrics for the YLB-PDL designs.

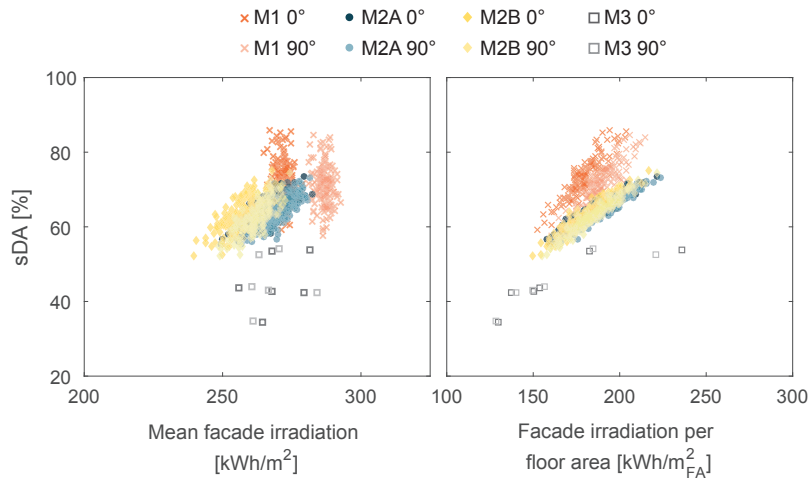


Figure 3.30 – sDA against irradiation-based metrics for the LN-PDL designs.

### 3.2.3 Correlation between geometry- and irradiation-based metrics and relative influence

In light of the trends observed for the irradiation-based metrics, it is of interest to verify the correlation level between the two categories of metrics tested. For example, we would like to see if the positive correlation between the heating need and the envelope irradiation per floor area for YLB-PDL (Fig. 3.26) could be linked to the effect of a dominating geometry-based parameter. This can be investigated through a correlation analysis, as done earlier for the geometry-based metrics, this time on both categories together. Results are shown in Fig. 3.31 through a partial correlation matrix, where the top part corresponding to results presented earlier (Fig. 3.17a) has been cut-off to avoid redundancy. A high  $R^2$  value is found between the irradiation per floor area and the plot ratio (negative) and surface-to-volume (positive) metrics. For the latter, this means that less compact designs have (logically) more solar exposure levels per floor area, yet these additional gains do not compensate the heat losses, as pointed out in section 3.2.2.

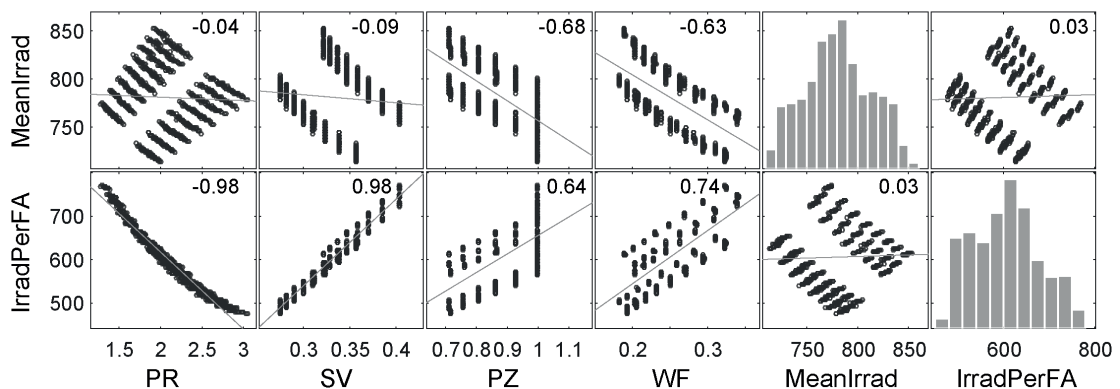


Figure 3.31 – Correlation matrix and Pearson coefficient between each pair of geometry- and irradiation-based metrics evaluated over the YLB-PDL designs. PR: plot ratio, SV: surface-to-volume, PZ: passive zone, WF: window-to-floor, MeanIrrad: mean envelope irradiation, IrradPerFA: envelope irradiation per floor area.

A natural continuation to the above correlation studies is to simultaneously consider multiple parameters to assess their relative influence on the performance metrics. This influence can be quantified by applying a linear regression fit on the set of parameters, previously standardized to eliminate the effect of units and differences in their order of magnitude. This analysis was done for the geometry-based metrics (cat. (i)) for the larger datasets of YLB-PDL and LN-PDL. The set of metrics were scaled (standardized) to have a mean of 0 and a standard deviation of 1 using the Matlab *zscore* function<sup>18</sup>. A linear fit was applied through Matlab's *fitlm* function<sup>19</sup>, providing the plotted coefficients including an intercept term (constant) representing the mean of each output.

<sup>18</sup><http://www.mathworks.com/help/stats/zscore.html> (last accessed on March 20, 2016)

<sup>19</sup><http://www.mathworks.com/help/stats/fitlm.html> (last accessed on April 18, 2016)

### **Chapter 3. Validity assessment of existing metrics through neighborhood case studies**

---

Results are shown in Fig. 3.32. For YLB-PDL, the fit was first done over the four metrics (Fig. 3.32a), and without the passive zone (Fig. 3.32c) to allow comparing the results with the LN-PDL study (Fig. 3.32b) for which the passive zone was not computed.

Not only does the influence of each parameter differ between the two outputs, it also differs from the trends we previously observed. For instance, the surface-to-volume has a negative vs positive effect over the heating vs sDA for YLB-PDL, although a positive correlation was found for both outputs in Fig. 3.16 and 3.20. When removing the passive zone, the effect of the surface-to-volume is negative for both outputs. Differences are also found between the two projects. In fact, all coefficients are opposite (bars below vs above 0) except for the window-to-floor influence over the sDA, however showing a much lower value for LN-PDL than YLB-PDL.

The coefficients of determination obtained through these fits are given in Fig. 3.32d. All are very close to 1 except for the sDA of LN-PDL (0.70). By considering and merging multiple metrics, we thus hypothesize that it is possible to 'create' a better performance indicator. Yet, the construct of this indicator is very sensitive to the underlying data. We will come back to this topic in the next chapter.

#### **3.2.4 Conflicting performance criteria**

An additional analysis of interest consists in plotting the simulation outputs (reference metrics) against each other to demonstrate the conflicting multi-objective situation that arises. This is done in Fig. 3.33 for the sDA versus heating need for the two largest datasets. Designs with the highest sDA are the ones with the worst heating performance. Non-dominated solutions defining the Pareto front are identified in red.

A point is considered a Pareto optimum if there is no other point that optimizes one criterion without worsening the other [Papalambros and Wilde, 2000]. If we focus on the first top-left red point in Fig. 3.33a and trace a line from this point to the next red one, the heating need increases (performance worsens) and so does the sDA (performance improves; note the reversed y-axis). This trade-off occurs across the Pareto front.

This visualization is in line with the opposite trends seen through the correlation graphs. The conflicting nature of certain performance criteria, despite being hard to address, should be captured and brought to light by a DDS tool for instance through such plots where partially optimal designs can be identified. The choice on which criterion to prioritize should remain in the hands of the decision-maker and be based for example on the project-specific goals and context.

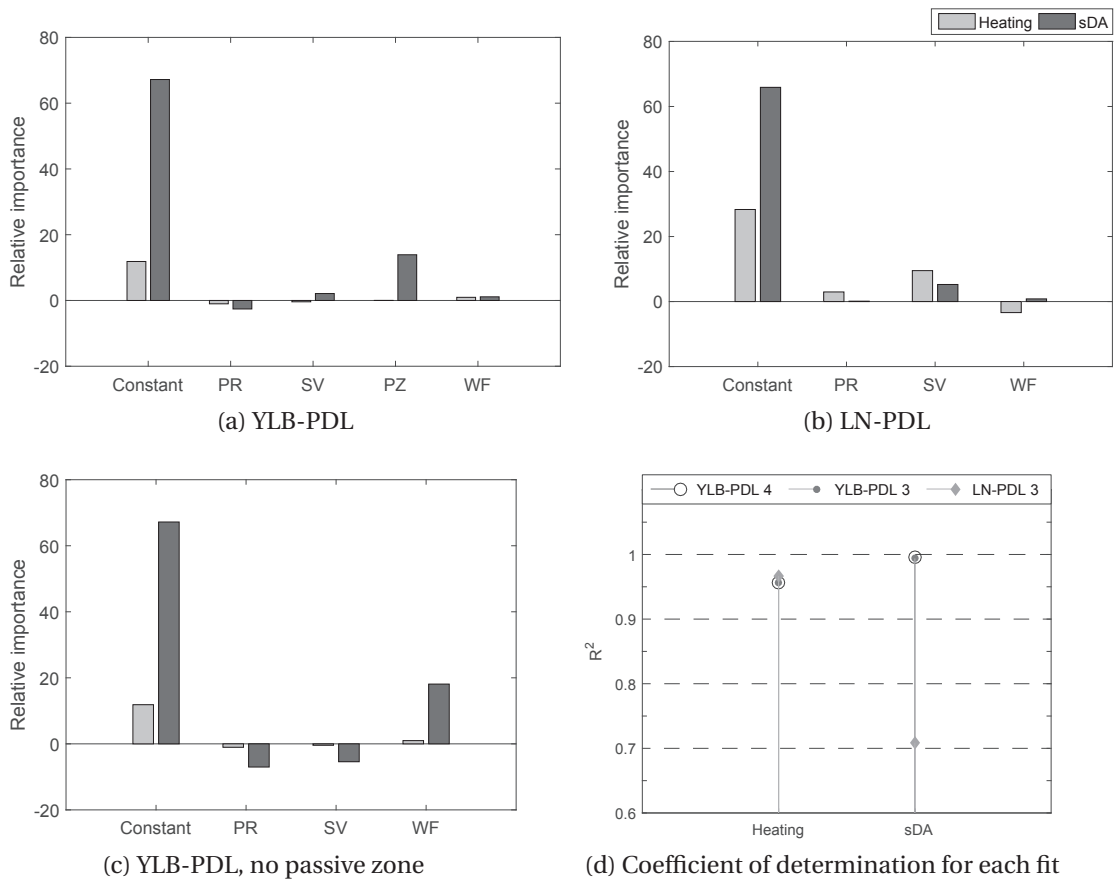


Figure 3.32 – Relative influence of geometry-based metrics over heating need and sDA for YLB-PDL and LN-PDL. Constant: intercept term in a linear regression (mean output when all parameters are 0). PR: plot ratio, SV: surface-to-volume, PZ: passive zone, WF: window-to-floor.

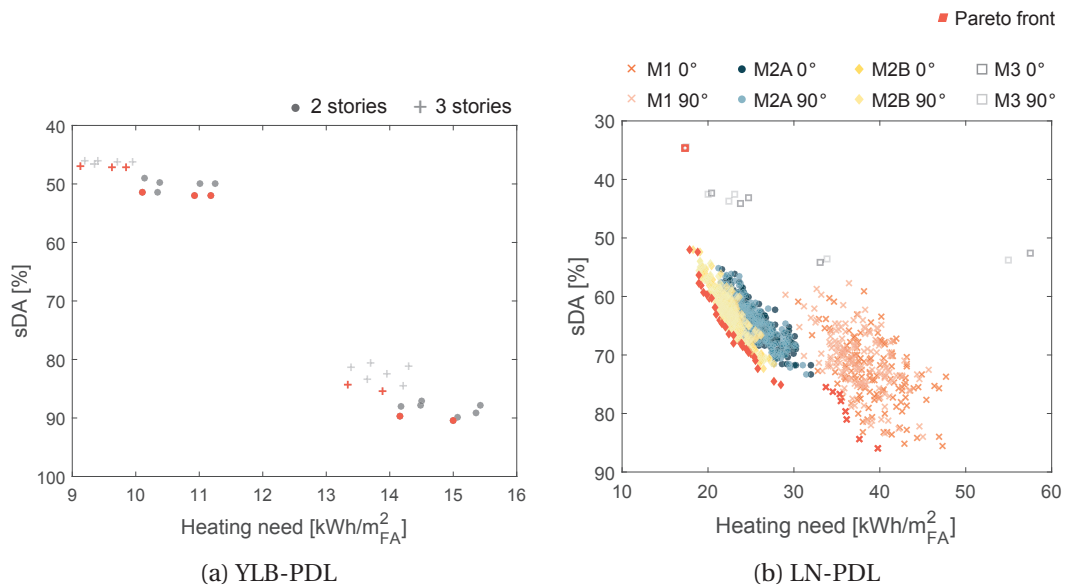


Figure 3.33 – sDA versus heating need for the YLB-PDL and LN-PDL designs, highlighting the conflicting nature of these two criteria. Pareto solutions are identified in red.

### 3.3 Discussion and limitations

We here present a synthesis of the different analyzes conducted in this chapter by highlighting the main observations. We discuss limitations of the tested metrics as well as of our experimental approach.

In this study, we considered that an increase in the passive solar potential, as quantified by any metric such as the ones tested here, should go hand in hand with energy consumption reductions. Similarly, an increase in the active solar potential should go together with higher production levels by PV and ST systems on roofs and facades. These correlations should be respected for both contexts of study: when different typologies are compared, as for the smaller datasets of BE and YLB, and when comparing variants generated from a base case design, as in the other two projects.

From the pairwise correlation analyzes, some metrics emerge as stronger indicators of the different performance criteria. However, results are not consistent over all projects, for instance in terms of strength of the relationship expressed through the  $R^2$  value, e.g. for the heating need vs window-to-floor between YLB-PDL and LN-PDL. According to our study, adopting a unique geometry- or irradiation-based metric as a performance indicator to support decision-making when comparing design alternatives could be misleading due to:

- Partial consideration of influential parameters;
- No consideration of how variants are generated;
- Use of metric can be based on 'false' correlation level and/or direction, caused by other dominating parameters correlated to the metric.

Combining the information brought by multiple complementary metrics can serve to address these issues. However, the possible interdependence between metrics can impede the interpretation of a multi-metric analysis, as highlighted in section 3.2.3.

It is important to note that it is practically impossible to detect causal relationships or even direct correlations. For example, although we observe a strong correlation between energy production by PV-F and the window-to-floor ratio, this relationship is caused by a non-direct effect linked to the parametric modeling method. To be able to more confidently evaluate the direct impact of a metric, it would have to be directly controlled keeping other parameters constant. Considering the nature of the metrics assessed in this chapter, this would not have been easily possible, as their values were derived from the 3D models and not used as design variables.

While we cannot generalize the results obtained, the fact that they differ stresses the need for more robust and flexible performance assessment methods, that can adapt to the specificity of the context proper to a project. Although specific design guidelines are typically sought by practitioners, it is very difficult in practice to provide this sort of information with confidence.



### 3.4. Towards a novel performance assessment method

---

As Oke [1988] stated:

*“These [vast range of possibilities and special cases] are associated with the almost infinite combination of different climatic contexts, urban geometries, climate variables and design objectives. Obviously there is no single solution, i.e., there is no universally optimum geometry. However, this should not stop us seeking general guidelines as long as they are flexible enough to cater to special needs and situations. We certainly do not want a rigid ‘solution’ whose blind application leads to further problems.” [p.103]*

We emphasize that the results presented in this chapter and the following ones should not be interpreted as proof of a clear cause-and-effect relationship between the parameters assessed. Our study does not aim at advocating specific designs, e.g. in terms of building typology. The data acquired through simulation is subject to the intrinsic limitations of the software used, especially since some tools were still in development. However, this issue is mitigated by the comparative nature of the study, which makes relative values more important than absolute ones. The small number of data points for BE and YLB restricts the depth of the analysis that can be conducted on these datasets, and the conclusions that can be drawn from it. While the YLB-PDL case study offers a much larger dataset, it must be recalled that the variations between the variants are smaller. Results between all datasets differ significantly due to distinct simulation settings, tools used, climate files and built context. The study could benefit from further work regarding the simulation details (e.g. natural ventilation) and the output metrics measures (e.g. energy for artificial lighting). Finally, the nature and amount of geometrical parameters considered were defined by the targeted (i.e. early) design phase and limited by the parametric modeling workflow; simple parameters were preferred and additional influential ones such as the location and proportion of windows with respect to each orientation were kept constant.

### 3.4 Towards a novel performance assessment method

The investigation presented in this chapter has brought out the difficulty in ascertaining trends that can be translated into valid performance indicators, independent from the problem under study. However, the preliminary work towards multiple linear regression presented in section 3.2.3 pushes us to investigate this path further. Building upon the metrics tested in this chapter and the various analyzes conducted, we propose to inquire into the feasibility of constructing a *predictive*<sup>20</sup> mathematical function as a performance assessment engine. Our goal is to address the main requirements highlighted throughout the previous chapters:

**Information required** to be limited to early-design knowledge, by imposing this restriction to the data needed by the predictive functions;

---

<sup>20</sup>In the context of this thesis, the term predictive is associated to a process that approximates the result from a full simulation, taken here as the ground truth.

### Chapter 3. Validity assessment of existing metrics through neighborhood case studies

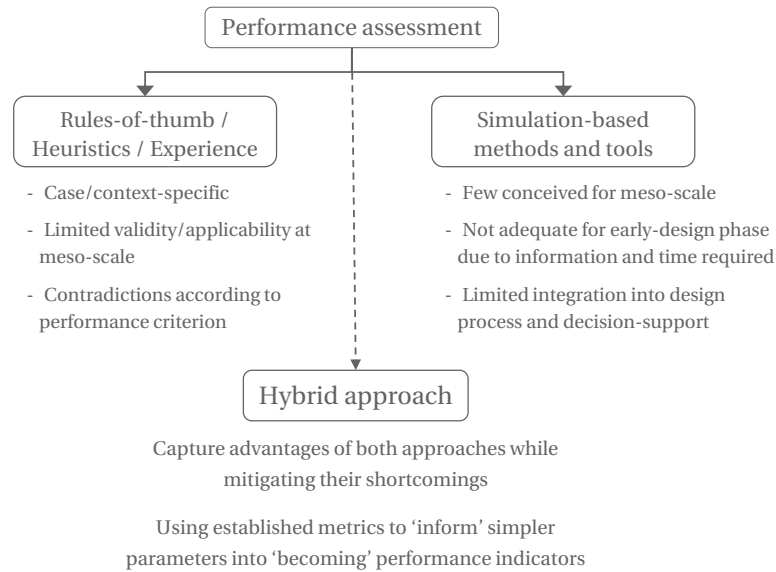


Figure 3.34 – Proposed ‘hybrid’ approach situated midway between simple rule-of-thumb like and simulation-based methods.

**Simulation time** to be minimized to allow real-time interaction, to be achieved by the predictive approach intrinsically designed for that purpose;

**Specificity** to be mitigated by adopting a multi-criteria approach, covering relevant solar performance aspects;

**Design scale** taking into consideration the interdependence of buildings, both by evaluating the performance at the meso scale and incorporating parameters capturing the influence of the surrounding context on individual buildings.

Design decision-support in the form of heuristics such as the morphological parameters tested in this chapter, practitioner knowledge, and many of the existing digital tools are difficultly applicable at the more abstract early design phase and complex neighborhood scale, where intuition, rules-of-thumb and detailed simulation lose in relevance, validity and appropriateness. However, we do not aim at discarding such methods, but instead try to adapt and exploit them in a way that can render them adequate for our targeted purpose. Detailed in the next chapter, the proposed approach can be seen as an in-between, hybrid method, exploiting the advantages of simple metrics and using more complex methods to ‘inform’ the former into becoming performance indicators. This vision is illustrated in Fig. 3.34.

## 4 Metamodel development

*“Essentially, all models are wrong, but some are useful.”*

George Box  
(mathematician, statistics professor)

This chapter describes the development process of our performance assessment engine, representing a core part of this research<sup>1</sup>. We begin in section 4.1 by laying down the basic theory of mathematical modeling (or metamodeling<sup>2</sup>), stemming from the statistics and machine learning domains. A brief review of the state-of-the-art regarding the use of such methods in the field of building performance is presented, followed by an overview of our workflow. The process for building a reference dataset and the choice of the model to derive from this data are detailed in sections 4.2 and 4.3. The dataset is analyzed in section 4.4 before proceeding with the function fitting in section 4.5.

From this work emerge predictive functions for rapidly estimating the passive solar and daylight potential from simple design parameters. The assessment of a third performance criterion - the active solar potential - is done through an algorithm detailed in section 4.6. The combination of these methods form the central piece of our DDS workflow, introduced in chapter 5. We conclude in section 4.7 with the limitations and foreseen work.

### 4.1 Theoretical framework and overview of approach

As seen in chapter 2, most existing performance assessment methods are based on solving equations that simulate the thermal behavior or the (day)light conditions of a building. This intrinsically makes it difficult to fulfill the requirements, identified throughout the previous chapters, to provide adequate early-design support. Evaluation methods based on machine learning techniques represent a promising alternative. Foucquier et al. [2013] and Zhao and

---

<sup>1</sup>Dr. Carlos Becker, computer scientist, contributed to sparking the main ideas behind this chapter, while also providing support and advice in the development of the research method.

<sup>2</sup>Different terms, introduced later on, can be used to refer to a predictive mathematical function.

## Chapter 4. Metamodel development

---

Magoulès [2012] conducted detailed reviews to compare different building energy assessment approaches, including the more common physics-based (or engineering), the alternative statistical and machine learning methods, and hybrids of the two. Table 4.1 presents a blend of their comparative analysis, including the main advantages and shortcomings of each method. To better understand the distinction between these approaches and their pros and cons, an explanation of machine learning methods is of order.

As illustrated in Fig. 4.1, machine learning is a multidisciplinary field: it employs techniques from analogous domains to build algorithms that can learn from data with minimal human intervention [Hall et al., 2014]. Our metamodeling approach, later detailed, stems from the specific branch of supervised machine learning, which consists of algorithms obtained by training an equation from a set of data. Such equations, known as metamodels, surrogate models or emulators, can then be used for prediction. The term metamodel is used in this thesis, sometimes replaced by (predictive) function or simply model to alleviate the text, the latter not to be confused with a 3D model (the sentence's context should prevent any mix-up).

Metamodels are used to “*replace the actual expensive computer analyses, facilitating multi-disciplinary, multi-objective optimization and concept exploration*” [Simpson et al., 2014]. As noted in Table 4.1, they are typically not as accurate as what they are meant to replace, i.e. thermal and daylight simulations in the present case. However, they are easier to apply in practice and provide fast estimates of the desired output. At the early design phase, when little is known about the design and accuracy is not a priority, such models are thus useful for facilitating rapid design space exploration.

The general metamodeling concept is presented in Fig. 4.2. First, in the development phase, a dataset linking a series of inputs (or predictors,  $\mathbf{x}$ )<sup>3</sup> and outputs (or responses,  $y$ ) is acquired by sampling the design decision space, through the available yet expensive simulation [Forrester et al., 2008]. A choice of model form is then selected and fitted to the data. The concept of fitting means that we attempt to learn a mapping  $y = f(\mathbf{x})$  that emulates the black box which is the simulation, but that veils its physics [Forrester et al., 2008]. The dataset of samples is thus used to construct an approximation  $\hat{f}$  of the simulation. Through this supervised (machine) learning or instance-based learning process, an approximate function is obtained that can then be used to cheaply predict the output for a given set of new inputs (application phase).

The use of such techniques in the field of building performance is fairly recent. A non-exhaustive list of studies employing statistical and machine learning methods is presented in Table 4.2. The type of technique, model and design space sampling method, as well as the context in which it is applied - base case building, inputs and outputs - are presented.

While metamodeling techniques are often used for building energy forecasting [Asadi et al., 2014; Ekici and Aksoy, 2009; Foucquier et al., 2013; Hygh et al., 2012; Tsanas and Xifara, 2012], machine learning methods can more generally be useful also for performance optimiza-

---

<sup>3</sup>Note on mathematical notation: scalars are italicized ( $y$ ), vectors are italicized and bold ( $\mathbf{x}$ ), and matrices are denoted by a bold capital letter ( $\mathbf{X}$ ).

#### 4.1. Theoretical framework and overview of approach

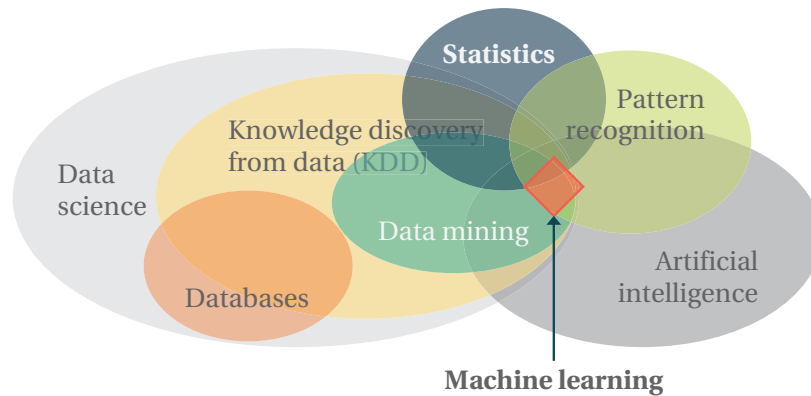


Figure 4.1 – Machine learning at the intersection of multiple domains. Figure adapted from Hall et al. [2014].

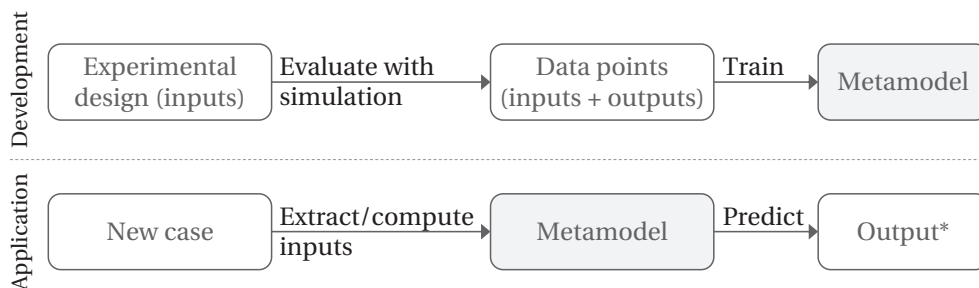


Figure 4.2 – Metamodeling concept: a metamodel is trained from a dataset of simulated cases (upper line), and applied to a new (unseen) case to obtain a predicted output\*, without simulation (lower line). Figure adapted from Couckuyt and Dhaene [2016]; The MathWorks [2014].

tion [Caldas, 2008; Evins, 2013; Evins et al., 2012; Kämpf and Robinson, 2010; Magnier and Haghghat, 2010; Nguyen et al., 2014; Wang et al., 2005; Yi and Malkawi, 2009] and sensitivity analyzes [Eisenhower et al., 2012; Hemsath and Alagheband Bandhosseini, 2015; Martins et al., 2014].

A large majority of studies have focused on a unique and isolated building, employing multiple linear regression, artificial neural networks (ANN), genetic algorithms (GA) or support vector machines (SVM). Different sets of parameters related e.g. to the building material, orientation and glazing area are typically used as inputs to the predictive function [Asadi et al., 2014; Ekici and Aksoy, 2009; Hygh et al., 2012; Tsanas and Xifara, 2012].

A much smaller number of studies have looked at the macro scale, either by exploiting city-wide data for predicting the distribution of energy consumption per building through a probabilistic approach [Kolter and Ferreira Jr, 2011], or for predicting the end-use energy consumption of existing districts, as done by Howard et al. [2012] for the city of New York.

For optimization purposes, the most common methods fall in the category of evolutionary algorithms, which have been used mainly at the building scale [Caldas, 2008; Magnier and

## Chapter 4. Metamodel development

---

Haghighat, 2010; Wang et al., 2005; Yi and Malkawi, 2009] and somewhat at the urban scale [Kämpf and Robinson, 2010; Martins et al., 2014].

Sensitivity analyzes, to assess the influence of certain parameters on a performance metric, can be done prior to optimization [Martins et al., 2014] and model fitting [Eisenhower et al., 2012] to decrease the dimension of the problem by removing parameters of low influence.

The demonstrated feasibility of applying machine learning methods at the building level for allowing a real-time performance assessment leads us to question its potential applicability to the meso scale. According to our knowledge, the work by Howard et al. [2012] represents one of the closest to this question. As detailed below, our approach however distinguishes itself by its specific scale and purpose of application, as well as by both the methods employed, e.g. for acquiring the data, and the information exploited for - and resulting from - the prediction. As such, this core thesis chapter details a novel contribution to the research field.

We therefore propose to investigate the feasibility of emulating thermal energy and daylight simulations at the neighborhood scale by developing a metamodel for each of these two performance criteria. The challenge consists in limiting the amount and, more importantly, the level of complexity and detail of the information required by the metamodels, while still achieving reasonable accuracy in the prediction. This shall ensure that the predictive performance assessment engine thus developed can be applied in the context of early-phase neighborhood design.

The main phases of our approach and their underlying steps are illustrated in Fig. 4.3 and further detailed in the next sections. To develop the metamodels, a reference dataset representing a sample of a delimited neighborhood design space is first acquired (section 4.2). Our choice of model form, multiple linear regression, is motivated and detailed in section 4.3. From the dataset, an analysis is conducted in section 4.4 prior to the metamodel fitting procedure, presented in section 4.5.

### 4.2 Data collection

The dataset, from which the metamodels are to be learned, should provide a good representation of the design space that we would like to be able to assess, once the functions are generated. In the current context of neighborhood-scale designs, this space is practically infinite. Designs can vary in terms of building typology, layout, program, construction and many more design parameters. It is thus necessary to define a bounded sub-space on which to focus to ensure the completion of the proposed approach as a proof-of-concept. These boundaries are exposed in the following sections.

The modeling and simulation approach including tools and some of the 3D designs used in this chapter have already been introduced in chapter 3. As such, we will regularly refer the reader to previous sections, in parallel with repeating some important phases and details.

Table 4.1 – Comparative analysis of methods used for predicting building energy consumption, according to/adapted from Fouquier et al. [2013]; Zhao and Magoules [2012]. Physical methods (above dashed line) are more common than machine learning techniques (below dashed line).

| Method  | Starting hypothesis   | Application field   | Advantages   | Drawbacks   |
|---|---|---|--|---|
| Elaborate physical  | -   |   | High accuracy  | High model complexity; De-tailed inputs needed; Low run-ning speed; Expertise required  |
| Simplified physical                                       | -   |   | Easy and quick to use; Simpli-fied inputs needed   | High model complexity   |
| Multiple linear re-gression                               | Starting hypothesis: linear relation between variables and the output                                     | Forecasting of the energy consumption; Evolution of the energy demand               | Regression function describing the system; Moderate to low model complexity; Easy to use                   | A large amount of training data; Non-collinearity between data  |
| Genetic algorithms (GA) (optimization technique)          | Starting hypothesis: equa-tion form imposed by the user; Final result is not nec-essary the best solution | Prediction of the energy consumption; Optimiza-tion of the equipment or load demand | Function describing the sys-tem; Powerful optimization al-gorithm  | A large amount of training data; Difficulties to adjust algorithm parameters; Large computation time                                    |
| Artificial neural net-works (ANN) (regres-sion technique) | No starting hypothesis but complex “black box” pre-venting physical interpreta-tions                      | Prediction of the energy consumption and energy uses                                | Large training faculty; High run-ning speed  | Large amount of exhaustive and representative data; No physical interpretation; High model complexity                                   |
| Support vector ma-chines (SVM) (regres-sion technique)    | Starting hypothesis: kernel function imposed by the user  | Forecasting of the energy consumption or tempera-ture                               | Reasonable amount of train-ing data; Minimization prob-lem based on structural risk minimization principle | Determination of the kernel function; Difficulty to adjust some parameters; High com-plexity and computational cost; Expertise required |

Table 4.2 – Non-exhaustive overview of studies using machine learning techniques in the field of building performance prediction and sensitivity analyzes.  
 \*Sample size of complete dataset including training and testing subsets. (?): not clearly stated; bldg.: building; FAST: Fourier Amplitude Sensitivity Test; LHS: Latin Hypercube Sampling; NYC: New York City.

| Ref.                     | Model/analysis type   | Base case   | Inputs  | Outputs  | Sampling method;<br>Sample size*                        |
|--------------------------|---|---|---|--|---|
| Asadi et al. [2014]      | Multi-linear regression (per building shape)                            | Two-story office bldg.  | Materials (incl. thickness), schedule   | Energy consumption (heating, cooling, lighting, ventilation) | Monte Carlo; 70 000                                     |
| Hygh et al. [2012]       | Multivariate regression (per climate)                                   | Office bldg.  | 27 parameters (incl. depth, orientation, U-value)   | Energy consumption (heating, cooling, total)                 | Monte Carlo; 20 000                                     |
| Karteris et al. [2013]   | Linear regression (per roof class)                                      | Multi-story-family bldg.  | Unavailable roof areas, orientation of roof's near south side, position of stairwell and elevator shaft on roof | Solar suitable flat roof-top area                            | 209 representative real buildings                       |
| Tsanas and Xifara [2012] | Linear regression and random forests                                    | Residential bldg.   | 8 parameters (incl. surface area, orientation, glazing area)  | Heating and cooling load                                     | Full factorial; 768                                     |
| Lam et al. [2010]        | Multiple regression (per climate)                                       | 40-story office bldg.   | 12 building design parameters (incl. window-to-wall ratio, U-value)   | Annual building energy use                                   | Full factorial and pseudo-random number generator; 1021 |
| Capozzoli et al. [2009]  | Variance decomposition with FAST (per climate); Multi-linear regression | Middle floor of multi-story office bldg.  | 6 parameters (incl. compactness, orientation)   | Energy needs for space heating and cooling                   | LHS and Monte Carlo; 600 (?)                            |
| Howard et al. [2012]     | Multivariate linear regression (per city area and bldg. function)       | Urban areas in NYC, covering 8 bldg. functions (residential, office, store, etc.) | Bldg. floor area and function   | Annual energy consumption (electricity and total fuel)       | NYC database  |



Table 4.2 – (Continued) Non-exhaustive overview of studies using machine learning techniques in the field of building performance for prediction and sensitivity analyses. \*Sample size of complete datasets including training and testing subsets. (?): not clearly stated; bldg.: building; incl.: including; ANFIS: Adaptive Neuro-Fuzzy Inference System; SVR: Support Vector Regression; PMV: Predicted Mean Vote; GSA: Global Sensitivity Analysis.

| Ref.                                | Model/analysis type   | Base case   | Inputs   | Outputs   | Sampling method;<br>Sample size*   |
|-------------------------------------|---|---|--|---|--|
| Ekici and Aksoy [2009]              | ANN (per building aspect ratio)                                   | Bldg.   | Transparency ratio, insulation thickness, orientation  | Heating energy  | Full factorial; 896  |
| Bektas and Aksoy [2011]             | ANFIS   | Bldg.   | Aspect ratio, transparency ratio, insulation thickness, orientation                                      | Heating and cooling energy  | Full factorial; 225  |
| Eisenhower et al. [2012]            | SVR with Gaussian kernel  | Two-story office and gym bldg.                                  | 1009 parameters (initially, incl. material, equipment, then 20 most influential)                         | Thermal comfort (PMV) and annual energy consumption                 | Quasi-Monte Carlo (deterministic); 5000  |
| Martins et al. [2014]               | Sensitivity analysis; Significance test                           | Real modern high-rise urban area (9 surrounded bldgs evaluated) | 12 parameters (incl. height, street width, floor area ratio)   | Irradiation and illumination on building envelope                   | Design of Experiment (DoE) fractional factorial; 8192 (?)                                  |
| Hemsath and Alagbandhosseini [2015] | Local sensitivity index and Morris GSA (per climate)              | Residential bldg.   | 9 parameters (incl. geometric e.g. aspect ratio and material e.g. insulation)                            | Heating and cooling loads   | GA (?); not stated   |
| Tso and Yau [2007]                  | Comparison of multiple stepwise regression, decision tree and ANN | Household in Hong Kong  | Housing type (e.g. private versus rental), household characteristics (e.g. size), presence of appliances | Seasonal electricity consumption                                    | Database through questionnaires and diaries  |
| Kolter and Ferreira Jr [2011]       | Linear regression; GP regression                                  | Residential and commercial buildings in Cambridge, US           | Tax assessor records and database (incl. e.g. roof height)   | Total and monthly (distribution of) energy consumption per building | Dataset of monthly electricity and gas bills for 6 500 buildings collected over many years |

## Chapter 4. Metamodel development

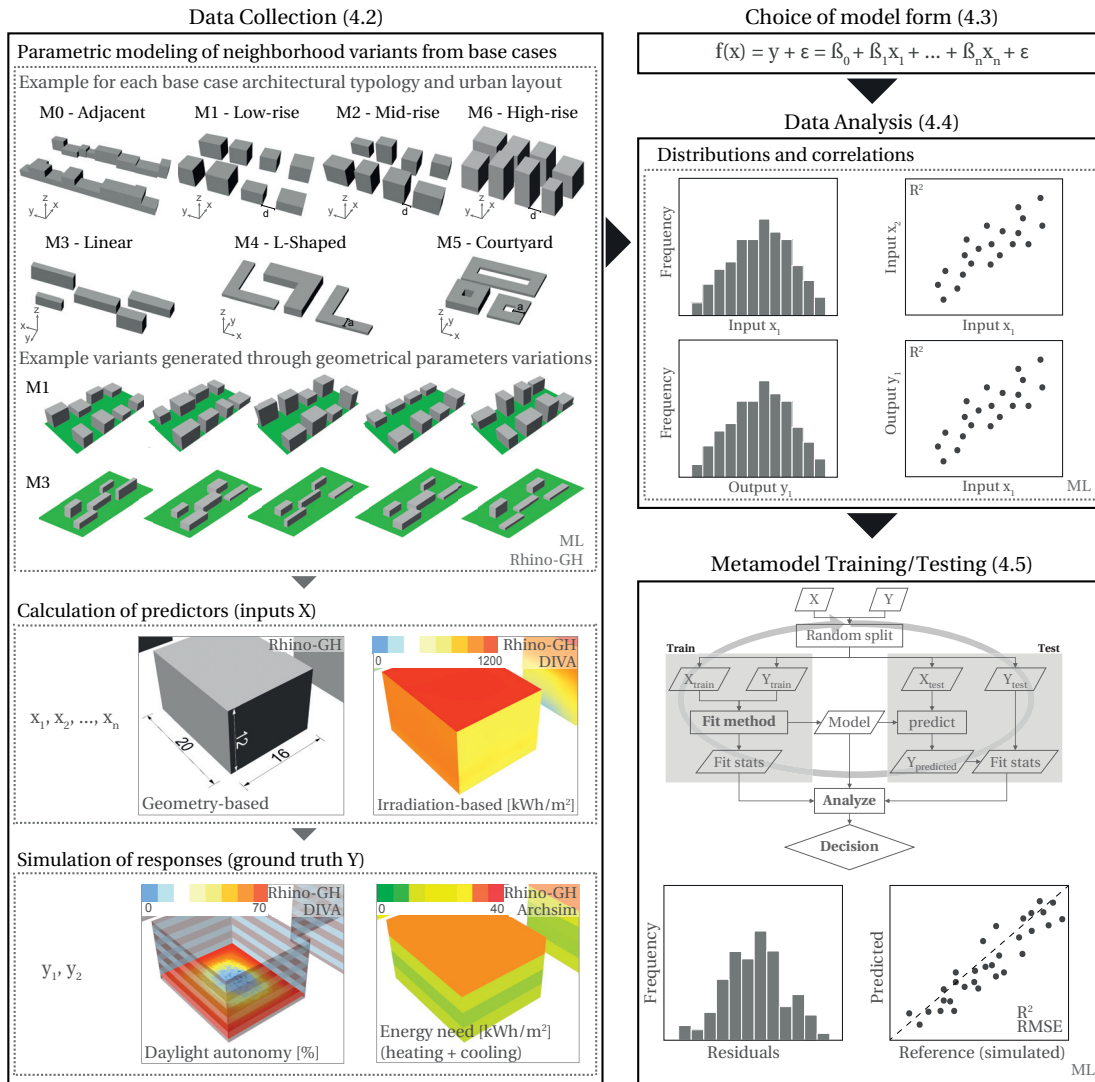


Figure 4.3 – Overview of metamodeling procedure including data collection and analysis, model selection and training and testing. The main tools used at each phase are annotated: ML: Matlab, Rhino, GH: Grasshopper, DIVA, Archsim. For a description of each program, we refer the reader to chapter 3. References are provided in the text.

### 4.2.1 Base case neighborhood designs

To construct our dataset we begin from base case designs, each consisting of a replicated building typology (or shape) according to a certain urban layout. An example variant for each base case is illustrated in the upper left corner of Fig. 4.3. The base case designs come from two earlier studies which were presented in chapter 3. M0 to M2 correspond to the series from the LN-PDL collaborative study with the urban design firm (Urbaplan, Fig. 3.4), here renamed so that what was previously M1-M2A-M2B become M0-M1-M2. M3 to M5 were inspired by three student projects from the BE study: 2-Transition, 3-Damier and 6-Hyperdensité in Fig. 3.1 (Green Density album [Rey, 2013]).

These designs were selected for their diversity yet simplicity of building shape, allowing us to cover common typologies: adjacent buildings and isolated, linear, L-shaped and closed (courtyard) blocks. M6 was later added to cover the tower typology, with the same layout as M0-M2. In what follows, we will refer to each base case as *case Mi*, as a term inclusive of both the building typology and the urban layout. Since these characteristics are fixed, the cases only encompass a small portion of the theoretically unbounded space of possible neighborhood designs. However, they do capture some of the main typologies recurrently encountered in early-stage projects. The following examples serve to support this point.

Figures 4.4 and 4.5 illustrate example neighborhood-scale designs from urban design competitions and master plan reports (*Plan Directeur Localisés (PDLs)*) [SDOL and Gauthier, 2012; Urbaplan, 2015]. By examining such design alternatives we can extract the Level of Detail (LoD) typically encountered at this early project stage, as well as the variations in terms of design features. For instance, we note that the building typology (shape) ranges from simple cubic volumes to courtyards, while the layout varies in terms of building replication, alignment and spacing. The dimensions also differ in height, width, length and depth in the case of L-shaped and courtyard buildings.

Multiple urban-scale studies have also focused on similar building typologies (using varying terminology), often with a regular replication pattern [Cheng et al., 2006; Kanters and Wall, 2014; Kristl and Krainer, 2001; Okeil, 2010; Pereira et al., 2009; Ratti et al., 2003; Tereci et al., 2010]. Examples are shown in Fig. 4.6 - 4.8.

In our approach, an irregular layout is preferred to the more commonly encountered regular grid of buildings. While the latter offers a simpler, more systematic generation of designs and analysis of results due to its repeated features, allowing more variations in the design brings us closer to real projects [Ratti et al., 2003].

### 4.2.2 Parametric modeling of design variants

#### Design variables, constants and constraints

To increase the design space sampling, a parametric modeling workflow was developed, as was done for the YLB-PDL and LN-PDL studies in chapter 3. Starting from the seven base cases portraying a diversity in terms of building typology and layout, specific design variables were varied in an iterative sequence. To define which parameters to vary versus keep constant, the following requirements were considered:

1. The design variables should represent parameters with which designers normally play at the early-design phase of neighborhood-scale projects,
2. have a significant impact on the solar access / energy performance of buildings,
3. be reasonably easy to vary parametrically and compute over a whole neighborhood design.

**Chapter 4. Metamodel development**

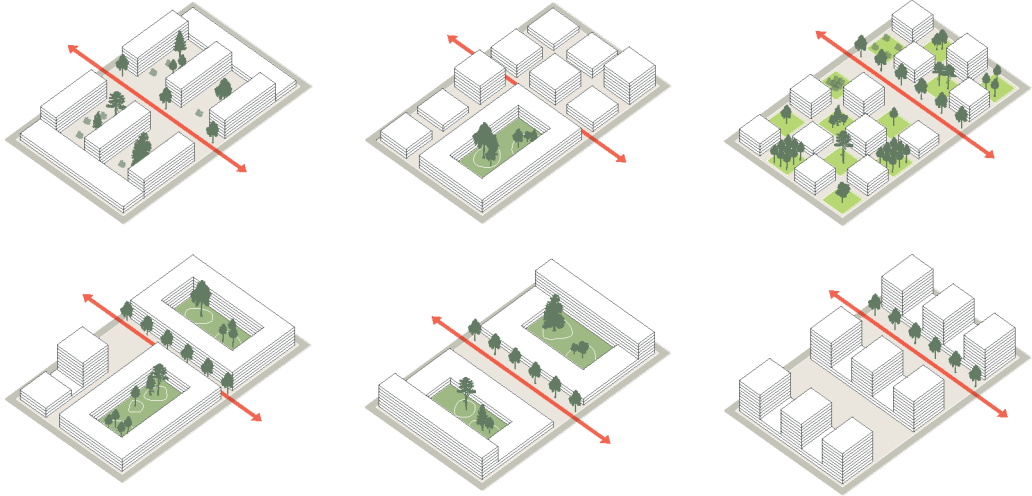


Figure 4.4 – Hypothetical designs proposed in the PDL for an area of Lausanne (Vernand) with a mixed program, highlighting the envisioned variations of building typology and layout for this mixed-used district. Source of images: Urbaplan [2015].

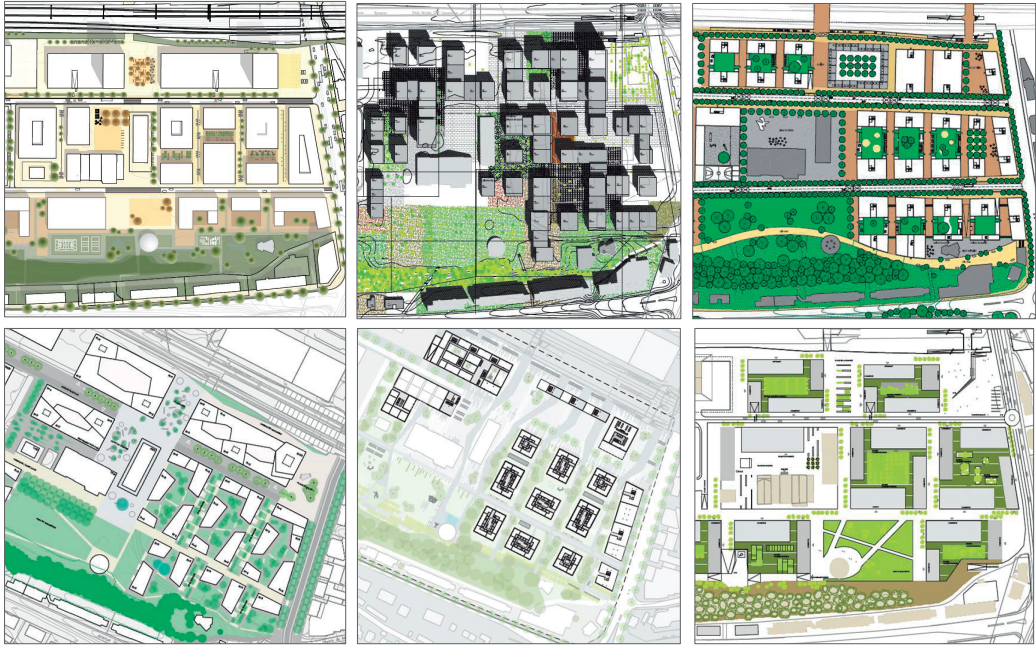


Figure 4.5 – Six example plans submitted to an urban design competition for an area of Lausanne (Malley) with a mixed program. Designs vary in terms of replicated versus mixed building typology (e.g. L-shape, cubic shape) and layout (e.g. different alignments, distances). Source of images: SDOL and Gauthier [2012].

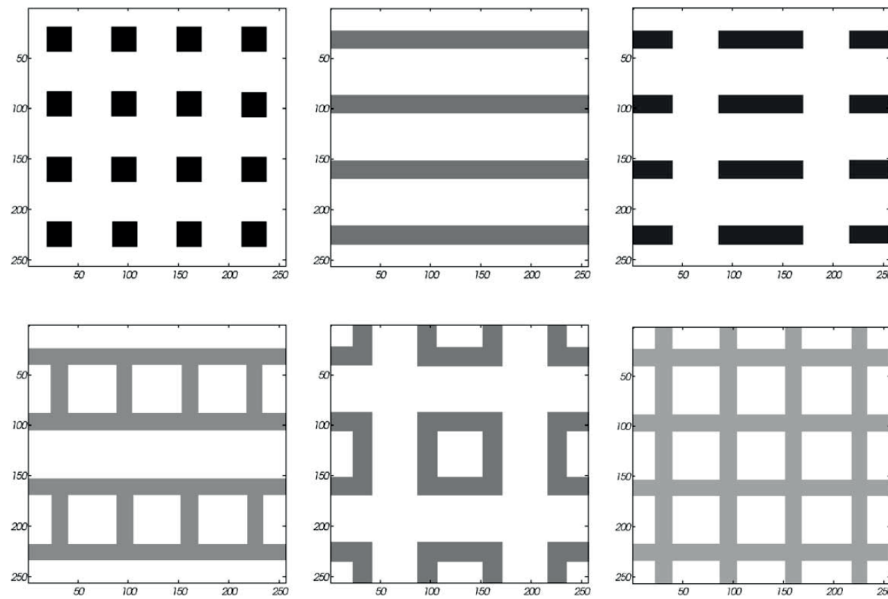


Figure 4.6 – Digital elevation models (DEMs) of the generic urban forms studied by Ratti et al. [2003] based on Martin and March [1972]. The shade of gray is indicative of the height (darker=higher). Top left to bottom right: pavilions, slabs, terraces, terrace-courts, pavilion-courts and courts. Source of image: Ratti et al. [2003].

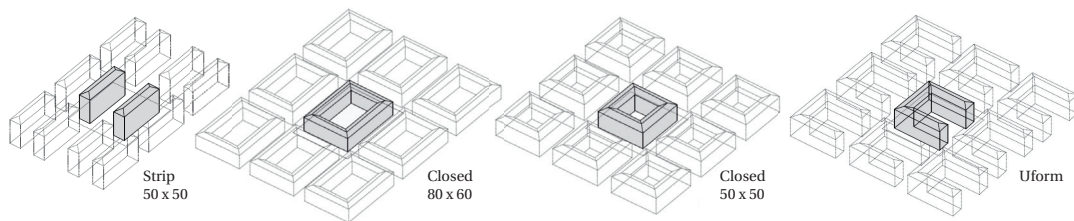


Figure 4.7 – Four typical building block designs identified and assessed by Kanters and Wall [2014]. Adapted from the original image found in the aforementioned source, licensed under CC BY 3.0.

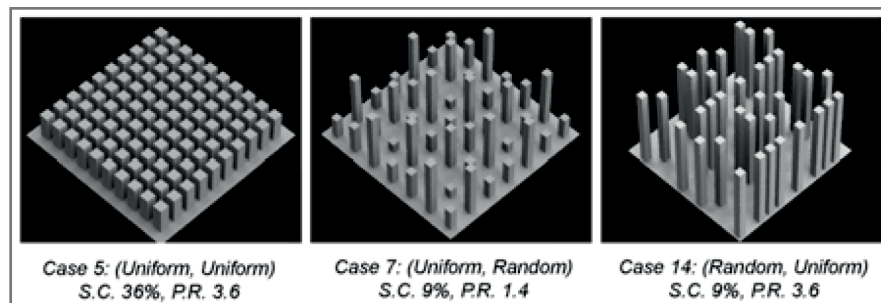


Figure 4.8 – Examples of models evaluated in Cheng et al. [2006] (source of the image).

## Chapter 4. Metamodel development

---

Relevant design parameters which did not conform to these criteria were considered either as fixed or as constraints to respect. Parameters related to point 1 were extracted from master plan documents including the ones cited above [SDOL and Gauthier, 2012; Urbaplan, 2015] and presented in chapter 3 (YLB-PDL study) [Bauart Architectes et Urbanistes SA et al., 2010], as well as through communication with the urban design firm that provided M0-M2 (Urbaplan).

Parameters most likely to affect building performance were identified through the outcome of our study presented in the previous chapter and by looking at multiple papers on the subject. From the main references listed in Table 4.3, we observe that building shape and layout - expressed by different measure such as the distance between buildings - were found to considerably affect the performance. To account for this impact both at the individual building scale and the neighborhood level, we judged that values quantifying the effect of the shading between buildings should be considered in addition to morphological parameters simultaneously capturing building and urban features.

When analyzing the highlighted parameters in the context of the third requirement above, a decision was made to separate design variables used for generating variants from the ones used as potential inputs to the metamodel. This distinction was necessary to ease the parametric modeling of variants while ensuring a relevant dataset for the metamodel training. For the 3D modeling, we needed one value per building, while in our metamodeling approach we wanted to use aggregated neighborhood values, as opposed to having a repetition of building-specific values. For example, if building height were to be used as an input to the metamodel, we would require one value per building, which would restrict the number of buildings to a fixed amount and increase the dimensionality of the inputs dataset. Instead, parameters considered as inputs, introduced in the next section, were chosen such that one value can be extracted for a set of buildings.

### Modeling workflow

In light of the above considerations, the height, depth and width of individual buildings were taken as variables for the 3D modeling, as well as the grid orientation. The ranges of design variables covered are presented in Table 4.4. The definition of each variable  $x$ ,  $y$ ,  $z$  and  $a$  can be seen in Fig. 4.9, with some example variants for each base case. For M0-M2, each variable's interval was specified by the urban design firm who provided the base designs (see also section 3.1.3). Similar values were used for M3-M5, for which only two dimensions were varied: height and length for the linear blocks and height and depth for the L-shaped and courtyard buildings. Values for M6 were set to generate 10- to 20-story high buildings.

Confining the design variables was necessary to bound the degrees of freedom in the parametric modeling. For this reason, the absolute position of each building was kept constant, except for the M0 case, where the number of buildings on each side and their length was randomly defined from the ranges specified in Table 4.4. Despite this condition, the relative layout of the buildings varies as a consequence of their dimension variations.

Table 4.3 – Examples of relevant sources regarding studies on the impact of geometrical parameters at the urban scale on various performance metrics.

| Source                          | Context   | Fixed parameters   | Variables   | Performance metric(s)  | Conclusions   |
|---------------------------------|---|--|---|--|---|
| Lobaccaro et al. [2012]         | Milan, individual versus surrounding building       | Urban context (9 blocks), volume of central building                                   | Central building shape (square, rectangular, triangular), height, footprint   | Maximize solar radiation (kWh/m <sup>2</sup> -y)   | 138% difference in facade radiation between building shapes; high reflectance > 60% can compensate shading, but with potential negative impacts e.g. glare, overheating   |
| van Esch et al. [2012]          | De Bilt, urban canyons, conventional solar dwelling | Building shape and size  | Street width, street direction, roof shape, envelope design   | Global radiation yield of canyon, direct irradiation on street, heat demand and solar heat gains   | Street width has significant influence on global radiation of canyon especially for E-W streets; street direction and roof shape have little impact on total radiation; solar dwelling with larger windows does not necessarily perform better than conventional dwelling |
| Takebayashi and Moriyama [2012] | Osaka, urban canyon                                 | Building materials and footprint   | Street width to building height ratio of canyon, street orientation, height and position of adjacent building                     | Surface temperatures, solar radiation gains  | Width/height ratio of canyon is the dominant factor on solar radiation gains on street and walls  |
| Hachem et al. [2012]            | Montreal, high efficiency residential dwellings     | Building height, floor area, window-to-wall ratio, materials, BIPV system and position | Building shape (rectangular versus L-shaped), aspect ratio, orientation, spacing between buildings, straight versus curved street | Relative heating and cooling energy consumption, relative electricity generation by south facing roof, spread of generation peak (hrs), energy balance | Main influencing parameters are shape of housing units and positioning on the site; heating load decreases with increasing distance and angle between buildings   |
| Pessenlehner and Mahdavi [2003] | Vienna, residential                                 | Volume, construction, internal gains, air change rate                                  | Compactness (shape), window-to-floor ratio per orientation  | Heating load, overheating index  | High correlation between heating load and compactness, higher when split between glazing ratios and orientations; weak correlation between overheating index and compactness, but higher when split between orientations  |

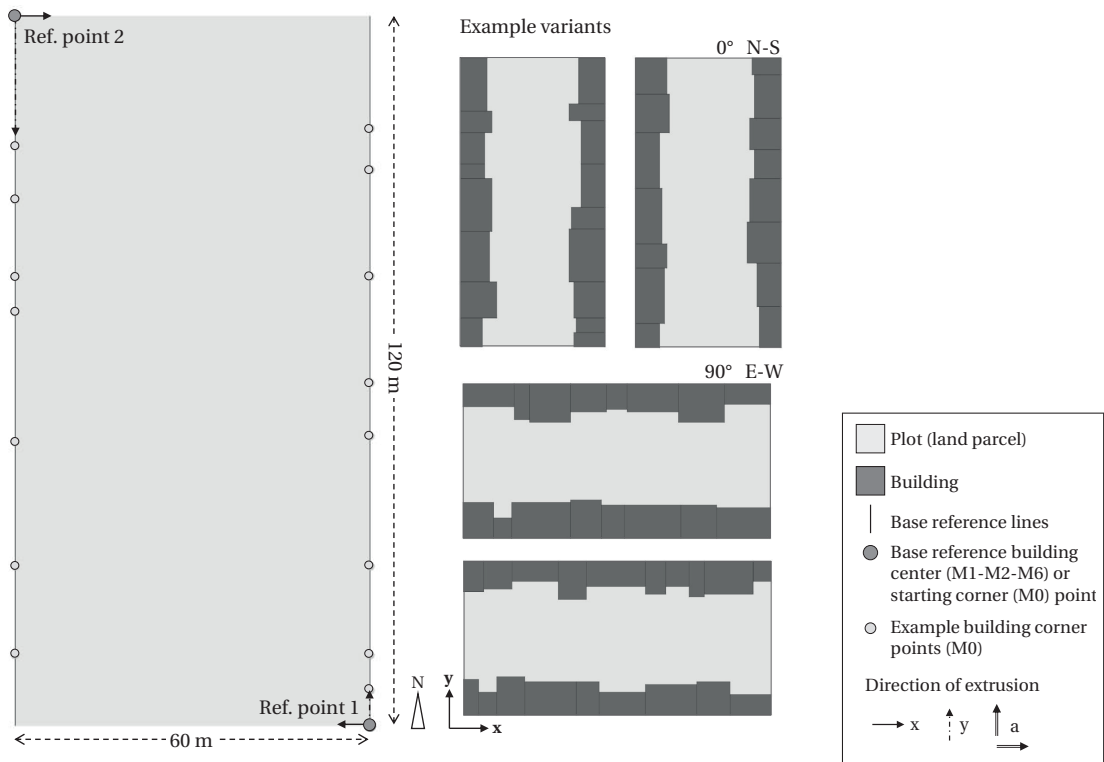
Table 4.4 – Variables range (in initial grid orientation coded as 0°), constraints when present and constant parameters. bldg(s): building(s), fp: building footprint. See Fig. 4.9 for definition of x, y, z, a.

|                           | M0          | M1       | M2       | M3                  | M4              | M5              | M6        |
|---------------------------|-------------|----------|----------|---------------------|-----------------|-----------------|-----------|
| Typology                  | Adjacent    | Low-rise | Mid-rise | Linear              | L-shaped        | Courtyard       | High-rise |
| Variable                  |             |          |          | Min:Step:Max        |                 |                 |           |
| Width (x) [m]             | 8:1:15      | 10:2:20  | 10:2:20  | fixed (75-122)      | fixed (54)      | fixed (28-71)   | 15:2:30   |
| Length (y) [m]            | 6:1:24      | 12:2:24  | 12:2:24  | 6:6:18 & 8:7:22     | fixed (54)      | fixed (28)      | 15:2:30   |
| Height (z) [story]        | 2:1:4       | 3:1:6    | 4:1:8    | 1:2:5 & 2:3:8       | 1:2:5 & 2:3:8   | 1:2:5 & 2:3:8   | 10:1:20   |
| Depth (a) [m]             | -           | -        | -        | -                   | 6:6:18 & 8:7:22 | 6:5:16 & 8:5:18 | -         |
| Constant/Constraint       |             |          |          | Condition/Value     |                 |                 |           |
| Floor height [m]          |             |          |          | 3 meters for all Ms |                 |                 |           |
| Dist b/w bldgs (d) [m]    | =0          | 6≤d≤20   | 6≤d≤20   | -                   | -               | -               | 6≤d≤20    |
| Number of bldgs (n)       | 8≤n/side≤14 | 4/side   | 4/side   | 5                   | 3               | 3               | 8/side    |
| Min plot ratio            | 0.9         | 0.9      | 0.9      | -                   | -               | -               | -         |
| Bldg fp [m <sup>2</sup> ] | 50          | 200      | 200      | -                   | -               | -               | -         |

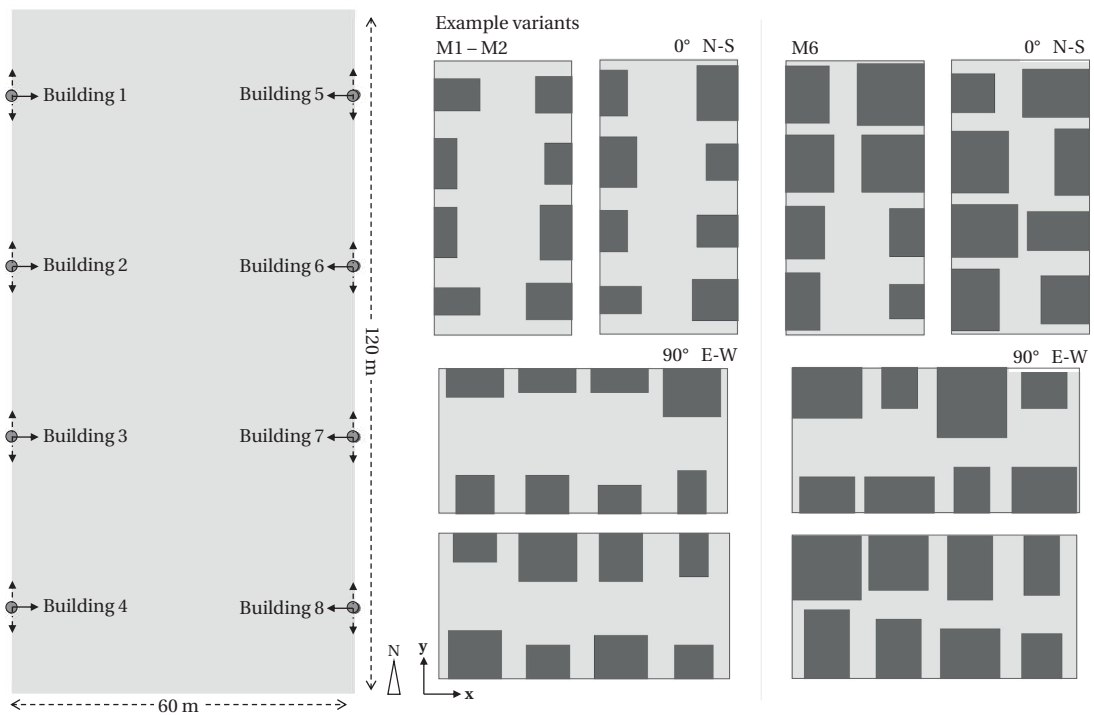
Table 4.5 – Comparison values for office building dimensions from Deru et al. [2011]; SIA [2015].

|                                    | Small office<br>(≤ 6 workplaces) | Medium-Large office<br>(> 6 workplaces) |
|------------------------------------|----------------------------------|---|
| Number of floors                   | -; 1                             | -; 12                                   |
| Story height (m)                   | 3; 3.05                          | 3; 2.74                                 |
| Total floor area (m <sup>2</sup> ) | -; 511                           | -; 46 320                               |
| Length of 1 room (m)               | 6;-                              | 12;-                                    |
| Depth of 1 room (m)                | 6;-                              | 12;-                                    |





(a) M0



(b) M1-M2-M6

Figure 4.9 – Top view of base case Rhino design (left) from which variants are generated (examples on the right) for each case  $M_i$ .

## Chapter 4. Metamodel development

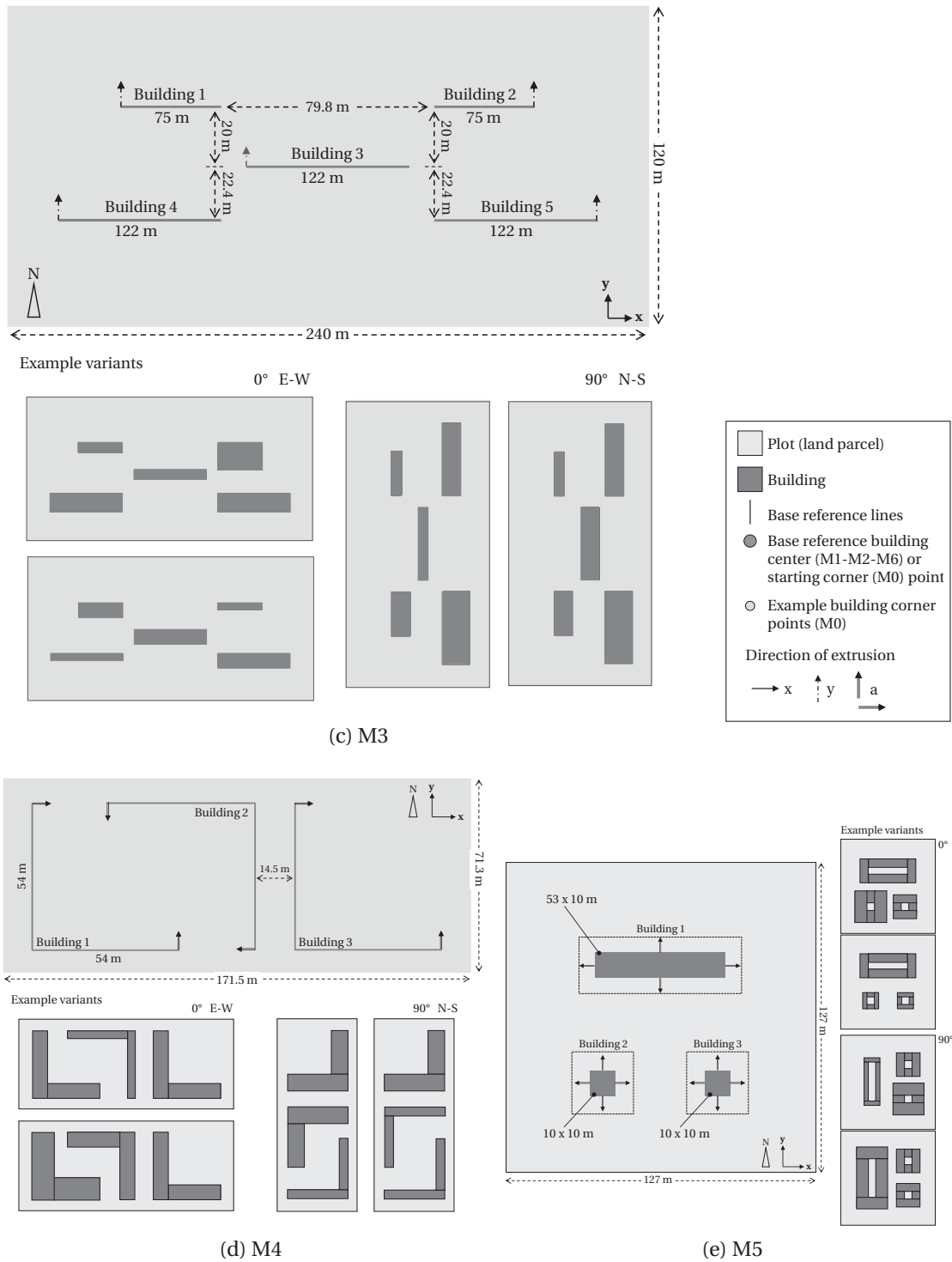


Figure 4.9 – (Continued) Top view of base case Rhino design (left) from which variants are generated (examples on the right) for each case  $M_i$ .

With these combinations of parameters, a generated building can theoretically have a total floor area between 96 and 21 472 m<sup>2</sup>. For comparison, Table 4.5 lists common values found in the Commercial Reference Building Models of the National Building Stock of the U.S. Department of Energy [Deru et al., 2011] and the SIA 2024 document *Données d'utilisation des locaux pour l'énergie et les installations du bâtiment* [SIA, 2015]. These dimensions correspond to small and medium to large office buildings, which is the program defined in our simulation as detailed later in section 4.2.4.

A parametric modeling workflow was set-up using Rhino<sup>4</sup> and Grasshopper<sup>5</sup>, in the same way as explained in section 3.1.3, and starting from the base case Rhino designs illustrated in Fig. 4.9. Windows were modeled equally on each facade, using constant distances (e.g. between window side and building edge) and sizes (e.g. window height), producing window-to-wall ratios ranging from 44% to 48%.

The 3D models were generated through an iterative sequence by reading the value of each variable to be applied to each building from an Excel file previously generated. The method for defining these values is explained below. At every iteration, i.e. for each design, a series of automated actions took place to extract all the information necessary to populate our database of inputs and outputs, needed for the metamodeling phase. This procedure is detailed in the next sections.

### Solution space sampling

From the ranges of design variables in Table 4.4 for each case  $M_i$ , a series of values had to be selected for each building to generate the design variants. For M0-M2 and M6, this selection was done via a random sampling algorithm as explained in section 3.1.3, which included a constraints verification to ensure all generated variants respected the specified minimum plot ratio and building footprint. For M3 to M5, we followed the Design of Experiment (DoE) approach and used a 3-level Box-Behnken design<sup>6</sup> to generate the variants. Illustrated in Fig. 4.10, the Box-Behnken design treats the minimum, median and maximum value, coded as -1, 0 and +1, of each design variable as possible options. It falls under the category of response surface designs, whose purpose is to allow estimating the interaction and eventual quadratic

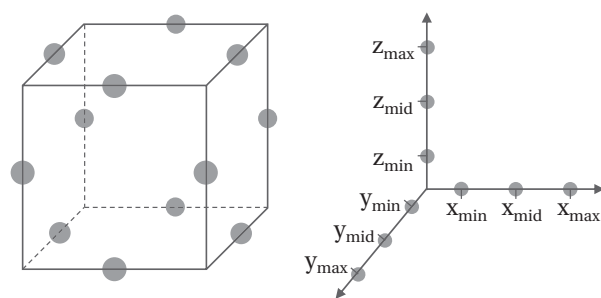


Figure 4.10 – Sampling technique for M3-M5: 3-level Box-Behnken Design of Experiment, visually directly translatable to our x, y, z design variables (Table 4.4).

<sup>4</sup><https://www.rhino3d.com/> (last accessed on March 20, 2016)

<sup>5</sup><http://www.grasshopper3d.com/> (last accessed on March 20, 2016)

<sup>6</sup><http://www.itl.nist.gov/div898/handbook/pri/section3/pri3362.htm> (last accessed on March 19, 2016)

effects between factors, while covering the design space in a more efficient way than by varying one factor at a time (referred to as a full factorial design). In our case, two Box-Behnken designs with a shifted range were used to increase the number of sampled points. All variants generated were duplicated with a 90° grid rotation with respect to their initial alignment.

Both the random sampling and DoE-based approaches for acquiring data are valid experimental methods found among multiple others [Simpson et al., 2014]. Although they ensure some level of coverage of the possible solution space, this is not explicitly exploited through our approach, since we are making a distinction between the parametric design variables and the input parameters to be used for predicting the performance, as aforementioned. The experimental methods for sampling the solution space apply only to the former, while the latter are subsequently derived instead of being directly controlled. Irrespective of this situation, some techniques exist to refine the selection of designs in order to improve the information gain, a topic that is addressed later on.

### 4.2.3 Computation of predictors (inputs)

We will interchangeably use the words inputs, predictors or parameters to refer to the set of potential inputs ( $\mathbf{x}$ ) to the predictive functions developed in upcoming sections.

The design variations prompted by the parametric modeling procedure affect multiple other parameters at the neighborhood scale such as the street width, density, and solar exposure levels of the buildings. To capture these changes and keeping in mind the design variable requirements exposed earlier, an extensive amount of geometry- and irradiation-based parameters were computed at the neighborhood scale and used to populate the inputs dataset. Table 4.6 lists the complete set, which includes most of the metrics tested in chapter 3, along with complementary parameters identified as relevant from the literature (see Table 4.3).

The process for extracting the predictors is similar to what was presented in section 3.1.3 and 3.1.4. All geometry-based parameters were computed via a Grasshopper script. The raw irradiation data was obtained through an annual simulation using GenCumulativeSky in DIVA-for-Grasshopper [Jakubiec and Reinhart, 2011; Robinson and Stone, 2004]. A grid of nodes with a resolution of 1 meter was used, and the number of ambient bounces<sup>7</sup> was set to 2. The EnergyPlus weather data file for Geneva, Switzerland [EnergyPlus, 2014] was used.

Both the geometrical information and the irradiation simulation output were exported to Excel using gHowl<sup>8</sup> and further processed in Matlab, where the irradiation-based parameters were computed.

---

<sup>7</sup>The number of ambient bounces (-ab) corresponds to the maximum number of diffuse bounces computed by the indirect radiation calculation. Other Radiance parameters were kept at their default values: number of ambient divisions -ad = 1000, number of ambient super-samples -as = 20, ambient resolution -ar = 300, and ambient accuracy -aa = 0.1 Full descriptions can be found at [http://www.siggraph.org/education/materials/HyperGraph/raytrace/radiance/man\\_html/rpict.1.html](http://www.siggraph.org/education/materials/HyperGraph/raytrace/radiance/man_html/rpict.1.html) (last accessed on April 8, 2016).

<sup>8</sup><http://www.grasshopper3d.com/group/ghowl> (last accessed on March 20, 2016)

Table 4.6 – List of geometry- and irradiation-based parameters representing potential performance predictors (inputs to the metamodells). Envelope includes all exposed facades and roof. TFA: total floor area; TEEA: total exposed envelope area

| Abbreviation              | Description  |
|---------------------------|--|
| <b>Geometry-based</b>     | [-]  |
| <i>PlotRatio</i>          | Density indicator: ratio between TFA and constructible land area   |
| <i>SiteCoverage</i>       | Density indicator: ratio between footprint area and constructible land area                                |
| <i>FormFactor</i>         | Compactness indicator: ratio between TFA and TEEA  |
| <i>RoofRatio</i>          | Total roof area divided by total exposed envelope area   |
| <i>NorthFacRatio</i>      | Total exposed north-facing facade area divided by TEEA   |
| <i>EastFacRatio</i>       | Total exposed east-facing facade area divided by TEEA  |
| <i>SouthFacRatio</i>      | Total exposed south-facing facade area divided by TEEA   |
| <i>WestFacRatio</i>       | Total exposed west-facing facade area divided by TEEA  |
| <i>WWRatio</i>            | Glazing ratio indicator of level of opening: ratio between total window area and total exposed facade area |
| <i>WFRatio</i>            | Glazing ratio indicator of level of opening: ratio between total window area and TFA                       |
| <i>MeanHeight</i>         | Average building height [meters]   |
| <b>Irradiation-based</b>  | [kWh/m <sup>2</sup> <sub>surface area or floor area</sub> ]  |
| <i>MeanEnvelopeIrrad</i>  | Average irradiation on all exposed envelope surfaces   |
| <i>MeanRoofIrrad</i>      | Average irradiation on all exposed roofs   |
| <i>MeanFacIrrad</i>       | Average irradiation on all exposed facades   |
| <i>MeanNorthFacIrrad</i>  | Average irradiation on north-facing facades  |
| <i>MeanEastFacIrrad</i>   | Average irradiation on east-facing facades   |
| <i>MeanSouthFacIrrad</i>  | Average irradiation on south-facing facades  |
| <i>MeanWestFacIrrad</i>   | Average irradiation on west-facing facades   |
| <i>EnvelopeIrradPerFA</i> | Total irradiation on all exposed envelope surfaces divided by total floor area                             |
| <i>RoofIrradPerFA</i>     | Total irradiation on all exposed roofs divided by total floor area   |
| <i>FacIrradPerFA</i>      | Total irradiation on exposed facades divided by total floor area   |
| <i>NorthFacIrradPerFA</i> | Total irradiation on north-facing facades divided by total floor area                                      |
| <i>EastFacIrradPerFA</i>  | Total irradiation on east-facing facades divided by total floor area                                       |
| <i>SouthFacIrradPerFA</i> | Total irradiation on south-facing facades divided by total floor area                                      |
| <i>WestFacIrradPerFA</i>  | Total irradiation on west-facing facades divided by total floor area                                       |

### 4.2.4 Simulation of responses (outputs)

The outputs, or values to be predicted by the metamodels, correspond to the reference metrics measured in chapter 3 falling under the passive solar performance criteria. However, from now on, we use the term passive solar potential as referring only to the energy need for heating and cooling, while the daylight potential is considered as a separate criterion. Using the EnergyPlus weather file for Geneva, these metrics are obtained through full climate-based simulations as detailed below. The algorithm for quantifying the third performance criterion considered, the active solar potential, is described in section 4.6.

#### Passive solar potential: energy need

As seen in chapter 1, the energy consumption distribution in buildings is dominated by the heating need in a climate like Switzerland's. To reduce this need and achieve the targets established by various regulations and labels, it is essential to prioritize passive measures related to the built form, in addition to complying with the imposed values regarding for instance the thermal envelope (e.g. U-value). The energy need for both heating and cooling is an indicator of how far we are from comfortable thermal conditions. Although the cooling need is sometimes absent if no systems are (allowed to be) installed, in highly insulated and glazed modern buildings, maintaining a comfortable indoor temperature in summer is often an important issue. As such, the cooling need quantifies the energy that would be needed to achieve these comfortable conditions. When settings related to internal gains and systems are maintained constant, one of the main influences<sup>9</sup> on the heating and cooling needs comes from solar heat gains and shading from the sun caused by surrounding buildings.

To obtain the floor-area-normalized energy need, the initial EnergyPlus input files (.idf) were generated via the Grasshopper plug-in Archsim<sup>10</sup>. They were then processed in Matlab before executing the simulation to obtain the annual energy need based on an ideal loads air system, as explained in section 3.1.4. Each building floor, of 3 meter high, was modeled as a thermal zone. The simulation results were summed over all zones and buildings and normalized by the total floor area for each design variant. In the following sections, we simply use the term energy to refer to this metric. Additional energy simulation settings are listed in Table 4.7, along with comparison values extracted from various standards.

It is to note that simulation batches were run in collaboration with a colleague<sup>11</sup> for different simulation settings, including three levels of U-values (low, medium, high). Since investigating interactions with such detailed parameters is out of the scope of this work, we have limited our study to a unique set of simulation settings. The moderate U-value case was retained, so as to ensure some level of variation in the energy need to facilitate the metamodel fitting. This

---

<sup>9</sup>Natural ventilation is also an important passive measure, which requires CFD simulations and falls outside the scope of this thesis.

<sup>10</sup><http://archsim.com/> (last accessed on March 20, 2016)

<sup>11</sup>Parag Rastogi, doctoral assistant at LIPID, contributed in defining the simulation settings and managing the computational resources for executing the simulation tasks.

topic is further discussed in section 4.7.3 and chapter 7, where we also show that low U-values attenuate the differences in the heating need across the design variants, diluting the effect of their diversity of features captured through urban morphological parameters. The U-values corresponding to the dataset used in this chapter are higher than the target from the SIA, yet closer to what can currently be encountered in other studies (e.g.  $1.15 \text{ W/m}^2\text{K}$  for walls in [LSE Cities and EIFER, 2014]) and contexts (e.g. climate- and construction period-referenced databases [Deru et al., 2011]). Moreover, considering that a larger amount of material with an associated higher cost and embodied energy are required for achieving low U-values, it is of interest to see the performance level that can be reached only through morphological changes. In any case and as mentioned in chapter 3, we emphasize that the purpose of the study is not to derive concrete design guidelines, which are dependent upon the simulation assumptions as further demonstrated in section 7.2.

An office function and associated occupancy schedule was defined. There was no specific motivation behind that choice except that it was considered a better match to the relatively high window-to-wall ratio, closer to an office than a residential building.

Future work, addressed in section 4.7 and chapter 7, includes looking at the additional data acquired. Along the same lines, work was initiated to define fully residential neighborhoods as well as mixed-used scenarios (including both office and residential units). Regardless of the source and underlying assumptions of the dataset, the main steps in the workflow described in the next section are applicable.

### **Daylight potential: spatial Daylight Autonomy**

The artificial lighting demand also weights heavily in the energy consumption, particularly in administrative buildings as seen in chapter 1. This need can be partly substituted through daylighting whose potential is here quantified by the sDA as defined in section 3.1.4. This metric was computed from illuminance data obtained through a DIVA-for-Grasshopper simulation, with the settings shown in Table 4.8. The occupancy schedule was defined to cover most daylight hours as opposed to representing a clear building function (e.g. office). This allows comparing between design variants without assuming any fixed function. To reduce computational time, simulation is done at the ground floor level only, representing a worst-case scenario with respect to upper building levels. No blinds were simulated due to limitations in the tool. Both the terms daylight and sDA are used to refer to this metric in this chapter.

## Chapter 4. Metamodel development

Table 4.7 – Settings for the energy need simulations with reference values for comparison. \*[SIA, 2015], \*\*[SIA, 2009b], \*\*\*[Deru et al., 2011].

| Parameter                           | Setting  | Comparison values  |
|-------------------------------------|--|--|
| Building function                   | Office   | (values below for offices as well)   |
| Heating/cooling set point           | 20/26°C  | 21/26°C *;<br>20°C ambient temperature **  |
| Loads                               |  |  |
| Equipment                           | 12 W/m <sup>2</sup>  | 7-10 W/m <sup>2</sup> *  |
| Lighting                            | 3 W/m <sup>2</sup> (300 lux set point)                         | 12.5-15.9 W/m <sup>2</sup><br>(500 lux set point) *  |
| Occupancy                           | 0.05 people/m <sup>2</sup><br>8.75 h/week-day                  | idem **/***; 0.07-0.1 *<br>7.2 h/week-day *  |
| Ventilation                         | 0.0125 m <sup>3</sup> /s person                                | 0.01 m <sup>3</sup> /s person *  |
| Infiltration                        | 0.1 ach  | 0.15-0.3 ach (target-existing) *;<br>0.62 ach ***  |
| Conductivity                        |  |  |
| Wall                                | U = 1.3 W/m <sup>2</sup> K                                     | 0.2 W/m <sup>2</sup> K limit **;<br>0.8 W/m <sup>2</sup> K (existing) *                                  |
| Roof                                | U = 1.84 W/m <sup>2</sup> K                                    | 0.2 W/m <sup>2</sup> K limit **;<br>0.8 W/m <sup>2</sup> K (existing) *                                  |
| Floor                               | U = 1.25 W/m <sup>2</sup> K                                    | 0.2 W/m <sup>2</sup> K limit **;<br>0.8 W/m <sup>2</sup> K (existing) *                                  |
| Windows<br>(double low e argon)     | U = 1.5 W/m <sup>2</sup> K<br>≈ 44-48% glazing ratio           | 1.3 W/m <sup>2</sup> K limit **;<br>1.5 W/m <sup>2</sup> K (existing)*<br>50% for west-oriented facades* |
| Solar protections<br>Activated when | Venetian blinds<br>Incident irradiation ≥ 180 W/m <sup>2</sup> |  |

Table 4.8 – Settings for the daylight simulation.

| Parameter                             | Setting      |
|---------------------------------------|--------------|
| Windows                               | double-argon |
| Occupancy                             | 8am - 10pm   |
| Illuminance target                    | 300 lux      |
| Sensor grid resolution                | 2 m          |
| Sensor grid height above ground floor | 0.8 m        |



### 4.3 Selection of metamodel form

The reference dataset of inputs and outputs is thus populated following the above-mentioned steps of modeling and simulation. A model function must be selected to guide the following steps of data analysis and metamodel development. While options from which to choose from are theoretically infinite, many of them would not perform well when applied to new, unseen data [Forrester et al., 2008], i.e. to predict the performance of a new neighborhood design. Our approach follows Occam's Razor: "*all things being equal, the simplest solution tends to be the best one*". That is, minimizing the complexity of a model tends to improve its generalization to unseen data [Forrester et al., 2008]. As such, a multiple linear regression model form is selected as a starting point. In section 4.5, trials are made with different settings e.g. to investigate the effect of including interaction terms.

As seen in Table 4.1, multiple linear regression assumes a linear relation between inputs and the output and is relatively easy to use and interpret. It takes the form of the following equation [Hastie et al., 2009]:

$$y = f(\mathbf{x}) + \varepsilon = \beta_0 + \sum_{i=1}^p \beta_i x_i + \varepsilon \quad (4.1)$$

where  $f(\mathbf{x})$  is the predictive function we want to define to estimate the real output  $y$ , which is in our case the simulated reference values.  $\varepsilon$  is the prediction error.  $\beta_0$  is a constant (or intercept) term and  $\beta_i$  the coefficient for input parameter  $x_i$ .

It is important to note that there are potential issues associated to the use of multiple linear regression. Some of the main ones, placed in the context of our study, are<sup>12</sup>:

- Strong dependency of the input coefficients and contribution to error reduction on the presence/absence of other parameters present in the model function. Linked to the possibility of having multi-collinearity among the inputs. If some parameters are strongly correlated, it is no longer possible to interpret outcomes during the metamodeling process. Considering our starting set of potential inputs, this is particularly relevant and further addressed in section 4.5.5.
- Extrapolation beyond the scope of the metamodel, occurring when the function is applied on new data whose input values are out of the range 'seen' by the metamodel. In such unknown regions, the prediction may be far from the expected output. This issue is investigated in chapter 6.
- Over-fitting: the  $\beta$  parameters are fitted too closely to the sample data, and capture more than the underlying relationships among the inputs and outputs [Forrester et al., 2008]. This extra information represents artifacts that we would like to avoid being included in the model, which we hope to be able to apply with confidence on new neighborhood designs for predicting their performance. We return on this risk of over-fitting in the next sections.

<sup>12</sup><https://onlinecourses.science.psu.edu/stat501/node/343> (last accessed on April 2, 2016).

### 4.4 Data analysis

Before proceeding with fitting the metamodel, the data must be examined for potential anomalies/outliers. An analysis is also conducted to identify any correlation between inputs and outputs, as well as among inputs. These checks respectively help identify the relevant and redundant parameters prior to fitting the metamodel. The significance of this information is further addressed in section 4.5.

It is to note that although both the energy and daylight simulations were automated from within the same modeling and simulation workflow via Grasshopper, the total number of design variants for which outputs were collected differs between the two performance metrics. Due to the simulation set-up, available computational resources, as well as the removal of some data due to errors detected, the energy dataset contains only a fraction of the designs present in the daylight dataset. In total, 624 variants (or data points) are included in the energy dataset, against 2060 in the daylight dataset. M2 is altogether absent in the former, due to errors detected in the simulated geometry. However, considering that this case falls between M1 and M6 in terms of morphology, layout and dimension ranges, its loss is considered as minor. In the following, we distinguish between the two datasets both in the text and figures.

#### 4.4.1 Distributions

Figures 4.11 and 4.12 show the distribution of each input for the energy and daylight datasets respectively, distinguishing between the seven case series. The histograms produced by merging all cases can be seen in appendix A.1.

As the geometry- and irradiation-based parameters were not directly controlled when generating the design variants, as explained earlier, non-uniform distributions like the ones observed for most inputs were to be expected. However, the ranges spanned are good representations of what can be found in real, constructed neighborhoods. Table 4.9 gives some comparison values from various sources for some of the geometry-based parameters.

Although higher frequencies are observed for the daylight dataset due to its larger size, the range spanned by each parameter and the shape of the histograms are similar to the ones observed for the energy dataset. When looking at individual case series, we observe clusters, for instance for the *PlotRatio* parameter where the tower typology of M6 pushes this series towards higher values, creating a gap around a plot ratio of 5. The higher values are above what is commonly found based on Table 4.9. In the current context of deriving a predictive function from a dataset, we are more concerned with covering a wide range than closely sticking to commonly encountered values. Our narrow *WWRatio* is caused by the window modeling method as previously explained. The latter parameter was explicitly kept close to a constant to reduce the number of variables and ease the parametric modeling. Transforming this parameter into a variable should be addressed in future work, as discussed in section 4.7. The *WFRatio* is instead used to capture the diversity in glazing ratio.

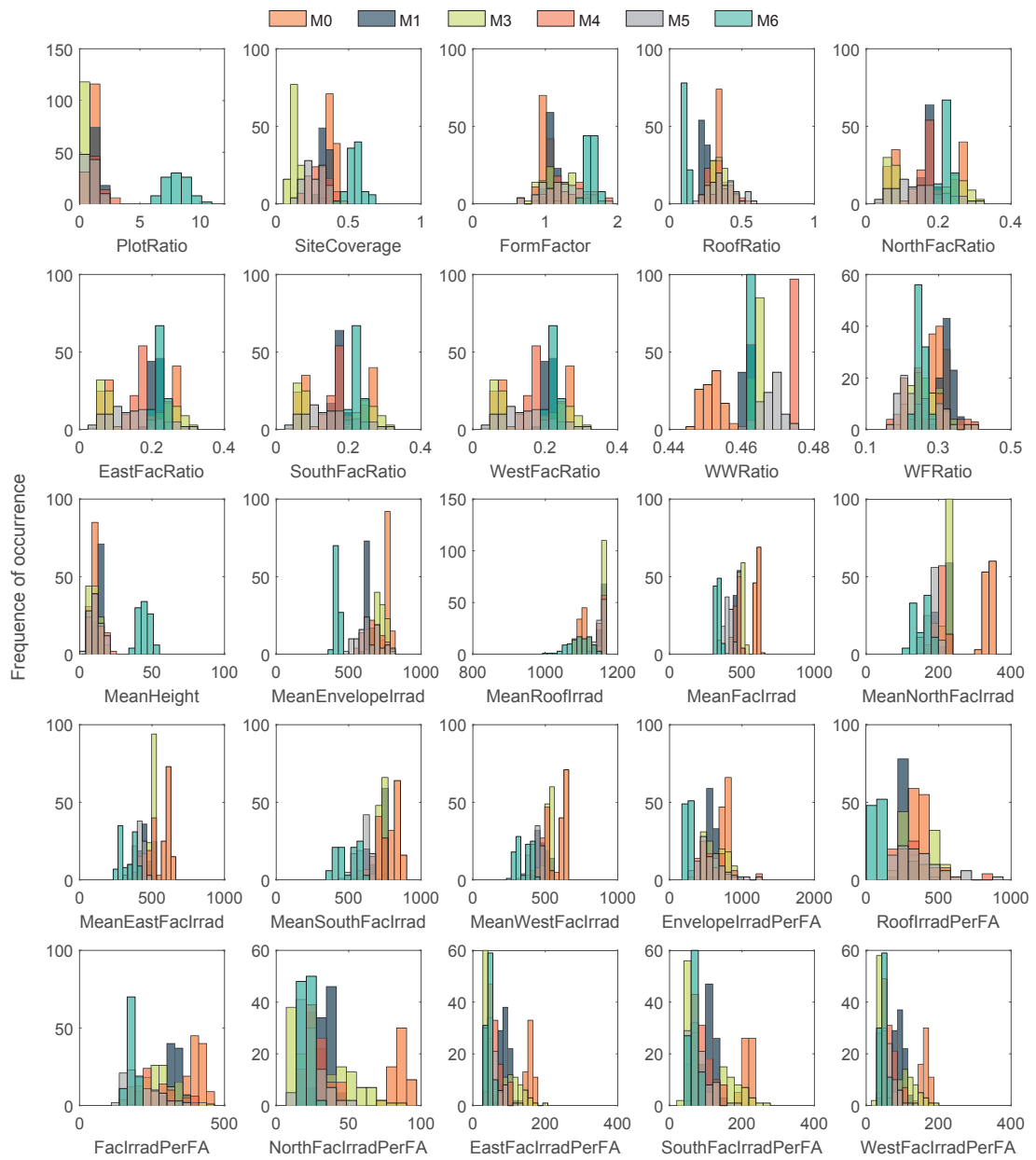


Figure 4.11 – Parameters distribution for each case series ( $M_i$ ) for the **energy** [ $\text{kWh}/\text{m}_{\text{FA}}^2$ ] dataset.

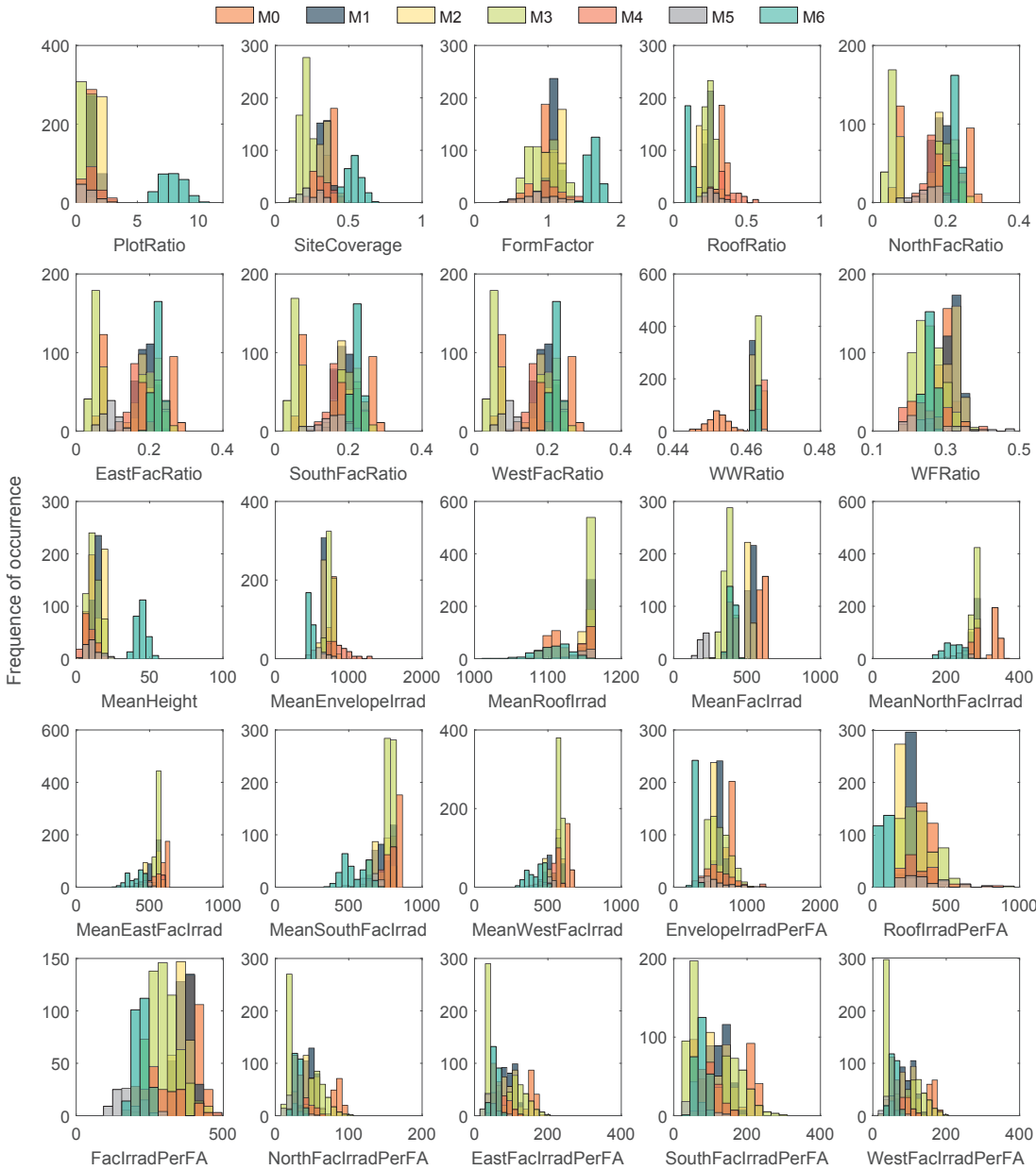


Figure 4.12 – Parameters distribution for each case series ( $M_i$ ) for the **daylight** [%] dataset.

Table 4.9 – Comparison values for some geometry-based parameters. Sources: (1) [LSE Cities and EIFER, 2014], (2) [Zhang et al., 2012a], (3) [Knowles, 2003], (4) [SIA, 2015], (5) [Steemers, 2003], (6) [Laëtitia et al., 2011].

| Parameter           | Range/Value | Context   | Source |
|---------------------|-------------|---|--------|
| <i>PlotRatio</i>    | 1.7-3.3     | regular urban block   | (1)    |
|                     | 1-5         | compact urban block   |        |
|                     | 0.2-1.7     | slab/terraced/detached housing  |        |
|                     | 1           | minimum recommended   |        |
|                     | 2.7-5.3     | range for studied zones in the cities of Amsterdam, Barcelona and Paris                     | (2)    |
| <i>SiteCoverage</i> | 30-50%      | regular urban block   | (1)    |
|                     | 30-65%      | compact urban block   |        |
|                     | 5-35%       | slab/terraced/detached housing  |        |
|                     | 20-75%      | range for studied zones in the cities of Amsterdam, Barcelona and Paris                     |        |
| <i>FormFactor</i>   | 1.7         | regular urban block   | (1)    |
|                     | 1-3.3       | compact urban block   |        |
|                     | 0.7-2.2     | slab/terraced/detached housing  |        |
|                     | 1.7         | minimum recommended   |        |
|                     | 0.3-5.3     | range for city of Los Angeles   |        |
| <i>WWRatio</i>      | 50%         | west-oriented facades of office buildings   | (4)    |
|                     | 40%         | modeling assumption in comparative study  | (1)    |
|                     | 25-38%      | range of optimal ratios (min. energy consumption) according to height for London case study | (5)    |
| <i>WFRatio</i>      | 17%         | French policy for optimal daylight and comfort  | (6)    |

The histograms of the simulated responses are shown in Fig. 4.13 and 4.14 for each case series as well as for the whole dataset. The majority of cases in the energy dataset fall near the 40 and 50 kWh/m<sup>2</sup> regions. For comparison, we have plotted the range of heating energy for existing small to large office buildings (hatched rectangle) [SIA, 2015], as well as the histogram of the SIA heating limits ( $Q_{h,lim}$ ), corresponding to new administrative (office) buildings and computed based on the formula and default values given in SIA [2009b]:

$$Q_{h,lim} = Q_{h,lim0} + \Delta Q_{h,lim} \times A_{th} / A_E \quad (4.2)$$

where  $Q_{h,lim0}$  and  $\Delta Q_{h,lim}$  are limit values depending on the type of building (here 65 MJ/m<sup>2</sup> and 85 MJ/m<sup>2</sup>),  $A_{th}$  is the surface of the thermal envelope and  $A_E$  the energy reference area (total floor area in our case). The limit is computed for each case by inserting its (inverted) form factor, one of the parameters already computed, in the formula and applying a conversion factor of 0.278 kWh/MJ to obtain kWh/m<sup>2</sup>.

The distribution associated to the limit values falls below our simulated energy needs, which is to be expected since the latter contain the cooling need in addition to the heating need. Moreover, as mentioned in section 4.2.4, our simulation settings do not exactly match the SIA

assumptions. Nevertheless, this comparison serves to demonstrate that our range covers a domain of realistic values and that it may be possible to fall below the SIA limit despite the unfavorable thermal envelope.

The sDA distributions shown in Fig. 4.14 vary between case series from narrow - e.g. M1, M6 - to wider - e.g. M4, M5 - ranges. In the graph holding all cases, dashed lines have been added for reference: the nominally accepted daylight sufficiency of 55% and the preferred daylight sufficiency of 75%, as recommended by IESNA [2012]. It must be remembered however that the official method for computing the sDA has not been exactly applied, as explained in section 3.1.4. Moreover, the values obtained are only for the ground floor level and are thus likely to be more conservative. For our purpose of learning a metamodel, it is of interest to have a wide span over the possible performance values, which correspond to [0, 100] in the case of the sDA. This is achieved through the combined M cases.

### 4.4.2 Correlations

It is important to look at the possible correlations, both between pairs of input parameters as well as between each input and output. This analysis can provide support in tuning and interpreting results in the metamodeling process detailed in the next section. The correlation level is here quantified using Pearson's linear correlation coefficient obtained via the *corr* Matlab function<sup>13</sup>.

Figure 4.15 shows a matrix view of the correlation level between each pair of inputs in the two datasets. White, gray and black squares respectively represent a perfect positive (+1), the absence of (0), and a perfect negative (-1) correlation. It is to note that, as observed in chapter 3, these correlation results stem from the parametric modeling, i.e. the way variants were generated and the fact that they were duplicated with a 90° rotation. As such, we observe some correlation among the North-East-South-West parameters and between the plot ratio, roof ratio and mean height. The presence of both white and dark zones highlights the need to take care of collinearity between the inputs when interpreting results from the model fitting. This is addressed in section 4.5.5.

To avoid redundancy there is thus a need to reduce the dimensionality of the inputs sets. Yet, we don't want to ignore parameters strongly linked to the output we are trying to predict. This link is shown in Fig. 4.16 and 4.17 for each dataset, with distinction between the different case series. The pairwise linear correlation coefficient, computed over all cases taken together, is displayed for combinations for which it was found to exceed ( $\pm$ )0.70. This is the case for the *FormFactor*, *EnvelopeIrradPerFA* and *FacIrradPerFA* in the daylight dataset, and for the same three parameters with the addition of the *RoofIrradPerFA* in the energy dataset. The same graphs plotted without distinction between the cases can be found in appendix A.1.

---

<sup>13</sup><http://www.mathworks.com/help/stats/corr.html> (last accessed on April 2, 2016)

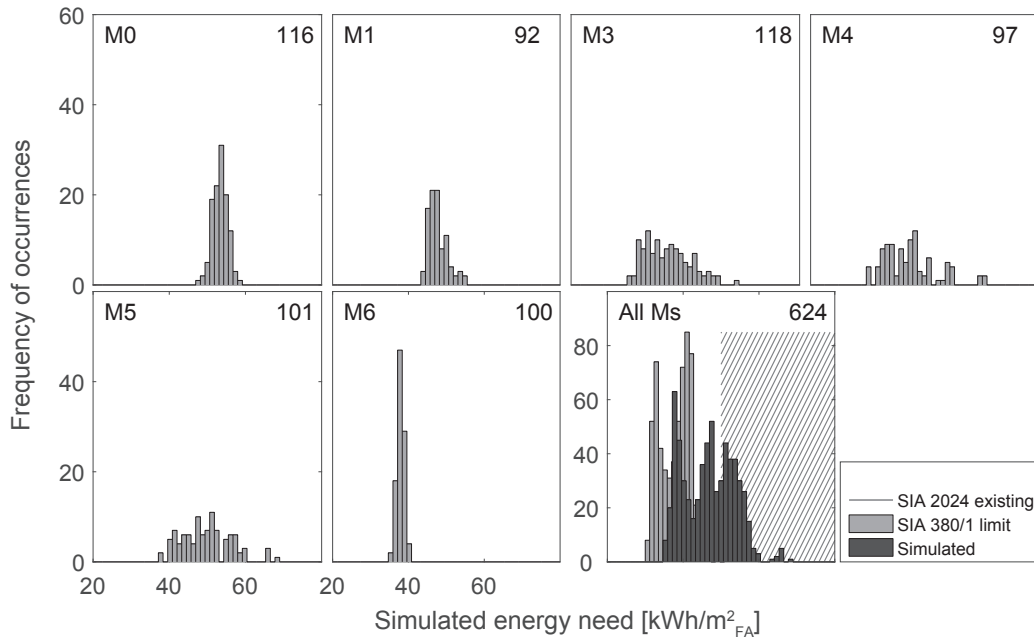


Figure 4.13 – Histograms of the simulated energy need distribution for each case series and over all variants together (bottom right graph). The number in the top right corner represents the amount of data points in the respective histogram. Comparative ranges - existing office buildings [SIA, 2015] (hatch) and SIA limits [SIA, 2009b] (light-gray histogram) - are shown in the background of the bottom right overall graph.

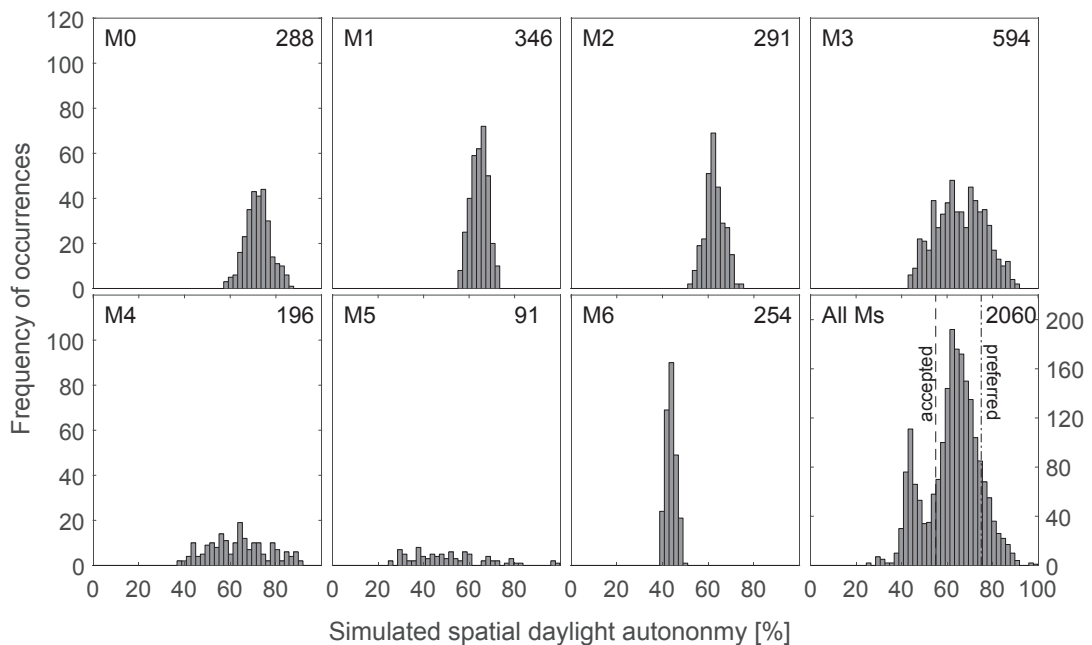


Figure 4.14 – Histograms of the simulated spatial daylight autonomy distribution for each case series and over all variants together (bottom right graph). The number in the top right corner represents the amount of data points in the respective histogram. The nominally accepted 55% and preferred 75% thresholds defined by the IESNA [2012] are shown on the bottom right overall graph.

## Chapter 4. Metamodel development

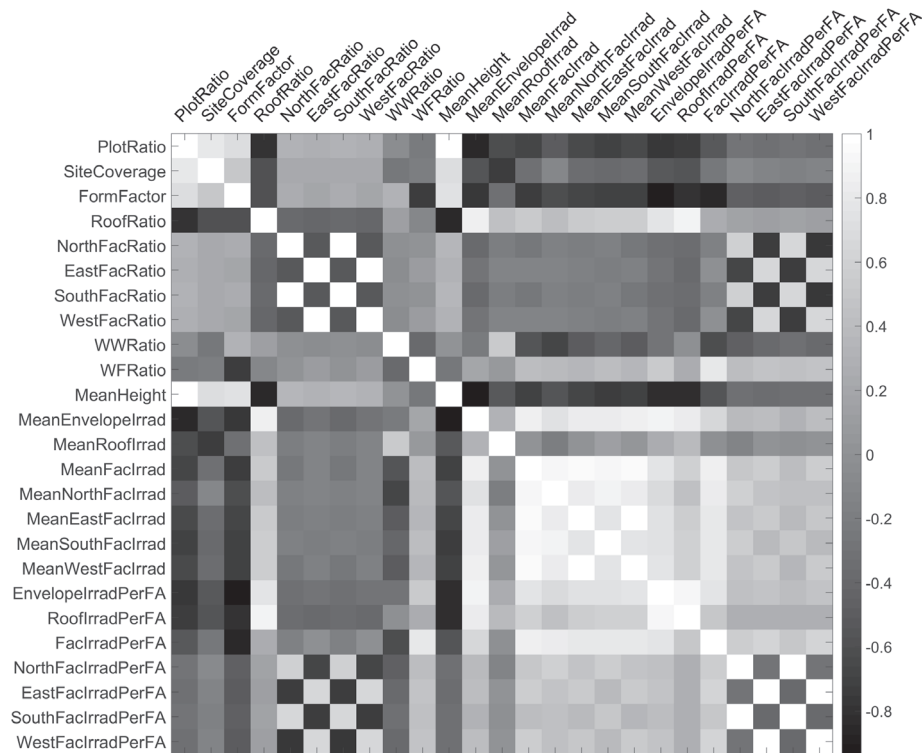
---

We see that the relationship differs between the seven cases. For example, M6 distinguishes itself from the other cases, showing a more clustered and localized group of points, with an often flatter slope such as for the *PlotRatio* and *MeanHeight* parameters. Despite these differences, in the following section we attempt to train the metamodels on all M-cases taken together, without any variable accounting explicitly for their difference in typology/layout. The advantages and drawbacks of this approach are discussed in section 4.7.

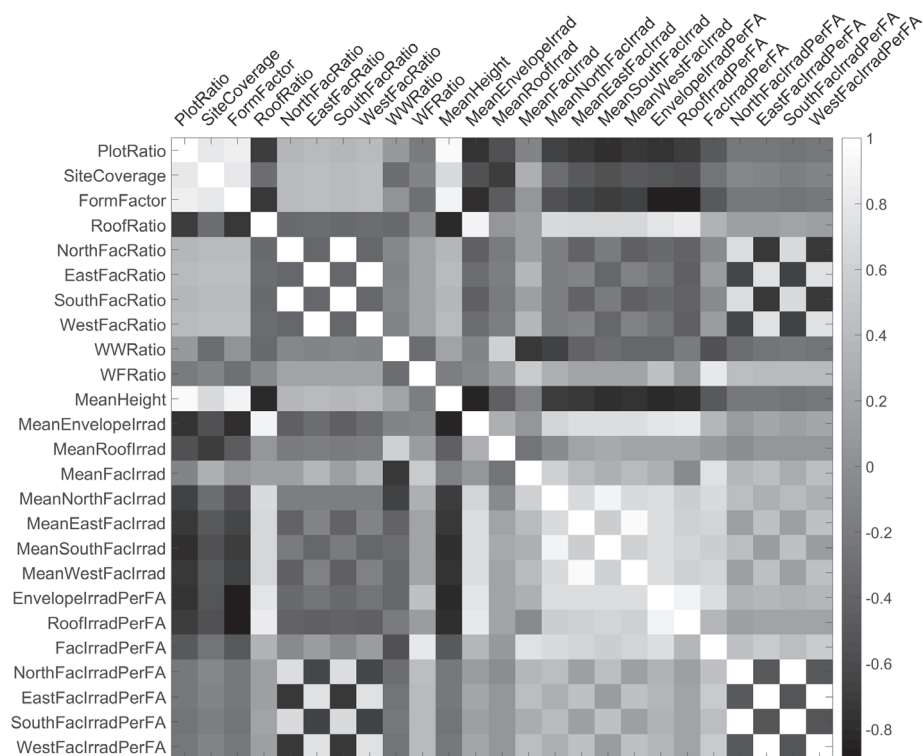
When selecting the list of ‘final’ inputs, that will effectively become the predictors in the energy and daylight functions, both types of correlations - i.e. between inputs and among inputs and outputs - are taken into account. We want to avoid redundant parameters while retaining influential ones. This is further addressed in the next section. The quasi-constant *WWRatio*, although it has until now been included in the figures, is removed from both datasets for the upcoming metamodeling training and testing phases.

It is important to highlight that the observed trends are strongly conditioned by the simulation assumptions, e.g. the U-values and building function in the case of the energy dataset. The results of the current correlation analysis are therefore not to be taken as design guidelines. In chapter 7, we demonstrate that, given different simulation settings, the observed trends differ to some extent.





(a) Energy dataset



(b) Daylight dataset

Figure 4.15 – Matrix of pairwise linear correlation coefficient between each combination of input parameters in the two datasets. From black (-1) to gray (0) to white (+1): negative to none to positive correlation.

Chapter 4. Metamodel development

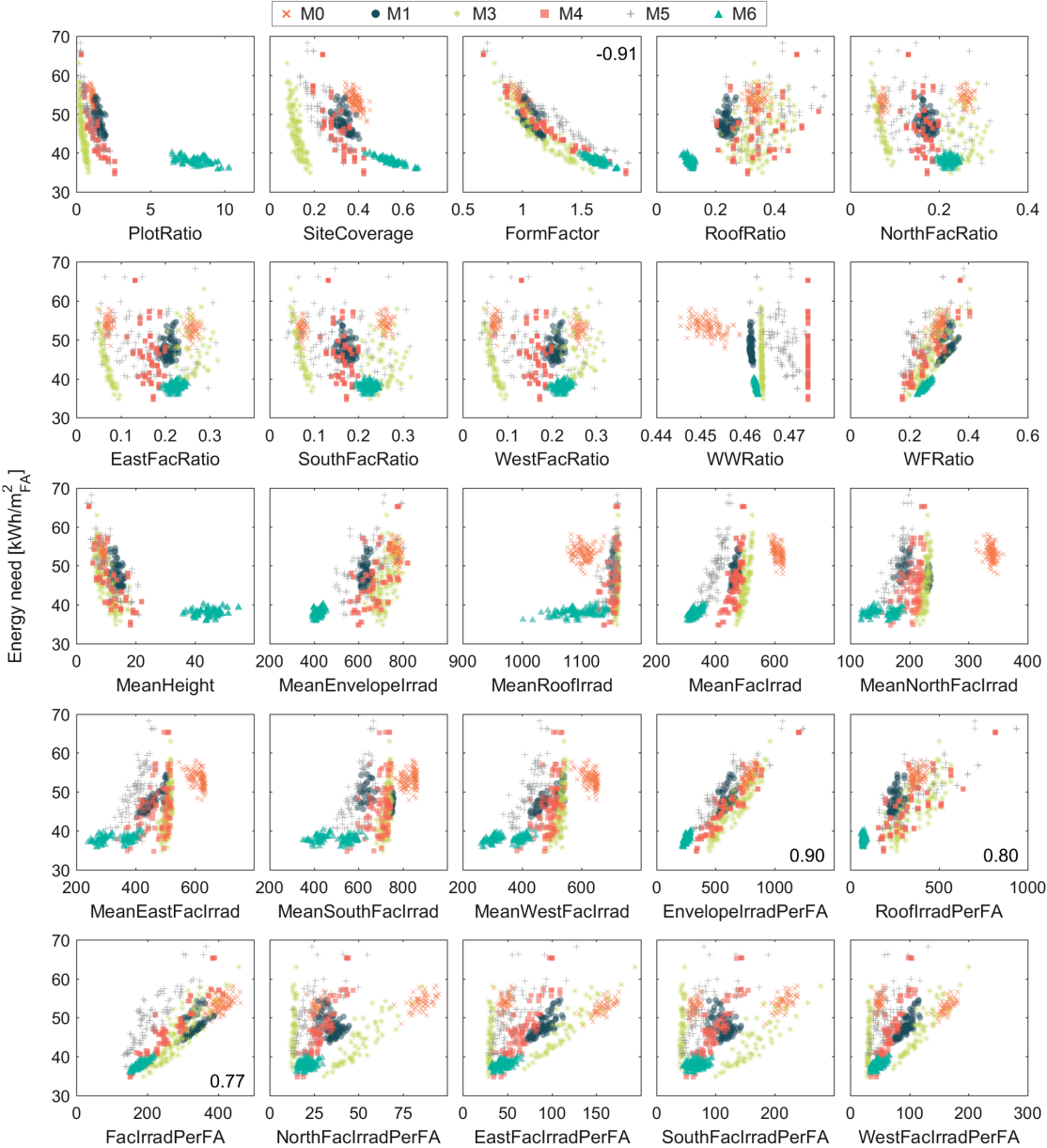


Figure 4.16 – Relationship between the energy need output and each input in the energy dataset, with distinction between the different cases.

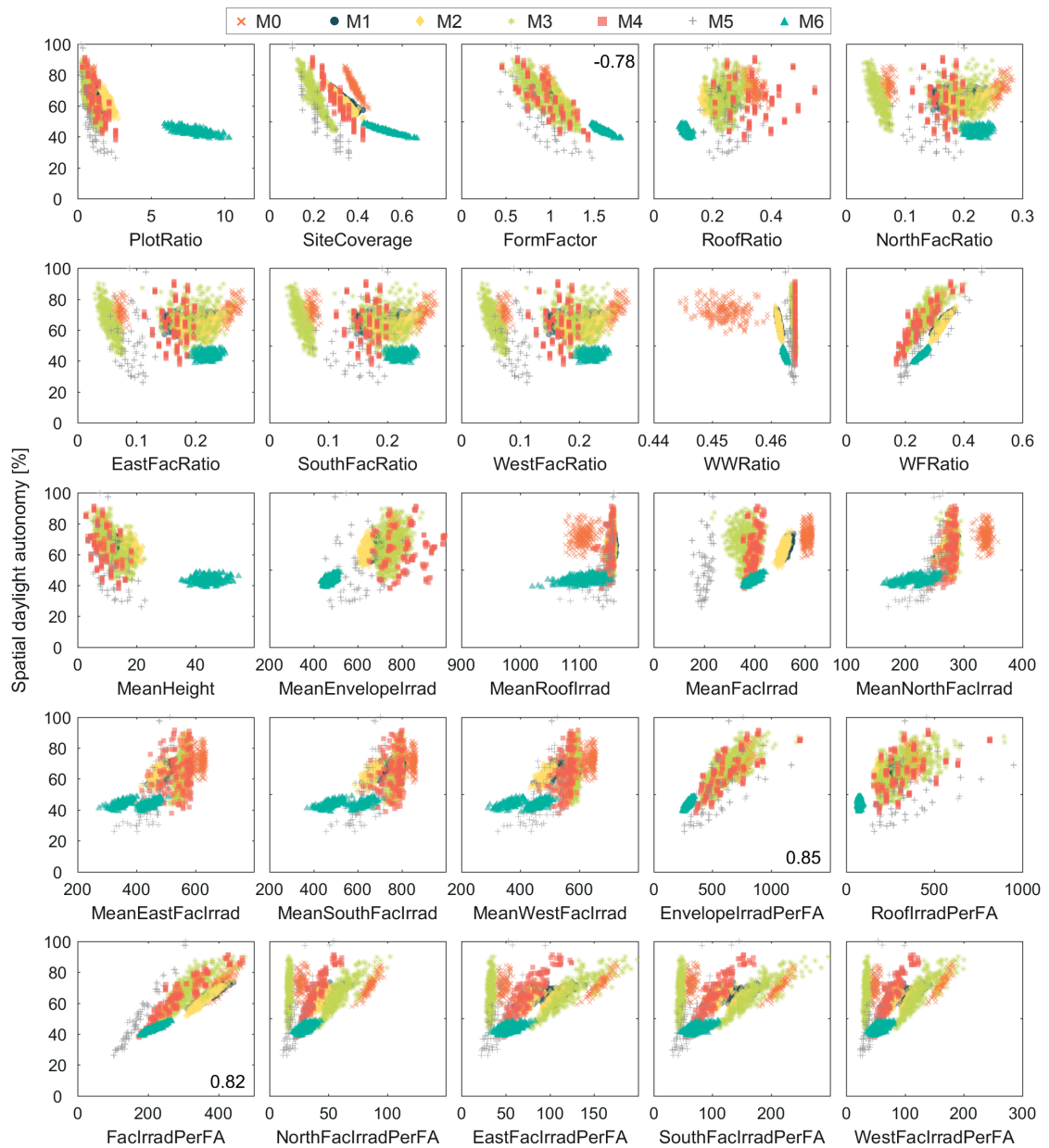


Figure 4.17 – Relationship between the sDA output and each input in the daylight dataset, with distinction between the different cases.

## 4.5 Metamodel training and testing

### 4.5.1 Overview of fitting procedure

This section details the procedure for fitting the metamodels to the energy and daylight datasets. This procedure is illustrated in an abstract way in Fig. 4.18. In the following subsections, we expose the content of the dark boxes, each consisting of a distinct iterative fitting process that allows us to progress in identifying, with some level of confidence, an adequate model form (e.g. linear, quadratic) and subset of inputs to be used when fitting the final predictive model.

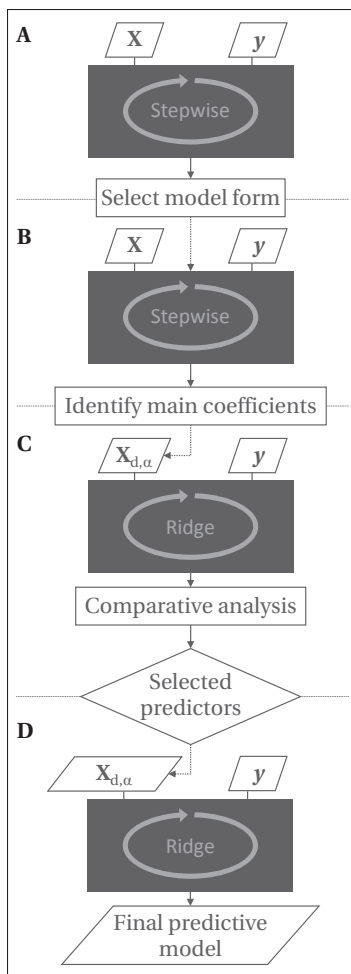


Figure 4.18 – Flowchart of the procedure for defining the predictors to use in the final predictive model fitting. Each block (top to bottom) is respectively detailed in sections 4.5.3 and 4.5.4.

As mentioned in section 4.3, a multiple linear regression model form is selected as a starting point. In steps **A** and **B** (section 4.5.3), a **stepwise selection** algorithm is used, first to compare model variations to see the effect of allowing interaction and quadratic terms, and secondly, to reduce the dimensionality of the inputs. Instead of randomly or manually searching for the best subset of the 25 possible predictors (listed in Table 4.6), we undertake a gradual elimination process using the information gathered through the distribution and correlation analysis of 4.4, combined with results from the stepwise selection. In phases **C** and **D** (section 4.5.4), a different algorithm, **ridge regression**, is used. The set of inputs is further reduced and fed to the final predictive function fitting algorithm. The final functions represent the metamodels to be implemented and subsequently used for predicting the performance of new, unseen neighborhood designs. This application phase is addressed in chapters 5 and 6.

Since each phase of the flowchart informs its successor, in the next sections we expose both the theory behind each algorithm and method as well as their respective results.

### 4.5.2 Particularities of deterministic simulations and consequences on metamodeling

Results from each fitting phase are analyzed using the statistical metrics listed in Table 4.10, indicators of the goodness-of-fit, i.e. how well the fitted model performs as a predictor of the response  $y$ . It is important at this point to highlight the precautions that must be taken when applying statistical techniques in our context, due to the deterministic

nature of the simulations we are attempting to emulate. Indeed, the thermal simulation in EnergyPlus is deterministic, meaning that re-running the simulation for an identical set of inputs will give the exact same output. In the case of daylight simulations, Radiance uses a hybrid deterministic-stochastic<sup>14</sup> (Monte Carlo) approach. However, the difference in the outputs for two simulation runs of the same design is small and gets reduced even more when computing the sDA over the whole neighborhood design.

The particularity of deterministic simulations with respect to stochastic experiments is that the concept of random error does not apply [Simpson et al., 2014]. That means that the error term  $\varepsilon$  in equation 4.3 only represents the approximation error and does not include a random component. The consequence is that many statistical measures, which rely on an assumed presence of a random error, lose their meaning. According to Simpson et al. [2014], the only values that can be used to verify the performance of a metamodel used to replace a deterministic computer experiment are the Coefficient of Determination ( $R^2$ ), which indicates the level of correlation between two sets of data, and its adjusted version, which takes into account the number of parameters. These should be combined with residuals plots to identify trends and outliers, where a residual is simply the difference between a simulated (reference) and predicted value. Moreover, validation using additional data points is indispensable. Maximum and mean absolute error and Root Mean Square Error (RMSE) can then be used to assess the metamodel's accuracy [Simpson et al., 2014]. We have retained the RMSE and added the Percentage Error (PercErr) as listed in Table 4.10. While the former quantifies the overall difference between the simulated and fitted values in the units of the response, the PercErr provides a relative reference to the order of magnitude of the output values. In some cases we will directly take the difference instead of the absolute value of the nominator in the PercErr equation, to preserve the sign which is an indicator of over (-) and under (+) prediction.

### 4.5.3 Model selection and inputs reduction - Stepwise linear regression

In phases A and B, a stepwise selection algorithm is employed, first to compare different levels of model complexity, and second to search for the inputs with the most statistical significance in explaining the output. We use the *stepwiselm* Matlab function<sup>15</sup>, whose algorithm proceeds by adding and removing terms in an iterative fitting process, comparing the explanatory power of each combination. There are two mechanisms possible for searching for the best model: forward-stepwise selection, which starts with an intercept term and adds the predictors that most improve the fit, and backward-stepwise selection, which begins with the full model and removes inputs that have the least impact on the fit [Hastie et al., 2009].

The Matlab function uses both techniques to determine the best fit, judged using the adjusted  $R^2$  as the performance criterion. Running the code results in a Matlab linear model object

---

<sup>14</sup><http://radsite.lbl.gov/radiance/framew.html> (last accessed on April 20, 2016)

<sup>15</sup><http://www.mathworks.com/help/stats/stepwiselm.html> (last accessed on April 6, 2016)

## Chapter 4. Metamodel development

Table 4.10 – Goodness-of-fit and error statistics used to compare and analyze results across the different fitting phases of Fig. 4.18.  $N$ : number of data points;  $P$ : number of input terms;  $y$ : simulated (reference) value;  $\hat{y}$ : predicted (fitted) value;  $\mu$ : mean.

| Name (acronym) [units]  | Equation  | Aim |
|---|---|-----|
| Coefficient of Determination ( $R^2$ ) [-]                          | $R^2 = 1 - \frac{SSE}{SST}$   | → 1 |
| Adjusted Coefficient of Determination ( $R^2_{adj}$ ) [-]           | $R^2_{adj} = 1 - \left(\frac{N-1}{N-P}\right) \frac{SSE}{SST}$              | → 1 |
| Residuals [units of $y$ ]   | $\Delta = y_i - \hat{y}_i$  | → 0 |
| Root Mean Square Error (RMSE) [units of $y$ ]                       | $RMSE = \sqrt{\frac{\sum_{i=1}^N (y_i - \hat{y}_i)^2}{N}}$                  | → 0 |
| Percentage Error (PercErr) [%] ( $\pm$ when without the  absolute ) | $PercErr = 100 \times \frac{\sum_{i=1}^N \frac{ y_i - \hat{y}_i }{y_i}}{N}$ | → 0 |

Where:

|  |  |
|--|--|
| Sum of Squared Error (SSE) [units of $y$ ] | $SSE = \sum_{i=1}^n (y_i - \hat{y}_i)^2$ |
| Total Sum of Squares (SST) [units of $y$ ] | $SST = \sum_{i=1}^N  y_i - \mu ^2$       |

with multiple properties, including the model's formula and its characteristics (e.g. number of inputs, coefficients), and error and fit measures (e.g. RMSE,  $R^2$ ).

### A - Model form

We first use the stepwise approach to compare different model forms (Fig. 4.19), distinct in terms of their complexity. The largest allowed model type, specified by the *'upper'* argument in the *stepwiselm* function, is iteratively set to: *'constant'*, *'linear'*, *'interactions'* and *'quadratic'*. Each setting represents a certain model complexity level, described in Table 4.11. An example of the Matlab output associated to each model type can be found in appendix A.2.

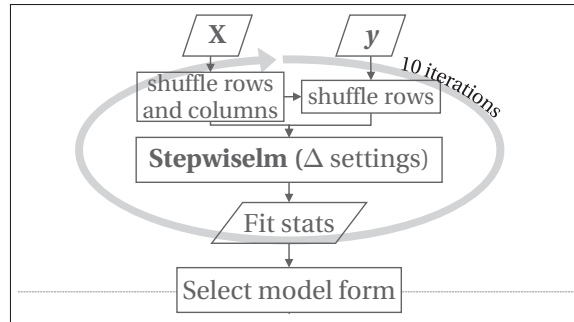


Figure 4.19 – Flowchart of the procedure for selected the model form using the Matlab *stepwiselm* function with different settings. 'Fit stats' corresponds to the metrics described in Table 4.10.

It is to note that the stepwise method is locally rather than globally optimal; the final model built may differ according to the terms in the initial model and the order in which inputs are added and removed. To address this potential variability, the columns and rows of  $\mathbf{X}$  (and by association the rows of  $\mathbf{y}$ ) are shuffled in a sequence of 10 iterations, in addition to varying the model settings as described above.

Results for both metrics are shown in Fig. 4.20. Figure 4.20a illustrates the histogram of the residuals, which are the differences between the simulated and the fitted (predicted) responses,

## 4.5. Metamodel training and testing

Table 4.11 – Model forms tested using the *stepwiselm* function with different settings.  $y$ : simulated (reference) value;  $\beta_0$ : constant term (bias, intercept);  $\beta_i$ : coefficient of input  $x_i$ ;  $\varepsilon$ : error term.

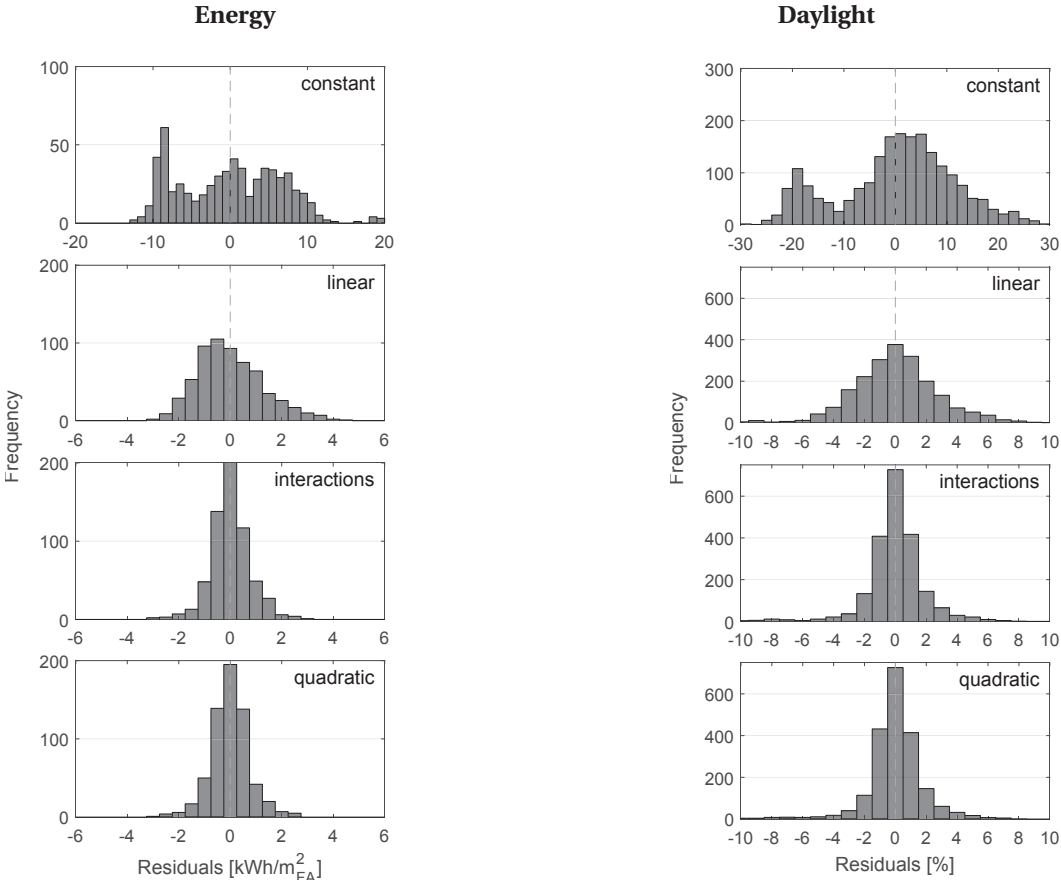
|               |   |   |
|---------------|---|---|
| Constant:     | containing only a constant term (intercept, no predictor terms)                 | $y = \beta_0 + \varepsilon$   |
| Linear:       | containing an intercept and linear terms  | $y = \beta_0 + \beta_1 x_1 + \beta_2 x_2 + \dots + \varepsilon$                                     |
| Interactions: | containing an intercept, linear terms, and products of pairs of distinct inputs | $y = \beta_0 + \beta_1 x_1 + \dots + \beta_n x_1 x_2 + \dots + \varepsilon$                         |
| Quadratic:    | containing an intercept and linear, interactions and squared terms              | $y = \beta_0 + \beta_1 x_1 + \dots + \beta_n x_1 x_2 + \dots + \beta_m x_1^2 + \dots + \varepsilon$ |

associated to one of the 10 iterations for each model form tested. The shape of the distribution can allow discovering outliers - i.e. instances further from the symmetric, Gaussian-like shape - and systematic over or under estimations - i.e. shift of the peak towards negative or positive values. In our case, the shape of the histograms were found to be the same across the 10 iterations, meaning that there was no effect of shuffling the data. This is the reason why only one example is here displayed.

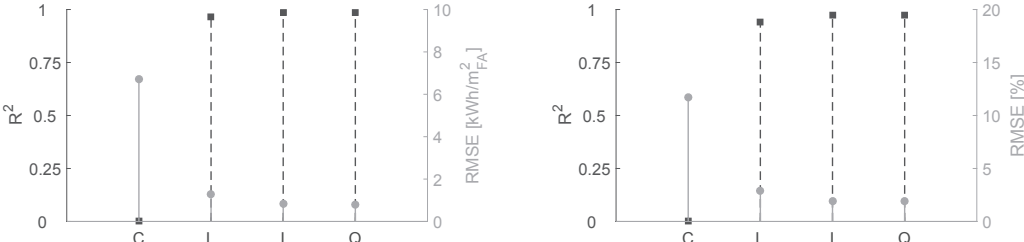
The constant model type is, not surprisingly, the worst with a wide spread in the residuals going up to a 20 kWh/m<sup>2</sup> and 25% error respectively for the energy and daylight metric. This range is greatly reduced for the other three models, with the linear type showing a more dispersed histogram than the interactions and quadratic models.

The predictive performance of each model is also reflected in Fig. 4.20b, showing the Coefficient of Determination ( $R^2$ ) and Root Mean Square Error (RMSE) corresponding to each type, averaged over the 10 iterations. Although values for the linear (L), interactions (I) and quadratic (Q) forms are similar, their structure is significantly different. That is, their level of complexity expressed through the number of terms present in each equation varies considerably, as seen in Fig. 4.20c. The linear form contains on average 20 terms, while this number jumps to nearly (resp. above) 100 terms for the quadratic energy (resp. daylight) model. An example output for each model type can be seen in appendix A.2.

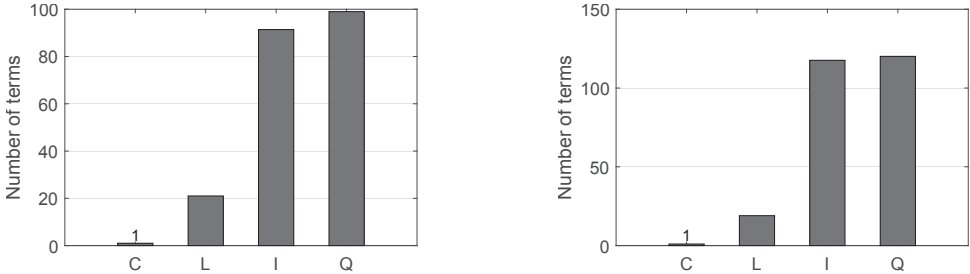
In light of the above results and analyzes, the linear model form is selected to pursue the fitting process for both metrics. The small loss in prediction performance compared to the I and Q options is counterbalanced by the simpler equation form. An important reason for this choice comes from the risk of over-fitting, which increases with the number of terms. This intermediate result leads us on to the next phase.



(a) Histogram of the residuals obtained over one iteration.



(b) Average  $R^2$  and RMSE over the 10 iterations.



(c) Average number of terms appearing in the model over the 10 iterations.

Figure 4.20 – Results from the stepwise selection for each type of model for the energy (left) and daylight (right) metric. C: constant, L: linear, I: interactions, Q: quadratic.



**B - Main coefficients**

With the model form set to a regression with linear terms only, we now use a similar iterative stepwise approach to identify the inputs that appear the most over 50 iterations (Fig. 4.21). At each run, the initial dataset is randomly split into a training and testing subset. A model is fitted on the training data and applied on the test data. The resulting predictions are compared to the responses in the test set. The iteration-specific inputs selected by the algorithm are analyzed along with the associated fit statistics.

The number of times each input appeared in a fitted model over the 50 iterations for the energy dataset is plotted in Fig. 4.22a. The value of each input's coefficient at each iteration is shown in Fig. 4.22b. The same two graphs for the daylight dataset are shown in Fig. 4.23.

In the coefficients' value graph, plots showing a straight line at the zero on the y-axis indicate that the corresponding input is not significant in explaining the response since its coefficient is always null. Inputs with a few non-zero values are linked to the random split at these instances and are thus not predominant. Conversely, we can be more confident that inputs consistently showing a non-null value, e.g. *PlotRatio*, *FormFactor*, are significant. Less clear are the inputs that appear about half the time such as the *RoofIrradPerFA* in the energy models. The number of inputs that appear in all 50 iterations is of 10 and 12 for the energy and daylight respectively.

Using the frequency of appearance information acquired in this phase, we proceed to the next step to further test the impact of including or not certain inputs.

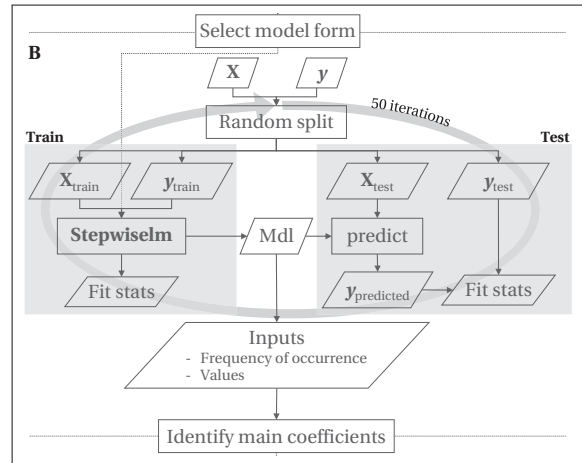
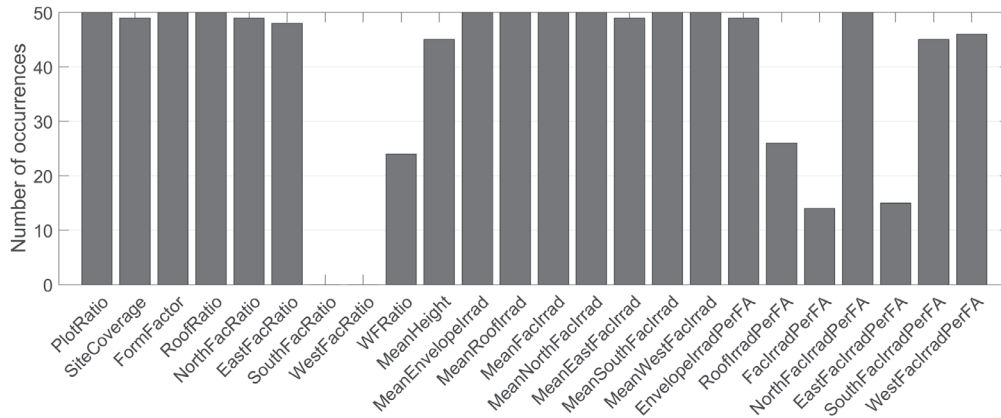
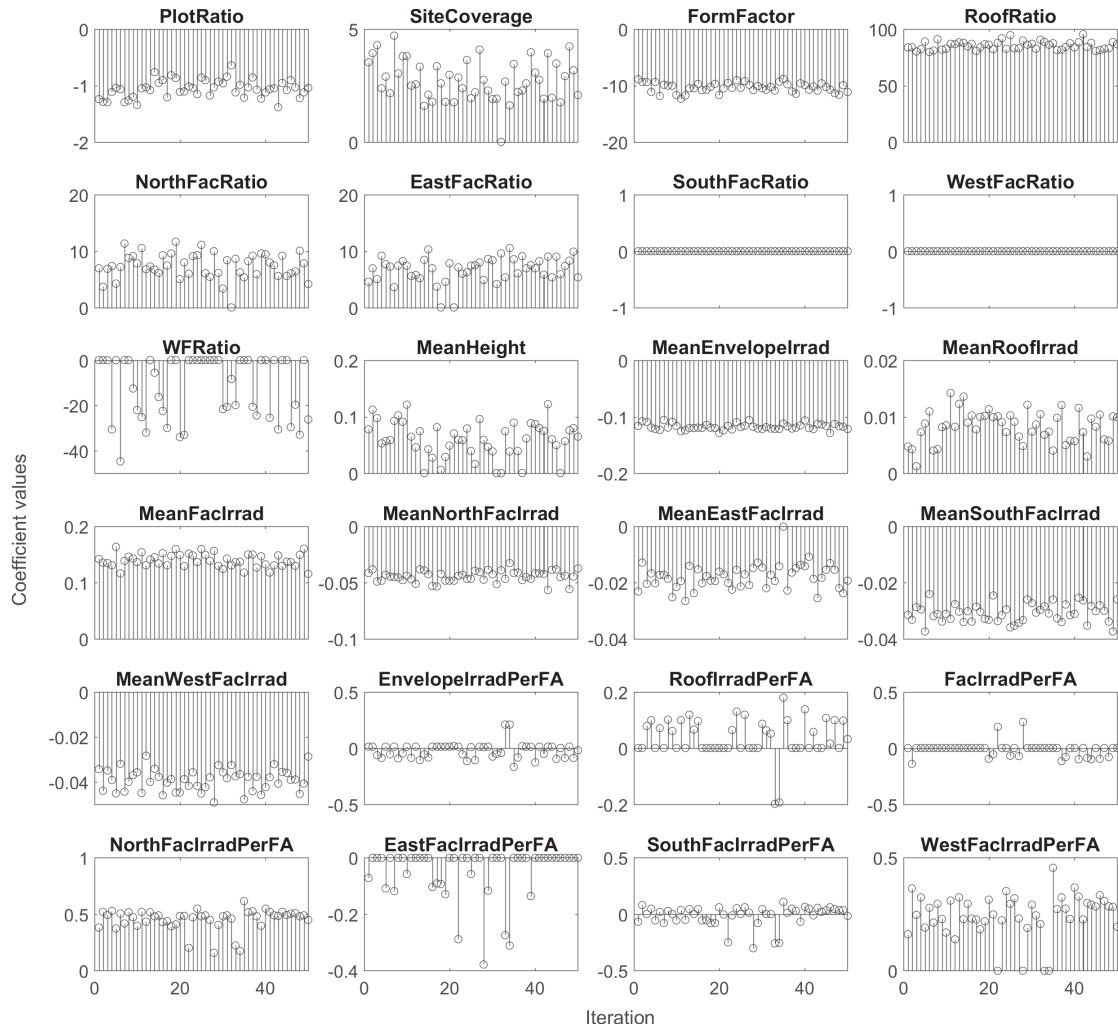


Figure 4.21 – Flowchart of the iterative process for identifying influential inputs using stepwiselm on different training data subsets.

## Chapter 4. Metamodel development



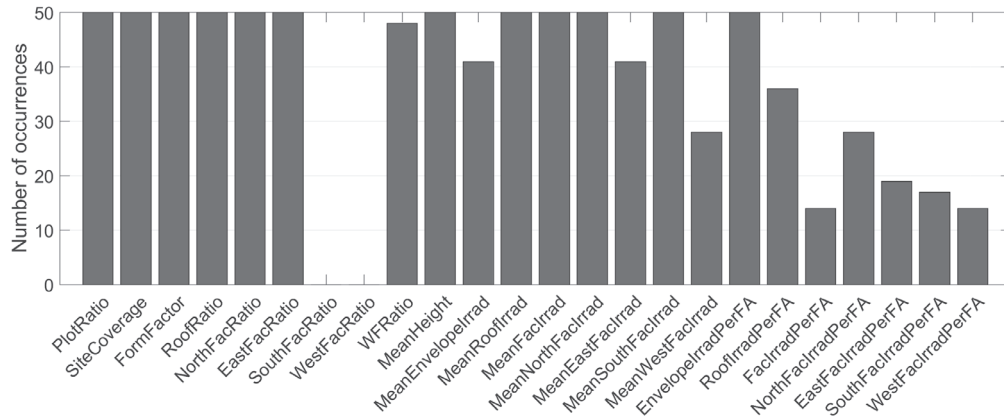
(a) Number of appearances of each input.



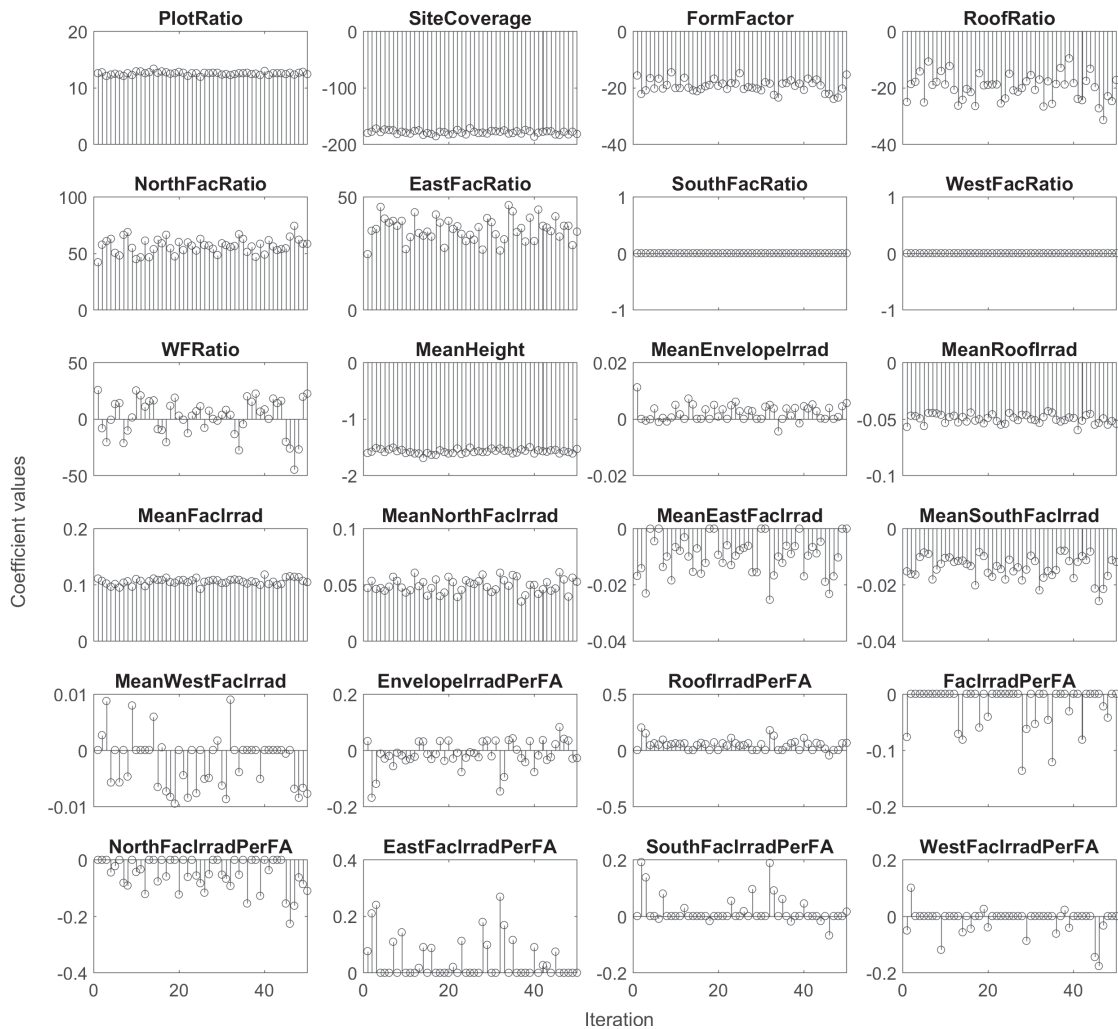
(b) Coefficient value of each input at each iteration.

Figure 4.22 – Occurrence and coefficient value for each input over 50 iterations of the **energy** model.

## 4.5. Metamodel training and testing



(a) Number of appearances of each input.



(b) Coefficient value of each input at each iteration.

Figure 4.23 – Occurrence and coefficient value for each input over 50 iterations of the **daylight** model.

### 4.5.4 Fitting the predictive functions - Ridge regression

In the next two phases C and D, we conduct additional tests this time using a different algorithm: ridge regression [Hastie et al., 2009], which we apply using the Matlab *ridge* function<sup>16</sup>. Ridge regression is a shrinkage method; it enforces a penalty on the coefficients to mitigate the consequences of potential multicollinearity between inputs. This is particularly relevant to our problem since some of the inputs are likely to be correlated, as highlighted in the data analysis phase of section 4.4.2. In such cases, a large positive coefficient on one input can be canceled out by an equally large negative coefficient on a correlated input [Hastie et al., 2009]. This issue is linked to the risk of over-fitting to our dataset, which decreases the generalization potential of the metamodel.

Considering our model equation:

$$y = f(\mathbf{x}) + \varepsilon = \hat{y} + \varepsilon = \beta_0 + \sum_{i=1}^P \beta_i x_i + \varepsilon \quad (4.3)$$

where  $\mathbf{x} \in \mathbb{R}^P$  contains the  $P$  input values,  $y$  is a reference (simulated) value,  $\hat{y}$  the model output (prediction),  $\beta$  the unknown coefficients and  $\varepsilon$  the experiment error. To estimate the model coefficients, we minimize:

$$\sum_{i=1}^N (f(\mathbf{x}) - y_i)^2 + \lambda \|\beta\|^2 \quad (4.4)$$

where  $N$  is the number of training samples and  $\lambda$  the regularization parameter which penalizes large coefficient values. The  $\beta$  minimizing equation 4.4 can be obtained as:

$$\hat{\beta} = (\mathbf{X}^T \mathbf{X} + \lambda \mathbf{I})^{-1} \mathbf{X}^T \mathbf{y} \quad (4.5)$$

where  $X \in \mathbb{R}^{N \times P}$ . Starting with 1000 values of  $\lambda$  between 0 and 1<sup>17</sup>, we use a technique called k-fold cross-validation to find the best  $\lambda$  [Hastie et al., 2009]. We split the data in k(=10) sets, take k-1 sets for training, then test the fitted model on the remaining set. The best  $\lambda$  corresponds to the value yielding a minimum RMSE averaged over the k-fold iterations. We then fit a model over the entire training set using  $\lambda_{\text{best}}$ , within a two-fold cross-validation to estimate the prediction error over the test set [Hastie et al., 2009]. The *ridge* function internally scales the inputs to have a mean of 0 and a Standard Deviation (std) of 1. The computed coefficients are then restored to match the scale of the original inputs.

---

<sup>16</sup><http://www.mathworks.com/help/stats/ridge-regression.html> (last accessed on February 23, 2016)

<sup>17</sup>Tests were conducted, starting from a larger range, to define these boundary values.

**C - Final predictors**

Using the information about the main inputs identified in the previous phase, we proceed with another iterative fitting sequence to further assess the fit obtained with different input subsets. As illustrated in Fig. 4.24, the  $\mathbf{X}$  matrix is recursively reduced to the inputs that appeared in  $\alpha = 25, 50, 75$  and  $100\%$  of the 50 iterations in the previous phase (see Fig. 4.22a and 4.23a). For example, the  $\alpha = 100\%$  case for the energy metric corresponds to fitting the model using the 10 inputs showing a full bar in Fig. 4.22a. To the four  $\alpha$  values is thus associated a  $P$  number of inputs. A ‘manual’ selection is also added, for which a smaller subset of inputs are retained, corresponding to the ones that were found to most influence the fit based on manual iterations. Starting from the  $\alpha = 100\%$  case, values corresponding to each input present were removed and the training/testing algorithm was repeated. By comparing the fit and error metrics obtained at each trial, a reduced set of main contributors was identified.

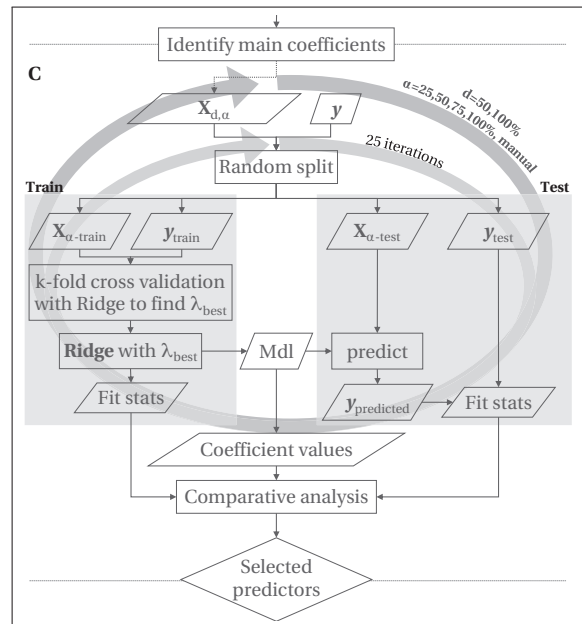


Figure 4.24 – Flowchart of the iterative process for testing different input combinations using the Matlab *ridge* function and leading to the final predictors’ selection.

In addition to the variations in the number of inputs, the sequence of Fig. 4.24 is first executed using all designs ( $d=100\%$ ) and then repeated using only half ( $d=50\%$ ). This test is done to see the effect of fitting using a smaller amount of reference data points.

To clarify both reductions, let us consider our matrix:

$$\mathbf{X} = \begin{bmatrix} x_{11} & x_{12} & x_{13} & \dots & x_{1P} \\ x_{21} & x_{22} & x_{23} & \dots & x_{2P} \\ \dots & \dots & \dots & \dots & \dots \\ x_{N1} & x_{N2} & x_{N3} & \dots & x_{NP} \end{bmatrix}$$

where  $x_{ij}$  is the value of input parameter  $j = 1, \dots, P$  (e.g. plot ratio) for design  $i = 1, \dots, N$  (e.g. variant 20 in M1 series). Reducing the number of designs consists in randomly cutting rows of  $\mathbf{X}$ , while removing some inputs means eliminating specific columns.

The train-test process described earlier is again executed, this time using the *ridge* function detailed above. For comparative purposes, the same random split is applied at each of the four  $\alpha$  runs.

## Chapter 4. Metamodel development

---

Results are shown in Fig. 4.25 and 4.26 for the energy and daylight metrics respectively. For each  $\alpha$ , the predicted versus simulated values over the 25 fitting runs are plotted along with the corresponding residuals histogram, for both the full series ( $d=100\%$ ) and half ( $d=50\%$ ) of the designs. Fit and residuals statistics are displayed as well as the number of terms associated to each  $\alpha$  value.

For the energy metric, results are very similar across  $\alpha = 25$  to  $75\%$  and between the full and half datasets. For  $\alpha = 100\%$ , the prediction accuracy slightly decreases as indicated by the lower  $R^2$  and wider spread in the residuals. From the scatter plots, we observe that values located at the extremities (e.g. energy need  $> 55 \text{ kWh/m}_{\text{FA}}^2$ ) are over-predicted. This situation is exacerbated in the bottom graphs showing the results for the manual reduction, which has the highest standard deviation of the residuals.

For the daylight metric, results are similar across all graphs, with a slight decrease in the prediction accuracy for the manual selection case (bottom graphs), as seen from the residuals' histograms. In all cases, we observe in the scatter plots both over- and under-predictions around simulated values of 75 to 85%.

For both metrics, we should as further work take a closer look at the extremes to identify potential outliers and eventually acquire new data points in those regions to improve the results.

The effect of reducing the dataset to half its original size - comparing  $d=100\%$  to  $d=50\%$  - is small. While the number of terms corresponding to each  $\alpha$  is slightly different and the number of data points present in the plots is lower (due to the smaller  $\mathbf{X}$ ), the fit and error statistics are only slightly worse. Considering the similarity between the different runs, we choose to retain the  $\alpha = 100\%$  and the manual reduction, both for  $d = 50\%$ , for proceeding with the next phase. Although the RMSE is higher for those settings, this choice is made to mitigate the risk of over-fitting to our reference dataset. It may seem contradictory to hypothesize that the risk of over-fitting can be reduced by removing some data. However, we believe that the high similarity between some design variants may cause the model to fit too closely to these specific characteristics, decreasing its accuracy when applied to distinct designs. Indeed, considering for example case M3 which has the most number of variants (see Fig. 4.13 and 4.14), it is possible that two or more of these variants have identical buildings in terms of dimensions, but with an inverted (or mirrored) layout, due to the sampling technique detailed in section 4.2.2. This would mean that all geometry-based parameters are equal between the two designs, with variations (possibly small) only in their irradiation-based parameters and outputs. As such, we are ready to sacrifice in accuracy based on the current results, in the hope of a better future generalization potential of the metamodel when applied to unseen designs. This test, essential to further probe the metamodels, is conducted in chapter 6.

## 4.5. Metamodel training and testing

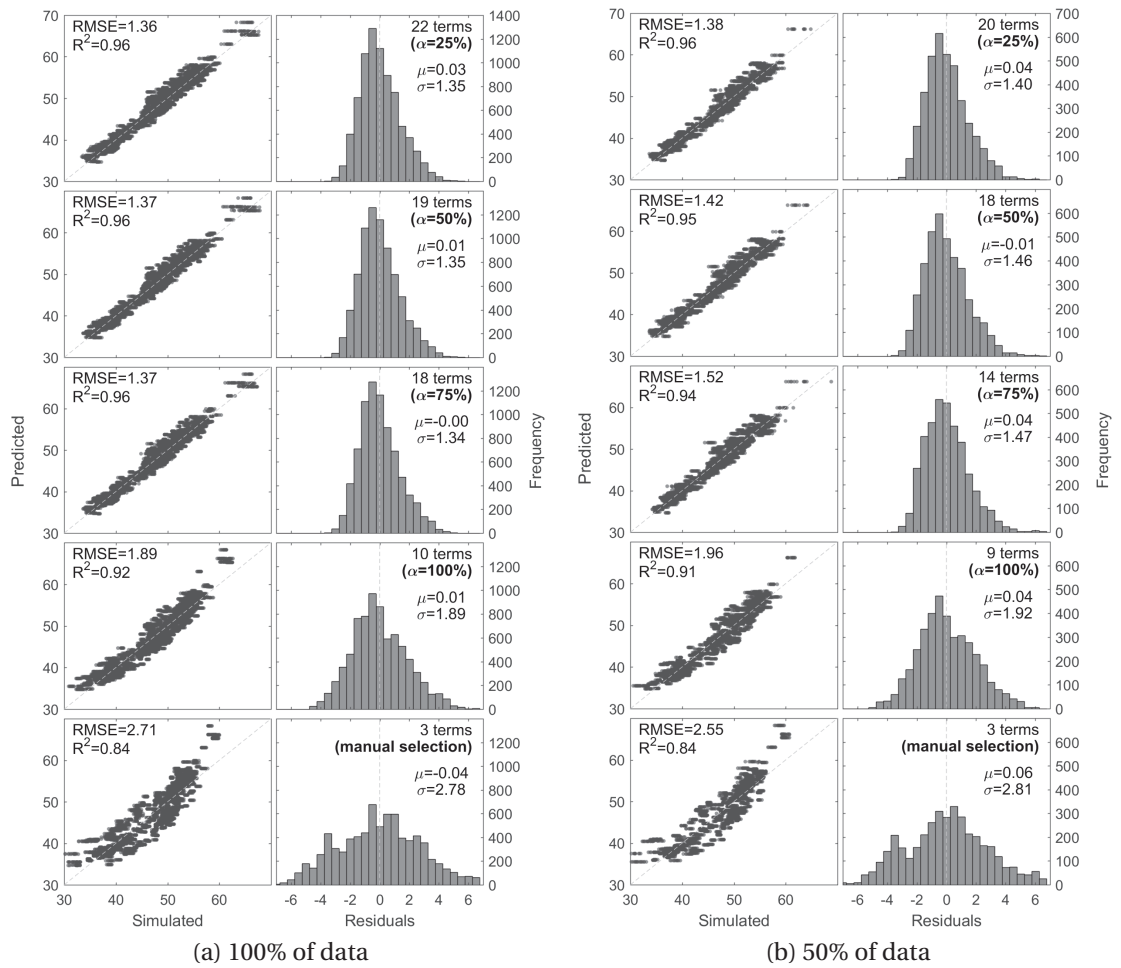


Figure 4.25 – Predicted versus simulated energy need values (left) with associated residuals histogram (right) over all 25 iterations for each  $\alpha$  (different subset of inputs included in each model), when training-testing using (a) the entire and (b) half of the dataset. The constant (intercept) is not counted in the displayed number of terms. Predicted, simulated and residual values are expressed in  $\text{kWh}/\text{m}_{\text{FA}}^2$ .

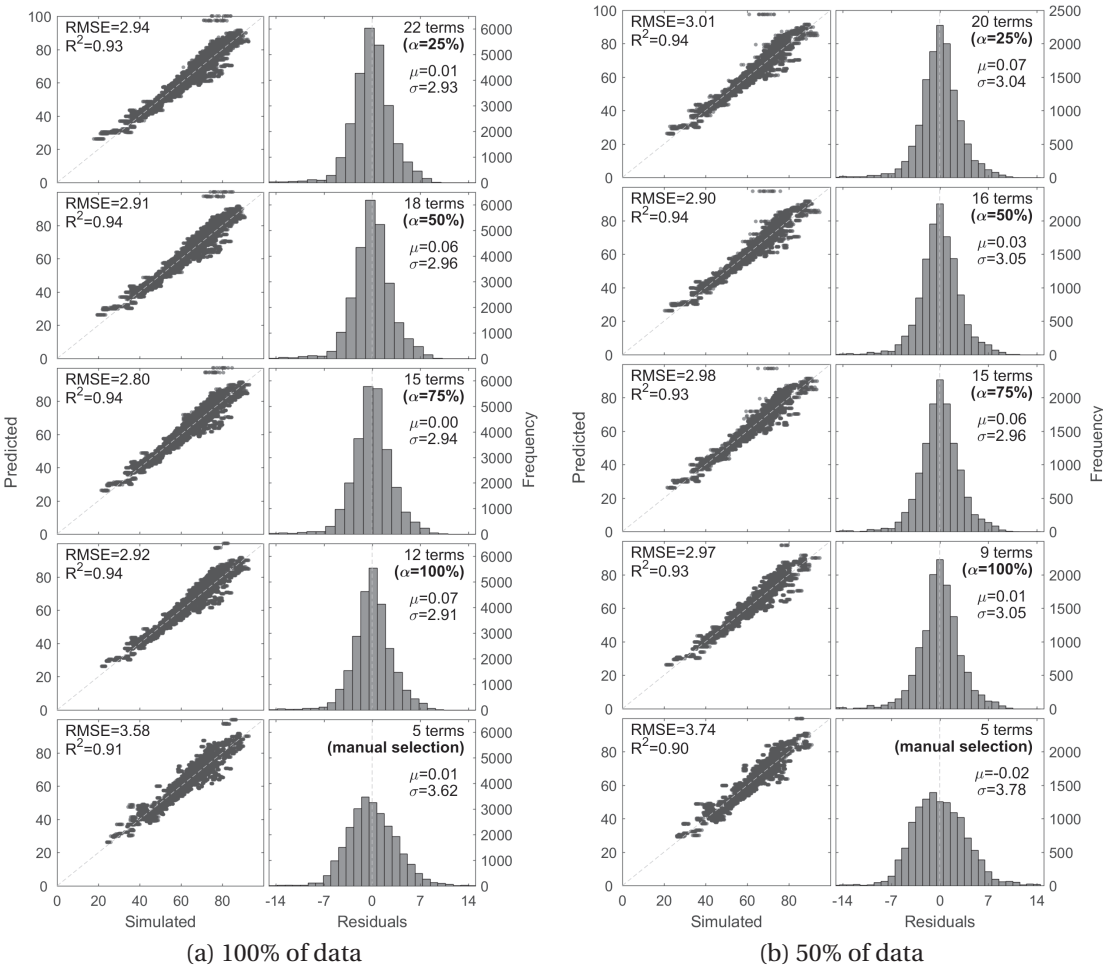


Figure 4.26 – Predicted versus simulated spatial daylight autonomy values (left) with associated residuals histogram (right) over all 25 iterations for each  $\alpha$  (different subset of inputs included in each model), when training-testing using (a) the entire and (b) half of the dataset. The constant (intercept) is not counted in the displayed number of terms. Predicted, simulated and residual values are expressed in %.



**D - Final energy and daylight metamodels**

The final metamodels are to be fitted using the same *ridge* function, in a simplified procedure illustrated in Fig. 4.27. This time, we do not split the data as no testing takes place. An internal 10-fold cross-validation is however used to define the best  $\lambda$  value.

The set of inputs  $X_{d,\alpha}$  to be included for fitting the final metamodels corresponds to the selected cases of  $\alpha = 100\%$  and the manual reduction, both with  $d = 50\%$ . They are listed in Table 4.12, along with their level of correlation with each output metric. Values range from a low (+)0.25 to a high of (-)0.91. The fact that some inputs are included despite their low correlation to the output may be caused by an interaction with another input present. Although the chosen model form does not allow explicit interaction terms (see Table 4.11), the inclusion of specific parameters in the model is a process that depends upon the other available input parameters. For instance, the *MeanRoofIrrad* in the daylight model may not be useful in predicting the output when considered on its own:  $\hat{y} = \beta_0 + \beta_1 x_1$ . However, its effect may be enhanced when accompanied by other inputs even though interactions terms (e.g.  $\beta_{12} x_1 x_2$ ) are not included:  $\hat{y} = \beta_0 + \beta_1 x_1 + \beta_2 x_2 + \dots + \beta_n x_n$ .

The predictive functions obtained are described in Table 4.13.  $f(x)$  corresponds to what we will refer to as the ‘full’ metamodel version ( $\alpha = 100\%$ ), while  $f_{red}(x)$  contains the reduced subset of inputs defined through the manual procedure previously explained. The reason for having two metamodel versions for each output metric comes from our hypothesis that simpler models may generalize better to new designs distinct from the ones used to construct the reference dataset. This hypothesis will be tested in section 6.2.2.

Table 4.12 – Correlation level between the output metric and each input selected for fitting the corresponding full and reduced (bold) final predictive models.

| Energy metric            |             | Daylight metric     |             |
|--------------------------|-------------|---------------------|-------------|
| Input                    | Correlation | Input               | Correlation |
| <b>PlotRatio</b>         | -0.62       | <b>PlotRatio</b>    | -0.67       |
| <b>FormFactor</b>        | -0.91       | <b>SiteCoverage</b> | -0.59       |
| RoofRatio                | 0.58        | FormFactor          | -0.78       |
| <b>MeanEnvelopeIrrad</b> | 0.69        | <b>WFRatio</b>      | 0.62        |
| MeanFacIrrad             | 0.64        | <b>MeanHeight</b>   | -0.68       |
| MeanNorthFacIrrad        | 0.57        | MeanRoofIrrad       | 0.25        |
| MeanSouthFacIrrad        | 0.58        | <b>MeanFacIrrad</b> | 0.36        |
| MeanWestFacIrrad         | 0.63        | MeanNorthFacIrrad   | 0.66        |
| NorthFacIrradPerFA       | 0.43        | EnvelopeIrradPerFA  | 0.85        |

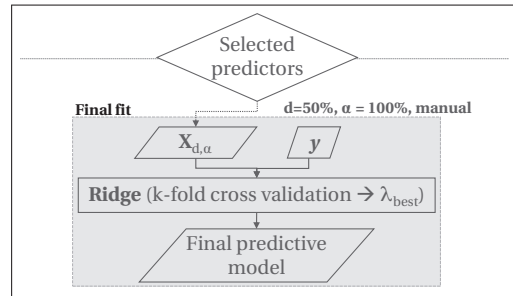


Figure 4.27 – Flowchart of the final metamodel fitting procedure using ridge regression.

## Chapter 4. Metamodel development

Table 4.13 – Full and reduced final fitted equations to be used for predicting the performance of new designs.

| <b>Energy metamodel [kWh/m<sub>FA</sub><sup>2</sup>]</b> |  |
|--|--|
| $f(\mathbf{x})$  | $= 105.30 - 0.45 \cdot PlotRatio - 25.16 \cdot FormFactor + 87.65 \cdot RoofRatio$<br>$- 0.13 \cdot MeanEnvelopeIrrad + 0.12 \cdot MeanFacIrrad$<br>$+ 0.021 \cdot MeanNorthFacIrrad - 0.028 \cdot MeanSouthFacIrrad$<br>$- 0.021 \cdot MeanWestFacIrrad + 0.011 \cdot NorthFacIrradPerFA$ |
| $f_{red}(\mathbf{x})$                                    | $= 72.76 + 0.19 \cdot PlotRatio - 22.75 \cdot FormFactor + 0.0024 \cdot MeanEnvelopeIrrad$   |
| <b>Daylight metamodel [%]</b>                            |  |
| $f(\mathbf{x})$  | $= 105.24 + 10.49 \cdot PlotRatio - 137.00 \cdot SiteCoverage - 16.43 \cdot FormFactor$<br>$+ 28.66 \cdot WFRatio - 1.23 \cdot MeanHeight - 0.031 \cdot MeanRoofIrrad$<br>$+ 0.076 \cdot MeanFacIrrad + 0.013 \cdot MeanNorthFacIrrad$<br>$+ 0.011 \cdot EnvelopeIrradPerFA$               |
| $f_{red}(\mathbf{x})$                                    | $= 74.44 + 16.41 \cdot PlotRatio - 179.89 \cdot SiteCoverage + 58.47 \cdot WFRatio$<br>$- 2.55 \cdot MeanHeight + 0.083 \cdot MeanFacIrrad$  |

### 4.5.5 Interpretation

At first view, it may seem like the metamodeling approach could allow investigating the relationship between the inputs and outputs. For instance, it is possible to apply the same fitting algorithm on a standardized version of the dataset to obtain the relative influence of each input present. Standardizing consists in scaling each series of input values, equivalent to each column of  $\mathbf{X}$ , so that they are centered with a mean of 0 and a std of 1. Using the Matlab function *zscore*<sup>18</sup>, this transformation is done to remove the effect of different units between the inputs and hence allow comparing their coefficient.

Figures 4.28 and 4.29 show the importance of each input respectively in the energy and daylight metamodel (full final version). In the bar plots of Fig. 4.28a and 4.29a, the position above versus below zero indicates the direction of the effect on the output. These coefficients are also found in the slope of each line in the Partial Dependence Plots (PDPs) of Fig. 4.28b and 4.29b, where the corresponding input histogram is also plotted to help interpretation by showing the range spanned by the data. A Partial Dependence Plot (PDP) describes the contribution of a predictor to the metamodel [Hastie et al., 2009]. It shows by how much, in average, the output varies in function of a unique input, when averaging the other parameters. For linear models like ours, a PDP also portrays a linear relation.

These results are intrinsic to the metamodels structure ( $f(\mathbf{x})$  in Table 4.13). That is, the information they portray is an artifact of the fitting process rather than a reflection of the trends observed in the raw data in section 4.4.2. Let us consider for example the *MeanEnvelopeIrrad* parameter in the energy metamodel. A negative effect is seen in Fig. 4.28b, where higher

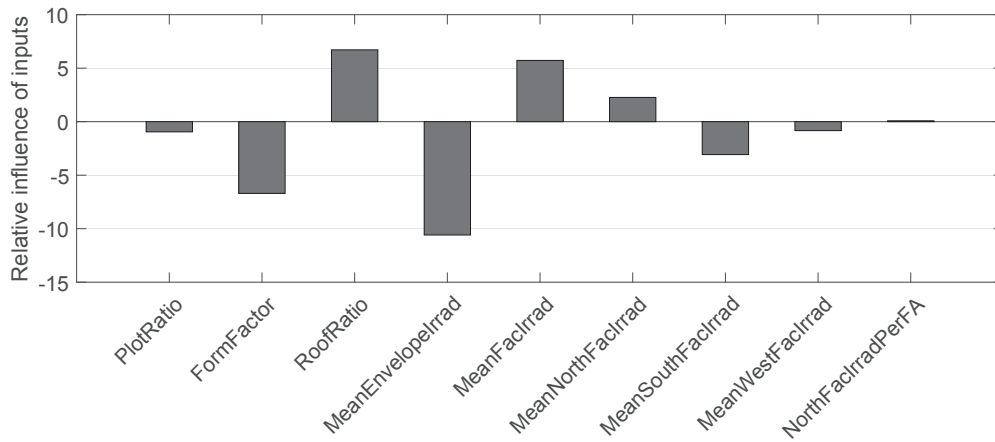
<sup>18</sup><http://www.mathworks.com/help/stats/zscore.html> (last accessed on April 4, 2016)

values are linked to a lower energy need. Yet, a positive correlation was previously observed in Table 4.12 and Fig. A.2a.

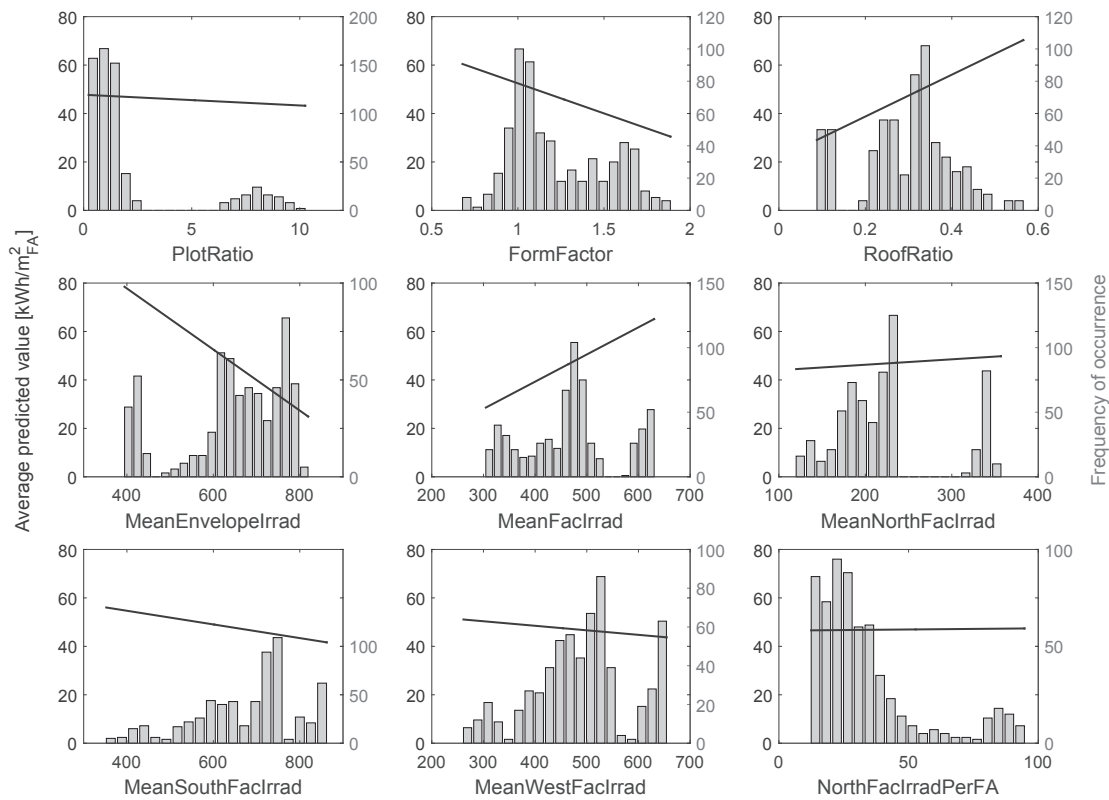
Other such inversions can be found, e.g. for the *PlotRatio* in the daylight metamodel. Interpreting the coefficients for instance for design-guidance is not a valid application of the metamodeling results. When the metamodels are fitted, there is no guarantee that the actual correlations are respected, as the algorithm only finds what works best for predicting the desired value, without accounting for the underlying relationships. What we observe from the above steps is that the structure of a metamodel is strongly dependent on the data from which it learns. Coefficients obtained for the set of included inputs are affected if one or more parameters are dismissed. This statement is further reinforced by the graphs presented in appendix A.3, showing the estimated main effect of each input for different fitting settings, i.e. different subsets of inputs based on the  $\alpha$  values in section 4.5.

In the context of this thesis, the metamodels are used for predicting the performance, to some level of accuracy which is further quantified in chapter 6. The functions can be seen as in constant evolution, a structure that feeds itself off the data it is given. Based on our experimental methods for the data acquisition, processing, and model fitting, it is not possible to extrapolate the application of the metamodels to investigate the relative importance of the parameters.

## Chapter 4. Metamodel development



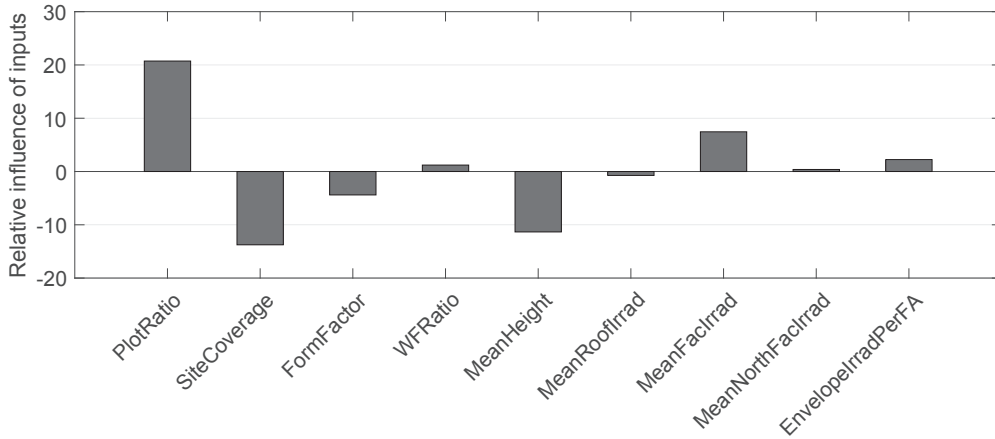
(a) Normalized coefficients



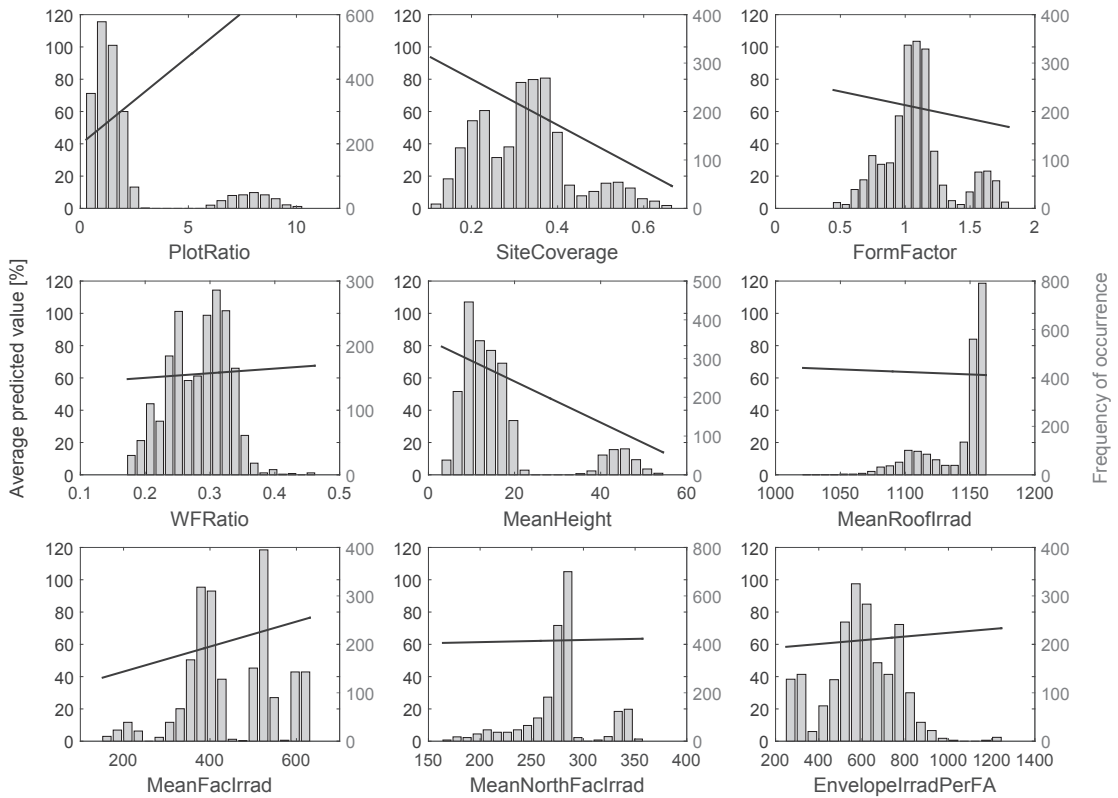
(b) Partial dependence plot (dark line) overlaid on corresponding input histogram (light gray)

Figure 4.28 – Relative importance and effect of each input according to the **energy**  $f(x)$  metamodel structure.

## 4.5. Metamodel training and testing



(a) Normalized coefficients



(b) Partial dependence plot (dark line) overlaid on corresponding input histogram (light gray)

Figure 4.29 – Relative importance and effect of each input according to the **daylight**  $f(x)$  metamodel structure.

#### 4.5.6 Additional metamodel version

A third metamodel version is shown in Table 4.14,  $f_{prelim}(\mathbf{x})$ , corresponding to preliminary functions fitted earlier in the course of this doctoral research, in view of the workshops described in chapter 5. These metamodels are the ones that were implemented in the DDS workflow also introduced in the next chapter. They were obtained from a slightly different dataset. Specifically, the total number of cases in the energy and daylight datasets were of 508 and 2263, respectively lower and higher than the current 624 and 2060 data points as noted in Fig. 4.13 and 4.14. In the initial energy dataset, the M0 case was absent, while the daylight dataset contained erroneous cases that were later identified and removed from the initial version. Moreover, the fitting procedure followed to derive these preliminary metamodels did not include all the steps presented in this chapter (e.g. the initial comparison of settings in the stepwise function in section 4.5.3).

In section 6.2, we bring back all metamodel versions when testing them on a new set of neighborhood designs, acquired through workshops conducted with professionals, as detailed in section 5.2.

Table 4.14 – Preliminary version of the predictive functions.

| <b>Energy metamodels [kWh/m<sub>FA</sub><sup>2</sup>]</b> |   |
|---|---|
| $f_{prelim}(\mathbf{x}) =$                                | $78.83 - 0.667 \cdot PlotRatio - 2.73 \cdot SiteCoverage - 8.15 \cdot FormFactor$<br>$+ 39.68 \cdot RoofRatio - 0.043 \cdot MeanEnvelopeIrrad$<br>$- 0.073 \cdot MeanNorthFacIrrad - 0.025 \cdot MeanEastFacIrrad$<br>$+ 0.014 \cdot FacIrradperFA + 0.169 \cdot NorthFacIrradperFA$<br>$+ 0.115 \cdot EastFacIrradperFA$   |
| <b>Daylight metamodels [%]</b>                            |   |
| $f_{prelim}(\mathbf{x}) =$                                | $47.67 + 4.78 \cdot PlotRatio - 97.98 \cdot SiteCoverage - 10.31 \cdot FormFactor$<br>$+ 69.21 \cdot RoofRatio + 63.60 \cdot WFRatio - 0.008 \cdot MeanEnvelopeIrrad$<br>$- 0.027 \cdot MeanRoofIrrad + 0.021 \cdot MeanFacIrrad + 0.013 \cdot MeanEastFacIrrad$<br>$+ 0.017 \cdot MeanSouthFacIrrad + 0.009 \cdot MeanWestFacIrrad$<br>$+ 0.049 \cdot FacIrradperFA$ |

### 4.5.7 Further investigation

#### Training and testing by case series

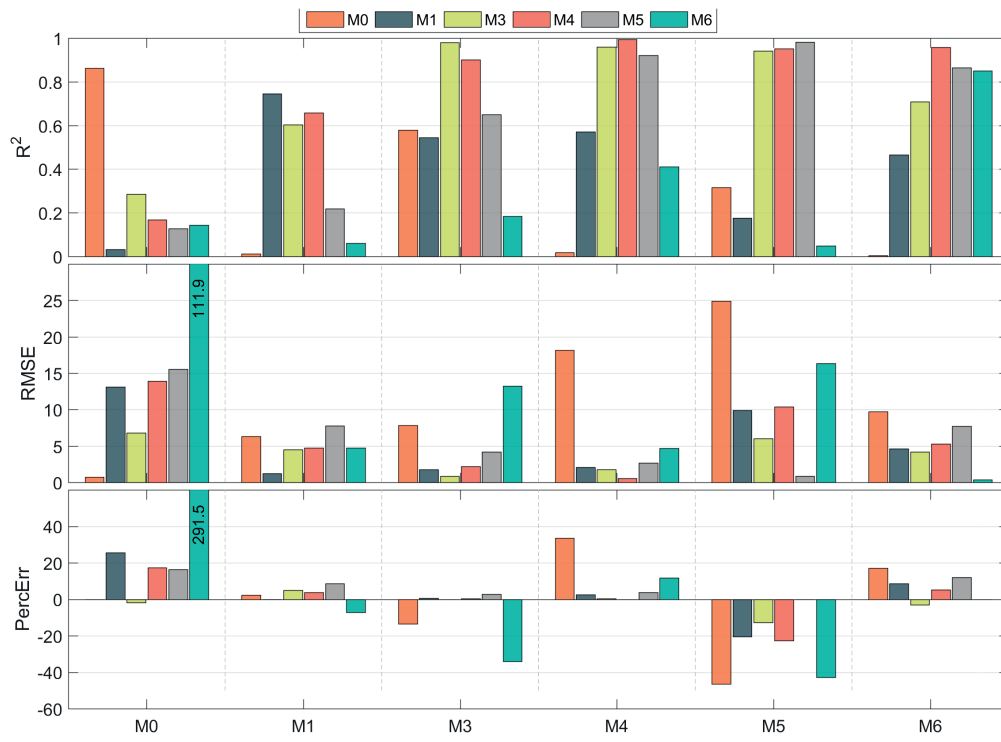
Until now, we have treated the dataset as a whole without distinguishing between the different case series of which it is composed. In the above steps, whenever a random split of the data was present, it was applied without controlling for the  $M$ -cases falling in the training and testing sets. It is of interest to verify what happens when we specifically use one or more case(s) for training and the remaining ones for testing. This sort of investigation can provide information on which type of design(s) contributes most to the metamodeling process. Specific cases may yield features that capture more explanatory information with respect to the output we are trying to predict.

Figure 4.30 shows the  $R^2$ , RMSE and Percentage Error (PercErr) statistics obtained when applying the stepwise algorithm on a unique case  $M_i$  (x-axis) and testing on each other case  $M_j$  (y-axis). As expected, the combinations where  $i = j$  lead to good results, since the training and testing datasets are the same. For combinations where  $M_i$  and  $M_j$  are further apart in terms of building typology such as M0-M6, the prediction error is higher. In that example case, the PercErr jumps to nearly 300%. However, for the opposite order where M6 is used for training and the resultant model is tested on M0, results are better (e.g. PercErr < 20%).

Based on our results, we observe that the energy model trained on M1 performs generally better across all other variants. For the daylight metric, the M4 and M6 models have the lowest prediction errors. This information could be exploited in future work to sample the solution space more efficiently, by adding designs characterized by features contributing most to improving the fit.

Although a higher prediction accuracy could be achieved by fitting a series of case-specific metamodels, their application range would be limited to similar typologies. We therefore consider a combined treatment, as done in the previous section, preferable to a separation by case series.

## Chapter 4. Metamodel development



(a) Energy



(b) Daylight

Figure 4.30 – Fit and error metrics for each combination of data subsets, where a model trained on case  $M_i$  (x-axis) is tested on case  $M_j$  (color-coded bar).



### Gaussian Processes

The choice of multiple linear regression applied in the previous sections conditions the function  $f(\mathbf{x})$  to be linear. A different supervised machine learning technique called Gaussian Processes (GP) regression detaches itself from the need to assume a fixed model form. GPs are probabilistic regression methods that can easily model non linear functions [Rasmussen and Williams, 2006].

To use a GP for prediction we must first define a prior distribution over functions, which is done by choosing an appropriate kernel (or covariance) function. This kernel function defines a ‘family’ of possible shapes or forms of the regression function we are trying to estimate. A popular and widely-used non-linear kernel function is the Radial Basis Function (RBF), also known as the squared exponential covariance function [Ebden, 2008; Rasmussen and Williams, 2006]:

$$\text{cov}(f(\mathbf{x}_i), f(\mathbf{x}_j)) = k(\mathbf{x}_i, \mathbf{x}_j) = \sigma_f^2 \exp\left(-\frac{1}{2l^2} |\mathbf{x}_i - \mathbf{x}_j|^2\right) \quad (4.6)$$

where  $\mathbf{x}_i$  and  $\mathbf{x}_j$  are a pair of inputs and  $\sigma$  and  $l$  parameters through which the level of smoothness of the function can be controlled.

Through a collaboration with Prof. Peter Moonen<sup>19</sup>, work was initiated to investigate the application of this method to our context. A technique further detailed in [Moonen and Allegrini, 2015] and based on the above kernel function was applied, leading to a metamodel employing the five inputs listed in Table 4.15, which were identified as most improving the fit for each model. The correlation coefficients, found through the analysis of section 4.4.2, have been included in the table in the same way as done in Table 4.12. Only two parameters, appearing in bold, are also found in the linear regression models presented earlier (see Table 4.13). This points again to the impossibility of drawing conclusions on the direct effect of specific inputs on the performance metrics just by judging from their presence/absence in the metamodels. Values such as the mean irradiation received on roof surfaces is not expected to affect the daylight conditions inside a building, yet this parameter is present in both the GP and linear models for that metric.

Results from the training-testing process of each metamodel containing the five respective inputs are shown in Fig. 4.31. The prediction accuracy achieved for both metrics is very similar to the results from our approach, previously shown in Fig. 4.25 and 4.26. However, the GP metamodels only contain about half the minimum number of terms we have considered ( $\alpha=100\%$  case).

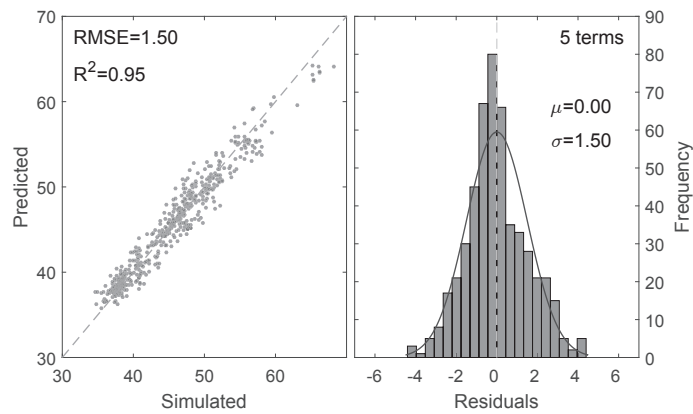
In section 6.2.2 we present the prediction results obtained by applying the GP metamodels on a new test set, to further assess the potential of this powerful yet more complex technique.

<sup>19</sup>Collaboration leading up to a joint publication (in preparation) is ongoing with Prof. Peter Moonen from the Université de Pau et des Pays de l'Adour. All results presented here reflect his contribution.

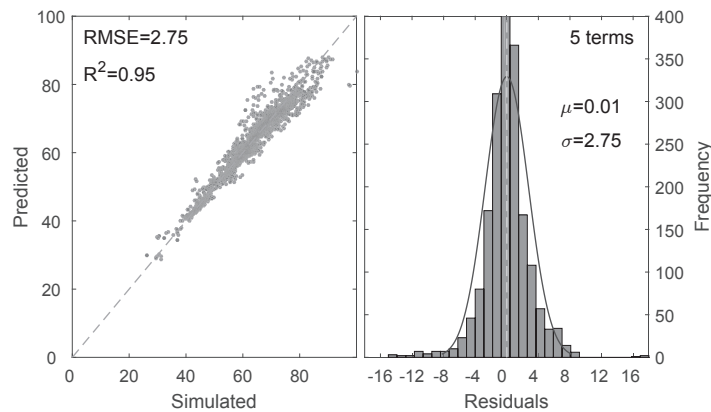
## Chapter 4. Metamodel development

Table 4.15 – Predictors found in the GP models along with their correlation level to the output metric. Bold terms denote predictors also contained in the final metamodels presented in section 4.5.4 (Table 4.13).

| Energy metric             |             | Daylight metric       |             |
|---------------------------|-------------|-----------------------|-------------|
| Input                     | Correlation | Input                 | Correlation |
| <b>FormFactor</b>         | -0.91       | <b>SiteCoverage</b>   | -0.59       |
| <i>NorthFacRatio</i>      | -0.29       | <i>EastFacRatio</i>   | -0.15       |
| <i>WFRatio</i>            | 0.66        | <i>WestFacRatio</i>   | -0.15       |
| <b>MeanWestFacIrrad</b>   | 0.63        | <b>MeanRoofIrrad</b>  | 0.25        |
| <i>EnvelopeIrradPerFA</i> | 0.90        | <i>RoofIrradPerFA</i> | 0.65        |



(a) Energy ( $\text{kWh/m}_{\text{FA}}^2$ )



(b) Daylight (%)

Figure 4.31 – Performance of the metamodels obtained by GP regression. For each metric: predicted versus simulated values (left) and residuals histogram (right). Each model contains the five input terms listed in Table 4.15.

### 4.6 Complementary algorithm: active solar criterion

The third performance criterion we want to include in our DDS workflow relates to the active solar potential of a neighborhood. Since we already have access to irradiation data, required to compute the irradiation-based predictors in the above metamodels, the exploitation of this information suffices to estimate the energy production by PV panels and ST collectors. Instead of a metamodel, an algorithm is therefore used, corresponding to a slightly modified version of the one presented in section 3.1.4.

Assuming an office function of all buildings and a DHW coverage of 50% over the year, equation 3.5 becomes simply:

$$\text{DHW} = 0.5 \times \text{FA} \times \text{Qhw5} = 3.47 \times \text{FA} \quad (4.7)$$

where FA is the total floor area and Qhw5 the annual demand per floor area for commercial buildings (25 MJ/m<sup>2</sup> converted to kWh/m<sup>2</sup>) [SIA, 2009b].

The remaining steps are the same, except that we take the annual instead of the winter irradiation value  $I_w, i$  in equations 3.6. This is done to avoid the need for a second irradiation simulation with a different period of time in DIVA, in view of the desired real-time calculation as explained in the next chapter.

In future work, this algorithm could be refined to include facades, by removing or lowering the irradiation threshold that is currently set to 1000 kWh/m<sup>2</sup>, and discarding glazed surfaces. Different assumptions, editable by the user, could be used for the each system's efficiency and relative coverage ratio, according to the building function and project-specific priorities.

### 4.7 Summary - Achievements, limitations and future work

This chapter has described the process of developing a novel multi-criteria method for rapidly predicting the solar performance of a neighborhood design in its early phase. The method combines predictive functions to estimate the energy need for heating and cooling and the spatial Daylight Autonomy, along with an algorithm for computing the potential energy production from active solar systems.

Trained on a series of design alternatives incorporating morphological variations, the metamodels perform well although they do not explicitly include parameters linked to the building typology (or shape). This is an advantage considering that there is no need to identify and categorize the typology when applying the metamodels. Their validity boundaries over neighborhood designs incorporating a mix of shapes is further assessed in chapter 6.

### 4.7.1 Reduction of computational cost

Inputs to the predictive functions consist of a mix of parameters capturing the essential features of a 3D model in terms of geometry and solar exposure levels. The computational cost of applying the metamodels is dictated by the irradiation simulation needed to obtain the irradiation-based predictors. Table 4.16 lists the time required to run a full simulation versus the metamodel for each metric. Depending on the size and complexity of the design, e.g. number of buildings, an energy and daylight simulation can respectively take up to (approximately) 10 and 180 times longer than applying the metamodel. In addition to time savings, our approach requires a simpler 3D model, i.e. empty boxes as opposed to the facade and internal (e.g. zoning) required for an energy and daylight simulations.

Table 4.16 – Comparison of computational cost of evaluating the performance through a simulation versus the metamodel. These times were recorded for simulations run on an Intel i7-4820K (4 cores) 3.70GHz computer with 16 GB of RAM. Ranges correspond to the min-max value measured across the seven M cases that were simulated to generate the dataset. Daylight simulation on ground floor level only.

| <b>Evaluation</b>                 | <b>Time per design variant</b> |
|-----------------------------------|--------------------------------|
| Energy simulation with EnergyPlus | ~1 to 5 minutes                |
| Energy metamodel                  | ~ seconds, max 1 minute        |
| Daylight simulation with DIVA     | ~30 minutes to over 1.5 hour   |
| Daylight metamodel                | ~ seconds, max 1 minute        |

### 4.7.2 Solution space sampling

Although an effort was made to obtain a large amount of data through the parametric modeling and different sampling techniques (DoE and random), we may have missed some important zones in terms of design features. This has an impact on the defined list of potential predictors as well as on the landscape of output values recorded, which may both be lacking some information. Complementary or alternative predictors could be tested in the future. The possibility of adopting an experimental design providing more control over the covered ranges of the input values should be investigated. Along the same lines, an infill strategy could be used to identify at which point additional simulations should be done to improve the dataset. The acquisition of so called infill or update points would allow improving the accuracy of the predictive function [Forrester et al., 2008].

Moreover, basing the data collection process on a thorough examination of contemporary urban developments would allow achieving a wider and more realistic coverage of the hypothetical design space in terms of building typology and layout.

### 4.7.3 Effect of simulation settings

As promised in section 3.2.1, we here come back to the question of the energy simulation settings. Considering that the metamodels are to be applied for quickly comparing design alternatives, what we want to investigate is whether or not these variants are ranked in the same order, according to their energy performance, when different simulation settings are applied in EnergyPlus.

Figure 4.32 shows the simulated heating need values for the same subset of designs, corresponding to the current M0 series, previously termed M1 in chapter 3 (LN-PDL study). For each orientation, the data corresponding to the LN-PDL study has been sorted from the lowest to highest value. The same order was applied on the current data. Looking at orientation  $0^\circ$  (light gray), we see that the heating need is lower for the current dataset and that the overall trend is slightly different. This means that the ranking in terms of heating need is not exactly the same between the two datasets. This difference is more important for the  $90^\circ$  orientation, corresponding to an East-West street alignment and hence dominant North- and South-facing building facades (see Fig. 4.9a). The two dark gray lines representing this orientation are closer in terms of order of magnitude, but show divergent rankings among designs. Not only do the distinct simulation settings have an effect on each design's heating need, but this effect is not the same across variants. Moreover, for larger North- and South-facing facade ratios, this difference in the effect is amplified.

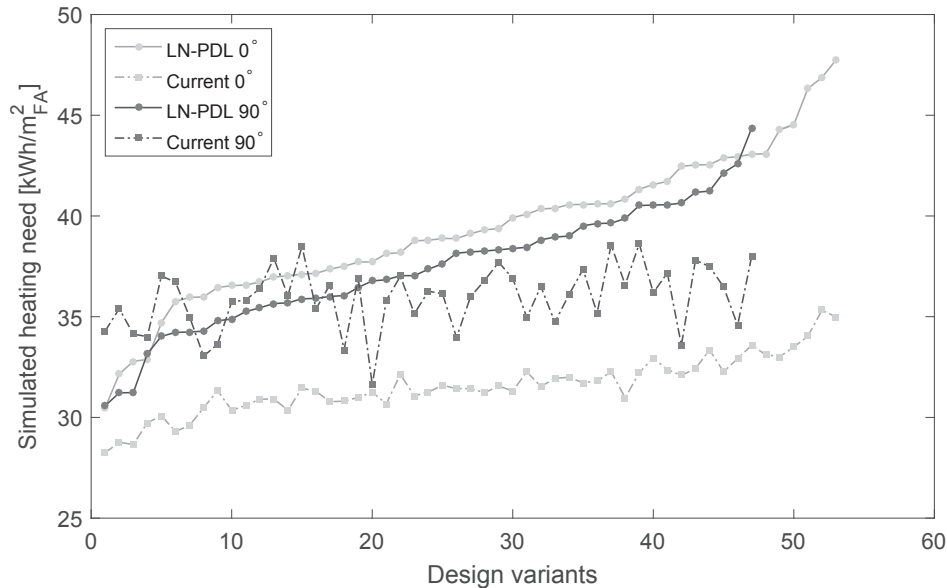


Figure 4.32 – Comparison of simulated floor-area-normalized heating need [kWh/m<sup>2</sup><sub>FA</sub>] between the current dataset and the LN-PDL results presented in chapter 3 for the adjacent M0 design series, in both orientations.

## Chapter 4. Metamodel development

---

To increase the scope of applicability of the metamodels, additional data should be analyzed and exploited, obtained through simulations with different underlying assumptions related to the climate and building function, materials, occupancy, etc. This has been initiated through preliminary work [Nault et al., 2015c].

Multiple versions of the metamodels should then be defined, generating a library of functions from which the adequate version could be retrieved based on the context. Another option would be to include predictors to account for the added variables linked to the climate, function, etc., assuming a robust metamodel could be derived. This topic is further discussed in chapter 7, where an additional analysis is presented to compare two datasets with different U-value settings.

### 4.7.4 Error sources

As for any computational experiments, results presented throughout the chapter are subject to deterministic experimental errors of both human nature - e.g. bugs in the Grasshopper scripts and Matlab code - and systematic type that can cause consistent under- or over-estimation of the measured values [Forrester et al., 2008].

Fitting results are conditioned by the choice of a linear regression and by the reference dataset. In future work, it would be of interest to investigate other types of models (e.g. non-linear) and techniques, such as the one presented in section 4.5.7 - Gaussian Processes - and ensemble methods, e.g. random forests based on decision trees, which were shown to be promising for predicting housing electricity energy consumption [Tso and Yau, 2007].

Further thoughts on the possible limitations and improvement and application prospects of the metamodels are presented in chapters 7 and 8. In the next chapter, we describe how the performance assessment engine consisting of the energy and daylight metamodels and the active solar potential algorithm are integrated into a DDS workflow to be tested among practitioners.

# 5 Application to the design process

*“We cannot solve our problems with the same thinking we used when we created them.”*

Albert Einstein  
(physicist)

The performance assessment method developed in the previous chapter offers the means to quickly and simply estimate the multi-criteria performance of a set of buildings. To further inquire into its accuracy as well as its usefulness and adequacy in the context of early neighborhood design, the assessment engine is integrated into a design decision-support (DDS) workflow. Described in this chapter, the workflow adopts a generative approach with the aim of providing user-guidance for exploring a space of design solutions from the perspective of their performance.

The implementation of the workflow as a computer-based prototype is detailed, as well as the approach adopted to test the prototype among practitioners through workshops<sup>1</sup>. Results of these workshops are presented in the next chapter.

## 5.1 Implementation as a design decision-support workflow

### 5.1.1 Related work and objectives

As mentioned in chapter 2, specific features built around a performance assessment engine can enhance the design-support aspect of a tool. We here briefly survey related work before presenting our implementation approach in the next section.

In the field of architectural design of structural elements with a focus on early-phase design, Mueller and Ochsendorf [2013] developed structureFIT<sup>2</sup>, an interactive web-based tool for exploring a solution space of planar trusses, linking geometrical variables to structural per-

<sup>1</sup>Some elements of this chapter have been presented in Nault et al. [2016a,b].

<sup>2</sup><http://digitalstructures.mit.edu/page/tools#structurefit> (*last accessed on April 5, 2016*)

formance. A surrogate model is used to compute the performance, while an evolutionary algorithm allows exploring the solution space and identifying optimal designs.

Focusing on room-level wind flows, Malkawi et al. [2005] developed an ‘evolution model’ using genetic algorithms (GA) and computational fluid dynamics (CFD). Conceived to minimize the deviation from a specified mean velocity inside a room, the optimization algorithm is used to make the design evolve by playing with relevant variables (e.g. position and length of supply duct).

Closer to our field are the Parametric Urban Design components developed by Schneider et al. [2011] for automating the generation of a street network, and the Animated Building Performance Simulation of Lagios et al. [2010] allowing the solar performance evaluation of multiple building-scale design variants. Both make use of the Grasshopper<sup>3</sup>graphical algorithm editor, linked to the Rhino<sup>4</sup>3D modeler.

Ritter et al. [2015] recently developed a design space exploration assistance method (DSEAM) that relies on a metamodel for predicting the energy use for heating and cooling and the maximum correspond loads for a building. From user-defined inputs consisting in a initial building design along with ranges for parameters such as the glazing ratio and envelope properties, the system automatically generates the design space and corresponding metamodel. Once this phase is completed, results are displayed in the form of graphs showing the impact of the different parameters on the outputs.

The approach we propose embraces the same vision of a semi-automated and interactive process for populating a solution space of design alternatives, supporting a visual comparison of their performance.

### 5.1.2 Implementation process and structure of workflow

The workflow is composed of the performance assessment engine, consisting of the passive solar and daylight metamodels and the active solar algorithm developed in chapter 4, complemented by additional elements as illustrated in the flowchart of Fig. 5.1. These elements, further detailed in the following sections, concern the acquisition of inputs from the user, the automatic generation of design alternatives (or variants), and the outputs visualization. It is important to note that we here use the term inputs to refer to both the data entered by users and the data passed to the performance assessment engine, i.e. the predictors  $\mathbf{x}$  in the functions  $f(\mathbf{x})$  as described in chapter 4. In the same way, the term outputs represents the performance values as well as the different formats in which these are presented to the user. The exact meaning of the words should be clear from the context.

---

<sup>3</sup><http://www.grasshopper3d.com/> (last accessed on March 20, 2016)

<sup>4</sup><https://www.rhino3d.com/> (last accessed on March 20, 2016)



## 5.1. Implementation as a design decision-support workflow

---

The structure of the workflow was conceived based on the outcome of our review presented in chapter 2, including the identified requirements that helped us configure the interface, the interaction with the user, and the multi-design-variants approach. This latter aspect was also inspired by the parametric modeling procedure developed for gathering data in section 4.2. Factors of technical nature linked to the implementation, which was done in collaboration with a student assistant<sup>5</sup> who provided coding support, also played a major role in shaping the workflow.

To transform this workflow into a CA(A)D-integrated digital prototype easily understood and directly usable by the concerned decision-makers (i.e. architects, urban designers), the implementation relied on the 3D modeler Rhino. Other existing tools, referred to in Fig. 5.1, were exploited and linked as illustrated in Fig. 5.2. Grasshopper became the central background program in which all elements of the workflow are linked. However, since this program quickly leads to complex graphical scripts (see Fig. 3.7) and is limited in terms of GUI, it was decided to transform parts of the workflow into a 'hidden' code and generate a custom interface to facilitate communication with the user. As such, the core of the prototype was coded in C# [Microsoft, 2013] and packaged as a Grasshopper plug-in for Rhino. This plug-in consists of three custom Grasshopper components illustrated in Fig. 5.3. The custom interface conceived for gathering user-inputs, shown in Fig. 5.4, is opened by double-clicking on the Parameters' component. The performance assessment engine is coded into the Evaluation component. Additional Grasshopper plug-ins are also used in the implementation: DIVA-for-Grasshopper [Jakubiec and Reinhart, 2011] for running the irradiation simulation and LunchBox<sup>6</sup> for exporting design variants as Rhino .3dm models and the performance data as an Excel file. The diagram in Fig. B.1 of appendix B.1 illustrates the internal functioning of the prototype and links between its constituents.

The DDS prototype thus produced was named Urban SOLar Visual Explorer (UrbanSOLve). The prototype is installed like any other Grasshopper plug-in, i.e. by placing it (a .gha file) in Grasshopper's Components folder. In its current status, the prototype requires some manual settings (e.g. components linking) in Grasshopper before it can be used. This is further explained in section 5.2.3. For now, we will assume these settings have been done to pursue below with detailing the workflow of Fig. 5.1. A screenshot-based demonstration of the workflow can also be found in appendix B.2.

It is to note that the text contained in most images referred to in this section - placed either herein or in the appendix - is in French, since the prototype was developed in view of the workshops presented in section 5.2 and in which local architects and urban designers (all French-speaking) participated. An effort is made in the description of the images and workflow to clarify/translate the important terms.

---

<sup>5</sup>The contribution of Mélanie Huck, architect and computer scientist, has been crucial in transforming the workflow into a usable prototype.

<sup>6</sup><https://provingground.io/tools/lunchbox/> (last accessed on April 22, 2016)

## Chapter 5. Application to the design process

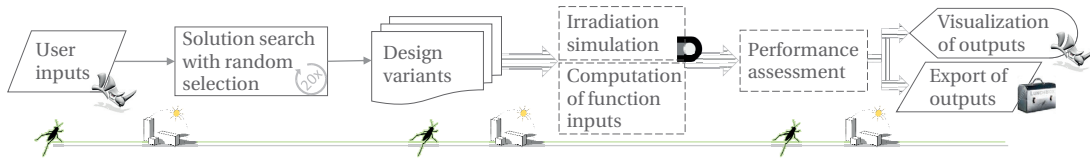


Figure 5.1 – Implementation flowchart. The developed performance assessment engine (dashed boxes), detailed in chapter 4, is integrated with additional components to complete the workflow. Tools used, indicated by their logo, are presented in Fig. 5.2.

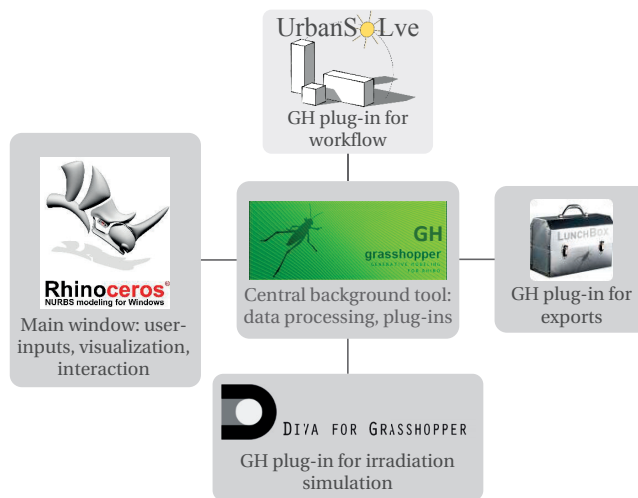


Figure 5.2 – Tools used in the development of the prototype to produce the workflow of Fig. 5.1. UrbanSOLve consists in a Grasshopper plug-in (.gha file) that holds three components presented in Fig. 5.3.

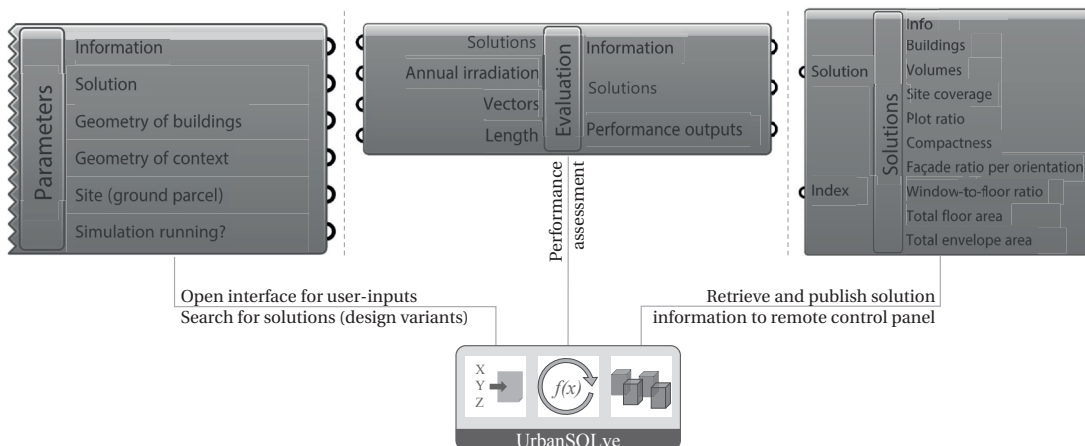


Figure 5.3 – Three custom Grasshopper components of the prototype (coded in C# by Mélanie Huck). These can be found in Grasshopper's Component Tab 'Extra'. Once selected, they must be placed in the current Grasshopper document and linked to/complemented by additional elements as explained in section 5.2.3 and Fig. 5.12.

## 5.1. Implementation as a design decision-support workflow

The screenshot shows the UrbanSOLVe software interface with the following sections:

- Buttons:** "Lancer la simulation", "Valider les paramètres", "Valider et fermer".
- Number of solutions:** "Nombre de solutions désirées" set to 20.
- Bâtiments:**
  - Typologie:** "Volume simple" (selected), "Îlot", "Volume en L".
  - Orientation:** Radio buttons for A, B, C, D with corresponding diagrams.
  - Alignement:** "Centre" (selected), "Bord", "Rotation" set to 0.
- Dimensions:**
  - Min X: 10, Max X: 30, Min Y: 10, Max Y: 60, Min Z (étage): 3, Max Z (étage): 10.
  - Min D - volumes L: 8, Max D - volumes L: 14, Min D - îlots: 8, Max D - îlots: 12.
- Buttons:** "Créer un bâtiment", "Créer plusieurs bâtiments".
- Contraintes:**
  - Indice d'utilisation du sol: IUS minimum (1.3), IUS maximum (1.8).
  - Taux d'occupation du sol: TOS minimum (0.2), TOS maximum (0.8).
  - Distance minimum entre bâtiments [m]: 10.0.
- Divers:**
  - Ratio fenêtres: 0.46
  - Hauteur d'étage [m]: 3.0
  - Fonction: résidentiel, commercial.
- Calques:**
  - Terrain: GH\_terrain
  - Bâtiments du contexte: GH\_contexte
- Logos:** LIPID (Interdisciplinary Laboratory of Performance-Integrated Design) and EPFL (ÉCOLE POLYTECHNIQUE FÉDÉRALE DE LAUSANNE).

Figure 5.4 – Custom interface of the prototype (coded by Mélanie Huck), opened by double-clicking on the Parameters' component (see Fig. 5.3). Boxes that are grayed-out correspond to variables that are currently fixed.

### User-inputs

The acquisition of user-inputs is made both through the custom interface developed (Fig. 5.4) and the Rhino window. First, users must draw the parcel of land on which they want to design, and on a distinct Rhino layer, the existing context i.e. surrounding buildings as simple volumes (optional). The name of each layer must be entered in the corresponding boxes in the UrbanSOLve interface (*Calques*).

The next step consists in defining an abstracted neighborhood base design by positioning building-specific reference points on the empty parcel. To do so, users must, for each building: (i) select the desired typology among the three options given in the UrbanSOLve interface: simple volume, courtyard or L-shaped<sup>7</sup>, and (ii) position a reference point (either corner or center)<sup>8</sup> on the empty parcel.

Once all points have been positioned, users must adjust the remaining parameters in the UrbanSOLve interface, which define the acceptable range (min/max) of values for each variable and constraint. Variables consist in the dimension X, Y and Z (in number of stories) of the buildings, as well as the depth (D) in the case of the courtyard and L-shaped typologies. These apply to all buildings as opposed to each individual one, in order to simplify the subsequent process detailed in the next section. Constraints to respect are linked to the density, expressed through the plot ratio (*IUS: indice d'utilisation du sol*) and site coverage (*TOS: taux d'occupation du sol*), and the minimum distance between buildings. Other items appearing in the UrbanSOLve window, currently grayed-out and fixed to a certain value, could become additional variables or constraints (e.g. glazing ratio and story height). These currently correspond to the assumptions made in chapter 4, when modeling and simulating our dataset from which the metamodels were derived.

The user-inputs phase is illustrated in Fig. 5.5: each numbered item is a schematic version of the selected typology and positioned building. To produce this visualization of the base design, fixed dimensions (independent from the data entered) are assigned to each item. In this example, items 0 to 3 have been positioned using the corner alignment as the reference point, while the center alignment was used for item 4. This distinction influences the way variants are generated in the subsequent phase of the workflow, i.e. how buildings 'grow' within the variables ranges. This is further explained in the following sections.

---

<sup>7</sup>This typological constraint comes from both the metamodeling approach, where we also limited ourselves to similar simple building shapes, and technical implementation limitations. However, users can mix these typologies, something which is not found in the reference dataset. This topic is further addressed in the next chapter.

<sup>8</sup>Additional settings can be chosen when positioning a point: the orientation (in the case of L-shaped buildings), and the alignment and rotation. The effect of these settings is illustrated in Fig. B.2 in appendix B.1.

## 5.1. Implementation as a design decision-support workflow

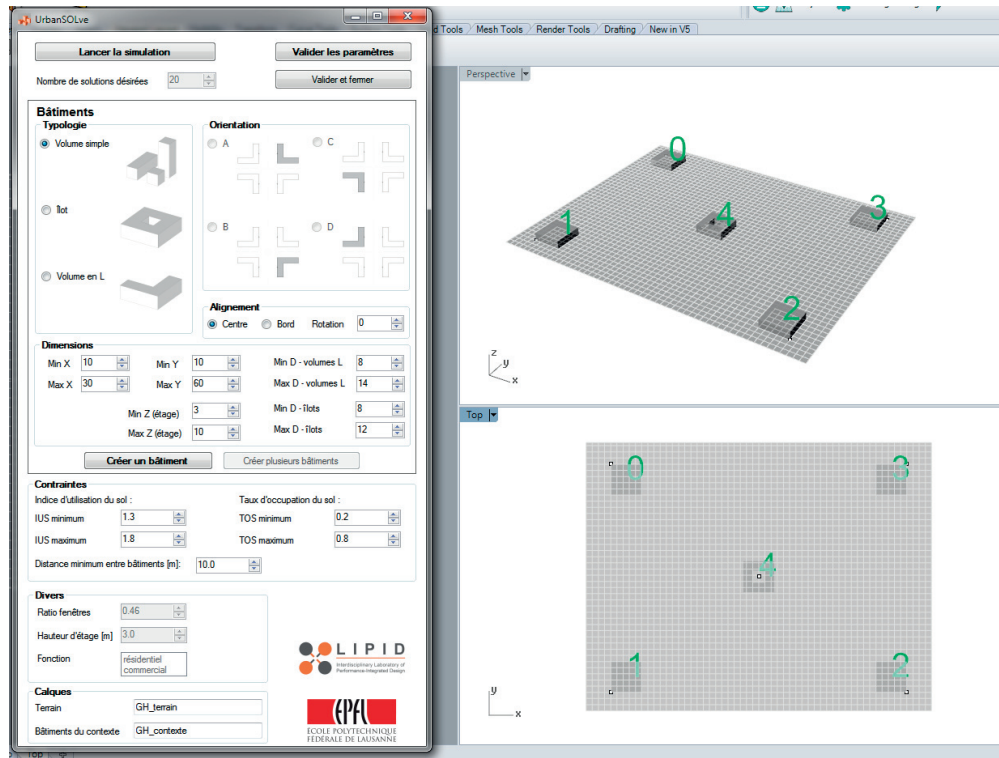


Figure 5.5 – User-inputs are acquired through the custom interface (left) and the Rhino window (right, example user-defined configuration).

### Generation and evaluation of design variants

Once all input-parameters have been provided and adjusted, users are ready to launch the simulation (*Lancer la simulation*), effectively the solution space population process. During this phase, which is hidden from the user, the prototype iteratively generates a design variant (or alternative) by randomly selecting a value for each variable and building from the user-defined ranges. It then verifies if the variant produced respects the density constraints. Additional checks are made to avoid any non-realistic situations such as buildings overlapping or extending beyond the defined parcel. This search process continues until 20 valid solutions have been found, populating to some extent the hypothetical design solution space defined by the user. Currently, this number of 20 design variants to be ‘found’, grayed-out in the UrbanSOLve window, is fixed due to technical implementation aspects linked to the use of DIVA. As one DIVA irradiation simulation component is required per design variant - leading to a repeated Grasshopper script illustrated in Fig. B.3 of appendix B.1 - it was necessary to freeze the number of variants. A value of 20 was arbitrarily defined, by considering also the simulation execution time. If users were given the option of changing the number of variants, a more direct communication pathway with the irradiation simulation would be necessary, to bypass the need for using DIVA. During the implementation, one solution considered was to directly use Radiance, an option that was then discarded due to time limitations in the development process and complications linked to creating the grid of nodes (a DIVA feature).

## Chapter 5. Application to the design process

---

For each variant, the geometry- and irradiation-based parameters required as inputs to the metamodels (chapter 4) are computed, the latter following the irradiation simulation. These inputs ( $\mathbf{x}$ ) are passed to the performance assessment engine that computes an estimate, through our predictive mathematical functions, of the energy need for heating and cooling (indicator of the passive solar potential) and sDA (indicator of the daylight potential). The third criterion (active solar potential) is computed using our irradiation-based algorithm also previously described.

This generation and evaluation phase occurs over a minimum time of about two minutes, conditioned by the irradiation simulations<sup>9</sup>. It can extend over slightly longer periods (> 5 minutes) when the user-inputs reflect strict boundaries within which it is harder to find valid designs (e.g. narrow density range).

### Outputs and visualization

Results from the generation and assessment of the design variants are shown in various formats that are produced in part by the UrbanSOLVe plug-in (in particular the Solutions component) and through some Grasshopper script. A .3dm Rhino model of each design is automatically created and saved in a folder. An Excel file containing the performance outputs of all variants is also exported to the same folder. In the Rhino window, the initial schematic model (Fig. 5.5) is overlapped with the irradiation map of the design variant selected by the user via a slider, as illustrated in Fig. 5.6. The slider, located at the top in the Grasshopper Remote Control Panel (green window), allows browsing through the 20 variants, which are numbered from 0 to 19. The information associated to the selected variant is displayed below the slider and includes parameters such as the plot (or floor area) ratio and total floor area, as well as the performance outputs and each building's dimensions.

Taking advantage of the multiple viewports in Rhino, a 3D graph, having one axis per performance criterion, can be visualized in 2D to compare the performance of the variants among each other and with respect to two criteria, as illustrated in Fig. 5.7. The three possible criteria combinations are displayed. The design showing the best performance in terms of active solar, passive solar and daylight potential is respectively colored in orange, green and purple.

By combining the different outputs, users can link a 3D model to its multi-criteria performance, while also comparing the performance of design alternatives whose morphologies are more or less distinct according to the user-inputs. An eventual weighting of the performance aspects is left to the user. The added-value and limitations associated to the prototype's functioning and GUI are further discussed in chapter 7.

---

<sup>9</sup>Time estimates obtained on an Intel i7-4820K (4 cores) 3.70GHz computer with 16 GB of RAM.

## 5.1. Implementation as a design decision-support workflow

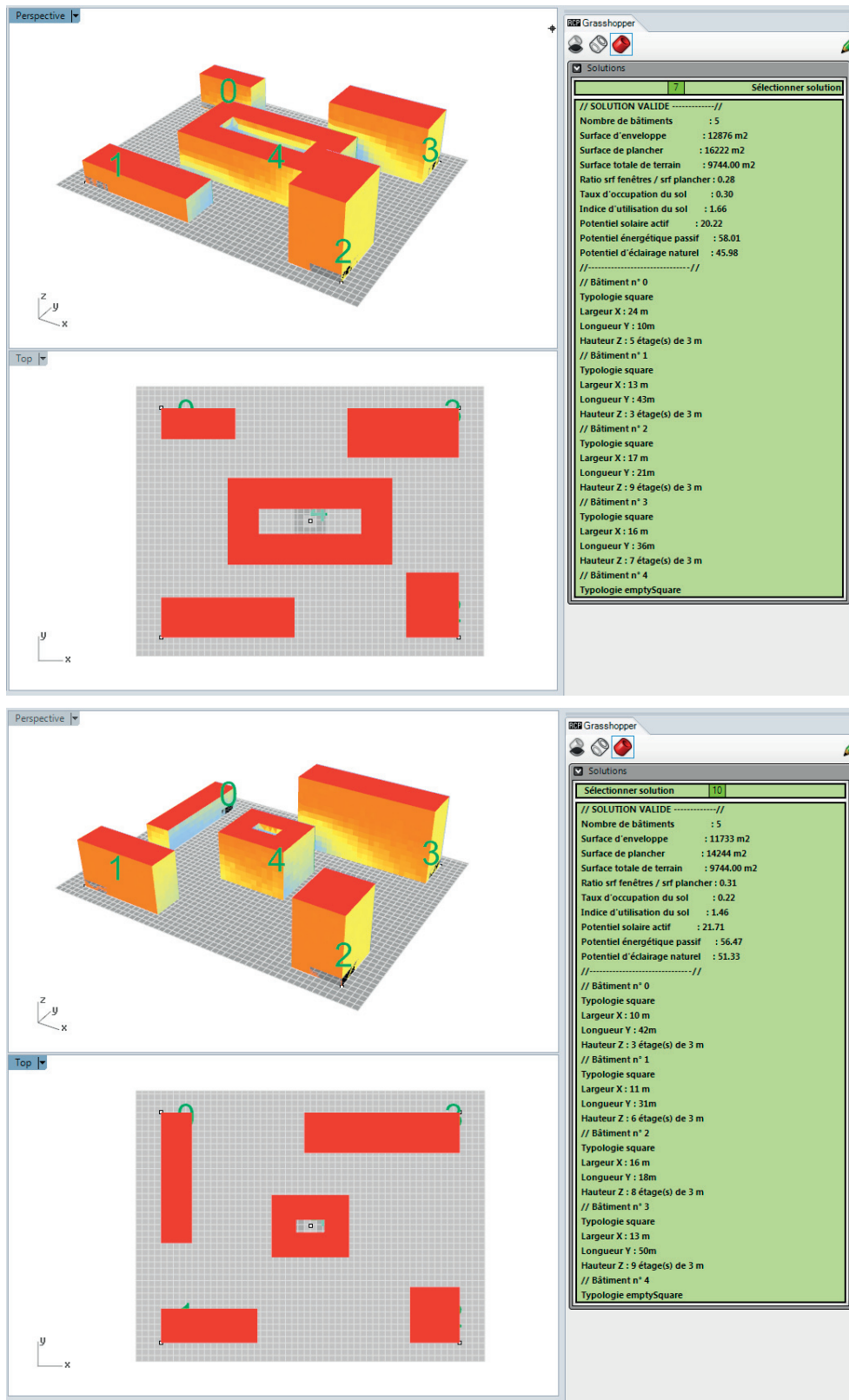


Figure 5.6 – Irradiation map (left) and solution's information (right) for two example design variants generated and evaluated by the prototype.

## Chapter 5. Application to the design process

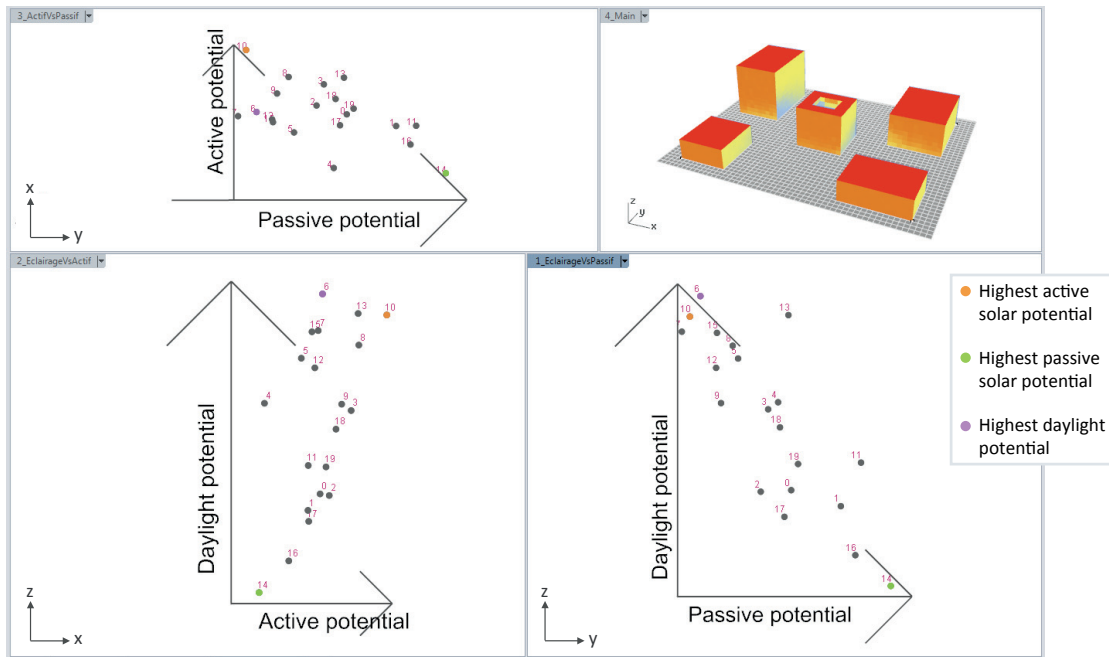


Figure 5.7 – 3D performance graph seen in 2D via three Rhino viewports. x-axis: active solar potential; y-axis: passive solar potential; z-axis: daylight potential. The 20 generated solutions are represented by numbered points (0-19).

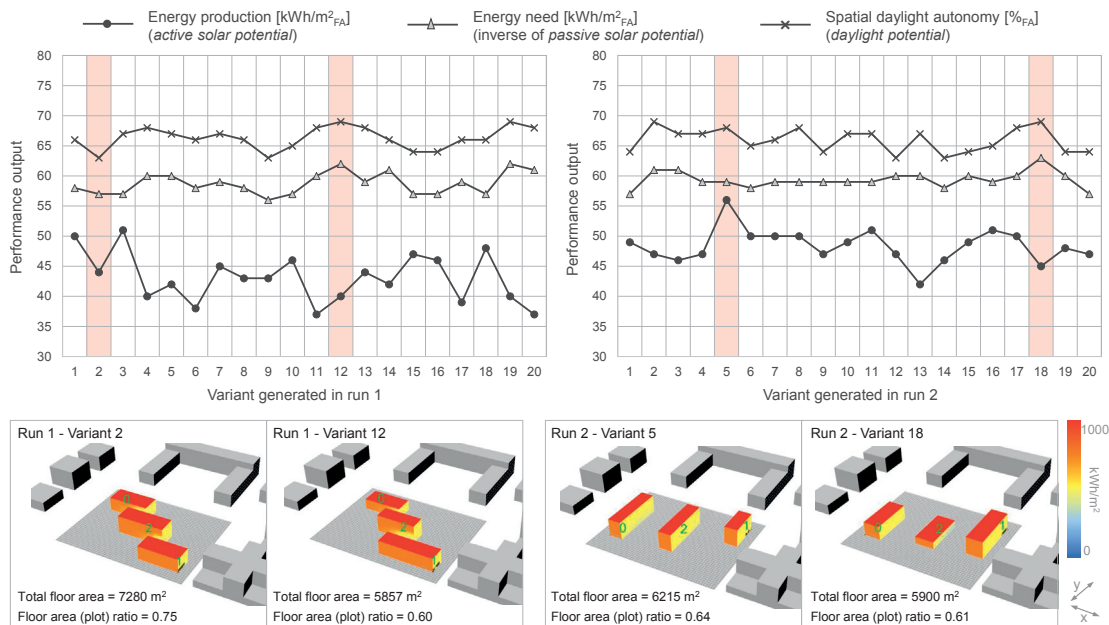


Figure 5.8 – Results from the two example runs of the prototype with a different starting base case (see Table 5.1). Top: performance of each variant generated in the first (left) and second (right) run. Bottom: irradiation map of example variants generated in each run, with distinct performance outputs.



### 5.1.3 Example application

While a step-by-step demonstration of the prototype can be found in appendix B.2, we here present an application example for two base case designs (i.e. two runs of the prototype) comprising three simple volumes each, with the user-inputs given in Table 5.1.

The performance outputs are plotted in Fig. 5.8 (top) for each variant generated in run 1 and 2. The example variants shown at the bottom of the figure (irradiation maps) present differences in their performance, despite similar geometry and total floor area.

This example could represent an investigation of the relative performance between design alternatives achieving a certain density level defined through a narrow plot (or floor area) ratio interval. Comparing results within each run as well as between the two allows exploring the effect of a larger dimension in Y versus X, which is equivalent to an orientation shift of 90°.

We observe that the range spanned by the daylight and passive solar potential is similar between the two runs, while the active solar potential shows more variation. Between variants, performance differences reach up to  $5 \text{ kWh/m}_{\text{FA}}^2$ , a number that can translate into a larger gap in terms of absolute values for the total floor area. The analysis of the results serve to get some insight on both the performance variations and similarities in relation to (sometimes small) changes in the geometry.

Table 5.1 – User-inputs for the first and second example runs.

|                         | Run 1     | Run 2     |
|-------------------------|-----------|-----------|
| Variables (min : max)   |           |           |
| X [m]                   | 20 : 46   | 10 : 16   |
| Y [m]                   | 10 : 16   | 20 : 46   |
| Z [stories]             | 2 : 5     | 2 : 5     |
| Constraints (min : max) |           |           |
| Floor area ratio [-]    | 0.6 : 0.8 | 0.6 : 0.8 |
| Site coverage [-]       | 0 : 1     | 0 : 1     |

### 5.2 Preparation of workshops with practitioners

To assess our proposed design decision-support workflow, we organized sessions where professionals were invited to test the implemented prototype. The structure of the workshops is detailed in this section, while their outcome is presented in chapter 6.

#### 5.2.1 Objectives and phases

Three workshop sessions were organized in October 2015, each lasting one afternoon. A first test-run was conducted with four colleagues with professional experience as architects. The outcome from this session, not reported in this thesis, served to identify bugs and refine the workshop schedule and tasks. The following two more official sessions held four professionals each and included architects, urban designers and one engineer. Recruitment was done by contacting professionals working in the Lausanne area, whose email was obtained through immediate colleagues at the EPFL. Registration was made on a voluntary basis by filling in an online Doodle form.

The main objectives of the workshops were to:

1. assess the potential of the proposed workflow as a solar/energy performance-based design decision-support method for the early-design phase of neighborhood projects;
2. verify if the workflow could bring new knowledge and help improve the performance of a design;
3. identify bugs and improvements in the interface and workflow;
4. assess the predictive accuracy of the underlying mathematical functions.

To fulfill these goals, we devised the workshop schedule as shown in Fig. 5.9, which is briefly introduced here and further detailed in the next section. Prior to the event, participants were asked to fill a questionnaire that included questions on their level of experience with tools and performance assessment methods. The workshop itself began with a brief introduction to the tasks and performance criteria addressed by the proposed prototype (daylight and passive and active solar potential). A design task was introduced, adapted from a real master plan, as illustrated in Fig. 5.10. Participants were first asked to come up with their own design - Variant A (VA) - for the identified plot, using their usual approach, methods and tools, and keeping in mind the three performance criteria introduced without trying to optimize for them. This design phase was followed by two ranking phases, devised to test the capacity of participants to estimate the relative performance of a set of designs based on their intuition and experience ('Initial rank'), and by seeing given examples ('Intermediate rank').

Participants were then shown a demo of the prototype before proceeding with the test. They were asked to re-create something similar to their VA and explore the variants generated by the tool to see if they could improve their design. Finally, they were asked to submit a (possibly improved) Variant B (VB), before proceeding with a last ranking phase ('Final rank'). The

## 5.2. Preparation of workshops with practitioners

workshop concluded with a questionnaire to collect the impression and suggestions from participants. This second questionnaire can also be found in appendix C.1 (in French only).

To ensure traceability of the material collected from participants while maintaining their anonymity, they were asked to note down the date and the number posted on their assigned work station (computer) on everything they submitted, and retroactively add this information on the initial questionnaire which was anonymously answered before the event.

The core part of the workshop, falling under the Design task section in Fig. 5.9, is further detailed in section 5.2.3. Throughout the session, slides were displayed as supporting material to explain each phase. The full presentation can be found in the Appendix in section C.2 (in French only).

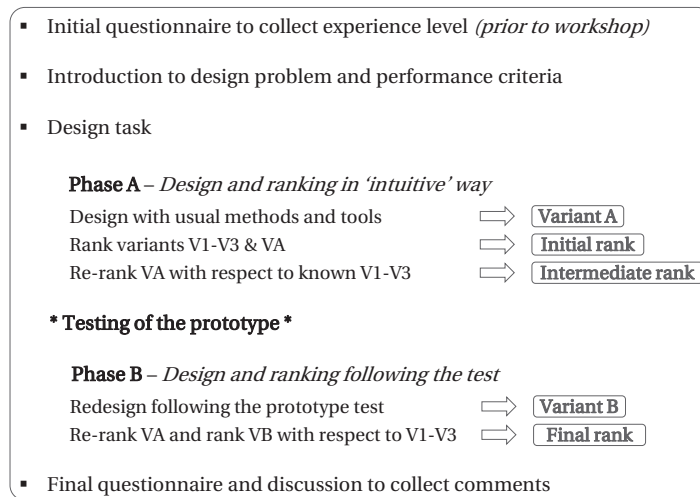


Figure 5.9 – Workshop phases and tasks.



Figure 5.10 – Images of the design task: the ‘empty’ plot, selected from the hypothetical plan for an area of Vernand part of the Lausanne-Vernand - Romanel-sur-Lausanne PDLi (*Plan Directeur Localisé intercommunal*) [Urbaplan, 2015], and its modified context.

### 5.2.2 Questionnaires

Both the initial and final questionnaires were formatted using Google Forms<sup>10</sup>, producing a private online document that was shared to the participants. Responses were stored automatically by Google in an Excel spreadsheet.

The full questionnaires can be found in appendix C.1 (in French only). Two main sources of reference were used when defining the question content and format as well as the choices of answers when present: similar workshop-based studies conducted by Attia et al. [2013a] and Gagne [2011], both in the same context of a doctoral thesis in which a decision-support tool was proposed and tested. These references also served as inspiration when defining the main phases of the workshop.

In the initial questionnaire, participants were first asked to provide information on their profession, years of experience and type of participation in neighborhood-scale projects through questions 1 to 4. They were then asked to specify if they used specific modeling and simulation tools, e.g. SketchUp, Rhino, Lesosai, and were given the option to specify any missing tool from the listed options (questions 5 to 10). Through questions 11 to 19, participants had to select out of the listed options or add by which means they typically assess the performance associated to: passive solar potential (for passive heating), thermal comfort (e.g. overheating in summer), active solar potential through PV and ST, and daylight potential. Options were: rules-of-thumb/heuristics, visualization (e.g. sun-path diagram), simulations, external consultant.

To get more precision on when the tools are typically used and the performance assessed, participant had to answer to all of the above questions by selecting one of the four possible answers: no, early phase, detailed phase, early and detailed phase. The questions were elaborated in order to get some insight, before the workshop, into the familiarity of participants with specific tools, including the ones part of the prototype (e.g. Rhino), as well as the performance criteria relevant to our proposed approach.

A second questionnaire, administered at the end of the workshop session, was developed to gather participants' feedback on their experience with the prototype. Questions 1 to 3 were posed as a list of statements to which participants had to answer in terms of level of agreement, based on the commonly used 5-point psychometric Likert scale [Likert, 1932; Nemoto and Beglar, 2014]. The questionnaire concluded with three open-ended questions (4-6) to gather any additional comments and suggestions. The exact content of this questionnaire is presented in the next chapter when revealing the results, in section 6.1 and appendix C.4.

---

<sup>10</sup><https://www.google.com/forms/about/> (last accessed on March 28, 2016)

### 5.2.3 Design task

#### Phase A

In this first design phase, participants were asked to work as ‘normally’ as possible given the different environment to come up with their Variant A. Working at individual work stations with one computer each as illustrated in Fig. 5.11, they were given access to typical tools: tracing paper and drawing/sketching sheets (including the base in Fig. C.1 of appendix C.3), material to build a scale model, and modeling software (SketchUp, Rhino and AutoCAD). A scale model of the context, seen in Fig. 5.11, was prepared prior to the event as supporting material for visualizing both the surroundings and variants that were built.

Participants had approximately one hour to complete this task. Designs were collected in various formats (e.g. 3D model, sketch), always including all the dimensional information that would later be necessary to complete a virtual 3D model for further analysis (e.g. simulation).

In addition to the fixed context and dimension of the empty parcel (9 744 m<sup>2</sup>) as illustrated in Fig. 5.10, they were asked to design buildings respecting a north-south-east-west alignment of their facades, with a plot ratio (total floor area / plot area) falling between 1.3 and 2, equivalent to having a total floor area of ~12 600 - 19 500 m<sup>2</sup>. This range was defined to fall within the major region found in the reference dataset (see Fig. 4.11 and 4.12) while also comprising the target of 1.75 found in the master plan document [Urbaplan, 2015].



Figure 5.11 – Workshop physical set-up: four work stations (computers) with installed software, scale model of the context (prepared prior to event) and material for making a scale model of the design.

## Chapter 5. Application to the design process

---

They were then asked to fill in the initial ranking sheet shown in Fig. 5.13, containing the 3D model of three example variants (V1-V3) to be ranked along with their VA in terms of the relative performance for each criterion. More specifically, they had to order the four variants from best to worst by writing the name (V1, V2, V3, VA) in the boxes from top to bottom for each of the three performance criteria. In addition, they were asked to provide an explanation for their ranking (to be written in the wider, rectangular boxes).

After completing this task in approximately 15 minutes, the second sheet shown in Fig. 5.14 was distributed, displaying the actual performance of the three example variants through images and bar graphs. Accounting for this new knowledge, participants were given the task to re-rank their VA, now in a more precise way by filling in the empty bars.

As will be seen in chapter 6, all Variants A were simulated after the workshops to assess the correctness of the rankings. While the initial phase probes the intuition of participants, the second ranking incorporates the added effect of learning from example cases which may or may not resemble each participant's VA.

### Testing of the prototype

In preparation for the workshops, the adapted master plan (Fig. 5.10) was modeled in Rhino, leading to a 3D model of the parcel (or plot) and context, illustrated in Fig. C.2 of appendix C.3. As mentioned in section 5.1, the prototype currently requires some setting-up in Grasshopper, as the custom plug-in in itself does not include all the workflow elements such as the outputs visualization. A Grasshopper script was thus specifically developed to avoid the need for user-intervention in setting-up the workflow. The script, illustrated in Fig. 5.12, includes the linked UrbanSOLve components and the algorithm for visualizing the results in the Rhino viewports. Users did not see or intervene with any part of this script except the circled component below 'Double-click to open interface', which allowed them to open the UrbanSOLve interface (Fig. 5.4).

After a short demo of the prototype, participants were given instruction sheets that can be found in appendix C.3 (in French only). They were asked to begin by trying to reproduce their Variant A through the tool's user-inputs - not by importing or drawing the exact 3D model as this option is not currently allowed by the prototype. Instead, the goal was to specify the relevant building typology, location, variable ranges and constraints (see Fig. 5.5), defining a solution space in which their VA could be found.

After launching the simulation process where 20 variants are generated and evaluated by the tool, participants could explore the results, extract interesting information and start over with adjusted input parameters. This testing phase lasted approximately 1.5 hour and was recorded using Rylstim Screen Recorder<sup>11</sup>, producing one .avi video file per participant.

---

<sup>11</sup><http://www.sketchman-studio.com/rylstim-screen-recorder/> (last accessed on March 16, 2016)

## 5.2. Preparation of workshops with practitioners

A screenshot-based demonstration of the workflow, representative of the participants' experience with using the prototype, can be found in appendix B.2.

### Phase B

Following or during the use of the prototype, participants were asked to design a second variant (VB), derived from VA, incorporating in their process whatever information they would have extracted from the trial phase. As such, there was freedom in how participants interpreted and made use of the results. We will come back to this topic in the next chapter when analyzing the workshop outcomes. As for VA, all VB variants were collected either in sketch or 3D format.

Participants were then asked to rank this second design using the provided sheet illustrated in Fig. 5.15. An empty bar was also included for an optional revision of the ranking of VA, given the insight possibly gained by using the tool. This final ranking task thus represented a means for investigating the impact of using the tool on participants' capacity to relatively evaluate a design's performance for each aspect considered.

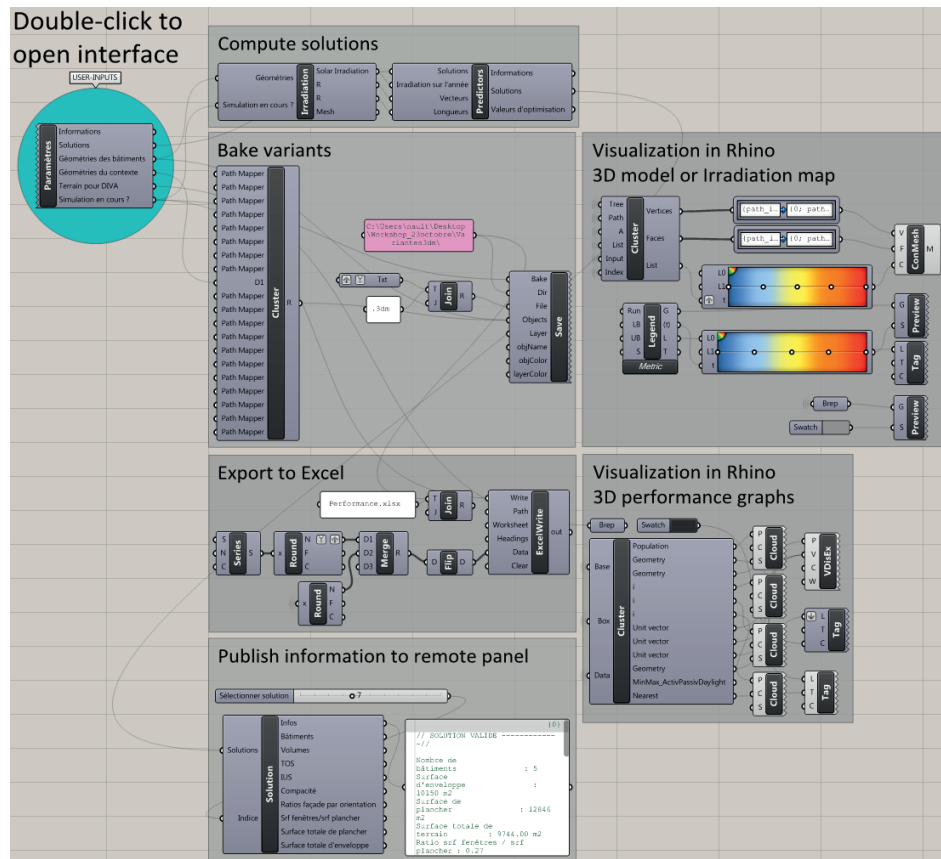



Figure 5.12 – Grasshopper script prepared for the workshops. The interface for gathering the user-inputs (see Fig. 5.4) is opened by double-clicking the circled (Parameters) component. The rest of the script is automated and does not require user intervention.

URBAN SOLAR VISUAL EXPLORER - URBANSOLVE (beta version)

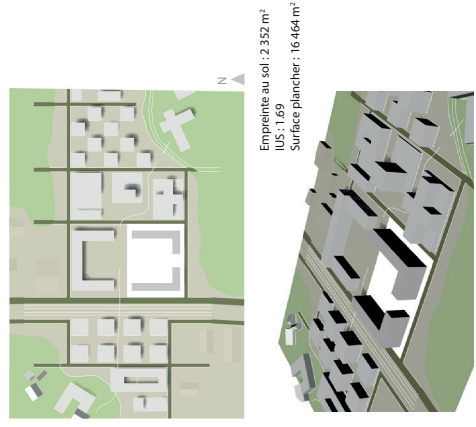


Date : \_\_\_\_\_ Poste de travail (#) :

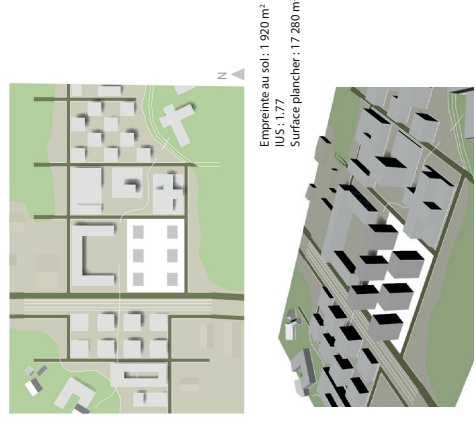
  

**Fiche 1a - Classement initial**

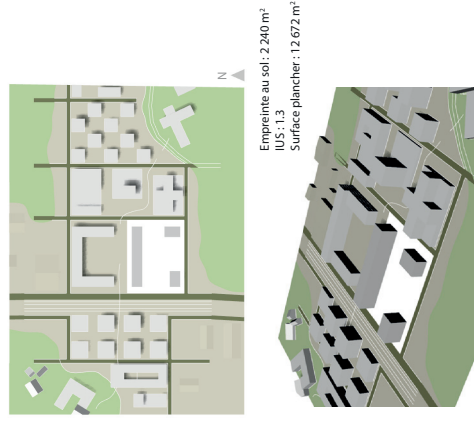
Trois variantes exemples :



V1



V2



V3

**Classement relatif des 3 variantes exemples et de votre Variante A (VA) :**

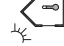

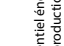
|  |  |   |  |
|--|--|---|--|
|  <p>Potentiel énergétique passif<br/>(consommation d'énergie)</p> |  <p>Eclairage naturel</p> |  <p>Potentiel énergétique actif<br/>(production d'énergie)</p> |  |
| meilleure performance  | meilleure performance  | meilleure performance   |  |
| Parce que...   | Parce que...   | Parce que...  |  |
| <input style="width: 100%; height: 30px;" type="text"/>  | <input style="width: 100%; height: 30px;" type="text"/>  | <input style="width: 100%; height: 30px;" type="text"/>   |  |
| <input style="width: 100%; height: 30px;" type="text"/>  | <input style="width: 100%; height: 30px;" type="text"/>  | <input style="width: 100%; height: 30px;" type="text"/>   |  |
| <input style="width: 100%; height: 30px;" type="text"/>  | <input style="width: 100%; height: 30px;" type="text"/>  | <input style="width: 100%; height: 30px;" type="text"/>   |  |
| <input style="width: 100%; height: 30px;" type="text"/>  | <input style="width: 100%; height: 30px;" type="text"/>  | <input style="width: 100%; height: 30px;" type="text"/>   |  |
| pire performance   | pire performance   | pire performance  |  |

Figure 5.13 – Initial ranking sheet.



## 5.2. Preparation of workshops with practitioners

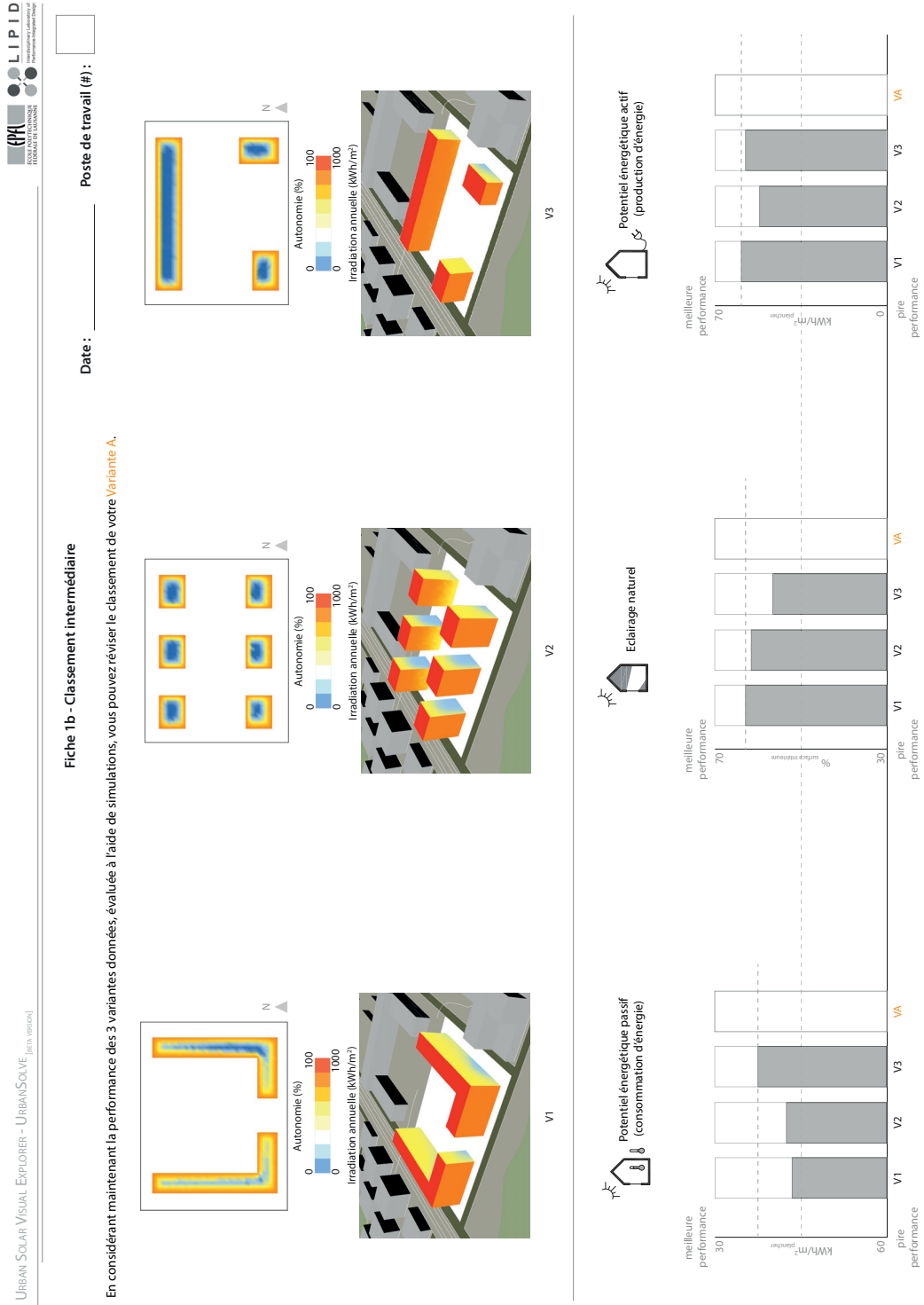


Figure 5.14 – Intermediate ranking sheet.

Fiche 2 - Classement final

Poste de travail (#) :

Date : \_\_\_\_\_

Classement de la Variante B et révision optionnelle de la Variante A :

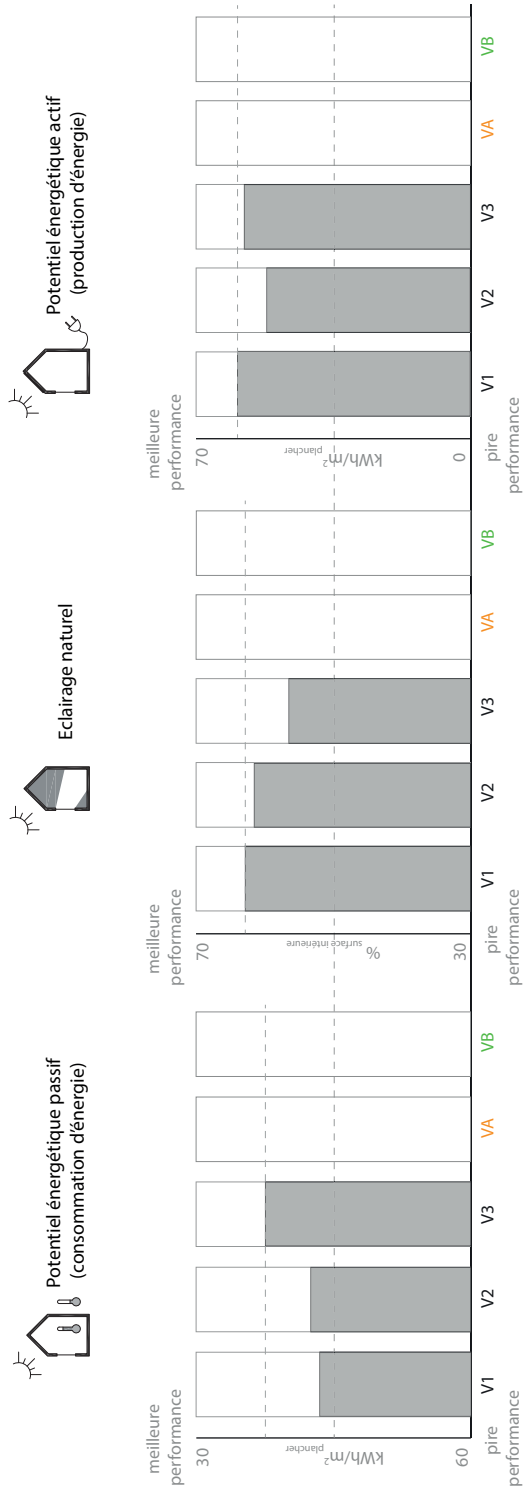


Figure 5.15 – Final ranking sheet.

## 6 Appraisal of developed prototype

*“Usability, fundamentally, is a matter of bringing a bit of human rights into the world of computer-human interaction.”*

Joel Spolsky  
(Software developer)

In this chapter, we analyze the outcomes from the workshops first, in section 6.1, to assess the general potential, usability and current limitations of the prototype as a design decision-support tool, and in section 6.2, to test the predictive power of its core performance assessment engine. Each section concludes with a summary of the main outcomes and lessons learned, including a discussion on the level of achievement respectively of first three objectives and the fourth one introduced in section 5.2.

### 6.1 Workshop outcome

The first workshop session, conducted with colleagues, was considered a test-run. It led to adjustments in the workshop schedule as well as changes to the prototype. As such, results from this preliminary session are not presented. For the subsequent two workshops, each conducted with four professionals, results are presented for all participants taken together. We also highlight some observations based on the analysis of each participant’s experience which can be found in appendix C.4. The main results of this section have been presented in Nault et al. [2016b].

#### 6.1.1 Initial questionnaire

Answers to the initial questionnaire, which can be found in appendix C.1, give us information on the level of experience of the participants, both with software and approaches for assessing different performance aspects. Within the group of eight participants, there were three architects, one engineer and four who declared themselves as both architects and urban designers,

## Chapter 6. Appraisal of developed prototype

with years of professional experience ranging from 2 to 15. All participants have some type of experience in neighborhood-scale projects, either through participating in competitions or in the elaboration of master or district plans, as shown in Fig. 6.1.

Answers regarding the use of various tools are shown in Fig. 6.2. Participants have more experience with drawing/modeling tools, in particular SketchUp and AutoCAD which are used both at the early and detailed design phase. The only simulation software used are Lesosai (four participants), a Swiss product, and the now obsolete Ecotect (one participant only).

Regarding the specific ways of approaching different performance aspects, results are summarized in Fig. 6.3. In cases where an assessment is done, it generally occurs at the early phase through the application of simple methods such as rules of thumb and visualization (e.g. sun path diagram). External consultants are solicited to some extent both at the early and detailed phases across all performance criteria, while simulation is conducted, here by a small portion of participants, mostly for daylight and active solar potential assessment.



Figure 6.1 – Participation in neighborhood-scale projects. PDL: (localized) master plan (*Plan Directeur Localisé*), PQ: district plan (*Plan de quartier*).

### 6.1.2 Performance of variants

Variants A and B submitted by the participants were collected in order to be modeled and evaluated through full simulations using the same tools and settings as in chapter 4. Since the metamodels are built from a dataset with underlying assumptions, these same settings must be applied to any new case for which we wish to compare the simulation results to the predictions from the metamodels.

While the design of all variants can be visualized in appendix C.4 for each participant, Fig. 6.4 and 6.5 illustrate examples in the form of sketches and 3D scale models.

It is to note that some participants experienced difficulties in reproducing variants similar to their VA in the prototype, due to limitations which are further discussed in section 6.1.5. Because of this situation, three participants did not submit a VB and final ranking.

Results from both the simulation and metamodels are presented in Fig. 6.6, where the y-axis of the energy need graph is inverted, so that higher bars across all graphs, i.e. all performance criteria, represent a better performance. The comparison between simulated and predicted values for investigating the metamodels' accuracy is conducted later in section 6.2. Unless stated otherwise, all results presented in this section are based on the simulated values. For the active solar criterion, there is no distinction between predicted and simulated values; this metric is evaluated through the algorithm described in section 4.6.

## 6.1. Workshop outcome

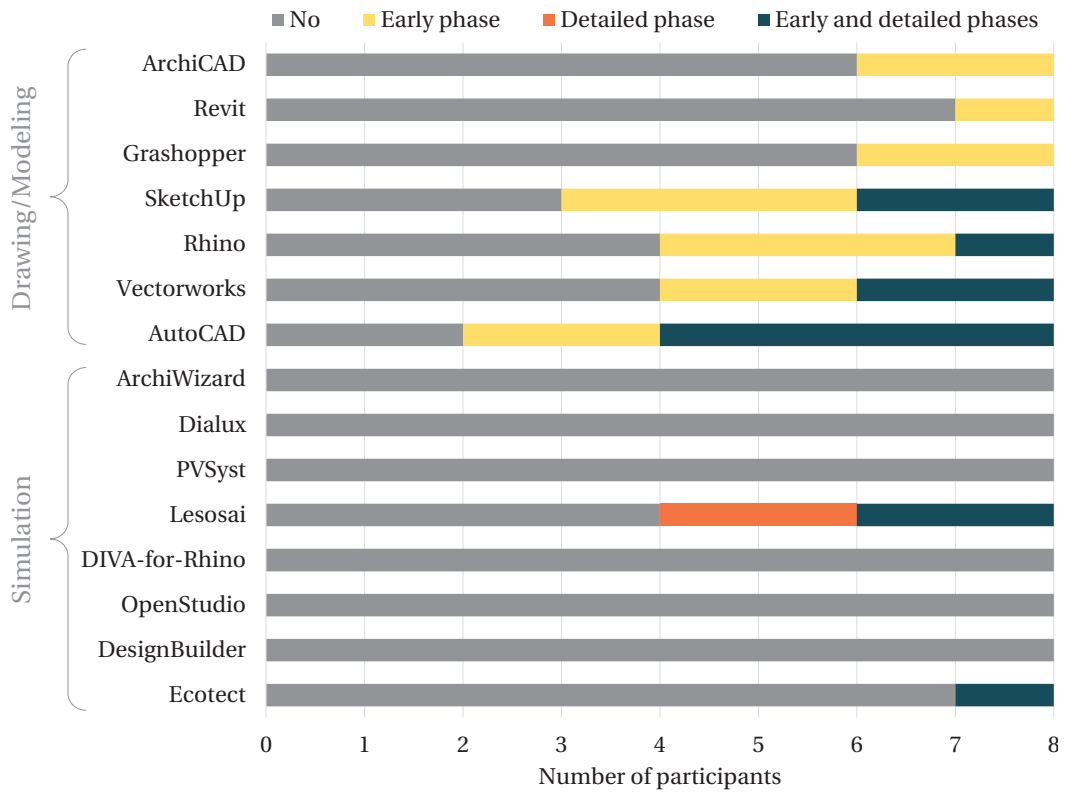


Figure 6.2 – Participants' experience with tools.

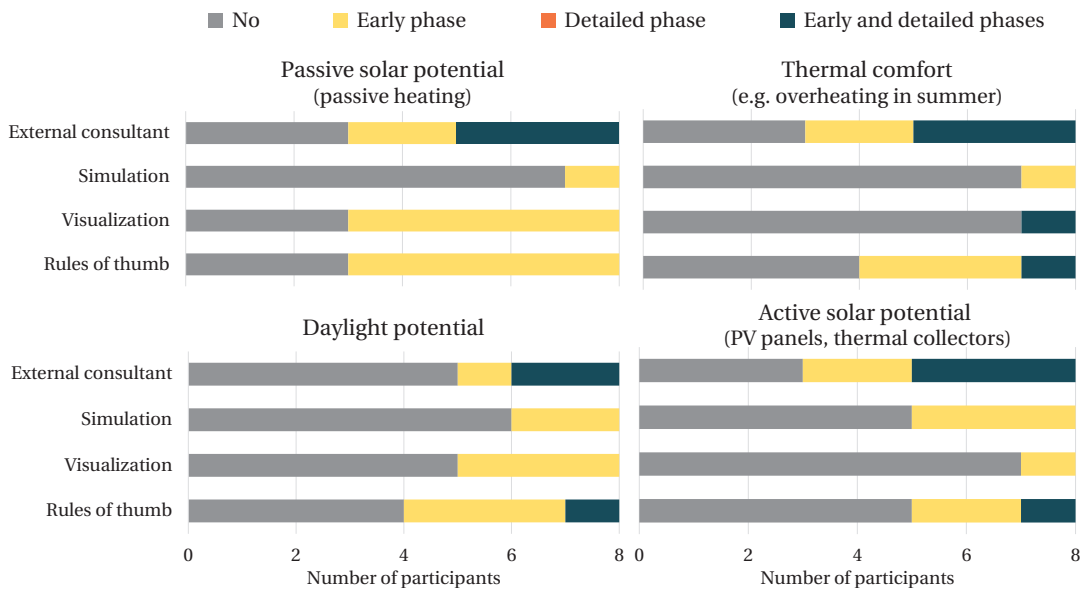
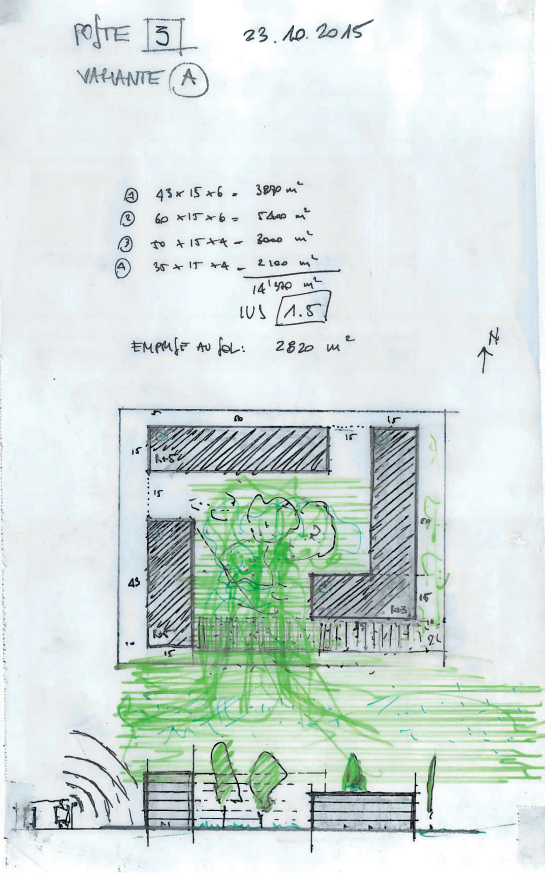
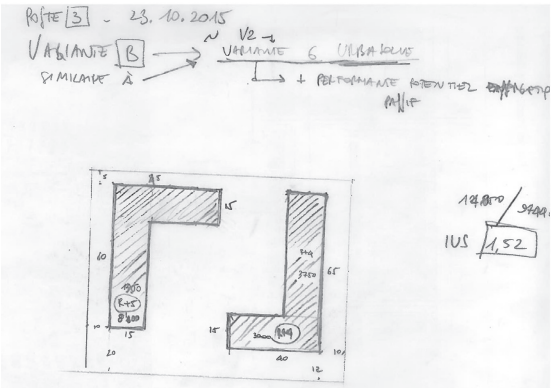


Figure 6.3 – Participants' experience with assessing different performance aspects.

Chapter 6. Appraisal of developed prototype



(a) Variant A



(b) Variant B

Figure 6.4 – Drawings and calculations from one participant, from (a) Variant A to (b) Variant B.

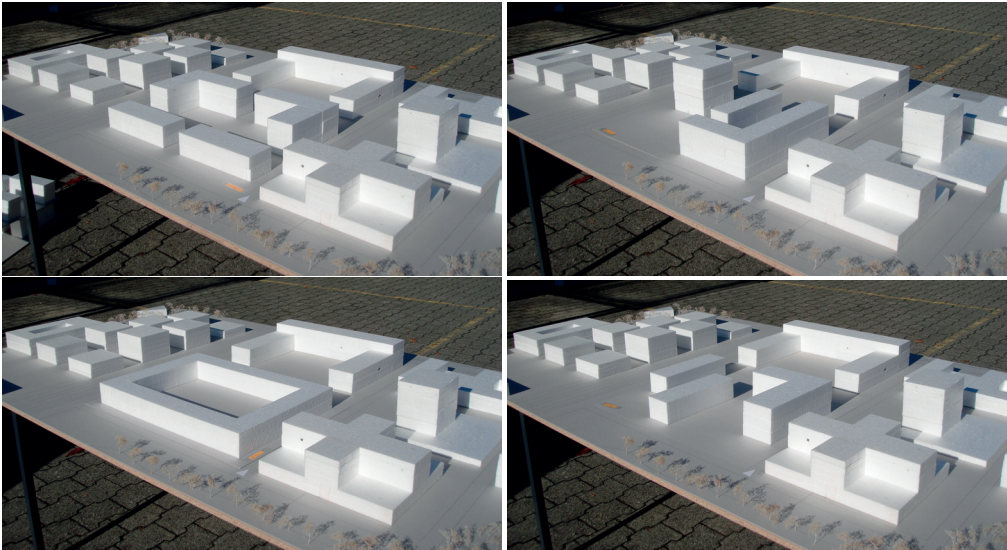


Figure 6.5 – 3D models of some of the participants' variant.

## 6.1. Workshop outcome

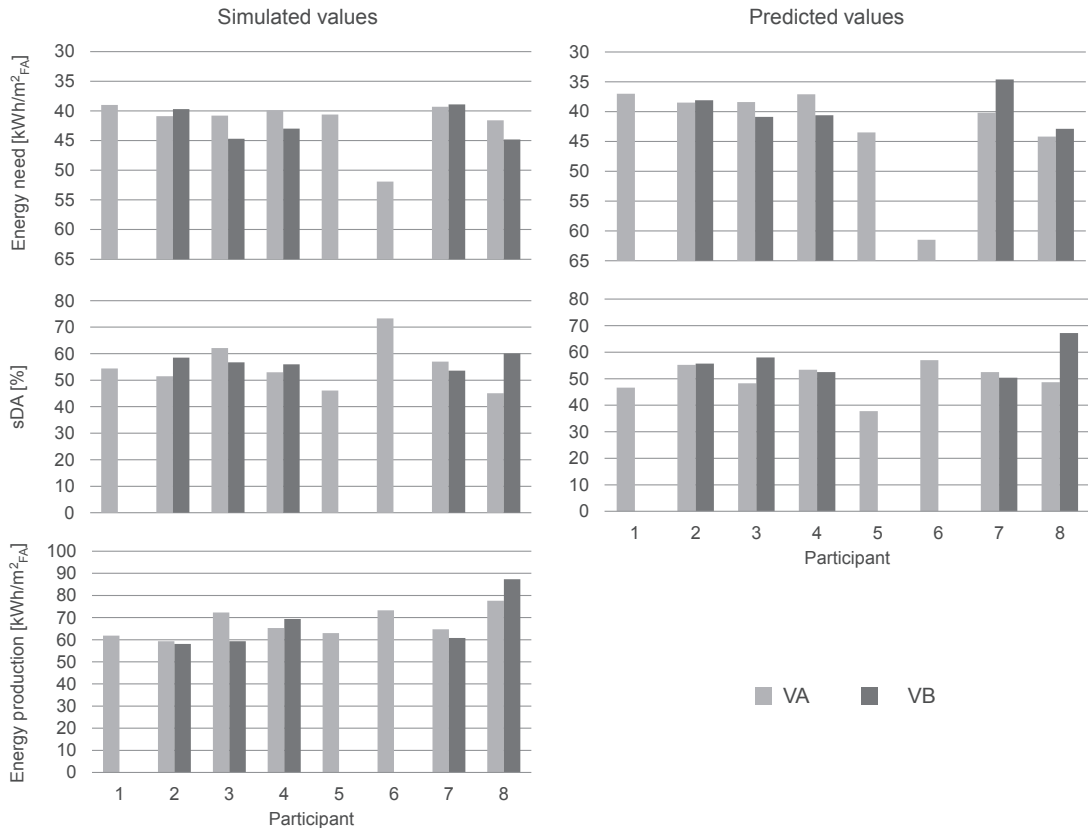


Figure 6.6 – Performance of each participant's VA and VB with respect to each criteria, evaluated through simulation (left) and the predictive functions implemented in the prototype (right).

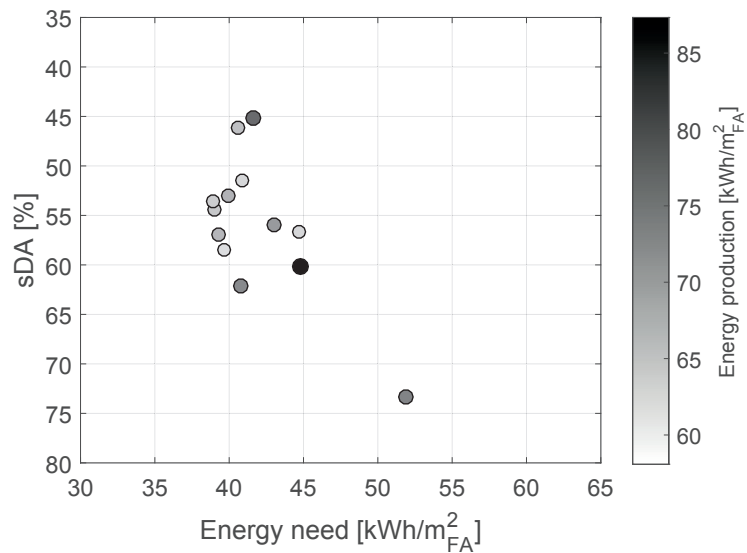


Figure 6.7 – Simulated values for the sDA versus energy need with the energy production coded in shades of gray, for all variants A and B created by the participants.

## Chapter 6. Appraisal of developed prototype

---

The difference between the highest and lowest performance is of  $13 \text{ kWh/m}_{\text{FA}}^2$ ,  $28.2 \%_{\text{FA}}$  and  $29.2 \text{ kWh/m}_{\text{FA}}^2$  for the energy need, sDA and energy production respectively. These differences are considerable, especially when applied to the whole set of buildings. For example, the design corresponding to the highest energy need value ( $51.9 \text{ kWh/m}_{\text{FA}}^2$ ) has a total floor area of  $18\,112 \text{ m}^2$ , leading to a total annual energy need of  $940\,000 \text{ kWh}$ . In comparison, the case having the lowest energy need ( $38.9 \text{ kWh/m}_{\text{FA}}^2$ ) achieves  $577\,665 \text{ kWh}$  in total considering its slightly smaller total floor area of  $14\,850 \text{ m}^2$ . This means that the difference of  $13 \text{ kWh/m}_{\text{FA}}^2$  stated above translates to a  $362\,335 \text{ kWh}$  gap in the annual energy need between the current 'best' and 'worst' design variant. Despite their difference in density -  $1.85$  versus  $1.52$  - these two designs could feasibly represent alternatives considered in a real project (e.g. urban design competition). Their distinct energy performance emphasizes the relevance and importance of incorporating energy-related criteria early-on in the decision-making process.

When comparing between VA and VB for participants that submitted both, we observe that the performance decreases from VA to VB in three out of five cases for the energy need and production, and in two out of five cases for the sDA. As previously mentioned, instructions given to the participants when designing VB were explicitly vague. No emphasis was put on any single performance aspect and participants were simply asked to create VB as a revised (or identical to) VA, based on their experience when exploring the solution space using the prototype. It is thus not possible to know the intention of each participant or if an effort was made to improve one or more performance criteria when designing VB.

Moreover, an error was detected in the energy production algorithm after the workshops, causing participants to see erroneous values for the active solar potential. This situation may well have induced them in error if they particularly focused on this criterion.

In any case, improving all aspects would have proven to be challenging, due to their conflicting nature as highlighted in chapter 3, section 3.2.4. This situation is observed for the participants' variants in Fig. 6.7, where for instance the design with the highest sDA (note the reversed y-axis) shows a relatively high energy production, but the worst passive solar potential (highest energy need). This sort of trade-off also appears in the output performance graph produced by the prototype (see Fig. 5.7). In its current format, the prototype does not provide any means for weighting the different performance aspects. However, it would be of interest to compute an aggregated performance metric that would allow comparing the variants using a comprehensive yet unique value. This shift would require translating the spatial daylight autonomy metric into the amount of artificial lighting needed to compensate the lack of daylight. A conversion into primary energy would offer a more accurate representation of the share for heating, cooling, and lighting. A balance between energy demand and production through PV and ST systems could also be added to the performance assessment. This topic is further discussed in chapter 7.



### 6.1.3 Ranking success rate

Computing the performance of variants A and B allows us to verify if the rankings done by the participants were correct. Despite the low number of participants, the overall results from each ranking task are analyzed using a statistical method, namely the Kendall rank correlation coefficient. This value, also termed Kendall's  $\tau$ , quantifies the degree of similarity between two sets of ranked data [Abdi, 2007]. The value computed using the Matlab function *corr* with the *type* parameter set to *Kendall* corresponds to the version known as  $\tau$ -b, which accounts for possible ties in the rankings. It ranges between -1 and +1, dictated by the number of inversions between the two sets. It is computed as follows:

$$\tau = \frac{K}{\left(\sqrt{\frac{N(N-1)}{2} - T_x}\right)\left(\sqrt{\frac{N(N-1)}{2} - T_y}\right)} \quad (6.1)$$

with

$$K = \sum_{i=1}^{N-1} \sum_{j=i+1}^N \text{sgn}(x(i) - x(j)) \cdot \text{sgn}(y(i) - y(j)) \quad (6.2)$$

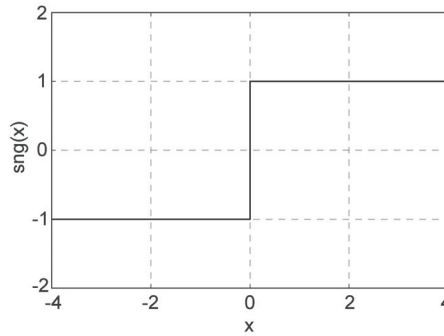
where  $N$  is the number of ranked objects,  $T_x$  and  $T_y$  the number of ties in rankings  $\mathbf{x}$  and  $\mathbf{y}$ , and  $\text{sgn}$  a function that performs the transformation illustrated in Fig. 6.8. Let us consider an example to clarify these equations, where we have  $N = 4$  design variants (V1, V2, V3, VA), which we represent by the vector [1, 2, 3, 4]. If we have two different rankings  $\mathbf{y} = [1, 2, 3, 4]$  (same as original order) and  $\mathbf{y} = [3, 2, 4, 1]$ , both  $T_x$  and  $T_y$  are null, since there are no ties (i.e. equal values) within the ranks. Computing  $K$ , we have:

$$\begin{aligned} i = 1 & \quad \text{sgn}(x(1) - x(2:4)) \cdot \text{sgn}(y(1) - y(2:4)) \\ & \quad = \text{sgn}([1] - [2, 3, 4]) \cdot \text{sgn}([3] - [2, 4, 1]) \\ & \quad = \text{sgn}([-1, -2, -3]) \cdot \text{sgn}([1, -1, 2]) \\ & \quad = [-1, -1, -1] \cdot [1, -1, 1] = -1 + 1 - 1 = \mathbf{-1} \\ i = 2 & \quad \text{sgn}(x(2) - x(3:4)) \cdot \text{sgn}(y(2) - y(3:4)) \\ & \quad = \text{sgn}([2] - [3, 4]) \cdot \text{sgn}([2] - [4, 1]) \\ & \quad = \text{sgn}([-1, -2]) \cdot \text{sgn}([-2, 1]) \\ & \quad = [-1, -1] \cdot [-1, 1] = 1 - 1 = \mathbf{0} \\ i = 3 & \quad \text{sgn}(x(3) - x(4)) \cdot \text{sgn}(y(3) - y(4)) \\ & \quad = \text{sgn}([3] - [4]) \cdot \text{sgn}([4] - [1]) \\ & \quad = \text{sgn}([-1]) \cdot \text{sgn}([3]) \\ & \quad = [-1] \cdot [1] = -1 = \mathbf{-1} \end{aligned}$$

$$\text{Which gives: } \tau = \frac{-1 + 0 - 1}{(\sqrt{6})(\sqrt{6})} = -0.33$$

Our compared sets of ranks correspond to the performance of the variants, for each criterion, ordered according to (i) the simulation values and (ii) each participant's ranking in the three phases (initial, intermediate, final). This provides a Kendall coefficient for each participant,

Figure 6.8 – Sign function where positive, null and negative values (x-axis) are respectively transformed to +1, 0 and -1 (y-axis).



performance criterion and ranking phase, which are presented in the next section. To obtain a coefficient over all participants  $P$ , assuming no ties, we compute:

$$\tau = \frac{1}{P} \frac{\sum_{j=1}^P K_j}{N(N-1)/2} \quad (6.3)$$

As seen in section 5.2.3, each ranking phase was slightly different both in the format of the sheet to fill in and the degrees of freedom in positioning the variants. These differences are however not explicitly taken into account in the above formulas. This means that between the initial and intermediate phases for instance, where  $N=4$  (V1-V2-V3-VA), the denominator in equation 6.1 is the same, although V1, V2 and V3 cannot possibly be inverted in the intermediate phase since their performance values are given. For the same reason, the numerator is likely to be higher, since less freedom exists in rankings  $\mathbf{x}$  and  $\mathbf{y}$ . Indeed, the probability of them being closer is higher, which translates to more occurrences of multiplications of identical numbers (e.g.  $[-1, 1] \cdot [-1, 1]$ ) in turn leading to higher  $K$  values. As such, Kendall rank coefficients will by default be higher for the intermediate phase than for the initial one. This limitation, further discussed in section 6.1.5, is intrinsic to how the ranking exercises were formulated. The value of  $N$  does however change between the initial/intermediate and the final phase, going from four to five to account for VB.  $P$ , the number of participants, also varies, decreasing from eight to five since three participants did not provide a VB and final ranking.

In light of the above considerations, the ranking success rate was evaluated through a second method, based on the ‘distance’ between the participants’ ranking and the real one (i.e. based on simulated values). We have termed it the level of closeness to the real rank,  $l$ . It is computed over all participants through the following equation:

$$l = 1 - \frac{\sum_{j=1}^P \left| \sum_{i=1}^N (\mathbf{x}_j - \mathbf{y}_j) \right|}{D_{\max} \times P} \quad (6.4)$$

where  $P$  is the number of participants,  $N$  the number of ranked objects,  $(\mathbf{x}_j - \mathbf{y}_j)$  the element-wise subtraction between the participant’s and the reference ranking (based on simulated values), and  $D_{\max}$  the maximum theoretical distance between the two rankings, that is, the largest possible argument of the absolute value found in the equation. This value is proper to each phase considering the variation in the level of freedom. In the initial phase, the maximum error is of eight, while in the intermediate phase, it is reduced to six due to V1-V2-V3 being

given. In the final ranking phase, it is of 10 considering the addition of VB. For example, the calculation of  $l$  for one participant (without the summation over  $P$ ) for the initial phase would be:

|  | V1                  | V2 | V3 | VA |
|--|---------------------|----|----|----|
| Participant's ranking ( $x_1$ )                                      | 4                   | 1  | 2  | 3  |
| Ranking based on simulated values ( $y_1$ )                          | 4                   | 3  | 1  | 2  |
| Difference ( $x_1 - y_1$ )   | 0                   | -2 | 1  | 1  |
| Sum absolute difference, normalize by $D_{\max}$ and subtract from 1 | $l = 1 - 4/8 = 0.5$ |    |    |    |

A perfect ranking would thus result in  $l = 1 - 0 = 1$ , while a complete opposite ranking would have a value of 0.

Results obtained by applying the Kendall and distance methods over all participants are shown in Fig. 6.9, where the y-axis goes from -1 to 1 for the Kendall coefficient  $\tau$  in Fig. 6.9a and from 0 to 1 in Fig. 6.9b to illustrate the level of closeness to a perfect rank. For both graphs, taller bars indicate higher success rate.

The overall trends are similar; there is an increase from the initial to the intermediate ranking phases across the three performance criteria, followed by a slight drop in the final phase. It is likely that the gap between the first and second phases are the effect of the visualization, by the participants, of the performance of the three example variants in the intermediate phase. Although there is a drop between the intermediate and final rankings, the latter still remains better than the initial ranking for the passive solar and daylight criteria.

Despite being shown in the graphs, the final ranking related to the active solar potential cannot be truthfully analyzed and interpreted, as erroneous values were shown to the participants due to the bug in the algorithm mentioned earlier. We can speculate that this may explain to some extent the drop in the final ranking's success rate compared to the initial and intermediate phases. Another potential factor blurring the results is linked to chance; luck in successfully ranking variants is something we cannot capture.

Figure 6.10 illustrates the same  $\tau$  and  $l$  values computed for each participant<sup>1</sup>. The ranking success rate improves from dark blue to yellow squares, with white spaces reflecting the absence of data corresponding to the three participants who did not submit a second variant and complete the final ranking sheet, as mentioned earlier. The overall trend is similar between the two methods. Considering the issues discussed earlier related to the structure of the ranking tasks, the methods used to compute the success rate, as well as the small number of participants (further reduced when we exclude the ones who did not complete all tasks), the conclusions that can be drawn from these quantitative results about the influence of using the prototype on the ability to rank are limited.

It is thus of interest to complement this quantitative analysis by looking at the qualitative data obtained in the initial phase, where participants were asked to justify their ranking using

<sup>1</sup>A detailed view of the participant-specific results can be found in appendix C.4.

## Chapter 6. Appraisal of developed prototype

the dedicated space (see Fig. 5.13). Table 6.1 lists the words and concepts written by the participants with respect to each performance criterion according to the terminology used in the sheet (translated from French). Despite the divided level of experience depicted by the questionnaire's answers (see Fig. 6.3), the terms brought up by participants illustrate a certain level of understanding and knowledge regarding the performance aspects. Indeed, these capture many of the parameters considered in this thesis, e.g. the input parameters to the metamodels. Yet, initial ranking results had the lowest success rate, supporting the need for adequate performance-based design guidance, one of the motivating arguments behind this thesis. We speculate that having to judge neighborhood designs, a scale intrinsically more complex than the building level due to interaction between buildings, has challenged participants. They may also have been confounded by the need to grasp an overall performance, where possible extreme values of individual buildings are averaged out. This latter aspect represents a limitation of our approach in its current status, further addressed in section 6.1.5.

Table 6.1 – Terms that appeared in the justifications provided by participants when ranking the variants in the initial phase.

| Passive energy potential<br>(energy consumption)   | Daylighting   | Active energy potential<br>(energy production)   |
|--|---|--|
| compactness, orientation and/or amount of exposed facades, shading and distance between buildings, spreading of facades, sun exposure level, density | (diversity in) orientation(s) and/or amount of exposed facades, shading and distance between buildings, solar exposure, spreading of facades, footprint, facing buildings | shading on roof, roof to floor area ratio, density, orientation, building height, roof surface |

### 6.1.4 Final questionnaire

Responses to the final questionnaire, which is shown in appendix C.1, are presented in Fig. 6.11 and Table 6.2 for the multiple choice and open-ended questions respectively. These answers bring a qualitative input, complementary to the measurements linked to the performance and ranking results.

Participants were generally in agreement with most statements listed in Fig. 6.11, with a few exceptions where the 'disagree' option was selected. This occurred for the statement on (i) the influence of using the prototype on the final concept (VB) and (ii) the satisfaction related to the relevance of the approach. Plausible explanations for these disagreements were identified when reviewing the participant-specific results (detailed in appendix C.4). The participant who did not agree with item (i) experienced difficulties in obtaining design variants similar to their Variant A. This same participant also disagreed with statement (ii). It was found that the second person to disagree with that statement was particularly focusing on the active solar potential when analyzing the performance graphs and working on their Variant B. The erroneous results displayed for that criterion likely caused some confusion to the participant.

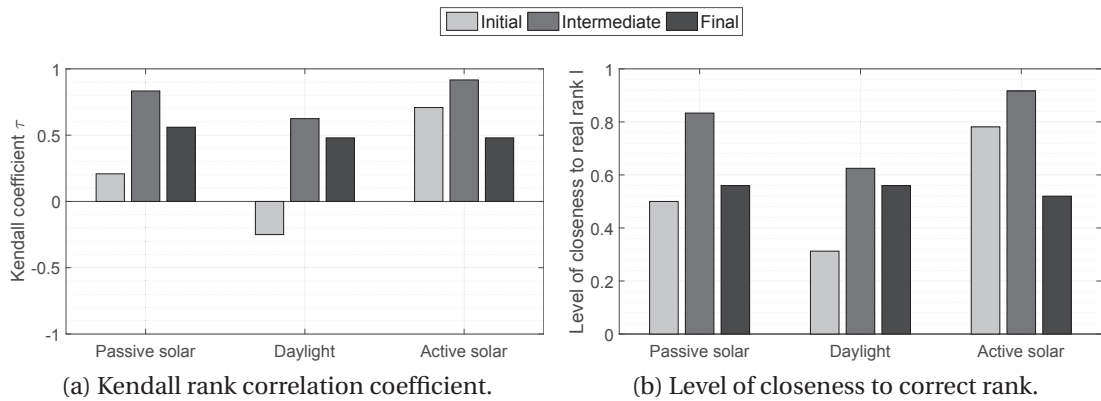


Figure 6.9 – Ranking success rate computed through the (a) Kendall rank and (b) distance method, over all participants for each criterion and phase.

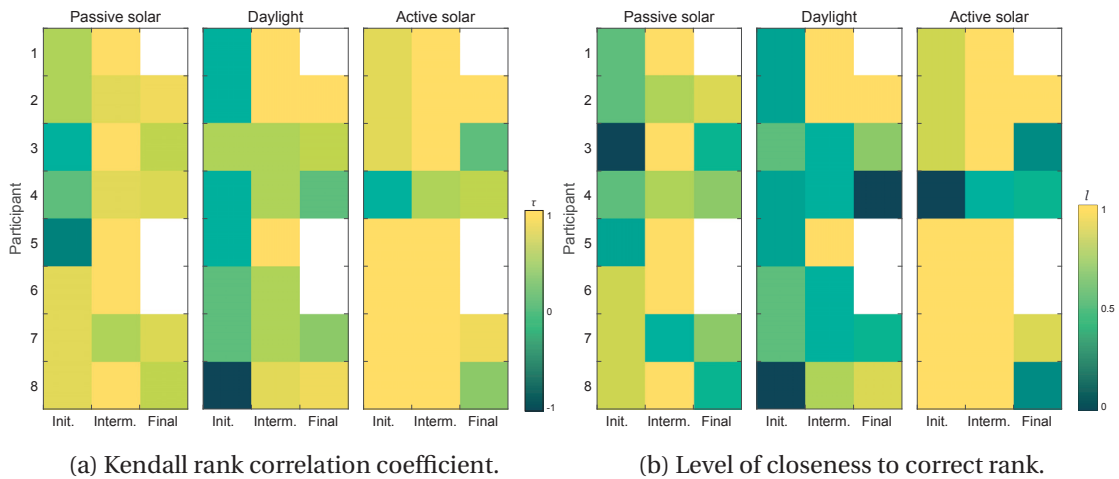


Figure 6.10 – Ranking success rate displayed as the color-coded (a) Kendall coefficient and (b) level of closeness, computed for each participant, criterion and phase. White squares correspond to no data.

A stronger consensus is found for the following points: (using the prototype) ‘influenced your approach to the problem’ and ‘allowed you to learn new elements useful in your approach to the problem’, as well as for the satisfaction level regarding the relevance of the interface and the information brought by the prototype. This qualitative insight demonstrates a perceived knowledge-gain by the participants from the usage of the prototype.

Results collected through the open-ended questions (Table 6.2) also shed an optimistic light on the overall outcome from the workshops. The main positive feedback gathered relates to the interface and general approach of the prototype, with qualifiers such as ‘intuitive’, ‘interactive’ and ‘promising’. The predominant weaknesses are linked to the current limitations in the number and types of user-inputs and the generation of variants. More flexibility or precision is required in the inputs to enforce specific typologies and ensure credible designs. Multiple

**Chapter 6. Appraisal of developed prototype**

suggestions were also given to overcome the current limitations and to expand the usability and relevance of the prototype, such as by adding specific parameters (e.g. maximum distance between buildings) and providing an automatically generated summary report.

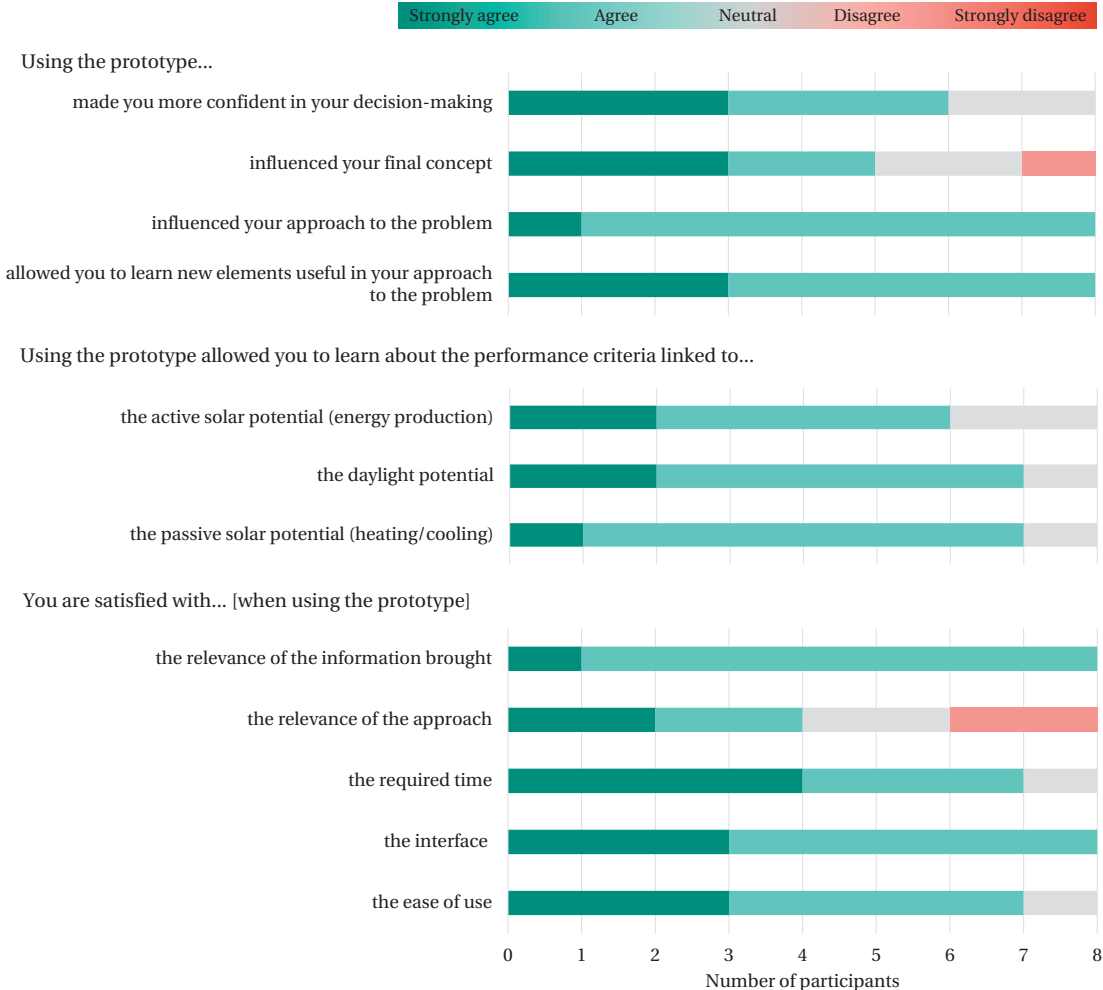


Figure 6.11 – Distribution of answers to the final questionnaire, in terms of agreement level on a 5-point Likert scale with specific statements. A strong level of agreement is observed for most statements, while the disagreement instances are likely mainly caused by technical limitations of the tested prototype.

## 6.1. Workshop outcome

Table 6.2 – Summary of feedback gathered through the open-ended questions in the final questionnaire, re-structured according to positive and negative aspects along with suggestions regarding different features of the prototype.

|   | <b>Positive aspect</b>   | <b>Negative aspects</b>   | <b>Suggestions</b>   |
|---|--|---|--|
| <b>Interface and visualization</b>                      | Intuitive, interactive, easy to understand, directly usable  | Difficult to visualize and compare variants and to read graphs, slow, points position imprecise on graphs | Visualize shadow on ground and initial model as background image, add 'restart' button to start from scratch, add scale on graphs, compare performance to absolute value for reference   |
| <b>User-inputs and automated generation of variants</b> | Does not attempt to impose an optimal solution   | Too restrictive, unrealistic variants generated, hard to recreate something similar to Variant A          | More precision and liberty in inputs, ungroup typology 1 to have 5 typologies in total whose dimensional characteristics can be controlled individually, add parameter for maximum distance between buildings, add 'entrance' point option |
| <b>Overall approach</b>                                 | Interesting to help architects choose between 2-3 options, complementary to existing tools, interesting and useful for (addressing performance criteria that are rarely part of) early-design phase, promising |   | Possibility to import/draw 3D model, integrate program types, add possibility of changing building parameters after simulation, provide automatically generated summary report   |

### 6.1.5 Synthesis - Potential of the prototype as design decision-support

The outcomes of the workshops presented in this section allow us to go over the first three main objectives that were introduced in section 5.2 (with the fourth one addressed in the next section):

1. assess the potential of the proposed workflow as a solar/energy performance-based design decision-support method for the early-design phase of neighborhood projects;
2. verify if the workflow could bring new knowledge and help improve the performance of a design;
3. identify bugs and improvements in the interface and workflow.

#### Potential as a DDS tool

We observe that the objectives which we intended to fulfill in terms of prototype features, namely: integration within the design process, relevance of approach, simplicity of user-inputs, intuitiveness of workflow and interface, were asserted by a majority of participants through their feedback collected in the final questionnaire. Despite a general low level of prior experience with existing tools and in particular programs exploited by the prototype (Rhino, Grasshopper, DIVA), users could all easily and quickly understand the workflow and use the interface. Based on the qualitative data, the prototype appears as highly promising in terms of the relevance and usefulness of its approach, as well as its intuitive and simple interface.

#### Knowledge-gain conferred by the prototype

Results from the ranking phases and comparison of VB to VA for each participant provide quantitative data for verifying if the workflow could bring new knowledge and help improve a design's performance (objective 2). Yet, it remains difficult to draw clear conclusions, due to the confluence of different factors including: the conflicting nature of the criteria, causing one performance value to improve while another one worsens; the technical difficulties (also detailed below) in reproducing and investigating variations of VA; the small number of participants, limiting the application of statistical analysis such as the descriptive Kendall rank coefficient; differences in the format and degrees of freedom between the ranking phases, restricting their comparison on equal grounds; possible intrinsic errors in the modeling and simulation of the variants performance, to which the ranking results are compared.

It would be desirable to obtain strong quantitative data that reflect the perceived knowledge-gain brought to light through the qualitative feedback. We note that this goal of verifying if the workflow can bring new knowledge and help improve a design's performance can only be achieved if design flexibility is increased significantly, so as to allow highly customized building massing options. Improvements in the visualization and interaction with the user can also contribute to enhancing the guidance feature of the prototype.



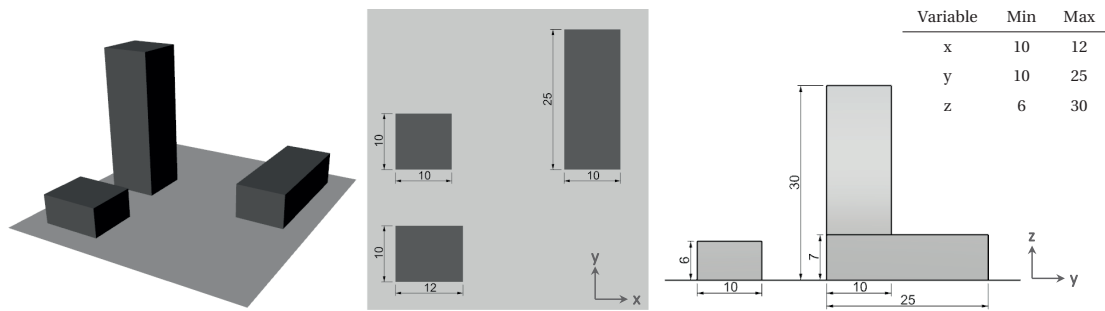


Figure 6.12 – Hypothetical design to attempt to reproduce in the prototype. The three buildings must be inputted by selecting the same ‘simple volume’. The minimum intervals of dimensions to input to ensure covering the ranges found in the design are listed in the top right corner table.

Moreover, a second series of workshops with a revised schedule and tasks, including more participants and an extended time-frame, would be necessary so as to enable a dedicated focus on assessing the educational potential of the prototype. Explicit directives should be communicated to participants to ensure they truly attempt to improve the performance of a design using the information given by the tool. In any case, it remains difficult to judge the level of effort made by participants in trying to understand, absorb and translate this information into a new design.

### Limitations of the prototype

Considering the early development status of the tested prototype, multiple elements were identified regarding objective 3, including suggestions made by participants through the open-ended questions of the final questionnaire. The main issues encountered are linked to the lack of flexibility in the design, caused by grouped building typologies and dimensions inputs being applied to all buildings. These two conditions have a combined effect of generating buildings often not corresponding to what is desired by the user. To better illustrate this issue, let us consider the example design illustrated in Fig. 6.12, hypothetically representing the initial concept of a practitioner. Using the prototype, it is possible to investigate the effect on the performance of varying, within certain boundaries, design parameters linked to the building dimensions. To do so, the design must be ‘inputted’ into the program, following the approach described in section 5.1 and using the interface of Fig. 5.4. All three buildings correspond to the same category of ‘Volume simple’. However, to cover the range of dimensions spanned by the buildings, large intervals must be specified for y and z, as shown in the top right corner of Fig. 6.12. Since the generation of design variants by the prototype is done through a random sampling of the possible variables’ values, there is no way to enforce searching in specific areas of the solution space domain. There is thus no guarantee that the mix of a tower, low block and bar will be obtained in the 20 generated variants. The reasons behind this way of functioning of the prototype are linked to technical feasibility issues in the coding and limited time in implementing the prototype in view of the workshops. Through suggestions made by participants and continued development following the workshops, improvement paths have

## Chapter 6. Appraisal of developed prototype

---

been identified and their implementation is foreseen. While we hint at some of these ideas in this section, they are further discussed in chapter 7.

The limited flexibility in the design is also linked to the underlying performance assessment engine. Building typologies were specifically restricted to the simple shapes present in the dataset used for training the metamodels, presented in section 4.2. This was done to ensure that predicted performance values, obtained when applying the functions on new, unseen designs, would remain realistic. The assessment of the predictive performance and validity boundaries of the metamodels is further addressed in the next section. Other design constraints were also the consequence of the underlying metamodels' input parameters and/or training dataset, e.g. the north-south-east-west alignment of facades and the climate file of Geneva.

### Outcome

In light of the qualitative information collected from the workshops, a general consensus on the high potential of the prototype was observed, despite its early development status. Issues encountered, mostly of technical nature, were to be expected due to the youth of the prototype and are judged as straightforwardly solvable, as further discussed in chapter 7.

In this section, we have assessed the prototype from the perspective of its usability, relevance and potential in becoming a DDS that can be seamlessly integrated into practitioners' work process. It is equally important to evaluate its level of accuracy in estimating the performance of neighborhood designs. This is done in the next section, by applying the predictive mathematical functions on the set of variants developed by the participants.

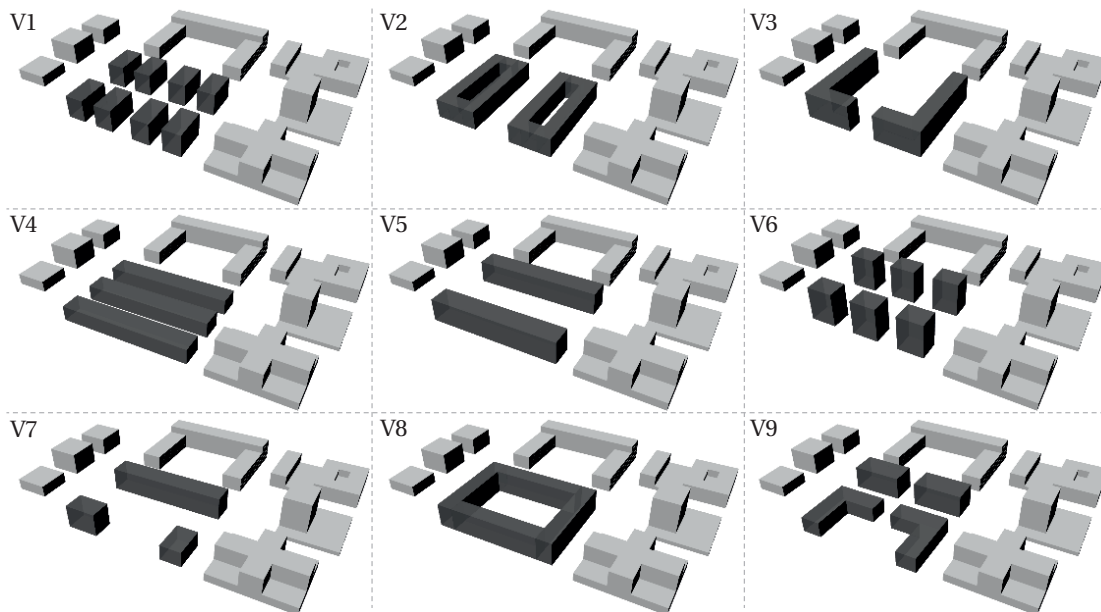


Figure 6.13 – Pre-workshop variants added to the participants' designs to form the test set.

### 6.2 Testing the metamodels' performance and boundaries

In this section, we focus on the performance results of the variants collected through the workshops, to further investigate the metamodels' predictive power. This study represents an 'external' test, which complements the internal training and testing procedure presented in chapter 4 when developing the predictive functions<sup>2</sup>.

The three example variants shown to participants during the ranking phases were selected from a set of nine test variants generated in preparation for the workshops. These are added to the 13 designs from the participants to form the external test set, comprising 22 variants in total. In the following, we refer to this group as the 'test set'.

#### 6.2.1 Computation of inputs and reference outputs for the test set

As explained in section 6.1, the modeling and simulation process following for acquiring the reference dataset in chapter 4 was applied on the workshop variants, to compute both the metamodels' inputs and reference outputs to allow verifying the prediction accuracy.

The nine variants added to the participants' variants are illustrated in Fig. 6.13. To facilitate the comparison of the test data, the input and simulated output values are standardized and displayed using a visualization technique called parallel coordinates [Few, 2006; Ritter et al., 2015]. As explained in chapter 4, standardization consists in scaling a list of values so that it is centered with a mean of 0 and a std of 1. The standardized values are plotted through the parallel coordinates graph shown in Fig. 6.14, where one line is associated to one design. The last parameter appearing on the x-axis corresponds to the simulated output and is preceded by the full list of inputs introduced in chapter 4. The ones in bold and starred are the predictors included in the full and reduced final versions of the metamodels respectively (detailed in Table 4.13). The reference dataset is plotted in the background in light gray.

Through these graphs, the variants' profile can be compared between the test data as well as with respect to the reference dataset used for fitting the metamodels. Participants' variants are denoted in the legend by the participant's number Px and the variant name A or B (full lines with marker). The nine post-workshop variants are listed from V1 to V9 (dashed lines).

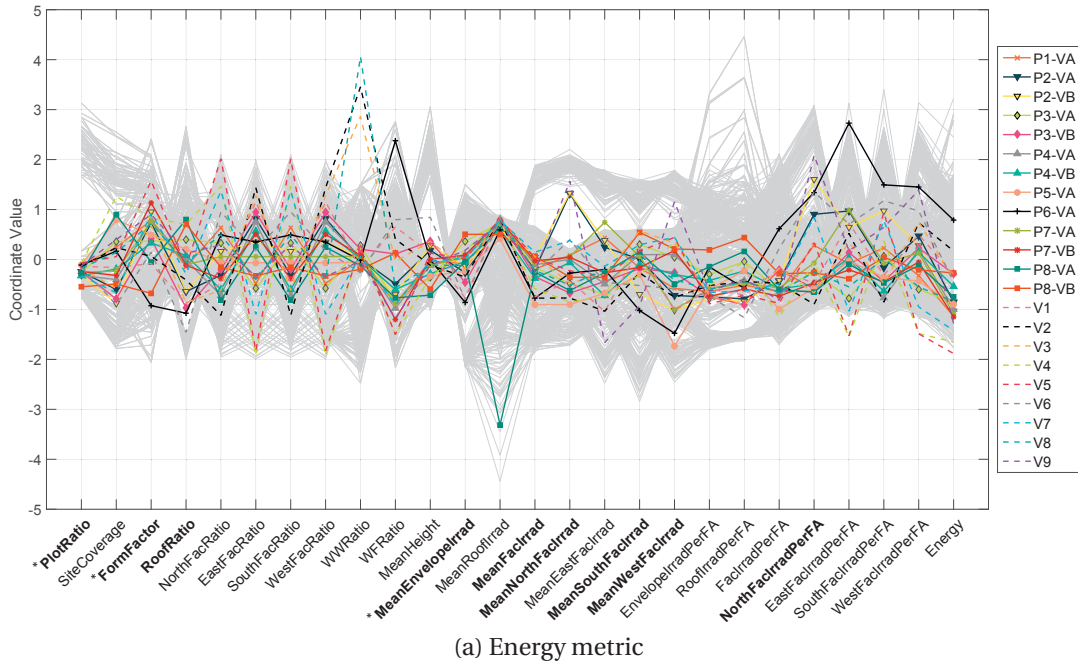
We observe a diversity of profiles, with extreme values located at or exceeding the boundaries defined by the reference data. For example, variant P8-VB is out of the reference range for its *PlotRatio*, *MeanHeight* and *MeanEnvelopeIrrad* value. Other designs with parameter values located out of the main range spanned are P8-VA, P6-VA and V5. In terms of the simulated responses, most variants are closely distributed within the reference data interval, with a few divergent designs e.g. P6-VA for both the energy and daylight metrics.

In the next section, we make use of this information for interpreting the prediction results.

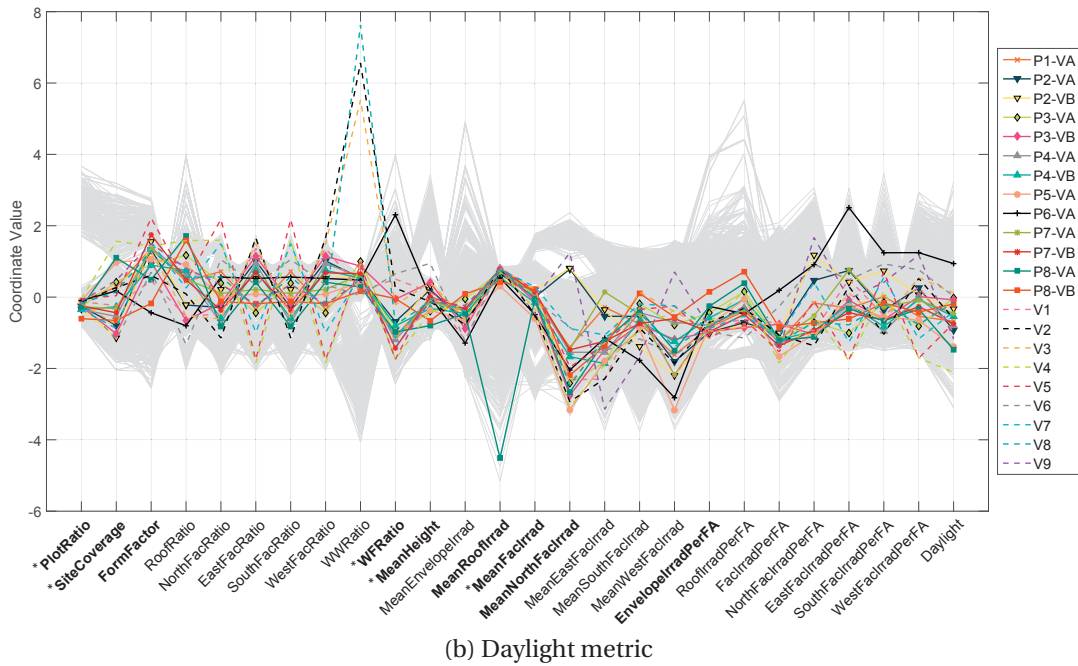
---

<sup>2</sup>Some of the following results have been presented in Nault et al. [2016a].

Chapter 6. Appraisal of developed prototype



(a) Energy metric



(b) Daylight metric

Figure 6.14 – Parallel coordinates plot showing the standardized value of the inputs and outputs corresponding to each test variants. Inputs in bold and starred are respectively the ones included in the full and reduced final versions of the metamodells.

### 6.2.2 Assessment of prediction accuracy

#### Multiple linear regression models

As explained in section 4.5.6, the metamodels implemented in the prototype correspond to a preliminary version,  $f_{prelim}(\mathbf{x})$ , detailed in Table 4.14. The second version  $f(\mathbf{x})$  presented in section 4.5.4 was later obtained from a slightly different dataset following a more extensive fitting procedure. From this second version, a 'reduced' variation  $f_{red}(\mathbf{x})$  was derived. Both are detailed in Table 4.13.

Results from applying each metamodel variation to the 22 variants are presented in Fig. 6.15 for the energy (left) and daylight (right) metrics. In each figure, the left-side plot shows the predicted versus simulated performance values along with the RMSE and  $R^2$ . The right-side plot displays the residuals across the 22 test variants, with information on the metamodel's number of inputs and the residuals' mean and std.

Comparing across model versions for the energy metric, we observe that the simpler (reduced) function that only uses three inputs (Fig. 6.15b) yields the lowest RMSE and highest  $R^2$  value. However, the residuals' mean is further from the desired zero, demonstrating a dominant over-prediction. Yet, due to the small dataset size, conclusions made by comparing the residuals distribution statistics are limited since outliers strongly condition the mean and std. For instance, residuals for the other two versions are not closer to the zero dashed line, yet the mean is nearly null due to the averaging effect involving points further above/below zero. Moreover, consistent under- or over-prediction may be beneficial to our purpose of comparing design alternatives, despite the fact that such a behavior may indicate that the model is missing a predictor<sup>3</sup>. In the current context, that would ensure that the relative ranking of the designs based on the predicted performance is closer to the one obtained based on the simulated (reference) values.

Some test variants may be categorized as outliers. For instance, P8-VA (over-estimated) and V3 (under-estimated) for the final version (Fig. 6.15a). Buildings in design P8-VA, shown in Fig. C.11a, have a larger base at the ground-floor level, a trait which is not found in the reference dataset and could not have been reproduced in the prototype. As for V3, possible reasons explaining the prediction error are harder to discern based on its design and inputs profile. Removing these two variants from the test set, the RMSE and  $R^2$  for the final energy metamodel improve to 2.76 [kWh/m<sub>FA</sub><sup>2</sup>] and 0.63 respectively, while the mean of the residuals stays similar with  $\mu = -0.24$ . Results for the reduced version  $f_{red}(\mathbf{x})$  show a slight improvement by ignoring the outliers, mainly reflected by the  $R^2$  which increases to 0.79.

The prediction accuracy achieved for the daylight metric is lower across all metamodel versions, with no clear 'winner'. This metric appears more challenging to predict than the energy need, at least from the predictors we have considered. The fact that the reference dataset used to generate the functions is over three times the size of the energy dataset may have

---

<sup>3</sup><https://onlinecourses.science.psu.edu/stat501/node/328> (last accessed on April 12, 2016)

## Chapter 6. Appraisal of developed prototype

---

caused these functions to over-fit due to similarities between variants within each case series, as explained in section 4.5.4.

Some test variants may be categorized as outliers. For instance, P6-VA, a design which was also highlighted in previous sections for its divergent input values (Fig. 6.14) and complex layout that could not be reproduced in the prototype (Fig. C.9a). The particularities of this design may well explain the prediction error, which is consistent across all daylight metamodels. Similarly for design P8-VB, which has input values bordering or exceeding the reference range in Fig. 6.14 and whose daylight performance is over-estimated by all three model versions.

If we remove these two variants from the test set, the predictive performance of the later metamodels improves: the RMSE decreases to 6.75 and 5.53 [%] respectively for  $f(\mathbf{x})$  and  $f_{red}(\mathbf{x})$ , with an associated increase in  $R^2$  to 0.52 and 0.48. The residuals mean remains close to its current value.

We can quantify the RMSE as a percentage of the simulated values by dividing it by the range of the corresponding test data output:

$$RMSE_{\%} = 100 \times \frac{RMSE}{(y_{max} - y_{min})} \quad (6.5)$$

The RMSE of the final energy and daylight metamodel respectively represent 22% and 21% of the range of each metric. For the reduced versions of the functions, these figures respectively reduce to 16% and 19%, getting closer to the 10% threshold defined by Forrester et al. [2008] to qualify a reasonable global model.

### Preliminary Gaussian Processes regression model

Using the Gaussian Processes (GP) regression model introduced in section 4.5.7, we obtain the results shown in Fig. 6.16. Compared to the above results (Fig. 6.15), we observe for the energy metric a higher  $R^2$  value, but a residuals' mean further from zero, showing a consistent over-estimation. All fit and error metrics for the daylight metric indicate a lower prediction accuracy for that metamodel. More tests should be conducted to verify the source of these behaviors, for instance by removing/adding one input at a time to verify the effect on the fit.

### 6.2.3 Synthesis - Generalization potential of metamodels

In this section, we have compared the predicted and simulated (reference) performance values computed for each of the 22 designs developed prior to and during the workshops. Results allow us to go over our initial goal, stated in section 5.2, of assessing the predictive accuracy of the DDS's underlying mathematical functions.

The predictive performance achieved by the metamodels is encouraging considering the following observations:

## 6.2. Testing the metamodels' performance and boundaries

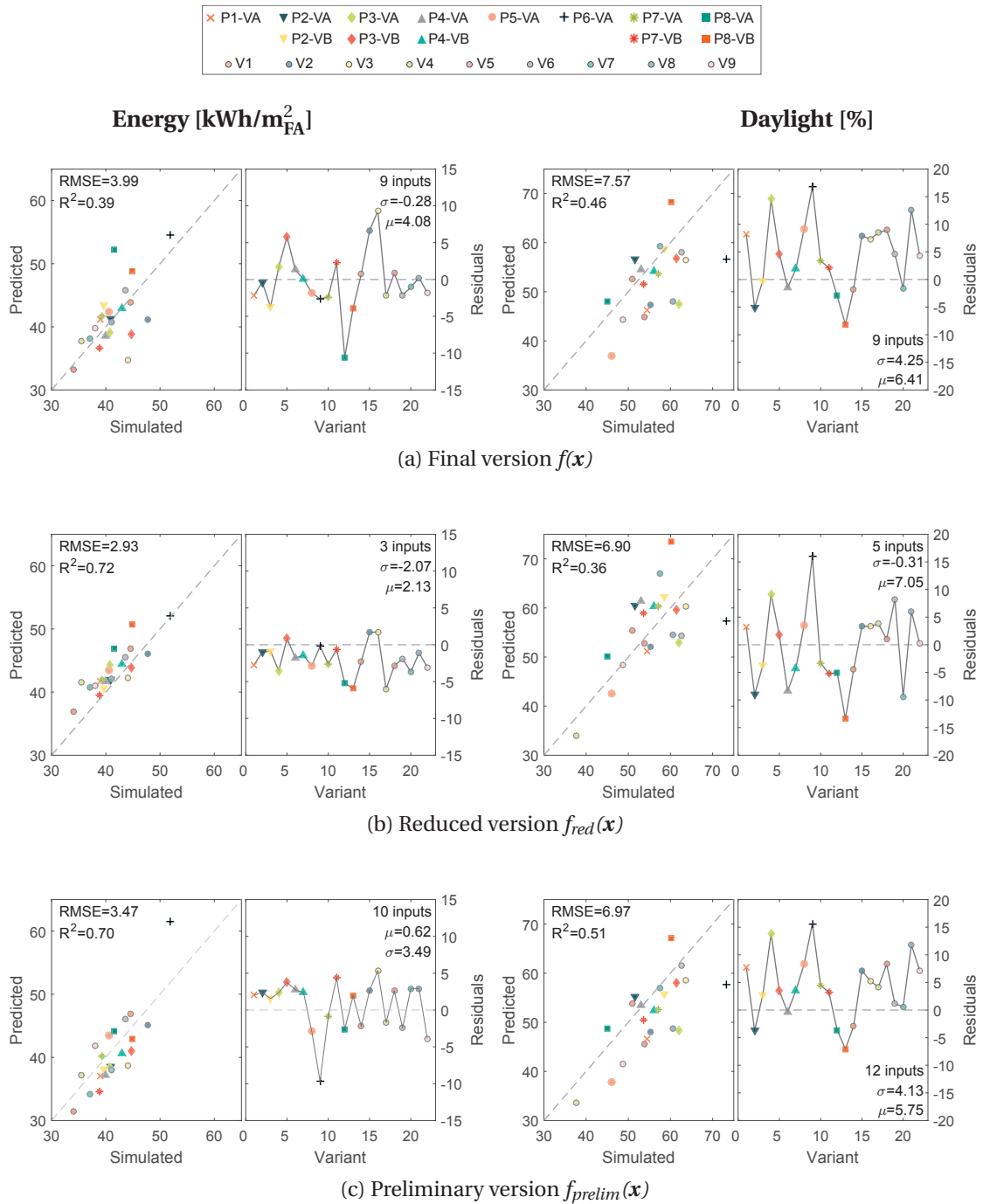


Figure 6.15 – Prediction accuracy of each energy (left) and daylight (right) metamodel version. For each figure: predicted against simulated performance values (left) and residuals (right) across the test variants.

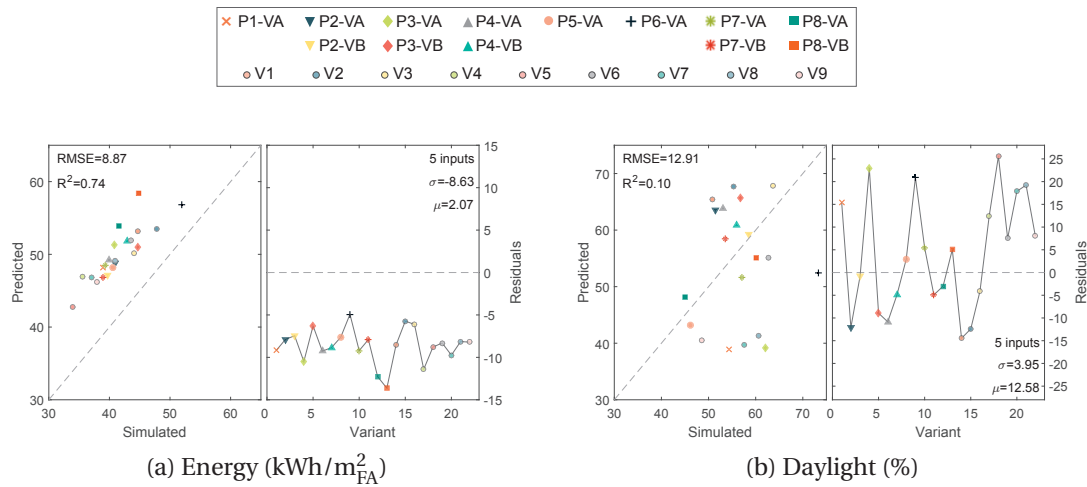


Figure 6.16 – Prediction accuracy of the (a) energy and (b) daylight GP metamodels. For each figure; predicted against simulated performance values (left) and residuals (right) across the test variants.

**Differences between reference designs and test variants.** Some degree of error was to be expected due to differences between the designs used to fit the functions and the workshop test set, specifically in terms of building layout and number as well as dimension of the parcel of land. Another dissimilarity of importance is the fact that some workshop variants present a mix of building typologies, a situation not found in the reference dataset. Yet, the metamodel was still able to accurately estimate the performance of such designs, for example P4-VA and V9, composed of both L-shaped and linear blocks.

**Application to designs beyond the prototype’s generative feasibility region.** As highlighted in section 6.1.2 and in the participant-specific analysis found in appendix C.4, some of the participants’ VA could not be reproduced in the prototype due to time and technical issues (discussed in section 6.1.5). Some of these limitations are linked to the hypothesized validity boundaries of the metamodels; the prototype was developed to allow reproducing designs that we assumed could be evaluated by the metamodels with some level of accuracy. As explained in section 5.1, design options were constrained to delimit the solution space and ensure some degree of similarity to the reference dataset, e.g. in terms of building typology and facade alignment. When applying the metamodels on the variants that could not be handled by the prototype mainly due to this design flexibility limitation, namely P5-VA and P6-VA, the prediction error is either low - P5-VA energy prediction from all versions and daylight prediction from the reduced version - or justifiably larger than average - P6-VA for preliminary energy model and all versions of daylight model.

We conclude that the predictive modeling approach adopted for constructing our DDS performance assessment engine is promising. To further improve the metamodels, multiple avenues can be explored as detailed in section 4.7 and further in chapter 7, such as enlarging the design diversity in the reference dataset and investigating other model forms and fitting techniques.



## 7 Discussion

In this chapter, we go over parts of this work to expand the discussion and highlight the main limitations and foreseen improvement possibilities, bringing complementary or additional observations to what has been presented in previous chapters.

### 7.1 Prediction error and fitting technique

The topic of prediction error or uncertainty has only been indirectly addressed in chapters 4 and 6, when looking at the residuals (e.g. Fig. 4.25, 4.26 and 6.15). It would be important to incorporate these notions particularly into the output visualization provided by the prototype. In that case, an error bar could be drawn around each performance value, enabling users to better distinguish significantly different variants.

Figure 7.1 presents results from a preliminary investigation where confidence intervals were obtained around each prediction for one iteration in the training-testing process in phase C of the metamodel development (see Fig. 4.24). The Matlab linear regression function *fitlm* was applied on the training set, giving a Matlab *LinearModel* object that was then used to obtain predictions and confidence intervals from the inputs in the test dataset. The intervals correspond to prediction bounds covering the likely values for a new simulated value (or observation  $y_{n+1}$ ) given a set of predictors  $(\mathbf{x}_{n+1})^1$ . The graphs show that the width of the 95% confidence interval is similar when fitting using 19 inputs (Fig. 7.1a) versus 10 inputs (Fig. 7.1b) with a mean of 4.95. It becomes wider with a mean width of 10.63 when reducing to three inputs (Fig. 7.1c). This means that there is a larger uncertainty in the prediction of new simulated values using the reduced function containing only three inputs. This sort of information could in the future be a useful complement to the other goodness-of-fit measures employed in chapter 4.

---

<sup>1</sup><http://www.mathworks.com/help/curvefit/confidence-and-prediction-bounds.html> (last accessed on June 27, 2016)

## Chapter 7. Discussion

Obtaining an uncertainty for each prediction could moreover be achieved by resorting to Gaussian Processes, introduced in section 4.5.7, or similar methods. Due to the probabilistic nature of GP, its prediction is a random variable. This means that it is possible to obtain a confidence range for each prediction, as illustrated in Fig. 7.2. The advantages conveyed by adopting a GP regression technique also include an added knowledge about the under- and over-sampled regions in terms of the predictor values, information that can guide the process of improving the metamodel.

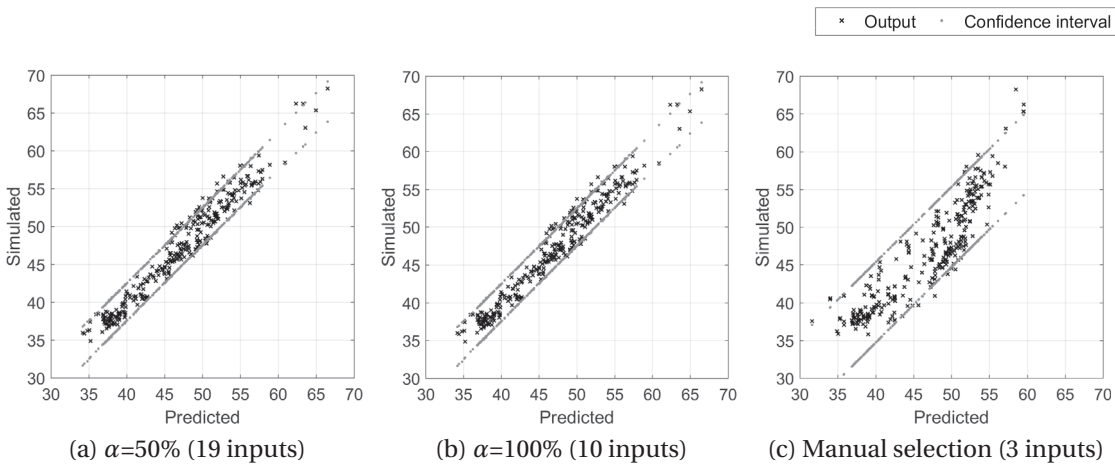


Figure 7.1 – Simulated against predicted energy need [ $\text{kWh/m}_{\text{FA}}^2$ ] with 95% confidence intervals for predicted values, for one example iteration in the training-testing procedure (see Fig. 4.24), when fitting using the entire dataset ( $d=100\%$ ) and (a) 19 inputs, (b) 10 inputs, and (c) 3 inputs (see also section 4.5 and Fig. 4.25). These graphs were produced using the *predict* and *fitlm* functions in Matlab.

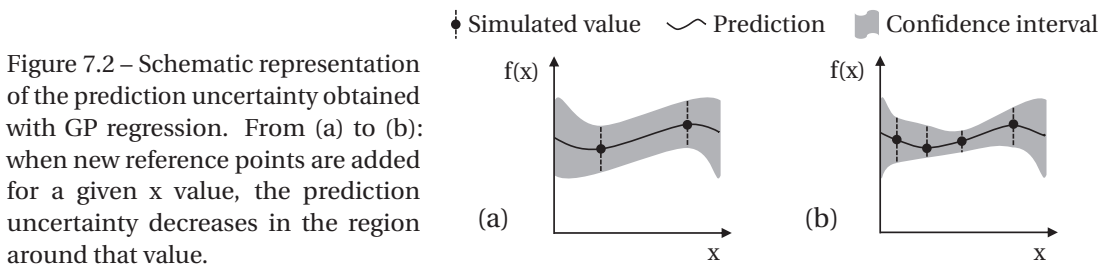


Figure 7.2 – Schematic representation of the prediction uncertainty obtained with GP regression. From (a) to (b): when new reference points are added for a given  $x$  value, the prediction uncertainty decreases in the region around that value.

## 7.2 Sensitivity to simulation settings

Sensitivity analysis to various simulation assumptions would be beneficial to allow making more sound conclusions on the results, e.g. in terms of metamodel validity. In addition to the preliminary investigation presented in section 4.7.3, further work was initiated by comparing two energy datasets distinct in terms of the U-value simulation settings for opaque surfaces: (i) the medium U-value set from which the metamodels were developed, and (ii) a low U-value set later acquired for a partial group of design variants (M-cases). The U-values for both settings are given in Table 7.1. All other parameters were identical (see Table 4.7).

Figure 7.3 shows the histogram for the simulated heating, cooling, and total energy need for each dataset, with a distinction between the five M-cases for which we had data for both U-value settings. The maximum difference observed in each graph is displayed ( $\Delta_{\max}$ ). The medium U-value dataset presents a wider and slightly narrower spread respectively for the heating and cooling need. The heating need values for the low U-value setting are particularly clustered, demonstrating that the effect of urban morphology is attenuated when high insulation standards are applied. However, the opposite effect is observed for the cooling need. In terms of energy for both heating and cooling, although a lower value ( $< 30 \text{ kWh/m}_{\text{FA}}^2$ ) is reached with the low U-value setting, the fact that medium and low U-value distributions partly overlap indicate that similar performance levels can be achieved with less insulation. These results lead us to speculate that the effect of poor insulation can potentially be counterbalanced by a proper urban form. Considering the evolution of the design process, this statement can be reformulated to: if the urban form is well planned, savings can potentially be made on insulation materials.

It is also important to note that the relative position of the M-specific peak is altered between the medium and low U-value histograms, e.g. the M0 and M1 designs that are switched. The ranking is different not only between series, but also between variants of a same series, as illustrated in Fig. 7.4, showing the difference between the medium and low U-value simulated energy need for each design. A flat line would indicate a constant difference, i.e.  $y_{\text{medU}} = y_{\text{lowU}} + \text{constant}$ . Such a situation would in turn signify an identical ranking between design alternatives. However, we observe variations across the variants, particularly for the M0 and M5 cases where the mean difference  $\mu$  exceeds 20%. This value is computed using the following equation:

$$\mu = \frac{100}{N} \times \left( \sum_{i=1}^N \frac{y_{i,\text{medU}} - y_{i,\text{lowU}}}{y_{i,\text{medU}}} \right) \quad (7.1)$$

where  $N$  is the number of designs and  $y_i$  is the simulated output of variant  $i$ .

A final comparison of the medium and low U-value datasets is presented in Fig. 7.5, which shows the input-output correlation graphs for each dataset and M-case. As in section 4.4.2, the pairwise linear correlation coefficient, computed over all cases taken together, is displayed when it was found to exceed  $(\pm)0.70$ . We observe that the spread of the points differ between

Fig. 7.5a and 7.5b, e.g. for the *PlotRatio* parameter, bringing out again the attenuation effect of the low U-value setting. This is also reflected in the reduced correlation level with the *FormFactor*. The input portraying the highest correlation with the energy metric in the low U-value dataset is the window-to-floor ratio, due to the larger difference between the wall and window U-values compared to the medium U-value setting (see Table 7.1).

We conclude that the underlying assumptions related to the dataset used in the metamodel development process are a matter of importance as they condition the observed trends. The current results indicate that a different metamodel structure, e.g. with other main inputs and coefficients, would most likely be obtained, were we to pursue the analysis of the low U-value dataset and apply the same metamodeling approach detailed in chapter 4. As highlighted earlier, the ranking of the variants based on their performance is also linked to the simulation assumptions, restraining the generalization of the results obtained with any one metamodel version into broader design guidelines. However, this thesis has contributed a method that can be extended/adapted to other design contexts than the one here used as a proof-of-concept. A future research path of interest would be to investigate the relative performance improvement achievable through early versus more detailed design variables, as well as the interaction between these two groups of parameters, e.g. through sensitivity analysis. As a second step, a robust and semi-automated method could be developed to allow conducting such a study and support the interpretation of its outcomes. This method could follow a similar workflow as developed in this thesis, starting from a user-defined base case with a range for each design variable and some constraints. This information would then be used by the underlying engine to generate the data required to perform a case-specific sensitivity analysis.

Further tests could be conducted, for instance on reflected light, linked to envelope material and likely to influence the energy consumption and daylight conditions in urban settings of a certain density [Strømman-Andersen and Sattrup, 2011]. Design characteristics for which specific parameters become influential could be identified in the form of thresholds. For example, density levels above which the contribution from inter-building reflection should be taken into account in the performance assessment could be defined.

Similarly for other design variables such as the window-to-wall ratio and glazing material. Figure 7.6 shows the effect of increasing the window-to-wall ratio on the energy demand for heating according to various glazing U-values for the climate of Paris, in the context of a study investigating different urban morphologies [LSE Cities and EIFER, 2014]. The heating demand increases with the glazing ratio from a U-value of 3.2 and 2.8 for the detached housing and compact urban block respectively.

The identification of such case-specific parameters would in turn influence the way metamodels are derived; according to the specificities of the project to be studied using the predictive DDS approach, the appropriate metamodel could be retrieved or even built. This idea is further detailed in section 8.3.

## 7.2. Sensitivity to simulation settings

Table 7.1 – U-values used in the energy need simulation for the medium and low U-value energy datasets. The medium setting corresponds to the dataset used to develop the metamodels in chapter 4.

|                              | Medium U-value<br>[W/m <sup>2</sup> K] | Low U-value<br>[W/m <sup>2</sup> K] |
|------------------------------|--|-------------------------------------|
| Wall                         | 1.3                                    | 0.18                                |
| Roof                         | 1.84                                   | 0.19                                |
| Floor                        | 1.25                                   | 0.18                                |
| Windows (double low e argon) | 1.5                                    | 1.5                                 |

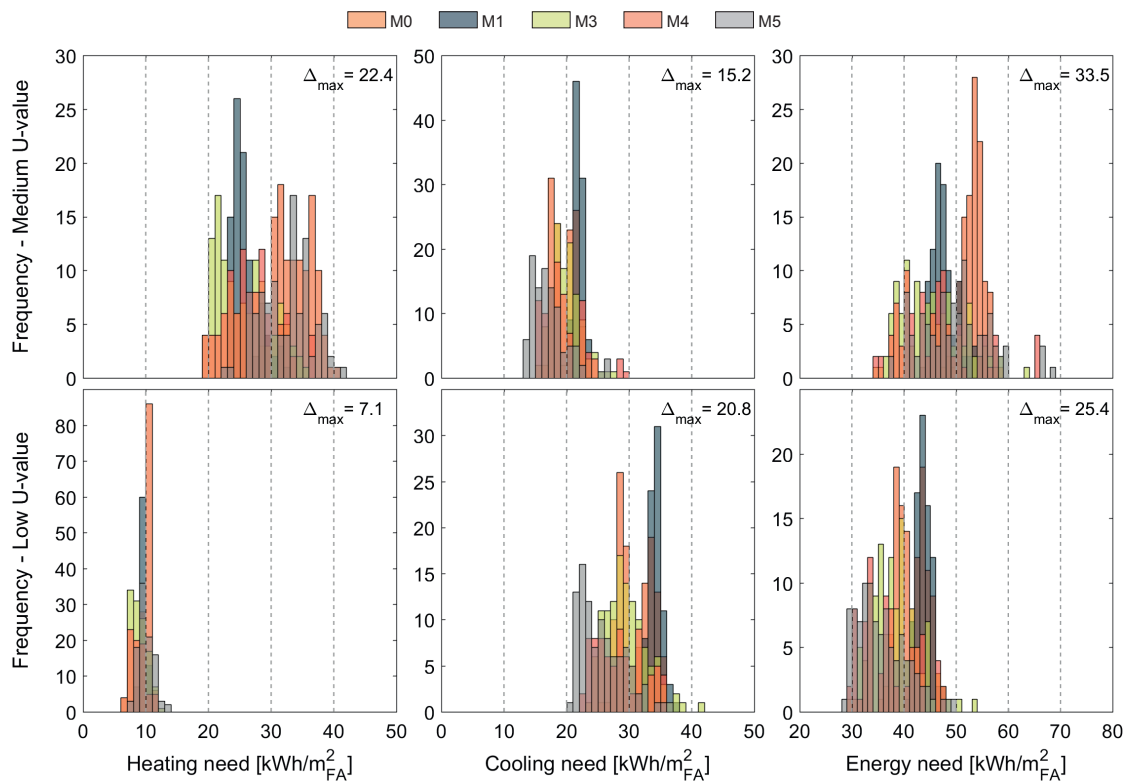


Figure 7.3 – Heating, cooling, and total energy need in the medium (top) and low (bottom) U-value datasets (see Table 7.1), with distinction between the different M-cases. The difference between the maximum and minimum value is displayed ( $\Delta_{\max}$ ).

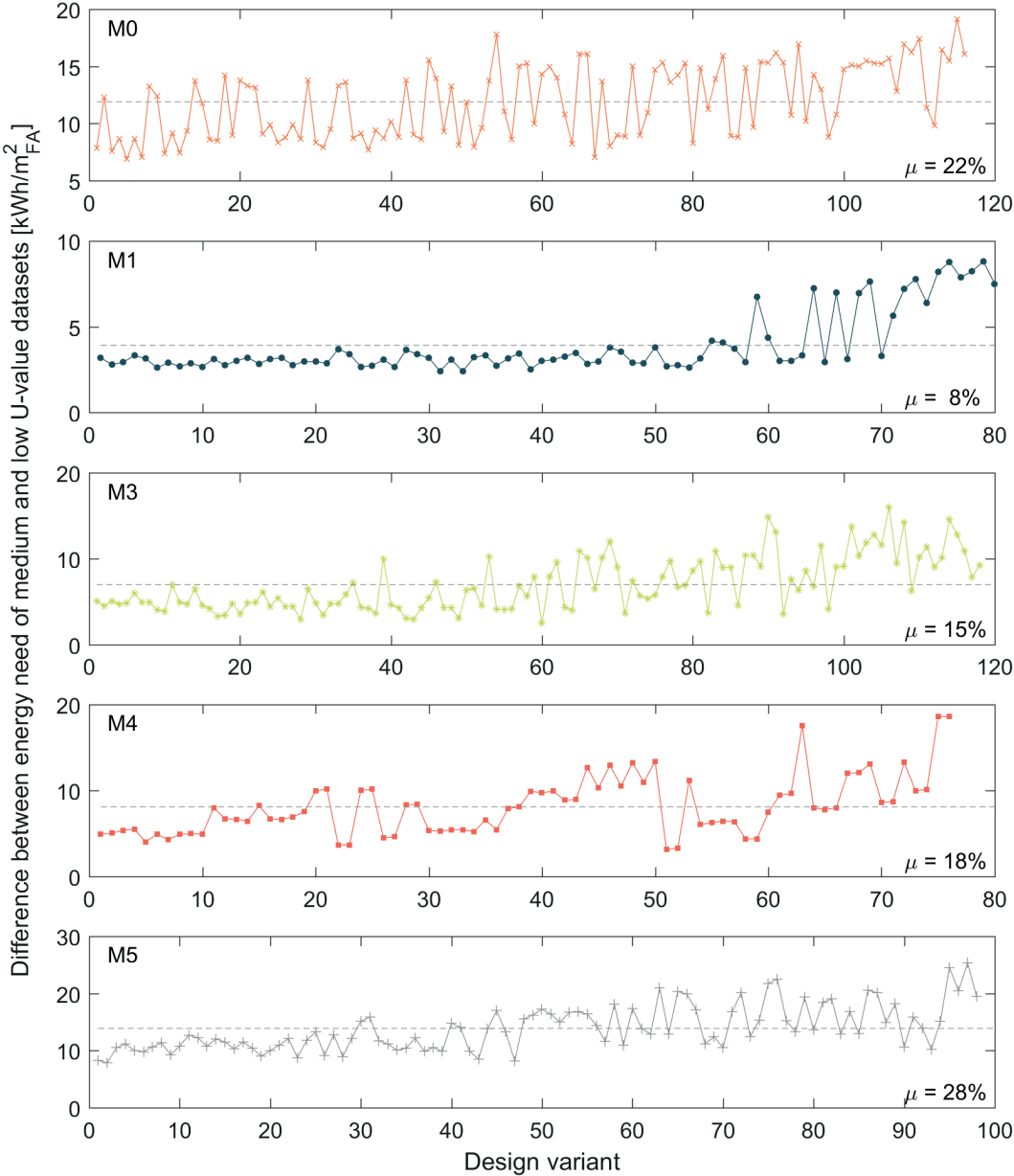


Figure 7.4 – Difference in the energy need between the medium and low U-value datasets (see Table 7.1), for each variant of each case series. The mean percentage difference, computed with respect to the medium U-value dataset, is displayed ( $\mu$ , see equation 7.1).

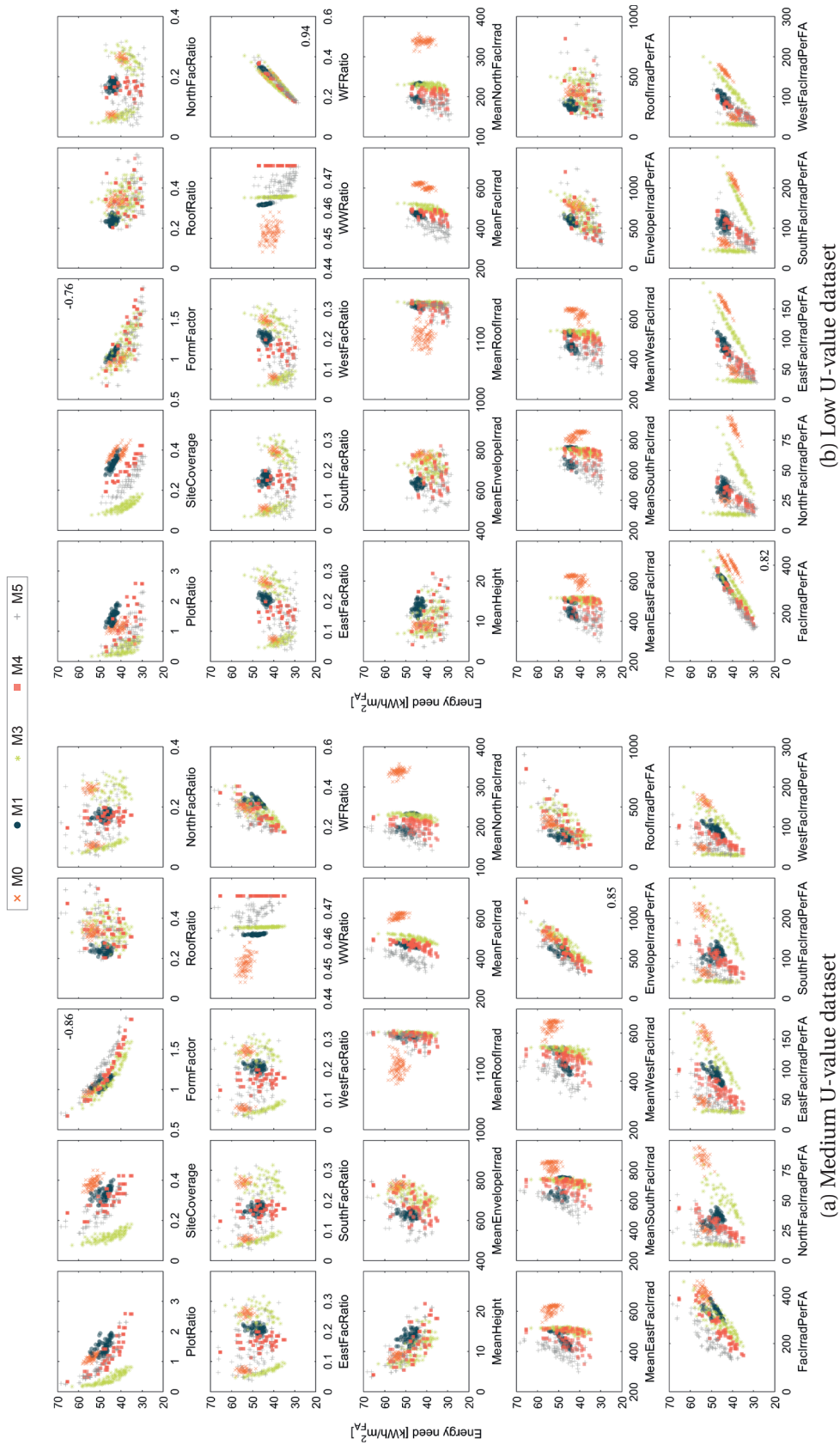


Figure 7.5 – Relationship between the energy need output and each input in the (a) medium and (b) low U-value energy datasets (see Table 7.1), with distinction between the different M-cases.

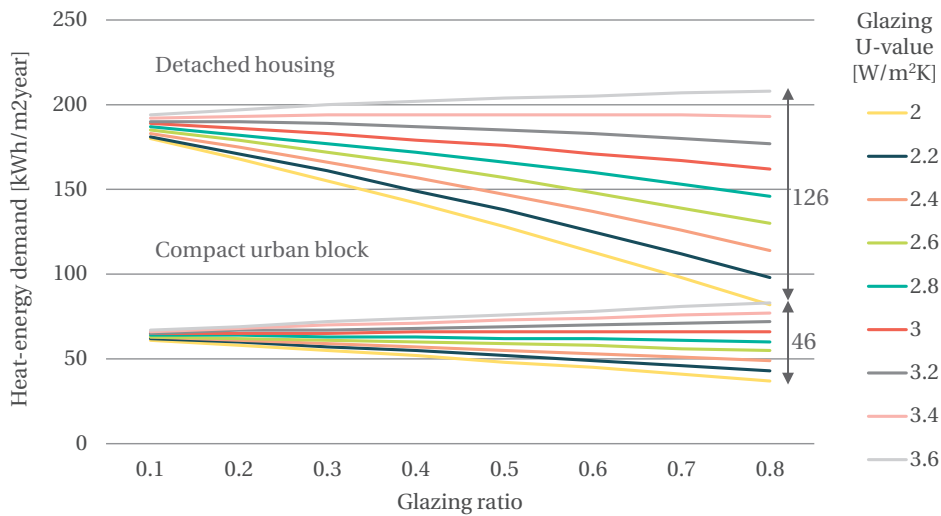


Figure 7.6 – Variation in the annual heating energy demand (normalized per floor area) obtained when increasing the window-to-wall ratio, for different glazing U-values, in the case of detached housing and compact urban block in Paris. Graphs made using data from [LSE Cities and EIFER, 2014].

### 7.3 Averaging effect and extension to existing context

The fact that the metamodels make use of inputs computed over all buildings taken together and output an estimated overall value blurs the individual building’s performance. For example, two buildings with opposite energy needs - low versus high - lead to the same average performance as two buildings with a mid-range value. However, the latter may be more desirable, especially if the mid-range value falls below the limit imposed by some standard or label. Future work should look into solving this potential pitfall, by including a verification of the individual building’s performance and avoid the possible misleading caused by the averaging effect. A way to do so would be to define thresholds in terms of performance per building, e.g. based on labels such as Minergie.

It would also be interesting to include an assessment of the effect of the new buildings planned on the existing surrounding context, to ensure that all buildings retain their solar rights and to mitigate the impact on the built environment. Along the same lines, an evaluation of the outdoor spaces, e.g. solar exposure in parks and on sidewalks, would also enrich the method by adding another element of importance of the conceptual design phase.

### 7.4 Refining the dataset

Through a random sampling approach, an extensive number of design variants were collected for building the reference dataset used to develop our metamodels. However, this method was used to assign values to the parameters varied in the parametric modeling, which are different from the ones we have used for training our metamodels. Indeed, the model inputs



were derived after the fact, i.e. once the design variants were modeled and their solar exposure levels computed. This disconnect between the sampled design variables and input parameters prevent us from controlling the distribution of the latter. Yet, it would be hard to start from fixed input values from which to define design variants. For instance, if we were to fix the plot ratio, form factor, window-to-floor ratio and other main parameters, it is not obvious how a corresponding design could be modeled from such a set of values.

Still, it would be of interest to refine the sampling method and the general approach for populating the dataset required to fit the metamodels. This is further discussed in section 8.2.

An alternative method for populating the database would consist in using available data from recently built projects. This would likely require significant work to collect all information needed, e.g. building plans, construction details and energy usage, including data often unavailable for confidentiality reasons.

### 7.5 Increase in design flexibility

Since the workshops of October 2015, the prototype has undergone modifications. One major change is the extended flexibility offered when defining the base case design through the custom interface and Rhino program. The ranges defined by the user for each design variable, defining the solution space within which the prototype searches for variants, was previously being applied to all buildings. The upcoming version will allow specifying a building-specific range, enabling more precision in the modeling and therefore producing variants closer to the user's expectations.

This extended flexibility will have to be matched by the metamodels' application range. Further work will involve adding new data to the reference dataset, e.g. the workshop variants, to inform and refine the predictive functions.

The current status of the forthcoming prototype's interface is shown in Fig. 7.7. Aside from the language change - the next workshop will be held in English - the only visible difference is the rearrangement of the interface's elements. However, the background code has been adjusted to allow the above-mentioned functionality and to facilitate applying the same settings to multiple buildings successively positioned.

### 7.6 Enhanced guidance and informative features of workflow

In its status as of the time of the workshops, the prototype's GUI was still rather crude. Changes were brought to the output performance graphs to address some of the participants' comments, in particular the difficulty in visualizing and comparing variants (see full list in Table 6.2). An example of the latest version of the graphs is illustrated in Fig. 7.8. Axes have been fixed and a grid with a constant separation of 5 [units] was added, facilitating the visualization

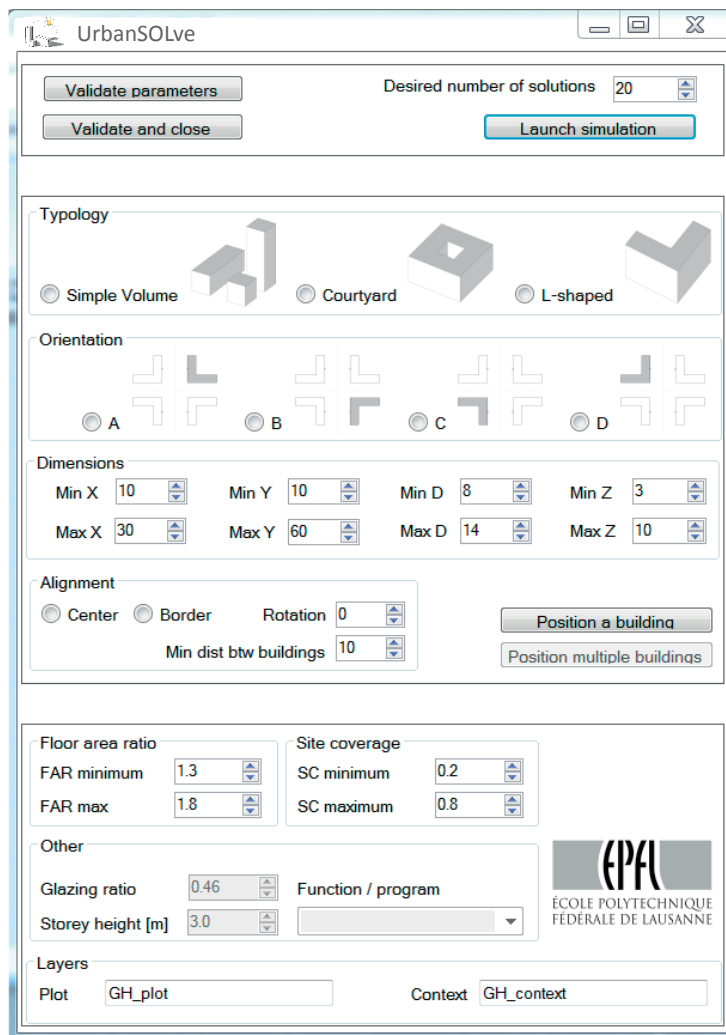


Figure 7.7 – New version of the custom interface for user-inputs (for comparison, see previous version in Fig. 5.4).

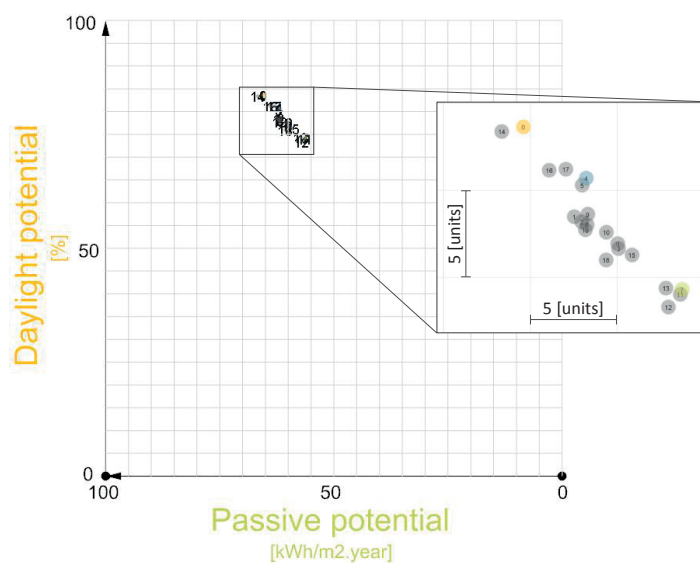


Figure 7.8 – Example graph for the new version of the performance visualization, with fixed axes allowing clearer comparison between the design variants from one run of the workflow, as well as between iterations starting with distinct initial user-inputs (for comparison, see previous version in Fig. 5.7).

Table 7.2 – Envisioned balance to compute an aggregated performance metric.

| Demand   |    | Partial coverage through          |
|--|----|-----------------------------------|
| Heating  | <– | Heat produced by ST collectors    |
| Cooling<br>(accounting for natural ventilation)        | <– | Electricity produced by PV panels |
| Artificial lighting<br>(exploiting daylight potential) | <– | Electricity produced by PV panels |

and comparison both across variants generated in one run of the prototype, as well as between different iterations (starting from another base case design). The clearer visualization of the relative difference in performance allows users to see not only which variants are better/worse, but also which ones are not significantly different. This information can be useful when incorporating other performance criteria in the decision-making process, such as morphological integration into the existing context, cost, etc.

As mentioned in section 6.1.2, potentially greater user-guidance could be achieved by providing an aggregated performance value, by merging the three criteria into an ‘autonomy’ metric quantifying the balance between energy demand and production (see Table 7.2). This translation could ideally benefit from an hourly analysis of the different values and a conversion into primary energy, which could allow computing additional performance metrics such as CO<sub>2</sub> emissions. Both interventions would however lead to an increased complexity of the whole assessment and pose new difficulties in the metamodeling approach. Alternatively, other performance metrics could also be computed, e.g. the thermal comfort in terms of overheating hours (replacing the cooling energy need yet preventing an aggregation) with a detailed natural ventilation assessment through CFD simulation, and the UHI effect.

A goal-based approach with user-defined performance targets could be adopted, facilitated by replacing the currently random population of the design space by an optimization-driven search. Both user-guidance and interactivity could be enhanced in parallel, by incorporating the user’s preferences into the optimization process to guide the generation of design alternatives. This is further discussed in chapter 8.

## 7.7 Revised workshop plan

From the lessons learned during the workshops and in parallel with the advancement of the forthcoming prototype version, a revised plan will be devised for the next tests with practitioners. The attention will be particularly placed on ensuring that results from each phase, e.g. ranking tasks, can be confidently compared to draw clearer conclusions on the added-value of using the prototype. According to the number of the participants, groups may be formed and assigned to a different design task to allow a comparative analysis.



# 8 Conclusion

## 8.1 Main outcomes and achievements

We began this thesis by highlighting the main challenges that remain in the specific field of methods for supporting urban designers and architects incorporate energy performance considerations early in their design process. In particular, a need was identified to facilitate real-time assessment of neighborhood designs in relation to decisions whose impact extends beyond the scale of the individual building.

This thesis has attempted to address this gap by proposing a design decision-support workflow whose features were defined so as to provide multi-criteria performance-based guidance in real-time, while respecting the ill-defined nature of early-phase meso-scale designs. Adopting the emerging generative design approach, the integration of the workflow into a digital prototype enabled us to demonstrate its accessibility among practitioners and its relevance to the exploratory early design stage. This was made possible by the underlying performance assessment engine, developed keeping in mind the limited available design information while capturing its effect at the neighborhood level. At the core of this engine, and concurrently of this thesis, are the daylight and energy neighborhood-scale metamodels, which represent a novel aspect of this research. The work was achieved by combining knowledge and methods coming from different fields, ranging from urban design to machine learning, while remaining cautious and attentive to the potential pitfalls or misinterpretations linked to such a cross-disciplinary approach.

Coming back to the three main questions introduced at the beginning of this thesis in section 1.4, we can further detail the main outcomes:

1. *How should we define the (energy/solar) performance of a (virtual) neighborhood and what metrics should be used to quantify each performance aspect, in a way that captures the interdependencies between buildings?*

Through the literature review and investigation presented in chapters 2 and 3, limitations associated to employing geometry- and/or irradiation-based parameters as

performance indicators were highlighted. Despite their advantageous simplicity, we observed that they lacked robustness and scope when used to compare and rank neighborhood designs in terms of their energy and daylight performance. This knowledge has led us to aim at ensuring a strong link to established performance metrics truly capturing the solar potential: the heating and cooling needs for expressing the energy required to maintain a comfortable indoor temperature, here associated to the (inverse of) passive solar potential, the spatial Daylight Autonomy (sDA) as a measure of the daylight conditions inside the buildings, and the energy production by photovoltaic (PV) and solar thermal (ST) systems as quantifying the active solar potential.

2. *How can we efficiently evaluate these metrics considering the available (low) amount of design information, in the context of a real-time interactive computer-based workflow?*

The time-consuming evaluation of the energy and daylight metrics require detailed building models and simulation assumptions, hindering their assessment at the conceptual design phase. As an alternative to simulation at this exploratory early stage, we have proposed in chapter 4 a data-driven method based on mathematical functions that can predict to some level of accuracy the value of each metric. Building upon the knowledge gained in chapter 3 when investigating the correlation between these established metrics and simpler parameters, the latter were combined to obtain a set of complementary information capturing the effect of urban morphology. As such, the metamodels generated only require early-phase friendly design information and can be seen as a temporary proxy of more advanced simulations that should nevertheless be conducted later on in the process. This approach thus promotes a temporal spread of the inclusion of energy-related considerations in design decision-making. Tested in chapter 6, the predictive accuracy was judged as satisfying, particularly considering the characteristics of the designs in the test set.

3. *What are the essential features of a design decision-support system, built around the performance assessment engine (defined through the previous questions), that will make it in line with the ill-defined nature of the design process?*

We have identified features judged relevant and of interest in the context of this thesis, through reviews, surveys, as well as recent developments found in the literature. Challenging the traditional generate-and-test workflow, we have adopted a generative approach that allows constructing a sample of a design solution space, from simple project-specific and user-defined inputs. These correspond to design variables that are typically decided upon early-on, and for which an exploration of their effect on the performance is highly desirable considering their strong influence on all criteria here considered. Described in chapter 5, the developed workflow was implemented as a digital tool to be tested by practitioners through workshops. This allowed distilling the technical, metamodel-based performance assessment method into an accessible and relevant format from the perspective of decision-makers. Results from the workshops, presented in chapter 6, demonstrate a solid potential of the prototype and of the proposed design approach.

### 8.2 Application potential

We have demonstrated, through the workshops outcomes, the potential of the proposed workflow as a DDS tool that could be seamlessly integrated into the early design process of practitioners. The focus has been placed on new neighborhood-scale projects, such as the ones that can be found in urban design competition or in master plans (e.g. Plan Directeur Localisé (PDL)). We argue that our method could provide support in these contexts both beforehand and afterwards, by helping the concerned actors when defining the ‘rules’ to be contained in urban planning instruments and competition briefs, while subsequently guiding designers who must respect the above documents in their exploration of design alternatives, decision-making, and communication. Moreover, the prototype could be adapted to become a useful teaching tool addressed mainly to architecture students.

We can envision that a similar approach could be extended or modified to application in renovation and renewal projects, considering the importance of current phenomena such as the densification and renewal of European cities [Riera Pérez, 2016] and of brownfield areas [Laprise et al., 2015].

Considering that 65% of the existing buildings in Switzerland were built before 1980 [OFS, 2014], it is indeed relevant to address the issues related to the renovation of the building stock. In such cases, databases of existing buildings including renovated examples could potentially be used to derive the metamodels. These could generate variants in the form of renovation options at the building envelope level [Aguacil Moreno et al., 2016], complemented by geometrical modifications through housing infill or roof raising strategies [Peronato, 2014]. The metamodels would predict the associated performance, having learned from existing cases.

The application of the method to projects differing in terms of size, e.g. expressed through the number/dimension of buildings, is theoretically possible. The validity of the metamodels should however be further tested on small (one building) to large urban settings. Similarly, the approach could be applied in other climates once the corresponding functions are developed, unless a unique robust version (for each criterion) can be obtained by including factors capturing the main climatic characteristics. This investigation was initiated through a collaborative study [Nault et al., 2015c].

In addition to the concrete improvement avenues highlighted throughout the thesis and in chapter 7, envisioned prospects for the future concern a revised string of actions for the workflow and enhanced features of the prototype. Figure 8.1 depicts this future vision. In Fig. 8.1a, the workflow is modified so that the solution search, currently random, is integrated to an optimizer such as the genetic algorithms offered by Octopus<sup>1</sup>, a Grasshopper plug-in. Accessing the background code of Radiance instead of passing through the front-end DIVA for the irradiation simulation allows more flexibility in the number of design variants generated

---

<sup>1</sup><http://www.grasshopper3d.com/group/octopus> (last accessed on April 5, 2016)

## Chapter 8. Conclusion

---

at each optimization iteration (see also section 5.1.2 and Fig. B.3 in the appendix). During the process, users are given the chance to interact with the tool to select or discard specific variants, guiding the optimization towards the desired solution space, based on user-specific criteria. A similar approach was adopted by Mueller and Ochsendorf [2013] in the development of structureFIT<sup>2</sup>, a web-based tool for incorporating structural considerations into early architectural design, also exploiting metamodeling and optimization techniques. The integration of an optimization-driven improvement-search mechanism could also facilitate the inclusion of user-defined performance goals.

Figure 8.1c portrays the idea of a tool that either (i) continuously ‘learns’ by adding to its database of neighborhood designs to cover areas in the solution space, e.g. in terms of building typology and layout, that are currently unknown by the metamodels, or (ii) builds case-specific metamodels by efficiently defining the designs - in terms of number and position in the solution space - necessary to achieve a reasonable prediction accuracy. This latter approach was adopted by Ritter et al. [2015] for building-level energy consumption prediction.

To deal with different climates, a library of metamodels could be developed, with associated simulation settings corresponding to context-specific best practice values, e.g. in terms of insulation levels. Another option would be to incorporate climate-based inputs into the metamodels, as discussed earlier.

### 8.3 Outlook

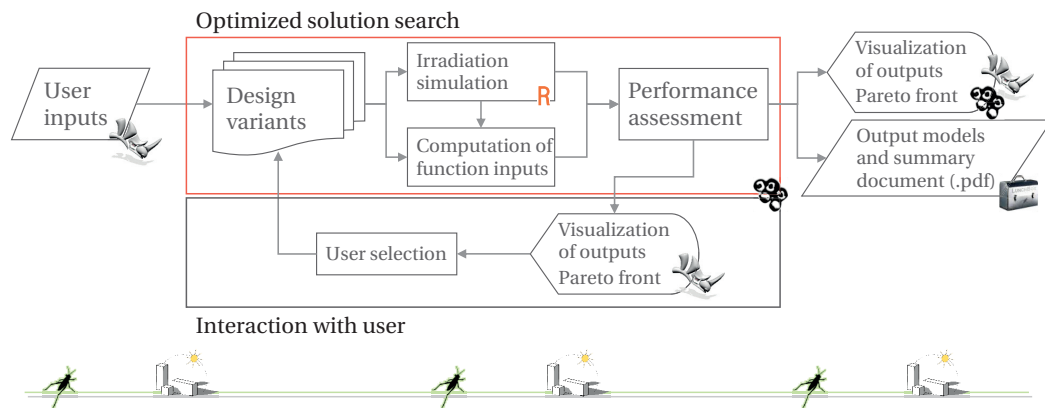
In a long-term perspective, the expansion of existing cities through the design of new neighborhoods induces a need to take into account sustainability parameters to provide comfortable housing and work places in harmony with the environment. Tools supporting the design of such neighborhoods, based on the passive use of local resources and renewable energy, will become key to the urban development of the future, not only making it possible to reduce energy consumption, but offering better daylight and healthier living spaces for occupants.

This research casts a light on a wide range of development opportunities that could further contribute toward achieving a sustainable built environment. By working at the junction between distinct yet complementary fields, we believe it is possible to develop high-impact methods and tools, for instance: by applying and automating powerful data generation, analysis, treatment, and visualization techniques related to architectural modeling, energy simulation, statistics, machine learning, and computer vision; by automating and linking pieces of a workflow using existing tools and custom scripts to facilitate the user’s experience and enhance user-interaction; by working on developing robust methods through the above-mentioned actions instead of conducting case-specific studies with limited application and generalization validity.

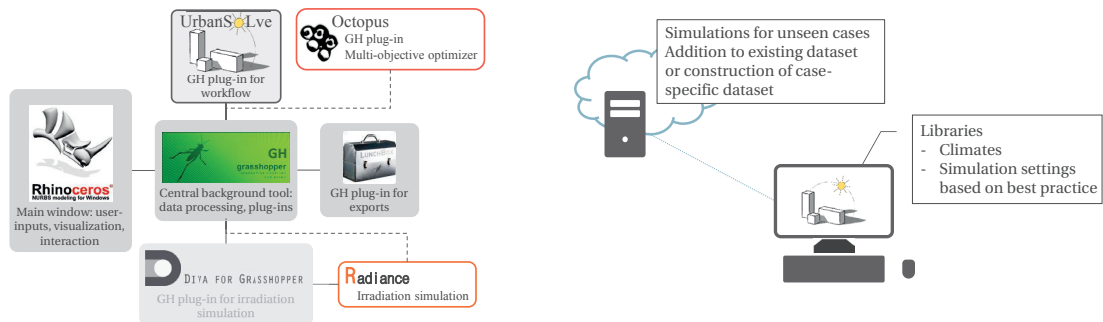
---

<sup>2</sup><http://digitalstructures.mit.edu/page/tools#structurefit> (last accessed on April 5, 2016)





(a) Modifications envisioned to the workflow, replacing the current random sampling by an optimization-based solution search, with enhanced interaction with the user. See Fig. 5.1 for comparison with the current workflow.



(b) Current and additional tools that would be used in the above workflow.

(c) Recourse to computational resources for continuous addition to the reference dataset or population of new case-specific dataset, respectively increasing or refining the solution space coverage and predictive power of the metamodels.

Figure 8.1 – Vision for future development avenues.

We have attempted through this research to make a contribution to a specific niche, to promote awareness and a performance-driven design approach within the process of decision-makers. Through an interdisciplinary work, an effort was made to reach out to professionals, as a step toward bringing our research to the practice world. Through its simple, design-oriented, and time-efficiency functioning, the proposed workflow appears as a relevant method that can complement other tools for incorporating crucial considerations throughout the design process toward efficient and comfortable buildings.



# A Metamodels

## A.1 Data analysis - Distributions and correlations

Figure A.1 shows the distribution each input in the energy and daylight datasets. Figure A.2 illustrates the relationship between each input and output for the corresponding dataset. Reference to these graphs is made in section 4.4.

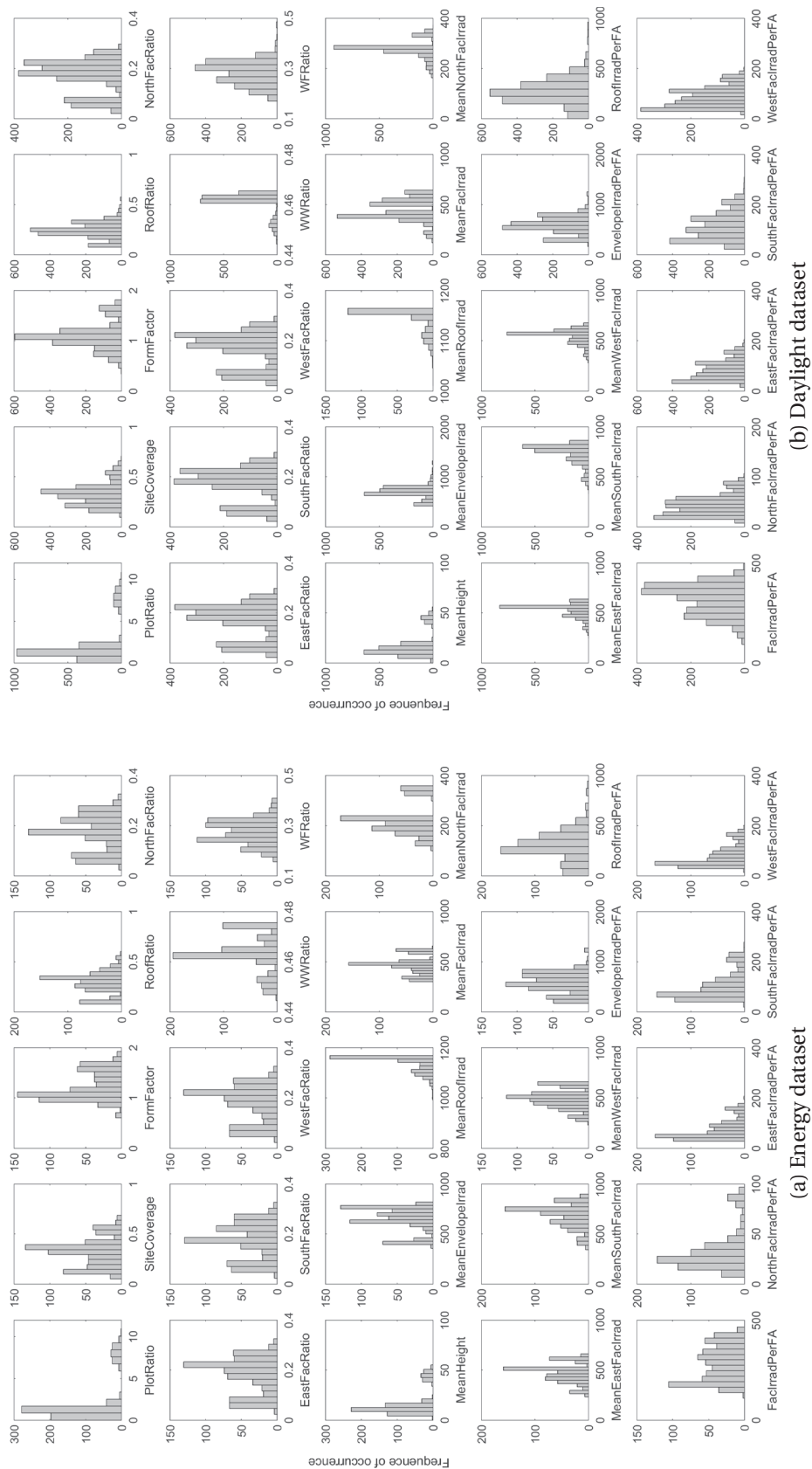


Figure A.1 – Distribution of each input. Reference to these graphs is made in section 4.4.1.

## A.1. Data analysis - Distributions and correlations

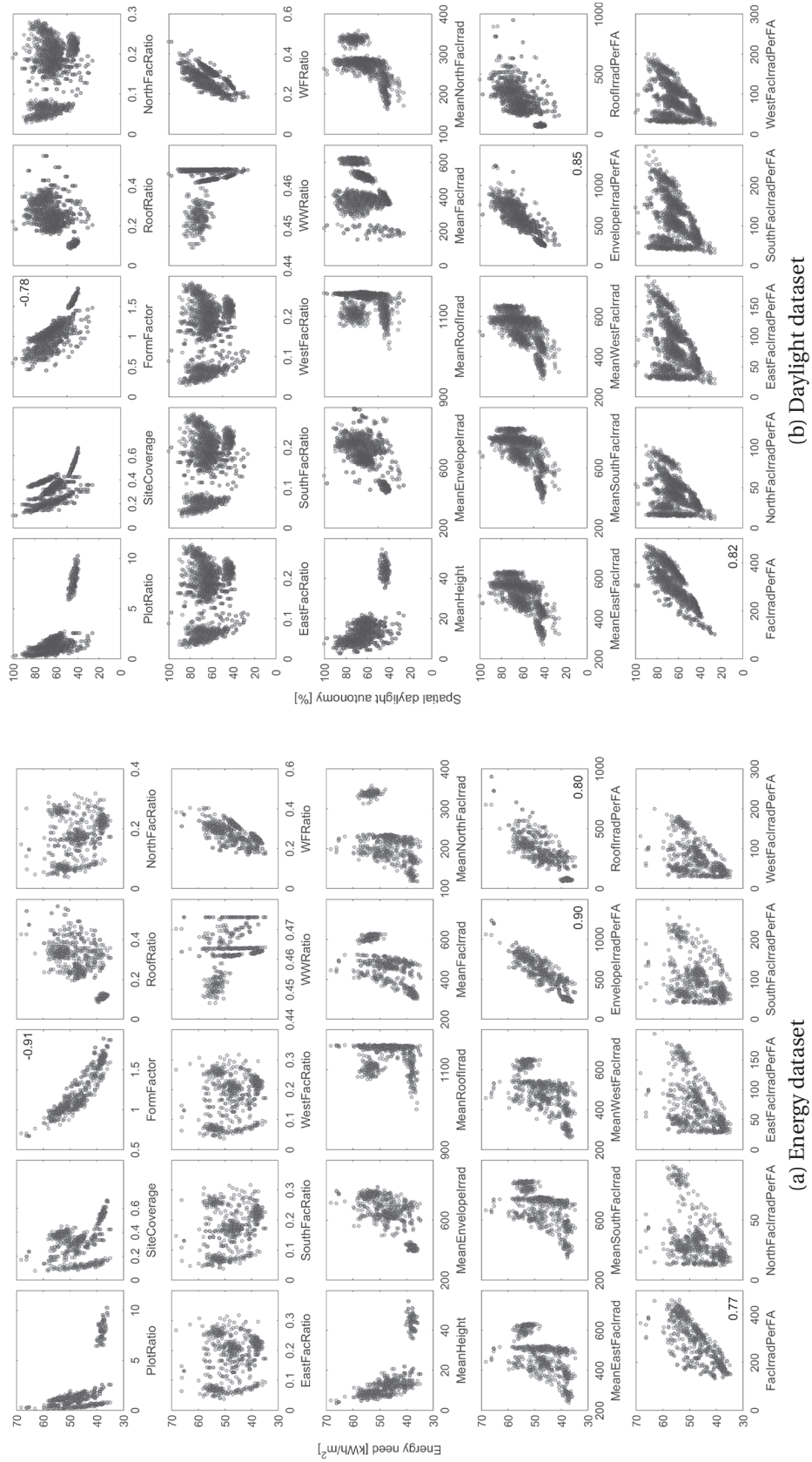


Figure A.2 – Relationship between the output and each input. Reference to these graphs is made in section 4.4.2.

## A.2 Stepwise selection

Example output from the stepwiselm algorithm, for each type of model tested in section 4.5.3, corresponding to an increasing level of complexity (see Table 4.11). Results are for the energy metric.

% Constant model type

Linear regression model:  
Energy ~ 1

| Estimated Coefficients: |          |    |       |        |      |
|-------------------------|----------|----|-------|--------|------|
|                         | Estimate | SE | tStat | pValue |      |
| (Intercept)             | 46.80    |    | 0.27  | 174.30 | 0.00 |

Number of observations: 624, Error degrees of freedom: 623  
Root Mean Squared Error: 6.71

% Linear model type

Linear regression model:  
Energy ~ [Linear formula with 21 terms in 20 predictors]

| Estimated Coefficients: |          |    |       |        |      |
|-------------------------|----------|----|-------|--------|------|
|                         | Estimate | SE | tStat | pValue |      |
| (Intercept)             | 74.38    |    | 7.49  | 9.93   | 0.00 |
| NorthFacRatio           | 6.63     |    | 3.17  | 2.09   | 0.04 |
| FormFactor              | -10.62   |    | 1.29  | -8.23  | 0.00 |
| RoofIrradPerFA          | 0.09     |    | 0.05  | 1.93   | 0.05 |
| WestFacIrradPerFA       | 0.29     |    | 0.09  | 3.18   | 0.00 |
| EnvelopeIrradPerFA      | -0.08    |    | 0.05  | -1.62  | 0.11 |
| SiteCoverage            | 2.74     |    | 1.17  | 2.35   | 0.02 |
| PlotRatio               | -1.09    |    | 0.22  | -5.02  | 0.00 |
| MeanEnvelopeIrrad       | -0.12    |    | 0.01  | -15.36 | 0.00 |
| WestFacRatio            | 6.92     |    | 2.98  | 2.32   | 0.02 |
| NorthFacIrradPerFA      | 0.50     |    | 0.05  | 9.13   | 0.00 |
| MeanNorthFacIrrad       | -0.04    |    | 0.01  | -6.21  | 0.00 |
| RoofRatio               | 84.71    |    | 6.70  | 12.64  | 0.00 |
| MeanFacIrrad            | 0.14     |    | 0.02  | 7.47   | 0.00 |
| MeanRoofIrrad           | 0.01     |    | 0.00  | 1.89   | 0.06 |
| SouthFacIrradPerFA      | 0.03     |    | 0.05  | 0.71   | 0.48 |
| MeanWestFacIrrad        | -0.04    |    | 0.01  | -5.11  | 0.00 |
| WFRatio                 | -16.79   |    | 15.87 | -1.06  | 0.29 |
| MeanEastFacIrrad        | -0.02    |    | 0.01  | -2.27  | 0.02 |
| MeanHeight              | 0.06     |    | 0.05  | 1.27   | 0.20 |
| MeanSouthFacIrrad       | -0.03    |    | 0.00  | -6.13  | 0.00 |

Number of observations: 624, Error degrees of freedom: 603  
Root Mean Squared Error: 1.3  
R-squared: 0.964, Adjusted R-Squared 0.962  
F-statistic vs. constant model: 797, p-value = 0

## A.2. Stepwise selection

% Interactions model type

Linear regression model:

Energy ~ [Linear formula with 95 terms in 17 predictors]

Estimated Coefficients:

|                                      | Estimate | SE | tStat   | pValue |       |      |
|--------------------------------------|----------|----|---------|--------|-------|------|
| (Intercept)                          |          |    | 321.35  | 130.62 | 2.46  | 0.01 |
| FormFactor                           |          |    | -3.34   | 34.49  | -0.10 | 0.92 |
| RoofIrradPerFA                       |          |    | -0.08   | 0.75   | -0.11 | 0.91 |
| EnvelopeIrradPerFA                   |          |    | 0.15    | 0.65   | 0.22  | 0.82 |
| SiteCoverage                         |          |    | -130.87 | 37.31  | -3.51 | 0.00 |
| PlotRatio                            |          |    | 11.20   | 3.66   | 3.06  | 0.00 |
| MeanEnvelopeIrrad                    |          |    | -0.77   | 0.54   | -1.44 | 0.15 |
| EastFacIrradPerFA                    |          |    | 0.26    | 1.05   | 0.25  | 0.80 |
| WestFacRatio                         |          |    | -81.19  | 44.13  | -1.84 | 0.07 |
| MeanNorthFacIrrad                    |          |    | -0.02   | 0.16   | -0.14 | 0.89 |
| RoofRatio                            |          |    | 1369.98 | 514.03 | 2.67  | 0.01 |
| MeanFacIrrad                         |          |    | -5.11   | 0.90   | -5.67 | 0.00 |
| MeanRoofIrrad                        |          |    | 0.02    | 0.02   | 0.80  | 0.42 |
| SouthFacIrradPerFA                   |          |    | 0.63    | 0.67   | 0.93  | 0.35 |
| MeanWestFacIrrad                     |          |    | 0.09    | 0.14   | 0.65  | 0.51 |
| WFRatio                              |          |    | -214.85 | 313.01 | -0.69 | 0.49 |
| MeanEastFacIrrad                     |          |    | 0.17    | 0.16   | 1.03  | 0.30 |
| MeanSouthFacIrrad                    |          |    | 0.09    | 0.16   | 0.56  | 0.57 |
| FormFactor:RoofIrradPerFA            |          |    | -4.20   | 0.94   | -4.48 | 0.00 |
| FormFactor:EnvelopeIrradPerFA        |          |    | 4.40    | 0.95   | 4.64  | 0.00 |
| FormFactor:SiteCoverage              |          |    | 14.67   | 14.25  | 1.03  | 0.30 |
| FormFactor:PlotRatio                 |          |    | -2.18   | 1.71   | -1.27 | 0.20 |
| FormFactor:MeanEnvelopeIrrad         |          |    | 0.06    | 0.12   | 0.52  | 0.60 |
| FormFactor:EastFacIrradPerFA         |          |    | 0.31    | 0.07   | 4.13  | 0.00 |
| FormFactor:RoofRatio                 |          |    | -311.42 | 119.14 | -2.61 | 0.01 |
| FormFactor:MeanWestFacIrrad          |          |    | 0.04    | 0.05   | 0.80  | 0.42 |
| FormFactor:WFRatio                   |          |    | -542.62 | 204.46 | -2.65 | 0.01 |
| FormFactor:MeanSouthFacIrrad         |          |    | 0.05    | 0.04   | 1.24  | 0.21 |
| RoofIrradPerFA:EnvelopeIrradPerFA    |          |    | -0.00   | 0.00   | -1.22 | 0.22 |
| RoofIrradPerFA:SiteCoverage          |          |    | -0.07   | 0.04   | -1.70 | 0.09 |
| RoofIrradPerFA:MeanEnvelopeIrrad     |          |    | -0.01   | 0.00   | -2.71 | 0.01 |
| RoofIrradPerFA:EastFacIrradPerFA     |          |    | -0.00   | 0.00   | -0.41 | 0.68 |
| RoofIrradPerFA:WestFacRatio          |          |    | 0.79    | 0.22   | 3.58  | 0.00 |
| RoofIrradPerFA:MeanNorthFacIrrad     |          |    | -0.00   | 0.00   | -2.53 | 0.01 |
| RoofIrradPerFA:RoofRatio             |          |    | 2.96    | 1.48   | 2.00  | 0.05 |
| RoofIrradPerFA:MeanFacIrrad          |          |    | 0.01    | 0.00   | 1.72  | 0.09 |
| RoofIrradPerFA:SouthFacIrradPerFA    |          |    | 0.00    | 0.00   | 1.95  | 0.05 |
| RoofIrradPerFA:MeanWestFacIrrad      |          |    | -0.00   | 0.00   | -4.17 | 0.00 |
| RoofIrradPerFA:WFRatio               |          |    | 1.32    | 0.63   | 2.10  | 0.04 |
| RoofIrradPerFA:MeanEastFacIrrad      |          |    | -0.00   | 0.00   | -1.62 | 0.11 |
| RoofIrradPerFA:MeanSouthFacIrrad     |          |    | 0.00    | 0.00   | 2.63  | 0.01 |
| EnvelopeIrradPerFA:PlotRatio         |          |    | -0.03   | 0.01   | -5.32 | 0.00 |
| EnvelopeIrradPerFA:MeanEnvelopeIrrad |          |    | 0.01    | 0.00   | 2.62  | 0.01 |
| EnvelopeIrradPerFA:EastFacIrradPerFA |          |    | 0.00    | 0.00   | 3.39  | 0.00 |
| EnvelopeIrradPerFA:WestFacRatio      |          |    | -0.53   | 0.21   | -2.50 | 0.01 |
| EnvelopeIrradPerFA:RoofRatio         |          |    | -2.65   | 1.45   | -1.83 | 0.07 |
| EnvelopeIrradPerFA:MeanFacIrrad      |          |    | -0.00   | 0.00   | -1.00 | 0.32 |
| EnvelopeIrradPerFA:MeanWestFacIrrad  |          |    | 0.00    | 0.00   | 2.62  | 0.01 |
| EnvelopeIrradPerFA:WFRatio           |          |    | -1.01   | 0.29   | -3.48 | 0.00 |
| EnvelopeIrradPerFA:MeanEastFacIrrad  |          |    | 0.00    | 0.00   | 1.29  | 0.20 |
| EnvelopeIrradPerFA:MeanSouthFacIrrad |          |    | -0.00   | 0.00   | -3.36 | 0.00 |
| SiteCoverage:PlotRatio               |          |    | -1.39   | 1.21   | -1.15 | 0.25 |

## Appendix A. Metamodels

---

|  |          |         |       |      |
|--|----------|---------|-------|------|
| SiteCoverage : MeanEnvelopeIrrad       | 0.36     | 0.09    | 4.18  | 0.00 |
| SiteCoverage : MeanNorthFacIrrad       | 0.01     | 0.05    | 0.20  | 0.84 |
| SiteCoverage : RoofRatio               | -223.74  | 77.63   | -2.88 | 0.00 |
| SiteCoverage : MeanWestFacIrrad        | 0.03     | 0.03    | 0.87  | 0.38 |
| SiteCoverage : MeanEastFacIrrad        | -0.04    | 0.03    | -1.14 | 0.26 |
| MeanEnvelopeIrrad : EastFacIrradPerFA  | -0.02    | 0.00    | -4.07 | 0.00 |
| MeanEnvelopeIrrad : RoofRatio          | -0.89    | 0.35    | -2.53 | 0.01 |
| MeanEnvelopeIrrad : MeanFacIrrad       | 0.00     | 0.00    | 3.68  | 0.00 |
| MeanEnvelopeIrrad : SouthFacIrradPerFA | -0.01    | 0.00    | -4.17 | 0.00 |
| MeanEnvelopeIrrad : MeanWestFacIrrad   | -0.00    | 0.00    | -2.14 | 0.03 |
| MeanEnvelopeIrrad : WFRatio            | 2.23     | 1.43    | 1.56  | 0.12 |
| MeanEnvelopeIrrad : MeanEastFacIrrad   | 0.00     | 0.00    | 3.02  | 0.00 |
| MeanEnvelopeIrrad : MeanSouthFacIrrad  | -0.00    | 0.00    | -2.71 | 0.01 |
| EastFacIrradPerFA : MeanNorthFacIrrad  | 0.00     | 0.00    | 1.61  | 0.11 |
| EastFacIrradPerFA : RoofRatio          | 9.70     | 2.77    | 3.51  | 0.00 |
| EastFacIrradPerFA : MeanFacIrrad       | 0.00     | 0.01    | 0.56  | 0.57 |
| EastFacIrradPerFA : MeanEastFacIrrad   | -0.00    | 0.00    | -0.86 | 0.39 |
| EastFacIrradPerFA : MeanSouthFacIrrad  | 0.01     | 0.00    | 4.51  | 0.00 |
| WestFacRatio : MeanNorthFacIrrad       | -0.13    | 0.17    | -0.73 | 0.47 |
| WestFacRatio : WFRatio                 | 518.32   | 192.20  | 2.70  | 0.01 |
| WestFacRatio : MeanSouthFacIrrad       | 0.03     | 0.09    | 0.36  | 0.72 |
| MeanNorthFacIrrad : RoofRatio          | 0.53     | 0.39    | 1.38  | 0.17 |
| MeanNorthFacIrrad : MeanFacIrrad       | 0.00     | 0.00    | 0.01  | 0.99 |
| MeanNorthFacIrrad : MeanWestFacIrrad   | -0.00    | 0.00    | -0.16 | 0.87 |
| MeanNorthFacIrrad : WFRatio            | -0.05    | 0.41    | -0.12 | 0.90 |
| MeanNorthFacIrrad : MeanEastFacIrrad   | -0.00    | 0.00    | -1.83 | 0.07 |
| MeanNorthFacIrrad : MeanSouthFacIrrad  | 0.00     | 0.00    | 1.48  | 0.14 |
| RoofRatio : SouthFacIrradPerFA         | 6.55     | 1.79    | 3.66  | 0.00 |
| RoofRatio : MeanWestFacIrrad           | 1.56     | 0.39    | 3.99  | 0.00 |
| RoofRatio : WFRatio                    | -4333.56 | 1137.10 | -3.81 | 0.00 |
| RoofRatio : MeanSouthFacIrrad          | 1.24     | 0.24    | 5.13  | 0.00 |
| MeanFacIrrad : SouthFacIrradPerFA      | 0.00     | 0.00    | 0.90  | 0.37 |
| MeanFacIrrad : MeanWestFacIrrad        | -0.00    | 0.00    | -1.52 | 0.13 |
| MeanFacIrrad : WFRatio                 | 2.24     | 1.40    | 1.59  | 0.11 |
| MeanFacIrrad : MeanSouthFacIrrad       | -0.00    | 0.00    | -1.33 | 0.19 |
| MeanRoofIrrad : MeanWestFacIrrad       | -0.00    | 0.00    | -2.02 | 0.04 |
| SouthFacIrradPerFA : MeanEastFacIrrad  | -0.00    | 0.00    | -0.74 | 0.46 |
| SouthFacIrradPerFA : MeanSouthFacIrrad | 0.01     | 0.00    | 4.19  | 0.00 |
| MeanWestFacIrrad : MeanEastFacIrrad    | -0.00    | 0.00    | -0.73 | 0.47 |
| MeanWestFacIrrad : MeanSouthFacIrrad   | 0.00     | 0.00    | 3.34  | 0.00 |
| WFRatio : MeanEastFacIrrad             | -0.74    | 0.56    | -1.32 | 0.19 |
| WFRatio : MeanSouthFacIrrad            | -0.44    | 0.46    | -0.95 | 0.34 |
| MeanEastFacIrrad : MeanSouthFacIrrad   | -0.00    | 0.00    | -5.58 | 0.00 |

Number of observations: 624, Error degrees of freedom: 529

Root Mean Squared Error: 0.827

R-squared: 0.987, Adjusted R-Squared 0.985

F-statistic vs. constant model: 431, p-value = 0



## A.2. Stepwise selection

% Quadratic model type

Linear regression model:

Energy ~ [Linear formula with 99 terms in 18 predictors]

Estimated Coefficients:

|  | Estimate | SE    | tStat    | pValue |       |      |
|--|----------|-------|----------|--------|-------|------|
|  | -----    | ----- | -----    | -----  |       |      |
| (Intercept)                            |          |       | 491.78   | 110.96 | 4.43  | 0.00 |
| NorthFacRatio                          |          |       | 277.28   | 116.56 | 2.38  | 0.02 |
| FormFactor                             |          |       | -40.60   | 50.27  | -0.81 | 0.42 |
| WestFacIrradPerFA                      |          |       | -0.44    | 0.57   | -0.78 | 0.44 |
| EnvelopeIrradPerFA                     |          |       | -0.02    | 0.04   | -0.52 | 0.60 |
| SiteCoverage                           |          |       | -173.23  | 29.34  | -5.90 | 0.00 |
| PlotRatio                              |          |       | 15.09    | 3.51   | 4.29  | 0.00 |
| MeanEnvelopeIrrad                      |          |       | -0.20    | 0.24   | -0.82 | 0.41 |
| EastFacIrradPerFA                      |          |       | -0.24    | 0.67   | -0.35 | 0.73 |
| NorthFacIrradPerFA                     |          |       | 1.56     | 1.60   | 0.97  | 0.33 |
| MeanNorthFacIrrad                      |          |       | -0.10    | 0.06   | -1.69 | 0.09 |
| RoofRatio                              |          |       | 308.47   | 232.23 | 1.33  | 0.18 |
| MeanFacIrrad                           |          |       | -0.33    | 0.33   | -1.00 | 0.32 |
| SouthFacIrradPerFA                     |          |       | -1.02    | 0.76   | -1.35 | 0.18 |
| MeanWestFacIrrad                       |          |       | -0.04    | 0.07   | -0.59 | 0.55 |
| WFRatio                                |          |       | -108.07  | 440.92 | -0.25 | 0.81 |
| MeanEastFacIrrad                       |          |       | 0.07     | 0.11   | 0.67  | 0.50 |
| MeanHeight                             |          |       | -6.01    | 2.17   | -2.77 | 0.01 |
| MeanSouthFacIrrad                      |          |       | 0.03     | 0.07   | 0.42  | 0.67 |
| NorthFacRatio : FormFactor             |          |       | -49.63   | 34.42  | -1.44 | 0.15 |
| NorthFacRatio : WestFacIrradPerFA      |          |       | 1.13     | 0.87   | 1.29  | 0.20 |
| NorthFacRatio : EnvelopeIrradPerFA     |          |       | 0.43     | 0.06   | 6.62  | 0.00 |
| NorthFacRatio : EastFacIrradPerFA      |          |       | -0.99    | 0.84   | -1.17 | 0.24 |
| NorthFacRatio : RoofRatio              |          |       | -497.02  | 122.28 | -4.06 | 0.00 |
| NorthFacRatio : WFRatio                |          |       | -1058.47 | 269.59 | -3.93 | 0.00 |
| NorthFacRatio : MeanEastFacIrrad       |          |       | -0.03    | 0.12   | -0.27 | 0.79 |
| FormFactor : EnvelopeIrradPerFA        |          |       | 0.03     | 0.05   | 0.53  | 0.59 |
| FormFactor : SouthFacIrradPerFA        |          |       | 0.07     | 0.07   | 1.01  | 0.31 |
| FormFactor : WFRatio                   |          |       | -619.31  | 248.41 | -2.49 | 0.01 |
| FormFactor : MeanEastFacIrrad          |          |       | 0.04     | 0.03   | 1.22  | 0.22 |
| FormFactor : MeanHeight                |          |       | 1.91     | 0.63   | 3.03  | 0.00 |
| FormFactor : MeanSouthFacIrrad         |          |       | 0.04     | 0.03   | 1.46  | 0.14 |
| WestFacIrradPerFA : PlotRatio          |          |       | 0.01     | 0.01   | 0.99  | 0.32 |
| WestFacIrradPerFA : EastFacIrradPerFA  |          |       | -0.04    | 0.01   | -2.93 | 0.00 |
| WestFacIrradPerFA : NorthFacIrradPerFA |          |       | 0.01     | 0.01   | 1.65  | 0.10 |
| WestFacIrradPerFA : MeanNorthFacIrrad  |          |       | 0.00     | 0.00   | 2.90  | 0.00 |
| WestFacIrradPerFA : RoofRatio          |          |       | 2.78     | 0.62   | 4.52  | 0.00 |
| WestFacIrradPerFA : MeanFacIrrad       |          |       | -0.01    | 0.00   | -3.70 | 0.00 |
| WestFacIrradPerFA : SouthFacIrradPerFA |          |       | -0.00    | 0.00   | -0.94 | 0.35 |
| WestFacIrradPerFA : MeanWestFacIrrad   |          |       | 0.01     | 0.00   | 3.72  | 0.00 |
| WestFacIrradPerFA : MeanEastFacIrrad   |          |       | 0.00     | 0.00   | 1.74  | 0.08 |
| WestFacIrradPerFA : MeanSouthFacIrrad  |          |       | -0.00    | 0.00   | -2.67 | 0.01 |
| EnvelopeIrradPerFA : SiteCoverage      |          |       | -0.05    | 0.02   | -2.79 | 0.01 |
| EnvelopeIrradPerFA : MeanNorthFacIrrad |          |       | -0.00    | 0.00   | -2.10 | 0.04 |
| EnvelopeIrradPerFA : MeanFacIrrad      |          |       | 0.00     | 0.00   | 5.28  | 0.00 |
| EnvelopeIrradPerFA : MeanWestFacIrrad  |          |       | -0.00    | 0.00   | -6.55 | 0.00 |
| EnvelopeIrradPerFA : MeanEastFacIrrad  |          |       | -0.00    | 0.00   | -2.76 | 0.01 |
| EnvelopeIrradPerFA : MeanSouthFacIrrad |          |       | -0.00    | 0.00   | -4.29 | 0.00 |
| SiteCoverage : MeanFacIrrad            |          |       | 0.39     | 0.05   | 7.66  | 0.00 |
| SiteCoverage : WFRatio                 |          |       | -21.73   | 40.57  | -0.54 | 0.59 |
| PlotRatio : MeanFacIrrad               |          |       | -0.02    | 0.01   | -4.16 | 0.00 |

## Appendix A. Metamodels

---

|  |          |        |       |      |
|--|----------|--------|-------|------|
| PlotRatio : MeanHeight                 | -0.13    | 0.04   | -3.09 | 0.00 |
| MeanEnvelopeIrrad : EastFacIrradPerFA  | -0.00    | 0.00   | -1.41 | 0.16 |
| MeanEnvelopeIrrad : NorthFacIrradPerFA | 0.01     | 0.00   | 3.38  | 0.00 |
| MeanEnvelopeIrrad : RoofRatio          | -1.60    | 1.32   | -1.22 | 0.22 |
| MeanEnvelopeIrrad : MeanFacIrrad       | -0.00    | 0.00   | -0.98 | 0.33 |
| MeanEnvelopeIrrad : SouthFacIrradPerFA | -0.01    | 0.00   | -4.66 | 0.00 |
| MeanEnvelopeIrrad : MeanWestFacIrrad   | 0.00     | 0.00   | 3.26  | 0.00 |
| MeanEnvelopeIrrad : MeanSouthFacIrrad  | 0.00     | 0.00   | 1.43  | 0.15 |
| EastFacIrradPerFA : SouthFacIrradPerFA | -0.00    | 0.00   | -1.18 | 0.24 |
| EastFacIrradPerFA : MeanWestFacIrrad   | -0.00    | 0.00   | -3.24 | 0.00 |
| EastFacIrradPerFA : MeanSouthFacIrrad  | 0.00     | 0.00   | 4.95  | 0.00 |
| NorthFacIrradPerFA : RoofRatio         | -6.32    | 2.20   | -2.87 | 0.00 |
| NorthFacIrradPerFA : MeanFacIrrad      | -0.02    | 0.01   | -4.02 | 0.00 |
| NorthFacIrradPerFA : MeanWestFacIrrad  | 0.00     | 0.00   | 3.31  | 0.00 |
| NorthFacIrradPerFA : WFRatio           | -9.23    | 3.72   | -2.48 | 0.01 |
| NorthFacIrradPerFA : MeanEastFacIrrad  | 0.00     | 0.00   | 3.73  | 0.00 |
| NorthFacIrradPerFA : MeanHeight        | 0.00     | 0.01   | 0.51  | 0.61 |
| NorthFacIrradPerFA : MeanSouthFacIrrad | 0.00     | 0.00   | 1.67  | 0.10 |
| RoofRatio : MeanFacIrrad               | -1.13    | 1.03   | -1.09 | 0.27 |
| RoofRatio : SouthFacIrradPerFA         | 4.79     | 0.86   | 5.60  | 0.00 |
| RoofRatio : WFRatio                    | -1419.10 | 361.01 | -3.93 | 0.00 |
| RoofRatio : MeanEastFacIrrad           | 0.45     | 0.19   | 2.39  | 0.02 |
| RoofRatio : MeanSouthFacIrrad          | 0.32     | 0.16   | 1.99  | 0.05 |
| MeanFacIrrad : SouthFacIrradPerFA      | 0.00     | 0.00   | 3.08  | 0.00 |
| MeanFacIrrad : MeanWestFacIrrad        | 0.00     | 0.00   | 0.57  | 0.57 |
| MeanFacIrrad : WFRatio                 | 1.66     | 0.40   | 4.17  | 0.00 |
| MeanFacIrrad : MeanSouthFacIrrad       | 0.00     | 0.00   | 3.01  | 0.00 |
| SouthFacIrradPerFA : WFRatio           | 3.72     | 1.44   | 2.59  | 0.01 |
| SouthFacIrradPerFA : MeanHeight        | -0.00    | 0.00   | -0.63 | 0.53 |
| SouthFacIrradPerFA : MeanSouthFacIrrad | 0.00     | 0.00   | 0.24  | 0.81 |
| MeanWestFacIrrad : MeanEastFacIrrad    | 0.00     | 0.00   | 3.66  | 0.00 |
| WFRatio : MeanHeight                   | 6.73     | 3.76   | 1.79  | 0.07 |
| MeanEastFacIrrad : MeanHeight          | -0.00    | 0.00   | -1.15 | 0.25 |
| MeanEastFacIrrad : MeanSouthFacIrrad   | -0.00    | 0.00   | -6.02 | 0.00 |
| NorthFacRatio^2                        | 26.80    | 72.24  | 0.37  | 0.71 |
| FormFactor^2                           | -8.61    | 9.02   | -0.96 | 0.34 |
| WestFacIrradPerFA^2                    | 0.02     | 0.01   | 3.16  | 0.00 |
| MeanEnvelopeIrrad^2                    | 0.00     | 0.00   | 0.67  | 0.50 |
| EastFacIrradPerFA^2                    | 0.02     | 0.01   | 2.66  | 0.01 |
| NorthFacIrradPerFA^2                   | 0.01     | 0.01   | 2.12  | 0.03 |
| RoofRatio^2                            | 760.78   | 437.66 | 1.74  | 0.08 |
| MeanFacIrrad^2                         | 0.00     | 0.00   | 0.32  | 0.75 |
| SouthFacIrradPerFA^2                   | -0.00    | 0.00   | -1.74 | 0.08 |
| MeanWestFacIrrad^2                     | -0.00    | 0.00   | -4.69 | 0.00 |
| WFRatio^2                              | 63.59    | 291.32 | 0.22  | 0.83 |
| MeanEastFacIrrad^2                     | -0.00    | 0.00   | -1.97 | 0.05 |
| MeanHeight^2                           | 0.02     | 0.01   | 2.27  | 0.02 |
| MeanSouthFacIrrad^2                    | -0.00    | 0.00   | -3.19 | 0.00 |

Number of observations: 624, Error degrees of freedom: 525

Root Mean Squared Error: 0.813

R-squared: 0.988, Adjusted R-Squared 0.985

F-statistic vs. constant model: 427, p-value = 0

### A.3 Interpretation - Main effects

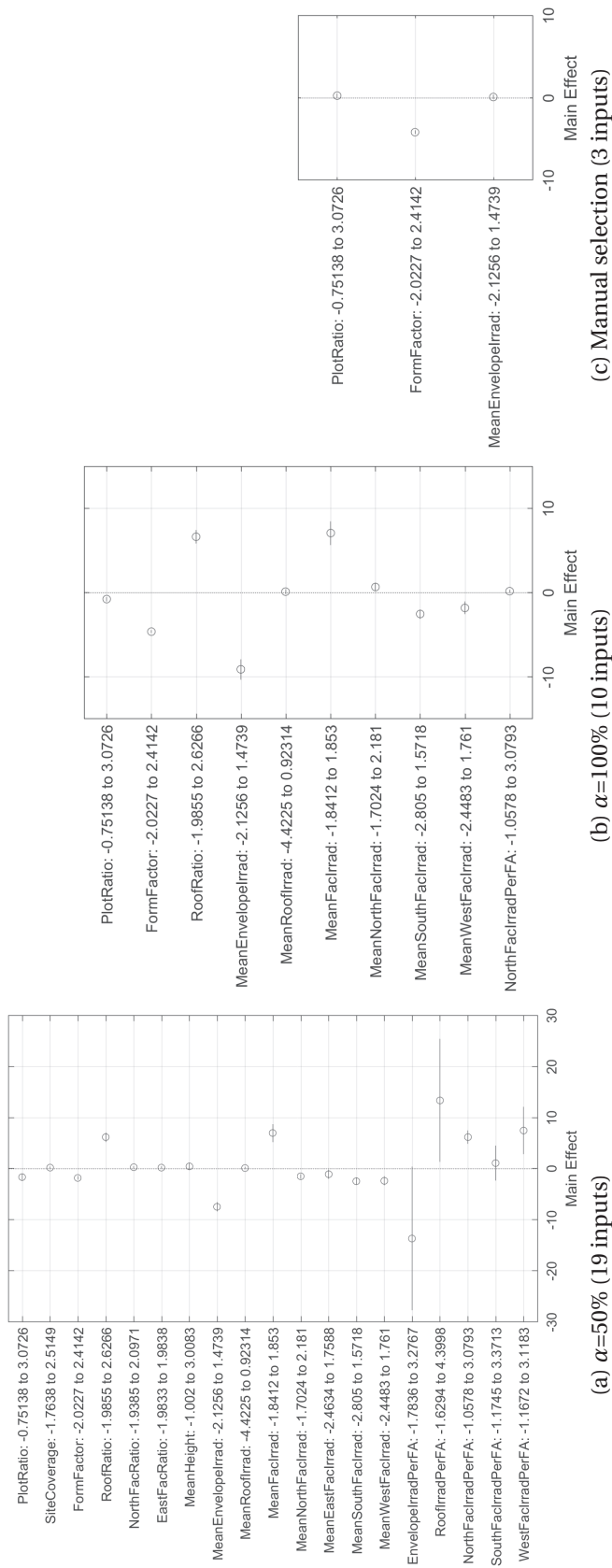


Figure A.3 – Main effects plot showing the estimated effect, on the energy metric, of each input, obtained when fitting using the entire dataset ( $d=100\%$ ) and (a) 19 inputs, (b) 10 inputs, and (c) 3 inputs (see also section 4.5 and Fig. 4.25). All values appearing on the graphs correspond to standardized data (inputs and output). The horizontal lines represent confidence intervals of 95% for these predictions, which are obtained by averaging over one input while changing the others. We observe that the effect of a given input changes from (a) to (c), e.g. the plot ratio whose effect goes from negative to positive. As mentioned in section 4.5.5, the influence of each input is dependent on the presence/absence of the others and as such, this data cannot be used e.g. as design guidelines. These graphs were produced using the *plotEffects* and *fitm* functions in Matlab.



# B Prototype

## B.1 Implementation

The following images are supporting material regarding the implementation of the prototype described in section 5.1. The diagram of Fig. B.1 presents the internal functioning and relationship between each part of the prototype. Figure B.2 illustrates the different building configurations possible when combining the alignment, rotation and orientation specifications in the user-interface of Fig. 5.4. Figure B.3 is a screenshot of the DIVA cluster (see Fig. B.1) holding 20 instances of the DIVA irradiation simulation component, i.e. one per design variant generated by the prototype.

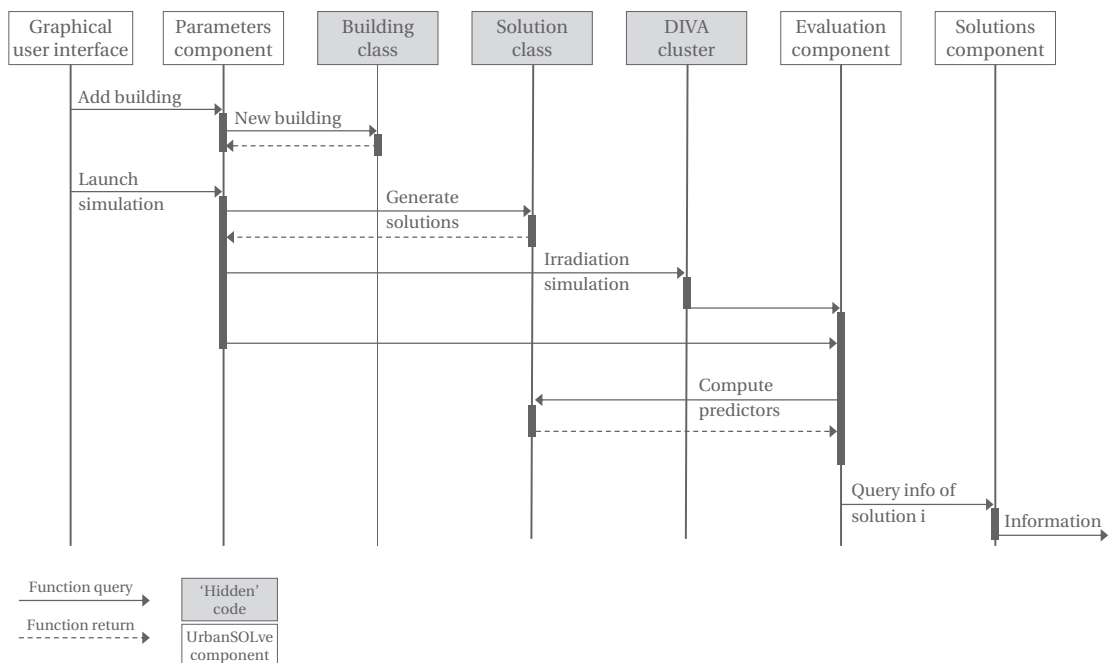


Figure B.1 – Implementation diagram showing the chronological communication between the different parts composing the prototype (diagram by Mélanie Huck).



Figure B.2 – Alignment and rotation settings: explanation of effect on each building typology.

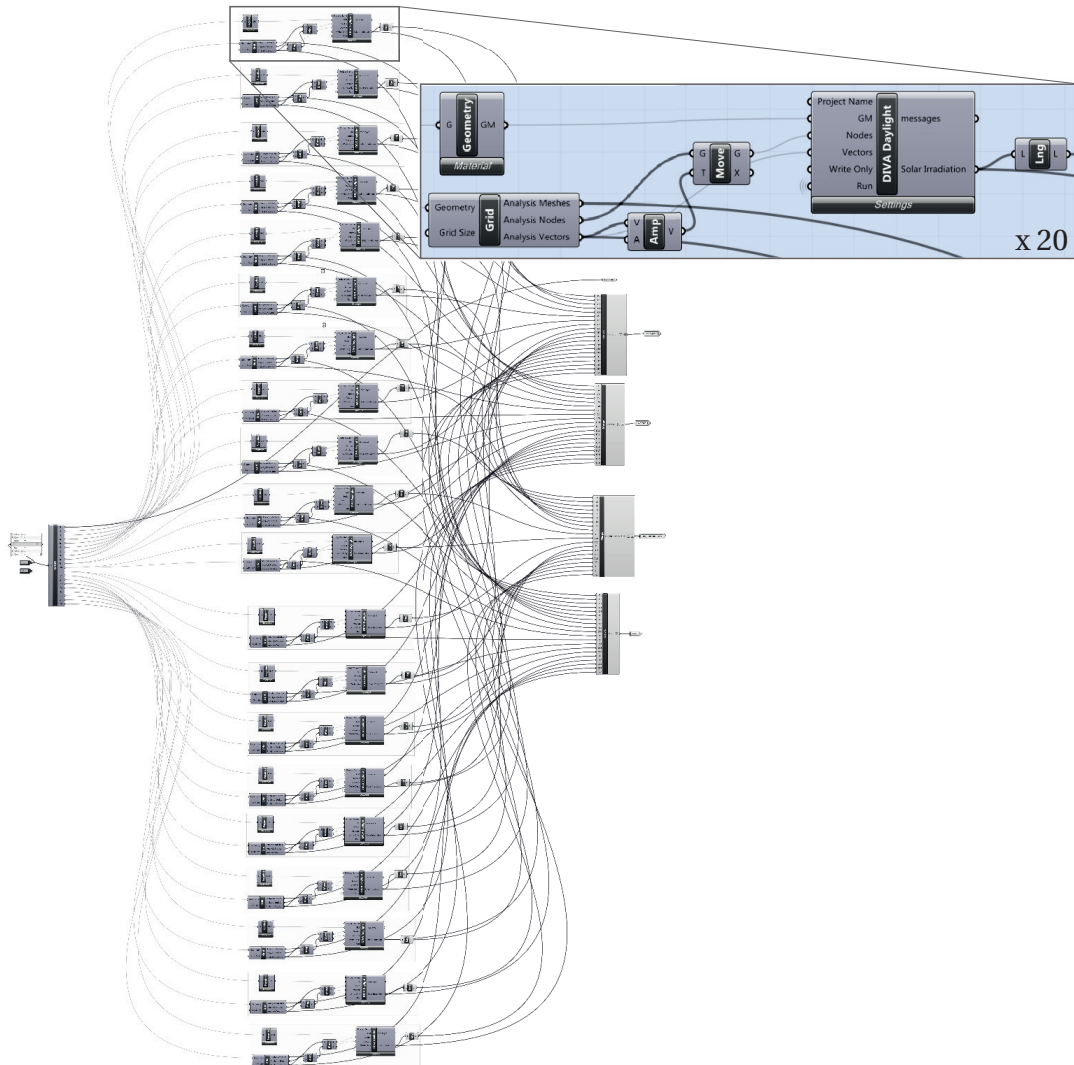
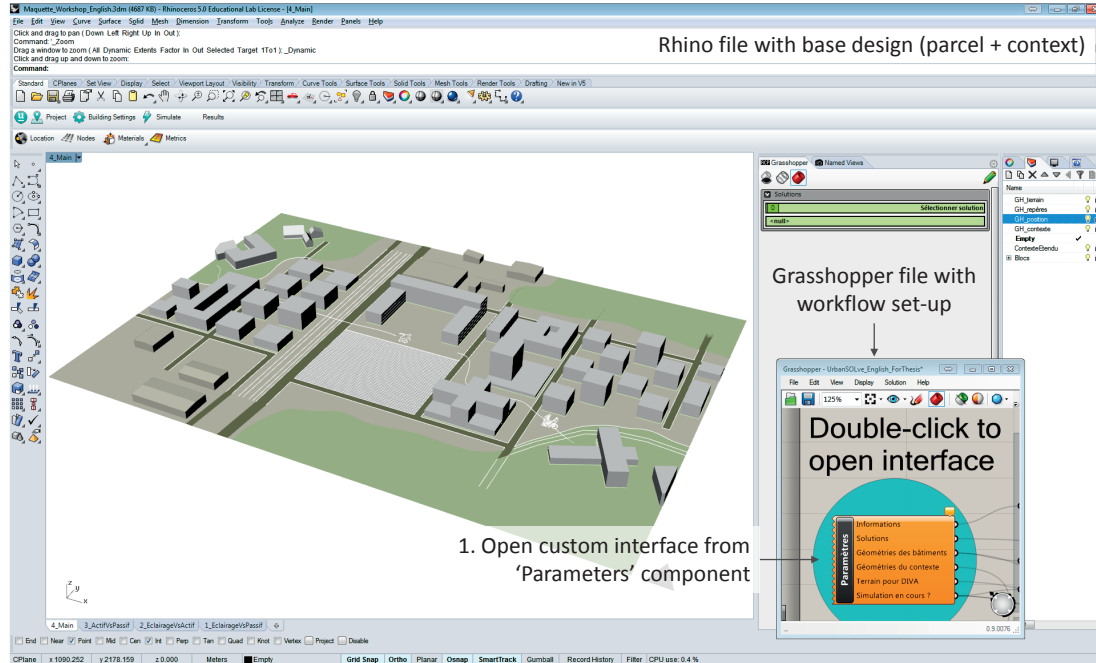


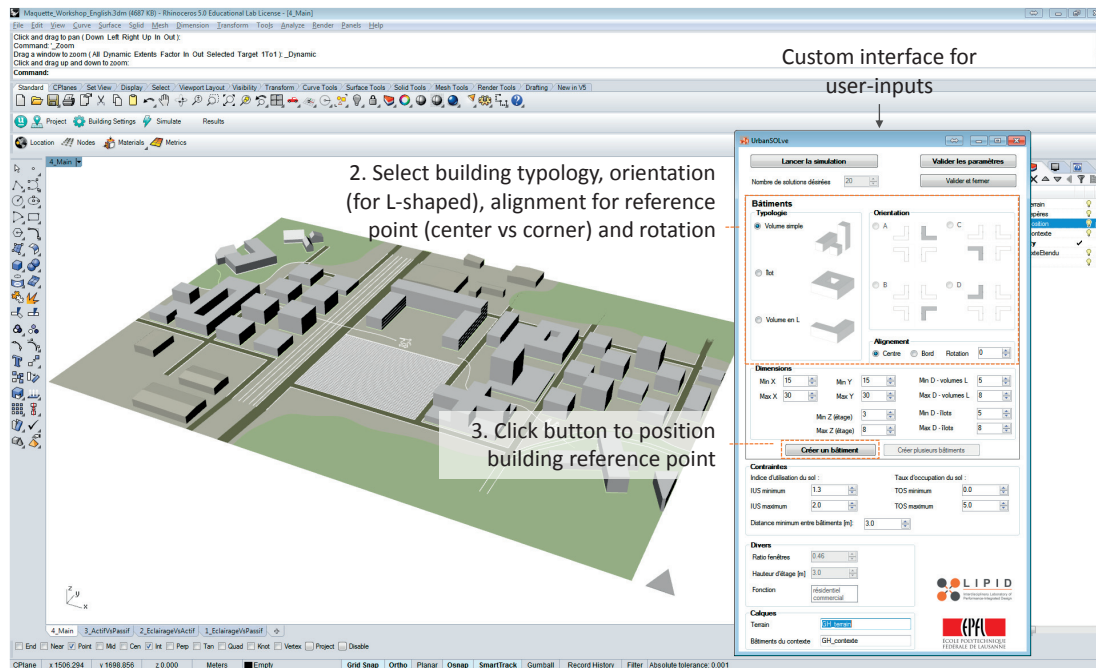
Figure B.3 – Irradiation cluster in Grasshopper, holding 20 instances of the DIVA irradiation simulation component.

## B.2 Static demo of prototype

The screenshots below illustrate the unfolding of the workflow through the use of the prototype, starting from the Rhino and Grasshopper files prepared for the workshops. The numbered items in the images represent user actions.



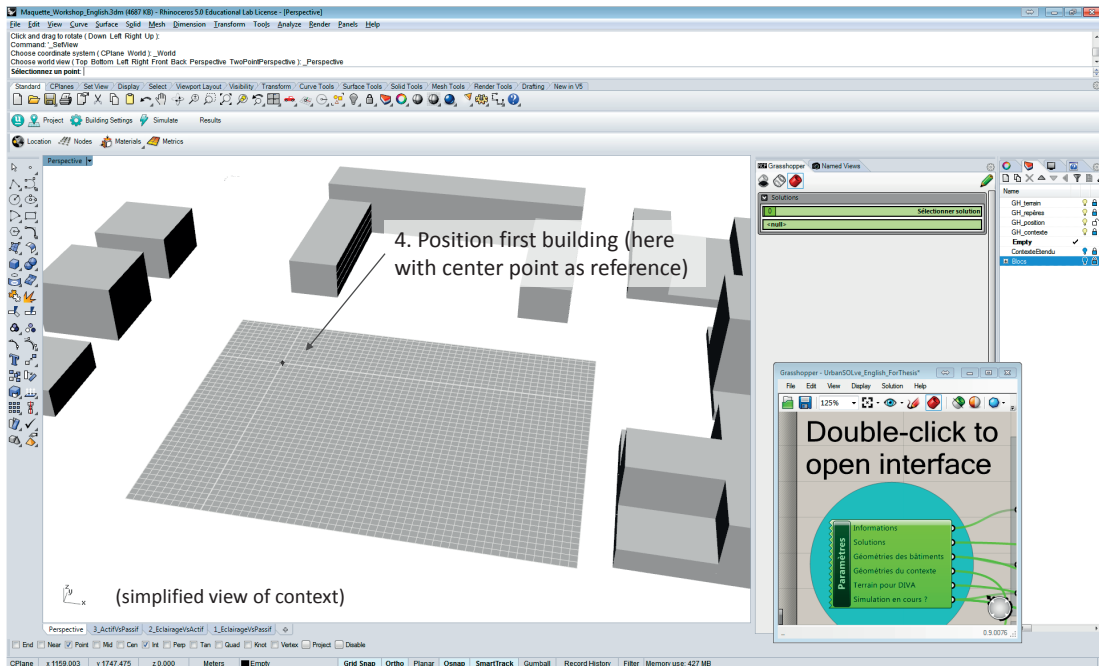
(a) Starting point: design context and parcel from the prepared Rhino file; Grasshopper file containing the implemented workflow and custom plug-in, from which the custom interface can be opened.



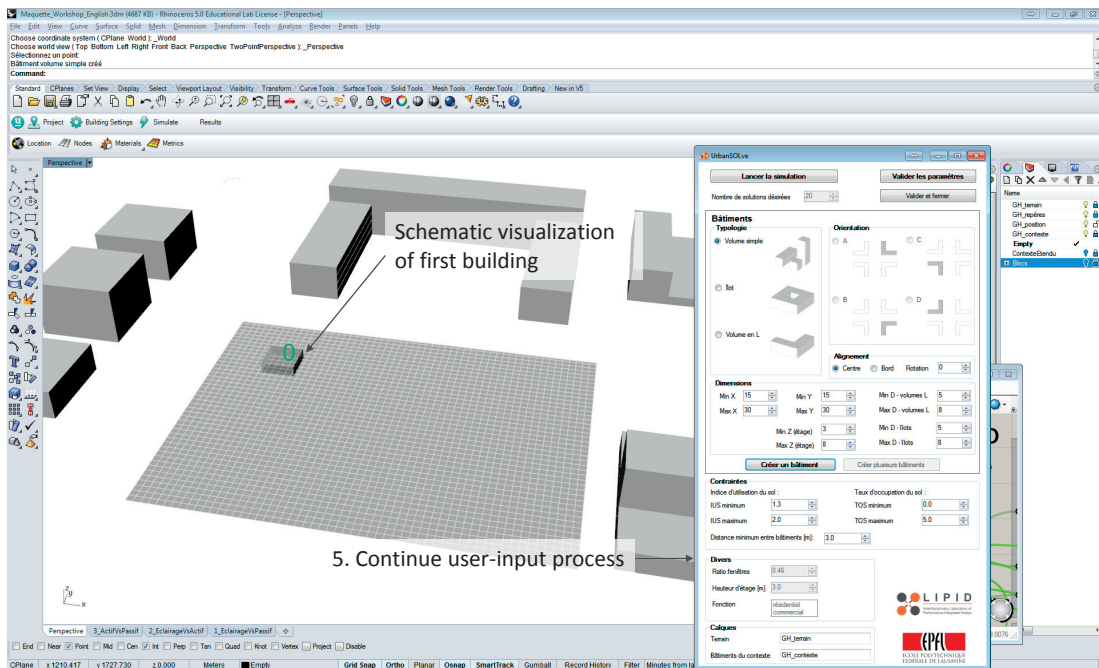
(b) Start of user-input phase via the custom interface and Rhino window.



## B.2. Static demo of prototype

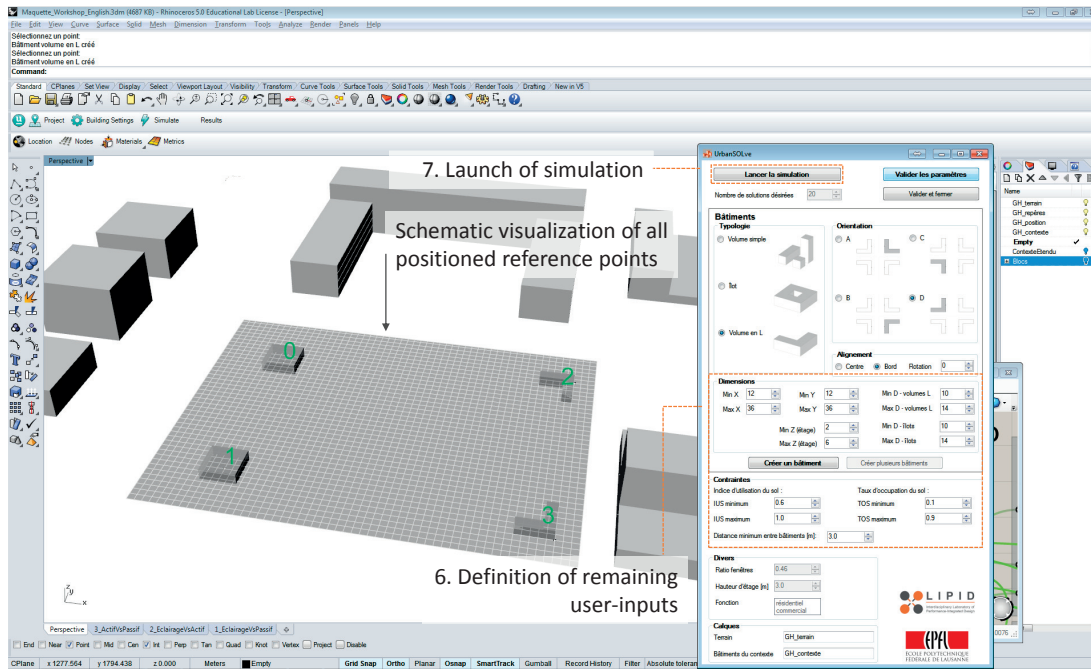


(c) Definition of a first 'abstracted building' by positioning a reference point on the parcel.

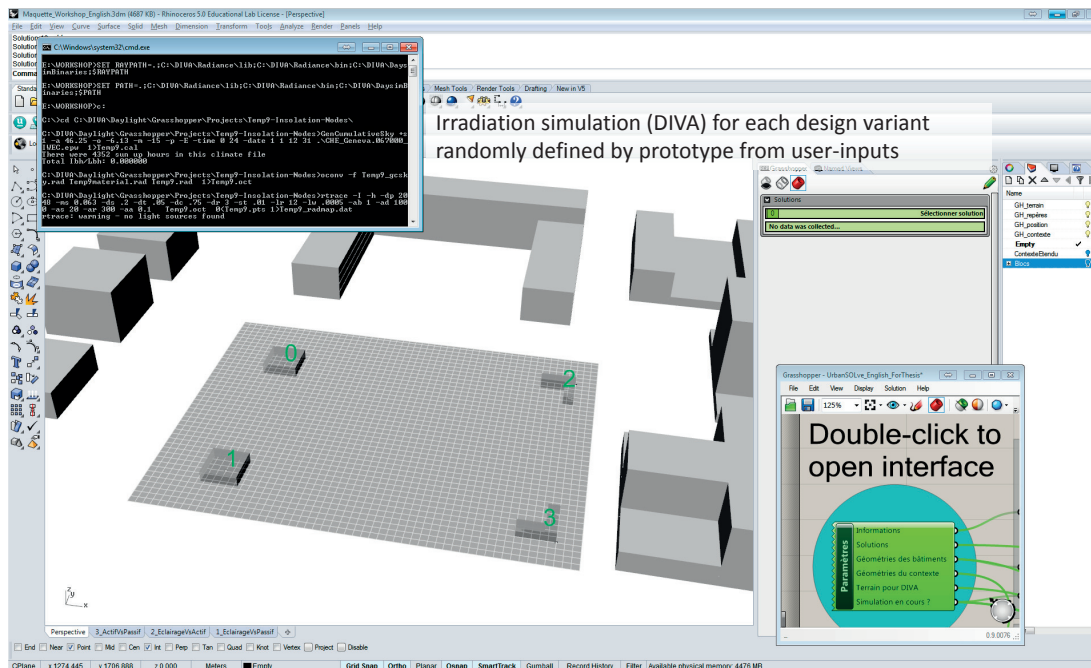


(d) A schematic view of each positioned building (numbered) is provided by the prototype.

## Appendix B. Prototype

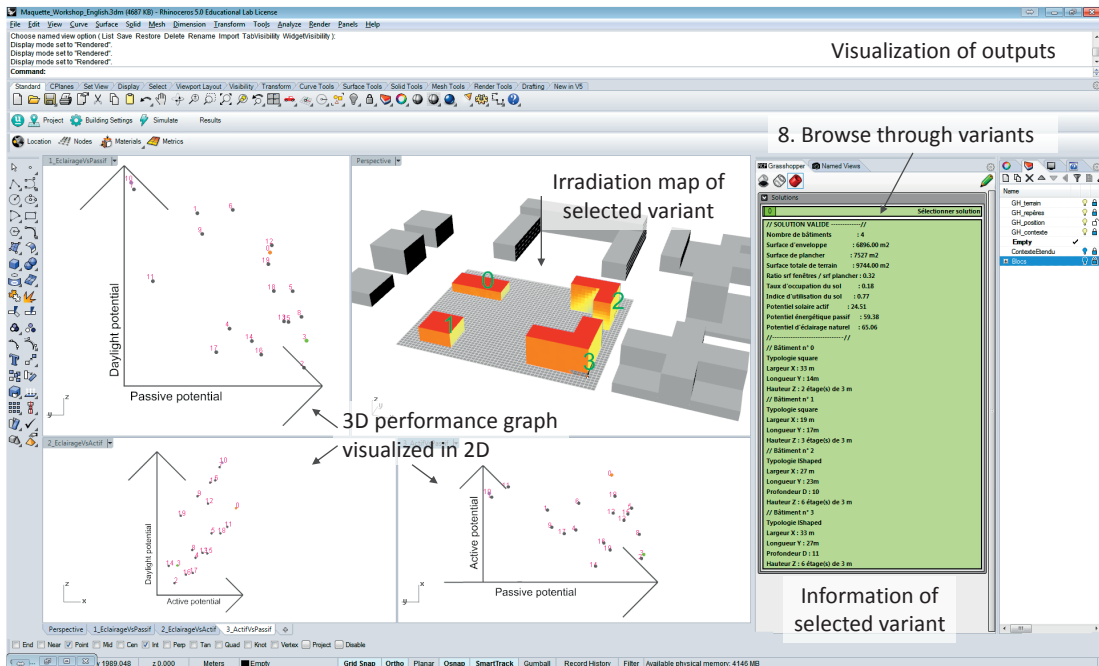


(e) Once the base case design has been completed (all reference points placed), the user must specify the remaining inputs: the parameterization of the design (minimum and maximum design variable values).

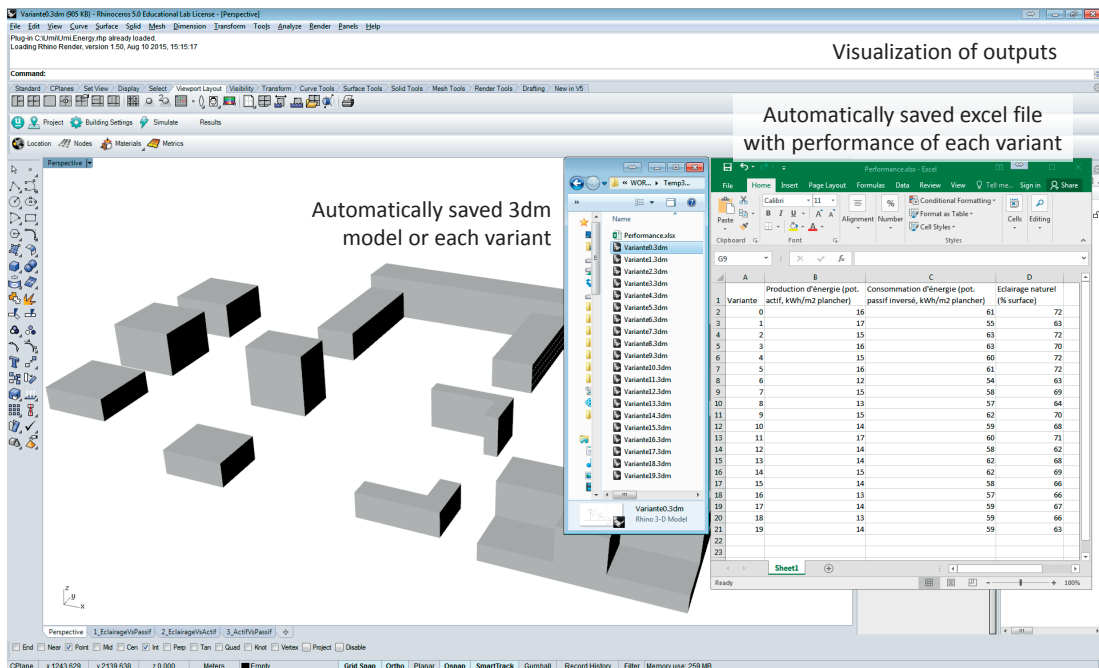


(f) When the user launches the simulation, the prototype searches for valid design variants and computes the required metamodel inputs (geometry- and irradiation-based parameters) for each one of them.

## B.2. Static demo of prototype



(g) Following the performance assessment by the prototype, results can be visualized in different formats: an irradiation map of the variant selected by the user via a slider; the relative performance in 2D graphs.



(h) Additional outputs from the prototype are a Rhino model for each variant and an excel file containing the performance data for all variants, all automatically exported in a folder.



# **C** Workshop

## **C.1 Questionnaires**

The original French version of the pre- (initial) and post- (final) questionnaires to which workshop participants had to answer are included in the following pages. They are introduced in section 5.2.2, while answers are shown in section 6.1 and appendix C.4.

[Edit this form](#)

## Questionnaire initial

\*Required

**1. Quelle est votre formation (niveau et domaine) ? \***

**2. Expérience professionnelle \***

Architecte  
 Urbaniste  
 Ingénieur  
 Etudiant(e) avec expérience dans un bureau d'architecte  
 Etudiant(e) avec expérience dans un bureau d'urbanisme  
 Etudiant(e) avec expérience dans un bureau d'ingénieur  
 Sans expérience professionnelle (ex: étudiant(e) niveau bachelior)  
 Other:

**Nombre de mois ou d'années d'expérience, le cas échéant:**

**3. Vous avez déjà participé à un projet à l'échelle du quartier**

Plan Directeur (Localisé)  
 Plan de Quartier  
 Concours  
 Other:

**4. Vous avez de l'expérience avec un/des outil(s) de modélisation 3D (incluant paramétrique)**

|             | Phase conceptuelle    | Phase détaillée       | Phases conceptuelle et détaillée | Non                   |
|-------------|-----------------------|-----------------------|----------------------------------|-----------------------|
| Rhino       | <input type="radio"/> | <input type="radio"/> | <input type="radio"/>            | <input type="radio"/> |
| SketchUp    | <input type="radio"/> | <input type="radio"/> | <input type="radio"/>            | <input type="radio"/> |
| Grasshopper | <input type="radio"/> | <input type="radio"/> | <input type="radio"/>            | <input type="radio"/> |
| Revit       | <input type="radio"/> | <input type="radio"/> | <input type="radio"/>            | <input type="radio"/> |
| ArchICAD    | <input type="radio"/> | <input type="radio"/> | <input type="radio"/>            | <input type="radio"/> |

**Autre(s) outil(s) de modélisation 3D que vous utilisez (pas dans la liste)**

**5. Vous avez de l'expérience avec un/des outil(s) de dessin assisté par ordinateur**

|             | Phase conceptuelle    | Phase détaillée       | Phases conceptuelle et détaillée | Non                   |
|-------------|-----------------------|-----------------------|----------------------------------|-----------------------|
| AutoCAD     | <input type="radio"/> | <input type="radio"/> | <input type="radio"/>            | <input type="radio"/> |
| Vectorworks | <input type="radio"/> | <input type="radio"/> | <input type="radio"/>            | <input type="radio"/> |

**Autre(s) outil(s) de dessin assisté par ordinateur que vous utilisez (pas dans la liste)**

**6. Vous avez de l'expérience avec un/des outil(s) de simulation (énergétique, irradiation, éclairage naturel, autre)**

|                | Phase conceptuelle    | Phase détaillée       | Phases conceptuelle et détaillée | Non                   |
|----------------|-----------------------|-----------------------|----------------------------------|-----------------------|
| Ecotect        | <input type="radio"/> | <input type="radio"/> | <input type="radio"/>            | <input type="radio"/> |
| DesignBuilder  | <input type="radio"/> | <input type="radio"/> | <input type="radio"/>            | <input type="radio"/> |
| OpenStudio     | <input type="radio"/> | <input type="radio"/> | <input type="radio"/>            | <input type="radio"/> |
| DIVA-for-Rhino | <input type="radio"/> | <input type="radio"/> | <input type="radio"/>            | <input type="radio"/> |
| Lesosai        | <input type="radio"/> | <input type="radio"/> | <input type="radio"/>            | <input type="radio"/> |
| PVSyst         | <input type="radio"/> | <input type="radio"/> | <input type="radio"/>            | <input type="radio"/> |
| DialLux        | <input type="radio"/> | <input type="radio"/> | <input type="radio"/>            | <input type="radio"/> |
| ArchiWizard    | <input type="radio"/> | <input type="radio"/> | <input type="radio"/>            | <input type="radio"/> |

**Autre(s) outil(s) de simulation que vous utilisez (pas dans la liste)**

**7. Vous avez de l'expérience par rapport à l'évaluation du potentiel solaire passif (pour le chauffage passif)**

|                                     | Phase conceptuelle       | Phase détaillée          | Phases conceptuelle et détaillée | Non                      |
|-------------------------------------|--------------------------|--------------------------|----------------------------------|--------------------------|
| Règles de la main / Heuristiques    | <input type="checkbox"/> | <input type="checkbox"/> | <input type="checkbox"/>         | <input type="checkbox"/> |
| Visualisation (ex: tracé du soleil) | <input type="checkbox"/> | <input type="checkbox"/> | <input type="checkbox"/>         | <input type="checkbox"/> |
| Simulations                         | <input type="checkbox"/> | <input type="checkbox"/> | <input type="checkbox"/>         | <input type="checkbox"/> |
| Consultant externe                  | <input type="checkbox"/> | <input type="checkbox"/> | <input type="checkbox"/>         | <input type="checkbox"/> |

**Autre(s) méthode(s) que vous utilisez pour évaluer le potentiel solaire passif (pas dans la liste)**

**9. Vous avez de l'expérience par rapport à l'évaluation du confort thermique (exemple: surchauffe en été)**

|  | Phase conceptuelle       | Phase détaillée          | Phases conceptuelle et détaillée | Non                      |
|--|--------------------------|--------------------------|----------------------------------|--------------------------|
| Règles de la main / Heuristiques             | <input type="checkbox"/> | <input type="checkbox"/> | <input type="checkbox"/>         | <input type="checkbox"/> |
| Visualisation (ex: graphique de température) | <input type="checkbox"/> | <input type="checkbox"/> | <input type="checkbox"/>         | <input type="checkbox"/> |
| Simulations                                  | <input type="checkbox"/> | <input type="checkbox"/> | <input type="checkbox"/>         | <input type="checkbox"/> |
| Consultant externe                           | <input type="checkbox"/> | <input type="checkbox"/> | <input type="checkbox"/>         | <input type="checkbox"/> |

**Autre(s) méthode(s) que vous utilisez pour évaluer le confort thermique (pas dans la liste)**

**8. Vous avez de l'expérience par rapport à l'évaluation du potentiel solaire actif (panneaux photovoltaïques, capteurs thermiques)**

|                                     | Phase conceptuelle       | Phase détaillée          | Phases conceptuelle et détaillée | Non                      |
|-------------------------------------|--------------------------|--------------------------|----------------------------------|--------------------------|
| Règles de la main / Heuristiques    | <input type="checkbox"/> | <input type="checkbox"/> | <input type="checkbox"/>         | <input type="checkbox"/> |
| Visualisation (ex: tracé du soleil) | <input type="checkbox"/> | <input type="checkbox"/> | <input type="checkbox"/>         | <input type="checkbox"/> |
| Simulations                         | <input type="checkbox"/> | <input type="checkbox"/> | <input type="checkbox"/>         | <input type="checkbox"/> |
| Consultant externe                  | <input type="checkbox"/> | <input type="checkbox"/> | <input type="checkbox"/>         | <input type="checkbox"/> |

**Autre(s) méthode(s) que vous utilisez pour évaluer le potentiel solaire actif (pas dans la liste)**

**10. Vous avez de l'expérience par rapport à l'évaluation du potentiel en éclairage naturel**

|                                  | Phase conceptuelle       | Phase détaillée          | Phases conceptuelle et détaillée | Non                      |
|----------------------------------|--------------------------|--------------------------|----------------------------------|--------------------------|
| Règles de la main / Heuristiques | <input type="checkbox"/> | <input type="checkbox"/> | <input type="checkbox"/>         | <input type="checkbox"/> |
| Visualisation (ex: rendering)    | <input type="checkbox"/> | <input type="checkbox"/> | <input type="checkbox"/>         | <input type="checkbox"/> |
| Simulations                      | <input type="checkbox"/> | <input type="checkbox"/> | <input type="checkbox"/>         | <input type="checkbox"/> |
| Consultant externe               | <input type="checkbox"/> | <input type="checkbox"/> | <input type="checkbox"/>         | <input type="checkbox"/> |

**Autre(s) méthode(s) que vous utilisez pour évaluer le potentiel en éclairage naturel (pas dans la liste)**

**11. Autre(s) tâche(s) similaire(s) que vous effectuez à l'aide de méthodes/outils spécifiques**

12. Vous avez été invité au workshop du \*

13. Vous participerez au workshop \*

Never submit passwords through Google Forms.

Powered by  This content is neither created nor endorsed by Google.  
Report Abuse - Terms of Service - Additional Terms



Edit this form

## Questionnaire final

\*Required

---

**1. L'utilisation de ce prototype... \***

|   | Pas du tout d'accord  | Pas d'accord          | Ni en désaccord ni d'accord | D'accord              | Tout à fait d'accord  |
|---|-----------------------|-----------------------|-----------------------------|-----------------------|-----------------------|
| vous a permis d'apprendre de nouveaux éléments utiles dans votre approche au problème | <input type="radio"/> | <input type="radio"/> | <input type="radio"/>       | <input type="radio"/> | <input type="radio"/> |
| vous a influencés votre approche au problème  | <input type="radio"/> | <input type="radio"/> | <input type="radio"/>       | <input type="radio"/> | <input type="radio"/> |
| vous a rendu plus confiant dans votre prise de décision                               | <input type="radio"/> | <input type="radio"/> | <input type="radio"/>       | <input type="radio"/> | <input type="radio"/> |

**2. L'utilisation de ce prototype vous a permis d'apprendre au sujet du critère de performance lié... \***

|  | Pas du tout d'accord  | Pas d'accord          | Ni en désaccord ni d'accord | D'accord              | Tout à fait d'accord  |
|--|-----------------------|-----------------------|-----------------------------|-----------------------|-----------------------|
| au potentiel solaire passif (énergie pour le chauffage et refroidissement) à l'éclairage naturel | <input type="radio"/> | <input type="radio"/> | <input type="radio"/>       | <input type="radio"/> | <input type="radio"/> |
| au potentiel solaire actif (pompes à chaleur solaires)   | <input type="radio"/> | <input type="radio"/> | <input type="radio"/>       | <input type="radio"/> | <input type="radio"/> |

---

**3. Vous êtes satisfait par rapport... \***

|  | Pas du tout d'accord  | Pas d'accord          | Ni en désaccord ni d'accord | D'accord              | Tout à fait d'accord  |
|--|-----------------------|-----------------------|-----------------------------|-----------------------|-----------------------|
| à la facilité d'utilisation du prototype                   | <input type="radio"/> | <input type="radio"/> | <input type="radio"/>       | <input type="radio"/> | <input type="radio"/> |
| à l'interface du prototype                                 | <input type="radio"/> | <input type="radio"/> | <input type="radio"/>       | <input type="radio"/> | <input type="radio"/> |
| au temps nécessaire lors de l'utilisation du prototype     | <input type="radio"/> | <input type="radio"/> | <input type="radio"/>       | <input type="radio"/> | <input type="radio"/> |
| à la pertinence de l'approche du prototype                 | <input type="radio"/> | <input type="radio"/> | <input type="radio"/>       | <input type="radio"/> | <input type="radio"/> |
| à la pertinence de l'information apportée par le prototype | <input type="radio"/> | <input type="radio"/> | <input type="radio"/>       | <input type="radio"/> | <input type="radio"/> |

**4. Commentaires généraux sur le prototype (interface, visualisation, modélisation, etc.)**

**5. Suggestions par rapport au prototype (interface, visualisation, modélisation, etc.)**

**6. Autres commentaires**

**Vous avez participé au workshop du \***

|  |   |
|--|---|
| <input type="text"/>   | <input type="text"/>  |
| <b>Numéro de poste de travail (post-it près de l'ordinateur) *</b> |   |
| <input type="text"/>   | <input type="text"/>  |
| <input type="submit" value="Submit"/>                              |   |
| <i>Never submit passwords through Google Forms.</i>                |   |
| Powered by   | This content is neither created nor endorsed by Google.<br><a href="#">Report Abuse</a> - <a href="#">Terms of Service</a> - <a href="#">Additional Terms</a> |

## C.2 Slides

# Workshop

Test d'une plateforme d'aide à la décision dans le processus de conception d'un plan de quartier

Urban Solar Visual Explorer – UrbanSolve\*

Emilie Nault  
Octobre 2015

\*Collège Mélorie Hock  
IAST | Interdisciplinary Laboratory of Architecture, School of Architecture, Civil and Environmental Engineering, EPFL, Switzerland

### Horaire et Phases

13h30 Introduction au problème de conception et critères de performance

14h **Problème de conception**  
*Design et classement de manière intuitive*  
 Phase I : Design avec méthodes et outils usuels (maquette, logiciels, etc.) tenant compte des critères de performance  
 Phase II : Estimation du classement par rapport aux trois critères exposés

15h30 **Design et classement avec le support UrbanSolve**  
 Phase III : Utilisation du prototype de la plateforme d'aide à la décision  
 Phase IV : Classements par rapport aux critères

17h Questionnaire et discussion pour récolte des impressions et commentaires  
 17h20 Synthèse

Octobre 2015 | Emilie Nault

### Horaire et Phases

13h30 Introduction au problème de conception et critères de performance

14h **Problème de conception**  
*Design et classement de manière intuitive*  
 Phase I : Design avec méthodes et outils usuels (maquette, logiciels, etc.) tenant compte des critères de performance  
 Phase II : Estimation du classement par rapport aux trois critères exposés

15h30 **Design et classement avec le support UrbanSolve**  
 Phase III : Utilisation du prototype de la plateforme d'aide à la décision  
 Phase IV : Classements par rapport aux critères

17h Questionnaire et discussion pour récolte des impressions et commentaires  
 17h20 Synthèse

Octobre 2015 | Emilie Nault

### Horaire et Phases

13h30 Introduction au problème de conception et critères de performance

14h **Problème de conception**  
*Design et classement de manière intuitive*  
 Phase I : Design avec méthodes et outils usuels (maquette, logiciels, etc.) tenant compte des critères de performance  
 Phase II : Estimation du classement par rapport aux trois critères exposés

15h30 **Design et classement avec le support UrbanSolve**  
 Phase III : Utilisation du prototype de la plateforme d'aide à la décision  
 Phase IV : Classements par rapport aux critères

17h Questionnaire et discussion pour récolte des impressions et commentaires  
 17h20 Synthèse

Octobre 2015 | Emilie Nault

### UrbanSolve – Urban SOLar Visual Explorer

- Création d'un espace de solutions (scénarios) à partir d'inputs spécifiés par l'utilisateur
- Workflow semi-automatisé
- Estimation de la performance (énergétique passif, actif, et éclairage naturel) via modèle mathématique
- Propre interface (plug-in pour Grasshopper) pour recueillir les inputs, et visualisation faite dans Rhino

Adapté du Plan Directeur Localisé Intercommunal  
Lausanne-Vernand – Romanet sur Lausanne  
(UrbanSolve)

CPH  
INSTITUT DE RECHERCHE  
EN HABITAT ET URBANISME

Octobre 2015 | Enlène Nault

LIPID  
LABORATOIRE  
D'INTEGRATION  
PROJECTION

### Situation



Adapté du Plan Directeur Localisé Intercommunal  
Lausanne-Vernand – Romanet sur Lausanne  
(UrbanSolve)

CPH  
INSTITUT DE RECHERCHE  
EN HABITAT ET URBANISME

Octobre 2015 | Enlène Nault

LIPID  
LABORATOIRE  
D'INTEGRATION  
PROJECTION

### Situation

- Surface de la parcelle : 9 744 m<sup>2</sup>
- Contexte pré-existant (modifié)
- Connexion avec axes de transport
- Entre deux espaces verts à valoriser



Adapté du Plan Directeur Localisé Intercommunal  
Lausanne-Vernand – Romanet sur Lausanne  
(UrbanSolve)

CPH  
INSTITUT DE RECHERCHE  
EN HABITAT ET URBANISME

Octobre 2015 | Enlène Nault

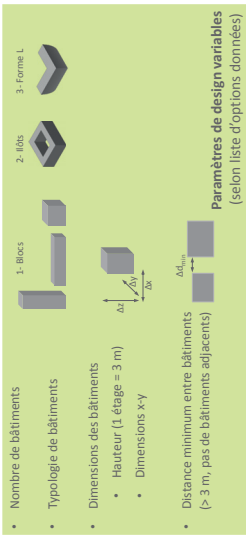
LIPID  
LABORATOIRE  
D'INTEGRATION  
PROJECTION

### Contraintes et Variables

- Surface de la parcelle : 9 744 m<sup>2</sup>
- Indice d'utilisation du sol (IUS) : 1,3 – 2
- Surface de plancher : 12 600 – 19 500 m<sup>2</sup>
- Alignement Nord-Sud-Est-Ouest

#### Contraintes à respecter

- Nombre de bâtiments
- Typologie de bâtiments
- Dimensions des bâtiments
  - Hauteur (1 étage = 3 m)
  - Dimensions x-y
- Distance minimum entre bâtiments (> 3 m, pas de bâtiments adjacents)



#### Paramètres de design variables (selon liste d'options données)

CPH  
INSTITUT DE RECHERCHE  
EN HABITAT ET URBANISME

Octobre 2015 | Enlène Nault

LIPID  
LABORATOIRE  
D'INTEGRATION  
PROJECTION

### Exemples

Facile à reproduire dans l'outil

Difficile à reproduire dans l'outil

Octobre 2015 | Erniele Nault

### Interface – Inputs

Choix de typologie pour chaque bâtiment

Intervalles communs à tous les bâtiments

Octobre 2015 | Erniele Nault

### Stratégie

Gabarit

→ Volumes plus définis

Octobre 2015 | Erniele Nault

### Stratégie

Gabarit

→ Volumes plus définis

Octobre 2015 | Erniele Nault

### Stratégie

Gabarit → Volumes plus définis

Echelle du bâtiment

CPH  
CENTRE DE PROJECTION  
URBAIN

LIPIID  
LABORATOIRE  
D'INTEGRATION  
PROJECTIONnelle

Octobre 2015 | Emille Nault

### Stratégie

Gabarit → Volumes plus définis

Echelle du bâtiment

CPH  
CENTRE DE PROJECTION  
URBAIN

LIPIID  
LABORATOIRE  
D'INTEGRATION  
PROJECTIONnelle

Octobre 2015 | Emille Nault

### Critères de Performance

**Solaire passif**  
Chauffage - Refroidissement

Moins de Chauffage (kWh/m²)

**Solaire naturel**  
Autonomie

Daylight Autonomy (%)

Au rez-de-chaussée  
Taux de vitrage 45%

**Solaire actif**  
Potentiel de production  
Photovoltaïque et Thermique

Emballéchauff (kWh/m²)

Sur les toitures

CPH  
CENTRE DE PROJECTION  
URBAIN

LIPIID  
LABORATOIRE  
D'INTEGRATION  
PROJECTIONnelle

Octobre 2015 | Emille Nault

### Critères de Performance

**Solaire passif**  
Chauffage - Refroidissement

**Solaire naturel**  
Autonomie

**Solaire actif**  
Potentiel de production  
Photovoltaïque et Thermique

CPH  
CENTRE DE PROJECTION  
URBAIN

LIPIID  
LABORATOIRE  
D'INTEGRATION  
PROJECTIONnelle

Octobre 2015 | Emille Nault

### Phase I (environ 1h)

Concevoir un design (3D) – Variante A – selon vos méthodes et critères habituels, à l'aide de vos outils usuels (dans la mesure du possible), mais tenant compte également des critères de performance.

[voir Données de l'exercice de conception]

Matériel à disposition :

- Maquette du contexte et matériel pour construire maquette
  - Plaques de *sogex* (30 mm) équivalente à deux étages de 3m
  - Machines à fil chaud pour couper le sagex et colle blanche
- Ordinateurs avec certains logiciels (SketchUp, Rhino, AutoCAD) et modèle de base avec contexte et parcelle (dossier Workshop\_(date))

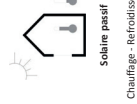


Octobre 2015 | Emeline Nault



### Phase II (environ 10min)

a. Classez votre Variante A ainsi que les 3 variantes données par rapport à chaque critère de performance. [voir Fiche 1a]



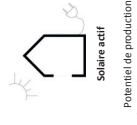
Solaire passif

Chauffage - Refroidissement



Eclairage naturel

Autonomie



Solaire actif

Potentiel de production Photovoltaïque et Thermique

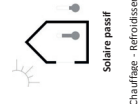


Octobre 2015 | Emeline Nault



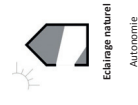
### Phase II (environ 10min)

- Classez votre Variante A ainsi que les 3 variantes données par rapport à chaque critère de performance. [voir Fiche 1a]
- En connaissant maintenant la performance des 3 variantes données, révisez votre classement précédent. [voir Fiche 1b]



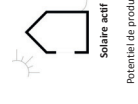
Solaire passif

Chauffage - Refroidissement



Eclairage naturel

Autonomie



Solaire actif

Potentiel de production Photovoltaïque et Thermique



Octobre 2015 | Emeline Nault



### Phase III (environ 1h)

À l'aide du prototype (plateforme d'aide à la décision), explorez l'espace de solutions en se basant sur votre Variante A, c'est-à-dire en essayant de la reproduire dans l'outil.

Soumettez ensuite une Variante B, qui peut être identique à la Variante A, ou une version révisée de celle-ci.

[voir instructions]

\* **Votre expérience contribuera au développement du prototype.**

\*\* **Vision test, ne pas considérer les résultats comme vérité absolue !**

Intervalle de confiance (90%)

Eclairage naturel : ± 5,4 kWh/m<sup>2</sup>

Potentiel énergétique passif : ± 3,8 kWh/m<sup>2</sup>



Demo



Octobre 2015 | Emeline Nault




### Phase IV (environ 10min)

Réviser vos classements précédents (1a et 1b) si vous le souhaitez, et **ajoutez-y votre Variante B** (si elle est différente de la Variante A).  
[voir Fiche 2]



October 2015 | Emile Nault



---


### Horaire et Phases

13h30 Introduction au problème de conception et critères de performance


14h *Problème de conception*  
*Design et classement de manière intuitive*  
Phase I : Design avec méthodes et outils usuels (maquette, logiciels, etc.)  
Phase II : Estimation du classement par rapport aux trois critères exposés

15h30 *Design et classement avec le support UrbanSolver*  
Phase III : Utilisation du prototype de la plateforme d'aide à la décision  
Phase IV : Classements par rapport aux critères

17h **Questionnaire et discussion pour récolte des impressions et commentaires**  
17h30 Synthèse



October 2015 | Emile Nault





### C.3 Supporting material

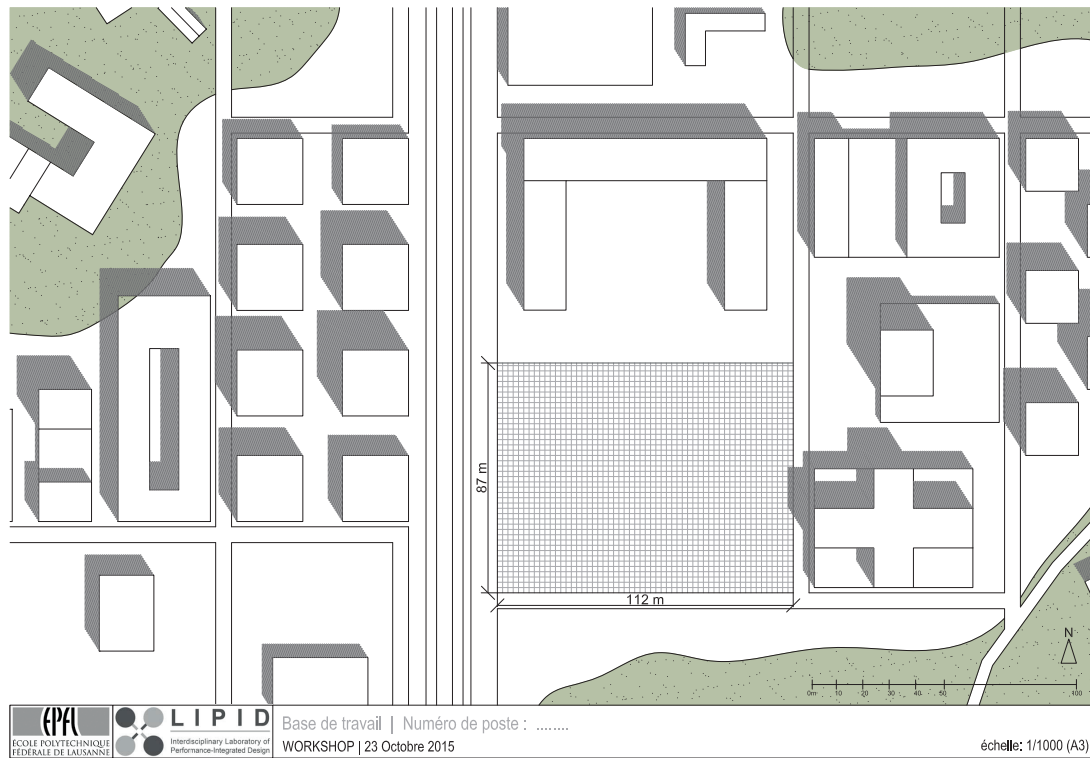


Figure C.1 – Drawing base provided to participants in Phase A.

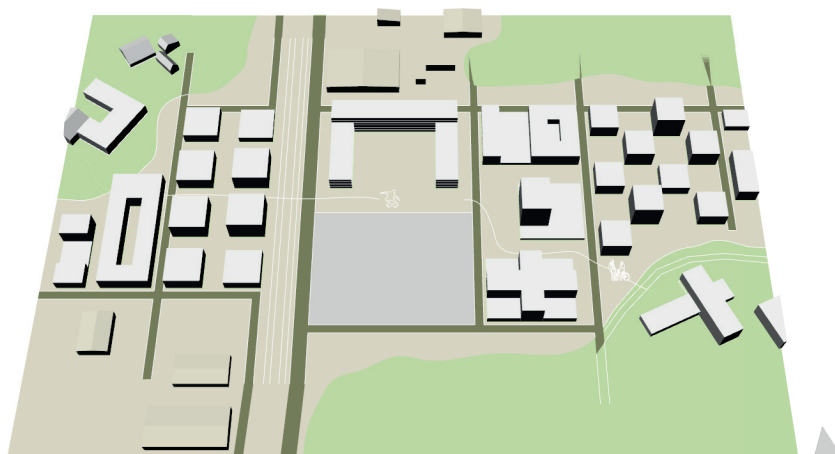
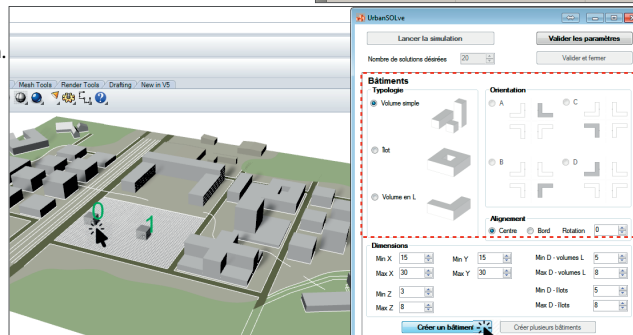
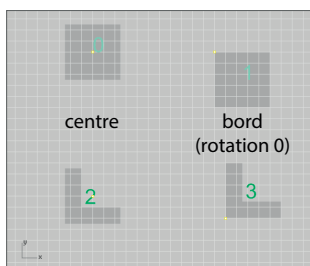
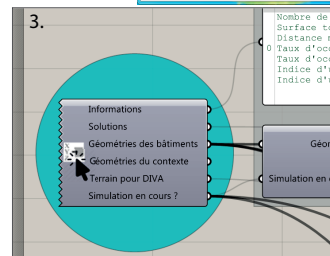
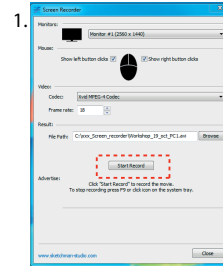


Figure C.2 – Rhino 3D model of the design task prepared for the workshops. Participants worked on the central empty parcel.

## Instructions - Inputs

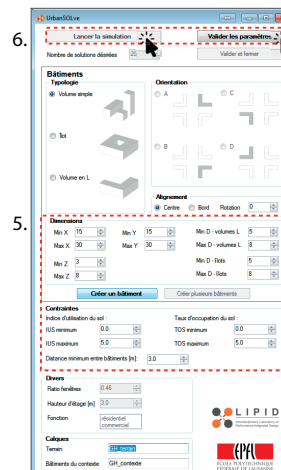
1. Démarrer la capture vidéo de l'écran.
2. Maximiser la fenêtre Rhino 'Maquette\_Workshop\_Final.3dm'.
3. Dans la fenêtre Grasshopper, double cliquer sur l'icône des Paramètres pour ouvrir l'interface UrbanSolve.
4. Création des bâtiments : choisissez d'abord la typologie, l'alignement voulu (centre ou bord), la rotation (0, 90, 180 et -90) et dans le cas de typologie en L, l'orientation.



Appuyez ensuite sur 'Créer un bâtiment'. Positionnez le bâtiment en cliquant sur la parcelle dans la fenêtre Rhino. Répétez pour chaque bâtiment. Vous pouvez à tout moment (avant l'étape 6) bouger ou éliminer un point.

5. Ajuster les paramètres restants :
  - Min et max pour les dimensions X, Y, Z (en nombre d'étages de 3 m)
  - Min et max pour la profondeur dans le cas de typologies en L ou en îlots
  - Min et max pour l'IUS (déjà fixé à 1.3 et 2)
  - Distance minimale à respecter entre bâtiments (3 m par défaut)
 Afin de faciliter et accélérer le processus de recherche de solutions, bien définir les paramètres par exemple à l'aide de quelques calculs.

6. Appuyer sur 'Valider les paramètres' et ensuite 'Lancer la simulation'. Vous devrez alors attendre un moment pendant que l'outil génère et évalue 20 solutions.



### Instructions - Outputs/Visualisation

7. La visualisation des résultats se fait dans les différentes fenêtres ('viewports') de Rhino.  
Pour faciliter la visualisation, minimiser la fenêtre Grasshopper (double-click sur la barre du haut).

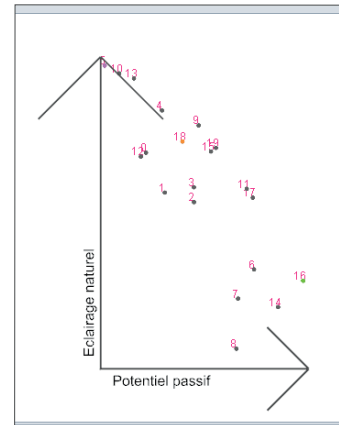
8. Les 3 graphes vous permettent de voir la performance relative des 20 variantes (numérotées de 0 à 19). Chaque graphique montre les résultats pour 2 des 3 critères de performance. Pour chaque critère, le scénario avec la meilleure performance est identifié :

**Vert** : meilleur potentiel énergétique passif

**Orange** : meilleur potentiel énergétique actif

**Mauve** : meilleur potentiel en éclairage naturel

Les limites de l'axe de chaque critère sont calculées à partir du minimum et maximum obtenus sur l'ensemble des 20 solutions pour ce critère en particulier. Ces limites changent donc à chaque exécution du programme (chaque nouvelle itération 'Lancer la simulation').



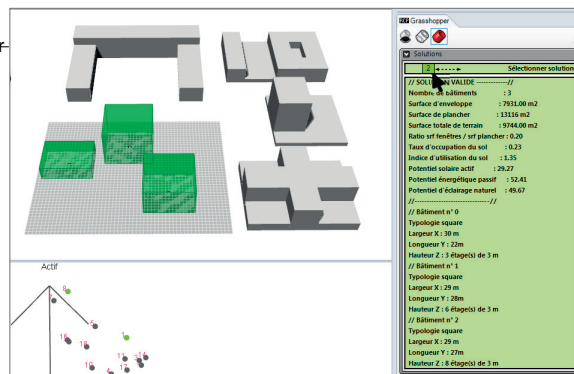
9. Vous pouvez visualiser un scénario en particulier, ainsi que les valeurs relatives à ce scénario, à l'aide du curseur ('slider')

'Sélectionner une solution, qui se trouve dans

la fenêtre Grasshopper intégrée à Rhino.

Soyez patient, le fait de bouger le curseur cause un temps d'attente dans la mise à jour de la solution affichée.

Truc : taper une commande (ex : 'distance') dans la fenêtre Rhino avant de bouger le curseur.



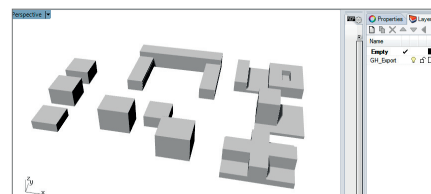
10. Pour chaque scénario, un fichier Rhino est créé et sauvegardé dans le dossier :

'Workshop\_[date]\Variantes3dm\'

Cela permet d'ouvrir un modèle .3dm pour un scénario en particulier que l'on voudrait examiner davantage et/ou utiliser ultérieurement.

Un fichier excel est également créé, contenant les valeurs de performance pour chaque critère et scénario.

Attention, ces fichiers sont écrasés à chaque fois qu'on relance la simulation (chaque fois que 20 nouvelles variantes sont créées).





## C.4 Results per participant

In this section, we present the results for each of the eight participants in a summary including, in this order: responses to the initial questionnaire, simulated performance of the variants along with ranking results for each phase, Variant A and B (when present) through an irradiation and DA false-color map, and answers to the final questionnaire. A brief synthesis concludes each part to highlight the main observations and, when relevant, issues encountered by the participant.

## Appendix C. Workshop

### Participant 1 - Architect / urban designer (15 years of experience)

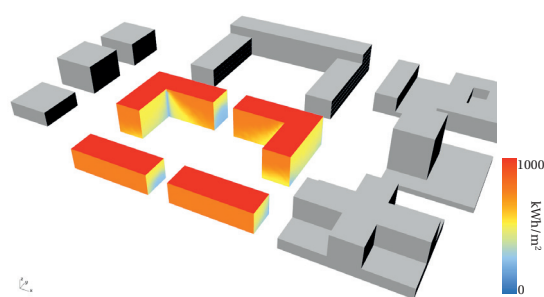
Table C.1 – Participant 1’s (a) answers to the initial questionnaire and (b) results in the ranking phases according to the simulated performance of each variant.

(a) Previous experience with tools and performance evaluation.

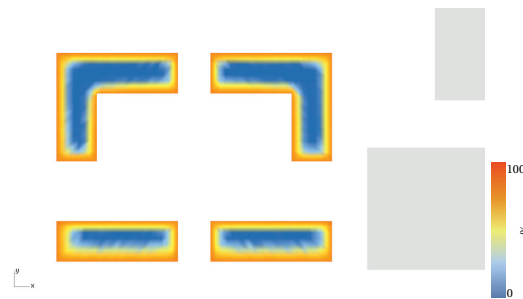
|                               |               | Conceptual        | Detailed | Both |
|-------------------------------|---------------|-------------------|----------|------|
| Experience with...            |               |                   |          |      |
| Modeling tools                |               | SketchUp, AutoCAD |          |      |
| Simulation tools              |               |                   |          |      |
| Experience with evaluating... |               |                   |          |      |
| Passive solar through:        | Rule-of-thumb | heating           |          |      |
|                               | Visualization | heating           |          |      |
|                               | Simulation    |                   |          |      |
| Daylight through:             | Rule-of-thumb |                   |          |      |
|                               | Visualization |                   |          |      |
|                               | Simulation    |                   |          |      |
| Active solar through:         | Rule-of-thumb |                   |          |      |
|                               | Visualization |                   |          |      |
|                               | Simulation    |                   |          |      |
| Ext. consultant               |               |                   |          |      |

(b) Simulated performance of variants and ranking results.

|  | V1                 | V2                 | V3                 | VA                 | VB | $\tau$ |
|--|--------------------|--------------------|--------------------|--------------------|----|--------|
| Simulated energy need [kWh/m <sup>2</sup> <sub>EAL</sub> ]       | 44.0               | 43.6               | 37.1               | 39.0               |    |        |
| Initial ranking  | Incorrectly ranked | Incorrectly ranked | Incorrectly ranked | Incorrectly ranked |    | 0.33   |
| Inter. ranking   | Correctly ranked   | Correctly ranked   | Correctly ranked   | Correctly ranked   |    | 1      |
| Final ranking  |                    |                    |                    |                    |    |        |
| Simulated sDA [% <sub>EAL</sub> ]                                | 63.7               | 62.6               | 57.5               | 54.4               |    |        |
| Initial ranking  | Incorrectly ranked | Incorrectly ranked | Incorrectly ranked | Incorrectly ranked |    | -0.33  |
| Inter. ranking   | Correctly ranked   | Correctly ranked   | Correctly ranked   | Correctly ranked   |    | 1      |
| Final ranking  |                    |                    |                    |                    |    |        |
| Simulated energy production [kWh/m <sup>2</sup> <sub>EAL</sub> ] | 61.3               | 56.4               | 60.8               | 61.9               |    |        |
| Initial ranking  | Correctly ranked   | Incorrectly ranked | Correctly ranked   | Correctly ranked   |    | 0.67   |
| Inter. ranking   | Correctly ranked   | Correctly ranked   | Correctly ranked   | Correctly ranked   |    | 1      |
| Final ranking  |                    |                    |                    |                    |    |        |



(a) VA - Irradiation map



(b) VA - sDA map

Figure C.3 – Variant submitted by participant 1.

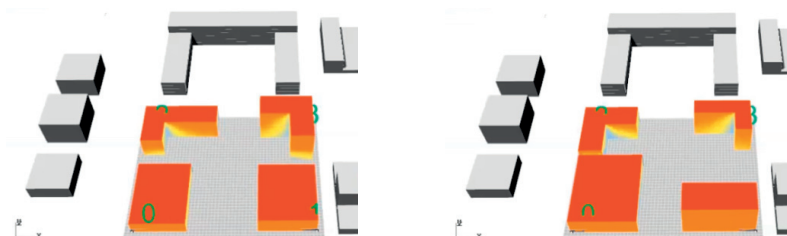


Figure C.4 – Example variants produced by the prototype, showing the building dimensions issue (screenshots of recorded session).

Table C.2 – Participant 1’s answers to the final questionnaire.

|   | strongly disagree   | disagree              | neither agree nor disagree       | agree                            | strongly agree                   |
|---|---|-----------------------|----------------------------------|----------------------------------|----------------------------------|
| The usage of this prototype...  |   |                       |                                  |                                  |                                  |
| allowed you to learn new elements useful in your approach to the problem                      | <input type="radio"/>   | <input type="radio"/> | <input type="radio"/>            | <input type="radio"/>            | <input checked="" type="radio"/> |
| influenced your approach to the problem   | <input type="radio"/>   | <input type="radio"/> | <input type="radio"/>            | <input checked="" type="radio"/> | <input type="radio"/>            |
| influenced your final concept   | <input type="radio"/>   | <input type="radio"/> | <input checked="" type="radio"/> | <input type="radio"/>            | <input type="radio"/>            |
| made you more confident in your decision-making   | <input type="radio"/>   | <input type="radio"/> | <input type="radio"/>            | <input type="radio"/>            | <input checked="" type="radio"/> |
| The usage of this prototype allowed you to learn about the performance criterion linked to... |   |                       |                                  |                                  |                                  |
| the passive solar potential   | <input type="radio"/>   | <input type="radio"/> | <input checked="" type="radio"/> | <input type="radio"/>            | <input type="radio"/>            |
| daylight  | <input type="radio"/>   | <input type="radio"/> | <input checked="" type="radio"/> | <input type="radio"/>            | <input type="radio"/>            |
| the active solar potential  | <input type="radio"/>   | <input type="radio"/> | <input checked="" type="radio"/> | <input type="radio"/>            | <input type="radio"/>            |
| You are satisfied regarding...  |   |                       |                                  |                                  |                                  |
| the facility of using the prototype   | <input type="radio"/>   | <input type="radio"/> | <input type="radio"/>            | <input checked="" type="radio"/> | <input type="radio"/>            |
| the prototype's interface   | <input type="radio"/>   | <input type="radio"/> | <input type="radio"/>            | <input checked="" type="radio"/> | <input type="radio"/>            |
| the time required when using the prototype  | <input type="radio"/>   | <input type="radio"/> | <input type="radio"/>            | <input checked="" type="radio"/> | <input type="radio"/>            |
| the relevance of the prototype's approach   | <input type="radio"/>   | <input type="radio"/> | <input type="radio"/>            | <input checked="" type="radio"/> | <input type="radio"/>            |
| the relevance of the information brought by the prototype                                     | <input type="radio"/>   | <input type="radio"/> | <input type="radio"/>            | <input checked="" type="radio"/> | <input type="radio"/>            |
| General comments  | Hard to use in practice in its current status due to difficulty in specifying realistic building dimensions for the 'simple volume' typology. The output table allows to easily identify optimal solutions. |                       |                                  |                                  |                                  |
| Suggestions   | Synthetic view of 20 solutions as output (pdf format). Ungroup 'simple volume' types for better dimension control. Add parameter maximum distance between building. Add axis limits on graphs.              |                       |                                  |                                  |                                  |

**Issue** This participant experienced some difficulties in re-creating something similar to their VA when using the prototype and as such, has not provided a VB and final ranking. The source of the problem seems to lie in the minimum and maximum y value required to cover the range of building dimensions, from the narrow bars to the longer L-shaped (see y dimension in Fig. C.3b). Indeed, as explained in section 5.1, the allowed range in terms of x, y, z specified by the user is applied to all buildings. The effect of the wide range in y caused the prototype to propose designs with large buildings instead of the desired narrow bars. In light of these encountered difficulties, this participant explicitly mentioned answering the final questionnaire based on the *potential* of the tool if further developed, particularly to solve the problem of unrealistic building dimensions and to allow reproducing with more accuracy the desired building typology and layout.

**Ranking** Between the initial and intermediate ranking phases, we observe a clear overall increase in the level of success in Table C.1b.

## Appendix C. Workshop

### Participant 2 - Architect / urban designer (4 years of experience)

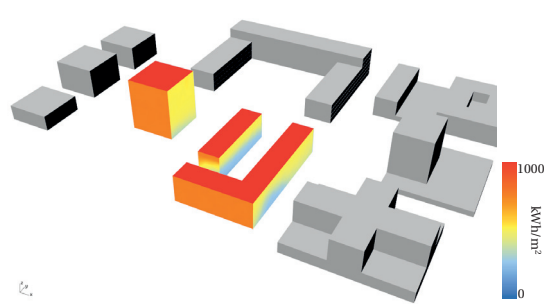
Table C.3 – Participant 2's (a) answers to the initial questionnaire and (b) results in the ranking phases according to the simulated performance of each variant.

(a) Previous experience with tools and performance evaluation.

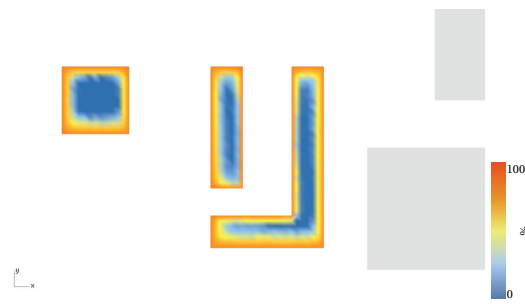
|                               |                 | Conceptual | Detailed | Both                  |
|-------------------------------|-----------------|------------|----------|-----------------------|
| Experience with...            |                 |            |          |                       |
| Modeling tools                |                 |            |          | SketchUp, Vectorworks |
| Simulation tools              |                 |            |          |                       |
| Experience with evaluating... |                 |            |          |                       |
| Passive solar through:        | Rule-of-thumb   |            |          |                       |
|                               | Visualization   |            |          |                       |
|                               | Simulation      |            |          |                       |
|                               | Ext. consultant |            |          |                       |
| Daylight through:             | Rule-of-thumb   |            |          |                       |
|                               | Visualization   |            |          |                       |
|                               | Simulation      |            |          |                       |
|                               | Ext. consultant |            |          |                       |
| Active solar through:         | Rule-of-thumb   |            |          |                       |
|                               | Visualization   |            |          |                       |
|                               | Simulation      |            |          |                       |
|                               | Ext. consultant |            |          |                       |

(b) Simulated performance of variants and ranking results.

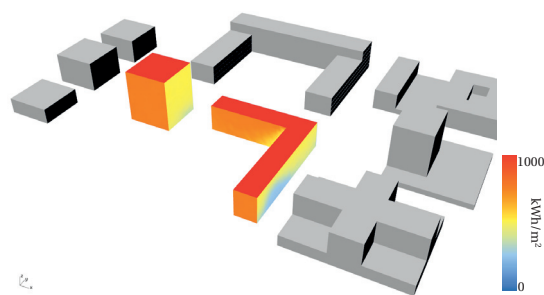
|   |                 | V1                 | V2                 | V3               | VA                 | VB               | $\tau$ |
|---|-----------------|--------------------|--------------------|------------------|--------------------|------------------|--------|
| Simulated energy need [kWh/m <sup>2</sup> <sub>Fa</sub> ]       |                 | 44.0               | 43.6               | 37.1             | 40.9               | 39.7             |        |
|   | Initial ranking | Correctly ranked   | Incorrectly ranked | Correctly ranked | Incorrectly ranked | Correctly ranked | 0.33   |
|   | Inter. ranking  | Correctly ranked   | Incorrectly ranked | Correctly ranked | Incorrectly ranked | Correctly ranked | 0.67   |
|   | Final ranking   | Correctly ranked   | Incorrectly ranked | Correctly ranked | Incorrectly ranked | Correctly ranked | 0.80   |
| Simulated sDA [% <sub>Fa</sub> ]                                |                 | 63.7               | 62.6               | 57.5             | 51.5               | 58.5             |        |
|   | Initial ranking | Incorrectly ranked | Correctly ranked   | Correctly ranked | Correctly ranked   | Correctly ranked | -0.33  |
|   | Inter. ranking  | Correctly ranked   | Correctly ranked   | Correctly ranked | Correctly ranked   | Correctly ranked | 1      |
|   | Final ranking   | Correctly ranked   | Correctly ranked   | Correctly ranked | Correctly ranked   | Correctly ranked | 1      |
| Simulated energy production [kWh/m <sup>2</sup> <sub>Fa</sub> ] |                 | 61.3               | 56.4               | 60.8             | 59.3               | 58.1             |        |
|   | Initial ranking | Incorrectly ranked | Correctly ranked   | Correctly ranked | Correctly ranked   | Correctly ranked | 0.67   |
|   | Inter. ranking  | Correctly ranked   | Correctly ranked   | Correctly ranked | Correctly ranked   | Correctly ranked | 1      |
|   | Final ranking   | Correctly ranked   | Correctly ranked   | Correctly ranked | Correctly ranked   | Correctly ranked | 1      |



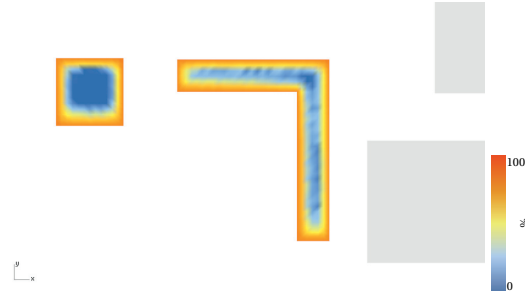
(a) VA - Irradiation map



(b) VA - sDA map



(c) VB - Irradiation map

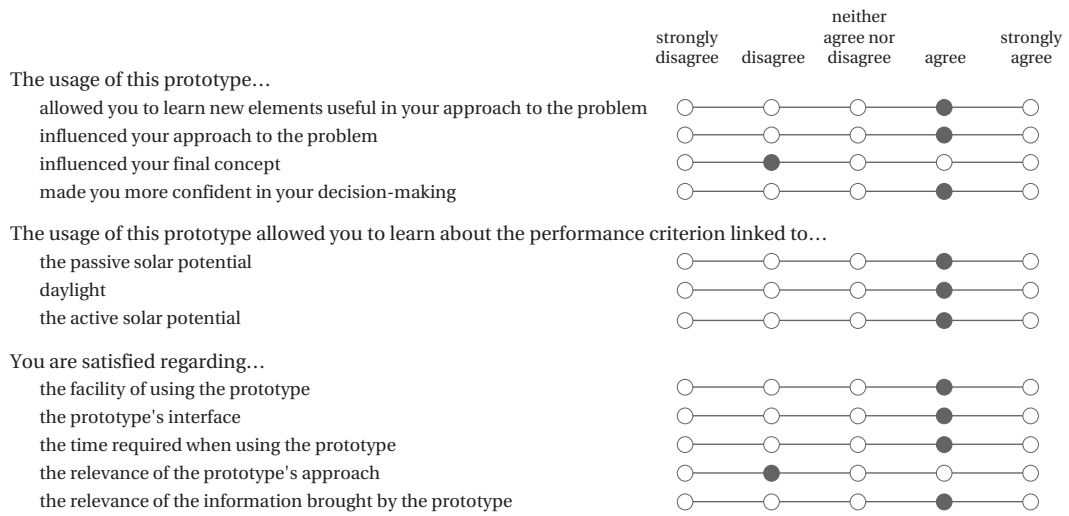


(d) VB - sDA map

Figure C.5 – Variants submitted by participant 2.



Table C.4 – Participant 2’s answers to the final questionnaire.



General comments The building generation is too restrictive, it was impossible to recreate my initial concept. The interface is simple to use and could be more complex if it allows modeling with more adequacy. Visualization is interesting although a little bit slow.

Suggestions Be able to distinguish between bars and more cubic volumes and to specify x, y, z for each building. Output a pdf to visualize all variants with a notation system with respect to an acceptable reference value. Be able to assess the exact initial variant to compare.

**Issue** This participant also experienced some difficulties in re-creating something similar to their VA when using the prototype. In addition to the issues explained earlier linked to the dimension ranges, the problem may have been caused also by the bar being positioned ‘within’ the L-shaped building. This participant’s VB is thus not derived from VA, but rather from a design they were able to explore using the tool.

**Ranking** Between the initial and intermediate ranking phases, we observe an increase in the level of success in Table C.3b, particularly for the daylight and active solar criteria. The final ranking is as good or better than the intermediate one.

**Performance** VB is similar to VA for the energy need and production criteria, while having a higher sDA value, as can be visualized in Fig. C.5.

Participant 3 - Architect (8 years of experience)

Table C.5 – Participant 3’s (a) answers to the initial questionnaire and (b) results in the ranking phases according to the simulated performance of each variant.

(a) Previous experience with tools and performance evaluation.

|                               |                 | Conceptual               | Detailed | Both        |
|-------------------------------|-----------------|--------------------------|----------|-------------|
| Experience with...            |                 |                          |          |             |
| Modeling tools                |                 |                          |          | Vectorworks |
| Simulation tools              |                 |                          | Lesosai  |             |
| Experience with evaluating... |                 |                          |          |             |
| Passive solar through:        | Rule-of-thumb   |                          |          |             |
|                               | Visualization   |                          |          |             |
|                               | Simulation      |                          |          |             |
|                               | Ext. consultant | heating, thermal comfort |          |             |
| Daylight through:             | Rule-of-thumb   |                          |          |             |
|                               | Visualization   |                          |          |             |
|                               | Simulation      |                          |          |             |
|                               | Ext. consultant | x                        |          |             |
| Active solar through:         | Rule-of-thumb   |                          |          |             |
|                               | Visualization   |                          |          |             |
|                               | Simulation      |                          |          |             |
|                               | Ext. consultant | x                        |          |             |

(b) Simulated performance of variants and ranking results.

|  |                | V1   | V2   | V3   | VA   | VB   | $\tau$ |
|--|----------------|------|------|------|------|------|--------|
| Simulated energy need [kWh/m <sup>2</sup> <sub>FAL</sub> ]       |                | 44.0 | 43.6 | 37.1 | 40.8 | 44.7 |        |
| Initial ranking  |                |      |      |      |      |      | -0.33  |
|  | Inter. ranking |      |      |      |      |      | 1      |
|  | Final ranking  |      |      |      |      |      | 0.40   |
| Simulated sDA [% <sub>FAL</sub> ]                                |                | 63.7 | 62.6 | 57.5 | 62.1 | 61.4 |        |
| Initial ranking  |                |      |      |      |      |      | 0.33   |
|  | Inter. ranking |      |      |      |      |      | 0.33   |
|  | Final ranking  |      |      |      |      |      | 0.40   |
| Simulated energy production [kWh/m <sup>2</sup> <sub>FAL</sub> ] |                | 61.3 | 56.4 | 60.8 | 72.3 | 59.3 |        |
| Initial ranking  |                |      |      |      |      |      | 0.67   |
|  | Inter. ranking |      |      |      |      |      | 1      |
|  | Final ranking  |      |      |      |      |      | 0      |

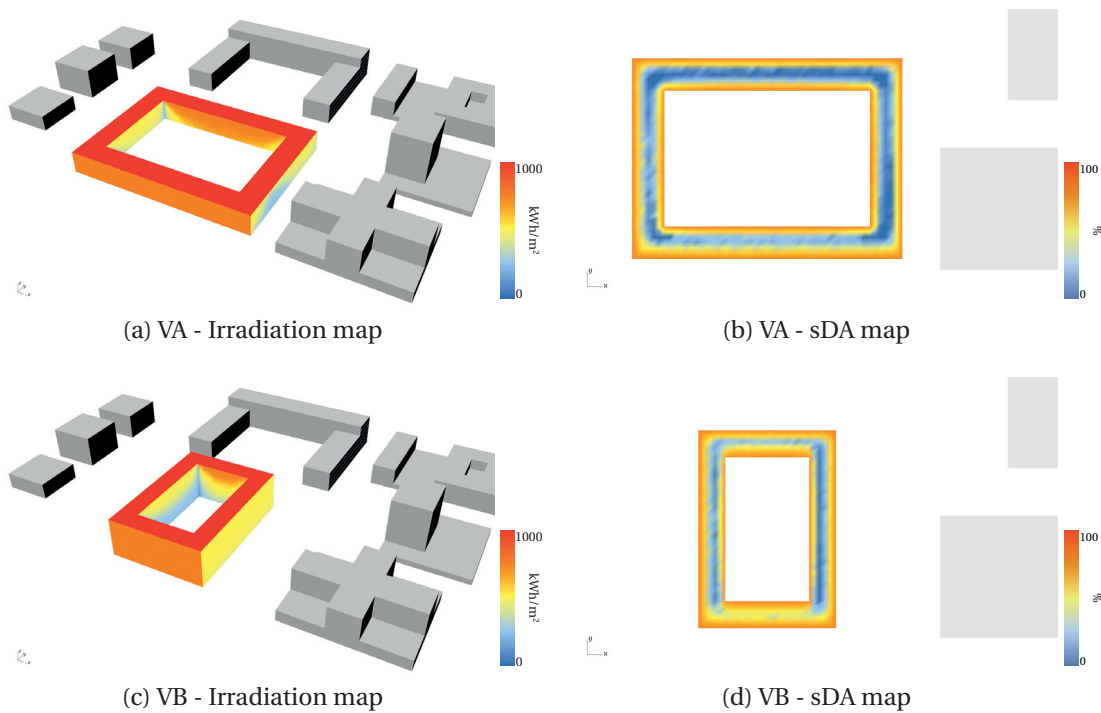


Figure C.6 – Variants submitted by participant 3.

Table C.6 – Participant 3’s answers to the final questionnaire.

|   | strongly disagree   | disagree                         | neither agree nor disagree       | agree                            | strongly agree                   |
|---|---|----------------------------------|----------------------------------|----------------------------------|----------------------------------|
| The usage of this prototype...  |   |                                  |                                  |                                  |                                  |
| allowed you to learn new elements useful in your approach to the problem                      | <input type="radio"/>   | <input type="radio"/>            | <input type="radio"/>            | <input checked="" type="radio"/> | <input type="radio"/>            |
| influenced your approach to the problem   | <input type="radio"/>   | <input type="radio"/>            | <input type="radio"/>            | <input checked="" type="radio"/> | <input type="radio"/>            |
| influenced your final concept   | <input type="radio"/>   | <input type="radio"/>            | <input type="radio"/>            | <input checked="" type="radio"/> | <input type="radio"/>            |
| made you more confident in your decision-making   | <input type="radio"/>   | <input type="radio"/>            | <input type="radio"/>            | <input checked="" type="radio"/> | <input type="radio"/>            |
| The usage of this prototype allowed you to learn about the performance criterion linked to... |   |                                  |                                  |                                  |                                  |
| the passive solar potential   | <input type="radio"/>   | <input type="radio"/>            | <input type="radio"/>            | <input checked="" type="radio"/> | <input type="radio"/>            |
| daylight  | <input type="radio"/>   | <input type="radio"/>            | <input type="radio"/>            | <input checked="" type="radio"/> | <input type="radio"/>            |
| the active solar potential  | <input type="radio"/>   | <input type="radio"/>            | <input type="radio"/>            | <input type="radio"/>            | <input checked="" type="radio"/> |
| You are satisfied regarding...  |   |                                  |                                  |                                  |                                  |
| the facility of using the prototype   | <input type="radio"/>   | <input type="radio"/>            | <input checked="" type="radio"/> | <input type="radio"/>            | <input type="radio"/>            |
| the prototype's interface   | <input type="radio"/>   | <input type="radio"/>            | <input type="radio"/>            | <input checked="" type="radio"/> | <input type="radio"/>            |
| the time required when using the prototype  | <input type="radio"/>   | <input type="radio"/>            | <input checked="" type="radio"/> | <input type="radio"/>            | <input type="radio"/>            |
| the relevance of the prototype's approach   | <input type="radio"/>   | <input checked="" type="radio"/> | <input type="radio"/>            | <input type="radio"/>            | <input type="radio"/>            |
| the relevance of the information brought by the prototype                                     | <input type="radio"/>   | <input type="radio"/>            | <input checked="" type="radio"/> | <input type="radio"/>            | <input type="radio"/>            |
| General comments  | The interface is directly usable without much preliminary instructions. Visualization in Rhino is pleasant and directly usable. I realized that my intuition is not necessarily just and that this type of decision-support tool would be very useful to me. The easy handling and intuitive interface are perfectly adapted for the purpose of the tool, which is complementary to other classical design tools. |                                  |                                  |                                  |                                  |
| Suggestions   | More complementary typologies when modeling.  |                                  |                                  |                                  |                                  |

**Ranking** Between the initial and intermediate ranking phases, we observe an increase in the level of success in Table C.5b, particularly for the energy need and production criteria. The final ranking is better than the intermediate one for the sDA and worse for the other two criteria. For the active solar potential, the participant may have been misled by the erroneous values displayed by the tool, due to the mistake in the algorithm as explained in section 6.1.

**Performance** VB is worse than VA for the energy need and production criteria, while very close in terms of sDA.

## Appendix C. Workshop

### Participant 4 - Engineer (3 years of experience)

Table C.7 – Participant 4’s (a) answers to the initial questionnaire and (b) results in the ranking phases according to the simulated performance of each variant.

(a) Previous experience with tools and performance evaluation.

|                               |                 | Conceptual               | Detailed | Both     |
|-------------------------------|-----------------|--------------------------|----------|----------|
| Experience with...            |                 |                          |          |          |
| Modeling tools                |                 | ArchiCAD, AutoCAD        |          | SketchUp |
| Simulation tools              |                 |                          |          | Lesosai  |
| Experience with evaluating... |                 |                          |          |          |
| Passive solar through:        | Rule-of-thumb   | heating, thermal comfort |          |          |
|                               | Visualization   |                          |          |          |
|                               | Simulation      |                          |          |          |
| Daylight through:             | Ext. consultant |                          |          |          |
|                               | Rule-of-thumb   |                          |          |          |
|                               | Visualization   |                          |          |          |
| Active solar through:         | Simulation      | x                        |          |          |
|                               | Ext. consultant |                          |          |          |
|                               | Rule-of-thumb   | x                        |          |          |
|                               | Visualization   |                          |          |          |
|                               | Simulation      |                          |          |          |
|                               | Ext. consultant |                          |          |          |

(b) Simulated performance of variants and ranking results.

|  |                | V1               | V2                 | V3               | VA                 | VB               | $\tau$ |
|--|----------------|------------------|--------------------|------------------|--------------------|------------------|--------|
| Simulated energy need [kWh/m <sup>2</sup> <sub>FAL</sub> ]       |                | 44.0             | 43.6               | 37.1             | 39.9               | 43.0             |        |
| Initial ranking  |                | Correctly ranked | Incorrectly ranked | Correctly ranked | Incorrectly ranked | Correctly ranked | 0      |
|  | Inter. ranking |                  |                    |                  |                    |                  | 0.67   |
|  | Final ranking  |                  |                    |                  |                    |                  | 0.60   |
| Simulated sDA [% <sub>FAL</sub> ]                                |                | 63.7             | 62.6               | 57.5             | 53.0               | 56.0             |        |
| Initial ranking  |                | Correctly ranked | Incorrectly ranked | Correctly ranked | Incorrectly ranked | Correctly ranked | -0.33  |
|  | Inter. ranking |                  |                    |                  |                    |                  | 0.33   |
|  | Final ranking  |                  |                    |                  |                    |                  | 0      |
| Simulated energy production [kWh/m <sup>2</sup> <sub>FAL</sub> ] |                | 61.3             | 56.4               | 60.8             | 65.3               | 69.4             |        |
| Initial ranking  |                | Correctly ranked | Incorrectly ranked | Correctly ranked | Incorrectly ranked | Correctly ranked | -0.33  |
|  | Inter. ranking |                  |                    |                  |                    |                  | 0      |
|  | Final ranking  |                  |                    |                  |                    |                  | 0.40   |

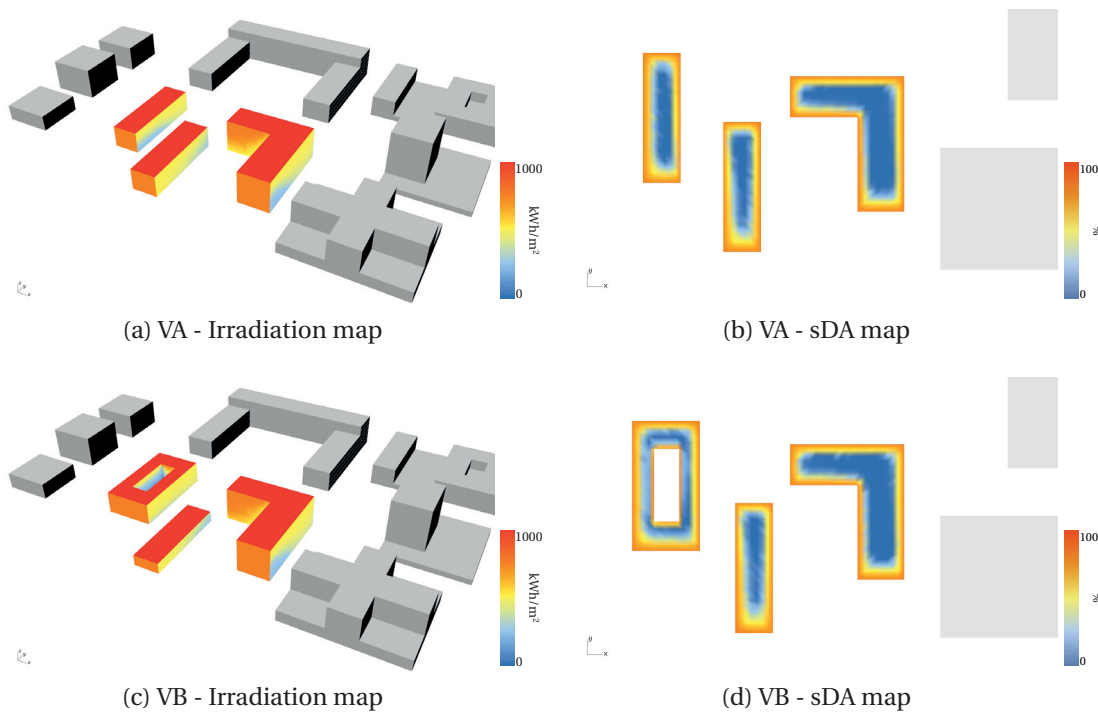


Figure C.7 – Variants submitted by participant 4.

Table C.8 – Participant 4’s answers to the final questionnaire.




|   | strongly disagree   | disagree              | neither agree nor disagree | agree                            | strongly agree                   |
|---|---|-----------------------|----------------------------|----------------------------------|----------------------------------|
| The usage of this prototype...  |   |                       |                            |                                  |                                  |
| allowed you to learn new elements useful in your approach to the problem                      | <input type="radio"/>   | <input type="radio"/> | <input type="radio"/>      | <input type="radio"/>            | <input checked="" type="radio"/> |
| influenced your approach to the problem   | <input type="radio"/>   | <input type="radio"/> | <input type="radio"/>      | <input type="radio"/>            | <input checked="" type="radio"/> |
| influenced your final concept   | <input type="radio"/>   | <input type="radio"/> | <input type="radio"/>      | <input type="radio"/>            | <input checked="" type="radio"/> |
| made you more confident in your decision-making   | <input type="radio"/>   | <input type="radio"/> | <input type="radio"/>      | <input type="radio"/>            | <input checked="" type="radio"/> |
| The usage of this prototype allowed you to learn about the performance criterion linked to... |   |                       |                            |                                  |                                  |
| the passive solar potential   | <input type="radio"/>   | <input type="radio"/> | <input type="radio"/>      | <input checked="" type="radio"/> | <input type="radio"/>            |
| daylight  | <input type="radio"/>   | <input type="radio"/> | <input type="radio"/>      | <input checked="" type="radio"/> | <input type="radio"/>            |
| the active solar potential  | <input type="radio"/>   | <input type="radio"/> | <input type="radio"/>      | <input checked="" type="radio"/> | <input type="radio"/>            |
| You are satisfied regarding...  |   |                       |                            |                                  |                                  |
| the facility of using the prototype   | <input type="radio"/>   | <input type="radio"/> | <input type="radio"/>      | <input type="radio"/>            | <input checked="" type="radio"/> |
| the prototype's interface   | <input type="radio"/>   | <input type="radio"/> | <input type="radio"/>      | <input checked="" type="radio"/> | <input type="radio"/>            |
| the time required when using the prototype  | <input type="radio"/>   | <input type="radio"/> | <input type="radio"/>      | <input type="radio"/>            | <input checked="" type="radio"/> |
| the relevance of the prototype's approach   | <input type="radio"/>   | <input type="radio"/> | <input type="radio"/>      | <input type="radio"/>            | <input checked="" type="radio"/> |
| the relevance of the information brought by the prototype                                     | <input type="radio"/>   | <input type="radio"/> | <input type="radio"/>      | <input checked="" type="radio"/> | <input type="radio"/>            |
| General comments  | Interesting exercise, somewhat unsettling to ask a computer to re-create by itself a representation of what we have imagined. Very interactive process, very positive for the evolution of the typology with respect to the three performance axes. Can be a very interesting tool to work on the first sketches taking into account the future solar performances. |                       |                            |                                  |                                  |
| Suggestions   | Differentiate in the interface between parameters that are building-specific versus those that apply to the whole design.   |                       |                            |                                  |                                  |
| Ranking   | There is an increase in the level of success between the initial and intermediate ranking phases in Table C.7b, with the final ranking similar to the intermediate one.   |                       |                            |                                  |                                  |
| Performance   | VB has a slightly higher daylight and active solar potential than VA.   |                       |                            |                                  |                                  |

## Appendix C. Workshop

### Participant 5 - Architect (6 years of experience)

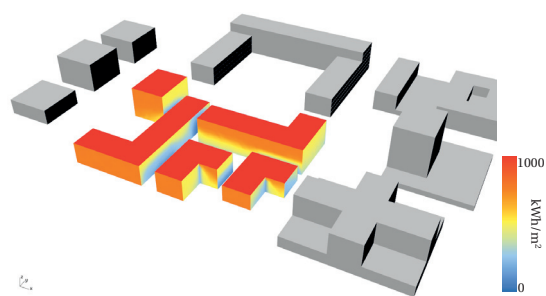
Table C.9 – Participant 5's (a) answers to the initial questionnaire and (b) results in the ranking phases according to the simulated performance of each variant.

(a) Previous experience with tools and performance evaluation.

|   |               | Conceptual               | Detailed                 | Both    |
|---|---------------|--------------------------|--------------------------|---------|
| Experience with...  |               |                          |                          |         |
| Modeling tools  |               | Rhino                    |                          | AutoCAD |
| Simulation tools  |               |                          |                          | Lesosai |
| Experience with evaluating...   |               |                          |                          |         |
| Passive solar<br>through:  | Rule-of-thumb | heating, thermal comfort |                          |         |
|   | Visualization | heating                  |                          |         |
|   | Simulation    |                          |                          |         |
| Daylight<br>through:       | Rule-of-thumb | x                        |                          |         |
|   | Visualization |                          |                          |         |
|   | Simulation    |                          |                          |         |
| Active solar<br>through:   | Rule-of-thumb | x                        |                          | x       |
|   | Visualization |                          |                          |         |
|   | Simulation    |                          |                          |         |
| Ext. consultant   |               |                          | heating, thermal comfort |         |
| Ext. consultant   |               |                          |                          | x       |
| Ext. consultant   |               |                          |                          | x       |

(b) Simulated performance of variants and ranking results.

|   | V1   | V2   | V3   | VA   | VB | $\tau$ |
|---|------|------|------|------|----|--------|
| Simulated energy need [kWh/m <sup>2</sup> <sub>Fa</sub> ]       | 44.0 | 43.6 | 37.1 | 40.6 |    |        |
| Initial ranking   |      |      |      |      |    | -0.67  |
| Inter. ranking  |      |      |      |      |    | 1      |
| Final ranking   |      |      |      |      |    |        |
| Simulated sDA [%F <sub>a</sub> ]                                | 63.7 | 62.6 | 57.5 | 46.1 |    |        |
| Initial ranking   |      |      |      |      |    | -0.33  |
| Inter. ranking  |      |      |      |      |    | 1      |
| Final ranking   |      |      |      |      |    |        |
| Simulated energy production [kWh/m <sup>2</sup> <sub>Fa</sub> ] | 61.3 | 56.4 | 60.8 | 63.0 |    |        |
| Initial ranking   |      |      |      |      |    | 1      |
| Inter. ranking  |      |      |      |      |    | 1      |
| Final ranking   |      |      |      |      |    |        |



(a) VA - Irradiation map



(b) VA - sDA map

Figure C.8 – Variant submitted by participant 5.

Table C.10 – Participant 5's answers to the final questionnaire.

|   | strongly disagree   | disagree              | neither agree nor disagree       | agree                            | strongly agree                   |
|---|---|-----------------------|----------------------------------|----------------------------------|----------------------------------|
| The usage of this prototype...  |   |                       |                                  |                                  |                                  |
| allowed you to learn new elements useful in your approach to the problem                      | <input type="radio"/>   | <input type="radio"/> | <input type="radio"/>            | <input checked="" type="radio"/> | <input type="radio"/>            |
| influenced your approach to the problem   | <input type="radio"/>   | <input type="radio"/> | <input type="radio"/>            | <input checked="" type="radio"/> | <input type="radio"/>            |
| influenced your final concept   | <input type="radio"/>   | <input type="radio"/> | <input checked="" type="radio"/> | <input type="radio"/>            | <input type="radio"/>            |
| made you more confident in your decision-making   | <input type="radio"/>   | <input type="radio"/> | <input checked="" type="radio"/> | <input type="radio"/>            | <input type="radio"/>            |
| The usage of this prototype allowed you to learn about the performance criterion linked to... |   |                       |                                  |                                  |                                  |
| the passive solar potential   | <input type="radio"/>   | <input type="radio"/> | <input type="radio"/>            | <input type="radio"/>            | <input checked="" type="radio"/> |
| daylight  | <input type="radio"/>   | <input type="radio"/> | <input type="radio"/>            | <input type="radio"/>            | <input checked="" type="radio"/> |
| the active solar potential  | <input type="radio"/>   | <input type="radio"/> | <input type="radio"/>            | <input type="radio"/>            | <input checked="" type="radio"/> |
| You are satisfied regarding...  |   |                       |                                  |                                  |                                  |
| the facility of using the prototype   | <input type="radio"/>   | <input type="radio"/> | <input type="radio"/>            | <input type="radio"/>            | <input checked="" type="radio"/> |
| the prototype's interface   | <input type="radio"/>   | <input type="radio"/> | <input type="radio"/>            | <input type="radio"/>            | <input checked="" type="radio"/> |
| the time required when using the prototype  | <input type="radio"/>   | <input type="radio"/> | <input type="radio"/>            | <input type="radio"/>            | <input checked="" type="radio"/> |
| the relevance of the prototype's approach   | <input type="radio"/>   | <input type="radio"/> | <input type="radio"/>            | <input checked="" type="radio"/> | <input type="radio"/>            |
| the relevance of the information brought by the prototype                                     | <input type="radio"/>   | <input type="radio"/> | <input type="radio"/>            | <input checked="" type="radio"/> | <input type="radio"/>            |
| General comments  | Pleasant interface. Results quickly and easily comparable. Pleasant visualization, except for graphs (hard to read). Very promising and interesting tool.   |                       |                                  |                                  |                                  |
| Suggestions   | Integrate program types. Increase resolution in decisions on dimensions for individual buildings. Be able to integrate street network, green areas, facade materials. Possibility of importing 3D models,.  |                       |                                  |                                  |                                  |
| Issue   | This participant experienced some difficulties in re-creating something similar to their VA when using the prototype. They did not provide a VB and final ranking. The problem is likely to have been caused by the complexity of the design, with multiple and closely positioned buildings of varying dimensions. Following the user-inputs, the prototype kept searching for valid solutions and had to be forced to restart considering the limited duration of the workshop. |                       |                                  |                                  |                                  |
| Ranking   | There is an increase in the level of success between the initial and intermediate ranking phases in Table C.9b for the passive solar and daylight criteria, the active solar showing a perfect ranking in both phases.  |                       |                                  |                                  |                                  |

## Appendix C. Workshop

### Participant 6 - Architect / Urban designer (6 years of experience)

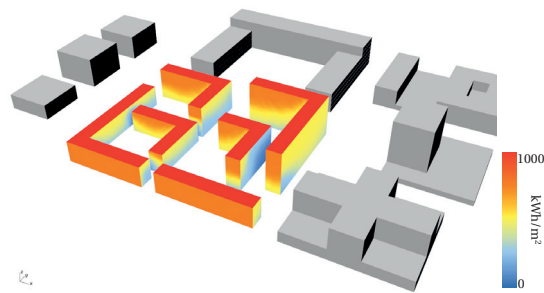
Table C.11 – Participant 6's (a) answers to the initial questionnaire and (b) results in the ranking phases according to the simulated performance of each variant.

(a) Previous experience with tools and performance evaluation.

| Experience with...            |                                 | Conceptual | Detailed | Both            |
|-------------------------------|---------------------------------|------------|----------|-----------------|
| Modeling tools                | Rhino, Grasshopper, Vectorworks |            |          | AutoCAD         |
| Simulation tools              |                                 | Lesosai    |          |                 |
| Experience with evaluating... |                                 |            |          |                 |
| Passive solar through:        | Rule-of-thumb                   | heating    |          | thermal comfort |
|                               | Visualization                   | heating    |          | thermal comfort |
|                               | Simulation                      |            |          |                 |
| Daylight through:             | Rule-of-thumb                   |            |          | x               |
|                               | Visualization                   | x          |          |                 |
|                               | Simulation                      |            |          |                 |
| Active solar through:         | Rule-of-thumb                   |            |          | x               |
|                               | Visualization                   | x          |          |                 |
|                               | Simulation                      |            |          |                 |
|                               | Ext. consultant                 |            |          |                 |

(b) Simulated performance of variants and ranking results.

|  | V1   | V2   | V3   | VA   | VB | $\tau$ |
|--|------|------|------|------|----|--------|
| Simulated energy need [kWh/m <sup>2</sup> <sub>FAL</sub> ]       | 44.0 | 43.6 | 37.1 | 51.9 |    |        |
| Initial ranking  |      |      |      |      |    | 0.67   |
| Inter. ranking   |      |      |      |      |    | 1      |
| Final ranking  |      |      |      |      |    |        |
| Simulated sDA [% <sub>FAL</sub> ]                                | 63.7 | 62.6 | 57.5 | 73.3 |    |        |
| Initial ranking  |      |      |      |      |    | 0      |
| Inter. ranking   |      |      |      |      |    | 0.33   |
| Final ranking  |      |      |      |      |    |        |
| Simulated energy production [kWh/m <sup>2</sup> <sub>FAL</sub> ] | 61.3 | 56.4 | 60.8 | 73.3 |    |        |
| Initial ranking  |      |      |      |      |    | 1      |
| Inter. ranking   |      |      |      |      |    | 1      |
| Final ranking  |      |      |      |      |    |        |



(a) VA - Irradiation map



(b) VA - sDA map

Figure C.9 – Variant submitted by participant 6.



Table C.12 – Participant 6’s answers to the final questionnaire.

|   | strongly disagree   | disagree              | neither agree nor disagree | agree                            | strongly agree                   |
|---|---|-----------------------|----------------------------|----------------------------------|----------------------------------|
| The usage of this prototype...  |   |                       |                            |                                  |                                  |
| allowed you to learn new elements useful in your approach to the problem                      | <input type="radio"/>   | <input type="radio"/> | <input type="radio"/>      | <input checked="" type="radio"/> | <input type="radio"/>            |
| influenced your approach to the problem   | <input type="radio"/>   | <input type="radio"/> | <input type="radio"/>      | <input checked="" type="radio"/> | <input type="radio"/>            |
| influenced your final concept   | <input type="radio"/>   | <input type="radio"/> | <input type="radio"/>      | <input type="radio"/>            | <input checked="" type="radio"/> |
| made you more confident in your decision-making   | <input type="radio"/>   | <input type="radio"/> | <input type="radio"/>      | <input checked="" type="radio"/> | <input type="radio"/>            |
| The usage of this prototype allowed you to learn about the performance criterion linked to... |   |                       |                            |                                  |                                  |
| the passive solar potential   | <input type="radio"/>   | <input type="radio"/> | <input type="radio"/>      | <input checked="" type="radio"/> | <input type="radio"/>            |
| daylight  | <input type="radio"/>   | <input type="radio"/> | <input type="radio"/>      | <input checked="" type="radio"/> | <input type="radio"/>            |
| the active solar potential  | <input type="radio"/>   | <input type="radio"/> | <input type="radio"/>      | <input checked="" type="radio"/> | <input type="radio"/>            |
| You are satisfied regarding...  |   |                       |                            |                                  |                                  |
| the facility of using the prototype   | <input type="radio"/>   | <input type="radio"/> | <input type="radio"/>      | <input type="radio"/>            | <input checked="" type="radio"/> |
| the prototype's interface   | <input type="radio"/>   | <input type="radio"/> | <input type="radio"/>      | <input type="radio"/>            | <input checked="" type="radio"/> |
| the time required when using the prototype  | <input type="radio"/>   | <input type="radio"/> | <input type="radio"/>      | <input type="radio"/>            | <input checked="" type="radio"/> |
| the relevance of the prototype's approach   | <input type="radio"/>   | <input type="radio"/> | <input type="radio"/>      | <input type="radio"/>            | <input checked="" type="radio"/> |
| the relevance of the information brought by the prototype                                     | <input type="radio"/>   | <input type="radio"/> | <input type="radio"/>      | <input type="radio"/>            | <input checked="" type="radio"/> |
| General comments  | Easy and intuitive.   |                       |                            |                                  |                                  |
| Suggestions   | With increased modeling capabilities, the development of unusual typologies can become very interesting with this tool. |                       |                            |                                  |                                  |

**Issue** This participant could not re-creating something similar to their VA when using the prototype and did not provide a VB and final ranking. Similarly to participant 5, the complexity of the design with nested L-shaped buildings could seemingly not be handled by the prototype, which kept searching for valid solutions.

**Ranking** The active solar potential shows a perfect ranking for both phases, while there is an increase in the level of success between the initial and intermediate rankings for the other two criteria in Table C.11b.

## Appendix C. Workshop

### Participant 7 - Architect / Urban designer (7.5 years of experience)

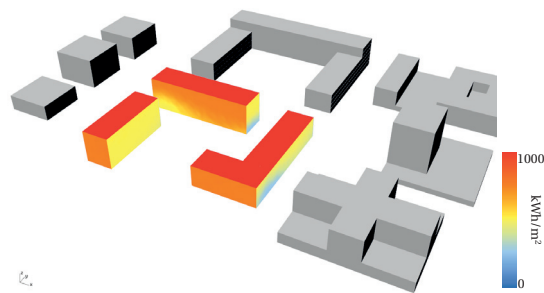
Table C.13 – Participant 7's (a) answers to the initial questionnaire and (b) results in the ranking phases according to the simulated performance of each variant.

(a) Previous experience with tools and performance evaluation.

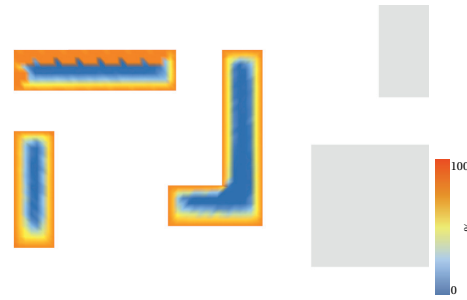
| Experience with...            | Conceptual                             | Detailed | Both              |
|-------------------------------|--|----------|-------------------|
| Modeling tools                | Rhino, SketchUp, ArchiCAD, Vectorworks |          | AutoCAD, ArchiCAD |
| Simulation tools              |  |          |                   |
| Experience with evaluating... |  |          |                   |
| Passive solar through:        | Rule-of-thumb                          |          |                   |
| Visualization                 | heating                                |          |                   |
| Simulation                    | thermal comfort                        |          |                   |
| Ext. consultant               | thermal comfort                        |          | heating           |
| Daylight through:             | Rule-of-thumb                          |          |                   |
| Visualization                 |  |          |                   |
| Simulation                    | x                                      |          |                   |
| Ext. consultant               | x                                      |          |                   |
| Active solar through:         | Rule-of-thumb                          |          |                   |
| Visualization                 | x                                      |          |                   |
| Simulation                    | x                                      |          |                   |
| Ext. consultant               |  |          |                   |

(b) Simulated performance of variants and ranking results.

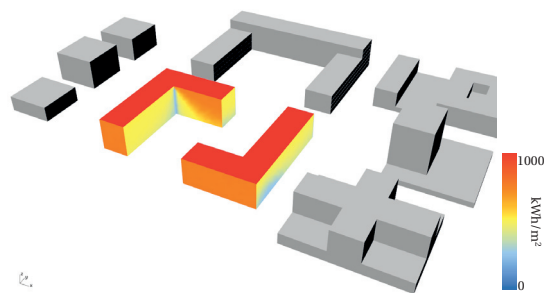
|  | V1                 | V2                 | V3               | VA               | VB                 | $\tau$ |
|--|--------------------|--------------------|------------------|------------------|--------------------|--------|
| Simulated energy need [kWh/m <sup>2</sup> <sub>FAL</sub> ]       | 44.0               | 43.6               | 37.1             | 39.3             | 38.9               |        |
| Initial ranking  | Incorrectly ranked | Incorrectly ranked | Correctly ranked | Correctly ranked | Correctly ranked   | 0.67   |
| Inter. ranking   | Incorrectly ranked | Incorrectly ranked | Correctly ranked | Correctly ranked | Correctly ranked   | 0.33   |
| Final ranking  | Incorrectly ranked | Incorrectly ranked | Correctly ranked | Correctly ranked | Correctly ranked   | 0.60   |
| Simulated sDA [% <sub>FAL</sub> ]                                | 63.7               | 62.6               | 57.5             | 57.0             | 53.6               |        |
| Initial ranking  | Correctly ranked   | Correctly ranked   | Correctly ranked | Correctly ranked | Correctly ranked   | 0      |
| Inter. ranking   | Correctly ranked   | Correctly ranked   | Correctly ranked | Correctly ranked | Correctly ranked   | 0.33   |
| Final ranking  | Correctly ranked   | Correctly ranked   | Correctly ranked | Correctly ranked | Incorrectly ranked | 0.20   |
| Simulated energy production [kWh/m <sup>2</sup> <sub>FAL</sub> ] | 61.3               | 56.4               | 60.8             | 64.7             | 60.8               |        |
| Initial ranking  | Correctly ranked   | Correctly ranked   | Correctly ranked | Correctly ranked | Correctly ranked   | 1      |
| Inter. ranking   | Correctly ranked   | Correctly ranked   | Correctly ranked | Correctly ranked | Correctly ranked   | 1      |
| Final ranking  | Correctly ranked   | Correctly ranked   | Correctly ranked | Correctly ranked | Incorrectly ranked | 0.80   |



(a) VA - Irradiation map



(b) VA - sDA map



(c) VB - Irradiation map

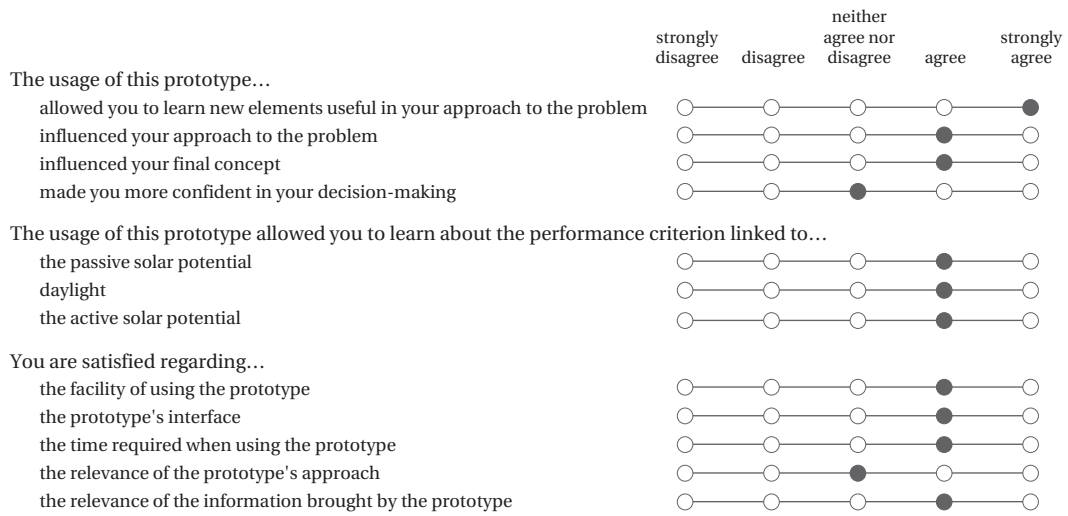


(d) VB - sDA map

Figure C.10 – Variants submitted by participant 7.

## C.4. Results per participant

Table C.14 – Participant 7's answers to the final questionnaire.



General comments Interesting and useful tool since it allows evaluating multiple variants through criteria that are not often present when designing an urban form at the beginning of a project. The impression I got is that the tool does not try to impose an optimal urban form based on energy-related criteria, which are surely important for sustainable development, but that do not necessarily generate 'urbanity' and quality of public spaces (which remain priorities in the urban project). Rather, the tool wants to attract the attention of the user on elements of thought that will anyway have to be integrated into the project. This tool allows addressing these in advance.

Suggestions The tool should not propose buildings that cannot be assigned a residential or other function due to their dimensions. The interface should allow more freedom in defining built forms.

Ranking Table C.13b displays no striking differences between the ranking phases. For the active solar criterion, the participant may have been misguided by the tool in the final ranking phase, due to the bug in the algorithm as mentioned earlier.

Performance VB is slightly worse than VA in terms of daylight and active solar potential.

## Appendix C. Workshop

### Participant 8 - Architect (2 years of experience)

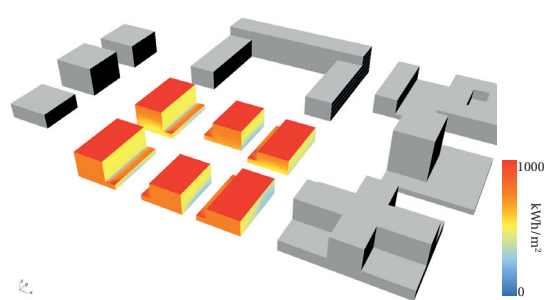
Table C.15 – Participant 8's (a) answers to the initial questionnaire and (b) results in the ranking phases according to the simulated performance of each variant.

(a) Previous experience with tools and performance evaluation.

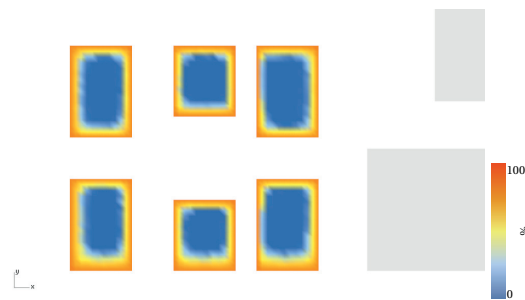
| Experience with...            |                 | Conceptual                   | Detailed | Both            |
|-------------------------------|-----------------|------------------------------|----------|-----------------|
| Modeling tools                |                 | SketchUp, Grasshopper, Revit |          | Rhino, AutoCAD  |
| Simulation tools              |                 |                              |          | Ecotect         |
| Experience with evaluating... |                 |                              |          |                 |
| Passive solar through:        | Rule-of-thumb   | heating, thermal comfort     |          |                 |
|                               | Visualization   | heating                      |          |                 |
|                               | Simulation      | heating                      |          |                 |
|                               | Ext. consultant | heating                      |          | thermal comfort |
| Daylight through:             | Rule-of-thumb   | x                            |          |                 |
|                               | Visualization   |                              |          |                 |
|                               | Simulation      | x                            |          |                 |
|                               | Ext. consultant |                              |          | x               |
| Active solar through:         | Rule-of-thumb   | x                            |          |                 |
|                               | Visualization   | x                            |          |                 |
|                               | Simulation      | x                            |          |                 |
|                               | Ext. consultant |                              |          | x               |

(b) Simulated performance of variants and ranking results.

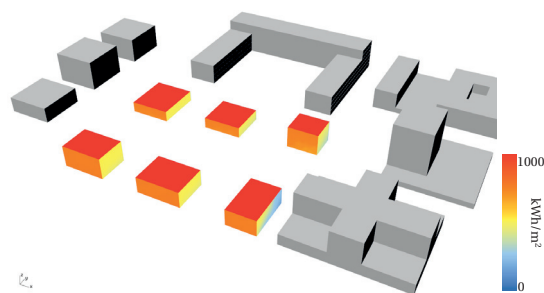
|   | V1   | V2   | V3   | VA   | VB   | $\tau$ |
|---|------|------|------|------|------|--------|
| Simulated energy need [kWh/m <sup>2</sup> <sub>Fa</sub> ]       | 44.0 | 43.6 | 37.1 | 41.6 | 44.8 |        |
| Initial ranking   |      |      |      |      |      | 0.67   |
| Inter. ranking  |      |      |      |      |      | 1      |
| Final ranking   |      |      |      |      |      | 0.40   |
| Simulated sDA [%Fa]   | 63.7 | 62.6 | 57.5 | 45.1 | 60.1 |        |
| Initial ranking   |      |      |      |      |      | -1     |
| Inter. ranking  |      |      |      |      |      | 0.67   |
| Final ranking   |      |      |      |      |      | 0.80   |
| Simulated energy production [kWh/m <sup>2</sup> <sub>Fa</sub> ] | 61.3 | 56.4 | 60.8 | 77.6 | 87.3 |        |
| Initial ranking   |      |      |      |      |      | 1      |
| Inter. ranking  |      |      |      |      |      | 1      |
| Final ranking   |      |      |      |      |      | 0.20   |



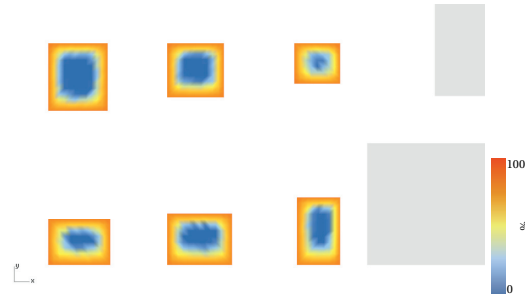
(a) VA - Irradiation map



(b) VA - sDA map



(c) VB - Irradiation map



(d) VB - sDA map

Figure C.11 – Variants submitted by participant 8.

Table C.16 – Participant 8’s answers to the final questionnaire.

|   | strongly disagree   | disagree              | neither agree nor disagree       | agree                            | strongly agree                   |
|---|---|-----------------------|----------------------------------|----------------------------------|----------------------------------|
| The usage of this prototype...  |   |                       |                                  |                                  |                                  |
| allowed you to learn new elements useful in your approach to the problem                      | <input type="radio"/>   | <input type="radio"/> | <input type="radio"/>            | <input checked="" type="radio"/> | <input type="radio"/>            |
| influenced your approach to the problem   | <input type="radio"/>   | <input type="radio"/> | <input type="radio"/>            | <input checked="" type="radio"/> | <input type="radio"/>            |
| influenced your final concept   | <input type="radio"/>   | <input type="radio"/> | <input type="radio"/>            | <input type="radio"/>            | <input checked="" type="radio"/> |
| made you more confident in your decision-making   | <input type="radio"/>   | <input type="radio"/> | <input type="radio"/>            | <input type="radio"/>            | <input checked="" type="radio"/> |
| The usage of this prototype allowed you to learn about the performance criterion linked to... |   |                       |                                  |                                  |                                  |
| the passive solar potential   | <input type="radio"/>   | <input type="radio"/> | <input type="radio"/>            | <input checked="" type="radio"/> | <input type="radio"/>            |
| daylight  | <input type="radio"/>   | <input type="radio"/> | <input type="radio"/>            | <input type="radio"/>            | <input checked="" type="radio"/> |
| the active solar potential  | <input type="radio"/>   | <input type="radio"/> | <input checked="" type="radio"/> | <input type="radio"/>            | <input type="radio"/>            |
| You are satisfied regarding...  |   |                       |                                  |                                  |                                  |
| the facility of using the prototype   | <input type="radio"/>   | <input type="radio"/> | <input type="radio"/>            | <input checked="" type="radio"/> | <input type="radio"/>            |
| the prototype's interface   | <input type="radio"/>   | <input type="radio"/> | <input type="radio"/>            | <input type="radio"/>            | <input checked="" type="radio"/> |
| the time required when using the prototype  | <input type="radio"/>   | <input type="radio"/> | <input type="radio"/>            | <input type="radio"/>            | <input checked="" type="radio"/> |
| the relevance of the prototype's approach   | <input type="radio"/>   | <input type="radio"/> | <input checked="" type="radio"/> | <input type="radio"/>            | <input type="radio"/>            |
| the relevance of the information brought by the prototype                                     | <input type="radio"/>   | <input type="radio"/> | <input type="radio"/>            | <input checked="" type="radio"/> | <input type="radio"/>            |
| General comments  | The tool works very well, we only have to understand the possibilities in terms of available form and the relation with our variant A.  |                       |                                  |                                  |                                  |
| Suggestions   | Directly see on the buildings a window with their dimensions. Be able to see our initial design as a background image. Have a middle or entrance point when positioning buildings. Be able to visualize the shadows on the ground (open space). |                       |                                  |                                  |                                  |

**Ranking** There is an increase in the level of success between the initial and intermediate ranking phases for the energy need and daylight criteria in Table C.15b. The final ranking is similar to the intermediate one for the sDA, but worse for the energy need and production, the latter possibly caused by the erroneous values seen by the participant.

**Performance** VB is better in terms of daylight and active solar potential.



# Acronyms

- ach** air changes per hour. 110
- ANN** artificial neural networks. 91, 93, 95
- ASHRAE** American Society of Heating, Refrigerating and Air-Conditioning Engineers. 34
- BIM** building information modeling. 31, 33
- BPS** building performance simulation. xi, 8, 14, 17, 19, 36
- CA(A)D** computer-aided (architectural) design/drafting. 14, 15, 17, 20, 22, 28, 31, 33, 41
- CFD** computational fluid dynamics. 30, 43, 109, 148
- DA** Daylight Autonomy. xiv, 31, 65, 67, 224
- DDS** design decision-support. ix, xii, 9–11, 13, 19–21, 36, 44–47, 54, 85, 87, 89, 138, 143, 146, 147, 149, 165, 175, 179, 183, 185, 187, 191–193
- DEM** digital elevation model. xv, 23, 26, 99
- DF** Daylight Factor. 27, 29, 31
- DHW** Domestic Hot Water. 63, 143
- DOE** US Department of Energy. 17
- DoE** Design of Experiment. xv, 95, 106, 144
- EU** European Union. 1
- FAR** Floor Area Ratio. 24, 47, 58
- GA** genetic algorithms. 38, 39, 91, 93, 95, 148, 193
- GHG** greenhouse gases. 1, 2
- GIS** geographic information system. 22, 28, 35, 95
- GP** Gaussian Processes. xvii, xviii, xxii, 95, 141, 142, 183, 185

## Acronyms

---

- GUI** graphical user interface. 14
- HVAC** Heating, Ventilation and Air Conditioning. 64
- IEA** International Energy Agency. 15, 17
- LCA** life cycle analysis. 15
- LoD** Level of Detail. 53, 54, 58, 59, 97
- LT** Lighting and Thermal. xii, 25, 26, 35
- MIT** Massachusetts Institute of Technology. 33, 36
- NZEB** Net Zero-Energy Building. 17
- PDL** Plan Directeur Localisé. xi, xv, xviii, xxi, 4, 6, 50, 57, 97, 98, 166, 193
- PDP** Partial Dependence Plot. 135
- PercErr** Percentage Error. 123, 124, 139
- PV** photovoltaic. xiv, xxi, 15, 28, 29, 45, 49, 60–63, 69, 70, 76–78, 85, 143, 158, 192
- R<sup>2</sup>** Coefficient of Determination. 123–126, 139, 182, 183
- RMSE** Root Mean Square Error. 123–126, 130, 132, 139, 182, 183
- sDA** spatial Daylight Autonomy. xiv–xvi, xviii, 48, 65, 67, 74–76, 79, 81–85, 111, 116, 121, 123, 143, 153, 169, 170, 192, 225, 227–231, 233, 235, 237, 239, 240
- SE** Solar Envelope. xii, 21–24, 43
- SHC** Solar Heating & Cooling programme. 15
- SIA** Société Suisse des ingénieurs et architectes. xvi, 2, 5, 33, 109, 113, 116, 117
- SSE** Sum of Squared Error. 124
- SST** Total Sum of Squares. 124
- ST** solar thermal. xiv, xxi, 15, 28, 29, 45, 49, 60–63, 69, 70, 77, 78, 85, 143, 158, 192
- std** Standard Deviation. 130, 135, 180, 182
- SV** Solar Volume. 22
- SVF** sky view factor. 23, 24, 30
- SVM** support vector machines. 91, 93
- UHI** urban heat island. 23
- UK** United Kingdom. 5
- US** United States. 5, 22, 28, 95



# Bibliography

- Abdi, H.** (2007). The Kendall Rank Correlation Coefficient. In *Encyclopedia of Measurement and Statistics*. Thousand Oaks (CA): Sage.
- Aguacil Moreno, S., Lufkin, S. and Rey, E.** (2016). Towards integrated design strategies for implementing BIPV systems into urban renewal processes: first case study in Neuchâtel (Switzerland). In *Proceedings of SBE16*. Zurich, Switzerland.
- Alsaadani, S. and De Souza, C. B.** (2012). The Social Component Of Building Performance Simulation: Understanding Architects. In J. Wright and M. Cook, eds., *Proceedings of BSO12*. Loughborough, UK. ISBN 978-1-897911-42-6.
- Andersen, M., Kleindienst, S., Yi, L., Lee, J., Bodart, M. and Cutler, B.** (2008). An intuitive day-lighting performance analysis and optimization approach. *Building Research & Information* **36**, 593–607.
- Andersen, M. and Nault, E.** (2013). Influence de la forme urbaine sur le potentiel solaire. In E. Rey, ed., *Green Density*. Lausanne: Presses Polytechniques et Universitaires Romandes (PPUR), pages 51–72.
- Asadi, S., Amiri, S. S. and Mottahedi, M.** (2014). On the development of multi-linear regression analysis to assess energy consumption in the early stages of building design. *Energy and Buildings* **85**, 246–255. ISSN 0378-7788.
- Attia, S., De Herde, A., Gratia, E. and Hensen, J. L. M.** (2013a). Achieving informed decision-making for net zero energy buildings design using building performance simulation tools. *Building Simulation* **6**, 3–21. ISSN 1996-3599, 1996-8744.
- Attia, S., Gratia, E., De Herde, A. and Hensen, J. L.** (2012). Simulation-based decision support tool for early stages of zero-energy building design. *Energy and Buildings* **49**, 2–15. ISSN 03787788.
- Attia, S., Hamdy, M., O'Brien, W. and Carlucci, S.** (2013b). Assessing gaps and needs for integrating building performance optimization tools in net zero energy buildings design. *Energy and Buildings* **60**, 110–124. ISSN 0378-7788.
- Baker, N.** (1992). The LT Method version 1.2 - Energy Design Tool for Non Domestic Buildings. Technical report, Commission of the European Communities, Directorate-General for Science, Research and Development.

## Bibliography

---

- Baker, N. and Steemers, K.** (1996). LT Method 3.0—a strategic energy-design tool for Southern Europe. *Energy and buildings* **23**, 251–256.
- Baker, N. and Steemers, K.** (2000). *Energy and environment in architecture: a technical design guide*. New York: E&FN Spon. ISBN 978-0-419-22770-0.
- Bauart Architectes et Urbanistes SA, Transitec Ingénieurs-Conseils, P+ Génie de l'environnement, raderschallpartner AG Landschaftsarchitekten, Vogt & Partner Lichtgestaltende Ingenieure, ADR Sàrl and Jaquier & Pointet SA** (2010). Plan Directeur Localisé Gare-Lac. Technical report, Yverdon-les-Bains.
- Beckers, B. and Rodriguez, D.** (2009). Helping architects to design their personal daylight. *WSEAS Transactions on Environment and Development* **5**, 467–477.
- Bektas Ekici, B. and Aksoy, U. T.** (2011). Prediction of building energy needs in early stage of design by using ANFIS. *Expert Systems with Applications* **38**, 5352–5358. ISSN 0957-4174.
- Birdsall, B., Buhl, W. F., Ellington, K. L., Erdem, A. E. and Winkelmann, F. C.** (1990). Overview of the DOE-2 building energy analysis program. LBL-19735m rev. w, Lawrence Berkeley Laboratory, Berkeley, CA.
- Boeykens, S. and Neuckermans, H.** (2003). Implementation strategy for an architectural design environment; Issues in the development of IDEA+. In *Proceedings of IPRC*. Lisbon, Portugal.
- Branko, K.** (2003). Computing the Performative in Architecture. In *Proceeding of eCAADe*. Graz, Austria.
- BRE** (2013). BREEAM Communities. Technical report, Building Research Establishment (BRE).
- Bruno, M., Henderson, K. and Kim, H. M.** (2011). Multi-objective Optimization in Urban Design. In *Proceedings of SimAUD'11*. San Diego, CA, USA: Society for Computer Simulation International.
- Burton, E., Jenks, M. and Williams, K.** (2003). *The Compact City: A Sustainable Urban Form?*. Routledge. ISBN 1-135-81698-0.
- Caldas, L.** (2006). GENE\_arch: an evolution-based generative design system for sustainable architecture. In *Intelligent Computing in Engineering and Architecture*. Springer, pages 109–118.
- Caldas, L.** (2008). Generation of energy-efficient architecture solutions applying GENE\_arch: An evolution-based generative design system. *Advanced Engineering Informatics* **22**, 59–70. ISSN 14740346.
- Caldas, L.** (2011). Generation of Energy-Efficient Patio Houses: Combining GENE\_arch and a Marrakesh Medina Shape Grammar. In *Proceedings of AAAI Spring Symposium: Artificial Intelligence and Sustainable Design*.
- Caldas, L. G. and Norford, L. K.** (2002). A design optimization tool based on a genetic algorithm. *Automation in construction* **11**, 173–184.

- Canton de Vaud** (2014). Loi sur l'énergie (LVLEne) - 730.01.
- Canton de Vaud** (2015). Plan Directeur Cantonal. Technical Report Adaptation 3, Département du territoire et de l'environnement, Service du développement territorial, Lausanne.
- Capeluto, I. and Shaviv, E.** (1999). Modeling the design of urban fabric with solar rights considerations. In *Proceedings of ISES Solar World Congress*.
- Capeluto, I. and Shaviv, E.** (2001). On the use of 'Solar Volume' for determining the urban fabric. *Solar Energy* **70**, 275–280.
- Capeluto, I., Yezioro, A., Bleiberg, T. and Shaviv, E.** (2005). From computer models to simple design tools: Solar rights in the design of urban streets. In *Proceedings of Building Simulation (IBPSA)*. Montréal, Canada.
- Capeluto, I. G., Yezioro, A., Bleiberg, T. and Shaviv, E.** (2006). Solar Rights in the Design of Urban Spaces. In *Proceedings of PLEA*. Geneva, Switzerland.
- Capozzoli, A., Mechri, H. E. and Corrado, V.** (2009). Impacts of architectural design choices on building energy performance applications of uncertainty and sensitivity techniques. In *Proceedings of Building Simulation (IBPSA)*. Glasgow, Scotland.
- Chatzipoulka, C., Compagnon, R. and Nikolopoulou, M.** (2015). Comparing the solar performance of urban forms in London. In *Proceedings of PLEA*. Bologna, Italy.
- Cheng, V.** (2010). Understanding density and high density. In E. Ng, ed., *Designing high-density cities for social and environmental sustainability*. pages 3–17.
- Cheng, V., Steemers, K., Montavon, M. and Compagnon, R.** (2006). Urban form, density and solar potential. In *Proceedings of PLEA*. Geneva, Switzerland.
- Claro, A., Pereira, F. O. and Ledo, R. Z.** (2005). APOLUX – An Innovative Computer Code for Daylight Design and Analysis in Architecture and Urbanism. In *Proceedings of Building Simulation (IBPSA)*.
- Compagnon, R.** (2000). PRECis: Assessing the Potential for Renewable Energy in Cities. *Annexe 3: Solar and Daylight availability in urban areas*.
- Compagnon, R.** (2004). Solar and daylight availability in the urban fabric. *Energy and Buildings* **36**, 321–328. ISSN 0378-7788.
- Compagnon, R., Antonutto, G., Longato, P. and Rotsch, A.** (2015). Assessing daylight and sunlight access in the built environment: A new tool for planners and designers. In *Proceedings of PLEA*. Bologna, Italy.
- Confédération Suisse** (1998). Loi sur l'énergie (LEne), status as of 2014 (revision).
- Conseil d'Etat du Canton de Vaud** (2014). Règlement d'application de la loi sur l'aménagement du territoire et les constructions (RLATC). Etat au 01.05.2014 (en vigueur).
- Couckuyt, I. and Dhaene, T.** (2016). SURrogate Modeling (SUMO) Toolbox: Tutorial (<http://www.sumo.intec.ugent.be/>, last accessed on January 18, 2016).

## Bibliography

---

- Crawley, D. B., Pedersen, C. O., Lawrie, L. K. and Winkelmann, F. C.** (2000). EnergyPlus: Energy Simulation Program. *ASHRAE Journal* **42**, 49–56.
- Cronemberger, J., Caamaño-Martín, E. and Sánchez, S. V.** (2012). Assessing the solar irradiation potential for solar photovoltaic applications in buildings at low latitudes – Making the case for Brazil. *Energy and Buildings* **55**, 264–272. ISSN 0378-7788.
- Danielski, I.** (2011). Energy variations in apartment buildings due to different shape factors and relative size of common areas. *District heating* **140**, 50.
- De Groot, E., Zonneveldt, L., Paule, B. and SA, E.** (2003). Dial Europe: A decision support tool for early lighting design. In *Proceedings of Building Simulation (IBPSA)*. Eindhoven, The Netherlands.
- Depecker, P., Menezo, C., Virgone, J. and Lepers, S.** (2001). Design of buildings shape and energetic consumption. *Building and Environment* **36**, 627–635.
- Deru, M., Field, K., Studer, D., Benne, K., Griffith, B., Torcellini, P., Liu, B., Halverson, M., Winiarski, D., Rosenberg, M., Yazdani, M., Huang, J. and Crawley, D.** (2011). U.S. Department of Energy commercial reference building models of the national building stock. Technical report.
- Doelling, M. C.** (2014). Space-Based Thermal Metrics Mapping for Conceptual Low-Energy Architectural Design. In *Proceedings of Building Simulation & Optimization (BSO)*. London, UK.
- Dogan, T., Reinhart, C. and Michalatos, P.** (2012). Urban Daylight Simulation : calculating the daylight area of urban designs. In *Proceedings of SimBuild*. Madison, Wisconsin, USA.
- Dogan, T., Reinhart, C. and Michalatos, P.** (2015). Autozoner: an algorithm for automatic thermal zoning of buildings with unknown interior space definitions. *Journal of Building Performance Simulation* **0**, 1–14. ISSN 1940-1493.
- E Source** (2006). Integrated Building Design - Design Brief.
- Ebden, M.** (2008). Gaussian Processes for Regression: A Quick Introduction. Technical report, University of Oxford.
- Eicker, U., Monien, D., Duminil, r. and Nouvel, R.** (2015). Energy performance assessment in urban planning competitions. *Applied Energy* **155**, 323–333. ISSN 0306-2619.
- Eisenhower, B., O'Neill, Z., Narayanan, S., Fonoberov, V. A. and Mezić, I.** (2012). A methodology for meta-model based optimization in building energy models. *Energy and Buildings* **47**, 292–301. ISSN 0378-7788.
- Ekici, B. B. and Aksoy, U. T.** (2009). Prediction of building energy consumption by using artificial neural networks. *Advances in Engineering Software* **40**, 356–362. ISSN 0965-9978.
- Elghazi, Y., Wagdy, A., Mohamed, S. and Hassan, A.** (2014). Daylighting driven design: optimizing kaleidocycle facade for hot arid climate. In *Proceedings of BauSIM*. RWTH Aachen University.

- EnDK and EnFK** (2014). Modèle de prescriptions énergétiques des cantons (MoPEC). Technical Report Edition 2014, Conférence des directeurs cantonaux de l'énergie.
- EnergyPlus** (2014). EnergyPlus Weather Data (<https://energyplus.net/weather>, last accessed on March 4, 2016).
- European Commission** (2015). *EU energy in figures: statistical pocketbook 2015*. Luxembourg: Publications Office of the European Union. ISBN 978-92-79-48359-2.
- Evins, R.** (2013). A review of computational optimisation methods applied to sustainable building design. *Renewable and Sustainable Energy Reviews* **22**, 230–245. ISSN 1364-0321.
- Evins, R., Pointer, P., Vaidyanathan, R. and Burgess, S.** (2012). A case study exploring regulated energy use in domestic buildings using design-of-experiments and multi-objective optimisation. *Building and Environment* **54**, 126–136. ISSN 0360-1323.
- Ewing, R.** (2011). Urban Design vs. Urban Planning: a Distinction With a Difference.
- Faucher, D. and Nivet, M.-L.** (2000). Playing with design intents: integrating physical and urban constraints in CAD. *Automation in Construction* **9**, 93–105. ISSN 0926-5805.
- Fazio, P., Bedard, C. and Gowri, K.** (1989). Knowledge-based system approach to building envelope design. *Computer-Aided Design* **21**, 519–527. ISSN 0010-4485.
- Few, S.** (2006). Multivariate Analysis Using Parallel Coordinates. *Business Intelligence Network - Perceptual Edge*.
- Forrester, A., Sobester, A. and Keane, A.** (2008). *Engineering design via surrogate modelling: a practical guide*. John Wiley & Sons.
- Foucquier, A., Robert, S., Suard, F., Stéphan, L. and Jay, A.** (2013). State of the art in building modelling and energy performances prediction: A review. *Renewable and Sustainable Energy Reviews* **23**, 272–288. ISSN 13640321.
- Gagne, J. M. L.** (2011). *An Interactive Performance-Based Expert System for Daylighting in Architectural Design*. Ph.D. thesis, Massachusetts Institute of Technology (MIT).
- Galasiu, A. D. and Reinhart, C. F.** (2008). Current daylighting design practice: a survey. *Building Research & Information* **36**, 159–174. ISSN 0961-3218, 1466-4321.
- Gallas, M. A., Bur, D. and Halin, G.** (2011a). Daylight and energy in the early phase of architectural design process. In *Proceedings of CAADRIA*. Hong Kong.
- Gallas, M. A., Bur, D. and Halin, G.** (2011b). A “green design” method to integrate daylight in the early phase of the design process. In *Proceedings of eCAADe*. Ljubljana, Slovenia.
- German Sustainable Building Council** (2013). The DGNB Certification System for Urban Districts.
- Goodman-Deane, J., Langdon, P. and Clarkson, J.** (2010). Key influences on the user-centred design process. *Journal of Engineering Design* **21**, 345–373. ISSN 0954-4828.

## Bibliography

---

- Graphisoft** (2016). ArchiCAD - Open BIM ([www.graphisoft.com/archicad/open\\_bim/](http://www.graphisoft.com/archicad/open_bim/)), last accessed on February 28, 2016).
- Grazziotin, P. C., Turkienicz, B., Sclovsky, L. and Freitas, C.** (2004). Cityzoom: A tool for the visualization of the impact of urban regulations. In *Proceedings of the Iberoamerican Congress of Digital Graphics*. Sao Leopoldo, Brazil.
- Grobman, Y. J., Yezioro, A. and Capeluto, I. G.** (2008). Building form generation based on multiple performance envelopes. In *Proceedings of PLEA*. Dublin, Ireland.
- Grobman, Y. J., Yezioro, A. and Capeluto, I. G.** (2010). Non-Linear Architectural Design Process. *International Journal of Architectural Computing* **8**, 41–54.
- Hachem, C., Athienitis, A. and Fazio, P.** (2012). Solar Optimized Neighbourhood Patterns: Evaluation and Guide-lines. In *Proceedings of eSim*. Halifax, Nova Scotia.
- Hachem, C., Fazio, P. and Athienitis, A.** (2013). Solar optimized residential neighborhoods: Evaluation and design methodology. *Solar Energy* **95**, 42–64. ISSN 0038092X.
- Hall, P., Dean, J., Kabul, I. K. and Silva, J.** (2014). An Overview of Machine Learning with SAS® Enterprise Miner™. In *Proceedings of SAS Global Forum*.
- Harzallah, A.** (2007). *Émergence et évolution des préconisations solaires dans les théories architecturales et urbaines en France, de la seconde moitié du XIXe siècle à la deuxième guerre mondiale..* Ph.D. thesis, Ecole nationale supérieure d'architecture de Nantes, Nantes.
- Hastie, T., Tibshirani, R. and Friedman, J.** (2009). *The Elements of Statistical Learning*. Springer, second edition.
- Hemsath, T. L. and Alagheband Bandhosseini, K.** (2015). Sensitivity analysis evaluating basic building geometry's effect on energy use. *Renewable Energy* **76**, 526–538. ISSN 0960-1481.
- Hensen, J. and Lamberts, R.,** eds. (2011). *Building performance simulation for design and operation*. London ; New York: Spon Press. ISBN 978-0-415-47414-6 978-0-203-89161-2.
- Hermund, A.** (2009). Building Information Modeling in the Architectural Design Phases, And Why Compulsory BIM can Provoke Distress Among Architects. In *Computation: The New Realm of Architectural Design*.
- Horvat, M. and Dubois, M.-C.** (2012). Tools and Methods for Solar Design—An Overview of IEA SHC Task 41, Subtask B. *Energy Procedia* **30**, 1120–1130. ISSN 1876-6102.
- Howard, B., Parshall, L., Thompson, J., Hammer, S., Dickinson, J. and Modi, V.** (2012). Spatial distribution of urban building energy consumption by end use. *Energy and Buildings* **45**, 141–151. ISSN 0378-7788.
- Hygh, J. S., DeCarolis, J. F., Hill, D. B. and Ranji Ranjithan, S.** (2012). Multivariate regression as an energy assessment tool in early building design. *Building and Environment* **57**, 165–175. ISSN 0360-1323.
- IEA** (2004). Types of Tools. Technical report, Canada Mortgage and Housing Corporation.

- IEA SHC Task 41** (2010). State-of-the-Art of Digital Tools Used by Architects for Solar Design. Technical Report Report T.41.B.1.
- IESNA** (2012). IES LM-83-12 IES Spatial Daylight Autonomy (sDA) and Annual Sunlight Exposure (ASE). Technical Report IES LM-83-12, New York, NY, USA.
- Jakubiec, A. and Reinhart, C. F.** (2011). DIVA 2.0: integrating daylight and thermal simulations using Rhinoceros 3d, DAYSIM and EnergyPlus. In *Proceedings of Building Simulation (IBPSA)*. Sidney, Australia: IBPSA.
- Kalay, Y. E.** (1985). Redefining the role of computers in architecture: from drafting/modelling tools to knowledge-based design assistants. *Computer-Aided Design* **17**, 319–328. ISSN 0010-4485.
- Kalay, Y. E.** (1998). P3: Computational environment to support design collaboration. *Automation in construction* **8**, 37–48.
- Kalay, Y. E.** (1999). Performance-based design. *Automation in Construction* **8**, 395–409. ISSN 09265805.
- Kalay, Y. E.** (2001). Enhancing multi-disciplinary collaboration through semantically rich representation. *Automation in Construction* **10**, 741–755. ISSN 0926-5805.
- Kanters, J., Horvat, M. and Dubois, M.-C.** (2014a). Tools and methods used by architects for solar design. *Energy and Buildings* **68, Part C**, 721–731. ISSN 0378-7788.
- Kanters, J. and Wall, M.** (2014). The impact of urban design decisions on net zero energy solar buildings in Sweden. *Urban, Planning and Transport Research* **2**, 312–332. ISSN 2165-0020.
- Kanters, J., Wall, M. and Dubois, M.-C.** (2014b). Typical Values for Active Solar Energy in Urban Planning. *Energy Procedia* **48**, 1607–1616. ISSN 1876-6102.
- Kanters, J., Wall, M. and Kjellsson, E.** (2014c). The Solar Map as a Knowledge Base for Solar Energy Use. *Energy Procedia* **48**, 1597–1606. ISSN 1876-6102.
- Karteris, M., Slini, T. and Papadopoulos, A. M.** (2013). Urban solar energy potential in Greece: A statistical calculation model of suitable built roof areas for photovoltaics. *Energy and Buildings* **62**, 459–468. ISSN 0378-7788.
- Kavgic, M., Mumovic, D., Summerfield, A., Stevanovic, Z. and Ecim-Djuric, O.** (2013). Uncertainty and modeling energy consumption: Sensitivity analysis for a city-scale domestic energy model. *Energy and Buildings* **60**, 1–11. ISSN 03787788.
- Kesser, F.** (2012). *Les enjeux techniques et commerciaux de la construction Minergie*. Ph.D. thesis, INSA de Strasbourg.
- Kämpf, J. H. and Robinson, D.** (2009). A hybrid CMA-ES and HDE optimisation algorithm with application to solar energy potential. *Applied Soft Computing* **9**, 738–745. ISSN 15684946.
- Kämpf, J. H. and Robinson, D.** (2010). Optimisation of building form for solar energy utilisation using constrained evolutionary algorithms. *Energy and Buildings* **42**, 807–814. ISSN 03787788.

## Bibliography

---

- Knowles, R. L.** (1974). *Energy and form: an ecological approach to urban growth*. Cambridge, MA, USA: The MIT Press.
- Knowles, R. L.** (1999). The Solar Envelope ([http://www-bcf.usc.edu/~rknowles/sol\\_env/sol\\_env.html](http://www-bcf.usc.edu/~rknowles/sol_env/sol_env.html), last accessed on February 24, 2016).
- Knowles, R. L.** (2003). The solar envelope: its meaning for energy and buildings. *Energy and buildings* **35**, 15–25.
- Kolbe, T. H., Gröger, G. and Plümer, L.** (2005). CityGML: Interoperable Access to 3d City Models. In P. D. P. v. Oosterom, D. S. Zlatanova and E. M. Fendel, eds., *Geo-information for Disaster Management*. Springer Berlin Heidelberg. ISBN 978-3-540-24988-7 978-3-540-27468-1, pages 883–899.
- Kolter, J. Z. and Ferreira Jr, J.** (2011). A large-scale study on predicting and contextualizing building energy usage. In *Proceedings of AAAI on Artificial Intelligence*. San Francisco, California, USA: Association for the Advancement of Artificial Intelligence. ISBN 978-1-57735-507-6.
- Kristl, Z. and Krainer, A.** (2001). Energy evaluation of urban structure and dimensioning of building site using iso-shadow method. *Solar Energy* **70**, 23–34. ISSN 0038-092X.
- Lagios, K., Niemasz, J. and Reinhart, C. F.** (2010). Animated Building Performance Simulation (ABPS)–Linking Rhinoceros/Grasshopper with Radiance/Daysim. In *Proceedings of SimBuild*. New York City, USA.
- Lam, J. C., Wan, K. K. W., Liu, D. and Tsang, C. L.** (2010). Multiple regression models for energy use in air-conditioned office buildings in different climates. *Energy Conversion and Management* **51**, 2692–2697. ISSN 0196-8904.
- Laprise, M., Lufkin, S. and Rey, E.** (2015). Towards sustainable regeneration of disused urban areas : a monitoring tool to integrate assessment into the projects dynamics. In *Proceedings of PLEA*. Bologna, Italy.
- Larson, G. W. and Shakespeare, R. A.** (1998). *Rendering with Radiance - The Art and Science of Lighting Visualization*. Morgan Kaufmann Publishers.
- Laëtitia, A., Olivier, B., Pascal, R. and Daniel, Q.** (2011). A Simple Method to Consider Energy Balance in the Architectural Design of Residential Buildings. In *Proceedings of SimAUD*. San Diego, CA, USA: Society for Computer Simulation International.
- Lechner, H. M.** (2009). *Heating, cooling and lighting*. New Jersey, USA: John Wiley and Sons Inc.
- Leidi, M. and Schlüter, A.** (2013). Exploring Urban Space: Volumetric Site Analysis for Conceptual Design in the Urban Context. *International Journal of Architectural Computing* **11**, 157–181. ISSN 1478-0771.
- Leung, K. S. and Steemers, K.** (2009). Exploring solar-responsive morphology for high-density housing in the tropics. In *Proceedings of CISBAT*. Lausanne, Switzerland.



- Likert, R.** (1932). A technique for the measurement of attitudes. *Archives of psychology* **22**, 101–119.
- Littlefair, P.** (1998). Passive solar urban design : ensuring the penetration of solar energy into the city. *Renewable and Sustainable Energy Reviews* **2**, 303–326. ISSN 1364-0321.
- Lobaccaro, G., Fiorito, F., Maserà, G. and Poli, T.** (2012). District geometry simulation: a study for the optimization of solar façades in urban canopy layers. In *Proceedings of SHC*.
- Long, N., Hirsch, A., Lobato, C. and Macumber, D.** (2010). Commercial Building Design Pathways Using Optimisation Analysis. In *Proceedings of ACEEE Summer Study*. Pacific Grove, California.
- LSE Cities and EIFER** (2014). CITIES AND ENERGY - Urban Morphology and Heat Energy Demand. Technical report, London.
- Luger, G. F.** (2005). *Artificial Intelligence: Structures and Strategies for Complex Problem Solving*. Addison-Wesley, fifth edition.
- Magnier, L. and Haghghat, F.** (2010). Multiobjective optimization of building design using TRNSYS simulations, genetic algorithm, and Artificial Neural Network. *Building and Environment* **45**, 739–746. ISSN 0360-1323.
- Mahdavi, A. and Gurtekin, B.** (2002). Shapes, Numbers, Perception: Aspects and Dimensions of the Design-Performance Space. In H. Timmermans, ed., *Part one: Architecture Proceedings*. The Netherlands.
- Malkawi, A. M., Srinivasan, R. S., Yi, Y. K. and Choudhary, R.** (2005). Decision support and design evolution: integrating genetic algorithms, CFD and visualization. *Automation in Construction* **14**, 33–44. ISSN 09265805.
- Mardaljevic, J. and Rylatt, M.** (2003). Irradiation mapping of complex urban environments: an image-based approach. *Energy and Buildings* **35**, 27–35. ISSN 0378-7788.
- Marin, P., Bignon, J.-C. and Lequay, H.** (2008). Generative exploration of architectural envelope responding to solar passive qualities. *Archive ouverte en Sciences de l'Homme et de la Société*.
- Martin, L. and March, L., eds.** (1972). *Urban Space and Structures*. Cambridge: University Press.
- Martins, T. A. d. L., Adolphe, L. and Bastos, L. E. G.** (2014). From solar constraints to urban design opportunities: optimization of built form typologies in a Brazilian tropical city. *Energy and Buildings* **76**, 43–56. ISSN 0378-7788.
- Mashood, P. K., Krishnamoorthy, C. S. and Ramamurthy, K.** (2007). KB-GA-based hybrid system for layout planning of multistory buildings. *Journal of computing in civil engineering* **21**, 229–237.
- McLean, D., Porter, J. and Halevi, T.** (2013). Integrated Design Education: Shifting the design paradigm. In *Proceedings of BESS-SB13*. Pomona, California, USA.

## Bibliography

---

- Meteotest** (2012). Meteonorm - global meteorological database (<http://www.meteonorm.com/>, last accessed on March 4, 2016).
- Microsoft** (2013). Visual Studio (<https://www.visualstudio.com/>, last accessed on January 20, 2016).
- Miguet, F.** (2007). A further step in environment and bioclimatic analysis: the software tool Solene. In *Proceedings of Building Simulation (IBPSA)*. Beijing, China.
- Miguet, F. and Groleau, D.** (2007). Urban bioclimatic indicators for urban planners with the software tool SOLENE. In *Proceedings of SB07*. Lisbon, Portugal.
- Milne, M.** (1991). Design Tools: Future Design Environments for Visualizing Building Performance. In *Proceedings of CAAD futures*. Liège, Belgium.
- Milne, M., Gomez, C., Leeper, D., Kobayashi, Y., Zurick, J., Weintraub, D. and Miranda, H.** (2001). A Drag-and-Drop Energy Design Tool. In *Proceedings of ASES*. American Solar Energy Society.
- Mindali, O., Raveh, A. and Salomon, I.** (2004). Urban density and energy consumption: a new look at old statistics. *Transportation Research Part A: Policy and Practice* **38**, 143–162. ISSN 0965-8564.
- Müller, S., Kresse, W., Gatenby, N. and Schoeffel, F.** (1995). A radiosity approach for the simulation of daylight. In *Rendering Techniques' 95*. Springer, pages 137–146.
- Moe, K.** (2008). *Integrated Design in Contemporary Architecture*. Princeton Architectural Press. ISBN 978-1-56898-745-3.
- Montavon, M.** (2010). *Optimisation of urban form by the evaluation of the solar potential*. PhD Thesis, École Polytechnique Fédérale de Lausanne (EPFL).
- Montavon, M., Scartezzini, J.-L. and Compagnon, R.** (2004a). Comparison of the solar energy utilisation potential of different urban environments. In *Proceedings of PLEA*. Eindhoven, The Netherlands.
- Montavon, M., Scartezzini, J. L. and Compagnon, R.** (2004b). Solar energy utilisation potential of three different Swiss urban sites. *Energie und Umweltforschung im Bauwesen, Zurich*, p. 503–510.
- Moon, P. and Spencer, D. E.** (1942). Illumination from a non-uniform sky. *Illum. Eng.* **37**, 707–726.
- Moonen, P. and Allegrini, J.** (2015). Employing statistical model emulation as a surrogate for CFD. *Environmental Modelling & Software* **72**, 77–91. ISSN 13648152.
- Morello, E. and Ratti, C.** (2009). Sunscapes: 'Solar envelopes' and the analysis of urban DEMs. *Computers, Environment and Urban Systems* **33**, 26–34. ISSN 01989715.
- Moudon, A. V.** (1997). Urban morphology as an emerging interdisciplinary field. *Urban Morphology* **1**.

- Mueller, C. and Ochsendorf, J.** (2013). An Integrated Computational Approach for Creative Conceptual Structural Design. In *Proceedings of IASS Symposium*.
- Nault, E., Peronato, G. and Andersen, M.** (2015a). Potentiel solaire et forme urbaine. In E. Rey, ed., *Urban Recovery*. Lausanne: Presses Polytechniques et Universitaires Romandes (PPUR), pages 97–106.
- Nault, E., Peronato, G., Rey, E. and Andersen, M.** (2015b). Review and critical analysis of early-design phase evaluation metrics for the solar potential of neighborhood designs. *Building and Environment* **92**, 679–691. ISSN 0360-1323.
- Nault, E., Rastogi, P., Rey, E. and Andersen, M.** (2015c). The sensitivity of predicted energy use to urban geometrical factors in various climates. In *Proceedings of PLEA*. Bologna, Italy.
- Nault, E., Rey, E. and Andersen, M.** (2013). Early design phase evaluation of urban solar potential: Insights from the analysis of six projects. In *Proceedings of BS 2013*. Chambéry, France.
- Nault, E., Rey, E. and Andersen, M.** (2016a). A multi-criteria performance-based decision-support workflow for early-stage neighborhood design. In *Proceedings of PLEA*. Los Angeles, USA.
- Nault, E., Rey, E. and Andersen, M.** (2016b). Urban planning and solar potential: assessing users' interaction with a novel decision-support workflow for early-stage design. In *Proceedings of SBE16*. Zurich, Switzerland.
- Nemoto, T. and Beglar, D.** (2014). Developing Likert-Scale Questionnaires. In *Proceedings of JALT2013*. Tokyo, Japan.
- Ng, E.** (2005). A study of the relationship between daylight performance and height difference of buildings in high density cities using computational simulation. In *Proceedings of Building Simulation (IBPSA)*. Montréal: IBPSA.
- Ng, E. and Cheng, V.** (2004). Daylight Design and Regulation for High Density Cities. In *Proceedings of ASES*.
- Nguyen, A.-T., Reiter, S. and Rigo, P.** (2014). A review on simulation-based optimization methods applied to building performance analysis. *Applied Energy* **113**, 1043–1058. ISSN 0306-2619.
- Niemasz, J., Sargent, J. and Reinhart, C. F.** (2011). Solar zoning and energy in detached residential dwellings. In *Proceedings of SimAUD'11*. San Diego, CA, USA.
- Ochoa, C. E., Aries, M. B., van Loenen, E. J. and Hensen, J. L.** (2012). Considerations on design optimization criteria for windows providing low energy consumption and high visual comfort. *Applied Energy* **95**, 238–245. ISSN 03062619.
- Ochoa, C. E. and Capeluto, I. G.** (2009). Advice tool for early design stages of intelligent facades based on energy and visual comfort approach. *Energy and Buildings* **41**, 480–488. ISSN 03787788.

## Bibliography

---

- OFEN** (2014). Graphiques de la statistique globale suisse de l'énergie 2014. Statistics, Confédération Suisse - Office fédéral de l'énergie.
- OFEN and DETEC** (2013). Perspectives énergétiques 2050 - Résumé. Technical report, Confédération Suisse - Office fédéral de l'énergie - Département fédéral de l'environnement, des transports, de l'énergie et de la communication.
- OFS** (2014). Statistique des bâtiments et des logements 2014. Statistics, Confédération Suisse - Office fédéral de la statistique.
- Oke, T. R.** (1988). Street design and urban canopy layer climate. *Energy and buildings* **11**, 103–113.
- Okeil, A.** (2010). A holistic approach to energy efficient building forms. *Energy and Buildings* **42**, 1437–1444. ISSN 0378-7788.
- Oliveira Panão, M. J. N., Gonçalves, H. J. P. and Ferrão, P. M. C.** (2008). Optimization of the urban building efficiency potential for mid-latitude climates using a genetic algorithm approach. *Renewable Energy* **33**, 887–896. ISSN 0960-1481.
- Otis, T.** (2012). Is solar design a Straitjacket for architecture? *Architecture & Sustainable Development-Proceedings-Vol. 1* **1**, 77.
- Oxman, R.** (2009). Performative design: a performance-based model of digital architectural design. *Environment and Planning B-Planning & Design* **36**, 1026–1037. ISSN 0265-8135.
- Papalambros, P. Y. and Wilde, D. J.** (2000). *Principles of Optimal Design: Modeling and Computation*. Cambridge University Press. ISBN 978-0-521-62727-6.
- Papamichael, K., La Porta, J. and Chauvet, H.** (1997). Building Design Advisor: automated integration of multiple simulation tools. *Automation in Construction* **6**, 341–352.
- Paule, B., Flourentzou, F., Pantet, S. and Boutillier, J.** (2011). DIAL+ suite: a complete, but simple, suite of tools to optimize the global performance of buildings openings. In *Proceedings of CISBAT*. Lausanne, Switzerland.
- Pereira, F., Leder, S. M., Moraes, L. N. and Lenzi, C.** (2009). Sky Obstruction and Daylight. In *Proceedings of PLEA*. Quebec City, Canada.
- Pereira, F. O. R., Silva, C. A. N. and Turkienikz, B.** (2001). A methodology for sunlight urban planning: a computer-based solar and sky vault obstruction analysis. *Solar Energy* **70**, 217–226. ISSN 0038-092X.
- Peronato, G.** (2014). *Built density, solar potential and daylighting: Application of parametric studies and performance simulation tools in urban design*. Tesi di Laurea Magistrale (Master's thesis), Università Iuav di Venezia, Venezia.
- Peronato, G., Nault, E., Cappelletti, E., Peron, F. and Andersen, M.** (2015). A parametric design-based methodology to visualize building performance at the neighborhood scale. In *Proceedings of BSA*. Bolzano: Bozen-Bolzano University Press. ISBN 978-88-6046-074-5.

- Pessenlehner, W. and Mahdavi, A.** (2003). Building morphology, transparency, and energy performance. In *Proceedings of Building Simulation (IBPSA)*. Eindhoven, Netherlands: IBPSA.
- Petersen, S. and Svendsen, S.** (2010). Method and simulation program informed decisions in the early stages of building design. *Energy and Buildings* **42**, 1113–1119. ISSN 03787788.
- Prazeres, L. M. R. and Clarke, J. A.** (2003). Communicating building simulation outputs to users. In *Proceedings of Building Simulation (IBPSA)*. Eindhoven, The Netherlands.
- Raboudi, K. and Saci, A. B.** (2013). A morphological generator of urban rules of solar control. In *Proceedings of PLEA*. Munich, Germany.
- Rasmussen, C. E. and Williams, C. K. I.** (2006). *Gaussian processes for machine learning*. Adaptive computation and machine learning. Cambridge, Mass: MIT Press. ISBN 978-0-262-18253-9.
- Rastogi, P.** (2016). *On the sensitivity of buildings to climate: the interaction of weather and building envelopes in determining future building energy consumption (in preparation)*. PhD, Ecole polytechnique fédérale de Lausanne, Lausanne, Switzerland.
- Ratti, C., Baker, N. and Steemers, K.** (2005). Energy consumption and urban texture. *Energy and Buildings* **37**, 762–776. ISSN 0378-7788.
- Ratti, C., Raydan, D. and Steemers, K.** (2003). Building form and environmental performance: archetypes, analysis and an arid climate. *Energy and Buildings* **35**, 49–59. ISSN 0378-7788.
- Ratti, C., Robinson, D., Baker, N. and Steemers, K.** (2000). LT Urban. In *Architecture, City, Environment*. Cambridge, UK: James & James.
- Reinhart, C., Bourgeois, D., Dubrous, F., Laouadi, A., Lopez, P. and Stelescu, O.** (2007). Daylight 1-2-3—a state-of-the-art daylighting/energy analysis software for initial design investigations. In *Proceedings of Building Simulation (IBPSA)*. Beijing, China.
- Reinhart, C., Dogan, T., Jakubiec, J. A., Rakha, T. and Sang, A.** (2013). Umi—an urban simulation environment for building energy use, daylighting and walkability. In *Proceedings of Building Simulation (IBPSA)*. Chambéry, France.
- Reinhart, C. and LoVerso, V.** (2010). A rules of thumb-based design sequence for diffuse daylight. *Lighting Research and Technology* **42**, 7–31. ISSN 1477-1535.
- Reinhart, C. F.** (2005). A simulation-based review of the ubiquitous window-head-height to daylit zone depth rule-of-thumb. In *Proceedings of Building Simulation (IBPSA)*. Montreal, Canada.
- Reinhart, C. F. and Cerezo Davila, C.** (2016). Urban building energy modeling – A review of a nascent field. *Building and Environment* **97**, 196–202. ISSN 0360-1323.
- Reinhart, C. F., Mardaljevic, J. and Rogers, Z.** (2006). Dynamic Daylight Performance Metrics for Sustainable Building Design. *LEUKOS* **3**, 7–31. ISSN 1550-2724.

## Bibliography

---

- Reinhart, C. F. and Wienold, J.** (2011). The daylighting dashboard – A simulation-based design analysis for daylit spaces. *Building and Environment* **46**, 386–396. ISSN 03601323.
- Rey, E.,** ed. (2013). *Green Density*. Lausanne: Presses Polytechniques Universitaires Romandes.
- Rey, E.,** ed. (2015). *Urban Recovery*. Lausanne: Presses Polytechniques Universitaires Romandes.
- Rickaby, P. A.** (1987). An approach to the assessment of the energy efficiency of urban built form. In D. Hawkes, J. Owers, P. Rickaby and P. Steadman, eds., *Energy and Urban Built Form*. pages 43–61.
- Riera Pérez, M. G.** (2016). *Méthodologie multicritère d'aide à la décision pour le renouvellement urbain à l'échelle du quartier*. PhD Thesis, Ecole polytechnique fédérale de Lausanne, EPFL, Lausanne, Switzerland.
- Ritter, F., Geyer, P. and Borrmann, A.** (2015). Simulation-based Decision-making in Early Design Stages. In *Proceedings of CIB W78 Conference*. Eindhoven, Netherlands.
- Roberts, A. and Marsh, A.** (2001). ECOTECT: environmental prediction in architectural education. In *Proceedings of ECAADE*. Helsinki, Finland.
- Robinson, D.** (2006). Urban morphology and indicators of radiation availability. *Solar Energy* **80**, 1643–1648. ISSN 0038092X.
- Robinson, D., Campbell, N., Gaiser, W., Kabel, K., Le-Mouel, A., Morel, N., Page, J., Stankovic, S. and Stone, A.** (2007). SUNtool – A new modelling paradigm for simulating and optimising urban sustainability. *Solar Energy* **81**, 1196–1211. ISSN 0038092X.
- Robinson, D., Haldi, F., Kämpf, J., Leroux, P., Perez, D., Rasheed, A. and Wilke, U.** (2009). CitySim: Comprehensive micro-simulation of resource flows for sustainable urban planning. In *Proceedings of Building Simulation (IBPSA)*. Glasgow, Scotland.
- Robinson, D., Scartezzini, J.-L., Montavon, M. and Compagnon, R.** (2005). SOLURBAN Project - Solar Utilisation Potential of Urban Sites. Technical report, Swiss Federal Office for Energy, Bern.
- Robinson, D. and Stone, A.** (2004). Irradiation modelling made simple: the cumulative sky approach and its applications. In *Proceedings of PLEA*. Eindhoven, The Netherlands.
- Rodríguez-Álvarez, J.** (2016). Urban Energy Index for Buildings (UEIB): A new method to evaluate the effect of urban form on buildings' energy demand. *Landscape and Urban Planning* **148**, 170–187. ISSN 0169-2046.
- Roudsari, M. S., Pak, M., Smith, A. and Gill, G.** (2013). Ladybug: a parametric environmental plugin for grasshopper to help designers create an environmentally-conscious design. In *Proceedings of Building Simulation (IBPSA)*. Chambéry, France.
- Saltelli, A., Tarantola, S., Campolongo, F. and Ratto, M.** (2004). *Sensitivity Analysis in Practice: A Guide to Assessing Scientific Models*. England: John Wiley & Sons Ltd.

- Samimi, M. and Nasrollahi, F.** (2014). *Intelligent design using solar-climatic vision: energy and comfort improvement in architecture and urban planning using SOLARCHVISION*. Number 09 in Young cities research paper series. Berlin: Univ.-Verl. der TU, Univ.-Bibliothek. ISBN 978-3-7983-2675-0.
- Sattrup, P. A. and Strømmand-Andersen, J.** (2013). Building Typologies in Northern European Cities: Daylight, Solar Access, and Building Energy Use. *Journal of Architectural and Planning Research* **30**, 56.
- Schneider, C., Koltsova, A. and Schmitt, G.** (2011). Components for Parametric Urban Design in Grasshopper from Street Network to Building Geometry. In *Proceedings of SimAUD'11*. San Diego, CA, USA: Society for Computer Simulation International.
- SDOL and Gauthier, R.** (2012). Malley Centre, Ouest Lausannois - Les coulisses de Malley. Concours d'urbanisme et d'espaces publics à un degré. Rapport du jury., Bureau du Schéma directeur de l'Ouest lausannois, Renens.
- Seong, Y.-B., Lim, J.-H., Yeo, M.-S., Goh, I.-D. and Kim, K.-W.** (2006). HELIOS: Solar rights analysis system for apartment buildings. *Solar Energy* **80**, 723–741. ISSN 0038-092X.
- Shaviv, E., Yezioro, A., Capeluto, I. G., Peleg, U. J. and Kalay, Y. E.** (1996). Simulations and knowledge-based computer-aided architectural design (CAAD) systems for passive and low energy architecture. *Energy and Buildings* **23**, 257–269. ISSN 0378-7788.
- Sherif, A., Sabry, H. and Gadelhak, M.** (2013). Daylighting simulation as means for configuring hospital intensive care unit windows under the desert clear skies. *Dimensions (m)* **5**, 3–00.
- SIA** (1999). SIA 180 Isolation thermique et protection contre l'humidité dans les bâtiments.
- SIA** (2009a). SIA 2031 Certificat énergétique des bâtiments.
- SIA** (2009b). SIA 380/1 Thermal Energy in Buildings.
- SIA** (2011). SIA 2040 La voie SIA vers l'efficacité énergétique. Technical Report SIA 2040, SIA, Zurich.
- SIA** (2015). SIA 2024 Données d'utilisation des locaux pour l'énergie et les installations du bâtiment.
- Simpson, T. W., Poplinski, J. D., Koch, P. N. and Allen, J. K.** (2014). Metamodels for Computer-based Engineering Design: Survey and recommendations. *Engineering with Computers* **17**, 129–150. ISSN 0177-0667, 1435-5663.
- Siret, D.** (1997). *Propositions pour une approche déclarative des ambiances dans le projet architectural: application à l'ensoleillement*. Ph.D. thesis, Université de Nantes.
- Siret, D.** (2013). Les sensations du soleil dans les théories architecturales et urbaines. De l'hygiénisme à la ville durable. In R. Beck, U. Krampfl and E. Retailaud-Bajac, eds., *Les cinq sens de la ville du Moyen Âge à nos jours*. Presses universitaires François-Rabelais (PUFR).

## Bibliography

---

- Smith, L., Bernhardt, K. and Jezyk, M.** (2011). Automated Energy Model Creation for Conceptual Design. In *Proceedings of SimAUD'11*. San Diego, CA, USA: Society for Computer Simulation International.
- Stemers, K.** (2003). Energy and the city: density, buildings and transport. *Energy and Buildings* **35**, 3–14. ISSN 0378-7788.
- Strømmandersen, J. and Sattrup, P.** (2011). The urban canyon and building energy use: Urban density versus daylight and passive solar gains. *Energy and Buildings* **43**, 2011–2020. ISSN 03787788.
- SuisseEnergie** (2014). Concept pour l'établissement du bilan de la société à 2000 watts (<http://www.2000watt.ch/fr/pour-les-ville-et-les-communes/concept-pour-etablissement-du-bilan/>, last accessed on January 4, 2016).
- SuisseEnergie** (2016). Société à 2000 watts (<http://www.2000watt.ch/fr/>, last accessed on January 25, 2016).
- Takebayashi, H. and Moriyama, M.** (2012). Relationships between the properties of an urban street canyon and its radiant environment: Introduction of appropriate urban heat island mitigation technologies. *Solar Energy* **86**, 2255–2262. ISSN 0038092X.
- Taleghani, M., Tenpierik, M., van den Dobbelen, A. and de Dear, R.** (2013). Energy use impact of and thermal comfort in different urban block types in the Netherlands. *Energy and Buildings* **67**, 166–175. ISSN 0378-7788.
- Teller, J. and Azar, S.** (2001). Townscope II—a computer system to support solar access decision-making. *Solar Energy* **70**, 187–200.
- Tereci, A., Kesten, D. and Eicker, U.** (2010). The impact of the urban form on heating, cooling, and lighting demand of cities. In *Proceedings of ICSU*. Hong Kong, China.
- The MathWorks** (2014). Supervised Learning (Machine Learning) Workflow and Algorithms (<http://www.mathworks.ch/ch/help/stats/supervised-learning-machine-learning-workflow-and-algorithms.html>, last accessed on January 18, 2016).
- Thomas, D., Miller, C., Kämpf, J. and Schlueter, A.** (2014). Multiscale co-simulation of EnergyPlus and CitySim models derived from a building information model. In *Proceedings of BauSIM*. RWTH Aachen University: International Building Performance Simulation Association.
- Tsanas, A. and Xifara, A.** (2012). Accurate quantitative estimation of energy performance of residential buildings using statistical machine learning tools. *Energy and Buildings* **49**, 560–567. ISSN 0378-7788.
- Tso, G. K. F. and Yau, K. K. W.** (2007). Predicting electricity energy consumption: A comparison of regression analysis, decision tree and neural networks. *Energy* **32**, 1761–1768. ISSN 0360-5442.
- Turkienicz, B., Gonçalves, B. B. and Grazziotin, P.** (2008). CityZoom: a visualization tool for the assessment of planning regulations. *International Journal of Architectural Computing* **6**, 79–95.



- Urban, B. and Glicksman, L.** (2006). The MIT Design Advisor - A fast, simple tool for energy efficient building design. In *Proceedings of SimBuild*. Cambridge, MA.
- Urbaplan** (2015). Plan Directeur Localisé Intercommunal Lausanne-Vernand - Romanel-sur-Lausanne. Cahier 1 - Rapport d'aménagement. Technical Report V.1.3.
- U.S. Department of Energy** (2011). Buildings Energy Data Book. Statistics.
- van Esch, M., Looman, R. and de Bruin-Hordijk, G.** (2012). The effects of urban and building design parameters on solar access to the urban canyon and the potential for direct passive solar heating strategies. *Energy and Buildings* **47**, 189–200. ISSN 03787788.
- Verdonck, E., Lieve, W., Verbeeck, G. and Froyen, H.** (2011). Design Support Tools in Practice. The Architects' Perspective. In *Proceedings of CAAD Futures*. Liège, Belgium. ISBN 978-2-87456-142-9.
- Vermeulen, T., Kämpf, J. H. and Beckers, B.** (2013). Urban Form Optimization for the Energy Performance of Buildings Using Citysim. In *Proceedings of CISBAT*, volume 2. Lausanne, Switzerland.
- Ville de Lausanne** (2010). Concept énergétique pour le quartier durable des Plaines-du-Loup. Technical report.
- Ville de Lausanne** (2013). Les Plaines-du-Loup - Plan directeur localisé en vue de la réalisation d'un écoquartier. Technical report, Ville de Lausanne - Service d'urbanisme, TRIBU Architecture, CITEC, PAYSAGESTION.
- Wang, W., Zmeureanu, R. and Rivard, H.** (2005). Applying multi-objective genetic algorithms in green building design optimization. *Building and Environment* **40**, 1512–1525. ISSN 03601323.
- Welch, A., Benfield, K. and Raimi, M.** (2011). A Citizen's Guide to LEED for Neighborhood Development: How to Tell if Development is Smart and Green. Technical report, Raimi + Associates and Natural Resources Defense Council.
- Wetter, M.** (2001). GenOpt®, "Generic Optimization Program. In *Proceedings of Building Simulation (IBPSA)*. Rio de Janeiro, Brazil.
- Weytjens, L. and Verbeeck, G.** (2009). Analysis of the impact of sustainability related design parameters in the architectural design process: A case study research. In *Proceedings of SASBE*. Delft University of Technology.
- Weytjens, L. and Verbeeck, G.** (2010). Towards' architect-friendly' energy evaluation tools. In *Proceedings of SpringSim*. San Diego, CA, USA.
- Yezioro, A.** (2009). A knowledge based CAAD system for passive solar architecture. *Renewable Energy* **34**, 769–779. ISSN 09601481.
- Yezioro, A., Capeluto, I. G. and Shaviv, E.** (2006). Design guidelines for appropriate insolation of urban squares. *Renewable Energy* **31**, 1011–1023. ISSN 09601481.

## Bibliography

---

- Yi, Y. K. and Malkawi, A. M.** (2009). Optimizing building form for energy performance based on hierarchical geometry relation. *Automation in Construction* **18**, 825–833. ISSN 0926-5805.
- Zeiler, W., Savanovic, P. and Quanjel, E.** (2007). Design decision support for the conceptual phase of the design process. In *Proceedings of IASDR07*. Hong Kong.
- Zemella, G., De March, D., Borrotti, M. and Poli, I.** (2011). Optimised design of energy efficient building façades via Evolutionary Neural Networks. *Energy and Buildings* **43**, 3297–3302. ISSN 03787788.
- Zhang, J., Heng, C. K., Malone-Lee, L. C., Hii, D. J. C., Janssen, P., Leung, K. S. and Tan, B. K.** (2012a). Evaluating environmental implications of density: A comparative case study on the relationship between density, urban block typology and sky exposure. *Automation in Construction* **22**, 90–101. ISSN 09265805.
- Zhang, J., Heng, C. K., Malone-Lee, L. C., Huang, Y. C., Janssen, P., Hii, D. J. C. and Ibrahim, N.** (2012b). Preliminary Evaluation of A Daylight Performance Indicator for Urban Analysis: Facade Vertical Daylight Factor per Unit Floor Area. In *Proceedings of SimBuild*. Madison, Wisconsin, USA: SimBuild.
- Zhao, H.-x. and Magoulès, F.** (2012). A review on the prediction of building energy consumption. *Renewable and Sustainable Energy Reviews* **16**, 3586–3592. ISSN 1364-0321.

## EMILIE NAULT

Nationality: Canadian  
Date of birth: 27/11/1986  
[emilie.nault@gmail.com](mailto:emilie.nault@gmail.com)



### EDUCATION

- 2011 - 2016 **PhD, Ecole polytechnique fédérale de Lausanne (EPFL), Switzerland**  
*(expected)* **Interdisciplinary Laboratory of Performance-Integrated Design (LIPID)**  
Development of a **decision-support workflow** for the **early-design phase of neighbourhoods**. Building physics, simulations (thermal, daylight, solar potential), data analysis, mathematical modeling.  
Supervisor: Prof Marilyne Andersen, Co-supervisor: Prof Emmanuel Rey
- 2009 - 2010 **Masters in Renewable Energy Engineering**  
Heriot-Watt University, Edinburgh, Scotland
- 2005 - 2009 **Bachelor in Physics**  
Université de Sherbrooke, Canada  
**Exchange year** at the Université de Genève, Switzerland

### WORK EXPERIENCE

- 2011 **Company QNORM, Qualitat I Medi Ambient, Girona, Espagne**  
(6 months) Development of internal tools, communication with companies, assistant in energy audits and research projects, translations
- 2010 **School of the Built Environment, Heriot-Watt University, Edinburgh, Scotland**  
(2 months) Review of steady-state domestic energy modeling software
- 2007 **Oceanographic Sciences Division, Fisheries and Oceans Canada, Maurice Lamontagne Institute, Mont-Joli, Canada**  
(8 months) Research in physical oceanography; study of ocean currents, creation of an oxygen atlas for the St. Lawrence Gulf; co-author of an article

### SPECIFIC COMPETENCES

Word and image processing software:

**Latex, Microsoft Office, Excel VBA, Adobe InDesign**

Parametric modeling and simulation tools (energy, daylight) for buildings:

**Rhino, DIVA-for-Rhino, Grasshopper (and associated plug-ins), DesignBuilder, EnergyPlus**

Data analysis and processing techniques; mathematical modeling:

Statistics, visualizations, regressions with **Matlab, Python, Excel**

### LANGUAGES

|                |                       |                |                             |
|----------------|-----------------------|----------------|-----------------------------|
| <b>French</b>  | Native language       | <b>Spanish</b> | Very good knowledge (B2-C1) |
| <b>English</b> | Bilingual proficiency | <b>German</b>  | Beginner (A1)               |

## PARTICIPATION IN RESEARCH PROJECTS AND VOLUNTEERING

- 2014 - Participation in the Synergistic Energy and Comfort through Urban Resource Effectiveness (SECURE) project, of the Competence Center Energy and Mobility (CCEM)  
*Contribution to the development of a holistic simulation and analysis framework*
- 2012 - Participation in the International Energy Agency (IEA) Task 51 on Solar Energy in Urban Planning  
*Review of legislation (urban planning and energy laws) in Switzerland, review and development of decision-support methods and tools, presentation of case studies*
- 2012 - Participant in the Energy Efficient Buildings and Communities (EEBC) project, GreenTech Initiative, EuroTech Universities  
*Exchanges with doctoral students from the 4 affiliated universities*
- 2013 - 2015 Member of the EPFL's Association of Research Scientists  
*Representation of members, organisation of various events*

## PUBLICATIONS

### Book chapters:

E. Nault, G. Peronato and M. Andersen (2015). **Potentiel solaire et forme urbaine**, in **Urban Recovery** (éd. : E. Rey), Architecture Albums, PPUR.

M. Andersen and E. Nault (2013). **Influence de la forme urbaine sur le potentiel solaire**, in **Green Density**, Architecture Albums, PPUR.

### Journal article:

E. Nault, G. Peronato, E. Rey and M. Andersen (2015). **Review and critical analysis of early-design phase evaluation metrics for the solar potential of neighborhood designs**, in *Building and Environment*, vol. 92, p. 679-691.

### Conference paper:

E. Nault, E. Rey, and M. Andersen (2016). **A multi-criteria performance-based decision-support workflow for early-stage neighborhood design**. Submitted to PLEA 2016 - 32th Passive and Low Energy Architecture Conference. Los Angeles, USA.

E. Nault, E. Rey, and M. Andersen (2016). **Urban planning and solar potential: assessing users' interaction with a novel decision-support workflow for early-stage design**. Accepted for SBE16. Zurich, Switzerland.

E. Nault, P. Rastogi, E. Rey and M. Andersen (2015). **The sensitivity of predicted energy use to urban geometrical factors in various climates**. PLEA 2015 - 31th Passive and Low Energy Architecture Conference. Bologna, Italy.

G. Peronato, E. Nault, F. Cappelletti, F. Peron and M. Andersen (2015). **A parametric design-based methodology to visualize building performance at the neighborhood scale**. Building Simulation Applications - 2nd IBPSA-Italy Conference, Bolzano, Italy.

E. Nault, E. Rey and M. Andersen (2013). **Early design phase evaluation of urban solar potential: Insights from the analysis of six projects**. Proceedings of IBPSA Conference. Chambéry, France.

E. Nault, E. Rey and M. Andersen (2013). **Towards climate-based irradiation recommendations for optimal solar design: insights from a parametric study**. sb13 - Sustainable Buildings: Implementing Sustainability, Barriers and Chances Conference. Munich, Germany.

